NONLINEAR DYNAMICS IN OPTICAL SYSTEMS

NDOS'95

Conference Digest

JUNE 5-7, 1995

University of Rochester

Rochester, New York, U.S.A.

REPORT DOCUMENTATION PAGE

OMB No. 0704-0188

1. AGENCY USE ONLY (Leave blank)	2. REPORT DATE	3. REPORT TYPE AND DATES COVERED
	January 15, 1996	Final, 4/1/95 - 11/30/95

4. TITLE AND SUBTITLE
Conference on Nonlinear Dynamics in Optical Systems (NDOS '95), June 5-7, 1995

5. FUNDING NUMBERS
Symposium Grant (G)
G#N00014-95-0530

6. AUTHOR(S)
Govind P. Agrawal

7. PERFORMING ORGANIZATION NAME(S) AND ADDRESS(ES)
University of Rochester
518 Hylan Building, ORPA
Rochester, NY 14627

8. PERFORMING ORGANIZATION REPORT NUMBER
NDOS-528838

9. SPONSORING/MONITORING AGENCY NAME(S) AND ADDRESS(ES)
Office of Naval Research
800 North Quincy Street
Arlington, VA 22217-5000

10. SPONSORING/MONITORING AGENCY REPORT NUMBER
R&T: 3107026-01

11. SUPPLEMENTARY NOTES
Symposium grant for NDOS '95 conference held at Rochester, June 5-7, 1995

12a. DISTRIBUTION/AVAILABILITY STATEMENT
Available for general distribution (UL)

12b. DISTRIBUTION CODE

13. ABSTRACT *(Maximum 200 words)*

The conference on "Nonlinear Dynamics in Optical Systems" (NDOS '95) was held at Rochester during June 5-7, 1995. About 150 scientists and graduate students from more than ten countries attended the conference. A joint session with the "Coherence and Quantum Optics Conference" was aheld on June 7, 1995.

14. SUBJECT TERMS
Nonlinear Optics, Optics Instabilities

15. NUMBER OF PAGES
5

16. PRICE CODE

17. SECURITY CLASSIFICATION OF REPORT	18. SECURITY CLASSIFICATION OF THIS PAGE	19. SECURITY CLASSIFICATION OF ABSTRACT	20. LIMITATION OF ABSTRACT
Unclassified	Unclassified	Unclassified	UL

FINAL REPORT on NDOS '95
Conference on
Nonlinear Dynamics in Optical Systems

The conference on Nonlinear Dynamics in Optical Systems (NDOS '95), was held in Rochester, New York, during the period June 5-7, just preceding the Seventh Coherence and Quantum Optics conference (CQO7), which was scheduled for June 7-10, 1995. On June 7, joint sessions were held with CQO7 that were planned in consultation with the organizing committee for that conference. The historic Coherence and Quantum Optics conferences have been held, since its beginning, seven times, consecutive meetings about six years apart. This year provided a rare opportunity to hold NDOS as a satellite meeting in concurrence with CQO7. As a historical footnote, three meetings on the general topic of nonlinear dynamics in optical systems have been organized before NDOS'95. The first was the Optical Instabilities conference in Rochester (1985). The second meeting was in Afton, Oklahoma (1990) with the title Nonlinear Dynamics in Optical Systems (NDOS). This title has been retained for the third and fourth meetings held in Alpbach, Austria (1992) and Rochester, NY (1995). These were highly successful meetings and demonstrated the growing interest in both the basic science and applied engineering aspects of optical instabilities. All the meetings were typically attended by 150 participants, and represented the truly international nature of this field of research because of the geographical distribution of the participants..

NDOS has come to be recognized as a unique meeting point for leading researchers in dynamical systems with expertise in the fields such as optical instabilities, chaos and its control, optical solitons and their applications, and laser physics. Advances in the mathematical discipline of dynamical systems have traditionally been aimed at fluid dynamics scientists and often at those studying the dynamics of chemical reactions and mechanical systems. In the past decade it has become evident that optical systems provide a novel setting for the exploration of nonlinear dynamics over a vast range of time scales and in one, two and even three spatial dimensions. It is perhaps the only meeting that has a goal of developing strong interdisciplinary ties between dynamical systems

researchers in the mathematical sciences and optical scientists and engineers. NDOS meetings have focused the attention of both communities on the similarities between fluid dynamical and optical pattern formation mechanisms, demonstrating the profound and deep connections of these disciplines. At the NDOS'95 meeting in Rochester, NY, reports on the control of chaotic behavior of laser systems and transverse pattern dynamics once again demonstrated the direct application of algorithms developed in a mathematical context to optical systems.

CONFERENCE ORGANIZATION

The conference was organized by a group of five scientists, all members of the Organizing Committee. They were helped in the selection of topics and invited speakers by the Advisory Committee. The program committee members helped in the review and selection of the contributed papers. The members of the three committees are listed here.

ORGANIZING COMMITTEE

G. P. Agrawal (Rochester)
P. Glorieux (Lille)
Y. Khanin (Nizhny-Novgorod)
M. Piché (Québec)
R. Roy (Atlanta)

PROGRAM COMMITTEE

M. Brambilla (Milan)
P. Colet (Palma de Mallorca)
O. Kocharovskaya (Novgorod)
N. Loiko (Minsk)
J. McInerney (Cork)
L. Melnikov (Saratov)
F. Mitschke (Münster)
J. Moloney (Tucson)

ADVISORY COMMITTEE

N. Abraham (Bryn Mawr)
F.T. Arecchi (Florence)
E. Arimondo (Pisa)
R. Boyd (Rochester)
G. Casati (Milan)
W. Firth (Glasgow)
R. Fork (Huntsville)

D. Lenstra (Amsterdam)
R. Harrison (Edinburg)
H. Haken (Stuttgart)
W. Lange (Muenster)
L. Lugiato (Milan)
A. Mak (St. Petersburg)
P. Mandel (Brussels)
A. Oraevsky (Moscow)
K. Otsuka (Tokyo)
M. San Miguel (Palma de Mallorca)
M. Scully (College Station)
M. Soskin (Kiev)
C. Stroud (Rochester)
J. Tredicce (Nice)
C. Weiss (Braunschweig)
H. Winful (Ann Arbor)

CONFERENCE PROGRAM

The meeting consisted of oral and poster presentations and discussions of recent developments on the dynamics of nonlinear optical systems. The reader is referred to the **Conference Digest** for a detailed listing of the session topics and the summary of the invited and contributed papers. A list of invited papers is included here for providing a flavor of the topics covered by NDOS'95.

Photorefractive Spatial Solitons, Mordechai Segev, *Greg Salamo, **George Valley and ***Bruno Crosignani, Princeton University, *University of Arkansas, **Hughes Research Laboratories, ***Universita' dell'Aquila

Synchronization of Chaotic Lasers in Master-Slave Relation, Maki Tachikawa, Toshiki Sugawara, Takayuki Tsukamoto and Tadao Shimizu, University of Tokyo

Transverse-Pattern Dynamics in Short-Pulse Lasers, Leonid A. Melnikov, Chernyshevsky State University

Laser Cooling: Physical Mechanisms and Ultimate Limits, C. Cohen-Tannoudji, Collège de France

Controlling Chaotic Lasers, R. Roy, Georgia Institute of Technology

Quantum Aspects of Optical Pattern Formation, L.A. Lugiato, Universita de Milano

Chaos in Semiconductor Lasers With Optical Injection, A. Gavrielides, Phillips Laboratory

Nonlinear Optical Properties of Quasi-One Dimensional Magneto-Excitons, Daniel S. Chemla, University of California at Berkeley

Phase-Controlled Photocurrents in Semiconductors, E. Dupont, P.B. Corkum and *H.C. Liu, National Research Council

Spatial Solitons in Wide-Aperture Nonlinear Optical Systems, N. N. Rosanov, S.I. Vavilov State Optical Institute

Cooperative Synchronization in a Laser Array with Eigenfrequency Spread, A. Napartovich, S.Y. Kurchatov and V.V. Likhanskii, Troitsk Institute for Innovation and Fusion Research

Financial Support

An important objective of NDOS'95 was to encourage the participation of the graduate students as much as possible. As a result, financial support was needed to cover local expenses for both the graduate students and the invited speakers (travel expenses of the foreign invited speakers were paid by the conference funds). Financial support was requested from both the AFOSR and ONR. The organizing committee was gratified and is thankful to both sponsors for their generous support.

Graduate students supported by the external funds

Name	Institute	Amount
R. Bridge	University of Rochester	$150
R. Essiambre	University of Rochester	$150
Z. Gilles	Georgia Institute of Technology	$284
D. L. Hart	Georgia Institute of Technology	$284
A. Hohl	Georgia Institute of Technology	$284
L. Liou	University of Rochester	$150

J. Marciante	University of Rochester	$150
M. Moller	Georgia Institute of Technology	$284
A. Pinto	University of Rochester	$150
A. Ryan	University of Rochester	$150
A. Teixieira	University of Rochester	$150
S. Thornburg	Georgia Institute of Technology	$284
P. van der Linden	Georgia Institute of Technology	$284
Q. L. Williams	Georgia Institute of Technology	$284
M. Yu	University of Rochester	$150

Invited Speakers supported by the external funds

M. Tachikawa	NIST, Boulder, Colarado	$284
L. A. Melnikov	Chernyshevsky State University	$284
A. Napartovich	Trisk Institute, Moscow	$309
N. A. Loiko	Institute of Physics, Minsk	$375
M. Segev	Princeton University, Princeton	$284
D. S. Chemla	Univerity of California, Berkeley	$284

Other Participants supported by the external funds

N. A. Loiko	Institute of Physics, Minsk	$375
I. V. Melnikov	General Physics Institute, Moscow	$284
N. N. Rosanov	Vavilov State Optical Institute	$375
L. Svirina	Institute of Physics, Minsk	$375
E. A. Viktorov	Vavilov State Optical Institute	$284

NONLINEAR DYNAMICS IN OPTICAL SYSTEMS

NDOS'95

Conference Digest

JUNE 5-7, 1995

University of Rochester

Rochester, New York, U.S.A.

ORGANIZING COMMITTEE

G. P. Agrawal (Rochester)
P. Glorieux (Lille)
Y. Khanin (Nizhny-Novgorod)
M. Piché (Québec)
R. Roy (Atlanta)

PROGRAM COMMITTEE

M. Brambilla (Milan)
P. Colet (Palma de Mallorca)
O. Kocharovskaya (Nizhny-Novgorod)
N. Loiko (Minsk)
J. McInerney (Cork)
L. Melnikov (Saratov)
F. Mitschke (Münster)
J. Moloney (Tucson)

ADVISORY COMMITTEE

N. Abraham (Bryn Mawr)
F.T. Arecchi (Florence)
E. Arimondo (Pisa)
R. Boyd (Rochester)
G. Casati (Milan)
W. Firth (Glasgow)
R. Fork (Huntsville)
D. Lenstra (Amsterdam)
R. Harrison (Edinburgh)
H. Haken (Stuttgart)
W. Lange (Münster)
L. Lugiato (Milan)
A. Mak (St. Petersburg)
P. Mandel (Brussels)
A. Oraevsky (Moscow)
K. Otsuka (Tokyo)
M. San Miguel (Palma de Mallorca)
M. O. Scully (College Station)
M. Soskin (Kiev)
C. Stroud (Rochester)
C. Weiss (Braunschweig)
H. Winful (Ann Arbor)

NDOS'95 is supported in part by the University of Rochester, U.S. Air Force Office of Scientific Research, and U.S. Office of Naval Research.

NDOS'95 PROGRAM

June 5, 1995 (Monday)

8:20-8:30 Opening of Conference (Hubbell)

Welcome Remarks R. Aslin, Vice Provost and Dean, University of Rochester

8:30-10:00 MA Plenary Session (Hubbell)
Chair: N. Abraham

MA1 Photorefractive Spatial Solitons (Invited) Mordechai Segev, *Greg Salamo, **George Valley and ***Bruno Crosignani, Princeton University, *University of Arkansas, **Hughes Research Laboratories, ***Universita' dell'Aquila

MA2 Synchronization of Chaotic Lasers in Master-Slave Relation (Invited) Maki Tachikawa, Toshiki Sugawara, Takayuki Tsukamoto and Tadao Shimizu, University of Tokyo

MA3 Transverse-Pattern Dynamics in Short-Pulse Lasers (Invited) Leonid A. Melnikov, Chernyshevsky State University

10:00-10:30 Coffee Break

10:30-12:00 MB Pattern Dynamics I (Hubbell)
Chair: C. Stroud

MB1 Transverse Mode Competition in a CO_2 Laser E. Louvergneaux, D. Hennequin, D. Dangoisse and P. Glorieux, Université des Sciences et Technologies de Lille

MB2 Circular Motion of Vortices in Lasers M. Vaupel, C. O. Weiss, Physikalisch-Technische Bundesanstalt

MB3 Roll Patterns and Transition to Turbulent State in a Laser System Dejin Yu, Weiping Lu and R. G. Harrison, Heriot-Watt University

MB4 Pattern Dynamics, Selection and Control in Large Aspect Ratio Lasers Joceline Lega, C. Bowman, J.V. Moloney, A.C. Newell, and *I Aranson, University of Arizona, *Bar Ilan University

MB5 Spatio-temporal Dynamics of Lasers with a Large Fresnel Number G. Huyet, S. Rica, J.R. Tredicce and N.B. Abraham, Institute Non Linéaire de Nice

MB6 The Effect of Mirror Curvature on Pattern Formation in Large Aspect Ratio Lasers G.K. Harkness, J.C. Lega, G.-L. Oppo, University of Strathclyde

12:15-13:15 Lunch: Danforth Dining Center

13:30-15:00 MC Chaos Control (Hubbell)
Chair: W. Firth

MC1 Control of Chaos in Multi Transverse Mode Lasers R. Martin, A.J. Kent, G. D'Alessandro, G.-L. Oppo, University of Strathclyde

MC2 Experimental Control of Chaos in CO_2 Laser with Feedback M. Ciofini, R. Meucci and F.T. Arecchi, Instituto Nazionale di Ottica

MC3 Adaptive Control of Chaos S. Boccaletti, F.T. Arecchi, University of Firenze

MC4 Control of Chaos in a Multimode Solid State Laser by Use of Small Periodic Preturbations Pere Colet, *Y. Braiman, Universitat de les Illes Balers, *Georgia Institute of Technology

MC5 Using the Control Duration to Stabilize a Multimode Laser Thomas W. Carr, Ira B. Schwartz, Naval Research Laboratory

MC6 Stabilizing or Destabilizing Lasers by Continuous Delayed Feedback Serge Bielawski, Dominique Derozier, Pierre Glorieux and *Thomas Erneux, Université des Sciences et Technologies de Lille, *Université Libre de Bruxelles

15:00-15:30 Coffee Break

15:30-17:00 MD Cavity Dynamics (Hubbell)
Chair: R. G. Harrison

MD1 Time Series Analysis of an Optically Turbulent System F. Mitschke, *G. Steinmeyer, *M. Heuer, *A. Schwache, I. Klopsch, Universität Münster, *Universität Hannover

MD2 Information Encoding in Passive Ring Resonators with Plane Mirrors Massimo Brambilla, L. A. Lugiato, M. Stefani, Università di Milano

MD3 Nonlinear Propagation in an Optical Fractal Structure M. Bertolotti, F. Moretti, C. Sibilia and *P. Masciulli, Università di Roma, *University of Palermo

MD4 On Instabilities and the Influence of Noise in a Nonlinear Resonator Mathew R. Semak, J. K. McIver Evangelos A. Coutsias, University of New Mexico

MD5 Nonlinear Dynamics, Delayed Bifurcation and Squeezing in a Triply Resonant Optical Parametric Oscillator K. Kasai, K. Petsas, C. Richy and C. Fabre, Laboratoire Kastler-Brossel

MD6 Dynamic Behaviors of Light Transmission of Thin Film with Mirror N.A. Loiko, Yu.A. Logvin and A.M. Samson, Institute of Physics of Academy of Sciences of Belarus

18:15-19:30 Dinner: Danforth Dining Center

20:00-22:00 ME Poster Session I
May Room, Wilson Common Building

ME1 The DFB of Counterpropogating Waves in a Periodically Modulated Medium with Relaxing Cubic Nonlinearity A.A. Afanas'ev, B.A. Samson, E.G. Tolkacheva, Belarus Academy of Sciences

ME2 Transverse Dynamics in a Laser with Fast-Relaxed Active Medium Leonid A. Melnikov, Irina V. Veshneva and Andrey I. Konukhov, Chernyshevsky State University

ME3 Controlling Chaos May Induce New Attractors in an Optical Device Paul Alsing, V. Kovanis and A. Gavrielides, *T. Erneux, Phillips Laboratory, *Université Libre de Bruxelles

ME4 Modelling Spectral Gain and Refraction Index in Semiconductor Lasers Salvador Balle, Universitat de les Illes Balears

ME5 Interaction of Soliton-Like Propagation in a Diffusive Nonlinear Planar Waveguide M. Bertolotti, S. Marchetti and C. Sibilia, Università di Roma

ME6 Pattern Formation in Bacteriorhodopsin Film with Mixed Absorptive-Dispersive Nonlinearity Mark Saffman, Jesper Glückstad, Risø National Laboratory

ME7 The Control of the Guiding Center Soliton by the Sliding Frequency Filter S. Burtsev, D.J. Kaup, Clarkson University

ME8 Semiconductor Laser Exposed to Optical Feedback from an External Cavity Containing an Atomic Absorber E. Cerboneschi, D. Hennequin, L. Guidoni, F. Di Teodoro and E. Arimondo, Universita di Pisa

ME9 Searching the Desired Periodic Orbit and Coding the Chaos in Semiconductor Laser Diodes for Message Transmission Jyh-Long Chern, Hong-Jyh Li, National Sun Yat-Sen University

ME10 Experimental Observation of Period Doubling Suppression in a Loss Modulated CO_2 Laser V.N. Chizhevsky, Belarus Academy of Science

ME11 Longitudinal Effects in Distributed Feedback Laser Diodes: Hole Burning Dynamics Pere Colet, Salvador Balle, Universitat de les Illes Balears,

ME12 Controlling Chaos in a Hybrid Optical Bistable System Jian-Hua Dai, Hua-Wei Yin and Hong-Jun Zhang, Chinese Academy of Sciences

ME13 Broad Turnability in an Intrinsic Passive (J = 1 to J = 0) Polarization Oscillator R.J. Ballagh, W. J. Sandle, University of Otago

ME14 Nonlinear Dynamics and Chaos of a Single Mode cw Nd: YAG Laser with Modulated Loss L. Dambly, P.M. Ripley, R.G. Harrison, Heriot-Watt University

ME15 Gain-Switching and Frequency Chirp of Injection-Locked Single-Mode Semiconductor Lasers Jaume Dellunde, *M.C. Torrent, J.M. Sancho and **M. San Miguel, Universitat de Barcelona, *Universitat Politècnica de Catalunya, **Universitat de les Illes Balears

ME16 Synchronization of Periodic and Chaotic CO2 Lasers with Saturable Absorber P.C. de Oliveira, Y. Liu, M.B. Danilov and J.R. Rios Leite, Universidade Federal de Pernambuco

ME17 Numerical Analysis of Non-Paraxial Beam Self-Focusing in Kerr Media Vladimir L. Derbov, Leonid A. Melnikov, Chernyshevsky State University

ME18 Generation of Ultrashort Pulses with Controlled Envelope Shape at Transient Double Resonance in the Regime of Instable Gain of Signal Wave Alexey Dmitriev, Oleg Parshkov, Andrey Vershinin, Saratov State Technique University

ME19 Relaxation Oscillation Dynamics and Stability of the Lang-Kobayashi Laser Thomas Erneux, *G.H.M. van Tartwijk, *A.M. Levine, *D. Lenstra, Université Libre de Bruxelles, *Free University (Amsterdam)

ME20 Average Symmetries in an Oscillator with Photorefractive Gain J . Farjas D. Hennequin, D. Dangoisse and P. Glorieux, Université des Science et Technologies de Lille

ME21 Polarization Competition and Transverse Effects in Sodium Vapor A. Gahl, A. Aumann, J.P. Seipenbusch, W. Lange, University of Münster

ME22 Dynamical Memory Function of a Hybrid Bistable Device with Delayed Feedback Self-Control of Chaos Jin-Yue Gao, Ying Zhang and Zhi-Ren Zheng, Jilin University

ME23 Fast Switching Unstable Orbits in Periodically Driving Laser V.A. Gaysenok, E.V. Grigorieva and *S. A. Kashchenko, Belarus State University, *Yaroslavl State University

ME24 Nonlinear Optical Response of Layered Composite Materials Russell J. Gehr, Robert W. Boyd, George L. Fischer and *J.E. Sipe, University of Rochester, *University of Toronto

ME25 "Hot" Reconstruction of Modes and Relaxation Oscillations of Solid-State Lasers A.V. Ghiner, Universidade Federal do Ceara

ME26 High-Order Spatial Mode Bifurcations in Nonlinear Interferometer with Delayed Feedback E.V. Grigorieva, *S.A. Kashchenko, Belarus State University, *Yaroslavl State University

ME27 Polarization Instabilities in Lasers with Weakly Anisotropic Cavities V.G. Gudelev, L.P. Svirina and Yu.P. Shurik, Academy of Science of Belarus

ME28 Mixed Period-Two and Fixed Point Attractor in Degenerate Optical Parametric Oscillations M. Haelterman, M.D. Tolley, Université Libre de Bruxelles

ME29 Dynamical Evolution of Four-Wave-Mixing Processes in an Optical Fiber Darlene L. Hart, Rajarshi Roy, Georgia Institute of Technology

ME30 Spatiotemporal Evolution of Femtosecond Pulses in Semiconductor Amplifiers Robert Indik J.V. Moloney and R. Binder, University of Arizona

ME31 Periodic Cycles, Bifurcations and Chaotic Behavior of the New Type of Optical Solitons in the Solid-State Lasers Mode-Locked by Linear and Nonlinear Phase Shift V.L. Kalashnikov, I.G. Polyko, V.P. Kalosha, V.P. Mikhailov, Belarus State University

ME32 Low Frequency Relaxation Oscillations in Class B Lasers with Feedback P. Khandokhin, Ya. Khanin, *J.-C. Celet, *D. Dangoisse and *P. Glorieux, Russian Academy of Science, *Université de Lille

ME33 Intensity Noise Suppression of External Cavity Semiconductor Laser via High Frequency Modulation Noriyuki Kikuchi, Yun Liu and Junji Ohtsubo, Shizuoka University

ME34 Multimode Instabilities in the Transit-Multistable Ring Cavity Jeong-Mee Kim, A. T. Rosenberger, University of Alabama in Huntsville

ME35 Nonlinear Dynamics in Additive Pulse Mode-Locked Lasers G. Sucha, *Sarah R. Bolton, and *D. S. Chemla, IMRA America, *University of California

ME36 Transverse Dynamics of a Phase-Conjugate Resonator with Phase Mismatch Dan Korwan, Guy Indebetouw, Virginia Tech

ME37 Pump Polarization Modulation in an Optically Pumped Laser A. Kul'minskii, R. Vilaseca and *R. Corbalan, Universitat Politècnica de Catalunya, *Universitat Autònoma de Barcelona

ME38 Control of Spatio-Temporal Chaos in Neural Networks and Its Application to Associative Memory Masanori Kushibe, Yun Liu and Junju Ohtsubo, Shizuoka University,

ME39 Optical Patterns Generated in the Single-Mirror Device with Polarization Instability M. Le Berre, D. Leduc, E. Ressayre, A. Tallet and *A. Maistre, Laboratoire de Photphysique Moléculaire du C.N.R.S., *Universite Pierre et Marie Curie

ME40 Instabilities of a Microcavity Laser with a Weak Optical Injected Signal Hua Li, T.L. Lucas, John G. McInerney, The University of New Mexico

ME41 Interaction of Counterpropagating Waves and Self-Organizing Distributed Feedback Laser in a Resonant Superfluorescence I.V. Mel'nikov, General Physics Institute RAS

June 6, 1995 (Tuesday)

8:30-10:00 TA Pattern Dynamics II (Hubbell)
Chair: L. Lugiato

TA1 Optical Patterns in Sodium Vapor: Experiment and Theory Thorsten Ackemann, Y. Logvin, A. Heuer, and W. Lange, University of Münster

TA2 Polarization Effects on Pattern Formation in Liquid Crystal Light Valves: Theory, Simulations and Experiments R. Neubecker, B. Thuering, T. Tschudi, G.-L. Oppo, University of Strathclyde

TA3 Competing Spatial Instabilities in a Coupled LCLV Feedback System Bernd Thüring, A. Schreiber, M. Kreuzer, and T. Tschudi, Technische Hochschule Darmstadt

TA4 Transport Induced Optical Instabilities in a Nonlinear Spatially Extended System P.L. Ramazza, S. Residori, E. Pampaloni, and F.T. Arecchi, Instituto Nazionale di Ottica

TA5 Pattern Formation in a Microfeedback System W.J. Firth, Yu. A. Logvin, *B.A. Samson, University of Strathclyde, *Belarus Academy of Sciences

TA6 Patterns, Pattern Dynamics, and Pattern Correlations in a Photorefractive Bidirectional Ring Resonator Z. Chen, D. McGee, N.B. Abraham, Bryn Mawr College

10:00-10:30 Coffee Break

10:30-12:00 TB Polarization Dynamics (Hubbell)
Chair: K. Otsuka

TB1 Polarization Pattern Dynamics in the Laser Vector Complex Ginzburg-Landau Equation A., Amengual, M. San Miguel, R. Montagne and E. Hernández-García, Universitat de les Illes Balears,

TB2 Polarization Pattern Forming Instabilities in Lasers Q. Feng, M. *San Miguel, J. V. Moloney and A.C. Newell, University of Arizona, *Universitat de les Illes Balears

TB3 Polarization Switching in Quantum Well Vertical-Cavity Surface Emitting Lasers J., Martín-Regalado, M. San Miguel, *N.B. Abraham and **F. Prati, Universitat de les Illes Balears, *Bryn Mawr College, **University of Milan

TB4 Transverse and Polarization Effects in VCSELs F. Prati, G. Tissoni, L.A. Lugiato, *J. Martin-Regalado, *M. San Miguel and *N.B. Abraham, Universita de Milano, *Universitat de les Illes Baleraes

TB5 Polarization Chaos in a Cavity-Isotropic Optically Pumped Laser C. Serrat, R. Vilaseca, R. Corbalán,

Universitat Politècnica de Catalunya, Universitat Autonomade de Barcelona

TB6 Polarization Instability in a Zeeman Laser Model Via On-Off Intermittency J. Redondo, E. Roldán and G.J. de Valcárcel, Universitat de València

12:15-13:15 Lunch: Danforth Dining Center

13:30-15:00 TC Ultrafast Dynamics (Hubbell)
Chair: M. Piché

TC1 Ultrashort Pulse Propagation in the Spatio-Temporal Regime Govind P. Agrawal, Andrew T. Ryan, University of Rochester

TC2 Chaotic Pulse Dynamics in Fiber Arrays Gregory G. Luther, Alejandro B. Aceves, University of New Mexico,

TC3 Femtosecond Nonlinear Dynamics of Periodic Structures through Direct Integration of Maxwell's Equations Stojan Radic, Nicholas George, Govind P. Agrawal, University of Rochester

TC4 Self-Induced Transparency in Bragg Reflectors: Gap Solitons Near Absorption Resonances Alexander Kozhekin, Gershon Kurizki, Weizmann Institute of Science

TC5 Picosecond Soliton Dynamics Beyond the Guiding-Center-Soliton Regime René-Jean Essiambre, Govind P. Agrawal, The University of Rochester,

TC6 Transmission of Solitons Generated by Modulation of Laser Diodes Using TDM and In-line Phase Conjugation, Claudio Mirasso, *Luis Pesquera, Instituto de Estructura de la Materia, *Universidad de Cantabria

15:00-15:30 Coffee Break

15:30-17:00 TD Laser Dynamics (Hubbell)
Chair: P. Mandel

TD1 Self-Pulsing in a Mesomaser C. Balconi, F. Casagrande, L.A. Lugiato, *W. Lange and *H. Walther, Università de Milano, *Max-Planck-Institute für Quantenoptik

TD2 Spatio-Temporal Dynamics in a Broad Area Laser Diode Ingo Fischer, *O.Hess, and W. Elsäßer, Philipps Universität Marburg, *Institut für Technische Physik

TD3 Nonlinear Dynamics in Lasers with Phase-Conjugate Optical Feedback George R. Gray, David H. DeTienne and *Govind P. Agrawal, University of Utah, *University of Rochester

TD4 Strongly Pulsating Oscillations in Lasers Subject to Continuous Delayed Feedback D. Pieroux, T. Erneux, Universite Libre de Bruxelles

TD5 Relaxation Oscillation in an Injection-Locked Semiconductor Laser Piet C. De Jagher, *Daan Lenstra, Eindhoven University of Technology, *Free University (Amsterdam)

TD6 Travelling Wave Model for the Multimode Behavior of a Fabry-Perot Laser M. Homar, J.V. Moloney and *M. San Miguel, University of Arizona, *Universitat de les Illes Balears

18:15-19:30 Dinner: Danforth Dining Center

20:00-22:00 TE Poster Session II
May Room, Wilson Common Building

TE1 Tunable Polarization Modulation Instability in Weakly Birefringent Fibers S.G. Murdoch, R. Leonhardt and J.D. Harvey, University of Auckland

TE2 Crtitical Phenomenon in a Hybrid Optical Bistable System Jian-Hua Dai, Hua-Wei Yin and Hong-Jun Zhang, Chinese Academy of Sciences

TE3 Bistability and Rectangular Pulses Under Second Harmonic Generation A.V. Ghiner, *G.I. Surdutovich and **N.P. Konopleva, Universidade Federal do Ceara, *Instituto de Fisica de Sao Carlos, **Novosibirsk State University

TE4 Nonlinear Dynamics of Chirped Solitons in Doped Fibers L.W. Liou, Govind P. Agrawal, University of Rochester

TE5 Noise and Chaos in a Multimode Solid State Laser Clif Liu, Henry D. Abarbanel, **Zelda Gills, and **Rajarshi Roy, University of California, **Georgia Institute of Technology

TE6 Suppression of Chaos in External Cavity Semiconductor Laser Yun Liu, Junji Ohtsubo, Shizuoka University

TE7 Chaos Control In a Modulated Class-B Laser N.A. Loiko, A.V. Naumenko and S.I. Turovets, Institute of Physics of Academy of Sciences of Belarus

TE8 Birfurcation to Antiphase Periodic Solutions in a Modulated Solid-State Fabry-Perot Laser Paul Mandel, T. Erneux, Université Libre de Bruxelles

TE9 Spatio-Temporal Dynamics of Gain Guided Semiconductor Laser Array J. Martín-Regalado, S. Balle and *N.B. Abraham, Universitat de les Illes Balears, *Bryn Mawr College

TE10 Nonlinear Dynamics and Chaos in a Periodically Driven SBS Oscillator: Experiment and Theory Weiping Lu, Paul M. Ripley and Robert G. Harrison, Heriot-Watt University

TE11 Coherent Effects on Ultrashort Pulse Interaction in a Doped Fiber I. V. Mel'nikov, A. W. Luchnikov, General Physics Institute

TE12 Spectral Features of a Short Pulse Self-Action in a Resonant Medium Leonid A. Melnikov, Andrey I. Konukhov and Irina V. Veshneva, Department of Optics - Chernyshevsky State University,

TE13 Chaos and Control in Semiconductor Lasers Govind P. Agrawal, *Charles M. Bowden and *Shawn D. Pethel, University of Rochester, *U.S. Army Missile Command

TE14 Three-order Nonlinearities as Mechanism of the Mode-Locking Victor P. Mikhailov, V.L. Kalashnikov, V.P. Kalosha, I.G. Poloyko, Belarus State University

TE15 Transmission of Laser Diode Pulses in Standard Optical Fibers: Different Compensation Techniques Claudio R. Mirasso, P. García-Fernández and C. Lozano, Instituto de Estructura de la Materia

TE16 Reflection of a Gaussian Beam from a Saturable Absorber: Experimental Results D. V. Petrov, A. S. L. Gomes and Cid B. de Araújo, Universidade Federal de Pernambuco

TE17 Multistability in a Thin Layer Laser with Inclined External Cavity I.E. Protensko, A.N. Oraevsky, *J.D. Graham, *R.T. Edmonson, and *D.K. Bandy, P.N. Lebedev Physics Institute, *Oklahoma State University

TE18 Nonlinear Dynamics of a CO_2 Laser with Externally Modulated and Re-Injected Optical Signal E.M. Rabinovich, *J.M. Kowalski, **M.A. Safonova and *C.L. Littler, Advanced Isotope Technologies, *University of Texas, **New York University,

TE19 Population Inversion Without Amplification via Field-Dependent Relaxation Yevgeny V. Radeonychev, Russian Academy of Sciences

TE20 Spatio Temporal Coupling Implications for Z-Scan Measurements Andrew T. Ryan, Govind P. Agrawal, University of Rochester

TE21 Pulsations of Transverse Drift Modes in Misaligned Linear and Ring Cavities Mark Saffman, Risø National Laboratory,

TE22 Self-Induced Gain and Stratification in Counter-Propagation of Light Beams in Dense Media B.A. Samson, W. Gawlik, Jagellonian University

TE23 Dye Laser with Polarized Pumping Dynamics S. Sergeyev, S.K. Gorbatsevich, S.A. Sakharuk, Belarus State University

TE24 Role of the "Cascading Effect" in a Ring Cavity Filled with a Quadratic Nonlinear Medium C. Sibilia, A. Re, E. Fazio, M. Bertolotti, Dipartimento di Energetica-Univ. Roma

TE25 Dynamic Transverse Patterns in a Two-Mode Laser D.V. Skryabin, A.G. Vladimirov, A.M. Radin, St. Petersburg State University

TE26 Spatial Instabilities in DH Stripe Semiconductor Injection Lasers: Effects of Thermal Nonlinearity G.A. Smolyakov, L.A. Melnikov, S.V. Ovchinnikov and *E.M. Rabinovich, Chernyshevsky State University, University of North Texas

TE27 Quasisoliton Inside a Dissipative Bistable Optical System G. I. Surdutovich, *A.V. Ghiner, Instituto de Fisica de Sao Carlos, *Universidade de Federal do Ceara'

TE28 Polariton Solitons as Asymptotic Solutions of Coherent Semiconductor Maxwell-Bloch equations in the low-density Regime Irina Talanina, *A. Knorr and *S.W. Koch, University of Ulm, *Philipps Universität

TE29 Simulation of Femtosecond Pulse Propagation in an Unpumped Er-doped Optical Fiber Xiaonong Zhu, Michel Piche, University Laval

TE30 Geometric Structure of Laser Models Vladislav Yu. Toronov, Vladimir L. Derbov, Saratov State University

TE31 Nonlinear Dynamics of a Two-Photon Laser with Injected Signal in the High-Q Cavity Limit J.F. Urchueguia, V. Espinosa, *G.J. de Valcarcel, *E. Roldan, Universitat Politecnica de València, **Universitat de València

TE32 Determinism and Stochasticity of Power Dropout Events in Semiconductor Laser Systems with External Feedback H.J.C. van der Linden, A. Hohl, R. Roy, School of Physics - Georgia Institute of Technology

TE33 Saddle Antiphase Dynamics of a Multimode Laser E. A. Viktorov, *D.R. Klemer and **M.A. Karim, S.I. Vavilov State Optical Institute, *Spectra-Physics Laserplane, **University of Dayton

TE34 Nonlinear Interaction of Transverse Modes in a Class-B Laser A.G. Vladimirov, D.V. Skryabin, St. Petersburg State University

TE35 Correlation Dimension Analysis of Heterodyne Detection of High-Frequency Chaotic Oscillation from a Laser Diode with Optical Feedback Nobuyuki Watanabe, Koichi Karaki, Olympus Optical Co.

TE36 Fast Dynamics of an Er^{3+} -doped fiber ring laser Quinton L. Williams, Rajarshi Roy, Georgia Institute of Technology

TE37 Transverse Spatial Modulation of a Gaussian Beam in BATi03:Ce Ping Xie, Jian-Hua Dai, Peng-Ye Wang and Hong-Jun Zhang, Chinese Academy of Sciences

TE38 Exciton Interaction Effects in Optical Transient Grating V. I. Yudson, TH. Neidlinger, P. Reineker, Universitat Ulm

June 7, 1995 (Wednesday)

8:30-10:05 WA Joint Session* I (Hubbell)
Chair: M. Lax

WA1 Laser Cooling: Physucal Mechanisms and Ultimate Limits (CQO7 Invited, one-hour Tutorial) C. Cohen-Tannoudji, Collège de France

WA2 Controlling Chaotic Lasers (CQO7 Invited) R. Roy, Georgia Institute of Technology

10:10-10:35 Coffee Break

10:45-11:50 WB Joint Session* II (Hubbell)
Chair: L. Allen

WB1 Quantum Aspects of Optical Pattern Formation (CQO7 Invited) L.A. Lugiato, Universita de Milano

WB2 Chaos in Semiconductor Lasers With Optical Injection (Invited) A. Gavrielides, Phillips Laboratory

12:00-13:00 Lunch: Danforth Dining Center

13:15-15:00 WC Joint Session* III (Hubbell)
Chair: R. W. Boyd

WC1 Nonlinear Optical Properties of Quasi-One Dimensional Magneto-Excitons (Invited) Daniel S. Chemla, University of California at Berkeley

WC2 Phase-Controlled Photocurrents in Semiconductors (Invited) E. Dupont, P.B. Corkum and *H.C. Liu, National Research Council

WC3 Spatial Solitons in Wide-Aperture Nonlinear Optical Systems (Invited) N.N. Rosanov, S.I. Vavilov State Optical Institute

13:15-15:00 WD Nonlinear Dynamics (Lander)
Chair: M. San Miguel

WD1 Self-Consistent Models of Lasing Without Inversion: Problems and Prospects Olga Kocharovskaya, Russian Academy of Science

WD2 Ball Bistability A.N. Oraevsky, *D.K. Bandy, P.N. Lebedev Physics Institute, *Oklahoma State University

WD3 Modelocking of a Titanium-Sapphire Laser Induced by Intracavity Frequency Shift Gerd Bonnet, Stefan Balle and Klaas Bergmann, Fachbereich Physik der Universität

WD4 Nonlinear Coupling in Self-Mode-Locked Lasers Robert Bridges, Robert W. Boyd and Govind P. Agrawal, University of Rochester

WD5 Periodic Antiphased States in Intracavity Second Harmonic Generation Paul Mandel, J.-Y. Wang, Université Libre de Bruxelles

WD6 The Effect of Noise Sources Correlation on the Form of Low-Frequency Intensity fluctuations spectra in multimode Class B Laser Ya. Khanin, P.A. Khandokhin and V.G. Zhislina, Institute of Applied Physics of Russian Academy of Sciences

15:00-15:30 Coffee Break

15:30-17:15 WE Chaos (Lander)
Chair: D. Lenstra

WE1 Cooperative Synchronization in a Laser Array with Eigenfrequency Spread (Invited) A. Napartovich, S.Y. Kurchatov and V.V. Likhanskii, Troitsk Institute for Innovation and Fusion Research

WE2 Dynamical Characterization of Globally Coupled Optical Systems Kenju Otsuka, *Jingyi Wang, *Paul Mandel, and *Thomas Erneux, Tokai University, *Universite Libre de Bruxelles

WE3 Unified Treatment of Spontaneous Pattern Formation in "2+1" Dimensional Optical Systems Ross F. McIntyre, Weiping Lu, Robert G. Harrison, Heriot-Watt University

WE4 Spatiotemporal Chaos Due to Attractor Merging in a Class-C Laser M. Sauer, F. Kaiser, Technical University Darmstadt

WE5 Controlling the Unstable Steady-States of Lasers Using Continuous Feedback Daniel J. Gauthier, Duke University

WE6 Instabilities and Synchronization of Coupled State Solid Lasers K. Scott Thornburg, Jr., Micheal Moller, Rajarshi Roy, Georgia Institute of Technology

18:15-19:30 Dinner: Danforth Dining Center

*Joint session with the Coherence and Quantum Optics (CQO7) Conference

Photorefractive Spatial Solitons

Mordechai Segev,(1) Greg Salamo,(2)

George Valley(3) and Bruno Crosignani(4)

(1) Electrical Engineering Dept., Princeton University, Princeton, NJ 08544.
Phone (609) 258-1949; Fax. (609) 258-1954; segev@ee.princeton.edu
(2) Physics Department, University of Arkansas, Fayetteville, AR 72701.
(3) Hughes Research Laboratories, Malibu, CA 90265.
(4) Dipartimento di Fisica, Universita' dell'Aquila, 67010 L'Aquila, Italy

We present an overview of the experimental and theoretical understanding on spatial solitons in photorefractive materials. There are three generic types at present: quasi-steady, screening and photovoltaic solitons. The ***quasi-steady-state solitons***, which were predicted and discovered first,[1-9] exist during the slow screening process of an externally-applied field in bright and dark realizations and in one and two transverse dimensions. The ***screening solitons*** are predicted and recently observed[10-12] (SBN) in a photorefractive material with an external applied field at steady state, when the field is nonuniformly screened. The ***photovoltaic solitons*** are predicted and observed[13,14] in photorefractive materials with a strong photovoltaic current ($LiNbO_3$) and use the refractive index perturbation associated with photovoltaic field to guide and confine the planar soliton. By and large, none of these solitons has properties similar to those of the conventional Kerr solitons. Perhaps the most important distinctions from Kerr solitons is the existence of photorefractive solitons at microWatts and lower power levels and in two transverse dimensions. This implies the practicality of using photorefractive solitons for beam steering, optical wiring and interconnects and other nonlinear optical devices.

We describe our recent experimental and theoretical results which include (i) observations of steady-state photorefractive screening solitons

trapped in one and two transverse dimensions, (ii) experimental studies of bright and dark quasi-steady solitons that serve as reconfigurable light-induced waveguides for other beams, (iii) theoretical predictions of vector solitons and of (iv) fast free-carrier screening-solitons at the high intensity regime.

References

(1) M. Segev, B. Crosignani, A. Yariv and B. Fischer, Phys. Rev. Lett. **68**, 923 (1992).

(2) B. Crosignani, M. Segev, D. Engin, P. DiPorto, A. Yariv and G. Salamo, J. Opt. Soc. Am. **B-10**, 449 (1993).

(3) D. N. Christodoulides and M. I. Carvalho, Opt. Lett. **19**, 1714 (1994).

(4) G. Duree, J. L. Shultz, G. Salamo, M. Segev, A. Yariv, B. Crosignani, P. DiPorto, E. Sharp and R^2 Neurgaonkar, Phys. Rev. Lett. **71**, 533 (1993).

(5) M. Segev, A. Yariv, G. Salamo, G. Duree, J. Shultz, B. Crosignani, P. DiPorto and E. Sharp, Opt. & Phot. News **4**, 8 (1993).

(6) M. Segev, A. Yariv, B. Crosignani, P. DiPorto, G. Duree, G. Salamo and E. Sharp, Opt. Lett. **19**, 1296 (1994).

(7) G. Duree, G. Salamo, M. Segev, A. Yariv, B. Crosignani, P. DiPorto and E. Sharp, Opt. Lett. **19**, 1195 (1994).

(8) G. Duree, M. Morin, G. Salamo, M. Segev, A. Yariv, B. Crosignani and P. DiPorto, ***Dark photorefractive spatial solitons and photorefractive vortex solitons***, to be published (accepted) in Phys. Rev. Lett., March 13, 1995.

(9) M. Segev, G. Salamo, G. Duree, M. Morin, B. Crosignani, P. DiPorto and A. Yariv, Opt. & Phot. News **5**, 9 (1994).

(10) M. Segev, G. C. Valley, B. Crosignani, P. DiPorto and A. Yariv, Phys. Rev. Lett. **73**, 3211 (1994).

(11) Observations of self-focusing effects in the screening regime were presented by M. D. Iturbe-Castillo, P. A. Marquez-Aguilar, J. J. Sanchez-Mondragon, S. Stepanov and V. Vysloukh, Appl. Phys. Lett. **64**, 408 (1994).

(12) M. Shih, M. Segev and G. C. Valley, ***Observation of photorefractive screening-solitons***, to be submitted, April 1995.

(13) G. C. Valley, M. Segev, B. Crosignani, A. Yariv, M. M. Fejer and M. Bashaw, Phys. Rev. A **50**, Rapid Comm., R4457 (1994).

(14) M. Taya, M. Bashaw, M. M. Fejer, M. Segev and G. C. Valley, ***Observation of dark photovoltaic spatial solitons***, submitted to Phys. Rev. Lett., November 1994.

SYNCHRONIZATION OF CHAOTIC LASERS IN MASTER-SLAVE RELATION

Maki Tachikawa,[+] Toshiki Sugawara, Takayuki Tsukamoto, and Tadao Shimizu[*]

Department of Physics, University of Tokyo, 7-3-1 Hongo, Bunkyo-ku, Tokyo-113.

[+]Present address: Time and Frequency Div., National Institute of Standards and Technology, 325 Broadway, Boulder, CO 80303.
Tel: 303-497-3174, Fax: 303-497-7845, E-mail: tachikaw@boulder.nist.gov
[*]Present address: Department of Physics, Science University of Tokyo, 1-3 Kagurazaka, Shinujuku-ku, Tokyo-162.

Summary

Synchronization between periodic oscillators is a well known phenomenon like Huygens' discovery of the two clocks on the wall. Then, it is quite interesting to ask whether chaotic systems can synchronize if they have mutual or one-way couplings. Recently, this problem has attracted considerable attention due not only to its fundamental importance in nonlinear dynamics but also to its practical applicability in neural networks, communications, and control of chemical and biological systems. In this paper, we demonstrate dynamic responses of a chaotic system to external driving signals by using a passively Q-switched (PQS) CO_2 laser[1].

We consider the situation where one chaotic laser (slave laser) is driven by the output of another chaotic laser (master laser). Fig.1 shows the experimental setup of the laser system. A saturable absorber inside the laser cavity induces self-sustained chaotic pulsation in a single-mode CO_2 laser. The infrared radiation from the master laser is injected into the absorption cell of the slave laser, modulating its saturable loss. Fig.2 shows the observed time sequences of the PQS pulsation from the two lasers. The amplitude correlation between the two signals is examined by plotting the intensity of the peak in the slave laser's output X_s against that of the peak in the master laser's output X_m which has appeared just before it. With no coupling, the two lasers are pulsating independently, and correspondingly, data points in the correlation plot are scattered in an erratic manner. The Lorenz plot analysis reveals that the two trajectories settle on slightly different strange attractors. When the injected power is raised up to 24.2 mW, the chaotic pulsation of the slave laser is synchronized to the driving pulsation with a certain delay, which is clearly shown by the linearity in the amplitude correlation.

Numerical calculation on our rate-equation model reproduces basic characteristics of the synchronization with a good fidelity. It is found that synchronization is realized when Lyapunov exponents of the modulated slave system are negative. Furthermore, the slave system is locked to the master system even when driven by a binary signal that is a

simplification of the time sequence of the master laser's output. Namely, the slave laser functions to recover the lost information of the master laser.

The frequency entrainment is generally observed in a nonlinear oscillator externally driven by a periodic force when the driving frequency is close to intrinsic frequencies of the system. Our observation demonstrates that the entrainment may occur even when the driving force is chaotic if it is based on a strange attractor nearly identical to that of the slave system.

Reference

1. T. Sugawara et al., Phys. Rev. Lett. **72**, 3502 (1994). In contrast to our observation, synchronization between mutually coupled lasers was reported by R. Roy and K. S. Thornburg, Jr., Phys. Rev. Lett. **72**, 2009 (1994).

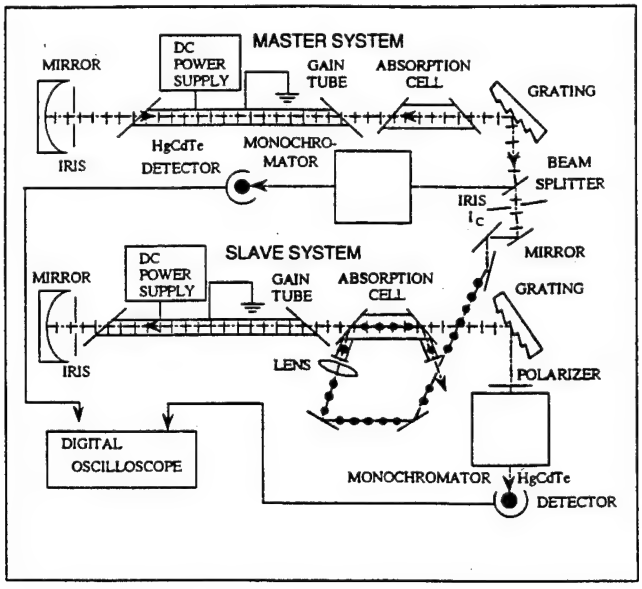

Fig.1. Experimental setup.

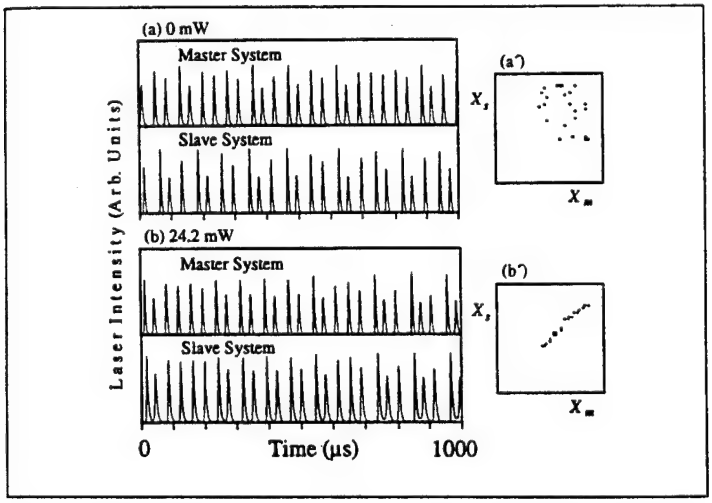

Fig.2. Observed chaotic PQS pulsations of the master and slave lasers for different powers of the injected beam together with the correlation plots between the peak heights.

Transverse-Pattern Dynamics in Short-Pulse Lasers

Leonid A.Melnikov

Department of Optics, Chernyshevsky State University
83 Astrakhanskaya str., Saratov 410071, Russia
phone: (845-2)51-51-95, fax: (845-2)24-04-46
e-mail: melnikov@scnit.saratov.su, melnikov@ire.saratov.su

Recently, different transverse-pattern dynamics have been demonstrated in various real laser systems or in the more or less complicated laser models. In the paper I present the results of the investigations (mostly numerical) of the transverse dynamics in the laser systems generating short and ultra-short pulses. These systems may be considered in some sense as the class A and B lasers, however its dynamics are described by mappings rather than differential equations especially when the "mean field limit" is violated. The regimes of short-pulse oscillations may be realized using the different mode-locking techniques. The transverse dynamical phenomena may manifest itself in the mode-locked lasers as the means to obtain mode-locking (for example, as in Kerr-lens mode-locking) and the effects accompanying the mode-locked regimes as the pulse-train regular or irregular (chaotic) modulation envelope. By the other hand the assumption of the short-pulse regime is the powerful means to simplify considerably the laser model. Three examples are discussed:

1. Transverse-pattern dynamics in solid-state mode-locked laser

The equations and corresponding mapping are presented for this laser using the approximations of scalar electric field (with given polarization) and of the pulse synchronously varying in transverse plane. The cavity considered is degenerate, when the transverse mode distance is near to the distance between adjacent axial modes. The numerical method include modal decomposition in terms of Laguerre-Gaussian modes with indices up to 10 (radial) and ± 9 (azimuthal). The results show the sensitivity of the regimes to the initial conditions, different dynamics, including pattern rotation, "colliding" spots, multiple vortices. The formation of valleys and phase-defect accumulation points are described. The defect dynamics and corresponding phase curves shapes "catastrophes" are analyzed.

2. The Kerr-lens mode-locking

This transverse dynamical effect occurs due to short pulse self-action in a Kerr media in the laser cavity leading to weak self-focusing and to the corresponding pulse shape temporal encoding at the aperture or at the nonuniform gain profile and to the pulse shortening. The results of the simulations of spatio-temporal dynamics of the pulse in nonlinear medium are discussed and compared with commonly used aberrationless approximation. The mapping describing laser pulse-train dynamics is presented and different regimes are performed.

The polarized transverse-pattern dynamics in the laser with fast nonlinearity and image-rotation cavity

The polarization effects in transverse dynamics in the unidirectional ring laser with large aperture are investigated numerically using the above mentioned in section 1 method out of the restriction of the number of transverse modes. The laser system is distinguished by the arbitrary values of the laser level momenta (the example of $J = 1 - J = 2$ transition is presented) and by the cavity configuration including the image rotation (the example is the non-planar cavity). Image rotation makes impossible to split the polarization and transverse coordinates, therefore, each of the transverse mode has its own distribution of polarization vector directions. The influence of the magnetic sublevel structure of active medium on transverse patterns are considered.

The partial support from ISF grant NS4000 and from the ESPRIT Contract P9282-ACTCS is acknowledged.

Transverse mode competition in a CO_2 Laser

E. Louvergneaux, D. Hennequin, D. Dangoisse and P. Glorieux.
Laboratoire de Spectroscopie Hertzienne
Unité associée au Centre National de la Recherche Scientifique (URA 249)
Université des Sciences et Technologies de Lille
F-59655 Villeneuve d'Ascq cedex (France)

Pattern formation resulting from transverse mode competition is studied in CO_2 lasers with a large transverse section. The laser is designed to support a large number of interacting modes with small frequency differences between their resonance frequency to allow for strong intermodal coupling since our aim is to investigate nonlinear regimes leading to spatio-temporal dynamics linked to the interaction of many modes or related to morphogenetic processes. We have used a multi-element degenerate resonator where the spot size of the TEM_{00} mode on the optical elements is considerably smaller than in conventional cavities and where the spacing between axial modes is large enough to avoid overlapping of axial mode families. We describe and analyze the particular situation that is met in the formation of ordered patterns in a cavity in which i) the cylindrical symmetry is broken by Brewter plates ii) the frequency degeneracy of modes belonging to the same family q is lifted by astigmatism and cavity aberrations. Spatial periodicity is associated with spectral periodicity. Indeed, the RF spectra of ordered patterns contain regularly spaced components typically separated by 500 kHz.

Modal expansion of the beam on the Hermite-Gauss (HG) basis has been privileged. If one considers these patterns as superpositions of HG modes with different frequencies, the thermal plate shows only the sum of their intensity as rapidly oscillating crossproducts are averaged to zero. We show by a least square method applied to experimental patterns that due to mode competition, the patterns are often composed of a few modes selected inside one transverse family and obeying "selection rules". Numerical reconstructions in good

agreement with experiments are obtained. In order to explain the behavior described above, we have integrated a model using modal expansion on the HG basis [1]. By comparing with experiments, the importance of the choice of the basis in which the beam is expanded is emphasized.

From the observation of patterns in which the eleven first transverse mode families are involved, two hypothesis based on integral overlap calculations may be formulated : (i) modal interaction is ruled by transverse hole burning. Modes are associated to minimize overlapping between their intensity distribution, (ii) the number of modes is determined to extract the maximum energy from the active medium. The selection of one transverse family in pattern formation, partially found in our experimental simulations is a result that comes out from the theoretical study of Harkness et al. [2]. They found that above threshold, the modes of only one transverse family appear in the pattern.

The observation of oriented patterns shows clearly that astigmatism of the cavity plays a dominant role in pattern formation. Comparison of these patterns with their counterparts in a cavity in which the astigmatism is much weaker has been made.

[1] L.A. Lugiato, F. Prati, L.M. Narducci, P. Ru, J.R. Tredicce and D. K. Bandy, Phys. Rev. **A37**, 3847-3866 (1988)

[2] G. K. Harkness, J. C. Lega and J. L. Oppo, to be published

Circular motion of vortices in lasers

M. Vaupel, C.O. Weiss
Physikalisch-Technische Bundesanstalt
38116 Braunschweig, Germany
Phone: +49 531 5924429, Fax: +49 531 5929292
e-mail: vaupe422@rz.braunschweig.ptb.d400.de

We have recently found that lasers can emit fields with moving vortices [1]. In [1] the motion of a single vortex was followed indirectly by using two strategically placed point detectors. If would seem difficult to follow more complex dynamical patterns with this technique. As the typical timescale of this motion of lasers is 10^{-8}s , there exists no real possibility to record films or even snapshots of the time-varying laser field. Photorefractive oscillators (PROs) are on the other hand largely equivalent to lasers of class A [2]. Since their gain-line widths are of the order of Hz, they show an extreme frequency pulling which results in dynamics with a characteristic time of 100ms. Thus dynamics can be observed with ordinary video equipment. As we work at low gain the differences between PRO and lasers should be negligible [2] and the experiments should give a proper picture of spatial laser dynamics of an ordered type. We use a ring resonator and a BSO crystal. The gain is obtained by two-wave mixing in BSO pumped by an Ar^+-Laser. The resonator contains two lenses for the selection of the number of transverse modes located between two neighbouring longitudinal modes. An iris is used to control the losses of the modes, so that the highest exciteable transverse mode is selected by the aperture. To excite reproducibly certain mode families, the resonator length is actively stabilized. The length is tunable, so that the modes of the passive resonator can be shifted relative to the gain line. 10% of the generated field is coupled out and recorded by a CCD-camera. Patterns will be shown on video film and as snapshots. We first concentrate on "doughnut-like" patterns which are essentially bright fields with a dark center at the optical axis. The optical field of those patterns contains a phase singularity (also called vortex). We observed such patterns with singularities of order up to 15.

If the n-th doughnut mode is emitted simultaneously with an adjacent longitudinal mode, the pattern consists of n circling vortices. We demonstrate an example in the case of $n = 4$. There approximately 4.1 transverse mode spacings per free spectral range are used. Reducing the detuning of the fundamental mode relative to the gain line increases the speed of circling, because the transverse and fundamental mode have different frequency

pulling according to their losses. When the two modes phase-lock, four stationary vortices result. As we tune the Gaussian mode away from and the fourth order mode family closer towards the gain line we find that the right hand circling changes into left hand circling at a particular detuning. Tuning the Gaussian back towards the gain line a second transition point is found where a change back to right hand circling occurs. The difference in frequency between these two points indicates hysteresis. The interferogram of the pattern shows an abrupt change of sign of the charge of the vortices at the transitions. It is plausible that there should be a hysteresis between circling directions because patterns are in general bistable with respect to helicity[3].

While there is hysteresis here between circling senses, it is also possible to phase-lock the two constituent modes. This corresponds to stopping of the circling motion and occurs when the modes are tuned so that their pulled frequencies become close enough. Phase locking requires resonator anisotropy.

With ~ 2.7 transverse mode spacings per free spectral range a stationary first order vortex at the center with seven vortices circling around can be realized. One can describe this pattern by interference between a charge-one and a charge-six doughnut.

In the case of simultaneous excitation of a charge-three- and a charge-five-dougnut together with the fundamental mode, three vortices move on a circle of a small radius while eight vortices move at a large distance from the optical axis. All these circling motions can be understood hydrodynamically as Magnus drifts.

To demonstrate other typical hydrodynamic effects, a one-dimensional mode flow was explored using cylindrical lenses in the resonator. The emitted patterns are mode cascades, vortex creation like in obstacle flow and interfering tilted waves.

References

[1] A.B. Coates et al., Phys. Rev. A, **49**, 1452 (1994)

[2] M.F.H. Tarroja, K. Staliunas, G. Slekys and C.O. Weiss, Analogy between photorefractive oscillators and class-A lasers, Phys. Rev. A accepted

[3] Chr. Tamm, C.O. Weiss, J. Opt. Soc. Am., **7**, 1034 (1990)

Roll Patterns and Transition to Turbulent State in a Laser System

Dejin Yu, Weiping Lu and R.G.Harrison
Department of Physics, Heriot-Watt University,
Riccarton, Edinburgh EH14 4AS, UK
Tel: 031-449 5111 Fax: 031-451 3136
E_mail: phydjy@uk.ac.hw.phy

In this paper, we report roll patterns and transition between rolls and turbulent states in the field intensity of emission from a coherently optically pumped three-level laser system. While such phenomena have been predicted and observed in various passive systems [1], our findings are to our knowledge the first to be reported for a laser, earlier attention being focused to phase singularities and defect-mediated turbulence evolving from travelling waves in laser systems [2].

We consider both pump and emission processes to be resonant in the model description [3]. The equations describing the coherently optically pumped three-level laser are derived from the semi-classical Maxwell-Bloch equations under the rotating-wave approximation and neglecting longitudinal effect and including transverse diffraction effect. Four control parameters involved in this nonlinear system are the pump strength A, the cavity damping constant σ, the unsaturated gain g and the ratio b of energy relaxation to dipole dephasing rates. The spatially homogeneous steady-state electric field amplitude $E^{(s)}$ has three branches, a nonlasing solution (N) and two symmetric lasing solutions (L). Linear stability analysis predicts that for the branch (N), the lowest instability threshold is always located at transverse wavenumber $K = 0$, in which the instability is identified to be *temporal*. For the lasing states (L), the instability occurs through a Hopf bifurcation where the unstable wavenumber K varies between $K = 0$ and $K = K_m$, indicative of possible spatio-temporal pattern formations. The latter limit K_m is determined by the termination of lasing due to pump-induced Rabi splitting [3].

For a typical parameter set: $g = 52$, $\sigma = 1.3$ and $b = 0.4$, we observe, from numerically integrating our nonlinear system, pure roll patterns, defects and a transition from rolls to a turbulent state and *vice versa*. The roll patterns not only appear in the real and imaginary parts of the complex electric field E but also in its intensity $|E|^2$, evolving from an initially uniform state which exists within the pump parameter window from the instability threshold value $A \simeq 2.4403$ at a critical wavenumber $K_c = 1.7818$ to $A = 2.512$. The spatial period of the roll patterns in $\mathrm{Re}(E)$ and $\mathrm{Im}(E)$ is identified to be the same as that in intensity $|E|^2$. The intensity pattern periodically changes with a period $T = 2\pi/\omega_A$ while both the real and imaginary parts of E also exhibit a slow amplitude modulation;

ω_A is the oscillatory frequency corresponding to the largest growth rate for the given pump A. When the pump parameter A is increased above $A = 2.52$, turbulent states are observed which span a pump parameter window from $A = 2.52$ to 2.56, beyond which the system evolves into a new roll state. Some typical intensity patterns near the transition point are shown in Fig. 1, in which on increasing A the roll pattern evolves through defect formation into a turbulent state. Figure 2(a) and (b) show the time evolution for the roll and the turbulent patterns, respectively.

In conclusion, we have provided first theoretical evidence of roll patterns and the dynamical transition between the roll states and turbulent structures in a resonant coherently optically pumped three-level laser model. These phenomena are found to exist only in the nonzero lasing branches.

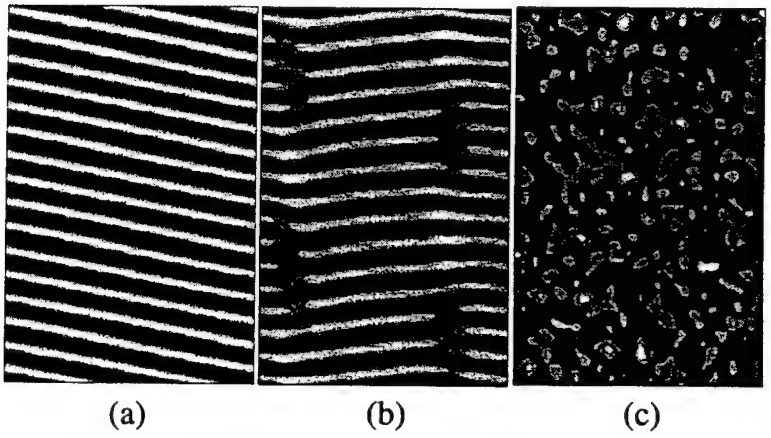

Fig. 1 Transverse field intensity $|E(x,y)|^2$ patterns. (a) $A = 2.51$, (b) $A = 2.515$ and (c) $A = 2.52$.

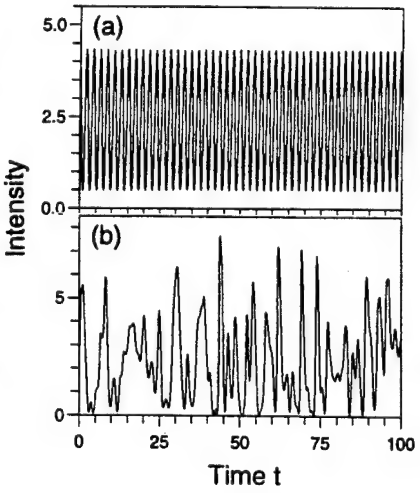

Fig. 2 Time series. (a) $A = 2.51$ and (b) $A = 2.52$.

REFERENCES

1. See, for example, M. Tlidi, M. Georgiou and P. Mandel, Phys. Rev. **A48**, 4605 (1993), G.-L. Oppo, M. Brambilla and L. Lugiato, Phys. Rev. **A49**, 2028 (1994), J. B. Geddes, J. V. Moloney, E. M. Wright and W. J. Firth, Opt. Commun. **111**, 623 (1994), and E. Pampaloni, S. Residori and F. T. Arecchi, Europhys. Lett. **24**, 647 (1993).

2. P. K. Jakobsen, J. Lega, Q. Feng, M. Staley, J. V. Moloney and A. C. Newell, Phys. Rev. **A49**, 4189 (1994).

3. W. Forysiak, J. V. Moloney and R. G. Harrison, Physica **D53**, 162 (1991).

Pattern Dynamics, Selection and Control in Large Aspect Ratio Lasers

J. Lega, C. Bowman, J.V. Moloney and A.C. Newell
Arizona Center for Mathematical Sciences
Mathematics Department
University of Arizona
Tucson AZ 85721
Tel: (602)-621-6755, Fax: (602)-621-1510 E-mail:lega@math.arizona.edu

I. Aranson
Department of Physics and Jack Pearl Resnick Institute of Advanced Technology
Bar Ilan University
Ramat Gan 52900, Israel

The emergence of transverse patterns near peak gain in large aspect ratio Class A, B and C lasers can be described by a complex Swift-Hohenberg equation (CSHE) coupled to a mean flow [1]. This model generalizes the conventional rate equation description to wide aperture lasers and avoids spurious high transverse wavenumber instabilities associated with the naive adiabatic elimination procedure [2]. The mean flow corresponds essentially to retaining the population inversion in the description of the laser dynamics even for the cases of Class A and C lasers and allows one to extend the validity of this complex order parameter description to well above lasing threshold. Robustness is a key observed feature, with the amplitude equations derived from the CSHE for negative (complex Ginzburg-Landau (CGLE)) and positive (complex Newell-Whitehead-Segel (CNWS)) detuning, agreeing precisely with those derived directly from the original laser equations [3]. The nonvariational character of the CSHE for a laser plays a fundamental role in determining the type of pattern that emerges above threshold.

A generalized rate equation descripton of a single longitudinal mode, homogeneously broadened 2-level laser is given by the complex Swift-Hohenberg equation coupled to the inversion (mean flow) [1]:

$$
\begin{aligned}
(\sigma+1)\psi_t &= \sigma[(r-1)-i\Omega]\psi + ia\nabla^2\psi - \frac{\sigma}{(\sigma+1)^2}(\Omega + a\nabla^2)^2\psi - \sigma n\psi \\
n_t + bn &= |\psi|^2
\end{aligned}
$$

This equation determines the space-time evolution of the complex order parameter ψ and has an obvious physical interpretation. The linear term (first term) on the RHS displays linear amplification (if the pump parameter $r > r_c = 1$) and frequency pulling ($\sigma\Omega$) where σ is the dimensionless cavity loss and Ω, the dimensionless cavity-atomic transition detuning. The second term accounts for diffraction and is responsible for the nonvariational character of the CSHE. The third diffusion term is all important in filtering the growth of unstable modes, by selectively amplifying the traveling wave with transverse wavenumber $k_c = \sqrt{\frac{\Omega}{a}}$ (gain discrimination). Otherwise all transverse modes would see equal gain. Without the additional degree of freedom n for Class A and C lasers, the CSHE would not reproduce the linear instability boundary (Busse balloon) well above threshold.

We will present a detailed study of pattern dynamics in wide aperture 2-level lasers comparing predictions of the complex order parameter description above with the 2-level Maxwell-Bloch model. The nonvariational aspect of the problem is all important, precluding static patterns, at least in an infinitely extended geometry. We will show how boundary driven pattern selection competes with pattern selection mechanisms in the bulk and, in particular, how boundary nucleated patterns invade the interior consuming core-unstable spiral waves. Preliminary results will be presented on the derivation of a *complex order parameter equation* description for wide aperture semiconductor lasers including inhomogeneous broadening and many-body effects where the latter impose a strong asymmetry on the neutral stability curves.Wide aperture Class B lasers will be shown to be inherently turbulent optical systems.

References

[1] J. Lega, J.V. Moloney and A.C. Newell, Phys. Rev. Lett., **73** 2978 (1994); J. Lega, J.V. Moloney and A.C. Newell, Physica D, (in press).

[2] P.K. Jakobsen, J.V. Moloney, A.C. Newell, and R.A. Indik, Phys. Rev. A. **45**, 8129 (1992).

[3] A.C. Newell and J.V. Moloney, *Nonlinear Optics*, Addison Wesley Publishing Co., Redwood City, California (1992).

Spatio-temporal dynamics of Lasers with a large Fresnel number

G. Huyet, S. Rica, J.R. Tredicce and N.B. Abraham
Institut Non Linéaire de Nice, UMR 129 CNRS-UNSA, 1361 Route des Lucioles, 06560 Valbonne, France.
FAX (33) 93 65 25 17, e-mail huyet @ecu.unice.fr

We report experimental evidence of spatio-temporal complexity and weak turbulence in lasers with large Fresnel numbers. We characterize the dynamics by measurements of the intensity cross correlation function of patterns emitted by a CO_2 laser with a Fresnel number around 60. We show that these patterns have limited spatial correlation and we have measured the correlation length. Our experimental results can be explain in a framework based on the Maxwell-Bloch equations. We show that two instabilities be present. The first is a long wavelength instability which is related to the phase invariance of the electromagnetic field and is described by a Kuramoto-Shivasinsky (KS) type equation. The second is a short wavelength instability which corresponds to a Hopf bifurcation which selects a very well-defined wavelength and is described by a complex Swift-Hohenberg (CSH) equation.

In this report, we summarize some of our recent results [1] for our Pérot-Fabry CO_2 laser which has an intracavity lens which can be moved to adjust up to 60 and then we give a theoretical approach based in the Maxwell-Bloch theory of lasers.

Time averaged intensity patterns are observed on an infra-red image plate and they may be as simple as concentric rings or may be of a more complex nature such as square lattices as reported in [2]. These averaged structures are induced by the geometrical symmetry of the cavity which can be adjusted with three piezoelectric (PZT) crystals for precise alignment of one of the cavity mirror. For a perfect alignment, the pattern has circular symmetry and when we move one of the PZT's from this setting we break the circular symmetry giving the pattern has a privileged axis of symmetry.

However, the observation of the spatial distribution of the time averaged laser intensity does not give any information about the temporal behavior. Moreover one may wonder if these structures are the time-averaged pattern of a complex field or are only generalized cavity modes. In other words, are we observing a low dimensional dynamics or a characteristic of spatio-temporal complexity and weak turbulence?

To obtain some answer to this question, the transverse profile of the intensity is measured with a rotating mirror which deflects the beam onto a *HgCdTe* detector (Fig.1b). We observed that the DC component is always large compared to the AC component. At relatively low pump rate, we observe periodic intensity oscillations at $150kHz$ over most of the pattern; this frequency is close to the relaxation oscillation frequency of the single mode laser. When the pump and/or the Fresnel number is increased the laser intensity becomes chaotic in time at each point, as we can see in FIG.1c. The intensity power spectrum shows a relative broad peak centered at a frequency of the order of magnitude of the relaxation oscillations, and a large broad spectrum at lower frequencies. The envelope of the oscillating auto correlation function decreases to zero with a correlation time of the order of $1ms$.

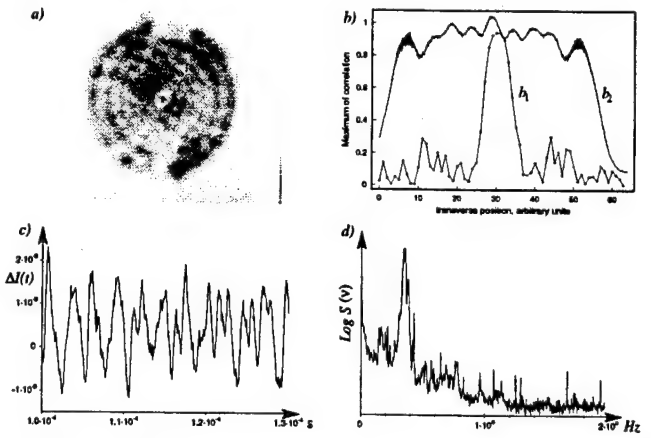

FIG. 1. *a)* The average pattern displayed by a thermal plate. *b)* The curve b_1 is a plot of the correlation function $C(x, x_0)$ with the reference detector positioned near the center of the pattern. The second curve b_2 is the averaged intensity coming from the rotating mirror. Curve b_2 is used as a spatial reference, and we can compare the correlation length with the radius of the beam and with the width of the "boundary layer" of the pattern. *c)* The AC component of the intensity at a point vs. time. *d)* The mean power spectrum of the signal in *c)*, in which we can distinguish a broad background characteristic of a chaotic signal and also a narrow band around a frequency between 350-400 kHz and a smaller band between $150 - 200kHz$.

We used two detectors to calculate the spatial correlation of the pattern. One detector is used to record the intensity at a reference point while the second measures the signal deflected by the rotating mirror. As the mirror rotates very slowly, we are able to measure the cross-correlation between the intensities at two different spatial points. With a digital oscilloscope we are able to acquire 1 million data points which are transferred to a computer for analysis.

The two data files obtained are divided into 64 files in set of which gives 64 separate regions in the pattern. We calculate the cross correlation between the such files as follows. Let us call $ref(x_0, t)$ and $mir(x, t)$ the x^{th} files obtained respectively from the reference file and from the

rotating mirror file. Then we calculate :

$$C(x,x_0) = \max_{\tau} \frac{\Sigma_{t=t_0}^{t=t_1} mir(x,t)\cdot ref(x_0,t+\tau)}{\sqrt{(\Sigma_{t=t_0}^{t=t_1} mir(x,t)^2)(\Sigma_{t=t_0}^{t=t_1} ref(x_0,t)^2)}}.$$

If the signals are perfectly correlated, then $C(x,x_0)=1$, and if they are uncorrelated $C(x,x_0)=0$. In FIG. 1-*b)* we show the function $C(x,x_0)$ plotted for 64 locations.

We measure this spatial correlation for different patterns as the Fresnel number is increased. For patterns which have periodic oscillations (low pump or low Fresnel number), the correlation is equal to one everywhere. When the complexity is increased the temporal behavior of the intensity becomes chaotic with a small number of modes; thus the spatial correlation function is no longer equal to one everywhere, but decreases with oscillations. This decrease of correlation comes from a superposition of modes which interact. But for high Fresnel number, we see that the spatial shape of the correlation changes dramatically. As we see in FIG. 1-*b)*, the correlation is a peaked function with a characteristic width which is about $\frac{1}{6}$ of the characteristic size of the pattern.

In the general electromagnetic Maxwell theory, the phase of the complex Fourier amplitude of the electromagnetic field (a real quantity) is not fixed. This property is valid either for a dissipative or conservative systems without an external forcing, which could lock the phase. According, the long wavelength laser dynamics (a dissipative system) is governed by a phase diffusion equation. Similar electromagnetic phase dynamics is a common feature for any laser and may lead under certain conditions to a "turbulent" state, which is uncorrelated in time and in space, through a modulation, mainly of the phase primarily of the electromagnetic field.

Some lasers, often called class-B lasers, also suffer from an oscillatory transition toward a periodic structure. These lasers exhibit a periodic modulations in space and time. In our case the measured electric field amplitude is modulated by both effects. As a consequence the laser intensity is locally chaotic on short time scales but the time-average intensity patterns retains the global symmetry of the system.

Coupled of partial differential equations for both a Hopf bifurcation and a (KS) phase dynamics, read:

$$\partial_t A = \mu A - iv(q_0^2+\nabla^2)A - \alpha(q_0^2+\nabla^2)^2 A - (\beta_1|A|^2 + \beta_2(\nabla\phi)^2)A + \beta_3\nabla\phi\cdot\nabla A; \qquad (1a)$$

$$\partial_t\phi = -k_0^2\nabla^2\phi - \frac{c_0}{2}\nabla^4\phi + c_1(\nabla\phi)^2 + c_2|A|^2. \qquad (1b)$$

The complex field A describes a Hopf bifurcation with a well defined spatial wavelength, while the real variable ϕ describes the dynamics of the phase of the electromagnetic field. μ and k_0^2 are the control parameters, v represents a group velocity of a Hopf bifurcation, q_0 is the spatial wavenumber, α is a complex coefficient representing diffusion and diffraction. c_0 is a positive coefficient which ensures the dissipation and it depends on the Fresnel number. β_i and c_j depend on laser parameters and ensure saturation. In general, equation (1b) leads to a "turbulent" behavior in time as well as in space. Its time scale ($\tau_c \sim c_0/k_0^4$) is much smaller than the characteristic time of the Hopf bifurcation, which is of the same order of magnitude as the relaxation oscillations of a single mode laser. Furthermore, the characteristic length of the phase instability ($\lambda_c \sim \sqrt{c_0}/k_0$) is larger than the wavelength of the Hopf bifurcation. As a result, we believe that the observed temporal oscillations come from the Hopf bifurcation, while a loss of correlation in time and space comes from the phase dynamics. Thus the overall correlation time and length in laser patterns should be of the order of τ_c and λ_c, respectively.

The phase dynamics reaches a "turbulent" state when the number of degrees of freedom is increased. Such a number grows in proportional to the Fresnel number (Fr), as Fr/Fr_0, where Fr_0 is dimensionless and depends on the laser parameters (detuning, pumping, *etc...*). Fr is the parameter which governs the transition from low dimensional chaos ($Fr \approx Fr_0$) to a weak turbulence regime ($Fr \gg Fr_0$). It is difficult to obtain detail of this kind of measurements of turbulent behavior of the laser intensity with measurements of the intensity as a function of time at a single point. Hence, we focus our attention on the correlation length. By dimensional analysis of equation (1b), we expect that the correlation length varies as $\lambda_c/R \sim \sqrt{Fr_0/Fr}$, with R the radius of the laser beam. For a low Fresnel number, that is for a system of only a few degrees of freedom, the pattern is completely correlated since $\lambda_c \approx R$. But as Fr increases (larger than Fr_0) the phase correlation length decreases becoming much smaller than R. In conclusion, as a result of these two instabilities, the laser intensity is disorganized in space and in time due to the turbulent behavior of the KS dynamics, yet the time-averaged pattern recovers the spatially periodic structure as selected by the CSH equation. The fact that "turbulent" patterns retain underlying symmetry on average, has been experimentally observed in Faraday instability [3].

[1] G. Huyet and S. Rica, "Pattern formation and phase turbulence in the transverse section of lasers", submitted Phys. Rev. Lett.; G. Huyet, M.C. Martinoni, S. Rica and J.R. Tredicce, "Measurement of spatio-temporal complexity in Lasers with a large Fresnel number", submitted to Phys. Rev. Lett.

[2] D. Dangoise, D. Hennequin, C. Lepers, E. Louvergneaux, and P. Glorieux, Phys. Rev. **A 46**, 5955 (1992).

[3] B.J. Gluckman, P. Marcq, J. Bridger, and J.P. Gollub, Phys. Rev. Lett. **71**, 2034 (1993); L. Ning, Y. Hu, R. Ecke, and G. Ahlers, *Ibid.*, p. 2216.

The Effect of Mirror Curvature on Pattern Formation in Large Aspect Ratio Lasers

G. K. Harkness, J. C. Lega[1] and G.-L. Oppo
Department of Physics and Applied Physics,
University of Strathclyde, 107 Rottenrow, Glasgow G4 0NG, UK
Tel: (UK) 141-552 4400 x3354 ; Fax: (UK) 141-552 2891
email: graeme@phys.strath.ac.uk

A number of recent publications have studied transverse pattern formation in broad area lasers [1-5]. One of the main results of these works has been to show that, in positively detuned lasers of infinite transverse extent, the first bifurcation is to a state corresponding to off-axis emission. One limitation of such work is that the effects of transverse boundaries are not included ; these may be important in describing real laser systems which have a transverse pump shape, intracavity apertures or curved cavity mirrors.

A recent study has considered transverse reflecting boundaries [6] but such reflectors are not commonplace in real lasers. Here we study the effect of mirror curvature on the first laser bifurcation by studying the bifurcation and above threshold behaviour of the mean-field Maxwell-Bloch equations [7],

$$\begin{aligned}
\frac{\partial F}{\partial t} &= -k\left[\left(1 - i\delta - ia\left[\frac{\nabla^2}{4} + \eta - \eta^2\rho^2\right]\right)F - R\right], \\
\frac{\partial R}{\partial t} &= -(1 + i\delta)R + F\Delta, \\
\frac{\partial \Delta}{\partial t} &= -\gamma\left[\Delta - \chi + \frac{1}{2}(F^*R + FR^*)\right].
\end{aligned}$$

These partial differential equations describe the interaction of the laser field, F, the polarisation, R, and the population inversion, Δ. The parameter χ describes the pumping, δ is the detuning and η is related to the curvature of the mirrors ; $\eta = 0$ corresponds to them being flat.

For small detunings, and close to threshold, we have reduced these Maxwell-Bloch equations to a modified Swift-Hohenberg equation and have performed linear analysis of both the reduced and full equations in a Gauss-Laguerre/Gauss-Hermite basis. Figure 1 shows how the curved mirror results converge to those for flat mirrors [3] (in a Fourier basis) when the parameter $\eta \to 0$.

Close to threshold, we have derived amplitude equations describing the nonlinear interaction of the cavity modes. For any arbitrary mirror curvature, the laser bifurcation is always to a pattern involving a single family of empty cavity modes, whereas for flat mirrors travelling waves are always expected. In this sense, the curvature of the mirrors introduces a singular perturbation. Away from threshold, a secondary transition occurs from patterns involving cavity modes to ones of a travelling wave nature. We have studied these transitions in detail in both one and two transverse dimensions. Figure 2 presents the results of two numerical simulations. The first, close to threshold, shows a final time independent state consisting of a few Gauss-

[1]Permanent address: INLN – UMR CNRS 129 – 1361 Route des Lucioles, 06560 Valbonne, France

Laguerre modes. The second, above the secondary threshold, shows a state dominated by travelling-waves, as described in the caption.

This work is, in part, supported by EPSRC grant GR/J/30998.

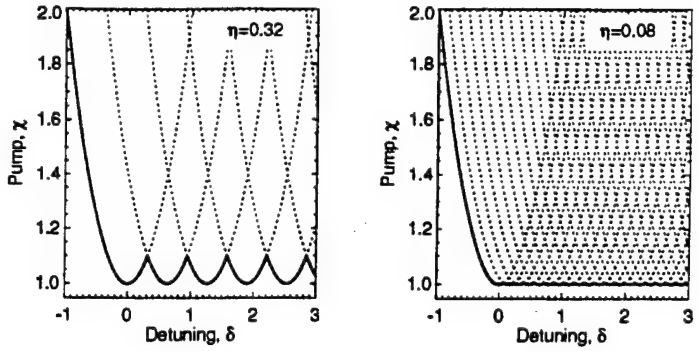

Figure 1: *The threshold for excitation of each family of Gauss-Laguerre modes for two values of the mirror curvature, η. On the right, the mirrors are nearly flat and the lowest of the threshold curved tends to that for the Fourier modes in the flat mirror case.*

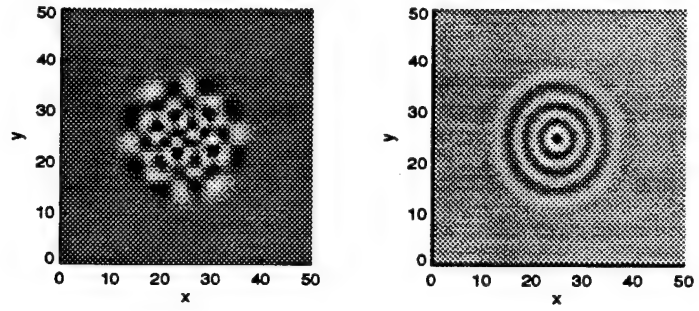

Figure 2: *The real part of the laser field, F, as a function of the transverse coordinates (x, y). On the left, the pump is close to threshold and the final output state is comprised of a few Gauss-Laguerre modes. On the right, travelling waves are generated at the boundary and travel inwards.*

References

[1] L. Gil, Ph.D. thesis, University of Nice, 1988.
[2] P. K. Jakobsen, *et al.*, Phys. Rev. A, Vol. **45**, No. 11, pp.8129–8137 (1992).
[3] J. V. Moloney and A. C. Newell, *Nonlinear Optics* (Addison-Wesley, Redwood City, CA, 1991).
[4] P. K. Jakobsen *et al.*, Phys. Rev. A, Vol. **49**, No. 5, pp.4189–4200 (1994).
[5] J. Lega, *et al.*, Phys. Rev. A, Vol. **49**, No. 5, pp.4201–4212 (1994).
[6] G. K. Harkness *et al.*, Phys. Rev. A, Vol. **50**, No. 5, pp.4310–4317 (1994).
[7] L. A. Lugiato *et al.*, J. Opt. Soc. Am. B, Vol. **7**, No. 6, pp.1019–33 (1990).

Control of Chaos in Multi Transverse Mode Lasers

R. Martin, A.J. Kent*, G. D'Alessandro and G.-L. Oppo**

Department of Physics and Applied Physics, University of Strathclyde
107 Rottenrow, Glasgow, G4 0NG, Scotland, UK
Tel + 44 - 141 - 552 - 4400 (ext. 3761)
Fax + 44 - 141 - 552 - 2891
Email : gianluca @ phys.strath.ac.uk

We show that a modified version of Hunt's Occasional Proportional Feedback (OPF) method [1] as applied to the chaotic single mode laser [2], can be used to control a multi transverse mode laser exhibiting weak spatio-temporal chaos.

We consider the diffractive Maxwell-Bloch equations for a single longitudinal ring cavity laser [3] and project the electric field variable onto a set of 15 Gauss-Laguerre modes for cavity configurations where only 6 modes have non-negligible amplitudes. The polarisation and population inversion variables are evaluated on a grid of 640 lattice nodes leading to a system of 2050 coupled ordinary differential equations. By perturbing global parameters of the system according to the OPF method, we have been able to stabilise periodic orbits in both the cases of cylindrically symmetric and asymmetric pump shapes. In order to describe experimentally feasible techniques, we have chosen to monitor the total output power of the laser and to sample it periodically at the frequency of the relaxation oscillations or at its harmonics/subharmonics. At these times a perturbation proportional to the difference between the sampled output power and a reference value was applied to a selected system parameter.

In the case of cylindrically symmetric pump shapes, orbits were controlled by perturbing either the magnitude of the pump or the cavity losses, the latter proving to be more effective. In all the controlled orbits, the modal projections of the final periodic state change little in spite of the different character of the dynamics which may range from period one to period nine and even above. The fact that we obtained a variety of periodic orbits all with very similar modal configurations indicates that Hunt's technique offers flexibility in temporal control but is less able in accessing spatial dimensions.

In order to describe more realistic laser configurations [4], we have broken the cylindrical symmetry of the Maxwell-Bloch equations by shifting the pump with respect to the centre of the spherical mirrors. Again, control of temporal chaos has been achieved by modulating the losses for weakly disordered cases. A first estimate of the correlation dimension gave values between 4 and 6 showing a low dimensionality of the attractor. Typical magnitudes of the control kicks are between 3 to 5% of the intensity but they can be reduced after control is achieved. Figure 1 shows the time evolution of the total power before and after the application of the control signal. Figure 2 displays the corresponding power spectra where the removal of the

continuum component via the control technique is apparent (see panel (b)).
From these measurements, it would appear that control using Hunt's technique is generically feasible even when a large number of coupled differential equations (2050 in our case) are present. It is important, however, to stress that control has been achieved only where the chaos is weak. As the pump is increased and the laser becomes more chaotic, the ability to control is lost. Whenever the dimension of the dynamics exceeds 8 or 10, the control technique appears to increase disorder instead of removing it. This is in agreement with recent attempts to control fully developed spatio-temporal disorder in partial differential equations [5] where the same relevance of attractors to the overall dynamics is questionable [6].
Support from EPSRC (GR/J/30998) is gratefully acknowledged.

References

[1] E. Hunt, Phys. Rev. Lett. **67**, 1953 (1991).
[2] R. Roy et al., Phys. Rev. Lett. **68**, 1259 (1992).
[3] L. Lugiato et al., J. Opt. Soc. Am. B **7**, 1019 (1990).
[4] C. Green et al., Phys. Rev. Lett. **65**, 3124 (1990).
[5] A. Kent, Ph.D. thesis, University of Strathclyde, Glasgow (1994).
[6] A. Politi et al., Europhys. Lett. **22**, 571 (1993) and references therein.

(*) Present address, Department of Physics, University of Buenos Aires, Argentina.
(**) Present address, Department of Mathematics, University of Southampton, UK.

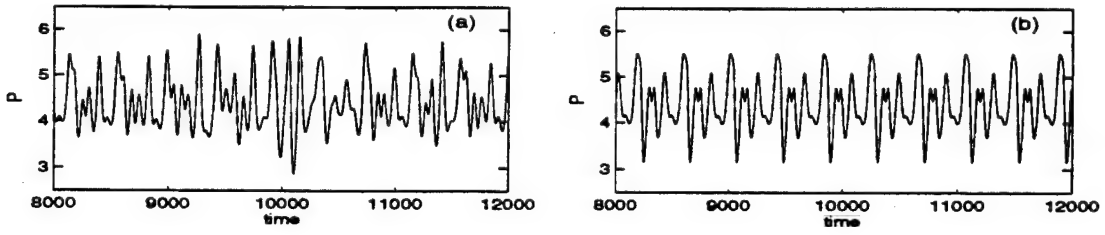

Figure 1: *Time evolution of the output power P of a multi-transverse mode laser before (a) and after (b) the application of the control signals.*

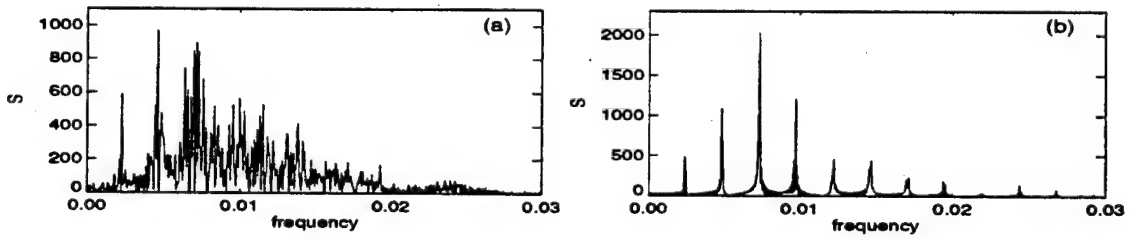

Figure 2: *Power spectrum S of the output power of a multi-transverse mode laser before (a) and after (b) the application of the control signals.*

EXPERIMENTAL CONTROL OF CHAOS IN CO_2 LASER WITH FEEDBACK

M.Ciofini, R.Meucci, and F.T.Arecchi
Istituto Nazionale di Ottica
1. E. Fermi 6, 50125 Florence, Italy
Tel. +39-55-23081, Fax +39-55-2337755
E-mail RIC@FIREFOX:INO:IT

We show that the chaotic behavior of a CO_2 laser with feedback can be stabilized by addition of a small sinusoidal perturbation in the feedback loop.

Robust stabilization of different periodic orbits can be achieved by a parametric perturbation with frequency close to that of the leading cycle embedded in the chaotic attractor and with relative amplitudes of the order of a few per cent. We call this stabilization "adaptive stabilization" since the perturbation parameters are suggested by a preliminary global measurement on the system itself. This method avoids the on-line tracking of a local feedback stabilization [1] which would imply too stringent requirements on the time resolution of the tracking apparatus; moreover it adapts to a global system property, that is, its power spectrum.

We recall that the chaotic behavior of a single mode CO_2 laser with feedback depends on some peculiarities of the feedback loop. In our case [2],the signal from a detector is fed back to an intracavity electro-optic modulator via an amplifier with a bias voltage B. B acts as the control parameter.When the system is in the chaotic region, the stabilization of periodic orbits has been obtained by adding to the bias voltage B a small sinusoidal perturbation so that it becomes

$$\bar{B} = B\,[1 + \varepsilon \sin(2\pi f t)]$$

The perturbation frequency f is chosen close to the frequency f^* of the peak (representing the remnant of the limit cycle) still present in the unperturbed chaotic spectrum. The relative perturbation amplitude ε is of the order of few per cent.

The stabilization region is presented in the parameter space $[\varepsilon,f]$ (Fig 1). We consider the difference $\Delta=S(f)-\bar{S}$ between the peak value of the power spectrum S(f) at the fundamental frequency of the stabilized orbit and the averaged spectrum $\bar{S}$ over the range 0-100 kHz as the robustness indicator. Figure 2 shows the dependence of $\Delta-\Delta_c$ on the perturbation frequency measured at $\varepsilon=0.027$, being Δ_c the value of Δ for the unperturbed chaotic spectrum. The boundaries of Fig. 2 correspond to the merging of the peak within the chaotic background, so that Δ

reduces to Δ_c.

Numerical simulations on a four-level model of the CO_2 laser are in good agreement with the experimental results [3].

References
1 - E.Ott, C.Grebogi and J.A.Yorke, Phys. Rev. Lett. 64, 1196 (1990).
2 - F.T.Arecchi, R.Meucci, and W.Gadomski, Phys. Rev. Lett. 58, 2205 (1987)

3 - M.Ciofini, R.Meucci and F.T.Arecchi, submitted to Phys. Rev E.

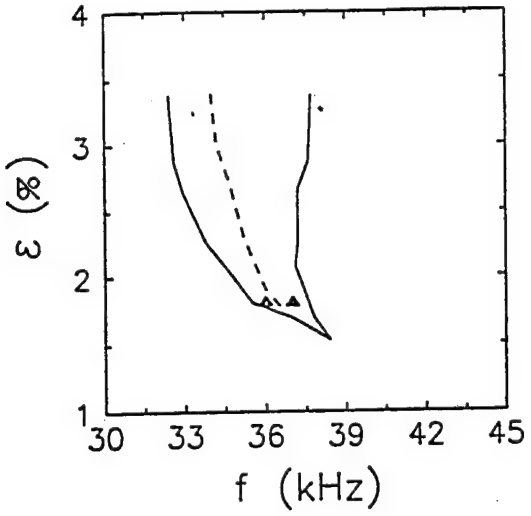

Fig. 1 - Experimental stability domain (area between the two solid lines) in the parameter space; The dashed line separates the regions of period-4 and period-2 stable orbits (right side and left side respectively).

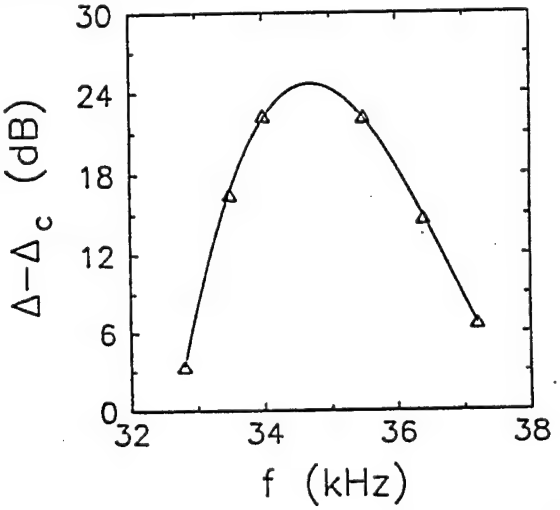

Fig. 2 - Dependence of the robustness indicator $\Delta-\Delta_c$ on the perturbation frequency f, for ε=0.027: symbols denote experimental points while the solid line represents a cubic fit.

Adaptive Control of Chaos

S. Boccaletti and F.T. Arecchi
Istituto Nazionale di Ottica, 50125 Firenze-Italy and
Dept. of Physics, University of Firenze, 50125 Firenze-Italy

We introduce an adaptive method for stabilizing the unstable periodic orbits embedded in a chaotic attractor. The control technique is based on a continuous correction of the dynamics with a forcing term driven by the local information extracted from the dynamics itself. The method easily controls systems in which more than one positive Liapunov exponent is present and can be implemented even for experimental situations which are too fast for standard off-line control methods.

Let us consider a system ruled by

$$\frac{d\mathbf{x}}{dt} = \mathbf{G}(x, \mu), \tag{1}$$

where $\mathbf{x}$ is a D-dimensional vector, $\mathbf{G}$ a nonlinear function and μ a set of control parameters chosen in such a way as to produce chaotic behavior.

In a previous work [1], an adaptive algorithm able to recognize a chaotic dynamics was introduced. This algorithm is based on a continuous readjustement of the observation time interval in order to minimize the second variations of the vector $\mathbf{x}$. For each component i ($i = 1, 2, ..., D$) of $\mathbf{x}$, one defines the variation over the time interval τ_n as

$$\delta x_i(t_{n+1}) = x_i(t_{n+1}) - x_i(t_n), \tag{2}$$

where $t_{n+1} = t_n + \tau_n$ (τ_n being specified later) represents the $(n+1)$th instant at which observation of the system is performed.

By use of Eq. (2) it is possible to evaluate the local variation rates λ's as

$$\lambda_i(t_{n+1}) = \frac{1}{\tau_n} \log \mid \frac{\delta x_i(t_{n+1})}{\delta x_i(t_n)} \mid, \tag{3}$$

and to update the observation interval as

$$\tau_{n+1}^{(i)} = \tau_n^{(i)} \left(1 - \tanh(g\lambda_i(t_{n+1}))\right). \tag{4}$$

In Eq. (4) the $\tau^{(i)}$ are the observation time intervals corresponding to the ith component of the vector $\mathbf{x}$. Once all $\tau^{(i)}$ have been calculated, the next time interval is selected as [1]

$$\tau_{n+1} = \min_i \{\tau_{n+1}^{(i)}\}, \tag{5}$$

and this fixes the new observation at the time $t_{n+2} = t_{n+1} + \tau_{n+1}$.

The analysis of the sequence of τ's permits to extract the main properties of the given dynamics $\mathbf{x}(t)$.

Now, in order to stabilize a periodic dynamics, we first need to extract the periods of the UPO's embedded in the chaotic motion [2].

We consider the maps τ_{n+k} vs. τ_n, $k \geq 2$. If the r.m.s. η of the distribution of points around the diagonal is plotted against the step interval k, the function increases, since the selfcorrelation of a chaotic signal lasts only for a finite time.

In fact, the chaotic trajectory visits phase space regions corresponding to neighborhoods of different UPO's. During the time in which the trajectory comes close to a generic UPO of period T_j, temporal selfcorrelation is rebuilt after such a period. Thus, for all k_j such that $k_j \cdot < \tau >$ approaches T_j ($< \tau >$ being the average of the τ distribution), the corresponding η vs. k_j plot should present local minima.
Once the periods T_j ($j = 1, 2, ...$) of the UPO's have been measured, stabilization of each one can be achieved when the system visits phase regions close to that UPO. For this purpose we modify the adaptive recognition algorithm as follows. At each new observation time $t_{n+1} = t_n + \tau_n$ and for each component i of the dynamics, instead of Eq. (2), we evaluate the difference between the observed and the desired values:

$$\delta x_i(t_{n+1}) = x_i(t_{n+1}) - x_i(t_{n+1} - T_j). \tag{6}$$

The local variation rates λ's are now redefined as

$$\lambda_i(t_{n+1}) = \frac{1}{\tau_n} \log \mid \frac{x_i(t_{n+1}) - x_i(t_{n+1} - T_j)}{x_i(t_n) - x_i(t_n - T_j)} \mid, \tag{7}$$

while Eqs. (4,5) are kept for the updating process of τ's.
Finally, we define $U_i(t)$ as the ith component (constant over each observation time interval) of the perturbing vector $\mathbf{U}(t)$ as

$$U_i(t_{n+1}) = \frac{1}{\tau_{n+1}}(x_i(t_{n+1} - T_j) - x_i(t_{n+1})), \tag{8}$$

and we add such a vector to the evolution equation, which now becomes

$$\frac{d\mathbf{x}}{dt} = \mathbf{G}(\mathbf{x}, \mu) + \mathbf{U}(t). \tag{9}$$

Therefore, once a given T_j has been preselected, it is the same adaptive dynamics which selects the correction terms to be added in Eq. (9). In summary, our method acts in two successive steps: a first recognition task in which the periods of UPO's are measured and a second control task in which the dynamics is constrained to shadow the desired periodic orbit.
Even though apparently similar to Pyragas' [3], our adaptive method is better at least in two ways. First, the adaptive nature of the forcing term (Eq. (8)) which is inversely proportional to the time intervals and hence is weighted by the information extracted from the dynamics itself. Second, while in Ref. 3 the control is readjusted at each computational time step, here interventions are done at the intermediate time scale, thus reducing the computational or experimental effort for the control task.
Work partly supported by EEC contract n. CI1*CT93-0331.
References:
[1] F.T. Arecchi, G. Basti, S. Boccaletti and A.L. Perrone, Europhys. Lett. **26**, 327 (1994).
[2] D. Auerbach, P. Cvitanovic, J.-P. Eckmann, G. Gunaratne and I. Procaccia, Phys. Rev. Lett. **58**, 2387 (1987).
[3] K. Pyragas, Phys. Lett. A **170**, 421 (1992).

Control of Chaos in a Multimode Solid State Laser by Use of Small Periodic Perturbations

Pere Colet
Departament de Física, Universitat de les Illes Balers, E-07071, Palma de Mallorca, Spain
Tel: 34 71 172537. Fax: 34 71 173426. e-mail: pere@hp1.uib.es
Y. Braiman
School of Physics, Georgia Institute of Technology, Atlanta, Georgia 30332

A great deal of attention has been paid in recent years to develop algorithms to convert the dynamical system from chaotic to periodic motion [1]. The algorithms are based on the fact that small changes applied to chaotic system can suppress and eliminate chaos. The different techniques in controlling chaos can be (mainly) classified in two categories: feedback and nonfeedback. Feedback techniques [2, 3] are very powerful and proved to be very efficient in different systems. In particular, the Occasional Proportional Feedback technique [3], has been successfully applied to control chaos in multimode solid state lasers [4]. The nonfeedback techniques have not been so actively studied, and are poorly understood and more challenging. The essential advantage of nonfeedback techniques lies in its speed; no on-line monitoring and processing is required. This speed makes them especially promising for controlling systems with many degrees of freedom, such as fast electro-optical systems, superconducting Josephson junction arrays, and hydrodynamical systems. Numerical and analytical studies of single a Josephson junction [5], Duffing oscillator [6], and Rossler model [7] are representative examples of the use of small periodic drive to stabilize chaotic system. Nonfeedback techniques have also been applied to stabilize the dynamics of a non-autonomous loss-modulated single mode CO_2. [8]

We numerically study the stabilization of periodic orbits in a multimode solid state laser by using small periodic perturbations of a externally controlled system parameter. The dynamics of a multimode Nd:YAG (neodynium doped ytrium aluminium garnet) laser with an intracavity KTP (potassium titanyl phosphate) frequency doubling crystal can be modelled in terms of the rate equations for the intensity I_k and G_k associated with each mode [9]

$$\tau_c \dot{I}_k = (G_k - \alpha - g\epsilon I_k - 2\epsilon \sum_{j \neq k} \mu_{kj} I_j) I_k \tag{1}$$

$$\tau_f \dot{G}_k = p - (1 + I_k + \beta \sum_j I_j) G_k \tag{2}$$

where N is the number of modes and $k = 1, \ldots, N$. Here τ_c is the cavity round-trip time (0.2 ns), τ_f is the fluorescence lifetime of the Nd^{3+} ion (240 μs), α is the cavity loss parameter (assumed to be the same for all the modes, $\alpha = 0.01$), p is the small signal gain, which is related to the pump parameter and $g = 0.1$ is a geometrical factor dependent on the phase delays due to the YAG and the KTP crystals and on the angle between the YAG and KTP fast axes. ϵ is the nonlinear coefficient associated with the conversion efficiency of the fundamental intensity into doubled intensity by the KTP crystal ($\epsilon = 5 \times 10^{-6}$). β is the cross-saturation parameter related to the competition among the different longitudinal modes (assumed to be the same for all the mode pairs $\beta = 0.65$). The coefficients μ_{jk} depend on the mode polarization. Each cavity mode can be polarized only in one of two orthogonal directions; $\mu_{jk} = g$ if modes j and k have the same polarization and $\mu_{jk} = 1 - g$ otherwise. We consider the case with three modes, two polarized in the one direction, and one in the orthogonal direction.

Increasing the pumping p; then the system evolves from a stable steady state to periodic and finally to chaotic behavior with one positive Liapunov exponent. To achieve stablization we perform small amplitude modulations of the losses $\alpha = \alpha_0(1 + \alpha_1 \sin(\omega t))$. Numerical simulations show that very small modulation amplitudes have a dramatic effect on the dynamics. Depending on amplitude and frequency, the applied modulation can either increase the chaos or eliminate it. Fig. 1 shows the value of the leading Liapunov exponent as function of loss modulation amplitude for $\omega = 166\ ms^{-1}$. Stabilization is possible for some small values of the modulation amplitude. For large modulation amplitudes, leading Liapunov exponent is higher that in absence of the modulation, thus, the amount of chaos in the system is increased.

For different amplitude and modulation frequencies it is possible to stabilize different kinds of orbits, with the different modes oscillating periodically in a symmetric or an assymmetric way. Also, for some frequencies of modulation, one can obtain short periodic peaks (with large peak intensity) separated by long periods of very small intensity at each modes. The pulses of each of the modes alternate showing an antiphase behavior with one pulse emitted at each period of the modulation for the losses.

P.C. acknowledges finacial support from the Comisión Interministrial de Ciencia y Tecnología, Project No. TIC93/0744. Y.B. work was supported by the Office of Naval Research, through contract N00014-91-J-1257.

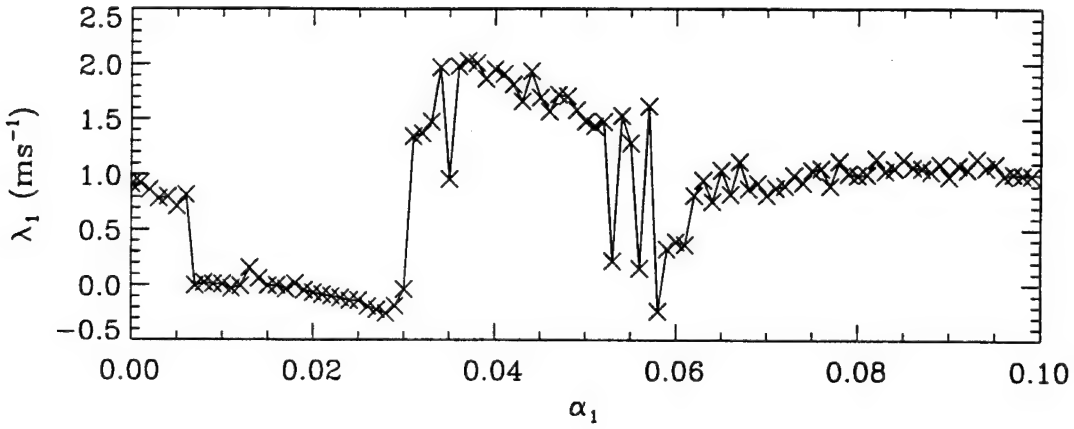

Fig. 1. Leading Liapunov exponent λ_1 as function of α_1 for $\alpha_0 = 0.01$ and $p = 0.03$.

References

[1] For a review, see for example, E. Ott, *Chaos in Dynamical Systems*, Cambridge University Press, 1993; S.Rajasekar and M.Lanshmanan,Physica D**67**, 282 (1993).

[2] E. Ott, C. Grebogi, and J. A. Yorke, Phys. Rev. Lett., **64**, 1196 (1990); T. ShinbroE. Ott, C. Grebogi, and J.A. Yorke, Nature, **363**, 411 (1993).

[3] E. R. Hunt, Phys. Rev. Lett., **67**, 1953 (1991).

[4] R. Roy, T. W. Murphy, T. D. Maier, Z. Gills, and E. R. Hunt, Phys. Rev. Lett., **68**, 1259 (1992).

[5] Y. Braiman and I. Goldhirsch, Phys. Rev. Lett., **66**, 2545 (1991).

[6] R. Lima and M. Pettini, Phys. Rev. A **41**, 726 (1990).

[7] V.V.Aleixeev and A.Yu.Loskutov, Dokl. Akad. Nauk SSSR **293**, 346 (1987).

[8] R.Meucci, W.Gadomski, M.Ciofini, and F.T.Arecchi, Phys. Rev. E**49**, R2528 (1994).

[9] C.Bracikowski and R.Roy, Chaos **1**, 49 (1991).

Using the control duration to stabilize a multimode laser

Thomas W. Carr and Ira B. Schwartz
Special Project in Nonlinear Science, Code 6700.3
Plasma Physics Division, Naval Research Laboratory
Washington, D.C. 20375
tel: 202-767-3195 fax: 202-404-8357
carr@nls7.nrl.navy.mil and schwartz@nls4.nrl.navy.mil

The use of a system's natural dynamics to force the system into a desired unstable state and thus achieve control offers an advantage over classical control methods. By applying small amplitude feedback to a readily available system parameter so that the system evolves towards the desired state, difficult or costly modifications to the system that alter its dynamics are unnecessary. This idea is apparent in a method to stabilize periodic orbits originated by Ott, Grobogi and Yorke (OGY)[1]. They used linear control theory and feedback to an available system parameter to direct the system to the stable manifold of the unstable state. Ideally, control could then be turned off as the natural dynamics along the stable manifold continued to contract the system towards the desired state.

A limitation of the OGY control method occurs in high-dimensional systems where control perturbations induce transients off the stable manifold that hinder the effectiveness of the method. It is interesting then that a related scalar control method called occasional proportional feedback (OPF)[3] has been successful in controlling the steady state and periodic orbits of a multimode laser, which is a high-dimensional system [4][5]. However, the OPF feedback method also requires the careful tuning of additional experimental parameters. In particular, the laser control experiment requires adjustment of control perturbation pulse width. This observation motivated us to develop a control method that explicitly uses the duration of time the control signal is applied, called control duration, as an additional feedback parameter to control steady states in high-dimensional systems [6]. An important difference between OPF and our method is that while in the case of OPF the control pulse width is fixed, we use the pulse width, or as we call it, the control duration, as an additional feedback parameter.

We have applied our method to the control of the model for a multimode Nd:YAG laser with an intracavity KTP crystal. This laser system is designed to convert infrared light to visible green light via frequency doubling. However, for moderate pump powers the steady state laser output undergoes a Hopf bifurcation and for higher pump powers exhibits chaos.

Fig. 1 shows the controlled steady state for approximately 40 ms, during which time there have been two-hundred control pulses. Control is then turned off so that the system evolves to splay-phase oscillations characteristic of the multimode laser. Specifying the duration of time for which control was activated as qT_{nat}, where T_{nat} is the natural period of the system, each control pulse lasted less than T_{nat}, so that $q < 1$. During the simulation shown in Fig. 1, it was found that $q \in (0.997, 0.014)$, the mean value was $\bar{q} = 0.384$, and the standard deviation was $\sigma_q = 0.263$. The fact that there is a low variance in q suggests a possible contributor to the success of the experiments using OPF when the control duration was held fixed.

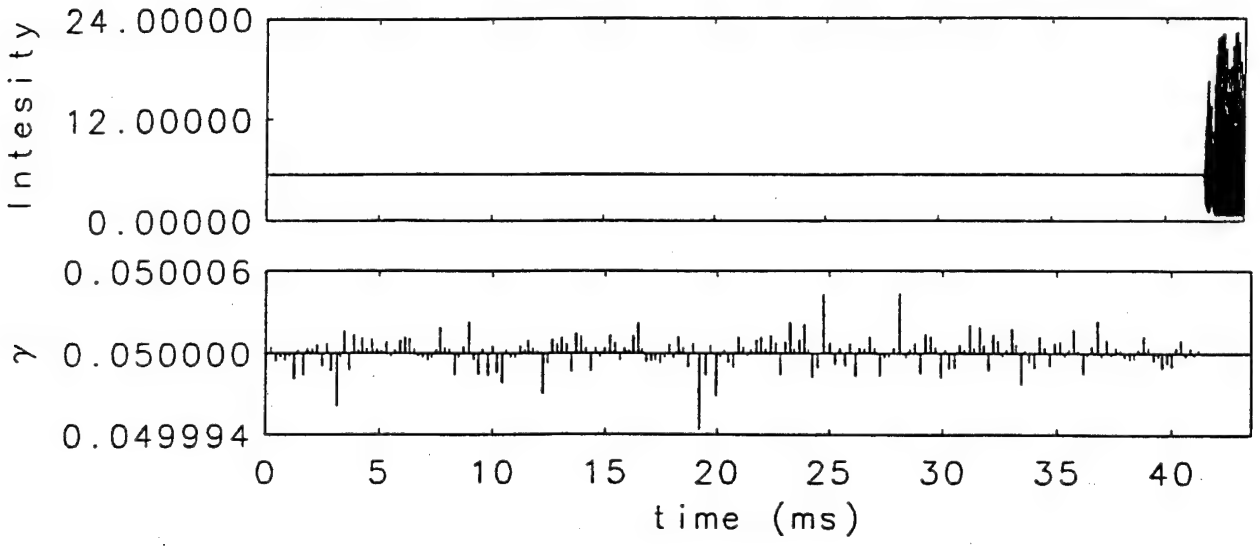

Figure 1: γ is related to the pump intensity of the laser and serves as the feedback parameter. The laser is controlled for approximately 40 ms at which time the feedback control is turned off and the system evolves to splay-phase oscillations.

References

[1] E. Ott, C. Grebogi, and J.A. Yorke, *Phys. Rev. Lett.* **64**, 1196 (1990)

[2] T. Sauer, J.A. Yorke and Martin Casdagli, *J. Stat. Phys.* **65**, 579 (1991)

[3] E.R. Hunt,*Phys. Rev. Lett.* **67**, 1953 (1991)

[4] R. Roy, T.W. Murphy, Jr., T.D. Maier, Z. Gills, and E.R. Hunt, *Phys. Rev. Lett.* **68**, 1259 (1992)

[5] Z. Gills, C. Iwata, R. Roy, I.B. Schwartz, and I. Triandaf, *Phys. Rev. Lett.* **69**, 3169 (1992)

[6] T.W. Carr and I.B. Schwartz, *Phys. Rev. E.* **50**, 3410 (1994)

STABILIZING OR DESTABILIZING LASERS BY CONTINUOUS DELAYED FEEDBACK

Serge Bielawski, Dominique Derozier, and Pierre Glorieux
Laboratoire de Spectroscopie Hertzienne, Université des Sciences et Technologies de Lille, 59655 Villeneuve d'Ascq Cedex, France
Fax:+ 33 20 43 40 84 email(GLORIEUX@LSH.CITILILLE.FR)
and
Thomas Erneux
Université Libre de Bruxelles, Optique Nonlinéaire Théorique, Campus Plaine, C.P. 231, 1050 Bruxelles, Belgium
Fax:+ 32 2 650 5824 email(TERNEUX@ULB.AC.BE)

ABSTRACT

Periodically modulated lasers exhibit cascade of period doubling bifurcations which have been studied experimentally [1,2], numerically [3,4] and analytically [5,6].

A comparative study between experimental and theoretical predictions requires informations on the unstable branches of periodic solutions. Stabilizing unstable orbits using feedback control methods became quickly an objective for several laboratories [7]. Chaotic outputs have been controlled on a Nd:YAG laser [8], an Nd:fiber laser [9], on a CO_2 laser [10] and on a NMR laser [11] but the actual mechanisms leading to successful stabilizations of unstable orbits are still unknown. The main objective of this paper is to show that stabilization is realized by moving the period doubling bifurcation point above which a particular branch of solutions is unstable.

Specifically, we consider a periodically modulated CO_2 laser controlled by delayed continuous feedback and investigate the stability of the Period 1 solution analytically, numerically and experimentally. We model the laser by the following dimensionless equations for the intensity I and the inversion of population D:

$$\frac{dI}{dt} = 2I[AD - 1 - k(t)], \tag{1}$$

$$\frac{dD}{dt} = \gamma[1 - D(1 + I)]. \tag{2}$$

Time t is measured in units of the cavity lifetime. $A = O(1)$ is the pump parameter and $\gamma = O(10^{-3})$ is the ratio of the population inversion relaxation rate to the cavity damping rate. k(t) is the additional loss term containing the modulation and the feedback terms:

$$k(t) = m\cos(\omega t) + \alpha(I(t) - I(t - \tau)). \tag{3}$$

The parameters m and ω are the amplitude and the frequency of the periodic modulations, respectively. α and $\tau = 2\pi\omega^{-1}$ are the amplitude and the delay of the feedback loop, respectively.

Assuming α and m small, we seek an asymptotic solution of Eqs. (1)-(3) of the form

$$I - I_0 \approx (C\exp(i\omega t) + c.c.) + (D\exp(i\omega t/2) + c.c.), \tag{4}$$

where $I_0 = A - 1$, and determine equations for C and D. We analyze these equations and obtain the stability boundaries for the Period 1 and Period 2 solutions. Figure 1 compares the exact numerical (dotted line) and approximate (full line) of the stability boundary for the Period 1 solutions (i.e., the period doubling bifurcation points $m = m_{PD}(\alpha)$; the values of the fixed parameters are $A = 2$, $\gamma = 4.17 \times 10^{-3}$ and $\omega = 2.01 \times (2I_0\gamma)^{1/2}$). Stabilization of a Period 1 orbit at a fixed value of m is realized because the period doubling bifurcation point m_{PD} increases as α increases. However, below a critical negative value of α (vertical line in Figure 1), the laser exhibits a new instability leading to quasiperiodic oscillations.

REFERENCES

1. F.T. Arecchi, R. Meucci, G.P. Puccioni, and J.R. Tredicce, Phys. Rev. Lett. 49, 1217 (1982).
2. D. Dangoisse, P. Glorieux, and D. Hennequin, Phys. Rev. A36, 4775 (1987); C. Lepers, J. Legrand, and P. Glorieux, Phys. Rev. A43, 2573 (1991).
3. I.B. Schwartz, Phys. Lett. A 126, 411-418 (1988); I.B. Schwartz, Phys. Rev. Lett. 60, 1359-1362 (1988).
4. H.G. Solari, E. Eschenazi, R. Gilmore and J.R. Tredicce, Opt. Comm. 64, 453 (1987).
5. T. Erneux, S.M. Baer and P. Mandel, Phys. Rev. A35, 1165-1171 (1987).
6. I.B. Schwartz and T. Erneux, SIAM J. Appl. Math. 54, 1083 (1994)
7. R. Roy, Z. Gills and K.S. Thornburg, Optics and Photonics news, May 1994, 8-15.
8. R. Roy, T. Murphy, Jr., T.D. Maier, Z. Gills, and E.R. Hunt, Phys. Rev. lett. 68, 1259 (1992).
9. S. Bielawski, D. Derozier, and P. Glorieux, Phys. Rev. A47, R2492 (1993), S. Bielawski, M. Bouazaoui, D. Derozier, and P. Glorieux, Phys. Rev. A47, 3276 (1993)
10. S. Bielawski, D. Derozier, and P. Glorieux, Phys. Rev. E49, R971 (1994).
11. C. Reyl, L. Flepp, R. Badii, E. Brun, Phys. Rev. E47, 267 (1993).

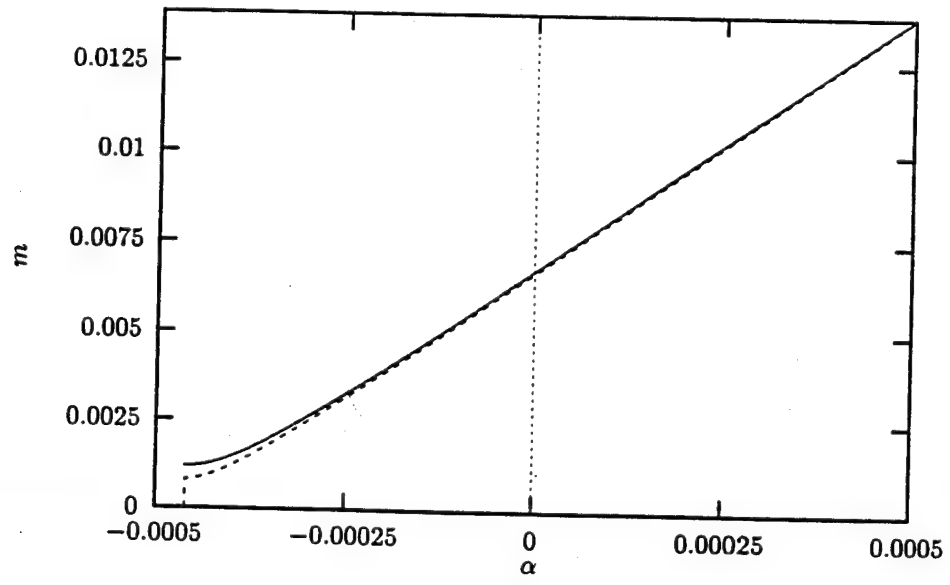

NDOS '95

Time series analysis of an optically turbulent system

F. Mitschke, G. Steinmeyer*, M. Heuer*, A. Schwache*, I. Klopsch*

Institut für Angewandte Physik
Universität Münster
Correnssstr. 2/4
48149 Münster, Germany
Tel. (49) 251 83-3535, Fax -3513

* Institut für Quantenoptik
Universität Hannover
Welfengarten 1
30167 Hannover, Germany

Time series analysis has developed into a powerful tool for the study of low-dimensional chaotic systems. Various algorithms to estimate attractor dimensions, Lyapunov exponents, etc. have been widely discussed. Surrogate techniques are now established which provide a degree of safety against spurious results that can lead to false interpretations. However, these techniques are usually limited to very low-dimensional systems. Turbulence, i.e. a situation when both temporal and spatial degrees of freedom undergo chaotic dynamics, is notoriously difficult to analyze in terms of time series.

We will discuss an optical system that develops in a chaotic fashion temporally. At the same time, there are spatial degrees of freedom which can, and do, lead to the formation of spatial structure, be it stationary, or periodically or nonperiodically evolving.

The experiment consists of a fiber optic ring resonator, where the optical Kerr effect in the fiber provides a nonlinearity. Such a system was first discussed theoretically by Ikeda and predicted to be chaotic /1/. In our experiment /2/, the resonator is synchronously driven by a train of picosecond pulses. We use single mode, polarization-preserving fiber, and either a color center laser or an additive-pulse mode-locked Nd:YAG laser as a light source. There are clean indications that an intricate substructure is generated in the pulses emerging from the resonator. On the other hand, standard photodetectors can only record the total energy per pulse so that much of this structure is washed out in the detector signal. Nevertheless, we work with these data in our time series analysis.

It is most remarkable that in the case of a true single mode fiber, all spatial degrees of freedom are in just one spatial dimension - the direction of propagation of the light. We can therefore speak of a *longitudinal instability* leading to *one-dimensional turbulence*. (It is also conceivable to add transverse degrees of freedom through choice of multimode fiber).

Group velocity dispersion in the fiber plays a role analogous to diffraction in the transverse plane. and thus controls how intricate the self-generated structures in the pulses can get. (The analogy between dispersion and diffraction is stretched a little, however, when one realizes that there can be dispersion of either sign, and also higher order dispersion). In a sense the number of spatial degrees of freedom can be selected through adjustment of dispersion. In the experiment we can choose the second order dispersion between about $-25ps^2/km$ and $-10ps^2/km$. In particular, we can tune around $\beta_2 = 0$ where higher order dispersion (β_3) becomes prominent.

Part of the information about the formation of structure can be extracted successfully from the experiment, in spite of the ultrashort time scales involved. Nevertheless, the full information is only accessible through detailed comparison with a computer simulation. Some interesting aspects about the formation of structurein the pulses, evident from simulations, will be discussed.

We ventured to run time series analysis of long strings of pulse energy measurements, recorded with state-of-the-art digitizing oscilloscopes. It turns out that with the use of certain extensions of the dimension concept the varying degree of complexity obtained through variation of dispersion can be seen quite clearly. In particular, the cases of anomalous and normal dispersion (soliton vs. non-soliton regime) are markedly different. We will present the first results which are already very encouraging for further research.

/1/ K. Ikeda, Opt. Comm. **30**, 257 (1979)
/2/ G. Steinmeyer, D. Jaspert, F. Mitschke, Opt. Comm. **104**, 379 (1994)

Information Encoding in Passive Ring Resonators with Plane Mirrors

M. Brambilla, L. A. Lugiato, M. Stefani
Dipartimento di Fisica dell' Università di Milano, via Celoria 16, 20133 Milano, Italy
Tel. +39-2-2392264, Fax +39-2-2392712, Email: lugiato@milano.infn.it

Summary

The spatial and spatio-temporal phenomena emerging in the transverse structure of the electromagnetic field, due to the coupling between diffraction and the nonlinearity of the medium, have attracted a lot of attention in recent years [1,2]. Modulational instabilities in passive systems with a cavity have been investigated widely and pattern-forming phenomena have been predicted and observed [2].
As it already occurred in the history of nonlinear optics, Kerr media driven by homogeneous external fields have been an ideal exploration land and, in fact, the existence of stationary modulational instabilties were readily discovered theoretically [3]. Further studies [4] proved the existence of a bifurcated branch where the stable emission profile of the field is a stationary hexagonal lattice. With an appropriate choice of the control parameters, this bifurcated branch can be made coexistent with a low transmission, homogeneous stationary emission. Under this operational condition, the system can realize also stable field patterns in which hexagons coexist with the homogeneous solution ; this phenomenon corresponds to what in other fields of physics were called *localized structures*(LS)[5]. The possibility of LS in a bistable optical system has been predicted in [6].
The occurrence of islands where a modulation (e.g. a single intensity peak of the hexagonal lattice embedded into the homogeneous background), is present immediately suggests the possibility of encoding information in the emitted transverse field profile of such a system, by 'writing' or 'erasing' the LS by acting on the profile of the driving field [7].

In this presentation we start considering a ring cavity with plane mirrors with a Kerr medium, as it was modeled in [3], where the governing equations for the emitted field include diffraction via the Laplacian operator and the critical parameters are the detuning θ, its amplitude E_{in} and the cooperativity parameter C. We find that the bifurcated branch extends over a wide range of values for the homogeneous input field E_{in} where a homogenous solution is also stable (corresponding to the lower branch of the plane wave steady state curve).
The process of encoding a high intensity dot is achieved by injecting an inhomogeneous field $E_{in}(x,y)$ having a 'hot spot' in that point of the transverse plane where the dot is to be emitted. The system excites a LS corresponding to one single peak (equal to those in the hexagonal lattice) at that point and sustains this modulated emission even when the 'hot spot' in the injected field is removed

and its profile is brought back to homogeneous . As many dots can be written in the transverse plane as one wishes, provided that they all remain independent. This is accomplished by exciting the dots at a distance larger than a minimum separation d_c which is on the order of the critical wavelength corresponding to the bifurcated lattice; when excited at a smaller distance the two dots will interact and in particular will annihilate when close enough.
This provides the mechanism for erasing a dot at any given location (x, y) in the transverse plane: the injected field is modified so to present a 'hot spot' at (x', y') (where the distance must be smaller than d_c) so that the original dot is annihilated. Then the profile of the driving field can be reset as homogeneous . Preliminary results from simulations on a saturable nonlinear 2-level absorber (the same model used in ref.8) seem to confirm the validity of this scheme: the high intensity peaks can still be excited as independent individuals as far as they are 'written' sufficiently far apart; while trying to excite a dot closer (than a certain critical distance) to an existing one can result in annihilation of both elements.

References

1. N. B. Abraham and W. J. Firth eds., Special issues on *"Transverse Effects in Nonlinear Optical Systems"*, J. Opt. Soc. Am. B**7**, June and July 1990; L.A. Lugiato, in Proceedings of the Solvay Conference on Quantum Optics, ed. by P. Mandel, Physics Reports, in press.
2. L. A. Lugiato ed., special issue on Transverse Effects, Chaos, Solitons and Fractals, **4** , (1994)
3. L. A. Lugiato and R. Lefever, Phys. Rev. Lett. **58**, 2209 (1987)
4. W. J. Firth, G. S. McDonald, A. J. Scroggie and L.A. Lugiato, Phys. Rev. A, **46**, R3609 (1992)
5. S.Fauve and O.Thual, J. Phys. France, **49**, 1829 (1988); S.Fauve and O.Thual, Phys. Rev. Lett., **64**, 282 (1990)
6. M. Tlidi, P. Mandel and R. Lefever, Phys. Rev. Lett. **73**, 640 (1994); M. Tlidi and P. Mandel, Chaos, Solitons and Franctals, **4**, 1475; A. J. Scroggie, G. S. McDonald, W. J. Firth, M. Tlidi, R. Lefever and L.A. Lugiato, Chaos, Solitons and Franctals, **4**, 1323
7. G. S. McDonald and W. J. Firth, J. Opt. Soc. Am. B **7**, 1328 (1990)
8. W. J. Firth and A. J. Scroggie, Europhys. Lett. **26**, 521 (1994)

Nonlinear Propagation In An Optical Fractal Structure.

M. Bertolotti, F. Moretti, C. Sibilia
Dipartimento di Energetica - Universita' di Roma I-
Via Scarpa 16, 00161 Roma Italy

Tel 06- 49916542, Fax 06 44240183, BERTOL88@ITCASPUR.CASPUR.IT

P. Masciulli

Dept. of Chemical Engineering, Processes and Materials, University of Palermo, V.le delle Scienze, 90128 Palermo

Phone: 039-6-49916541,Fax: 039-6-44240183

In this paper we study the input-output characteristic of a fractal nonlinear optical Fabry-Perot resonator. The 1D dielectric integrated resonator is obtained alternating two nondispersive planar dielectric layers of unperturbed refractive index n_2 and n_1 ($n_2 > n_1$) of thickness such that their optical path is the same. The initiator is the layer of refractive index n_2. If L is the optical path of the initiator, the generator is obtained substituting the central part of the initiator having an optical path of $L/3$ with the layer of refractive index n_1 and thickness such that the optical path is $L/3$ again. The resonator is obtained iterating the operation on the left and right third optical path, and stopping the iteration at the N-th step.

We consider the resonator embedded between two equal semi-infinite nondispersive layers of refractive index n less than both n_2 and n_1. The incident light is assumed to be a plane TE wave with normal incidence. The transmission properties of this linear resonator have been just studied [1, 2], by using the transfer matrix formalism . The isolated transmission peaks in a forbidden frequency gap [1, 2] suggest the possibility of obtaining optical switching at low threshold intensity. In the case of a nonlinear device we have therefore studied the same resonator with the layers of refractive index n_2 made by a Kerr-type medium. As a consequence, the transmitted intensity is a nonlinear function of the incident one, at a given e.m. frequency . The calculations of the transmitted intensity versus the incident one are based on a generalization of the dummy method [3]. In order to evaluate the nonlinear behaviour of the resonator, we consider the wave nonlinear phase shift due to the propagation in one nonlinear layer as follows [3]

$$\varphi_{NL_h} = 3k_0\gamma\int_0^{\delta_h}\left(|a_h|^2 + |b_h|^2\right)dz$$

where k_0 is the vacuum wave number, γ is the Kerr coefficient of the nonlinear layers whose refractive indices are given by $n_{NL} = n_m + \gamma|E|^2$ ($m = 1,2$ depending on which of the two basic dielectric layers is the nonlinear one), δ_h, a_h, b_h are the geometrical thickness, the forward and backward waves amplitudes respectively of the *h-th* nonlinear layer. The material's losses are taken into account by considering complex refractive indices. Multistable behaviour has been found, with switch input power depending on which of the two basic layers (of linear refractive index n_1 or n_2) is nonlinear. The considered resonator shows a reduction of the input switch power, if compared with the analogous periodic structure. A comparison with nonlinear interferential filters is also presented .
The simulations show that it is possible to have a multistable behaviour with a relatively low first switch threshold.
The spatial field profile inside the structure is also calculated.

References

[1] M. Bertolotti, P. Masciulli, C. Sibilia, Optics Letters (1994), 19, p. 777.
[2] M. Bertolotti, P. Masciulli, C. Sibilia, Proceedings of Integrated Optics Conference, Lindau (Germany), 11-15 April 1994.
[3]H. M. Gibbs, "Optical Bistability: Controlling Light with Light", Academic Press, 1985, Chapter 2.

On Instabilities and the Influence of Noise in a Nonlinear Resonator

Matthew R. Semak and John K. McIver
Center for Advanced Studies,
Department of Physics and Astronomy,
University of New Mexico
Albuquerque, New Mexico 87131-1156
msemak@aquarius.phys.unm.edu
jmciver@aquarius.phys.unm.edu

Evangelos A. Coutsias
Department of Mathematics and Statistics,
University of New Mexico
Albuquerque, New Mexico 87131
coutsias@bootes.unm.edu

Jan. 27, 1995

ABSTRACT

We study the nature of the instabilities which arise in the Maxwell-Bloch system where an adiabatic approximation is made by which the polarization follows the field. Moreover, a retarded-time integration is performed and the system is placed in the setting of an optical resonator containing a nonlinear

element. With this, one can construct a pair of coupled differential-delay equations for the scaled field and the scaled population inversion. Of the various limits in which the latter can be examined, the dispersive, or Kerr, limit forms the backdrop for this study. Indeed, several limits have been considered. Following the work of Ikeda, as well as others, one can take the limit of fast longitudinal relaxation and weak feedback fraction and derive a real, non-invertible map for the intensity in which time develops discretely in integer steps of the cavity transit time. This mapping can be shown to display an intermittency route to chaos by the same mechanism seen in such cases as the logistic map. This mechanism can be most easily appreciated by considering a particular instance of its occurrence - the period three solution. The period three and all odd periodic cycles come about by an inverse tangent bifurcation. In our work, we allow for a non-negligible feedback fraction in developing the backdrop for creating methods for the study of multiple element systems, where relaxation and delay times may be comparable. With the limit of fast relaxation not enforced, the evolution of the differential delay system is considered in the presence of white noise. The most interesting behavior appears to occur in chaotic regions which are being stochastically perturbed. The characterization of this behavior can be sought in the transitional nature of the correlation dimension. In our computational work, we consider a highly accurate integration scheme that is applied to ensembles of initial conditions to assure minimal contamination from round-off errors. Finally, a description is also discussed in terms of the properties of the probability density function of the motion.

NON LINEAR DYNAMICS, DELAYED BIFURCATION AND SQUEEZING IN A TRIPLY RESONANT OPTICAL PARAMETRIC OSCILLATOR

K. Kasai, K. Petsas, C. Richy, C. Fabre

Laboratoire Kastler-Brossel, associé au CNRS, ENS and Université P. et M. Curie
Tour 12, Case 74, 75252 Paris cedex 05, France
Tel : 33 1 44 27 73 27, Fax : 33 1 44 27 38 45, e-mail : fabre@spectro.jussieu.fr

Triply resonant OPOs (TROs), in which the signal, idler and pump modes are simultaneously resonant in the optical cavity, are of great interest if one wants to obtain very low pump power oscillation thresholds in the c.w. regime, that can be reached for example by semiconductor single mode lasers. Such c.w. OPOs have a high frequency stability and can be used to inject high power pulsed OPOs for spectroscopic applications.

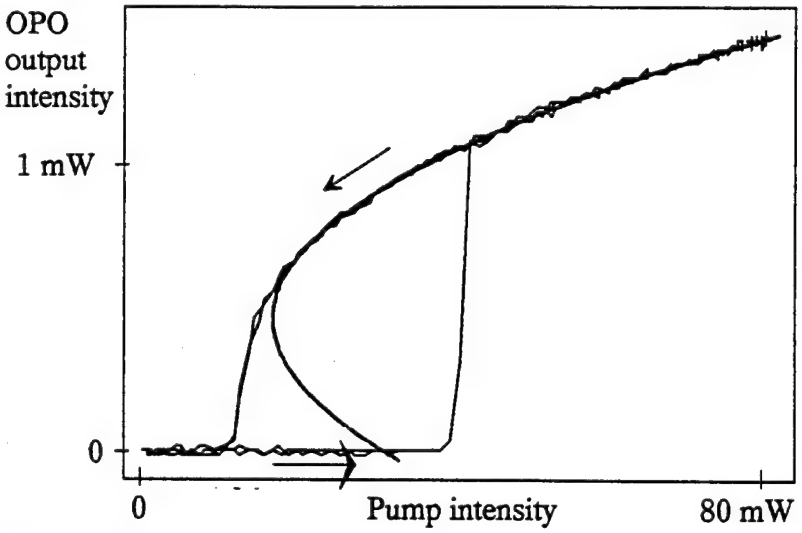

Figure 1

We have built a "semi-monolithic" OPO, made of a 1 cm long KTP crystal with flat ends, that is anti-reflection coated on one side and has a multidielectric coating on the other side (finesse of 45 for the pump beam, and about 10^3 for the signal and idler modes), pumped by a single mode c.w. frequency doubled YAG laser. The *minimum observed oscillation threshold was 0.6 mW*. Figure 1 shows the variation of the OPO signal or idler intensity as a function of pump intensity. One observes[1] a hysteresis loop characteristic of *bistability*, which is in very good agreement with the theoretical curve obtained from[2] (parabolic curve in figure 1). At high pump powers, of the order of 100 mW, we have also observed a *self-pulsing* behaviour of the OPO.

Figure 2

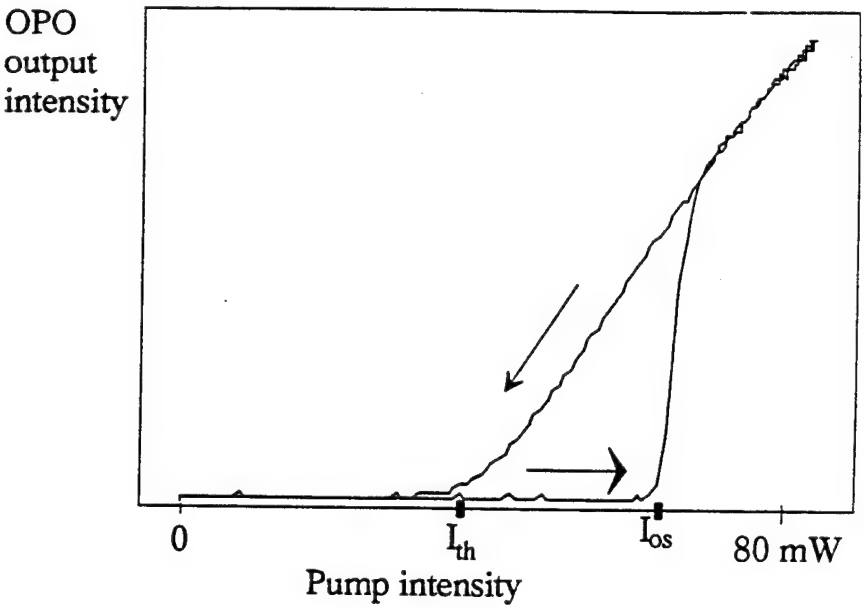

Figure 2 shows the variation of the OPO output power when the pump power is swept linearly with time, in conditions where no bistability occurs in the steady state regime. When the pump intensity increases, the system crosses the oscillation threshold I_{th} but does not start oscillating, until it reaches a value I_{os}, where it switches abruptly to a non zero output intensity. On the contrary, when the pump intensity decreases with time, the OPO output intensity decreases smoothly with time, and the system follows a curve which looks similar to what is obtained in the steady state regime. One thus observes in this regime a *delay to oscillation,* of the order of 4 μs, i.e. very long as compared to the characteristic build-up times t_{cav} of the intracavity intensity, either for the pump mode ($t_{cav} \approx 2\,ns$), or the signal and idler modes ($t_{cav} \approx 60\,ns$). Such "delayed bifurcations" have been first theoretically predicted[3], and have been observed so far in optical systems only in CO_2 and Ar^+ lasers. Using a model derived from [3], we have obtained a very good agreement between experimental and theoretical curves.

In this kind of system, there is an interesting interplay between dynamical behaviour and quantum noise : on the one hand, the quantum noise is responsible for the starting of the OPO. Its characteristics influence the transient behaviour of the system and the onset of delayed bifurcations. On the other hand, the pump field reflected by the TRO can be squeezed, and the regions of significant squeezing are found close to the bifurcations points connecting the different dynamical regimes. We are presently studying the quantum noise properties of this device.

Acknowledgements:

This work has been supported in part by the ESPRIT programme QUINTEC 6934.

References

(1) C. Richy, K.I. Petsas, E. Giacobino, C. Fabre, L. Lugiato, to appear in Phys Rev A (1995)

(2) L. Lugiato, C. Oldano, C. Fabre, E. Giacobino, R. Horowicz, Nuovo Cimento, **10**, 959 (1988)

(3) P. Mandel, T. Erneux, Phys. Rev. Letters **53**, 1818 (1984)

DYNAMIC BEHAVIOURS OF LIGHT TRANSMISSION OF THIN FILM WITH MIRROR

N.A. Loiko, Yu.A. Logvin, A.M. Samson

Institute of Physics of Academy of Sciences of Belarus
70 F.Skaryna Prosp., Minsk 220072, Belarus
Phone: 7(0172)395521, fax: 7(0172)393131
E-mail: ifanbel%bas03.basnet.minsk.by@demos.su

The work is devoted to investigations of an light interaction with a system consisting of a thin film whose length is much less than an input wavelength and a feedback mirror. It is known, the thin film itself displays an optical bistability due to a creation of a necessary nonlinearity by both a superradiance and a Lorentz defined local field effect /1/. The presence of an additional reflecting surface (when, for example, such film is put on a dielectric substrate) provides one more feedback mechanism. It increases the dynamic range of bistability and can lead to selfpulsings of the transmitted field/2,3/. The considerations of this problem, as rule, take into account the superradiance only, suppose the resonance tune of the light field frequency to the centre of absorption line of the film (absorption bistability) and very short times of relaxations processes in comparison with a delay time in the feedback loop. At present work we have studied a role of both the local field and superradiance in the instability appearance. The influence of a detuning of the input field frequency has been analysed. The special attention has been concentrated on the delay effect connected with a finiteness of the time of the light passage from the film to the mirror as well as on the phase displacement arising in the feedback loop.

The analysis of the thin film element has been carried out in the framework of the two-level approximation. The differential difference equations have been formulated on the basis of Bloch equations /1/ taking into account the external delayed feedback. In the parameter space, domains with different orders of instability of the system's steady state have been derived. In the instability domains the structure of arising pulsations

has been investigated. Bifurcations taking place with changing the delay have been retraced. Mechanisms of the pulsation appearance and their chaotization have been elucidated.

As a result, the routes for control of the light transmission of the system have been found out. In particular, we have determined a change in the dynamic range of bistability because of a change in the phase displacement in the feedback loop. We have shown that by an increasing of delay the bistabilty character can be changed: the bistability state can include a stable steady state and stable pulsations instead of two stable steady states. Such increasing can also lead to the change in the transmission behaviour from the bistability to regular or chaotic pulsations.

It has been shown that the structure of pulsations in the main depends on the ratio of longitudinal and transverse relaxation times and on the delay time in the feedback. If the ratio is more bigger than unity, an increase in the delay results in the change of pulsation shape to asymptotically rectangular pulses whose duration closed to the delay. The pulsations develop due to the same reasons that the bistability takes place when there is the phase displacement in the feedback loop. The domains of their existence have only a lower boundary on the delay. At the certain value of input field the pulsations are destabilized. When the longitudinal relaxation time is close to the transverse one approximately harmonic pulsations arise in limited intervals of the delay. Their appearance is connected with the excitement of Rabi oscillations. With increasing the input field the sequence of the pulses periodically invert the population of levels of the film.

The revealed properties of the light transmission of thin film with mirror extends scope for the use of such device for the control of light.

REFERENCES

1. A.N.Oraevsky, D.J.Jones, D.K.Bandy, F.K.Tittel,in Nonlinear Dynamics in Laser and Optical Systems, L.Melnikov, Ed.,Proc. SPIE 2099, 152 (1994).

2. A.M.Basharov. Sov.Phys.JETP, 67,1741(1988)

3. Yu.A.Logvin,A.M.Samson. Sov.J.Quantum Electron.,22,N%8(1992)

The DFB of counterpropagating waves in a periodically modulated medium with relaxing cubic nonlinearity

A.A.Afanas'ev, B.A.Samson and E.G.Tolkacheva

Institute of Physics, Belarus Academy of Sciences,
F.Skoriny ave.,70, Minsk, 220602, Belarus

The interest to the investigation of the features of the radiation propagation in a periodically modulated nonlinear media is stimulated by the prospects of using such media ("nonlinear" gratings) in optical fibre communication lines, to get subshort durations pulses and so on. The different nonlinear effects, such as bistability [1], self-pulsing and chaos [2], formation of the solitons [1,3,4] and so on arise under the radiation propagation in the "nonlinear" gratings. The above mentioned effects are predicted in assumption of the medium instantaneous nonlinear response. So, that appeared characteristic nonstationary phenomena are connected with the radiation propagation prosess, i.e. with the wave nonstationarity.

In this report the radiation propagation in a periodically modulated medium with the relaxing cubic nonlinearity is investigated for the first time. An equations for the counterpropagating waves amplitudes were obtained and their analytical solution under the low distributed feedback (DFB) approximation was shown. It is determined, that the nonstationary energy exchange (NEE) between the power forward wave and the low backward wave can take place because of the phase mismatching of interference picture of electromagnetic field and light-induced grating. We made a numerical modelling of the equations obtained for the arbitrary values of the coupling coefficient k, Bragg detuning Δ and the input pulse parameters. The dynamics of the regular temporal modulation of continuous radiation [5] in dependence of relation of the radiation trip time through the medium to the time of relaxing of the nonlinear medium response (parameter $\mu = L/ct_0$) is investigated.

The equations for the normalized counterpropagating waves amplitudes in the problem under consideration are

$$\pm\frac{\partial\mathcal{E}_\pm}{\partial z}+\frac{1}{c}\frac{\partial\mathcal{E}_\pm}{\partial t}=ik\mathcal{E}_\mp e^{\pm i\Delta z}+\frac{i}{t_0}e^{-t/t_0}\left\{\mathcal{E}_\pm\int\limits_{-\infty}^{t}|\bar{\mathcal{E}}|^2e^{t'/t_0}dt'+\mathcal{E}_\mp\int\limits_{-\infty}^{t}\mathcal{E}_\pm\mathcal{E}_\mp^*e^{t'/t_0}dt'\right\},$$

where $|\bar{\mathcal{E}}|^2=|\mathcal{E}_+|^2+|\mathcal{E}_-|^2$, $\mathcal{E}_\pm=\sqrt{Kn_2}E_\pm, K=\omega/c, n_2>0$, and the boundary conditions are $\mathcal{E}_+(0,\tau)=\mathcal{E}_0(\tau), \mathcal{E}_-(L,\tau)=0$.

In approximation of the low DFB ($kL\ll 1$) if assuming that $(I_0+|\Delta|)L\ll 1$ the next expression for the reflected wave intensities followed from obtained equations

$$I_-(0,\tau)=(kL)^2I_0\left\{1-\frac{L^2}{12}\left[(\Delta-3I_0)^2+f(\tau,I_0)\right]\right\},$$

in which

$$f(\tau,I_0)=3I_0e^{-\tau}\left[2\Delta-I_0(2+e^{-\tau}+4\tau)\right],$$

where $I_0=|\mathcal{E}_0|^2=const$ at $\tau\geq 0$. It is obviously, that in the region $f(\tau)<0$ the sluggishness of the medium nonlinear response leads to the increasing of the low refclected wave which is caused by the NEE between the waves on the light-induced grating phase-mismatched by the radiation [6]. In particular for $\Delta=3I_0$, $f(\tau)<0$ in the region $\tau\geq 0.9$. In this case the low wave maximum amplification is reached at the time moment $\tau_0=2$.

The basic characterictics of the output pulses in dependence of the "nonlinear" grating parameters and gauss-form input pulse $\mathcal{E}_0(\tau)$ are investigated with the help of the numerical modelling of the system of equations obtained. The regularities of the passed pulses temporal modulation are discussed.

We investigated the regime of the radiation temporal modulation in the "nonlinear" grating [5] in dependence of the parameter μ in the case of the $I_0 = const$. The results of the numerical modelling at $\Delta = 0, kL = 2, I_0 = 2$ are shown on the Fig., from which one can see, that the frequency of the appeared pulsations of the passed radiation $I_+(L,\tau)$ increase with the μ increasing. The stabilization of the modulation frequency corresponding to the case of the sluggishless nonlinearity [5] occur at $\mu \geq 30$.

So, the "nonlinear" grating can be used as a continuous radiation modulator with the certain frequency, which depend of the relaxation time of the nonlinear medium response. The transformation of the continuous radiation to the train of the short stable pulses of any duration can has a practical interest for the various devices of the quantum electronics and integral optics.

References

1. H.G.Winful, J.H.Marburger and E.Garmire, *Appl. Phys. Lett., v.35, p.379, 1979*
2. H.G.Winful and G.D.Cooperman, *Appl. Phys. Lett., v.40, p.298, 1982*
3. D.N.Christodoulides and R.I.Joseph *Phys. Rev. Lett., v.35, N15, p.1746, 1989*
4. J.Feng and F.K.Kneubuhl, *IEEE J of QE, v.29, N2, p.590, 1993*
5. H.G.Winful, R.Zamir and S.Feldman, *Appl. Phys. Lett., v.58, p.1001, 1991*
6. P.A.Apanasevich, A.A.Afanas'ev and S.P.Gvavy, *Izvestiya AN USSR, ser.fis., v43, N2, p.350, 1979*

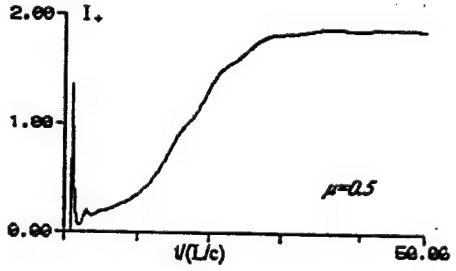

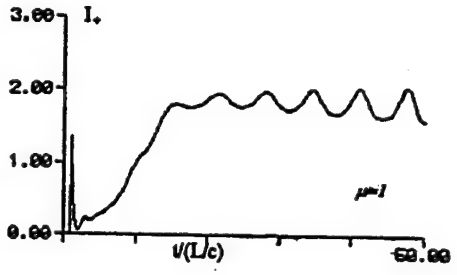

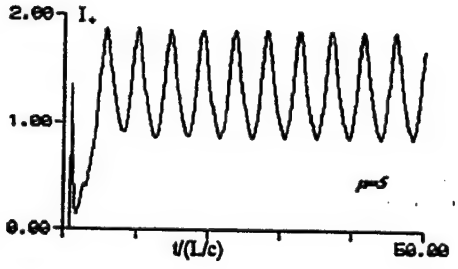

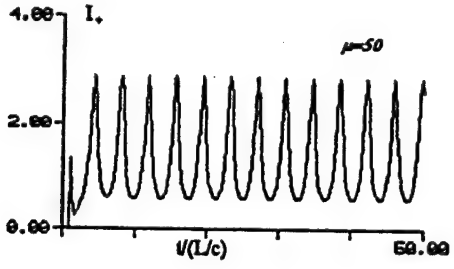

Transverse Dynamics in a Laser with Fast-relaxed Active Medium

Leonid A. Melnikov, Irina V.Veshneva, Andrey I.Konukhov

Department of Optics, Chernyshevsky State University, 83 Astrakhanskaya str., Saratov 410071, Russia
phone: (845-2)51-51-95, e-mail: melnikov@scnit.saratov.su, melnikov@ire.saratov.su

Pattern formation in lasers and associated space-time dynamics in the output of a laser beam are problem of growing interest in recent years. Many of the nontrivial features including phase singularities, and regular pattern dynamics are investigated [1]. However, most of the theoretical models are restricted by the limitations of single longitudinal mode and small field variation on a round-trip in a laser cavity, which are valid for a small gain medium and a cavity with near-flat mirrors (generalized 'mean field limit'). In this paper we present some results of numerical simulations of transverse dynamics in a laser with high round-trip gain and arbitrary cavity configuration including near confocal or concentric cavities in the approximation of fast-relaxed medium with homogeneously broadened gain line. Therefore, the effect of active medium can be described through a nonlinear susceptibility. The comparison of the results of 'mean field limit' theory with these results allows to underline the net effect of transverse field structure on laser dynamics.

The numerical model include the solution of initial problem for the paraxial wave equation in the active medium:

$$2i\partial E(z,\vec{r})/\partial z + \nabla_{\perp}^2 E = (\delta + i)E/(1 + \delta^2 + |E|^2), \tag{1}$$

where δ is the normalized detuning of carrier frequency of the slowly varying electric field envelope $E(z,\vec{r},t)$, z is the axial coordinate, $\vec{r} = (r,\varphi)$ are polar coordinates, g is the unit-length gain. This equation was solved numerically using of the step-splitting method. The modal decomposition in terms of Laguerre-Gaussian modes of empty cavity was used at the diffraction step without of the restriction of axial symmetry. More than 200 modes $TEM_{m,n,q}$ were included into consideration with radial and azimuthal indices $n \leq 10$ and $m \leq 9$, respectively.

To complete the field transformation in empty-space part of a cavity and transformations on intracavity elements the corresponding modal amplitude transformation were included. Thus the multidimensional mapping for transverse scalar field was obtained. It should be noted that the temporal behavior of the field within round-trip temporal interval does not vary from one round-trip to another owing to the lack of second-order dispersion in the equation (1). It may occur in pulse laser with actively or passively compensated pulse spreading or in lasers with small numbers of longitudinal modes. Thus the results will be the same for both small and great numbers of longitudinal modes. Obviously, the mapping dynamics represents the actual dynamics of laser output at the temporal interval from round-trip time to infinity.

The cavity configuration of unidirectional symmetric ring cavity with one spherical mirror and gaussian aperture [2], [3] was used in numerical experiments. Starting with standard set of initial values of modal amplitudes after some thousands round-trips the dynamical regimes were recorded and analyzed. The cavity detuning characteristics was of special interest in the paper.

As previously, we have observed the deformed modes (cooperative frequency locking) with stationary amplitudes, some locking regimes when transverse mode beat frequency coincides with subharmonics of c/L. The diagram of the dynamics regimes in the case of zero detuning in the plane of G (round-trip gain) and F (mirror focal power) is shown in the Fig.1, presenting the region of zero intensity $St0$, threshold curve, region of the stationary regimes with nonzero intensity St, bifurcation curve of power oscillation appearance, and the region of quasiperiodic oscillation of output power QP. The pattern evolution in the narrow locking regions $nT, n = 2, 3, ...$ corresponds to colliding and repulsing maxima, while in the regimes of quasiperiodic oscillation the pattern rotates with angular velocity approximately proportional to the transverse mode spacing. The mean radius of the pattern also oscillate with a doubled period. At moderate values of the gain the pattern dynamics corresponds to the evolution of the linear sum of empty cavity modes (Fig. 2a),

with the modal amplitudes slowly varying within the mode-beating period (Fig. 2b, the dependencies of the intensity of TEM_{00q}, TEM_{10q}, and total power W from round-trip number are shown). The increase of the gain leads to more complicated pattern with arising valleys (Fig. 3a), while the modal amplitudes begin to oscillate (Fig. 3b).

We have observed that the width of locking region increased essentially in the case of nonzero detuning. In the Fig. 4a,b the patterns, corresponding to $\delta = \pm 1$,respectively, at $G = 2.2$ and the same value of$F$ are shown. As the period-2 oscillations of power exist in this regimes, both pictures of consequent round-trip are shown, demonstrating the drastic differences among the pictures corresponding to different values of detuning.

This work was supported by the Commission of the European Communities under ESPRIT Contract P9282-ACTCS, EU-Russia Collaboration, and ISF grant NS4000.

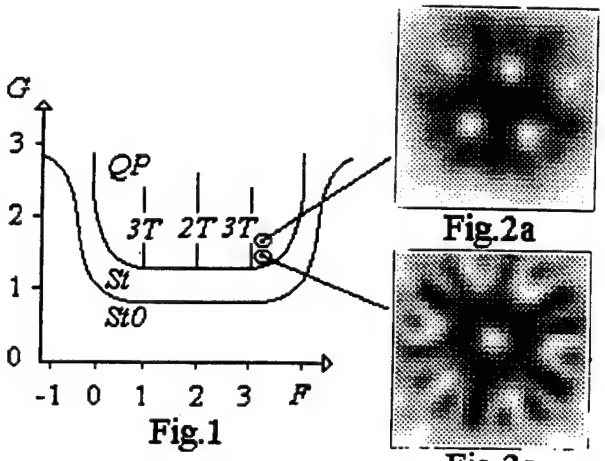

Fig.1

Fig.2a

Fig.3a

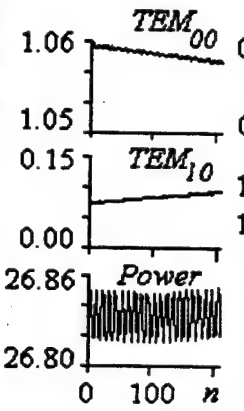

Fig.2b

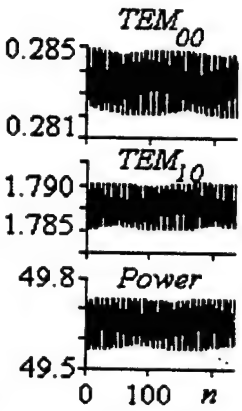

Fig.3b

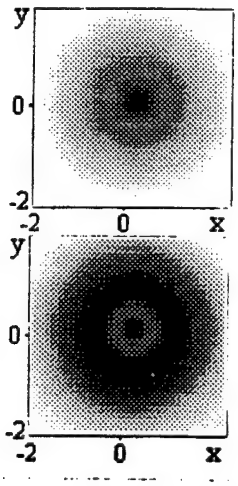

Fig.4a

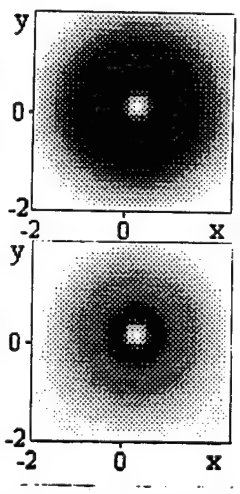

Fig.4b

[1] Brambilla M., Cattaneo M., Lugiato L.A., Pirovano R. et al. *Phys. Rev. A*,**49**, 1427(1994); Coates A.B., Weiss C.O., Green C., D'Angelo E.J. et al. *Phys. Rev. A*,**49**, 1452(1994)

[2] L.A.Melnikov, I.V.Veshneva, A.I.Konukhov. *Chaos, Solitons, and Fractals*, **4**, 1535 (1994)

[3] L.A.Melnikov, S.A.Tatarkova, G.N.Tatarkov *J.Opt.Soc.Amer.*, **B7**, 1286 (1990)

Controlling Chaos May Induce New Attractors in an Optical Device

P.M. Alsing, V. Kovanis and A. Gavrielides
Nonlinear Optics Center, Phillips Laboratory, PL/LIDN, Kirtland AFB, NM 87117-5776

T. Erneux
Université Libre de Bruxelles, Optique Nonlinéaire Théorique, Campus Plaine, C.P. 231, 1050, Bruxelles, Belgium

The logistic map has been used to describe period doubling bifurcations for periodically modulated lasers. It also represents an asymptotic approximation of Ikeda's map for a passive ring cavity. Because various control methods have been used recently to stabilize branches of periodic solutions in lasers, we investigate the logistic map with a standard Ott, Grebogi and Yorke (OGY) control. We explore the structure of this map plus perturbations and find considerable modifications to its bifurcation diagram. In addition to the original fixed points, we find a new fixed point and new period doubling bifurcations. We show that for certain values of small perturbations the new fixed point of the perturbed logistic map is stable, while its original fixed point becomes unstable. Our analysis suggests that new branches of solutions may exist in lasers as a result of the feedback control.

I. INTRODUCTION

Experimental observations of cascading period doubling bifurcations in periodically modulated lasers [1,2] have been compared to the bifurcation properties of simple maps such as the logistic map. Although the logistic map has not been derived from the original laser equations, essential features of the experimental bifurcation diagram has been explained by contrasting experimental and theoretical bifurcation diagrams [2]. This includes predictions of the harmonic cascades, the inverse cascade, and the universal sequence. More recently, period doubling cascades in lasers have been further investigated experimentally by using a variety of control methods [3,4]. The main objective of these experiments is to stabilize branches of unstable periodic solutions so that a complete understanding of the laser dynamics is possible. Because these methods are motivated by local arguments (a shift or the elimination of a bifurcation point responsible for the change of stability of a specific periodic solution), the question has been raised whether the control method may induce new branches of solutions.

In this paper, (see also [5]) we investigate this problem by studying the logistic map with the standard OGY algorithm and explore the bifurcation properties of the resulting perturbed map. The Ott, Grebogi, and Yorke (OGY) [6] control method was developed to stabilize unstable periodic orbits by introducing a feedback on an accessable control parameter. It was later successfully applied experimentally in chaotic lasers [7] and both experimentally and theoretically in a host of other chaotic systems.

The OGY algorithm perturbs a map locally about an unstable fixed point x_F. Considered as a map in its own right, the OGY perturbed map also has x_F as a fixed point. However, new fixed point(s) are created as well. Typically, these newly created fixed points lie outside the local region in which the OGY perturbation is applied. However, in certain cases these new fixed points may lie close to the original fixed point and can even swap stability with it. Although this latter phenomenon can occur more generally in other maps, in this paper we will demonstrate this effect in the case of an OGY peturbed logistic map

$$x_{n+1} = F(x_n, \alpha) = \alpha x_n(1 - x_n). \tag{1}$$

The logistic map is shown in [5] to be a local approximation of the Ikeda map [8]

$$X_{n+1} = a\,[1 - \xi \sin(X_n)] \tag{2}$$

where X_n is proportional to the field intensity in a ring laser cavity containing a nonlinear dispersive medium.

II. THE LOGISTIC MAP AND THE OTT, GREBOGI AND YORKE CONTROL METHOD

The logistic map Eq. (1) is a one dimensional map which becomes chaotic when the the control parameter α exceeds a critical value, $\alpha_c = 3.569946$. It admits two fixed points given by $x_*^{(1)} = 0$ and $x_F \equiv x_*^{(2)} = 1 - \alpha^{-1}$. The slope of the map at the zero solution $x_*^{(1)}$ is given by $\partial F/\partial x_n|_{x_n = x_*^{(1)}} = \alpha$ and, therefore, is stable for $0 < \alpha < 1$ and unstable for $\alpha > 1$. At the nonzero fixed point x_F the map has slope $\partial F/\partial x_n|_{x_n = x_F} = 2 - \alpha$. Thus x_F is a stable fixed point for $|2 - \alpha| < 1$ or $1 < \alpha < 3$ and unstable for $\alpha > 3$.

Ott, Grebogi and Yorke [6] observed that the set of unstable fixed points are dense in a chaotic attractor. By using simple control techniques, they realized that the unstable periodic orbits embedded in the chaotic attractor could be stabilized. The OGY control formula is derived by requiring $\delta x_{n+1} = x_{n+1} - x_F \to 0$ as the result of a specific perturbation $\delta\alpha_n$. For the logistic map Eq. (1) this yields (at x_F)

$$\delta\alpha_n = -\frac{\partial F/\partial x_n}{\partial F/\partial \alpha}\,\delta x_n = \frac{\alpha^2(\alpha - 2)}{\alpha - 1}\,\delta x_n \equiv \beta_0(\alpha)\,\delta x_n \tag{3}$$

Let us now consider the new map F^c consisting of the logistic map with the OGY perturbation

$$F^c(x_n, \alpha, \delta) = [\alpha + \{\beta_0(\alpha) + \delta\}\,\delta x_n]\,x_n(1 - x_n). \tag{4}$$

where $\delta x_n = x_n - x_F$ and we have introduced an additional parameter δ which controls the amplitude of the feedback. The introduction of the second parameter δ is motivated by the laser experiments. In these experiments both the amplitude of the feedback and the main bifurcation parameter can be modified independently.

For $\delta \equiv 0$, the main effect of the OGY perturbations Eq. (3), is to locally alter the map F in the neighborhood of the unstable fixed point x_F, so that the perturbed map F^c has zero slope at x_F. To guarantee control of the unstable fixed point, it is sufficient for the slope of the perturbed map

at x_F to have magnitude less than unity. This ensures that the perturbed map is a contraction mapping in the neighborhood of the fixed point. The OGY algorithm, in which this slope is set equal to zero, represents the prescription for optimal control. For a fixed, maximum allowed value of the perturbation $\delta\alpha_{max}$ the extent of the change in x_n, called the *controlling region* $\delta\tilde{x}$, is found by inverting Eq. (3), $\delta\tilde{x} = |\delta\alpha_{max}/\beta_0|$.

III. NEW FIXED POINTS

The map F^c admits the fixed points $x_*^{(1)} = 0$ and x_F as well as a new one at

$$x_*^{(3)} \equiv 1 - \frac{\alpha}{\beta_0 + \delta}. \tag{5}$$

Note that the fixed point x_F is the same as in the unperturbed map. This is obvious from Eq. (4). However, the slope at x_F is now significantly altered. A simple calculation shows that at x_F $\partial F^c/\partial x_n = \delta\, x_F(1 - x_F) = \delta\,(\alpha - 1)/\alpha^2$. The slope at the other fixed point $x_*^{(3)}$ is given by $\partial F^c/\partial x_n = \alpha(1 - \alpha/\beta_0 + \delta) + (2 - \beta_0 + \delta/\alpha)$. Note that the fixed points $x_*^{(3)}$ and x_F coalesce at $\delta_{cr_1} \equiv 1/x_F(1 - x_F) = \alpha^2/(\alpha - 1)$ where both have slope unity. For $\delta < \delta_{cr_1}$, x_F is stable and $x_*^{(3)}$ is unstable. For $\delta > \delta_{cr_1}$ x_F is unstable and $x_*^{(3)}$ is stable for $\delta_{cr_1} < \delta < \delta_{cr_2}$, where $\delta_{cr_2} \equiv \alpha/2\,(\alpha + 3 + \sqrt{\alpha^2 + 2\alpha + 9})$. This is depicted in Fig. 1(a). For $\delta > \delta_{cr_2}$ a period doubling route to chaos occurs as shown in Fig. 2, for the case $\delta > 0$. The previous discussion remains essentially unaltered for the case of $\delta < 0$. Again there is a period doubling route to chaos for increasing $|\delta|$, only in this case no new period 1 fixed point is created.

The perturbed OGY map F^c, has an additional fixed point $x_*^{(3)}$, even for $\delta = 0$ (see Fig. 1(a)). This fixed point may be observed in the controlling region near x_F provided δ is nonzero. To this end, it is worthwhile to examine the total changes of the map as δ is progressively increased from zero (with α fixed).

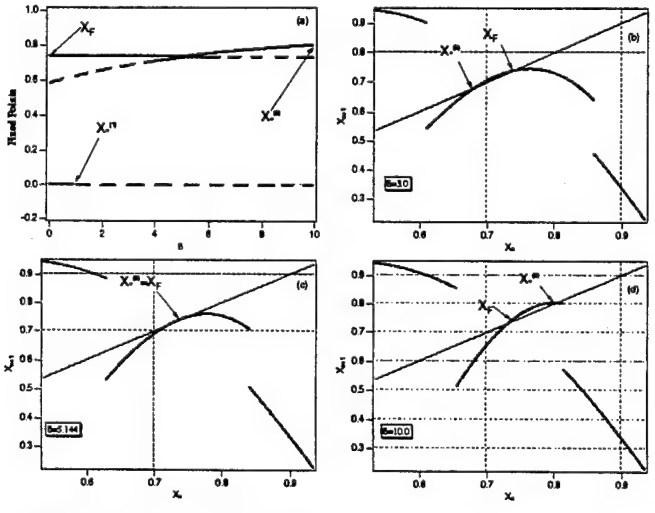

Fig. 1: (a) Stability of fixed points of peturbed logistic map F^c for $\alpha = 3.785$, solid line stable, dashed line unsatble; (b) $\delta = 3.0$, x_F stable, $x_*^{(3)}$ unstable; (c) $\delta = 5.144$, the slope at both x_F and $x_*^{(3)}$ is unity; (d) $\delta = 10.0$, x_F unstable, $x_*^{(3)}$ stable, {(b)-(d): x_{n+1} vs. x_n}.

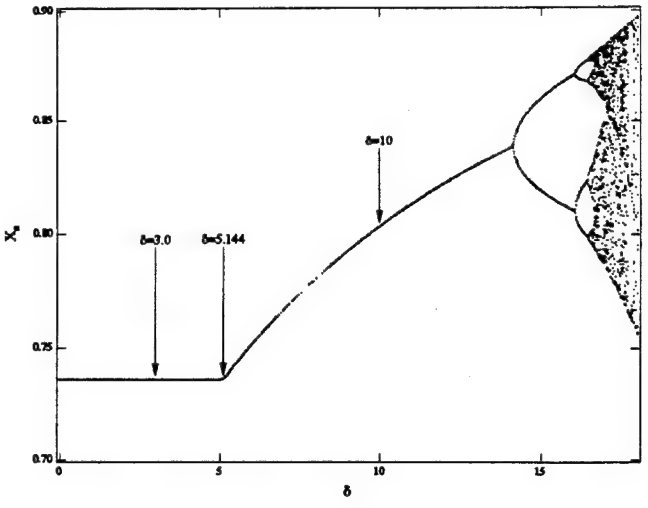

Fig. 2: x_{n+1} vs. δ for the peturbed logistic map F^c, Eq. (4).

Figures 1(b)-(d) show the local change that occurs in the controlling region $|x_n - x_F| \leq \delta\tilde{x}$, where $\delta\tilde{x}$ is now defined by: $\delta\tilde{x} \equiv |\delta\alpha_{max}/(\beta_0 + \delta)|$ Note that the line running across the figures at an angle of 45° represents the bisector $x_{n+1} = x_n$. Its intersection with the return map gives the current fixed points. The figures have been plotted with a value of $\alpha = 3.785$, and $|\delta\alpha_{max}/\alpha| = 0.4$, which is typically much larger than would be implemented in the usual OGY algorithm. In Fig. 1(b) $\delta = 3.0$; the slope at x_F is less than unity. The maxima of F^c in the controlling region no longer coincides with x_F and is shifting to the right for increasing δ. The slope at the new fixed point $x_*^{(3)}$ is greater than unity. However, for increasing δ, the value of $x_*^{(3)}$ increases as its slope decreases. At $\delta = \delta_{cr_1} = 5.144$ the two fixed points coalesce and both have slope unity. For $\delta = 10.0 > \delta_{cr_1}$, x_F has become unstable and while $x_*^{(3)}$ has become stable.

The above figures have been shown with a value of $\delta\alpha/\alpha \lesssim 0.4$. However, even in the limit of very small $\delta\alpha/\alpha$ conforming to the spirit of the OGY algorithm, the new fixed point $x_*^{(3)}$ can be seen. For example, as shown in [5] if we allow for an OGY perturbation of no more than 5%, then for $\delta = 5.85$ we find that the map locks onto the new period 1 stable fixed point $x_*^{(3)} = 0.7482$ instead of the now unstable, original fixed point $x_F = 0.7358$. For values of $\delta > 5.85$ the stable fixed point $x_*^{(3)}$ lies outside the controlling region $\delta\tilde{x}$, while x_F remains inside, yet unstable. The map F^c is unable to lock onto any stable fixed point and remains chaotic.

[1] FT Arecchi, R Meucci, GP Puccioni, and Tredicce, Phy Rev Lett **49** 1217 (1982).

[2] D Dangoisse, P Glorieux, and D Hennequin, Phy Rev A **36** 4775 (1987); C Lepers, J Legrand, P Glorieux, Phy Rev A **43** 2573 (1991).

[3] R Roy, TW Murphy Jr, TD Mailer, Z Gills and ER Hunt, Phy Rev Let **65** 3211 (1991).

[4] C Reyl, L Flepp, R Badii and E Brun, Phy Rev E **47** 267 (1993); S Bielawski, D Derozier, P Glorieux, Phy Rev E **49** R971 (1994).

[5] A Gavrielides, PM Alsing, V Kovanis, and T Erneux, (to appear in) Optics Comm (1995).

[6] E Ott, C Grebogi, and JA Yorke, Phy Rev Let **64** 1196 (1990).

[7] R Roy, Z Gills, and KS Thornburg, Opt Phot News **5** 8 (1994).

[8] K Ikeda, H Daido and O Akimoto, Phy Rev Let **45** 709 (1980).

Modelling spectral gain and refraction index in semiconductor lasers

Salvador Balle
Departament de Física, Universitat de les Illes Balears, E-07071 Palma de Mallorca, Spain
Tel: +34-71-173234, Fax: +34-71-173426, E-mail: dfssbm0@ps.uib.es

When multimode rate equations (RE) are used to model semiconductor laser dynamics, different modal gain coefficients describe the spectral shape of the gain [1], but the spectral shape of the refraction index is neglected. AM/FM coupling due to carrier density variations is simply described by means of a Henry's α factor [2]. In this way, coherent couplings of the fields and Four-Wave Mixing effects are not fully incorporated.

In order to include these effects, two-level models (TLMs) have been sometimes applied to semiconductor lasers [3]. However, TLMs neglect the semiconductor bandstructure and assume a constant energy difference between electronic states which leads to severe failures of TLMs when applied to semiconductor lasers [4].

Microscopic models for calculating the gain and refraction index spectra from the electronic bandstructure of the semiconductor have been developed [5,6], showing that, due to the electronic structure of the semiconductor, the gain peak does not occur at zero dispersion. However, these models are much more complicated than TLM and RE, and they are computationally expensive and strictly applicable only to CW operation or small-signal analysis.

This has stimulated the search for models which incorporate the main results of microscopic theories in a phenomenological way, while preserving the simplicity of the RE/TLM descriptions [7]. Here I present a simple modification of the TLM that allows to reproduce the qualitative trends of the complex susceptibility of a semiconductor laser in the spectral regions of net gain [8], namely 1) Asymmetric spectral shapes of the gain and refraction index, 2) Reasonable dependence of these spectral shapes on the carrier number, 3) Maximum gain not coinciding with zero dispersion, and 4) Reasonable α values for small detunings.

The model is based on the TLM optical Bloch equations in the rotating-wave and slowly-varying amplitude approximations [9], where the evolution equation for the slowly varying amplitude of the material polarization is modified to

$$\partial_t P = \left[-\frac{1}{T_2(N)} + i(\omega_0 - \omega_g(N))\right] P - i\frac{|\mu|^2}{\hbar}(N - N_t + i\alpha_0 N_t)E \,. \qquad (1)$$

where E is the slowly varying amplitude of the optical field, ω_0 is the carrier angular frequency, N is the carrier density and N_t is its value at transparency for $\omega_0 = \omega_g$. The particular form chosen for the α_0 term can be justified as an heuristic extension of the exact results obtained for a two-band semiconductor system at zero temperature from microscopic theory. In general, both the polarization decay rate T_2 and its natural frequency ω_g may depend on both N and on Joule heating related to the value of J [6,10]. To simplify the following analysis, I assume $1/T_2 = 1/T_2^0 + r(N - N_t)$ and $\omega_g = \omega_g^0 + s(N - N_t)$, and I define the normalized detuning $\theta_0 = (\omega_0 + \omega - \omega_g^0)T_2^0$. The steady-state complex susceptibility is then given by

$$\chi(\omega) = \chi' + i\chi'' = -i\frac{|\mu|^2 T_2}{\epsilon_0 \hbar}\frac{N - N_t + i\alpha_0 N_t}{1 - i\theta} \,. \qquad (2)$$

The corresponding gain spectrum $g(\omega)$ (Fig. 1) is not lorentzian. The frequency where we have maximum gain does not correspond to zero dispersion, and it increases for increasing carrier density [11]. The asymmetry of $g(\omega)$ depends only on the value of α_0; the N-dependence of both T_2 and ω_g affects both the frequency of the gain peak and the gain bandwidth but does not affect the spectral shape of the gain.

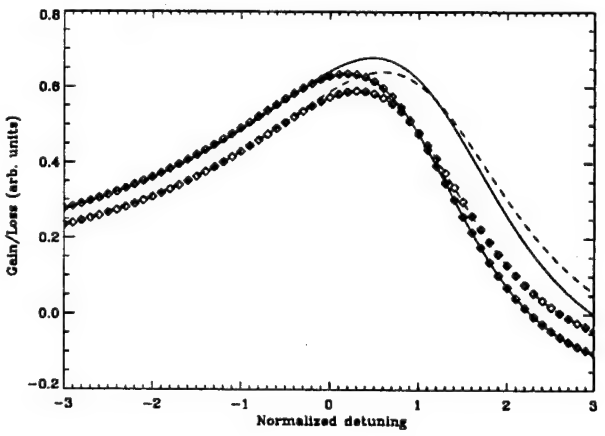

FIG. 1. Gain spectrum obtained for $rT_2^0 N_t = 0.75$ and $sT_2^0 N_t = -1.2$ for $\alpha_0 = 0.9$ (solid line) and $\alpha_0 = 0.7$ (dashed line). Lines with no symbols correspond to $N = 1.99N_t$ and lines with symbols to $N = 1.79N_t$.

The effective α parameter, $\alpha = (\partial\chi'/\partial N)/(\partial\chi''/\partial N)$, depends on both the frequency and carrier-density, as shown in Fig. 2. It must be noted that, in order to match the measured values of α, the N-dependence of both ω_g and T_2 is crucial, otherwise α essentially corresponds to detuning and hence it is too small around the gain peak.

The Amplified Spontaneous Emission spectrum for a multi-longitudinal-mode Fabry-Perot laser operating in a single transverse and lateral mode has been calculated for different levels of current injection (Fig. 3), showing the experimentally observed asymmetric shape of the gain curve with the longitudinal modal resonances superimposed on it [11,12].

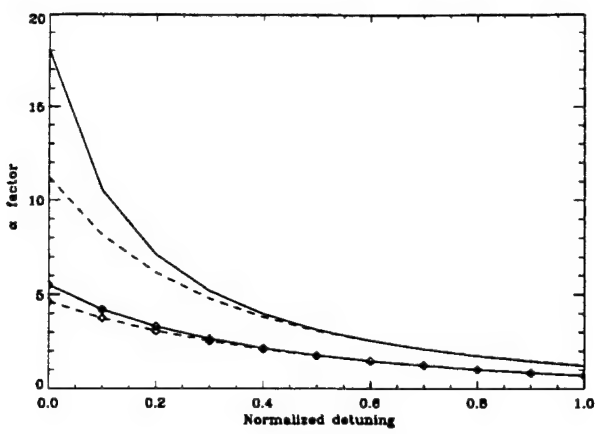

FIG. 2. α in the region of maximum gain in Fig. 1

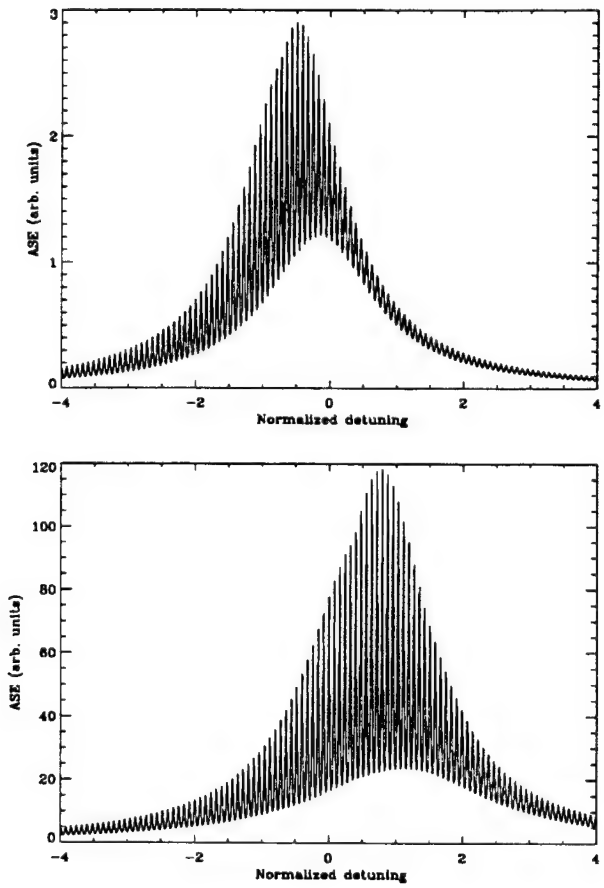

FIG. 3. Amplified Spontaneous Emission spectrum for the parameters in Fig. 1. The upper pannel corresponds to $N = N_t$, while the lower pannel corresponds to $N = 1.99N_t$. These results closely resemble the experimental measurements in [11].

In summary, I have presented here a simple extension of the TLM which preserves its simplicity while incorporating the fundamental results of microscopic theories. The model allows to adjust experimental results for a variety of materials and situations for operation of the laser below threshold.

Acknowledgements I acknowledge financial support from Comisión Interministerial de Ciencia y Tecnolog/'/i a, project TIC93-0744. I also acknowledge Profs. M. San Miguel and N. B. Abraham for many useful suggestions and comments.

[1] C. L. Tang, H. Statz and G. deMars, J. Appl. Phys. **34**, 2289 (1963).

[2] C. H. Henry, IEEE J. Quantum Electron. **QE-18**, 259 (1982).

[3] P. Mandel, C. Etrich and K. Otsuka, IEEE J. Quantum Electron. **29**, 836 (1993).

[4] R. Raghuraman, N. Yu, R. Engelmann, H. Lee and C. L. Shieh, IEEE J. Quantum Electron. **29**, 69 (1993); M. Hofmann, M. Koch, H.-J. Heinrich, G. Weiser, J. Feldmann, W. Elsässer, E. O. Gobel, W. W. Chow and S. W. Koch, IEE Proc.-Optoelectron. **141**, 127 (1994).

[5] F. Stern, J. Appl. Phys. **47**, 5382 (1976); D. S. Citrin and Y.-C. Chang, IEEE J. Quantum Electron. **29**, 97 (1993); T. Yamanaka, Y. Yoshikuni, K. Yokoyama, W. Lui and S. Seki, IEEE J. Quantum Electron. **29**, 1609 (1993).

[6] H. Haug and S. W. Koch, Phys. Rev. A **39**, 1887 (1989)

[7] G. P. Agrawal, J. Appl. Phys. **63**, 1232 (1988); M. Lindberg and S. W. Koch, Phys. Rev. B **38**, 3342 (1988); C. M. Bowden and G. P. Agrawal, Optics Commun. **100**, 147 (1993); J. Yao, G. P. Agrawal, P. Gallion and C. M. Bowden, preprint.

[8] A. Yariv, *Quantum Electronics*, (Wiley, New York, 1989) sect. 21.6, p. 592.

[9] See Ref. [13], ch. 8, p. 155.

[10] J. Manning, R. Olshansky and C. B. Su, IEEE J. Quantum Electron. **19**, 1365 (1983).

[11] V. Kozlov, A. Salokatve, A. V. Nurmikko, D. C. Grillo, L. He, J. Han, Y. Fan, M. Ringle and R. L. Gunshor, Appl. Phys. Lett. **65**, 1863 (1994).

[12] S. L. Chuang, J. O'Gorman and A. F. J. Levi, IEEE J. Quantum Electron. **29**, 1631 (1993).

Interaction of Soliton -Like Propagation in a Diffusive Nonlinear Planar Waveguide

M.Bertolotti, S.Marchetti, C.Sibilia

Dipartimento di Energetica, Università di Roma,
Via A.Scarpa 14,00161 Roma, Italy -
Phone 39 6 49916542, FAX 39 6 49766541

The aim of this work is to study the existence of interaction properties of a localised field propagating in a nonlinear planar waveguide under the assumption that confinement is provided in the transverse dimension by a linear refraction index difference and that in the orthogonal dimension the nonlinear interaction, known as self-focusing is of use, when the nonlinearity is of thermal origin and therefore it is a diffusive and non local nonlinearity.

Under slowly varying envelope approximation (SVEA) , the equation describing the propagation in a Kerr -type nonlinear waveguide , under stationary conditions is

$$2i\left(\frac{\partial F}{\partial z}\right) = -\left(\frac{\partial^2}{\partial x^2} + \frac{\partial^2}{\partial y^2}\right)F - LF - N|F|^2 F = 0 \qquad (1)$$

where

$$L = \left(\frac{k_o n}{\beta}\right)^2 - 1,$$

$$N = \frac{1}{2}\left(\frac{k_o}{\beta}\right)^2 n_f c\varepsilon_0 n_{nl} \ ,$$

and β is the mode wavevector, k_0 is the vacuum propagation constant , n_{nl} is the nonlinear part of the refractive index , and a suitable change of variable has been performed : Z=ßz, X=ßx , Y=ßy. If a thermal diffusive nonlinearity is studied , the last

term of eq. (1) is replaced by one containing information about a temperature field obtained by solving a coupled problem with the heat conduction equation. To realise a strong confinement of the field in the waveguide , so that to reduce the study of the field propagation along the Z direction , whit a control of the diffraction along the X dimension , suitable boundaries conditions must be introduced on the evaluation of the temperature field, so for example the presence of a dissipation in the Y-X plane . Under this hypothesis . Eq. (1) for the e.m. field propagation is reduces to a NSE - like form ,

$$i\frac{\partial Q}{\partial Z} = -\frac{1}{2}\frac{\partial^2 Q}{\partial X^2} - \tilde{k}|Q|^2 Q \qquad (2)$$

where $\tilde{k}$ is proportional to the nonlinear thermal behaviour of refractive index, depending on the thermal characteristics of the medium, and on the contrary of the local electronic case , now is a function of the spatial variables .

To study the propagation we have solved numerically the coupled e.m. and thermal problem, by using the FDBPM method.

For a low absorbing material and for a propagation length shorter that $1/\alpha$ (α is the absorption coefficient) , we have found the existence of spatial soliton -like propagation: stabe propagation with a control of the diffraction for a propagation length of the order of $1/\alpha$.

We have studied the interaction properties of two close localised excitations of input space profile as sech, finding attractive properties of soliton like of equal phase , and repulsive behaviour when the phase is π , in a very similar way as spatial solitons in a local nonlinear waveguides.

A value of the level of power and thermal nonlinearities to reach this kind of interaction is also presented and discussed.

References

-R.Horak, M.Bertolotti and C.Sibilia, in press on J.of Mod.Optics

-R.Horak, M.Bertolotti and C.Sibilia, to be published .

-M.Bertolotti, S.Marchetti, C. Sibilia , to be published.

Pattern Formation in bacteriorhodopsin film with mixed absorptive-dispersive nonlinearity

Mark Saffman and Jesper Glückstad

Department of Optics and Fluid Dynamics,
Risø National Laboratory, DK-4000 Roskilde, Denmark

tel: +45 46 77 45 03
fax: +45 46 75 40 64
e-mail: saffman@risoe.dk

We report on the formation of transverse patterns in thin films of the nonlinear material bacteriorhodopsin [1]. The geometry of a thin nonlinear film with feedback mirror [2-7] was used as shown in Fig. 1. Bacteriorhodopsin has attracted considerable interest in recent years as a nonlinear optical medium [8], and is characterized by a combined absorptive-dispersive nonlinearity [9], in addition to relatively high values of the background linear absorption. The dispersive part of the nonlinearity stems both from photochromic effects, and, at high intensities, a thermal nonlinearity.

Previous theoretical work on pattern formation in thin films has centered on Kerr type media where the nonlinearity is purely dispersive. Bacteriorhodopsin, on the other hand, is characterized by a mixed absorptive-dispersive nonlinearity. We have modeled the nonlinearity as a sluggish saturable Kerr medium with complex index of refraction

$$n = n_0' + in_0'' + \left(n_2' + in_2''\right)\frac{I}{1+I/I_s},$$

where I_s is the saturation intensity. The presence of absorption results in two effects. The loss due to linear absorption increases the threshold intensity for pattern formation. What is more significant is that a linear stability analysis shows that the nonlinear absorption, as described by the imaginary part of the complex n_2, results in frequency detuning of the patterns but does not otherwise affect the threshold intensity. This result differs from that found in the original analysis of this geometry [2], where a purely dispersive material response was assumed. In that case the threshold is a minimum for static instabilities. The detuning predicted here is analogous to that found in photorefractive media where a

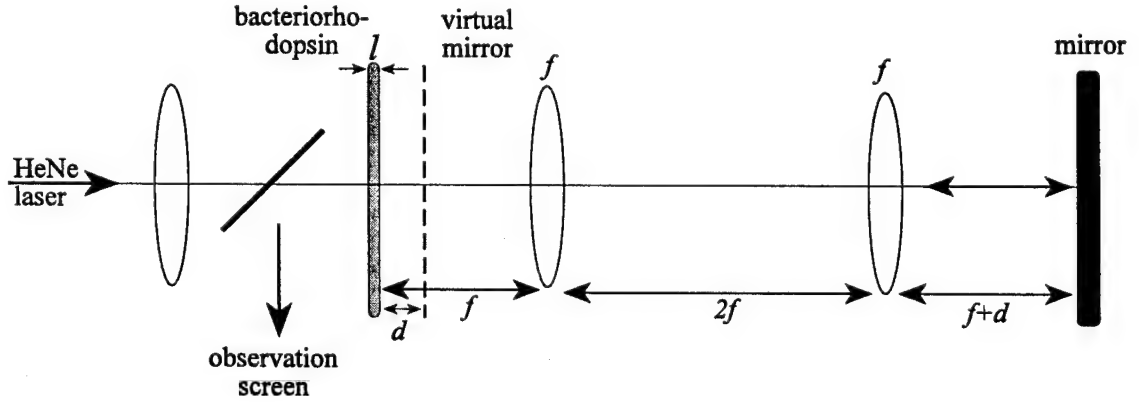

Fig. 1. Experimental geometry.

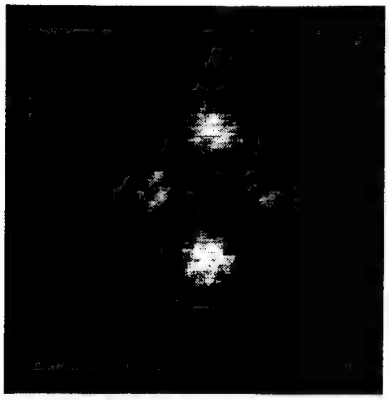

Fig. 2. A typical transverse structure, observed with $d=3$ mm.

sluggish complex nonlinearity also results in frequency detuning of the spatial sidebands[10,11].

The experimental setup is shown in Fig. 1. A 15 mW beam from a HeNe laser with wavelength 633 nm is focused to a spot with Gaussian beam radius $w \cong 26\mu$m giving a peak intensity of $1400\ W/cm^2$. The bacteriorhodopsin in gelatin film had a thickness of $l \cong 40\mu$m and a refractive index of about 1.5. The film was prepared to have a pH of about 9, resulting in a high saturation intensity of about $900\ W/cm^2$. A virtual mirror [12] based on a $4f$ lens system with real mirror allows small mirror spacings d to be investigated conveniently. A typical transverse structure is shown in Fig. 2.

The measured values of the intensity needed for pattern formation were found to agree, within a factor of two, with the predictions of the linear stability analysis.

This work was supported by a grant from the Danish Natural Science Research Council.

References

1. J. Glückstad and M. Saffman, to appear Opt. Lett., 1995.

2. W.J. Firth, J. Mod. Opt. **37**, 151 (1990).

3. G. D.'Alessandro and W.J. Firth, Phys. Rev. Lett. **66**, 2597 (1991); Phys. Rev. A **46**, 537 (1991).

4. G. Giusfredi, J.F. Valley, R. Pon, G. Khitrova, and H.M. Gibbs, J. Opt. Soc. Am B **5**, 1181 (1988).

5. R. Macdonald and H.J. Eichler, Opt. Commun. **89**, 289 (1992).

6. M. Tamburrini, M. Bonavita, S. Wabnitz, and E. Santamato Opt. Lett. **18**, 855 (1993).

7. G. Grynberg, A. Maître, and A. Petrossian, Phys. Rev. Lett. **72**, 2379 (1994).

8. V. Yu. Bazhenov, M.S. Soskin, V.B. Taranenko, and M.V. Vasnetsov, in *Optical Processing and Computing* (Academic, Boston, 1989), Ch. 4.

9. D. Zeisel and N. Hampp, J. Phys. Chem. **96**, 7788 (1992).

10. M. Saffman, D. Montgomery, A.A. Zozulya, K.Kuroda, and D.Z. Anderson, Phys. Rev. A **48**, 3209 (1993).

11. M. Saffman, A.A. Zozulya, and D.Z. Anderson, J. Opt. Soc. Am B **11**, 1409 (1994).

12. E. Ciaramella, M. Tamburrini, and E. Santamato, Phys. Rev. A **50**, R10 (1994).

The Control of the Guiding Center Soliton by the Sliding Frequency Filter

S. Burtsev*
burtsevs@sun.mcs.clarkson.edu, tel.:(315)268-6595
D.J. Kaup
kaup@sun.mcs.clarkson.edu, tel.(315)268-2360, Fax(315)268-6670
Institute for Nonlinear Studies and Department of Mathematics
Clarkson University, Potsdam, NY 13699-5815, USA
*On leave from Russian Branch of International Institute for Nonlinear Studies, Moscow, Russia

The installment of filters [1] helps to suppress the Gordon-Haus effect [2] of timing jitter of solitons in fibers caused by amplifier noise. The filters not only suppress the noise, but also cause the exponential growth of a linear waves. In order to overcome this problem, Mollenauer et al., [3] proposed the use of sliding frequency filters, whose peak frequency slowly changes linearly along the transmission line, as an alternative to ordinary filters. This idea was confirmed experimentally in [4]. Kodama and Wabnitz [5] applied conservation laws of the nonlinear Schroödinger equation and used computer simulation to analyze the performance of the sliding frequency filter.

In this paper, we apply the singular perturbation method to the "averaged" equation[3, 7]:

$$iq_z + q_{TT} + 2q^2q^* = i\epsilon[\delta q + \beta_2(\partial_T + i\epsilon\beta_0 Z)^2 q] \tag{1}$$

to analyze the effect of the sliding frequency filter on the guiding center soliton. The results we obtain may help to optimize the performance of the filter. In Eq.(1) $\beta_2 > 0$ is a parameter representing filter strength, δ is an excess gain and β_0 parameterizes the sliding of the peak frequency ω_0 of filters installed after each amplifier, so that the peak frequency is a linear function of distance Z: $\omega = \omega_0 + \epsilon\beta_0 Z$ along the fiber. According to [6] one may expand unknown solutions of the perturbed NLS (1) in the series about a single soliton:

$$q = q_0 + \epsilon q_1 + ..., \quad q_0 = \frac{2\eta \exp[i(-2\xi(T-\overline{T}) + \overline{\alpha})]}{\cosh[2\eta(T-\overline{T})]} \tag{2}$$

Here $2\eta, 1/\eta, \overline{T}$ and $\overline{\alpha}$ are the soliton's amplitude, width, position and phase, respectively. In the absence of perturbation

$$\overline{T}_z = -4\xi, \quad \overline{\alpha}_z = 4(\eta^2 + \xi^2) \tag{3}$$

Omitting calculations, let us present the main results. Under the sliding frequency filter the soliton parameters evolve according to the following system:

$$\eta_{z_1} = 2\delta\eta - 8\beta_2\eta(\xi'^2 + \eta^2/3), \quad \xi'_{z_1} = -\beta_0/2 - (16/3)\,\beta_2\eta^2\xi', \quad Z_1 = \epsilon Z \tag{4}$$

provided the modulus of the sliding parameter β_0 is under the critical value of $\beta_{0_{cr}} = \frac{8}{3\sqrt{3}}\delta\sqrt{\delta/\beta_2}$. To make (4) more compact we factored out the sliding frequency from ξ by introducing a new notation: $\xi' = \xi - \epsilon\beta_0 Z/2$. The sliding filter does not affect the equations for the soliton's position $\overline{T}$ and phase $\overline{\alpha}$(up to the ϵ^2), but does change the equations for the soliton's amplitude η and frequency ξ considerably. According to (4), the soliton's frequency ξ would *follow* the sliding frequency. The fixed points of the system (4) are fixed by a cubic equation with respect to the η^2. This cubic equation has only two positive roots [5]: $(\eta_a, \xi_a), (\eta_b, \xi_b)$ where $\eta_a > \eta_b$. Only the first point is a stable one. If the sliding parameter has an overcritical value, then the soliton frequency ξ is no

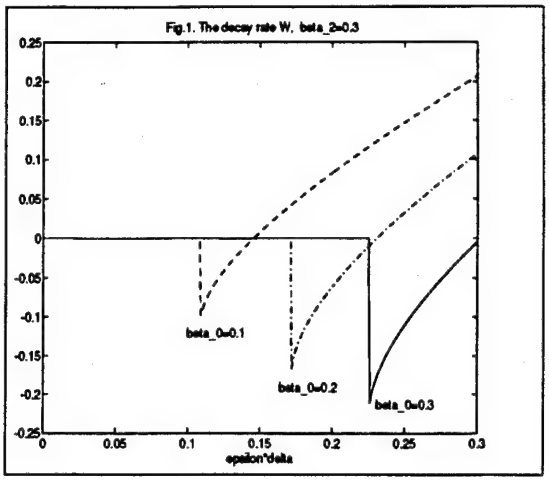

longer able to follow the sliding frequency. Equation for the radiation part is very complicated. But, in fact, we really only need to understand the dynamics in the limit $Z \to \infty$. The zero-mode: $k = 0$ is, potentially the fastest growing mode. Moreover, this mode defines the change of area $A = \int_{\infty}^{\infty} d\theta q_1$ with distance. So, we need to derive its asymptotics. Straightforward calculations gives the following estimate of the modulus of the linear mode:

$$A \sim \exp[WZ], \quad W = \epsilon(\delta - \frac{\pi|\beta_0|}{4\eta_a} - 4\beta_2\xi_a^2) \tag{5}$$

Let us fix the filter's strength $\epsilon\beta_2 = 0.3$ and plot Fig.1 which represents 3 characteristic slices of $W = W(\epsilon\delta, \epsilon\beta_0)$ for $\beta_0 = 0.1, 0.2, 0.3$. ¿From Fig.1 it follows there is a critical range of parameters, only inside of which the sliding frequency filter would operate. First, one must use a sufficiently large extra gain, δ, because otherwise one would be in the overcritical regime (the horizontal line in Fig.1 contains this overcritical regime). Just above this critical value of δ_{cr}, the curve dips down and one has the maximum suppression of radiation. Then, as δ is increased more, the value of W increases also and at certain value of δ, parameter W becomes positive. Now, instead of suppression one has growth of the linear mode. It's obvious that, although, one should like to work close to the critical value of δ_{cr} in order to provide the maximum suppression of radiation, nevertheless one must be careful so that fluctuations would not slip one into the overcritical regime.

References

[1] Mecozzi, A., Moores, J.P., Haus, H.A., and Lai Y, Opt. Lett., **16**, 1841 (1991).

[2] Gordon, J.P., Haus, H.A., Opt. Lett., **11**, 665 (1986).

[3] Mollenauer, L.F., Gordon, J.P., and Egvangelides, S.G., Opt. Lett **17**, 1575 (1992).

[4] Mollenauer, L.F., Lichtman, E., Neubelt, M.N., Harvey, G.T., Lett. **29**, 910 (1993).

[5] Kodama, Y., Wabnitz, S., Opt Lett.,**18**, 1311 (1993)

[6] Kaup, D.J. , Phy. Rev. A. **42**, 5689 (1990).

[7] A. Hasegawa and Y. Kodama, Opt. Lett. **15**, 443 (1990).

Semiconductor laser exposed to optical feedback from an external cavity containing an atomic absorber

E. Cerboneschi, D. Hennequin*, L.Guidoni, F.di Teodoro, and E. Arimondo**

Dipartimento di Fisica, Università di Pisa, Piazza Torricelli 2, 56100 Pisa, Italy

**Permanent address: Laboratoire de Spectroscopie Hertzienne, Unité associée au CNRS, Université des Sciences et Technologies de Lille, 59655 Villeneuve d'Ascq Cedex, France.*

***Present address: JILA, University of Colorado at Boulder, Boulder, CO 80309-0440, USA.*

In recent years, semiconductor laser systems including an absorber medium have been extensively investigated, mainly with the purpose of improving the spectral performance of the lasers. The incorporation of an absorber in the laser cavity provides a dispersive loss mechanism, which can be used to produce frequency dependent changes in the laser gain and refractive index, such as to correct for the amplitude and phase fluctuations of the laser field. In this way, quenching of the spectral linewidth and improvement of the frequency stability of the laser are achieved if, as dispersive loss mechanisms, the saturated absorption [1] or the Faraday rotation [2] in atomic vapours are used. Semiconductor laser systems with intracavity absorber attract also interest from the point of view of the fundamental research on nonlinear dynamics and chaos. Up to now, investigations have been conducted on lasers with saturable absorber (LSA) introduced in the semiconductor cavity itself, either by doping or by controlled optical damage of the active layer. Passive Q-switching and transitions to chaos have been observed [3], like in the more widely investigated LSA with CO_2 laser [4].

We have performed experimental observations of the dynamics and the spectral behaviour of a semiconductor laser coupled to an external cavity containing a cell of Cs vapour. Our laser system consists, unlike the LSA, which is an unique resonator containing both gain medium and absorber, in a compound resonator composed by two coupled cavities: the one formed by the cleaved facets of the semiconductor laser, and the exernal cavity, constituted by the output facet of the laser and a grating placed 68 cm away. We have used a laser Spectra Diode SDL-5400, with 100 mW maximum power, tuned, by means of the rotation and the fine translation of the feedback grating, to the D_2 absorption line of the Cs atoms. In Fig. 1 we show three Fabry-Perot spectra and the respective fluorescence profiles, recorded at different laser frequencies. The frequency has been varied within the Doppler-broadened D_2 line of the Cs atoms. The fluorescence profiles represent the fluorescence intensity emitted by the atoms inside the cell as a function of the position, along a direction orthogonal to the laser axis. Contemporarily with the laser spectra and the atomic fluorescence, the temporal dynamics of the intensity of the laser output has been monitored. Fabry-Perot spectra corresponding, in (a), to self-locking, in (c), to the competition between two modes and, in (e), to the excitation of many resonance modes of the external cavity (separated by 220 MHz) are shown. While the self-locked situation corresponds to a stable laser emission with low noise level, the spectra shown in (c) and (e) are respectively accompanied by bistability and by the low-frequency fluctuation instability, typical of

semiconductor laser under certain conditions of optical feedback [5]. The fluorescence profiles corresponding to the three situations are markedly different from each other, displaying maximum intensity either at the center (in (d) and (f)) or at each side of the laser beam (in (b)). The self-locked situation is obtained through the above-mentioned spectral stabilization mechanism due to the dispersive losses produced by saturated absorption.

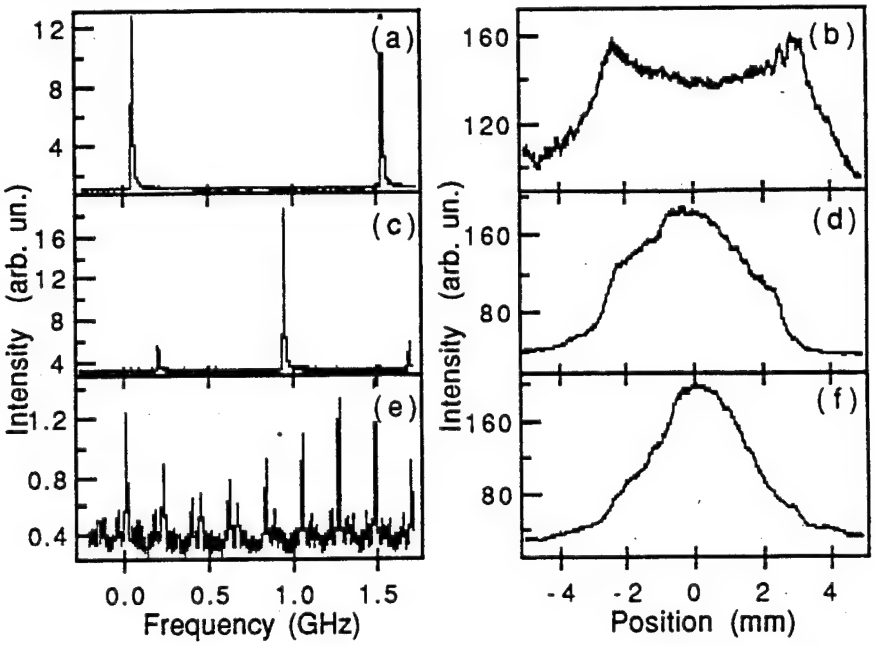

Fig. 1: In (a), (c) and (e), Fabry-Perot spectra of the field emitted by a semiconductor laser exposed to feedback from an external cavity with an absorber of Cs vapour. The three spectra have been recorded at different values of the laser frequency within the D2 absorption line of the Cs atoms. The FSR of the spectrum analyzer is 1.5 GHz. In (b), (d) and (f), the corresponding intensity profiles of the fluorescence emitted by the Cs vapour, versus a space coordinate transverse with respect to the laser axis. The origin of the space coordinate coincides with the center of the laser beam.

Different shapes of the fluorescence profiles can be due to optical pumping mechanisms. In order to gain an insight into the physical origin of such profiles we plan to perform precise measurements of the laser frequency with the aim of identifying which of the hyperfine structure transitions are involved in the radiation-atom interaction. The connection of the fluorescence profile with the spectral features of the laser output could turn out suitable to implement intacavity spectroscopy. Deeper investigations are also required to undestand the mechanisms underlying the dynamical features associated with the excitation of either two or many laser modes, and to identify the modifications that the presence of the absorber in the external cavity introduces in the nonlinear dynamics of the semiconductor laser with external feedback.

[1] C. J. Cuneo, J. J. Maki, and D. H. McIntyre, Proceedings of *Symposium on Nonlinear Optics I*, 1714 (1993).

[2] Y. Shevy, J. Iannelli, J. Kitching, and A. Yariv, Opt. Lett. **17**, 661 (1992).

[3] H. G. Winful, Y.C. Shen, and J. M. Liu, Appl. Phys. Lett. **48**, 616 (1986).

[4] F. de Tomasi, D. Hennequin, B. Zambon, and E. Arimondo, JOSA **B6**, 45 (1989).

[5] E. Cerboneschi, F. de Tomasi, and E. Arimondo, SPIE Vol. 2099 *Nonlinear Dynamics in Lasers and Optical systems*, 183 (1994).

Searching the Desired Periodic Orbit and Coding the Chaos in Semiconductor Laser Diodes for Message Transmission

Jyh-Long Chern and Hong-Jyh Li

Department of Physics, National Sun Yat-Sen University

Kaohsiung, Taiwan 80424, Republic of China

Phone: (Taiwan) +886-7-5320796; Fax: (Taiwan) +886-7-5310546

email: chern@venus.phys.nsysu.edu.tw

Recently, interest has been growing in the use of chaos for communication. Its potential applicability to high-speed optical systems is of technological importance. At least three typical methods have currently emerged in the literature to achieve the use of chaos in communication. The first involves synchronized chaos [1]. With synchronization achieved, the chaotic replica of the original chaotic signal is subtracted from the received composite signal and this leaves the message signal. This method is basically a masking method. The second method [2] concerns the utilization of controlling chaos [3]. This method, however, needs fast feedback mechanisms for high-speed signal processing that make it complicated to implement. The third method [4] uses the unstable periodic orbits embedded within a chaotic attractor to achieve communication. However, for high-speed system this method requires a non-trivial modulation technique to transmit correct information. Unlike the methods described above, we utilize a novel characteristic of chaos that a variety of dynamic states can be created by imposing a weak periodic perturbation [5]. Since these states can be further classified by some characteristic index, here the Shannon entropy, we suggest that by guiding the entropy, we can search the desired periodic orbit and a temporal programming of small parameter switching between these dynamic states can lead to a new mean of message coding without greatly modifying the system. Specifically, we quantify the system's output time series by measuring its some successive maxima and evaluating the Shannon entropy according to these data. In this manner, we can construct a mapping table between the parameter and the entropy and an alphabet table in terms of the entropy. The information

transmission is achieved by applying well-prepared weak perturbations successively. In communication, we prescribe the coding length and the alphabet table. After receiving a coded message, the receiver can decode it by calculating the entropy with a reference to the alphabet table. Here we theoretically demonstrate the proposed scheme in a directly modulated semiconductor laser and a laser diode with orthogonal polarization feedback [6] where an additional current modulation is used as the weak periodic perturbation. We have also exercised the proposed scheme in a semiconductor diode experimentally.

References:

[1]. K. Cuomo and A. V. Oppenheim, Phys. Rev. Lett. 71, 65 (1993).

[2]. S. Hayes, C. Grebogi, and E. Ott, Phys. Rev. Lett. 70, 3031 (1993); S. Hayes, C. Grebogi, E. Ott, and A. Mark, *ibid.* 40, 643 (1993).

[3]. E. Ott., C. Grebogi, and J. A. Yorke, Phys. Rev. Lett., 64, 1196 (1990).

[4]. H. D. I. Abarbanel and P. S. Linsay, IEEE Trans. Circuit Syst. II Analogy and Digital Signal Processing, 40, 643 (1993).

[5]. Y. Braiman and I. Goldhirsch, Phys. Rev. Lett. 66, 2545 (1991).

[6]. G. P. Agrawal, Appl. Phys. Lett. 49, 1013 (1986); K. Otsuka and J.-L. Chern, Opt. Lett. 16, 1759 (1991).

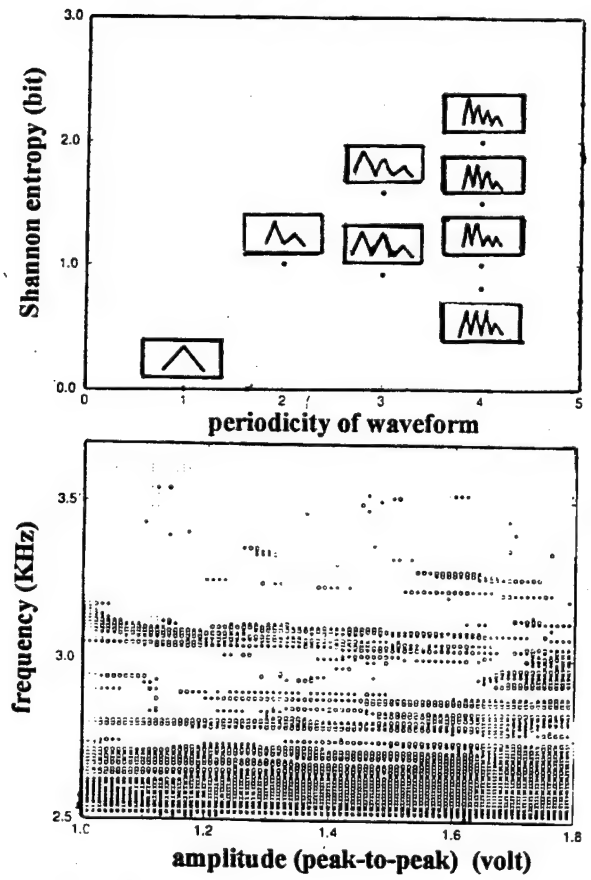

A state diagram created by imposing a weak periodic perturbation to a diode chaos. Different symbols mean different ranges of entropy value. The axes x and y are the amplitude and frequency of weak perturbation respectively. (experiment in a diode)

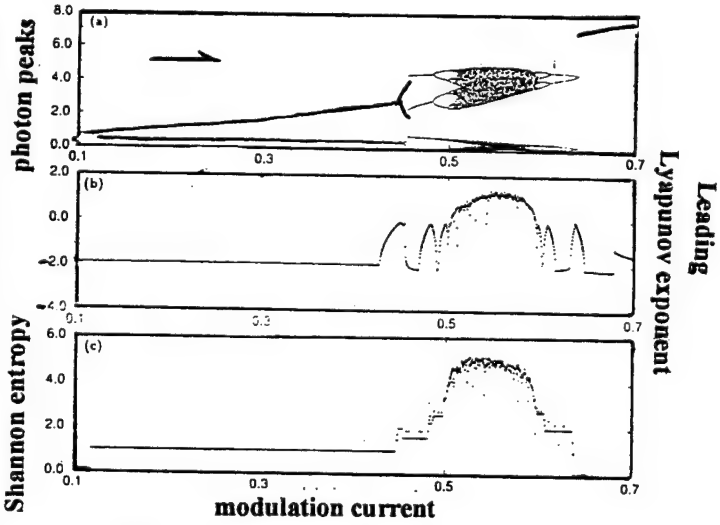

Dynamic features of a semiconductor laser model.

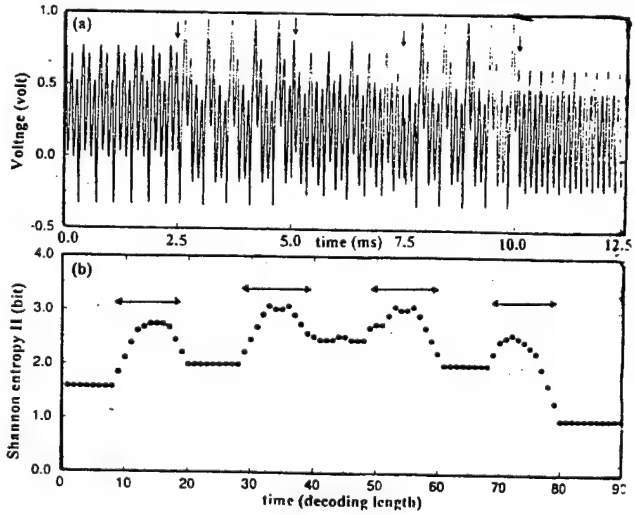

Coded waveform and decoded message (experiment in a diode)

EXPERIMENTAL OBSERVATION OF PERIOD DOUBLING SUPPRESSION IN A LOSS MODULATED CO_2 LASER

V.N.Chizhevsky
Institute of Physics, Belarus Academy of Sciences
220072 Minsk, Republic of Belarus
Phone: (0172) 395-658, Fax: (0172) 393-131
E-mail: ifanbe%bas03.basnet.minsk.by@demos.su

Over the last years the influence of periodical perturbations on dynamics of nonlinear systems near critical points is the matter of great interest, especially in the case when their frequencies are close to parametric resonancies of the unperturbed system. An existence of great number of nonlinear parametric effects near the period doubling bifurcation (PDB) in nonautonomous systems has been theoretically predicted in Ref.1. Experimentally, the most of them have been observed in the strain dynamics of a magnetostrictive ribbon [2] and other nonoptical dynamical systems.. In loss driven CO_2 lasers, such types of effects as small signal amplification and classical squeezing (deamplification) have been experimentally demonstrated as well as its strong phase dependencies [3-6].

In this paper we present the first experimental observation in optical systems of the effects of the period doubling suppression and the shift of bifurcation point due to periodical loss perturbations in the loss modulated CO_2 laser. A scaling law relating to the shift of the bifurcation point and the amplitude of the loss perturbations was also found, as well as others related nonlinear parametric effects predicted in Ref.1. Besides, a scaling law for the idler power near the bifurcation point was found which is in the perfect agreement with a theoretical prediction obtained in Ref.7.

The investigations were performed with a cw single mode frequency-stabilized CO_2 laser. Two acousto-optic modulators placed inside the cavity have been used for sinusoidal pump and perturbation loss modulations. The laser parameters were tuned so that the pump modulation frequency f_p (=100 kHz) was approximately twice the relaxation-oscillation frequency of the CO_2 laser. The frequency of the perturbation signal was equal $f_p/2+d$, where d=0.5 kHz. The laser output intensity was measured by a HgCdTe detector with time resolution of 50 ns and a digital oscilloscope coupled to PC/AT486. The spectral components near $f_p/2$ in the laser response were found on the base of Fourier transform of time series.

The results of the experimental investigation of the period doubling suppression are shown in the figure (a). The curve (1) is the amplitude of the laser response at $f_p/2$ that

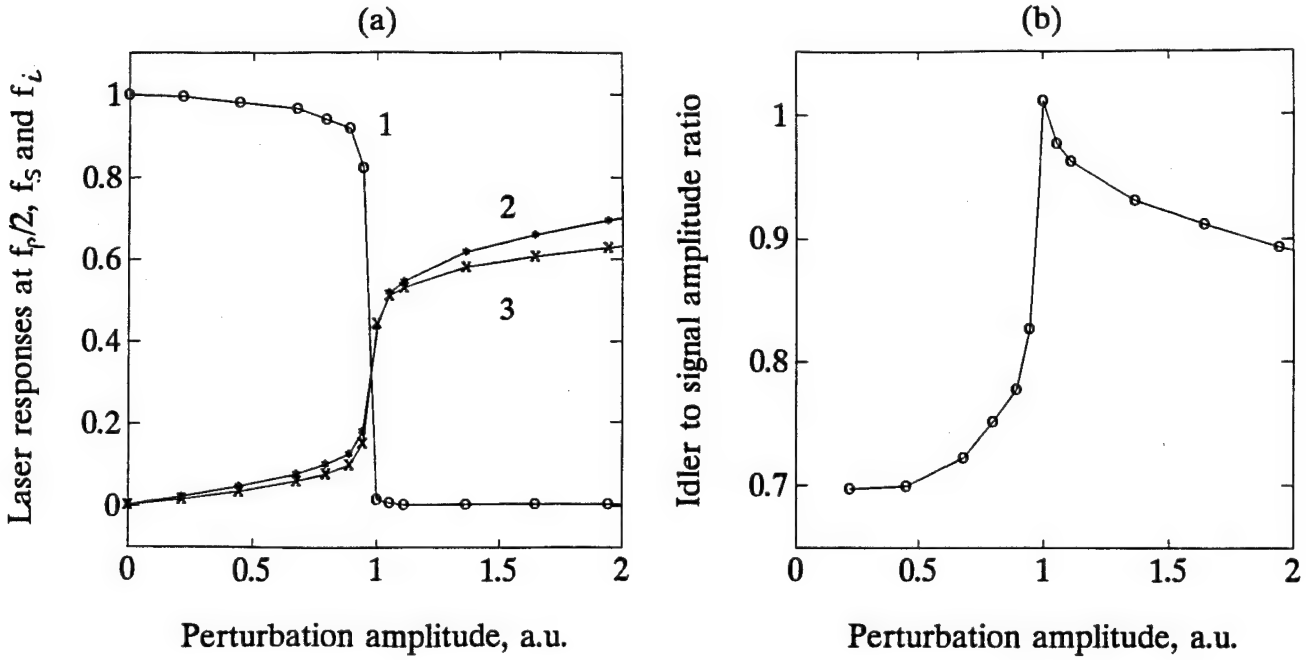

corresponds to the amplitude of PDB. It is clear seen the switchlike behavior in the laser response at $f_p/2$ when the amplitude A_s of the perturbing signal reaches the critical value. This means that the periodical loss perturbation suppresses the PDB in CO_2 laser and stabilizes the system. The bifurcation point is shifted to a new value that is higher the value of the unperturbed system. Under the experimental conditions the shift of the bifurcation point is proportional to A_s in power of a = 0.85±0.02 that has a some difference from the predicted value of 2/3 which was obtained for very small detuning. d [1]. In general, the power in the scaling law depends on the detuning d. The curves (2) and (3) show the components in laser response at signal f_s at idler f_i frequencies. A similar behavior is observed also at $f_p/2+md$, where m is an odd integer.

The fig..(b) shows the idler-to-signal amplitude ratio as a function of the amplitude of perturbation.When the PDB is suppressed the ratio reaches a maximal value which depend in general on a dissipation and the detuning [7] as well as the perturbation amplitude.

The research described in this publication was made in part by Grant No. MX3000 from International Science Foundation.

References.

1. P.Bryant, K.Wiesenfeld, Phys.Rev.A33 (1986) 2525.
2. S.T.Vohra, F.Bucholtz, K.P.Koo, D.M.Dagenais, Phys.Rev.Lett. 66 (1991) 212; Phys. Rev. Lett. 66 (1991) 2843.
3. C.Lepers, J.Legrand, P.Glorieux, Phys.Lett. A161 (1992) 493.
4. A.M.Samson, S.I.Turovets, V.N.Chizhevskii, V.V.Churakov. Sov. Phys. JETP 74 (1992) 628.
5. V.N.Chizhevsky, S.I.Turovets, Optics Commun. 102 (1993) 175.
6. R.Corbalan, J.Cortit, A.N.Pisarchik, V.N.Chizhevsky, R.Vilaseka, Phys. Rev. A51 (1995) No.1.
7. H.Swensmark, K.Wiesenfeld, Phys.Rev. A46 (1992) 787.

Longitudinal effects in distributed feedback laser diodes: Hole Burning dynamics.

Pere Colet and Salvador Balle
Departament de Física, Universitat de les Illes Balears, E-07071 Palma de Mallorca, Spain
Tel # : +34 71 173234, Fax #: +34 71 173426, e-mail: dfspcr4@ps.uib.es

Spatial hole burning (SHB) is the phenomenon of a localized reduction in carrier density due to stimulated recombination and the finite diffusion length of the carriers. In semiconductor lasers, carrier density provides gain, but it also induces frequency-dependent changes in the index of refraction. SHB has shown to originate instabilities gain-guided semiconductor lasers [1]. In addition, it is considered to play a dominat role in the spectral degradation of the emission of distributed feedback (DFB) lasers. In these devices, a modulation of the device refrative index is implemented in order to obtain higher spectral purity as compared to conventional Fabry-Perot devices. However, since SHB involves a spatial redistribution of the gain, it might cause lasing of secondary modes [2]. Different attempts to study the influence of SHB on the static and dynamical behaviour of DFB lasers have been carried out using a variety of models [3]. However, the inclusion of SHB and spontaneous emission noise in a large-signal, dynamical model based on the Maxwell-Bloch description of the optical field and its interaction with the active medium has not been considered until very recently [4]. Similar descriptions are frequently used in connection with a modal expansion for the electric field [2, 5], although they have been applied only to the analysis of the CW operation of the diode.

The model considers the wave equation for the SVA of the optical field $E(z,t)$ and carrier frequency Ω, and Bloch equations for the material variables, which we take as a two-level system. The equations read:

$$\partial_t E = \frac{1}{2n^2 - i\gamma/\Omega}\left\{-i\frac{c^2}{\Omega}\left(\partial_z^2 E + \frac{\Omega^2 n^2}{c^2}E\right) + P - \gamma E\right\} \quad (1)$$

$$\partial_t N = J - \gamma_e N - (E^* P + E P^*)/2 + D\partial_z^2 N + \sqrt{2\gamma_e N}\chi_N + \sqrt{\zeta}\chi_J \quad (2)$$

$$\partial_t P = -\gamma_P(1+i\theta)P + g_0(N-N_t)(1-i\alpha)E + \sqrt{2\gamma_e N}\chi_s \quad (3)$$

where $P(z,t)$ is the SVA of the material polarization. The longitudinal distribution of refractive index is given by $n(z)$, which has a mean value $\bar{n}$. γ describes the losses and g is the gain coefficient for the electric field. $N(z,t)$ stands for the minority carrier density and N_t its value at transparency. $J(z,t)$ is the current density injection (in carriers per unit length and unit time), γ_e is the inverse carrier lifetime due to spontaneous recombination, and D is the diffusion coefficient for the carriers. Spontaneous emission noise is modeled through the Gaussian complex noise term $\chi_E(z,t)$, which we assume to be of zero mean and delta correlated in both space and time. $\chi_N(z,t)$ models spontaneous non-radiative recombination of the minority carriers, and $\chi_J(z,t)$ models fluctuations in the injection current due to circuit parasitics. χ_N and χ_J are taken as independent Gaussian white noises with zero mean, and they are also independent of spontaneous emission noise.

We consider non-reflecting facets as the boundary conditions for the electric field at the lasing frequency, and no current flow through the faces as the boundary condition for the carriers. The DFB element is a $\lambda/4$-shifted cosinusoidal grating for a lasing wavelength of 1.53 μm.

We have numerically integrated these equations for a stepwise change of the injected current J from a bias level below threshold to a given level above it. When a uniform current injection is considered, the light

output at the facets obtained from our model features (see figures) the same pulse emission characteristics obtained from the simpler rate equation approach, though it can be seen that SHB yields non-linear gain saturation. The results in this case are also similar to those obtained from other models [6]. We have also determined the light-current characteristic from this solution, determining the threshold current density as a function of the step in the refractive index grating.

In addition, we show that, for moderate values of κL, higher order modes destabilize the CW output as the current injection is increased.

However, the numerical results show that, due to the modelling of the material as a two-level system, the α parameter describing AM/FM coupling corresponds to detuning away from resonance. In order to match the observed values of $\alpha \sim 5$, the gain peak is largely detuned from the Bragg wavelength, so a quite large modulation amplitude of the refraction index is required in order to achieve lasing at the Bragg wavelength. This shows that a better modelling of the material polarization is required to reproduce the behaviour of real DFB lasers.

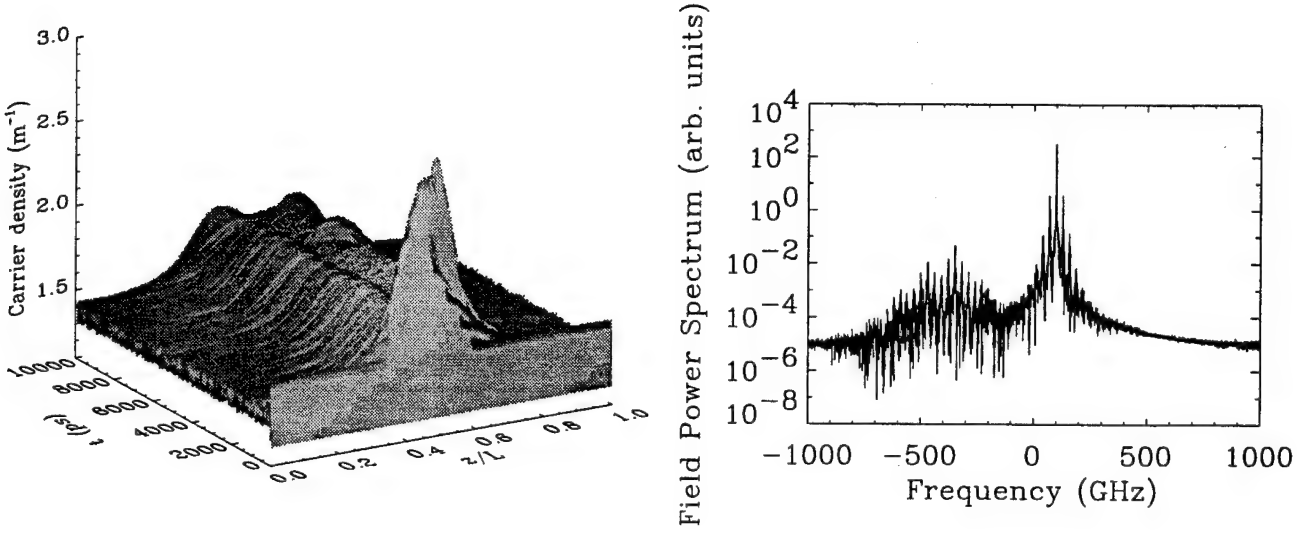

References

[1] B. W. Hakki, J. Appl. Phys. **46**, 292 (1975); N. Chinone, J. Appl. Phys. **48**, 3237 (1977).

[2] B. Tromborg, H. Olesen and X. Pan, IEEE J. Quantum Electron. **27**, 178 (1991).

[3] See e. g. A. J. Lowery, A. Keating and C. N. Murtonen, IEEE J. Quantum Electron. **28**, 1874 (1992).

[4] P. Colet and S. Balle, in "Integrated Photonics Research", 1994. Technical Digest Series Vol. 3, pp. 108 (Optical Society of America, Washington, DC, 1994)

[5] H. Kogelnik and C. V. Shank, J. Appl. Phys. **43**, 2327 (1972).

[6] A. J. Lowery, IEE Proc. J: Optoelectronics **139**, 402 (1992).

Controlling Chaos in a Hybrid Optical Bistable System

Jian-Hua Dai, Hua-Wei Yin, Hong-Jun Zhang

Institute of Physics, Chinese Academy of Sciences, P. O. Box 603, Beijing 100080, China

FAX: 86-1-2562605, E-Mail: user307@aphy01.iphy.ac.cn

OGY's method to control chaos [1] inspired the recent research in chaos application [2]. In this paper, we numerically and experimentally study the control of chaos in a hybrid optical bistable system using the piece-wise function model. Whether the perturbation in an accessible system parameter is large or small, the dynamic behavior of each iteration can be described by the piece-wise function map and the process of controlling chaos can be described by a new map which intersects the original map at the fixed point (or desired controlled orbits). The fixed point is a common orbit for both maps, and it is unstable in the original map but stable in the new map. In such a way we can convert the chaotic dynamics to the fixed point. The one-dimension mapping is $x_{n+1} = f(x_n, p)$, where p is an accessible system parameter. A piece-wise function is defined as

$$x_{n+1} = \begin{cases} f(x_n, p_0) & \text{for } x_n \le x_0 \\ f(x_n, p_n) & \text{for } x_n > x_0 \end{cases}, \qquad (1)$$

where x_0 is a piece-wise point that divides the function curve into two part . The process of controlling chaos can be expressed as

$$\begin{cases} x_{n+1} = f(x_n, p_n) \\ p_n = \varepsilon (x_n - x_f) + p_0 \end{cases}, \qquad (2)$$

where ε is the feedback strength and x_f is the unstable point fixed embedded in the chaotic attractor. Eq.(2) is a new map which is different from the original map Eq. (1). Choosing a suitable value of ε, we can control the chaos to the fixed point x_f. Suppose that x_n is close enough to x_f, then a linear approximation can be applied. From Eq.(2), we obtain $\varepsilon_0 - \Delta\varepsilon < \varepsilon < \varepsilon_0 + \Delta\varepsilon$. Here, $\varepsilon_0 = -\lambda/[(\lambda-1)g]$, $\Delta\varepsilon = 1/[(\lambda-1)g]$, $\lambda = \partial f / \partial x$, $g = \delta x_f(p_0) / \delta p$, and these partial derivatives are evaluated at $x = x_f$ and $p = p_0$. These variables can be derived from experiment data. The choice $\varepsilon = \varepsilon_0$ is optimal for it minimizes the average time during which the orbit wanders chaotically before it can be stabilized.

The experimental apparatus[3-5] used in this study consists of a He-Ne laser used as the light source and a $LiNbO_3$ crystal as a nonlinear medium. The feedback loop delay is controlled by a computer. When the delay time of the feedback loop is much larger than the relaxation time of the medium, the hybrid optical bistable system can be described by the following mapping $x_{n+1} = A_0 \sin^2(x_n - b)$, where A_0 and x_n are proportional to the input and output intensity respectively, and b is a bias voltage. If the value of $A=A_0$, the system is chaotic. As long as the iteration falls near x_f, we changed A from A_0 by $\Delta A = \varepsilon_0 (x_n - x_f)$. The experimental results are shown in Figures 1. Fig. 1(a) shows the return map, 1(b) the controlled time series, and 1(c) the perturbation of parameter A. We estimate the noise level to be 2% from Figure 1(a). Similar numerical results are shown in Figures 2. Both are in good agreement with each other.

References

[1] E.Ott, C. Grebogi, and J. A. Yorke, Phys. Rev. Lett. **64**, 1196 (1990).
[2] W.L.Ditto, S.N. Rauseo, and M.L.Spano, Phys. Rev. Lett. 65, 3211 (1990).
[3] K. Ikeda, H. Daido, and O. Akimoto, Phys. Rev. Lett **45**, 709 (1980).
[4] H. M. Gibbs, F. A. Hopf, D. L. Kaplan, and R. L. Shoemaker, Phys. Rev. Lett. **46**, 474 (1981).
[5] Hong-Jun Zhang, Jian-Hua Dai, Peng-Ye Wang, and Chao-Ding Jin, J. O. S. A. **B3**, 231 (1986).

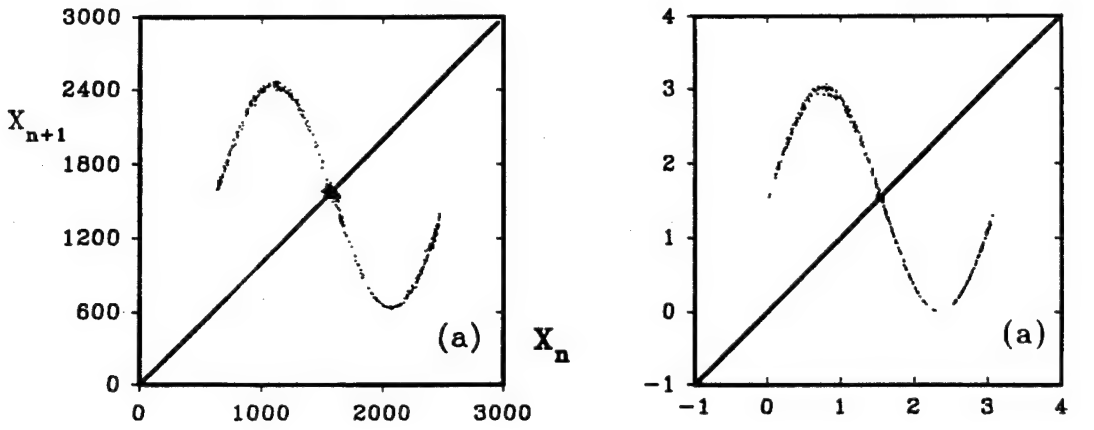

The return map

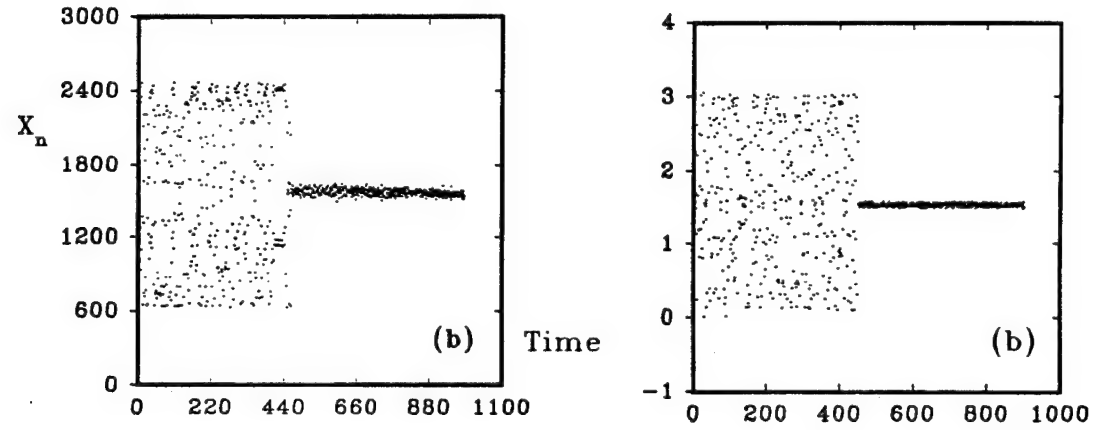

Time series

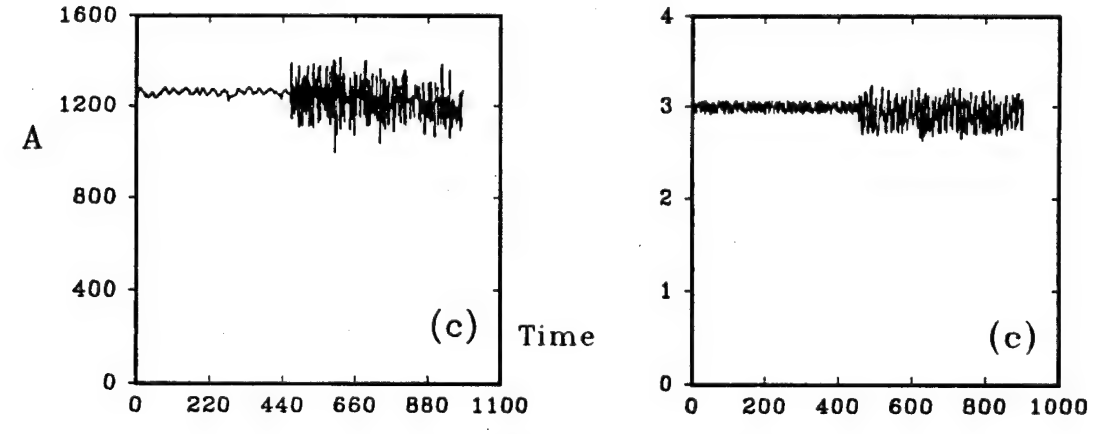

perturbations of A

Figures 1 Experiment results

Figures 2 numerical results

Broad tunability in an intrinsic passive (J=1 to J=0) 'polarization oscillator'

R J Ballagh and W J Sandle

Physics Department, University of Otago, Dunedin, NEW ZEALAND

A "polarization oscillator" is an unstable optical device utilizing nonlinear birefringence or dichroism to spontaneously modulate a transmitted laser beam for steady-state input. Such a device may hold considerable application potential: for example in optical communications and optical data processing it could provide the optical equivalent of an electronic voltage-controlled oscillator—producing an output modulation frequency linearly related to input intensity. We present in this paper a model for such a device, based upon a system of J=1(lower)↔J=0(upper) atoms in a ring cavity. An important feature of the proposal is the presence of a magnetic field, longitudinal to the beam propagation direction, which provides overall control of the modulational instability.

The semiclassical model for the system is developed for a homogeneously-broadened (J=1↔J= 0) transition driven by a linearly-polarized continuous-wave field. The atomic response is solved to all orders of the field intensity by using a density-matrix approach, and the evolution of the circularly-polarized components of the plane-wave field in the cavity is treated in the mean-field approximation. In the absence of the magnetic field, the output is also linearly polarized and has a stable constant intensity in almost all circumstances. However, there are large parameter regimes for which the output field may undergo steady oscillation between states of left- and right-circular polarization when a non-zero longitudinal magnetic field is applied. The incident laser intensity controls the onset of oscillation, which may have large (temporal) gain. The oscillation frequency is sensitive to cavity detuning and magnetic field, but in general is also dependent on the laser intensity. The wide parameter range over which the oscillations for the J = 1↔ J = 0 medium occur is in marked contrast to the case for instabilities with two-state atoms[1,2], and is illustrated in Fig. 1. Here, the pulsation frequency is plotted as a function of the magnetic field strength (Larmor frequency ω) and the cavity detuning (ϕ).

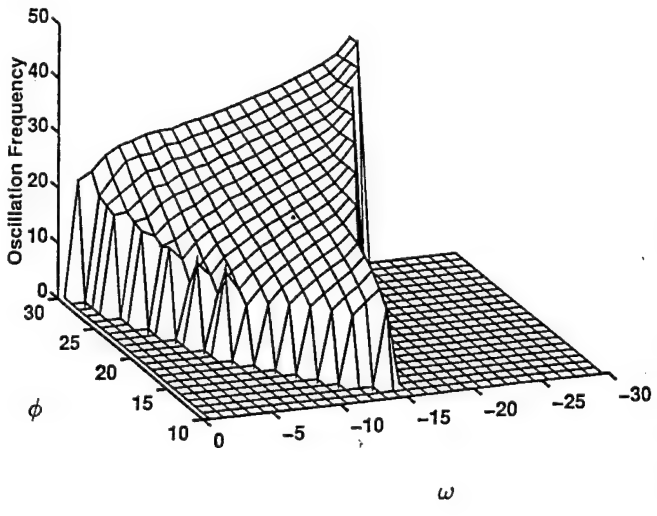

Fig. 1. Oscillation frequency as a function of cavity detuning ϕ and Larmor frequency ω for a laser-atom detuning, Δ, of 100. The incident laser intensity is adjusted at each value of ϕ and ω for maximum gain. All other system parameters are held constant: cooperativity = 2400 (600 times the critical value of 4 for onset of optical bistability at zero magnetic field); lower-level relaxation rate 0.0875; upper-level radiative decay rate 0.25; and cavity relaxation rate 1.2. The Larmor and oscillation frequencies, decay rates and detunings (except for the laser-cavity detuning, which is expressed in terms of the empty-cavity half-width at half-height) are all measured in units of the optical-dipole dephasing rate.

The case chosen in Fig. 1 is for large detuning from resonance (see caption). All system parameters are constant except for the incident laser intensity which is adjusted at each value of ω and ϕ to give maximum gain. A broad tuning range of oscillation frequency can be obtained simply by varying the input intensity, as is illustrated in Fig. 2: the range of frequencies obtained by varying the incident laser intensity is plotted, corresponding to each point in Fig. 1.

Acknowledgements

We are grateful to Dr C. Parigger and to J. Hooley for assistance with earlier phases of this work. We acknowledge support from the New Zealand Foundation for Research, Science and Technology under Public Good Science Fund Contract UOO308.

References

1. R. Bonafacio and L. A. Lugiato, Lett. Nuovo Cimento 21, 510 (1978).
2. V. Benza, L. A. Lugiato, and P. Meystre, Opt. Commun. 33, 113 (1980).

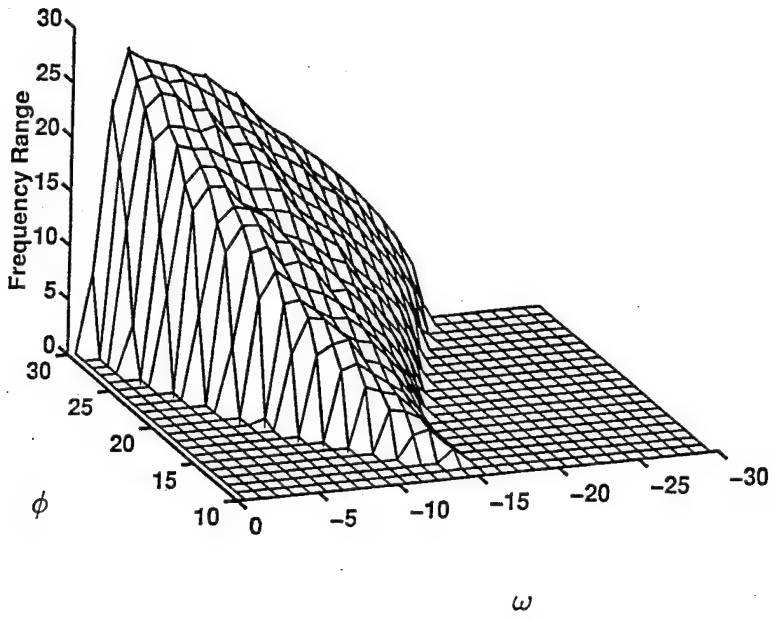

Fig. 2. Tuning range of the oscillation frequency corresponding to each point in Fig.1, obtained by varying only the incident laser intensity.

Nonlinear Dynamics and Chaos of a Single Mode cw Nd:YAG Laser with Modulated Loss.

L. Dambly, P.M. Ripley and R.G. Harrison

Department of Physics, Heriot-Watt University
Riccarton, Edinburgh EH14 4AS, UK
e-mail: phydl@uk.ac.hw.phy

We report on the nonlinear dynamic and chaos of a cw unidirectional, single mode Nd:YAG laser with modulated loss. These observations are, to our knowledge, the first to be reported for such a system which in many respects is a paradigm of Class B solid state lasers. Further, our investigations are to the application of new control algorithms to this system to stabilise its dynamical and in particular chaotic behaviour.

The experiments were carried out with a CW Nd:YAG laser[1] comprising a ring cavity of two flat mirrors and a 10% flat output coupler. An intra-cavity Faraday rotator and a half-wave plate were introduced to ensure unidirectional propagation, single mode operation being ensured through appropriate choice of cavity length and the inclusion of intra-cavity apertures. Intra-cavity loss modulation was implemented by an accousto-optic modulator provided with control of both amplitude A_m and frequency ν_m of modulation; these were used as the principle control parameter for our investigations of dynamical behaviours.

This driven system had a resonance ($\nu_R \approx 8kHz$) corresponding to the radiative life-time of the upper level of the lasing transition. All the dynamics appeared for a frequency of modulation in the neighborhood of the resonance and its harmonics. Outside these domains of frequency, the modulation had no effect and the dynamical behaviour was reduced to the steady state of the non-driven Nd:YAG laser. Figure 1 shows the different dynamical behaviour for various amplitudes of modulation when the frequency of modulation was close to the first harmonic ($\nu_m \approx 2\nu_R$). For small amplitude ($A_m = 1\%$), we observed a periodic state with a frequency of approximately $50kHz$ (Fig. 1 (a) and (d)) characteristic of the pump process rate. For higher amplitude, the system jumped to another limit cycle ($A_m = 4\%$) with a frequency close to ν_m (Fig. 1 (b) and (e)) and reached a chaotic state ($A_m = 16\%$)

(Fig. 1 (c) and (f)).

The representative data of Figure 1, both time series and phase portraits, were recorded using a Lecroy digitiser. A full characterisation and modelling of the dynamical behaviour will be reported together with the results of our current application of continuous feedback control[2,3] to the system utilising the intra-cavity modulator as the control element interfaced to a PC for programmable control.

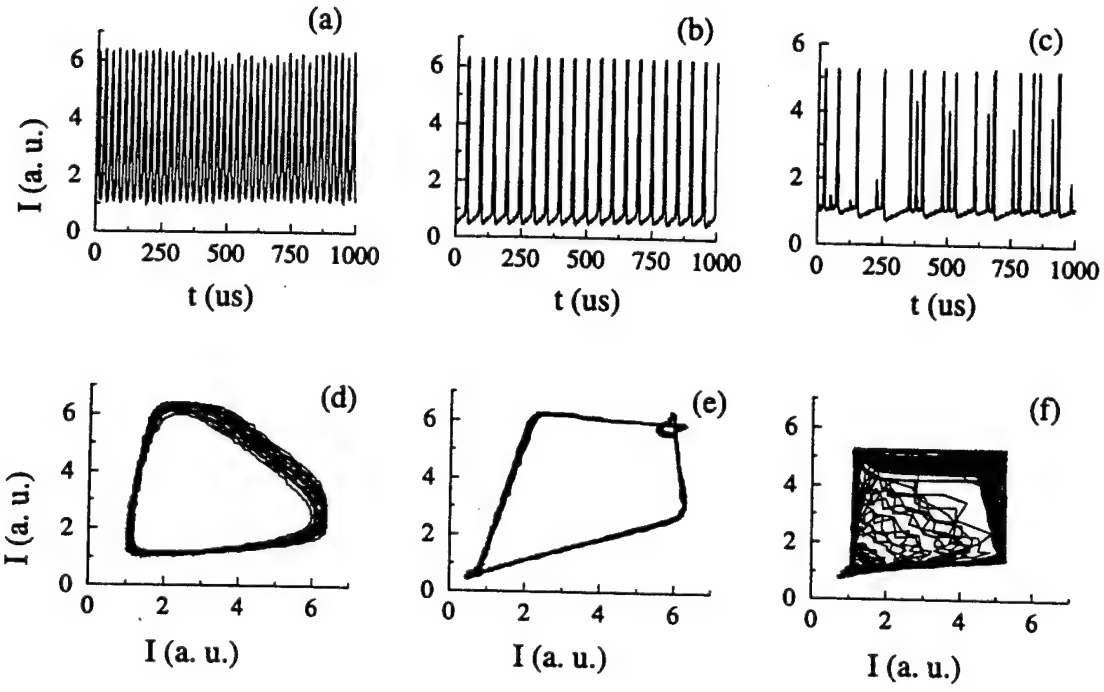

Figure 1: Example of dynamical behaviour (a, b and c) and the corresponding phase portraits (d, e and f). $\nu_m = 20kHz$ *and* $A_m = 1\%(a,d), 5\%(b,e) and 16\%(c,f)$ *of losses.*

References

1) W. Koechner [1976]: *Solid state laser engineering*; Springer Series in Optical Sciences, **1**, Springer-Verlag

2) K. Pyragus [1992]; Phys. Lett. A, **170**, p 421

3) J. Socolar *et al* [1994]; Phys. rev. E, **50**, p 324

GAIN-SWITCHING AND FREQUENCY CHIRP OF INJECTION-LOCKED SINGLE-MODE SEMICONDUCTOR LASERS

J. Dellunde*, M.C. Torrent**, J.M. Sancho* and M. San Miguel***
* *Departament d'Estructura i Constituents de la Matèria, Facultat de Física, Universitat de Barcelona, Diagonal 647, E-08028 Barcelona, Spain. Fax: (343) 402 11 98 Phone: (343) 402 11 83 E-Mail: dellunde@noise.ecm.ub.es, jmsancho@ebubecm1.ecm.ub.es*
** *Departament de Física i Enginyeria Nuclear, EUETIT, Universitat Politècnica de Catalunya, Colom 1, E-08222 Terrassa, Spain. Fax: (343) 7398225 Phone: (343) 7398222 E-mail: carme@noise.ecm.ub.es*
*** *Departament de Física, Universitat de les Illes Balears, E-07071 Palma de Mallorca, Spain. Fax: (3471) 173426 Phone: (3471) 173229 E-mail: dfsmsm0@ps.uib.es*

Injection locking of semiconductor lasers has been used as an effective method for frequency locking and linewidth reduction in CW operation [1]. Modulated operation of laser diodes can also be improved with light injection, showing both frequency chirp and time jitter reduction [2]. The laser with an external field exhibits interesting physical phenomena, such as optical bistability, four-wave mixing, frequency conversion and optical chaos [3].

Depending on the intensity of the external field, several regimes can be appreciated for different values of the detuning between the master and the slave lasers. Stable steady-state operation of the slave is only possible inside an asymmetric locking range of detunings. The emission frequency of the slave laser becomes identical to that of the master and shows a smaller linewidth than in the unlocked case.

In this work, we investigate the frequency dynamics and switching time of gain-switched single-mode semiconductor lasers under light injection. An study of the turn-on time with a laser subject to a small external field was presented in [4] in the context of detection of weak optical signals. We use the same stochastic coupled rate equations, including gain compression effects. Results are based on numerical simulations.

A sudden increase in the current injection drives the laser from below to above threshold. A range of dynamical locked operation can be observed with a low chirp, where only phase modulation and noise remains. This range of detunings depends on the injection level and can be broader than the one corresponding to CW operation. Figure 1 shows an asymmetric dynamical locking range as large as 90 GHz with an injected intensity around a 5% of the intensity of the solitary slave laser in the on state.

The switch-on time is considered as the delay time between the current step and light emission at a given intensity reference level. The mean switch-on time shows a minimum for a given detuning. This minimum can be found outside both the CW and the dynamical locking range. Time jitter is highly reduced for all detunings, except at special locations linked to the switch-on time minima, where time jitter is dramatically increased. Mean switch-on time and time jitter at two reference levels are plotted in figure 2, for a injected intensity of a 0.1%. The values corresponding to the solitary laser are also plotted for completeness. Appearance of an

a given detuning, that can be found outside both the CW and the dynamical locking range. Time jitter is highly reduced for all detunings, except at special locations linked to the switch-on time minima, where time jitter is dramatically increased. Mean switch-on time at two reference levels is plotted in figure 2, for a injected intensity of a 0.1%. The values corresponding to the solitary laser are also plotted for completeness. Appearance of an intensity prepulse triggers the switch-on before the exponential grow of the intensity, making the precise position of the minima dependent on the intensity reference.

The turn-on of the slave laser can be triggered by the external field, even if the carrier number has not reached its threshold value, corresponding to the slave laser acting as an optical amplifier. This effect can be observed in figure 2, at the reference level of a 12%, being the mean switch-on time of the solitary laser of 161 ps.

REFERENCES

[1] R.Lang, IEEE JQE, **QE-18** p. 976 (1982)

[2] S.Mohrdiek, H.Burkhard and H.Walter, IEEE J.Light. Tech. **12** p. 418 (1994)

[3] K.B.Dedushenko and A.N.Mamaev, Opt. Comm. **96** p. 78 (1993)
J.M.Iannelli, A.Yariv, T.R.Chen and Y.H.Zhuang, Appl.Phys.Lett **65** (16) p. 1983 (1993)
G.H.M. van Tartwijk, G. Mujires, D. Lenstra, M.P. van Exter and J.P. Woerdman,
Elect. Lett. **29** p.137 (1993)
T.B. Simpson, J.M. Liu, A. Gavrielides, V. Kovanis and P.M. Alsing,
Appl.Phys.Lett. **64** (24) p.3539 (1994)

[4] M.C.Torrent, S.Balle, M.San Miguel and J.M.Sancho, Phys.Rev. **A47** p. 3390 (1993)

Figure 1

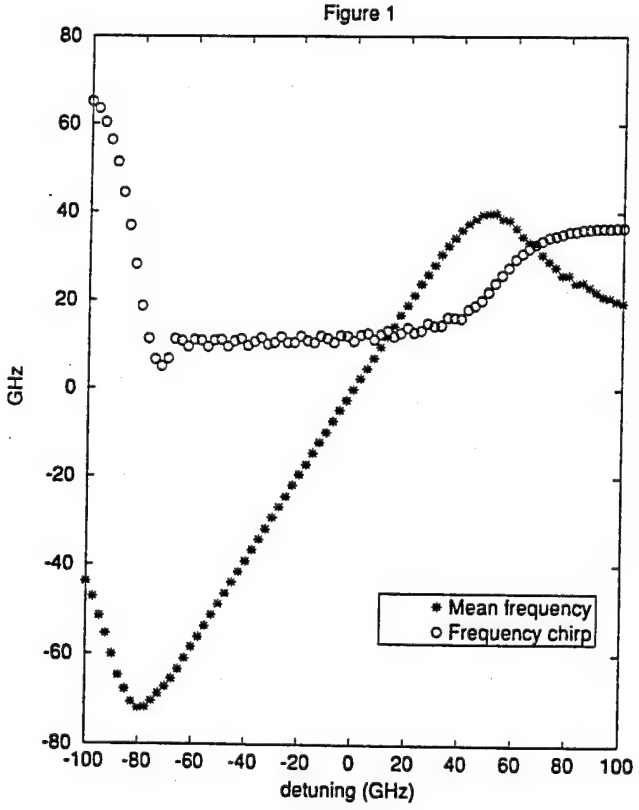

Figure 2

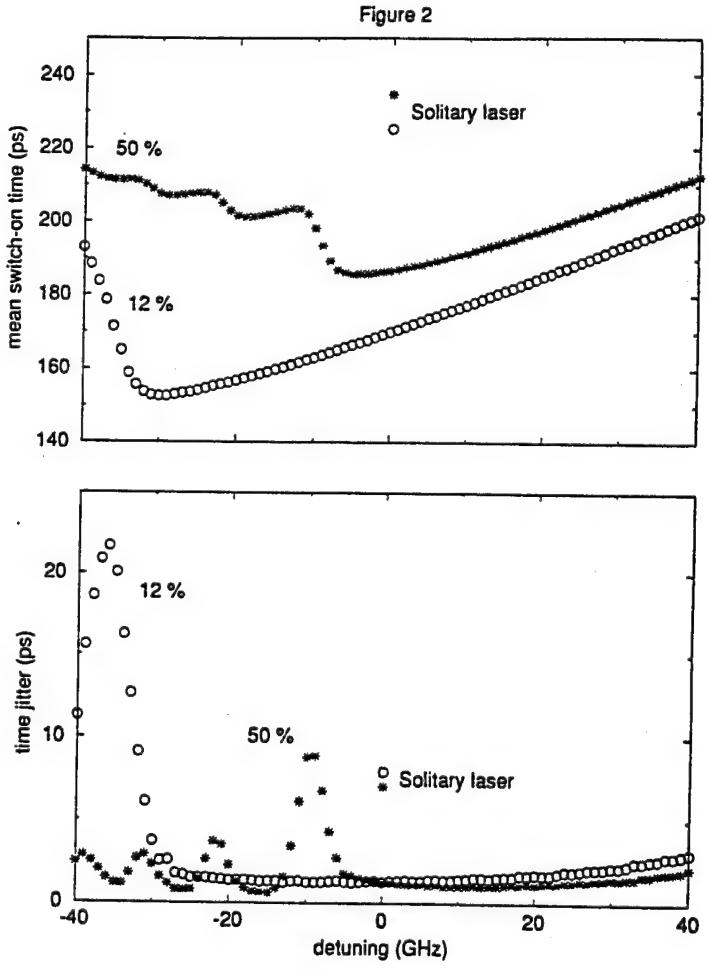

Synchronization of Periodic and Chaotic CO_2 Lasers with Saturable Absorber

P.C. de Oliveira , Y. Liu, M.B. Danailov and J.R. Rios Leite

Departamento de Física, Universidade Federal de Pernambuco, 50732-910 Recife PE Brazil

We studied experimentally and numerically the dynamics of two single mode CO_2 lasers with intracavity saturable absorber when they are submitted to variable amount of optical coupling. This type of laser has been extensively studied [1]. Changes in a control parameter, like the absorber gas pressure or the cavity tuning, produces alternating periodic and chaotic pulsations, cascades of period doubling and type I intermittency with Shil'nikov homoclinic orbits giving routes to chaos verified experimentally and numerically [1,2]. These instabilities have pulse rate in the range of $50kHz$. Two such lasers refered as A and B were $15m$ apart and a portion of the output of A was sent into B with a small misalignment to avoid standing wave coupling. Conversely a variable amount of the B power was also sent into A. Their optical coupling was measured to be $5.0 \pm 0.5\%$, with their gratings selecting the $10.6\mu m$ P(18) CO_2 lines. A spectrum analiser was used to monitor the beatnote of the lasers. An observed high frequency relative jitter ($\geq 500kHz$) indicates that in the time scale of their Q-switching ($\geq 20\mu s$) any interference between the two laser fields was averaged to zero. All coupling effect was then interpreted as intensity and population changing rates.

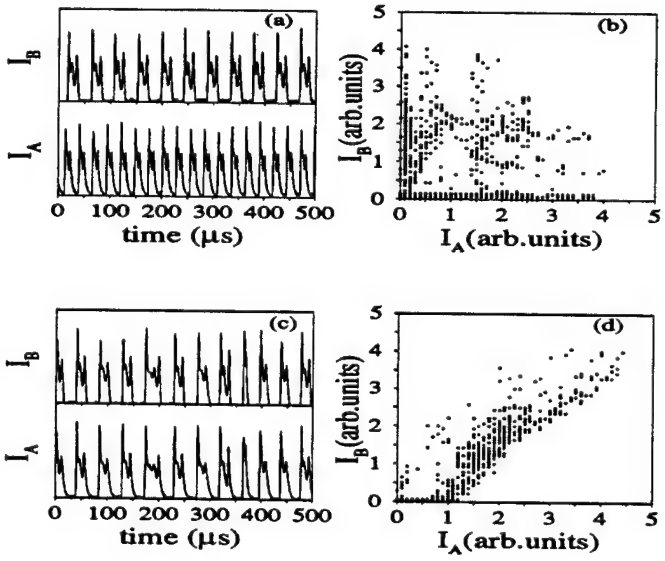

The above figure shows the output pulses of the lasers when the intracavity cell of laser

A had $40mTorr$ of SF_6 mixed with $600mTorr$ of CO_2 as a buffer gas (in the cell the CO_2 is mostly in its vibrational ground state and will not absorb the laser light), while laser B had $20mTorr$ of SF_6 plus $700mTorr$ of CO_2 . Choosing the appropriate frequency tuning, the uncoupled lasers were set in periodic pulsation as given in Fig. a. After coupling, the lasers gave pulses as Fig. c. They became chaotic and syncronized their pulsations. Both lasers had lower saturation intensities in their absorbers, as compared to their amplifiers, so their coupling acted mostly as absorber coupling when they had their optical frequencies separated by less than $5MHz$. Thus positive correlation between their pulsation resulted as shown in Fig. d. Figs. b and d are the two intensities correlations of Figs. a and c, respectively.

For other values of PZT tuning, the two lasers could be set in chaotic regime and then syncronized. For small frequency detunings, positive correlation between their pulsation resulted. Anticorrelated synchronization was obtained when the optical frequency detuning of the lasers was $20MHz$. For instance, before coupling they were periodic, in $P^{(1)}$ and $P^{(2)}$ regime, respectively. After the coupling each laser kept the same type of periodic pulse shape but they adjusted their pulse rate and separation to meet the negative correlation condition.

The theoretical model uses the two-level three-level systems of rate equations for each laser[1,2], with coupling terms to account for cross saturation of the absorbers and amplifiers,as described in [3]. Numerical solutions of the equations for each laser, with apropriate choice of parameters was made to produce pulsed solutions as previously observed in experiments[1]. The calculated pulses for the coupled lasers did compare well with the experimental observation[3]. Similar synchronization studies were recently obtained on CO_2 [4] and $NdYag$ [5] lasers. Our model neglects standing wave effects, inhomogeneous broadening in the absorber medium, transverse beam profile effects, etc... and yet there is a very good agreement between the calculations and our experiments.

References

[1] M. Tachikawa, F.L. Hong, K. Tanii and T. Shimizu, Phys. Rev. Lett. **60**, 2266 (1988).

[2] M. Lefranc, D. Hennequin and D. Dangoisse, J. Opt. Soc. Am. B **8,** 239 (1991).

[3] Y.Liu, P.C.de Oliveira, M.B.Danailov and J.R.Rios Leite, Phys. Rev. A **50,** 3464 (1994).

[4] T. Sugawara *et al.*, Phys. Rev. Lett. **72,** 3502 (1994).

[5] R. Roy and K. S. Thornburg, Jr. Phys. Rev. Lett. **72,** 2009 (1994).

Numerical Analysis of Non-Paraxial Beam Self-Focusing in Kerr Media

Vladimir L.Derbov and Leonid A.Melnikov

Department of Optics, Chernyshevsky State University, 83 Astrakhanskaya str., Saratov 410071, Russia
phone: (845-2)51-51-95, e-mail: derbov@scnit.saratov.su, melnikov@scnit.saratov.su

We suggest a new numerical algorithm for modelling the beam self-action and transverse pattern formation in the situations when the focal beam spot or the typical scale of the transverse pattern is comparable with the wavelength, so that the conventional paraxial theory yields singular behavior of the beam at the focal point [1]. For Kerr self-focusing Feit and Fleck [2] have shown that this singularity is due to the commonly used parabolic approximation and suggested a more sophisticated scheme of reducing the Helmholtz equation to a first-order one. Numerical calculations of wide-angle self-focusing in [2] showed multiple foci with a finite value of the field and a sudden drop of the total beam power at each of them. The power loss was attributed to the reflection of the wide-angle components of the beam by the focal region. If it is so, a considerable backward wave may arise, which, however, could not be observed in [2] since only the forward wave was considered explicitly. Formally the second-order Helmholtz equation has both forward and backward waves as solutions, so the role of backward waves in nonparaxial self-focusing is an open question. There seem to be at least two physical reasons for the backward wave to appear: 1) linear reflection due to fast transverse variation of the nonlinear refraction index n; 2) reflection from 3D structure of n induced by the interference of the opposite waves.

We solve directly the scalar Helmholtz equation:

$$(\partial^2/\partial z^2 + \nabla_\perp^2 + k^2 n^2) E(r,\varphi,z) = 0, \tag{1}$$

where $E(r,\varphi,z)$ is the coordinate-dependent amplitude of the electric field. For Kerr media n is given by $n = n_0 + n_2|E(\vec{r},z)|^2$. We make use of the field decomposition in terms of Laguerre-Gaussian modes of free space [3]:

$$E(r,\varphi,z) = \sum_{m,n} A_n^m(z)\psi_{mn}(r,\varphi), \tag{2}$$

$$\psi_{mn}(r,\varphi) = (n!/(n+m)!)^{-1/2} L_n^{|m|}(\eta(z)r^2)(\eta r^2)^{\frac{|m|}{2}} exp(-Pr^2/2 + im\varphi) \tag{3}$$

where L_n^m is the Laguerre polynomial, $P = \eta + i\xi$ is the inverse complex beam parameter which is, generally, z-dependent. If we choose P to be constant, the modal amplitudes in the free space obey the set of equations

$$\frac{d^2 A_n^m}{dz^2} + k^2 n_0^2 A_n^m + \eta \sum_{n'} D_{nn'}^m A_{n'}^m = 0, \tag{4}$$

where n_0 is the linear part of the refraction index, D^m is a symmetric three-diagonal matrix

$$D_{nn'}^m = -(2n + |m| + 1)\delta_{nn'} - [(n+1)(n+1+|m|)]^{1/2}\delta_{n',n+1} - [n(n+|m|)]^{1/2}\delta_{n',n-1}, \tag{5}$$

Diagonalization of the matrix (5) yields a new basis set of functions

$$\Phi_{mj}(r,\varphi) = \sum_n B_{nj}^m \psi_{mn}(r,\varphi), \tag{6}$$

the columns of the matrix B^m being the eigenvectors of the matrix (5). Using the new basis the field amplitude may be presented as $E(r,\varphi,z) = \sum_{m,j} C_{mj}(z)\Phi_{mj}(r,\varphi)$, where the new modal coefficient satisfy the set of equations

$$\frac{d^2 C_{mj}}{dz^2} + \alpha_{mj}^2 C_{mj} = -4\pi k^2 P_{mj}, \tag{7}$$

where $\alpha_{mj} = (k^2 n_0^2 + \eta d_j^m)^{1/2}$, d_j^m is the $j-$th eigenvalue of the matrix (5), P_{mj} is the modal coefficient for the nonlinear part of the polarization. To solve (7) we used the fourth-order Runge-Kutta scheme. Forward and backward transformation (2) is carried out at each step of the process to calculate the nonlinear polarization. Rigorously one should solve a boundary (scattering) problem to account for the reflected wave. As a first step, however, it is natural to solve a Cauchy problem with initial conditions imposed on the field and its derivative at $z = 0$.

Using the method described the propagation of beams through nonlinear media was numerically modelled for various types of initial conditions. As one of the examples, consider the propagation of an axially symmetric ($m = 0$) beam having the initial profile $E_0(r) = exp(-\eta_0 r^2)$. To make our results comparable with [2] we put $\lambda = 1$, λ being the wavelength, $\Delta z = 0.01$, $n_2 = 0.015$, the initial $1/e$ diameter of the Gaussian beam is 5.0, the initial value of $I_{\max} = 1$. We used up to 60 Gauss-Laguerre modes defined by their values in 60 points, corresponding to zeros of Laguerre polynomials and covering the interval of r^2 from 0 to 202.9. It was shown that nearly 50 modes provide the accuracy of nearly one per cent in reproducing the z-dependence of the on-axis intensity. In Fig. (a) and (b) solid curves show the on-axis intensity versus z for two types of initial conditions imposed on the z-derivative of the modal coefficients $C'_{mj}(0)$. In case (a) we set $C'_{mj}(0) = i\sqrt{\alpha_{mj}^2 + 4\pi k^2 P_{mj}(0)/C_{mj}(0)}C_{mj}(0)$ which provides asymptotically no backward wave at the input. In case (b) $C'_{mj}(0) = 0$, which means that the forward and backward waves have equal amplitudes at the input. Dashed line in Fig.(a) shows the numerically found value of the sum $i\sum_{mj}(C^*_{mj}C'_{mj} - c.c.)$, which may be easily shown to be a rigorous integral of motion in transparent media.

Our analysis have shown that the representation of the total AC field as the sum of forward and backward waves is unambiguous only in the asymptotic sense, namely in the regions far from the self-focus. For the parameters considered in case (a) we observed zero backward wave both before and after the focus. Since the latter is the correct boundary condition, one may conclude that no back reflected wave appears at the focus. If the backward wave is already present for some reason, Fig.(b) shows that its amplitude is not significantly affected while passing the focal region. Hence the results of [2] may be interpreted as the power loss at the absorbing boundary due to wide-angle beam divergence rather than as the manifestation of the backward reflected wave.

This work was supported by the Commission of the European Communities under ESPRIT Contract P9282-ACTCS, EU-Russia Collaboration.

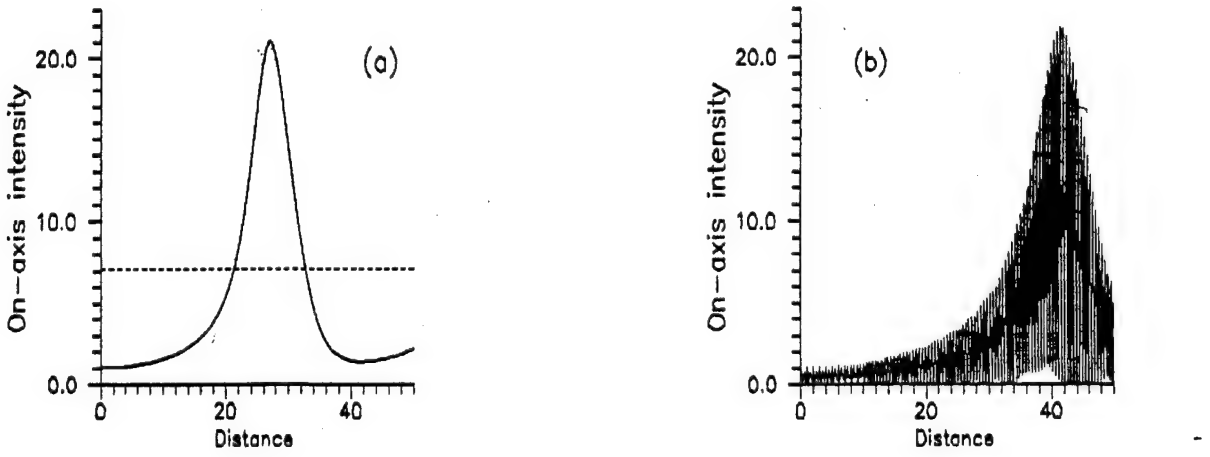

[1] J.H.Marburger. *Progr. Quantum. Electron.*,**4**, 35 (1976)
[2] M.D.Feit and J.A.Fleck, Jr., *J. Opt. Soc. Amer.*, **5**, 633 (1988)
[3] L.A.Melnikov, I.V.Veshneva, and A.I.Konukhov. *Journ. of Chaos, Solitons and Fractals*, **4**, 1535 (1994)

GENERATION OF ULTRASHORT PULSES WITH CONTROLLED ENVELOPE SHAPE AT TRANSIENT DOUBLE RESONANCE IN THE REGIME OF INSTABLE GAIN OF SIGNAL WAVE

Alexey E. Dmitriev, Oleg M. Parshkov, Andrey L. Vershinin
Saratov State Technique University.
77, Polytekhnitcheskaya ul., Saratov,410057, Russia

In the given report one offers the theory of transient double resonance in the medium with inhomogeneously broadening lines of quantum transitions in the field of 2π-pulse of self-induced transparency. Theory is developed on the base of treatment of boundary problem

$$\frac{\partial A}{\partial x} - \frac{\partial A}{\partial w} = i \int_{-\infty}^{\infty} g(\delta)\ \sigma\ d\delta \qquad (1)$$

$$\frac{\partial \sigma}{\partial w} + \left[\tanh w + i\ \frac{\delta_o - \omega_1 \delta_1}{\omega_2} \right] \sigma = - i\ n^2\ \frac{\alpha(\varepsilon_o).\operatorname{sech}^2 w.\ A}{\omega_2^2 + (\delta - \delta_o + \omega_2 \varepsilon_o)^2} \qquad (2)$$

$$A(w, x=0) = \mathcal{F}(w), \qquad \sigma(w=-\infty, x) = 0, \qquad (3)$$

Here A and σ - normalized magnitudes of signal radiation and polarization of medium on signal frequency; w and x - normalized values of time in pump pulse frame and of coordinate along the propagation direction; δ_o, ω_1, ω_2, ε_o - parameters that depends on the frequencies; n - parameter of coupling between the pump and signal transitions;

$$g(\delta) = \frac{T_2}{\tau\sqrt{\pi}} \exp\left[-\left(\frac{T_2}{\tau} \right)^2 (\delta - \delta_o)^2 \right]$$

$$\alpha(\varepsilon_o) = \frac{\omega_2^2 \cdot \tau \cdot \sqrt{\pi}}{T_1} \left\{ \int_{-\infty}^{\infty} \frac{\exp\left[- \left(\frac{T_1}{\tau} \right)^2 (\varepsilon - \varepsilon_o)^2 \right]}{1 + \varepsilon^2}\ d\varepsilon \right\}^{-1}$$

where τ is duration of 2π-pulse; T_1 and T_2 are times of polarization dephasing caused to the Doppler effect.

Analytical solution of (1)-(3) was produced for the cases when one of following simplified suppositions is valid

$$\tau/T_1 = \tau/T_2, \qquad T_1/\tau = T_2/\tau = 0, \qquad \omega_1 = 0 \qquad (4)$$

The analysis of it has shown that at $n > (1+\gamma)/2$ and $x \to \infty$ it

becomes possible to form the stationary mode of p-th order - the pulse of asymptotically stable shape that amplifies exponentially on x wih undimensional gain $G = 2\,(n\text{-}p)\text{-}\gamma\text{-}1$, where p = 0, 1 ... $[n\text{-}(\gamma+1)/2]$. Here γ - parameter depending on the type of selected simplified supposition (4). The mode of p-th order arises as asymptotical solution at $x \to \infty$ only when following p conditions for the input signal pulse shape, $\mathcal{F}(w)$ are meeting

$$\int_{-\infty}^{\infty} \mathcal{F}(w)\,\frac{\exp\,[(2p - n - 2l + \gamma + 1)w]}{\cosh^{n} w}\,dw = 0, \qquad l = 1, 2 \,..\, p \quad (5)$$

When any conditions are failed the process of signal pulse formation is essentially unstable and the mode of p-th order ($p \geq 1$) dominates only on any stage of transient process that ends by the 0-th order mode formation.

To determine the possibility of stationary mode formation and the area of given order mode stability in the case of non-fulfilment of any suppositions in (4) one carries out the numerical simulation of the signal pulse evolution on the base of the equations (1)-(2) with initial condition (3). The results of such modeling for one case are represented in fig.1. The curves 1, 2, 3 in it describe the 1-th order mode but curve 4 coresponds to the 0-th order mode formation that ends the transient process.

To conclude note that shape and duration of stationary modes do not depend on the initial signal pulse shape, $\mathcal{F}(w)$.It permits to make the conclusion that transient double resonance can be applied for the transformation and stabilization of ultrashort laser pulse characteristics.

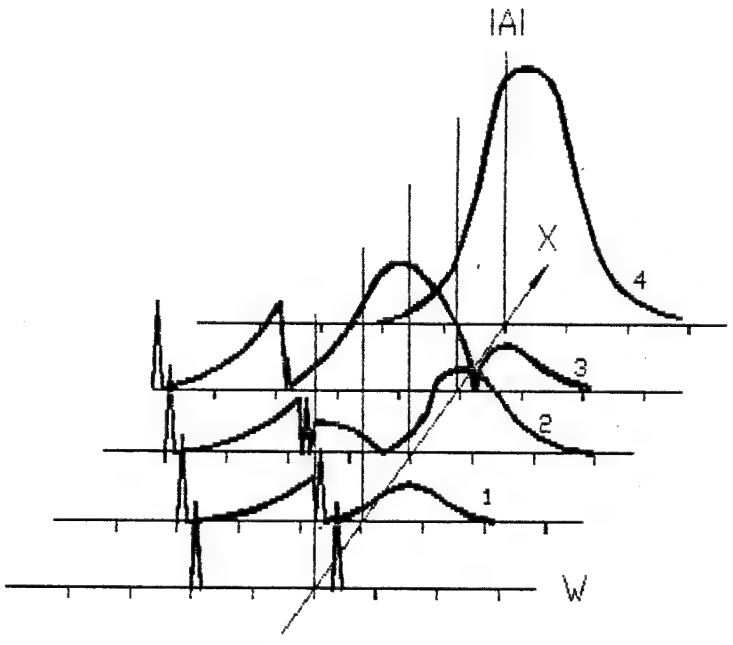

Fig. 1.

RELAXATION OSCILLATION DYNAMICS AND STABILITY OF THE LANG-KOBAYASHI LASER

Thomas Erneux
Université Libre de Bruxelles, Optique Nonlinéaire Théorique,
Campus Plaine, C.P. 231, 1050 Bruxelles, Belgium
Fax:+ 32 2 650 5824 email(TERNEUX@ULB.AC.BE)
and

G.H.M. van Tartwijk, A.M. Levine*, D. Lenstra
Department of Physics and Astronomy, Free University,
De Boelelaan 1081, 1081 HV Amsterdam, The Netherlands
Fax:+ 31 20 444 7899 email(GUIDORT@NAT.VU.NL)

ABSTRACT

Semiconductor lasers are extremely sensitive to external signals. Unwanted optical feedback is the main source of instability and is leading to various forms of chaos. Recently, the physical mechanisms leading to the so-called low frequency fluctuations (LFF) have been studied in detail [1,2]. LFF consist of sudden drops in light intensity each followed by a gradual increase. They have been observed at moderate feedback levels and near the lasing threshold. But little is known on the instabilities that may appear near threshold. This motivates a new analysis of the Hopf bifurcation point above which the intensity becomes pulsating.

A minimal model for a semiconductor laser subject to optical feedback has been proposed by Lang and Kobayashi in 1980 [3]. A basic state corresponding to a single mode periodic solution is known but its stability cannot be found analytically. We propose to determine approximations of the Hopf bifurcation point by taking advantage of two large parameters in the problem. Our analysis differs from previous approximative theories [4] by the fact that we are using a singular perturbation method. The method allows a systematic analysis of the Hopf bifurcation point in terms of all the parameters.

Lang and Kobayashi model is described by two ordinary-delay-differential equations for the complex electrical field Y and the excess carrier number Z. In dimensionless form, these equations are given by

$$Y' = (1 + i\alpha)ZY + \eta\exp(-i\tilde{\Omega}\theta)Y(s - \theta) \qquad (1)$$

$$TZ' = P - Z - (1 + 2Z)|Y|^2. \qquad (2)$$

$T \equiv \tau_n/\tau_p = O(10^3)$ is the ratio of carrier and photon lifetimes. $\theta \equiv \tau/\tau_p = O(10^3)$ is the ratio of the diode cavity round-trip time and the photon lifetime. $P < 1$ is the dimensionless pumping current above threshold. $0 < \eta < 1$ is the amplitude of the feedback. $\alpha \approx 3$-5 is the linewidth enhancement factor. $\tilde{\Omega}$ is the frequency of the solitary laser. The single mode solutions are solutions of the form

$$Y = A_s\exp[i(\Omega_s - \tilde{\Omega})t] \text{ and } Z = Z_s \qquad (3)$$

where A_s, Ω_s and Z_s are constants. These constants are determined in terms of the effective feedback strength C and the feedback phase ϕ_0 defined by

$$C \equiv (1 + \alpha^2)^{1/2}\eta\theta \text{ and } \phi_0 \equiv \bar{\Omega}\theta + \arctan(\alpha). \qquad (4)$$

Figure 1 shows the stability boundaries in (C,ϕ_0) parameter's space. The dotted lines correspond to saddle-node bifurcation points which separate regions of equal numbers of single mode solutions [5]. The full lines correspond to the approximative Hopf bifurcation points found from our analysis which is based on the double limit T large and $\theta = O(T^{1/2})$ large. The condition $\eta > 0$ requires the inequality

$$\cos(\Delta - \arctan(\alpha)) < 0 \qquad (5)$$

where $\Delta \equiv \Omega_s\theta$ is defined as the external cavity mode frequency. We have analyzed (5) for various Δ and have found that a mode close to the maximum gain mode ($\Delta = 0$) is stable because it does not verify (5). This observation is substantiated by independent numerical studies.

Our analysis of the Hopf bifurcation requires separate studies near resonance points and in the low pump limit. Of particular interest is the low pump limit which exhibits a Hopf bifurcation at the lasing threshold.

REFERENCES

* permanent address: The College of Staten Island, The City University of New York, 2800 Victory Boulevard, Staten Island, New York 10314

1. T. Sano, Phys. Rev. A50, 2719 (1994).
2. G.H.M. van Tartwijk, A.M. Levine, D. Lenstra, IEEE, J. Quant. Electron., to appear (1995).
3. R. Lang and K. Kobayashi, IEEE J. Quant. Electr., QE-16, 347 (1980).
4. A. Ritter and H. Haug, JOSA B10, 130 (1993).
5. G.A. Acket, D. Lenstra, A.J. den Boef, and B.H. Verbeek, IEEE J. Quantum Electron., QE-20, 1163 (1984).

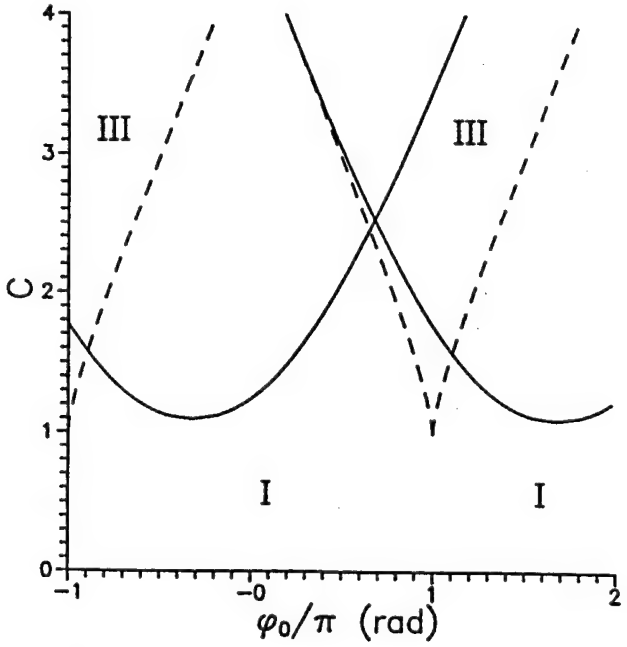

Figure 1. The roman numbers denote the number of solutions. T = 1000, θ = 1092, P = 0.5, α = 4.

AVERAGE SYMMETRIES IN AN OSCILLATOR WITH PHOTOREFRACTIVE GAIN

J. Farjas, D. Hennequin, D. Dangoisse and P. Glorieux
Laboratoire de Spectroscopie Hertzienne
Unité associée au CNRS # 249
Université des Sciences et Technologies de Lille
F-59655 Villeneuve d'Ascq - FRANCE

Oscillators with photorefractive gain (OPG) have been shown to be very convenient to study spatio-temporal dynamics. In particular, defect mediated turbulence has been experimentally evidenced [1]. The defects are here the so-called optical vortices, which are phase singularities of the optical field [2]. Recently, Arecchi et al [1] described the optical turbulence through the statistics of the vortices, and showed the existence of two main regimes: at low Fresnel number $\mathcal{N}_F$, typically $\mathcal{N}_F<10$, the dynamics is governed by the transverse boundaries, while at $\mathcal{N}_F>10$, it becomes intrinsic.

We propose here to use a simpler statistical measure, namely the time average of the patterns, to differentiate the regimes. We use as an indicator the symmetry of the pattern, which is compared to that of the system. In the latter, we separate two contributions: the boundary symmetry σ_b, imposed by e.g. the shape of an iris, and the intrinsic symmetry σ_i, usually cylindrical, but which can be changed by using e.g. a ring cavity with an odd number of mirrors in order to privilege an axis.

Using this method, three types of behavior have been identified. For $\mathcal{N}_F<10$, the averaged patterns are exclusively depending on σ_b. In particular, when only σ_i is cylindrical, the patterns no more exhibit circular structures. For $10<\mathcal{N}_F<100$, σ_i mainly determines the symmetry of the patterns. The shape of the iris affects only its borders while the

center exhibits the σ_i symmetry. Finally, when $\mathcal{N}_F$>100, we are no more able to detect any symmetry in the averaged pattern, except that the borders remain imposed by σ_b.

Thus it appears that through this simple statistical test, it is possible to put in evidence three types of behavior of the OGP, and in particular, for $\mathcal{N}_F$>100, dynamics where the memory of the intrinsic symmetry is lost, probably due to the fact that the transverse instability wavelength becomes smaller than the coherence length of the system.

[1] F. T. Arecchi, S. Bocaletti, P. L. Ramazza and S. Residori, Phys. Rev. Lett. 70 2277 (1993)

[2] P. Coullet, L. Gil and F. Rocca, Opt. Commun. 73 403 (1989)

Polarization competition and transverse effects in sodium vapor

A. Gahl, A. Aumann, J. P. Seipenbusch and W. Lange

Institute of Applied Physics, University of Münster, Corrensstr. 2/4, D-48149 Münster
Tel. +49-251-83 3522, FAX: +49-251-83 3513, e-mail: gahl@nwz.uni-muenster.de

In addition to the transverse effects which occur in Kerr media, a wealth of phenomena can be observed if the nonlinearity of the medium has tensor properties. This is true for sodium vapor, since the creation of ground state orientation is a pronounced nonlinear mechanism which brings the vector properties of the light field into play and may e. g. induce a spatial separation of different polarization components of the light field [1,2]. In a recent paper [2] we have described the experimental observation of self–induced planar and cylindrical splitting of a laser beam into different polarization components in a single transit through sodium vapor and have given evidence that it is a completely deterministic phenomenon.

In this contribution we give additional experimental results some of which are unexpected and counterintuitive. We present further analytic and numerical studies of the beam propagation which are in good qualitative agreement with the observations. We also discuss the physical principles underlying the results.

One of the striking experimental results is the observation that the total power of a laser beam transmitted by sodium vapor in a nitrogen atmosphere can strongly decrease with increasing input power in a certain parameter range (see Fig. 1a). The phenomenon occurs on the self–focusing side of the D_1–line. It is observed that the sudden decrease is coupled with a strong change in the transmitted beam profile which displays a spatial splitting into right– and left–hand circularly polarized components (see Fig. 1c – 1e) in the same parameter range. It should be noted that the position of the spots is nonlinearly shifted in Fig. 1c to 1e.

In [2] we have presented a model which treats the sodium atoms as two–level atoms with two–fold spin–degeneracy. It includes Zeeman pumping and the presence of the light–shift phenomenon of the atomic sublevels as the important features of the atomic interaction with the light field. In small magnetic fields light–shift induced level crossings can occur which have strong impact on the optical properties of the sample and introduce intensity–dependent contributions to the refractive index whose spatial distribution is not washed out by atomic diffusion. These level crossings are the origin of a very pronounced dependence of the system on the magnetic field. Using this microscopic description of the medium we compute the propagation of the light field by means of a split–step FFT beam–propagation method.

In the interpretation of the numerical results most of the observations find a physical explanation based on the idea of a competition between different polarization components. Also the result displayed in Fig. 1a can be reproduced qualitatively in the calculations (Fig. 1b).

Another counterintuitive result is presented in Fig. 2 for an experimental situation in which the cylindrical symmetry is conserved. In the case of an elliptically polarized input beam, experimental parameters exist (e. g. those of Fig. 2b) that make the initially weaker circular component become the stronger one at the end of the sodium cell. Fig. 2a, which has been obtained analytically, predicts a certain range of the external longitudinal magnetic field that allows the on–axis concentration of the initially weaker σ_-–component. Since the *intensity* in the σ_-–spot is larger than the one in the wide σ_+–ring (see Fig. 2b), the σ_-–component is less absorbed during the propagation and finally also the *power* in the σ_-–component is larger. When the longitudinal component of the magnetic field is variied, ring structures are observed (see Fig. 2b, c) which agree with the order predicted by the analytic treatment.

[1] A. C. Tam, W. Happer, Phys. Rev. Lett. **38**, 278 (1977)
[2] A. Gahl, J. P. Seipenbusch, A. Aumann, M. Möller, W. Lange, Phys. Rev. **A50**, R917 (1994)

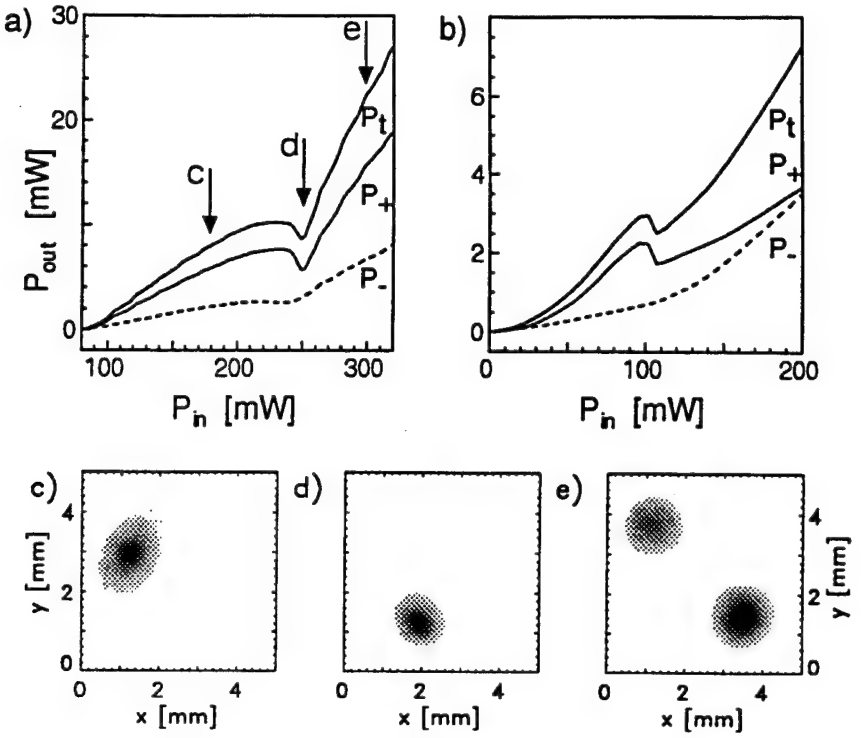

Fig. 1: a) Transmitted power vs. input power. P_t: total power, $P_\pm$: power of $\sigma_\pm$–component.
b) Numerical simulation using control parameters similar to the experimental ones.
c – e) Intensity distribution on the CCD–camera at input power levels indicated by c,d,e in Fig. 1a. The upper left spot in Fig. 1e is σ_- polarized, the others are σ_+ polarized.

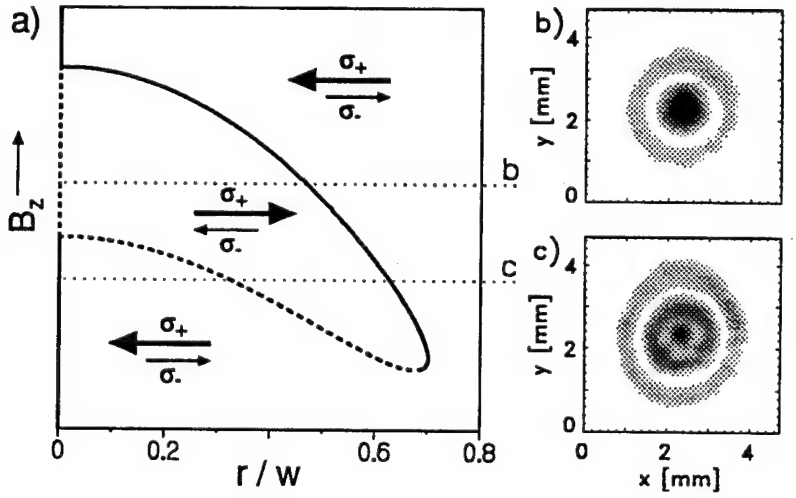

Fig. 2: a) Position of local extrema of the ground state orientation as a function of the radial position r/w in dependence on the longitudinal magnetic field B_z. The bold/dashed lines indicate a maximum/minimum for an initially elliptically polarized gaussian beam with weaker σ_-–component. During the propagation the resulting gradient of the refraction index causes a transverse flow of the $\sigma_\pm$–intensity as denoted by the arrows. From a cut along the line "b" a σ_-–polarized central spot and a σ_+–polarized ring are expected, from a cut along "c" a σ_+–polarized central spot surrounded by a σ_-– and a σ_+–polarized ring.
b, c) Intensity distribution on the CCD–camera for two values of B_z. Polarisation of the central spot in b) and the inner ring in c) is σ_-, while the ring in b) and the central spot and the outer ring in c) are σ_+–polarized.

Dynamical memory function of a hybrid bistable device with delayed feedback self-control of chaos

Jin-Yue Gao, Ying Zhang, Zhi-Ren Zheng
Physics Department, Jilin University,
Changchun, Jilin 130023, China

FAX: 86-431-892-3907
E-mail: JYGAO@JILIN.IHEP.AC.CN

Dynamic chaos is a very interesting nonlinear effect which has been intensively studied during the last two decades. The effect is very common, it has been detected in a large number of dynamic systems of various physical nature. In practice, however, this effect is usually undesirable. Many researchers have been interested in controlling undesirable chaos and applying chaos. Ott, Grebogi and Yorke [1] (OGY) have suggested an efficient method of chaos control that can eliminate chaos. Pyragas [2,3] proposed two new methods, external force control and delayed feedback self-control, to control chaos. We apply the method of delayed feedback self-control of chaos to dynamic memory of an electro-optical bistable device, A binary code data have been written to and read from this system. The mathematical description of this system can be summarized by the following simple-looking delayed differential equation [4]:

$$dV(t)/dt+V(t)=0.5Y\{1-K\cos[V(t-T)+\theta]\} \qquad (1)$$

for the feedback voltage or the output intensity V(t) applied to the modulator. In Eq. (1), Y is the input intensity, and the time t and the delay T are both measured in units of the system's natural relaxation time. In turn, θ denotes a fixed bias voltage applied to the modulator in units of the half-wave voltage, and K is the extinction coefficient of the device. Eq. (1) links the input and the output intensity signals and describes the steady state transmittance when dV/dt=0.

Ikeda et al. have clarified the bifurcation structure of the oscillation modes of a similar delayed feedback system and suggested potential applicability as a memory device, utilizing the multistable modes of oscillation [5]. Following this suggestion, Davis et al. proposed a method called seeded bifurcation switch [6] , in which dynamical storage was carried through the system being switched frequently between the bifurcation region and reverse bifurcation region. A similar system was studied by Gao et al [7], and up to 51 binary code has been demonstrated.

Based on the previous works, we proceed the idea of self-control of chaos into the dynamical memory device, so that memory function can be completed in one developing chaos region only, and the experimental setup is simplified. We have completed writing binary data to the following experimental system and the results are coincident with computer simulation. A

3mw He-Ne laser was used as the input source; it was modulated by a $LiNbO_3$ crystal with an electric field applied perpendicularly to the direction of propagation of the incident light beam. The input intensity was monitored by a detector D_2 and was partially transmitted through a second $LiNbO_3$ modulator whose applied voltage consisted of the sum of a fixed bias and the output of the feedback loop. The feedback signal itself was produced by a photomultiplier and two amplifiers, and could be delayed by a Z-80 microprocessor which was connected with a NEC personal computer for data injection and recording. The behavior of the output intensity was monitored by an oscilloscope.

In our experiment, the open loop relaxation time of the system is 0.15±0.02ms. With delay time T_r=7.3±0.2ms in Z-80 microprocessor, we introduce self-control of chaos into the process loop, and tuned the input intensity and bias voltage until a chaotic oscillation waveform in order 2 inverse bifurcation region of chaos was observed on the oscilloscope. The "write" procedure is done as follows. We generated one of (n, m=2) oscillation patterns in order 2 period doubling bifurcation region in NEC computer with two different peaks and two different valleys. This peak and valley values are the same as the corresponding values in (n=1, m=2) oscillation waveforms which can be read from Z-80 microprocessor by the NEC computer earlier before the "write" signal was produced. The "write" oscillation patterns with one delay time length and arbitrary n element binary code was injected from NEC computer to Z-80 as seed signal. After code injection, the system shows order n harmonic chaotic oscillation and the waveforms transits continuously among (n, m=2) class. when desired n element binary coded waveform emerges, we keep it in the system by completing the loop of controlling-chaos in time. The n-bit binary coded data was written into the memory, and the oscillation patterns with n-bit binary coded waveform can be seen on the oscilloscope and can be recorded in NEC computer through Z-80 microprocessor.

Because of the instabilities and noise from the amplifiers and detector, the steady working regions of input intensity for (n, m=2) class is very limited, the regions for higher order harmonics (larger n) are even small. We are going to stabilize the coded waveforms more and identify the phase of the different oscillation patterns by an external reference clock, so that higher stable harmonic could be used and more binary information signals could be "write" into and read out from the memory device.

References

[1] E. Ott, C. Grebogi, Y. A. Yorke, Phys. Rev. Lett. 64, (1990)1196.

[2] K. Pyragas, Phys. Lett. A 170, (1992) 421.

[3] K. Pyragas, Phys. Lett. A 180, (1993) 99.

[4] J. Y. Gao, J. M. Yuan and L. M. Narducci, Opt. Commun. 44, (1983) 201.

[5] K. Ikeda and K. Matsumoto, Physica 29D, (1987) 223.

[6] T. Aida and P. Davis, IEEE J. Quantum Electronics 28,(1992) 686.

[7] J. Y. Gao, J. H. Huang, Z. R. Zheng, Optical Engineering, March(1995).

Fast switching unstable orbits in periodically driving laser

V.A.Gaysenok, E.V.Grigorieva
Department of physics, Belarus State University, 220050 Minsk, Belarus, e-mail:root@mfp.bsu.minsk.by
S.A.Kashchenko
Department of mathematics, Yaroslavl State University, 150000 Yaroslavl, Russia, e-mail:uni@cnit.yaroslavl.su

Abstract

Theory to find periodic unstable orbits due to large perturbations is given for class B laser systems. The method allows to determine nonlocal organization of phase space, in particular,boundaries of attractive basins of attractors and stable manifold of repellers.

Recently the different algorithms have been developed for dynamical chaos control in nonlinear systems. In [1,2] specific targeting of unstable periodic orbits has been achieved experimentally by using large amplitude perturbations in CO_2 laser with intracavity modulated losses. Contrary to the small perturbation control methods , the last technique allows to obtain both unstable orbits embedding inside the basin of attractor (as a result of period doubling bifurcation) and unstable orbit created by saddle-node bifurcation of coexisting attractors.

It would be useful for such purposes to know global construction of phase space . Here we present the analytical approximation of Poincare mappings for class B lasers with periodic modulation of intracavity losses or pumping rate. The method allows:

- to found key points for reconstruction of both stable and unstable limit cycles (repellers);
- to determine the main characteristics of multistable periodic attractors, in particular amplitude of oscillations, period, energy of pulse and average energy of nonstationary process in dependence on driving frequency ;
- to found threshold conditions on creation of regimes with periods multiple driving period, i.e. conditions for saddle-node bifurcations;
- to obtain analytically instability threshold via period doubling bifurcation;
- to calculate analytically the direction of stable manifold of the repeller using the values of its multiplicators;
- to give the recipe to reach targeting unstable orbit, i.e. the amplitude and optimum timing of additional losses perturbation following the experimental technique of [1].

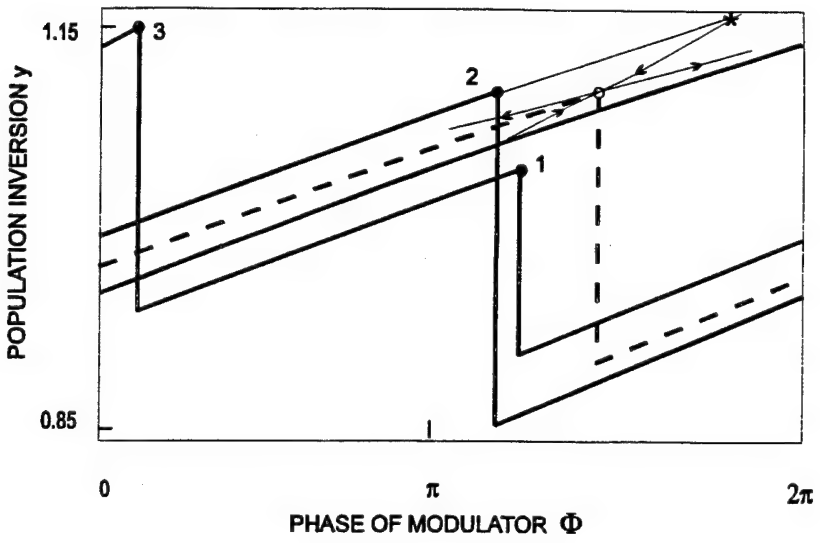

The example of three-points attractor of the mapping is present in fig.1. It is identical with $3T$-periodical window in chaos. The right black point 1 corresponds to the start of a middle pulse, point 2 - to the start of a small pulse and point 3 - to the start of a big pulse. Arrows denote the directions of stable and unstable manifolds of the repeller. The last one is presented by white point. We can calculate the value of additional losses perturbation to move to move $(c_2, \phi_2) \rightarrow (c_*, \phi_*)$ denoted by $*$. The timing of optimum perturbation should be chosen between small and big pulses to reach the stable manifold of the repeller.

We also take into account small external illumination, impurities with saturable absorption , and small optical delayed feedback. The phenomenon of quasiperiodisity is shown analytically for such systems.

The possibilities of controlling unstable orbits by small coupling periodic perturbation and by small external feedback are discussed on the base of mapping dynamics.

1. V.N.Chizhevsky, P.Glorieux, Phys.Rev.E, Oct.-Nov.(1994).
2. V.N.Chizhevsky, S.I.Turovets, Phys.Rev.A 50 (1994) 1340.

Nonlinear Optical Response of Layered Composite Materials

Russell J. Gehr,[1] George L. Fischer,[2] Robert W. Boyd,[1] J. E. Sipe[3]

[1]Institute of Optics, University of Rochester, Rochester, New York 14627

[2]Department of Physics and Astronomy and Institute of Optics, University of Rochester, Rochester, New York 14627

[3]Department of Physics, University of Toronto, Toronto, Ontario M5S 1A7, Canada

The nonlinear optical properties of composites materials are of current interest, since composites can exhibit enhanced nonlinear response. We have analyzed previously the second- and third-order nonlinear susceptibilities of layered composites under the assumption that the layer thicknesses are much smaller than an optical wavelength and have found that significant enhancement is possible under certain circumstances: namely, the constituent with the larger nonlinear response must have the lower linear index of refraction and the light must be polarized normal to the layers. [1] The enhancement takes the form of local field correction factors in the expression for the susceptibility. Note that the effective medium of the composite is uniaxial, with the optic axis oriented normal to the layers.

We have constructed layered composites from titanium dioxide and the conjugated polymer poly (p-phenylenebenzobisthiazole) (PBZT) by spin casting alternating layers 500 A and 400 A thick, respectively. The fill fraction of the PBZT was thus 44%, which was nearly ideal given the relative linear refractive indices of the two constituents. According to the theory [1] we expect an effective third-order susceptibility 35% larger than that of PBZT.

To determine the value of $\chi^{(3)}$ of our samples, we performed z-scan measurements with the samples tilted with respect to the beam axis. For p-polarized light incident on the samples, there was a component of the electric field normal to the layers. This component

Gehr: Phone: (716) 275-5030, Fax: (716) 244-4936
email: gehr@optics.rochester.edu

experienced the enhanced nonlinear susceptibility. The data from the experiments [2] consisted of the nonlinear phase shift acquired by the laser beam versus the sample angle.

The analysis of this data required a new theoretical formalism determining the nonlinear phase shift acquired by a laser beam in passing through a uniaxial material oriented at an arbitrary angle with respect to the beam. We have developed a solution to this problem based on a Green function formalism, similar to one reported previously. [3] We will present the theory and the subsequent analysis of our experimental data. The good agreement found indicated that the model is accurate. (See figure 1.)

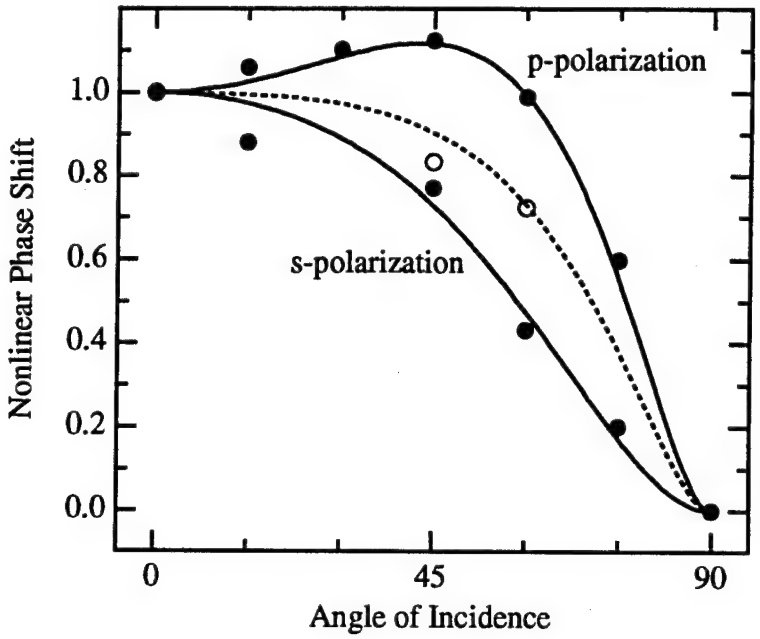

Figure 1: Theory and experimental data for s- and p-polarized light at various angles of incidence. The dashed curve represents the theory without local field enhancement of the nonlinear susceptibility and the open circles represent data for pure PBZT.

1. R. W. Boyd and J. E. Sipe, J. Opt. Soc. Am. B **11**, 297 (1994).

2. G. L. Fischer, R. W. Boyd, R. J. Gehr, J. E. Sipe, S. A. Jenekhe, J. A. Osaheni, L. A. Weller-Brophy, Phys. Rev. Lett. **74**, 1871 (1995).

3. J. E. Sipe, J. Opt. Soc. Am. B **4**, 481 (1987).

"HOT" RECONSTRUCTION OF MODES AND RELAXATION OSCILLATIONS OF SOLID-STATE LASERS

A.V.Ghiner

Universidade Federal do Ceara, C.P.6030, CEP 60450-970, Fortaleza CE, Brazil
fax 55(85)2434138,e-mail ghiner@fisica.ufc.br

A mode's competition due to spatial hole burning effect (SHB) is a reason of nontrivial nonlinear dynamical properties of solid-state lasers [1]. From the other hand the nonstationary generation of such kind of lasers is a low - damping process due to fact that the relaxation rate γ of the inverse population $N(\vec{r},t)$ much less then inverse lifetime of the photon in cavity $\sigma_j(\vec{r})$. In such situation it is essential in theory to obtain the exact results because in principle any approximations may change qualitatively the conclusion about stability of the stationary state of laser.

To push forward the problem of stability of stationary generation the analogy of Boltzman H-theorem was derived in general suppositions for multimode rate equations taking into account the SHB-effect [2]:

$$\frac{d}{dt}\left[\frac{1}{2}\int\frac{(\Delta N)^2}{N_S}d^3\vec{r}+\sum_j\left(M_j-M_{jS}-M_{jS}\ln\frac{M_j}{M_{jS}}\right)\right]=-\int\frac{(\Delta N)^2}{N_S}\left(\gamma+\sum_j D_j M_j\left|\vec{U}_j\right|^2\right)d^3\vec{r}$$

Here $M_j(t)$ is the intensity of mode with number "j", D_j is Einstein coefficient of induced radiation and $\vec{U}_{jS}(\vec{r})$ is a spatial eigenfunction of j-th mode. Indice "S"denotes the stationary values of magnitude, $\Delta N(\vec{r},t)=N(\vec{r},t)-N_S(\vec{r})$. It was shown that SHB-effect leads not only mode's competition in frame of usual rate equations but produces some kind of "hot" reconstruction of the mode's structure of the laser [3]. As a result some additional term appears in right-hand side of the eq.(1).

$$\Delta F=\sum_j\int\left[M_j\left(D_jN_S-\sigma_j\right)-M_{jS}\left(D_jN-\sigma_j\right)\right]\left(\left|\vec{U}_j\right|^2-\left|\vec{U}_{jS}\right|^2\right)d^3\vec{r} \qquad (2)$$

Here $\sigma_j(\vec{r})$ is the cavity losses, $\vec{U}_j(\vec{r},t)$is the eigenfunction of j-th mode of "hot"cavity. So the problem of the stability of stationary solution arises again. Now we could calculate

the "hot" reconstruction by expansion of the $\vec{U}_j(\vec{r},t)$ on the set of eigenfunctions $\vec{U}_{Ck}(\vec{r})$ of the "cold" $(N=0,\sigma=0)$ cavity:

$$\vec{U}_j = \vec{U}_{Cj} + \sum_{k\neq j} \frac{1}{\omega_j - \omega_{Ck}} \left[\sigma_{jk} - \left(1 + \frac{\omega_j - \omega_0}{\Gamma} \right) \nu_{jk} \right] \vec{U}_{Ck} \qquad (3)$$

Here $\sigma_{jk} = \int \sigma_j \vec{U}_{Cj} \bullet \vec{U}_{Ck} d^3\vec{r}, \nu_{jk} = \int D_j N \vec{U}_{Cj} \bullet \vec{U}_{Ck} d^3\vec{r}$, ω_j is the frequency of j-th mode of the "hot" cavity, ω_{Ck} is the frequency of k-th mode of the "cold" cavity, ω_0 is the frequency and Γ is the linewidth of the atomic laser transition (the expression (3) holds true under conditions that $\sigma_{jk}(\omega_j - \omega_{Ck})^{-1}$ and $\nu_{jk}(\omega_j - \omega_{Ck})^{-1}$ both are much less then unity). So one can rewrite the expression (2) by such a way:

$$\Delta F = 2\sum_j \frac{\omega_j - \omega_0}{\Gamma} \left[M_{jS} \sum_{k\neq j} \frac{(\nu_{jk} - \nu_{jkS})^2}{\omega_j - \omega_{Ck}} + (M_j - M_{jS}) \sum_{k\neq j} \frac{(\nu_{jk} - \nu_{jkS})(\nu_{jkS} - \sigma_{jk})}{\omega_j - \omega_{Ck}} \right] \qquad (4)$$

One can see that under neglecting of the detuning $(\omega_j - \omega_0)\Gamma^{-1}$ there is no any influence of the "hot" mode's reconstruction on the stability of the stationary generation. With the taking into account this factor to obtaine the rough condition of stability we can compare ΔF with the right-hand side of eq. (1). For generation close to the center of the line it leads to inequality $\gamma \cdot \Gamma > \sigma^2$. So one can conclude that "hot" reconstruction of the mode structure doesn't violate the stability and uniqueness of the stationary state of the solid-state laser in the case of good quality cavity and generation close to the center of line.

The possibilities of the existence of bistability and instabilities of the stationary generation outside the frames of mentioned conditions are discussed.

1.Ya.I.Khanin, Dynamics of Lasers, Sov. radio, Moscow, 1975

2.A.V.Ghiner, K.P.Komarov, K.G.Folin, Opt.Comm.,**19**,350(1976)

3.A.V.Ghiner, K.G.Folin, Dynamics of Free Generation of Solid-State Lasers, "Nauka", Novosibirsk, 1979

High-order spatial mode bifurcations in nonlinear interferometer with delayed feedback

E.V.Grigorieva
Department of physics, Belarus State University, 220050 Minsk, Belarus, e-mail:root@mfp.bsu.minsk.by
S.A.Kashchenko
Department of mathematics, Yaroslavl State University, 150000 Yaroslavl, Russia, e-mail:uni@cnit.yaroslavl.su

Abstract

The properties of different spatial structures in nonlinear resonator with spatial transformer in feedback are investigated. The parameter regions, amplitudes and rotation frequency of complex optical reverberators are determined on the base of normal form theory. High-order spatial mode bifurcation results multistability of neutral stable travelling waves . The direction of their evolution are obtained by second normalization procedure.

Recently different types of instability of a light field were observed by controlling the spatial scale and the topology of the transverse interactions of light fields in a medium with cubic nonlinearity, in particular rotating patterns and optical turbulence [1-3].

The mathematical description of these phenomena is based on parabolic equation with a retarded argument:

$$\frac{\partial u}{\partial t} + u = D\frac{\partial^2 u}{\partial \theta^2} + K\sin[u(t, \theta - \Delta)]$$

and periodic boundary conditions:

$$u|_{\theta=0} = u|_{\theta=2\pi}, \ \frac{\partial u}{\partial \theta}|_{\theta=0} = \frac{\partial u}{\partial \theta}|_{\theta=2\pi},$$

where u is the phase shift of the field in the medium, K is proportional to input intensity of light, θ is the angle coordinate, Δ is an effective diffusion coefficient. The equation corresponds to experimental situation when the light beam has the form of a thing light.

In this communication the existence of different structures (slowly and fast oscillating ones) are shown on the base of normal forms theory. Some important cases must be distinguished in dependence on peculiarities of stability destruction for finite and small values of diffusion D and rotation shift Δ (i.e. local and large-scale transverse interactions).

Finite D and Δ. There are four situations when the critical conditions are valid for the different numbers (from one to six) of spatial modes. Then

there are finite-dimensional manifolds on which the local dynamics of (1) is determined by universal normal form. The main characteristics of travelling waves (optical reverberators) and mode beating corresponding complex spatio-temporal patterns are obtained.

Small D and Δ. Slowly oscillating spatial structures occur if radius of light ring is large (diffusion is small) and rotation shift Δ is close to rational number multiple π. Here the central manifold with infinite dimension takes place. If odd modes are existed only then we get quasi-normal form :

$$\frac{\partial z}{\partial s} = (1 + \frac{\Delta_1^2}{2})\frac{\partial^2 z}{\partial \theta^2} - p_1 z - (\frac{1}{6} + \frac{u_0^2}{4})z^3.$$

with antiperiodic boundary conditions.

The conditions of realization of different stable states and spatial inhomogeneous and slowly rotating in time solution are obtained. The frequency of the last one is proportional to the small factor of diffraction and amplitude tends to "step".

Small D and small Δ. The fast oscillating patterns are formed by the set of high-order spatial modes with wave numbers close to $D^{-1/2}$. Quasi-normal form presents the dynamics of travelling waves with neutral stability. The second normalization leads to normal equation:

$$\frac{\partial \xi}{\partial s} = \frac{\partial^2 \xi}{\partial \Theta^2} + \frac{\partial \xi}{\partial \Theta}(A_1 + iA_2) + (B_1 + iB_2)\xi + (C_1 + iC_2)\xi \mid \xi \mid^2,$$

with periodic boundary conditions. Here $s = Dt$ is slow temporal variable, $\Theta = \theta - \sqrt{D}t(-\delta p \cos(S\delta))$ - travelling angle variable.

The obtained equation describes the phenomenon of multistability and determines the evolution direction of travelling waves under change of the 2nd-order infinitesimal parameters. In particular, infinite process of creation and destruction of spatial structures takes place as geometrical size of system is increased infinitely.

The quasi-normal forms are universal for the same critical cases with infinite dimension in different systems and determine the universal roads of self-organization.

1. S.A.Alhmanov, M.A.Vorontsov. In "Nonlinear waves. Dynamics and evolution." Moscow, 1989.
2. S.A.Akhmanov, et.al. JOSA B 9 (1992) 78.
3. S.A.Kashchenko. Sov.J. of Num.Math. and Math.Phys. 31 (1991) 467.

Polarization instabilities in lasers with weakly anisotropic cavities

V.G. Gudelev, L.P. Svirina and Yu.P. Zhurik

Institute of Physics, Academy of Science of Belarus,
70 Skaryna Avenue, Minsk 220072, Belarus
Fax: 007(0172) 393131
E-mail:ifanbel%bas03.basnet.belpak.minsk.by@demos.su

The nonstationary behaviour of polarization parameters without any time-dependent external influence (polarization instability) was observed experimentally in single-mode He-Ne [1,2] and He-Xe [2] lasers at $j_1 = 1 \rightarrow j_2 = 2$ transition and linear phase anisotropy of the cavity as well as in He-Ne [3] laser at $j_1 = 1 \rightarrow j_2 = 1$ transition and circular phase anisotropy of the cavity.

On the basis of the proposed mathematical model [4] we have studied in details the influence of the active medium and empty cavity anisotropies, as well as the longitudinal magnetic field on polarization instability phenomenon.

According to the theoretical predictions this phenomenon has been observed experimentally in He-Ne ($\lambda = 1.15\mu m$) laser at elliptical orthogonal eigenstates of the empty cavity with not too large values of ellipticity.

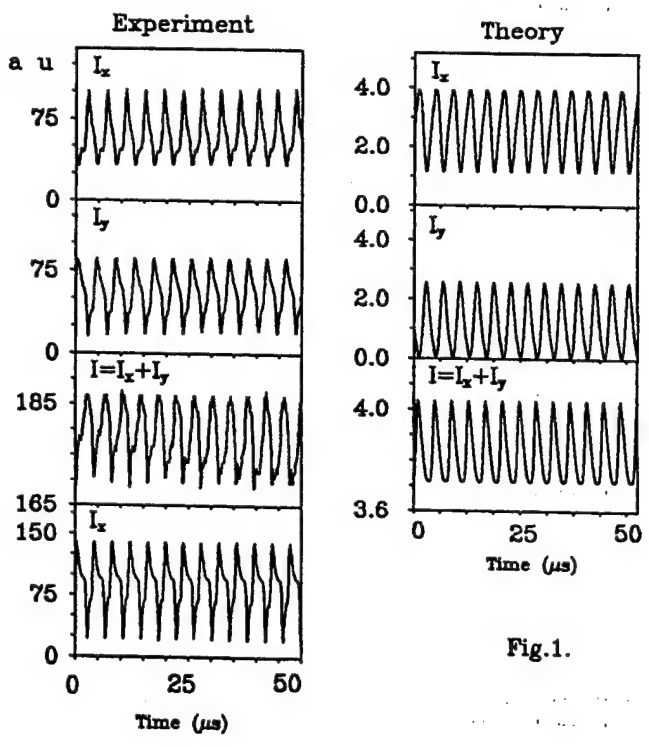

Fig.1.

Periodic oscillations of two qualitatively different forms, represented in terms of xy components of the intensity of two standing waves in Fig.1 and Fig.2, have been found. The first of them occurs near the Hopf's bifurcation point. The second solution has been observed at the line center tuning when the frequency difference between the emitted waves is decreased, or at the detuning from the line center.

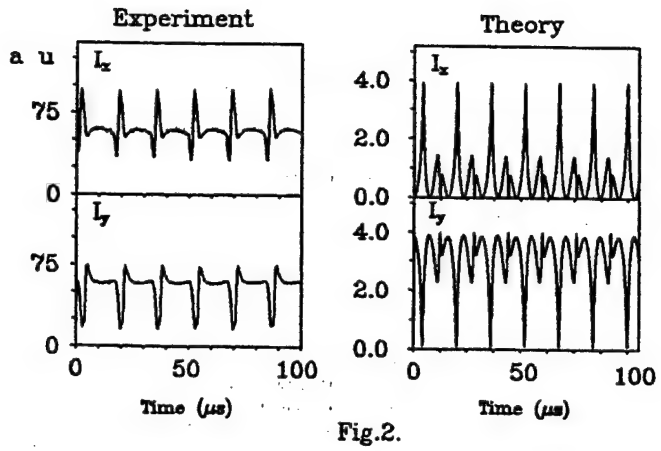

Fig.2.

Polarization instability in the system under consideration is very much the same as it is at linear orthogonal eigenstates of the empty cavity, observed in [2] in He-Ne ($\lambda = 3.39\mu m$) laser.

In the vicinity of the line center tuning the transition between two stationary orthogonal elliptically polarized waves has been observed, which occurs through the region of tunings with polarization instability. Analogous polarization behaviour has been found in [1] and [3] at linearly and circularly polarized eigenstates of the empty caviy, respectively.

It has been shown also that polarization instability phenomenon in a single-mode gas laser with weakly anisotropic cavity exists whilst the empty cavity or the external field anisotropy changes the active medium eigenstates, or in other words, the scheme of connection of atomic sublevels, which forms the state of polarization of the emitted radiation. So, this phenomenon, according to the predictions of [2], could be considered as the exhibition of the dynamics of atomic variables. It can be found in other laser systems at comparable in value active medium and empty cavity or (and) external field anisotropies.

The research described in this publication was made possible in part by Grant N RWVOOO from the International Science Foundation.

References

1.A. Le Floch, G.Ropars and J.Lenormand. *Phys. Rev. Lett.* Vol.52 (1984) 918.

2.G.P. Puccioni, G.L. Lippi , N.B. Abraham and F.T. Arecchi. it Optics Commun. Vol.72 (1989) 361.

3.J.C. Cotteverte, F.B. Bretenaker and A. Le Floch. *Optics Letters.* Vol.16 (1991) 572.

4.L.P. Svirina. *Optics Commun.* Vol.111 (1994) 370, *Optika i Spectroscopiya* Vol. 77 (1994) 124.

Mixed period-two and fixed-point attractor in degenerate optical parametric oscillations

M. Haelterman[1] and M. D. Tolley[2]
Service d'Optique Théorique et Appliquée[1], Service de Mathématique[2]
Université Libre de Bruxelles, 50 Av. F. D. Roosevelt, CP194/5
tel: +32 2 650 4494, fax: +32 2 650 4496, E-mail: mhaelter @ulb.ac.be

In recent years, significant improvements in crystal quality, laser sources, and cavity designs have led to the development of optical parametric oscillators (OPO's) operating in the continuous-wave regime with thresholds as low as a few milliwatts.[1] Such thresholds have been made possible thanks to drastic cavity loss reduction (overall loss of 0.1% leading to finesse of up to 6000 has been recently reported).[2] Besides their practical interest, the high finesse OPO's are attractive for the study of nonlinear dynamics.[1] In particular, since they operate with low internal intensities (i.e., weak pump depletion over each cavity round-trip), they can be described by the mean-field theory which predicts a variety of complex behaviors such as self-pulsing, period-doubling cascades, and chaos.[3]

The aim of our communication is to present a new remarkable dynamical feature of the high finesse OPO. We deal here with the particular case of second harmonic generation. Instead of considering the situation which is relevant to the application of the mean-field theory (i.e., both fields near resonance), we study the case where the pump field is tuned between two cavity resonances. This is the situation in which Ikeda instability occurs when considering a Kerr medium in the cavity.[4] Owing to the Kerr-like nonlinear phase changes in the pump field resulting from the cascaded second order nonlinearity, we can expect that Ikeda-type instabilities will also occur in the off-resonance OPO.

We treat this problem by means of the procedure we developed in ref.[4] for the Kerr nonlinearity. The propagation equation together with the resonator boundary conditions yield the following four dimensional map

$$E_1^{n+1}(0) = T_1 S + R_1 E_1^n(L) \exp(ik_1 L) \qquad (1.a)$$

$$E_2^{n+1}(0) = R_2 E_2^n(L) \exp(ik_2 L) \qquad (1.b)$$

where E_1 and E_2 are the pump and signal amplitudes in the cavity, S is the input pump amplitude, T_i and R_i are the transmission and reflexion coefficients of the cavity input coupler (see fig.1) and L is the cavity length. Assuming phase-matching ($k_2 = 2\,k_1$), $E_1(L)$ and $E_2(L)$ are given by integration of the normalized propagation equations $dE_1/dz = i\,E_1^* E_2$ and $dE_2/dz = i\,E_1^2$ over a cavity round-trip. In order to study Ikeda-type instability, we assume that the pump field is tuned between two cavity resonances, i.e., $k_1 L = (2m+1)\pi - \delta$ where δ is the linear phase detuning (we assume $\delta << 2\pi$). If the coupling coefficients T_i and R_i are real, the phase matching condition implies that the signal field is close to resonance [$k_2 L = 2(2m+1)\pi - 2\delta$]. This is the situation we consider here. As in the mean field theory of ref.[3], we assume weak pump depletion over one round-trip. This allows us to integrate the propagation equations in a first order approximation which yields[5] $E_1(L) = E_1(0) + iL\,E_1^* E_2$ and $E_2(L) = E_2(0) + iL\,E_1^2$. Introducing these

expressions into the map (1) and applying a first order expansion in terms of the cavity losses T_i and detuning δ, we get a simplified algebraic map from which it it easy to calculate the fixed-point (P1) and period-two (P2) attractors. Straightforward calculations reveal the existence of a period-doubling bifurcation (onset of Ikeda instability) characterized by P2 oscillations in the pump field while the signal field remains on a fixed-point attractor. The amplitude of the signal on this fixed-point, $E_2^n = E_2^{n+1}$, is given by

$$E_2^n = E_2^{n+1} = \frac{iL}{T_2^2 + 4i\delta}\left[(E_1^n)^2 + (E_1^{n+1})^2\right] \qquad (2)$$

Fig.2 shows this peculiar mixed P1-P2 attractor as calculated from the map (1). We verify the validity of the approximate algebraic expression (2) with an accuracy of the order of 3%. Note that with the map (1) the degeneracy in the signal field predicted by (2) is slightly broken. We observe two close but separate lines (the separation being only of a few percents). As expected, the accuracy of eq.(2) decreases for higher values of the losses.

In conclusion, our analysis reveals that off-resonance OPO's exhibit an Ikeda-type instability characterized by a mixed P1-P2 attractor which constitutes a remarkable example of self-organized behavior in a two-mode nonlinear system.

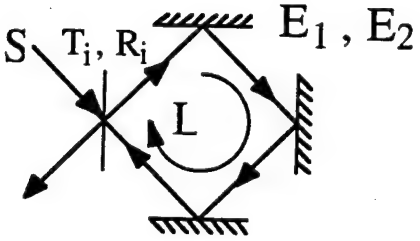

Fig.1 Schematic of the OPO cavity. We consider a monolithic ring design analogous to that of ref.[2]

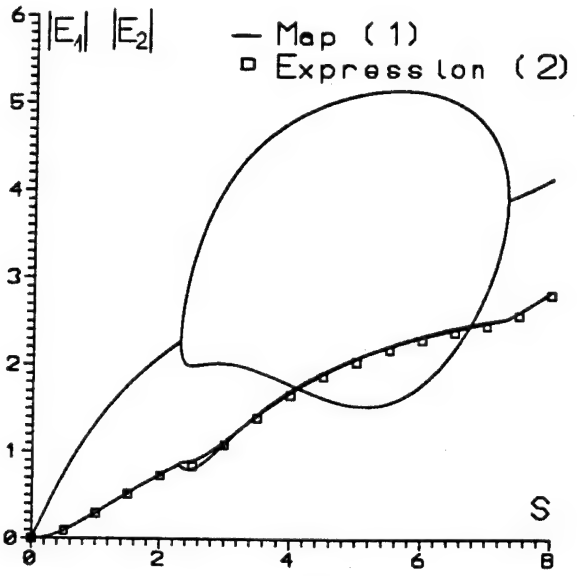

Fig.2 Pump and signal field amplitudes $|E_1|$ and $|E_2|$ versus input pump amplitude S with T1 = T2 = 0.25 and $\delta = 0.1$.

References

[1] J. Opt. Soc. Am. B 10, 1655, Special Issue on Optical Parametric Oscillation (1993).
[2] R. L. Byer et al., Opt. Lett. 19, 1046 (1994).
[3] C. M. Savage and D. F. Walls, Opt. Acta 30, 557 (1983).
[4] M. Haelterman, Opt. Commun. 100, 389 (1993).
[5] T. Debuisschert et al., J. Opt. Soc. Am. B 10, 1665 (1993).

Dynamical Evolution of Four-Wave-Mixing Processes in an Optical Fiber

D.L. Hart and R. Roy
Georgia Institute of Technology
Atlanta, GA 30332
Office: 404-853-0027 Fax: 404-853-9958
Internet: darlene@socrates.physics.gatech.edu

Two waves at different frequencies copropagating through a fiber can generate sidebands at new frequencies due to nonlinear interactions in the fiber medium. Earlier investigations, using short lengths of fiber (1-2m), found good agreement between experimental measurements and theoretical predictions.[1,2] A conservation law, derived from theoretical models, for the asymmetry between the pumps and sidebands, has been experimentally verified for short fiber lengths.[2,3] Here, we report the results of both theoretical and experimental investigations of the nonlinear dynamics of four-wave mixing (FWM) processes along a long optical fiber. Experimental measurements of the dynamical evolution of the FWM spectra in a long length of optical fiber are compared with numerical solutions of the nonlinear Schrodinger equation (NLSE), used to model wave propagation in an optical fiber. We also discuss the effect of multimode laser inputs on the dynamics of the FWM processes along the optical fiber and show how the dynamics are altered significantly compared to single mode laser inputs.

The experiments are performed on a 50 m length of fiber with a pump frequency detuning of 366 GHz in the normal dispersion regime of the fiber. The output spectrum from the fiber was imaged using a low noise, high resolution CCD camera placed at the output of a spectrometer. A typical FWM spectrum is shown in Figure 1, the sidebands are centered around the two pump peaks. The power in the first order sidebands, normalized to the total power, was measured along the length of fiber and is compared with numerical solutions of the NLSE. In Figure 2(a) we show the results for pump inputs with 2W peak power, while Fig. 2(b) shows the results for 5W peak power. The NLSE predicts periodic and quasi-periodic energy exchange between the pumps and sidebands, whereas the experiments indicate that the energy in the sidebands tend to steady state values. It is interesting to note that despite the disagreement, the asymmetry conservation law[2,3] was found to be preserved throughout the fiber, independent of length. At the long lengths of fiber this asymmetry relation proved to be a sensitive test to detect other nonlinear processes, such as stimulated Raman scattering.

Pump fluctuations in the detuning and power were included in the numerical simulations and do not fully explain the evolution to the steady state values as seen in Figure 2. The experimental results also show that the individual sidebands exhibit distinct dynamics. The power generated in the blue-shifted sideband along the fiber (Figure 3(a)) has a higher value at the maximum of the cycle and a shorter period than the red-shifted sideband (Figure 3(b)). A more accurate description of this behavior is found by modelling one of the input pumps as a two mode laser and the other as a single mode laser. Numerical solutions of the NLSE including the effects of pump fluctuations and a two mode laser input yield good agreement with experimental measurements of the average sideband dynamics, Figures 3(a) and 3(b). However, measurements of the standard deviation of the average values along the fiber are still not explained by this model.

References

1. J.R. Thompson and R. Roy, Phys. Rev. A **43**, 4987 (1991).
2. J.R. Thompson and R. Roy, Phys. Rev. A **44**, 7605 (1991).
3. D.L. Hart, A. Judy, T.A.B. Kennedy, R. Roy and K. Stoev, Phys. Rev. A **50** 1807 (1994).

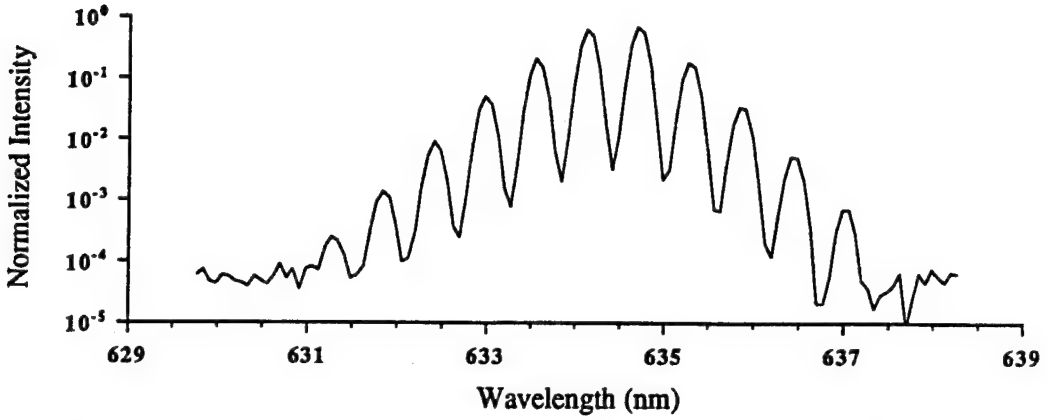

Figure 1. Measured FWM spectrum at the output of an optical fiber with bichromatic input.

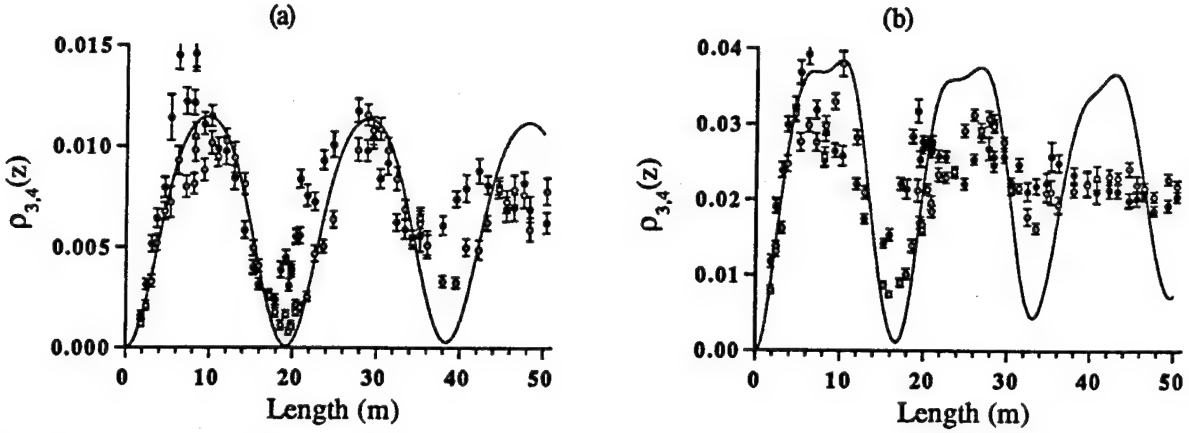

Figure 2. Comparison of the NLSE with experiment. Sideband power vs length along the fiber with input powers of (a) 2W and (b) 5W. —— NLSE with single mode pump input. Experiment: • Blue shifted sideband. o Red shifted sideband.

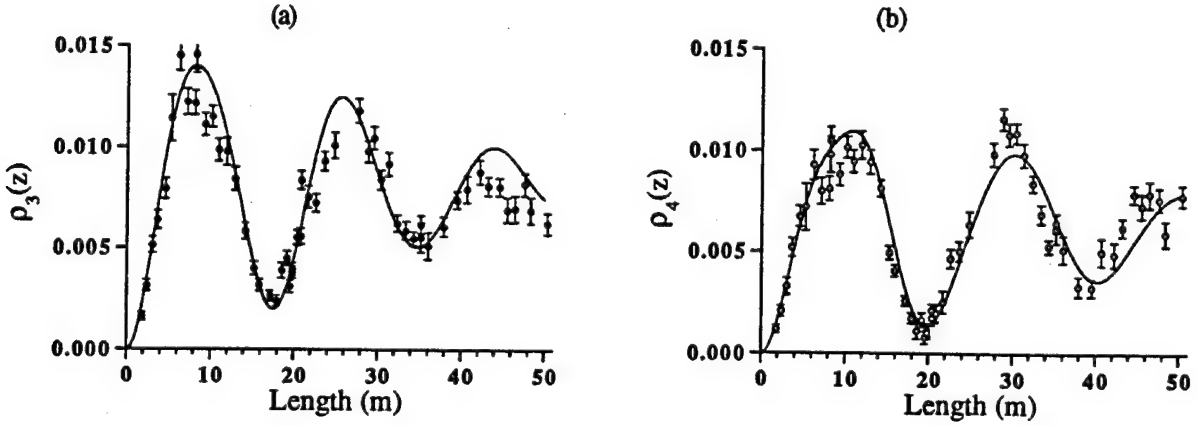

Figure 3. Comparison of experiment and the NLSE including a two mode laser input as well as pump fluctuations with an input power of 2W.

Spatiotemporal Evolution of Femtosecond Pulses in Semiconductor Amplifiers

R.A. Indik and J.V. Moloney
Arizona Center for Mathematical Sciences
Mathematics Department
University of Arizona
Tucson AZ 85721
Tel: (602)-621-6755, Fax: (602)-621-1510 E-mail:indik@math.arizona.edu

R. Binder
Optical Sciences Center
University of Arizona
Tucson, AZ 85721

Many-body effects have been shown to be important in describing femtosecond pulse propagation in semiconductor amplifiers. Physical mechanisms such as dynamic bandgap renormalization, Coulomb screening, spectral hole-burning, plasma heating and cooling etc. have all been shown to play an important role in determing the nature of the pulse evolution along the amplifier [1]. An important experimental observation at low carrier densities is the so-called Urbach tail[3], which corresponds to an exponential rather than Lorentzian-like decay of the exciton absorption tails away from the peak. This observed phenomenon has been ascribed to memory effects [2] and requires a modification to the Maxwell-Semiconductor Bloch equations (MBSE) describing the interaction of light with the semiconductor material. The MBSE are given by:

$$\begin{aligned}
\frac{\partial E}{\partial \xi} - \frac{1}{2ik_0}\nabla_\perp E &= \frac{id_{cv}\mu_0\omega_0^2}{k_0 V}\sum_q P_q \\
\frac{\partial P_q}{\partial \eta} &= -i(\Delta_q - \omega_q)P_q - i\Omega_q(f_q^e + f_q^h - 1) + \left.\frac{\partial P_q}{\partial \eta}\right|_{coll} \\
\frac{\partial f_q^{e/h}}{\partial \eta} &= iP_q^*\Omega_q + c.c + \left.\frac{\partial f_q^{e/h}}{\partial \eta}\right|_{coll}
\end{aligned}$$

with the renormalized Rabi frequency $\Omega_q = \Omega/2 + \frac{1}{h}\sum_{q'} V_{q-q'}P_{q'}$ and the renormalized transition energy $\Delta_q = \varepsilon_q - (1/h)\sum_{q'} V_{q-q'}(f_{q'}^e + f_{q'}^h)$. In the usual relaxation rate approximation, the collision terms are replaced by an

effective k-dependent damping constant i.e $\frac{\partial P_q}{\partial \eta}\Big|_{coll} = -\gamma_q P_q$. This amounts to representing each homogeneously broadened lineshape by a Lorentzian profile. In order to account for memory effects in the polarization decay we consider $\frac{\partial P_q}{\partial \eta}\Big|_{coll} = \int_{-\infty}^{t} \gamma_q(t-t')P_q(t')dt'$.

This generalized manybody problem offers a formidable computational challenge. We utilize forms for $\gamma_q(t)$ which correspond to both a hyperbolic secant lineshape [3] and a series of multiple pole approximations to account for faster than quadratic fall-off for the tails of the homogenously broadened lineshape. In the low density approximation, we recover the rapid fall-off in the exciton feature showing that a truncated multiple-pole approximation is reliable in this case. The effect of faster fall-off in the tails is to recover a linear gain profile which asymptotes to zero absorption at the band edge. Lorentzian tails yield an artificial net absorption which is nonzero at the band edge and extends to lower energy [3].

We will report on a study of femtosecond pulse propagation in semiconductor amplifiers including inhomogeneous broadening, many-body interactions, plasma cooling and memory effects. Plasma cooling provides more *cold carriers* for gain on the tail of the pulse and leads to strong pulse distortion. Memory effects significantly affect the saturation behavior of the amplifier and reduce the predicted absorption from high-lying carrier momentum states following saturation. Plane wave calculations are extended to a broad-area amplifier, introducing the diffraction degree of freedom to the problem. A femtosecond pulse will be shown to undergo transient self-focusing to form an self-induced index waveguide near its peak with diffraction occuring on the outer edges.

References

[1] A. Knorr, R. Binder, E.M. Wright and S.W. Koch, Opt. Lett. **18**, 1538 (1993); R. Indik, A. Knorr, R. Binder, J.V. Moloney and S.W. Koch, Opt. Lett., **19**, 966 (1994).

[2] L. Banyai, T. Wicht and H. Haug, Z. Phys. B, **77**, 343 (1989).

[3] W.W. Chow, S.W. Koch and M. Sargent, *Semiconductor Laser Physics*, (Springer Verlag, New York, 1994)

Periodic cycles, bifurcations and chaotic behavior of the new type of optical solitons in the solid-state lasers mode-locked by linear and nonlinear phase shift

V. L. Kalashnikov, V.P.Kalosha, I.G.Poloyko and V.P.Mikhailov

International Laser Center of Belarus State University, 7 Kurchatov Str., Minsk, 220064, Belarus, Tel/fax.: (7-0172)78-57-26, E-mail:user3@mikhai.bsu.minsk.by

As has been shown recently a spontaneous formation of the solitons in the laser systems takes place without any additional modulators [1,2]. Main feature of these lasers is the low frequency beatings produced by a shift of the carrier generation frequency from the center of the luminescence band. Moreover, the existence of the traditional mechanism of the soliton formation based on the interaction between the group-velocity dispersion and the self-phase modulation (SPM) may sufficiently increase the mode locking efficiency.

The purpose of this paper was to perform a detailed research of new type of soliton lasers with SPM, negative group-velocity dispersion and frequency shift from the luminescence band center. These investigations were based on the self-consistent field theory, analysis of the soliton stability and the numerical simulation of the generation dynamics performed with the help of the split-step Fourier method and the fluctuation model.

We have shown that a mechanism of the soliton formation for the new type of mode-locking may be understood by analogy with soliton propagation in the media with the negative group-velocity dispersion and SPM. A transform-limited pulse propagating through nonlinear media becomes a frequency modulated. SPM leads to growth of the instant frequency along the pulse profile. It was assumed also that the soliton carrier frequency has shift from the center of the luminescence band (ω) owing to a move of the resonator mirror creating the cumulative Doppler effect, a shake of the laser cavity elements (for example, the rotating prisms or plates), intracavity long-pass wavelength filter consisting of a knife edge introduced between the prism pairs, the gain line splitting. Then pulse obtains an additional linear frequency modulation. If $\omega < 0$ (longer-wavelength shifted soliton) the instant frequency decreases along the pulse profile. The combined action of these processes may produce a self-reproduction of the pulse propagating in the system. If this state is stable, a competition between initial amplifying pulses in the laser system may lead to formation of the single stable pulse.

We have considerated the dissipative nonlinear equation describing the field propagation in the laser system with frequency shift from the center of the luminescence band and being an analogue of the generalized Landau-Ginzburg equation. It has the soliton solutions:

$a = a_0 \exp(i\omega t)\cosh^{-1-i\psi}\theta t$, where $\theta = -\omega\dfrac{\sqrt{-(d\psi)+2\tau}}{\sqrt{\psi(d-d\psi^2+2\psi\tau)}}$ is the reverce soliton width,

$a_0^2 = \dfrac{\omega^3\tau(-2d\psi-2d\psi^3+4\tau+4\psi^2\tau)}{\alpha\psi^2(d-d\psi^2+2\psi\tau)}$ is the soliton intensity,

$\alpha = \gamma + \frac{2\omega^2\tau - 2d^2\omega^2\psi}{d - d\psi^2 + 2\psi\tau} + \frac{4d\omega^2\tau}{d - d\psi^2 + 2\psi\tau} - \frac{2\omega^2\tau^2}{\psi(d - d\psi^2 + 2\psi\tau)}$ is the gain in the soliton maximum, ψ is the chirp, τ is the time delay on the spectral filter, γ is linear losses, d is group velocity dispersion coefficient. The chirp and the frequency shift are found from implicit equations. We described the main features of these solitons. The results of the soliton analysis are in excellent agreement with experimental dates presented in [2,3].

Fig.1

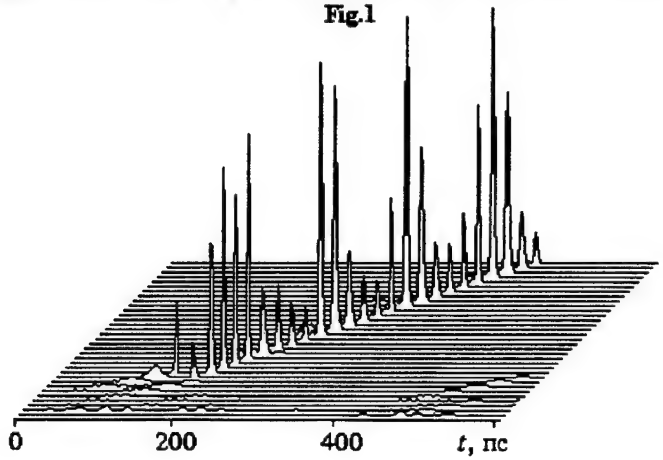

We found that the rise of the soliton energy result in Hopf bifurcation. The soliton acquires the nonrelaxating oscillations with frequencies ~10 MGz. Such oscillations correspond to the deflection of the laser parameters from the zone of the efficient mode locking (see fig.1, where the result of the numerical simulation of the laser dynamics is shown). The further rise of the soliton energy breaks the regular character of the oscillation. The additional frequency dependent on amplitude of the oscillation appears. If the oscillation frequencies are rationally independent, there is a quasi-periodical oscillation. The vector "wanders" on the bifurcation tore and the oscillations become irregular (see fig.2). The layer of the ergodic motion expands around initial trajectory.

Later on the systems suffers the bifurcation cascade when the motion becomes regular again but with new rational ratios between the oscillation frequencies. New regular trajectories appear on the boundaries of the ergodic motion zones. Such state is supported on the finite interval of the soliton energy increase. On this interval a frequency-lockin regime exists. Then the formation of the ergodic layer is repeated and each bifurcation is accompanied by the states with ergodic motion. Further rise of the soliton energy leads to increase of the oscillation amplitude and the appearance of the new oscillation frequencies ratios. We have observed the trajectories corresponding to four frequencies relations. At last, the soliton becomes fully unstable and the system behavior becomes a chaotic.

Fig.2

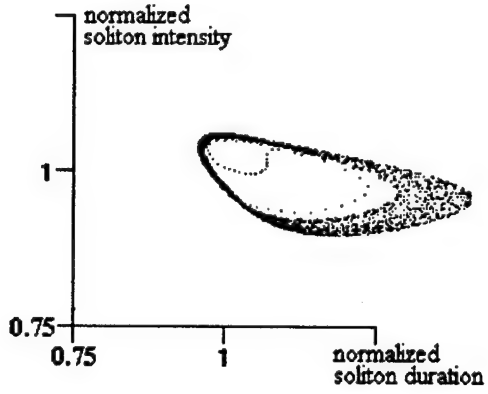

We believe that new type of soliton mechanisms enables to generate stable ultra-short pulse trains in a wide range of the laser parameters without the need of additional modulators.

REFERENCES:

[1]. C.C.Cutler. IEEE J. Ouantum Electronics, 28, 282 (1992).

[2]. Q.Wu, J.Y.Zhou, X.G.Huang, Z.X.Li, Q.X.Li. J. Opt. Soc. Am., 10, 2080 (1993).

[3]. D. Kopf, F. X. Kartner, K. J. Weingarten, U. Keller. Dig. Sym. CLEO'94, Anaheim (USA), 183-184 (1994).

LOW FREQUENCY RELAXATION OSCILLATIONS IN CLASS B LASERS WITH FEEDBACK

P. KHANDOKHIN, Ya. KHANIN, Institute of Applied Physics, Russian Academy of Science, 46 Uljanov Street, 603600 Nizhny-Novgorod, Russia. Fax : + 7 8312 362061 e-mail : khando@appl.nnov.su
J.-C. CELET, D. DANGOISSE and P. GLORIEUX, Laboratoire de Spectroscopie Hertzienne, UA CNRS 249, Université de Lille I, 59655 Villeneuve d'Ascq Cedex, France. Fax: + 33 20 33 70 20 e-mail: glorieux@lsh.univ-lille1.fr

Relaxation oscillations have been studied both theoretically and experimentally in a multimode YAG laser in presence of a derivative feedback. Feedback which is often used to reduce the fluctuations in the laser output [1] has also been considered from a dynamical point of view[2]. Continuous feedback is useful to stabilize unstable steady states and to track them over a wide range of parameters in which the laser is usually spiking periodically or chaotically [3]. We report here on a detailed investigation of relaxation resonances of a multimode class B laser with a derivative feedback built from a combination of the total intensity and of the intensity in a given mode. Such a combined feedback is represented by the expression

$$A = A_0 + K_{total} \sum \frac{dI_j}{d\tau} + K_\nu \frac{dI_\nu}{d\tau} \qquad (1)$$

where A is the pump parameter and I_j the intensity in mode j. We have considered here the case of multimode operation of this laser when up to 4 modes are simultaneously excited above threshold and up to 4 relaxation frequencies may play a significant role in the dynamics of such a laser.

In this presentation, we use a rate equation model describing the operation of the class-B laser [4]:

$$\begin{aligned} \frac{dI_j}{d\tau} &= G\, I_j\, (N_0 + N_j - 1 - C_j) \\ \frac{dN_0}{d\tau} &= A - N_0\,(1 + \Sigma I_j) - \Sigma\, N_j\, I_j \\ \frac{dN_j}{d\tau} &= -\,N_j\,(1 + \Sigma I_j) - \frac{1}{2}\, N_0\, I_j \end{aligned} \qquad (2)$$

using the loss distribution of the form $C_j = \beta\,(j-1)$, and standard notations of laser theory. Steady-state solutions are given and their stabilities are linearly analysed. Numerical simulations have shown that depending on the

feedback coefficients the laser may destabilise through excitation of specific relaxation oscillations and eventually switch to chaos.

The experiments have been performed on a YAG laser with a feedback made of a combination of the total intensity and the intensity in one longitudinal mode. The radiofrequency noise spectra have been measured for each of the longitudinal modes and for the total intensity. In absence of feedback, all spectra display a resonance peak at the standard relaxation oscillation frequency of the laser. The RF noise spectra in each longitudinal mode also exhibit several resonances at frequencies lower than 80 kHz typically. All these lower resonance frequencies which are observed on individual mode fluctuations are almost absent from the total intensity. They correspond to antiphase oscillations which globally compensate each other. Special attention has been paid to the case where the coefficients K_{total} and K_v fulfill the conditions $K_{total} < 0$ and $K_v > 0$ to realize both the compensation of the high frequency ω_0 and the excitation of a low frequency. Various dynamical features have been obtained depending on the amplitude and the sign of the feedback and in particular on the relative weight of the selected mode intensity. They include regenerative amplification and selective excitation of low frequency quasi-sinusoidal oscillations and chaos.

The model derived in the theoretical section provides an excellent description of the influence of a combined derivative feedback on the multimode YAG laser as seen in the experiments. These effects include

- shift, narrowing and enhancement (reduction) of relaxation oscillation peaks in the radiofrequency spectrum of laser noise.
- destabilization of the laser by two scenarios either through a Hopf bifurcation or directly to chaos.

REFERENCES

[1] R. Roy, A. W. Yu and S. Zhu, "Colored noise in dye laser fluctuations" in *Noise in Nonlinear dynamical systems* , p. 90-118, F. Moss and P. V. E. McClintock eds., Cambridge U. Press, (Cambridge, 1989).

[2] F. T. Arecchi, R. Meucci and W. Gadomski, Phys. Rev. Lett. **58**, 2205 (1987).

[3] S. Bielawski, M. Bouazaoui, D. Derozier and P. Glorieux, Phys. Rev. A **47**, 3276 (1993), D. J. Gauthier, D. Sukow, H. M. Concannon and J. E.S. Socolar, Phys. Rev. E**50**, 2343 (1994)

[4] K. Otsuka, M. Georgiou and P. Mandel, Jpn. J. Appl. Phys. **31**, L1250 (1992).

Intensity Noise Suppression of External Cavity Semiconductor Laser via High Frequency Modulation

Noriyuki Kikuchi, Yun Liu, and Junji Ohtsubo
Faculty of Engineering, Shizuoka University, Johoku 3-5-1, Hamamatsu, 432, Japan
Tel: +81-53-471-1171 Fax: +81-53-478-1251 e-mail: ohtsubo@oeme.shizuoka.ac.jp

Abstract

The theoretical investigation of high frequency injection modulation technique in semiconductor laser with external optical feedback is conducted for the reduction of relative-intensity-noise (RIN). The modulation frequency is determined from a linear stability analysis.

1 Introduction

In some of optical systems such as an optical disk system, the system performance is largely affected by the optical feedback (OFB) induced laser intensity noise. The relative intensity noise (RIN) of a semiconductor laser suddenly increases at a certain feedback level and deteriorates the signal-to-noise ratio. In this report, we apply the high frequency injection modulation technique[1] to suppressing the feedback induced RIN in a compound laser system and control the chaos in the laser output. To optimize the modulation frequency, we give the theoretical background of the noise reduction by the high frequecy modulation based on a linear stability analysis.

2 Rate Equation Model

For a semiconcuctor laser system with weak optical external feedback, the dynamics is governed by the following rate equations[2]

$$\frac{dE(t)}{dt} = \left[j\omega(N) + \frac{1}{2}\left\{G(N) - \frac{1}{\tau_p}\right\}\right] E(t) + \frac{\kappa}{\tau_{in}} E(t-\tau) + F_E(t), \quad (1)$$

$$\frac{dN(t)}{dt} = J - \frac{N(t)}{\tau_s} - G(N)|E(t)|^2 + F_N(t), \quad (2)$$

where $E(t)$ is the field amplitude, $N(t)$ is the carrier number, and J is the injection current. ω is the laser cavity frequency, G is the gain coefficient, and τ_p, τ_{in}, and τ_s are the photon life time, the optical round trip time in the laser diode cavity, and the carrier life time, respectively. The feedback parameter κ is given by $\kappa = (1-r_2{}^2)r_3/r_2$, where r_2 and r_3 are the reflectivities of the front laser facet and the external reflector, respectively. F_E and F_N are the Langevin forces of spontaneous emission noise.

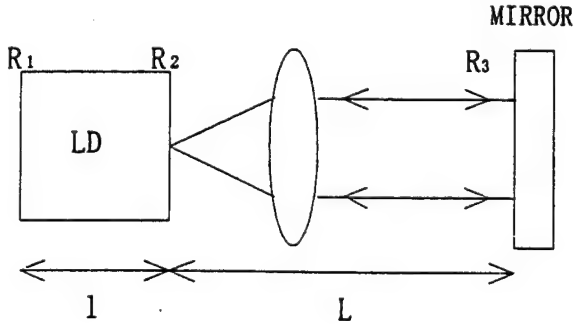

Fig. 1 Cavity model for a semiconductor laser with external optical feedback. l,L : lengths of laser diode cavity and external cavity, R_1,R_2 : reflectivities of the laser facet, R_3 : reflectivity of the external mirror.

The effect of a high frequency modulation to the injection current at a frequency f_m is described by $J = J_b + J_m \sin(2\pi f_m t)$, where J_b and J_m are the bias and modulation currents, respectively. To optimize the modulation frequency f_m for the reduction of the RIN, we carry out a linear stability analysis[3] for the perturbation to the stationary solutions and obtain the transcedental equation. Fig.1 shows the mode distribution calculated by the transcedental equation.

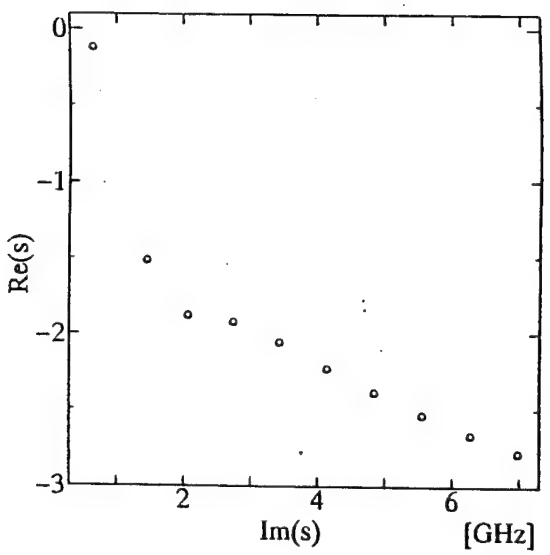

Fig. 2 Mode distribution for J_b=1.07J_{th}, L=21cm, and $r_3{}^2$=1.6%. s is the perturbation parameter.

By employing frequencies that are equal to or near the mode frequencies, the numerical integration of Eqs.(1) and (2) were carried out by using a fourth-order Runge-Kutta algorithm. Fig.3 shows an example of the laser output powers for J_b=1.07J_{th} (J_{th} is the threshold current), the external cavity length L=21cm, $r_3{}^2$=1.6%, and f_m =1.44GHz. The chaotic behavior in Fig.3(a) is controlled to a period two cycle as shown in Fig.3(b). The Corresponding RIN spectra are shown in Fig.4.

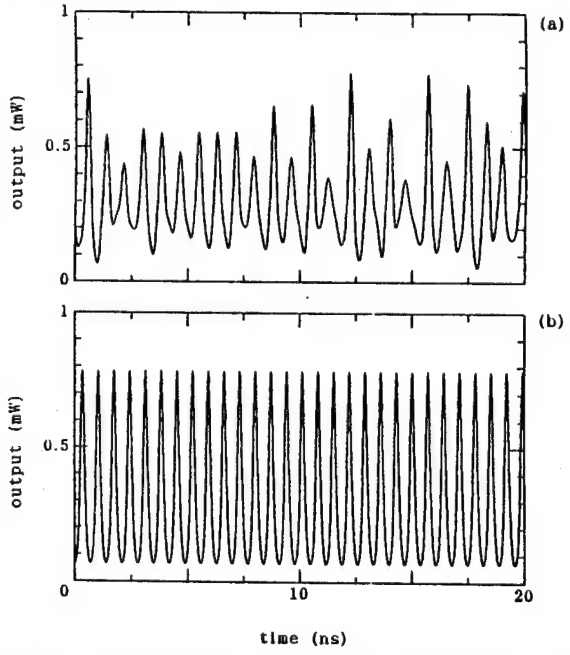

Fig.3 Laser output power for J_b=1.07J_{th}, L=21cm, and $r_3{}^2$=1.6%.(a) without modulation and (b) with modulation.

It is recognized from the figure that the RIN with high frequency modulation at the low frequency region is suppressed about 20dB/Hz compared with that without the modulation.

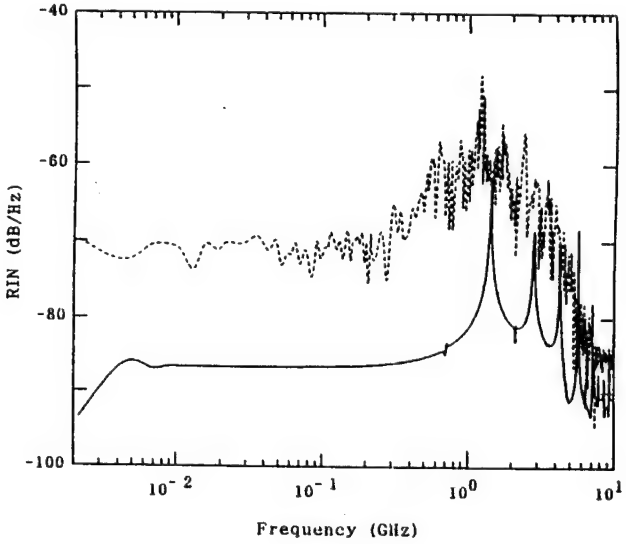

Fig. 4 RIN spectra corresponding to Fig. 3. solid line: with modulation; dotted line: without modulation;

3 Conclusion

We have investigated the elimination or suppression of the chaotic bahavior in a semiconductor laser with external optical feedback. The feedback induced intensity noise has been suppressed by a high frequency injection modulation technique, in which the modulation frequency is chosen to be equal to or near the mode frequency. The RIN at lower frequency region has been reduced by the optimized modulation frequency. It is proved that the high frequency injection modulation technique is a promising method for the control of chaos in semiconductor laser with external optical feedback.

References

[1] G. R. Gray, A. T. Ryan, G. P. Agrawal, and E. C. Gage, Optical Engineering. **32(4)**, 739 (1993).

[1] J. Mørk, B. Tromborg, and J. Mark, IEEE J. Quantum Electron. **QE28**, 93 (1992).

[3] B. Tromborg, J. H. Osmundsen, and H. Olesen, IEEE J. Quantum Electron. **QE20**, 1023 (1984).

Multimode Instabilities in the Transit-Multistable Ring Cavity

Jeong-Mee Kim and A. T. Rosenberger

Department of Physics
University of Alabama in Huntsville
Huntsville AL 35899, USA
Phone: (205) 895-6276 ext. 218
Fax: (205) 895-6873
E-mail: rosenbergera@email.uah.edu

It was recently shown [1-3] that a cw-driven ring resonator, in which the nonlinear medium is a beam of two-level atoms, can exhibit multistability as a result of the Rabi cycling of the atoms as they pass through the cavity mode. In the present work, we investigate multimode instabilities in this system.

For the case of absorptive (atoms resonant with the driving field) transit multistability [1,2], we have extended the single-mode stability analysis of Ref. 1 to the multimode case. For the n^{th} mode, where n is the mode's detuning from the driving laser in units of half the cavity's free spectral range, a perturbative analysis shows that instability will occur when

$$\mathrm{Re}(\lambda_n) = -k\,\mathrm{Re}[1-\{2C\tau/(x^2-n^2\pi^2\tau^2/\tau_r^2)\}J_i(x, in\pi\tau/\tau_r)] > 0$$

where k is the cavity decay rate, C the cooperativity, x the normalized intracavity field, τ the transit time, and τ_r the cavity round-trip time (times in units of $\gamma_\perp^{-1}$). The quantities J_i (i = 1,2) are given by

$$J_1(x,\lambda\tau) = 1-e^{-\lambda\tau}\cos(x)-\frac{1}{\lambda\tau}(1-e^{-\lambda\tau}+\frac{\lambda^2\tau^2}{x^2})x\sin(x),$$

$$J_2(x,\lambda\tau) = \cos(x)-e^{-\lambda\tau}-\lambda\tau\,\mathrm{sinc}(x).$$

As first pointed out by Carmichael [4], regions of negative slope in the state equation (x vs. y, the normalized input field) of the driven mode (n = 0) in the resonant cavity correspond to regions of instability in the modes of the cavity driven midway between resonances. For the multistable system, there are many such regions, as illustrated in the figure.

In the figure, regions inside the curves are unstable; here $C\tau = 10$. The J_1-type regions intersect the x-axis at the limits of the negative-slope branches of the multistability state equation. The J_2-type regions are closed curves, and exist only for the lowest negative-slope branch at this value of $C\tau$. Curves for three values of n (n = 1, 2, 3) are shown; the vertical extent of each curve decreases with increasing n. Even values of n denote neighboring cavity modes when the driving laser is resonant with a mode; odd n apply when the laser is tuned midway between modes. Note that the J_2-type instabilities,

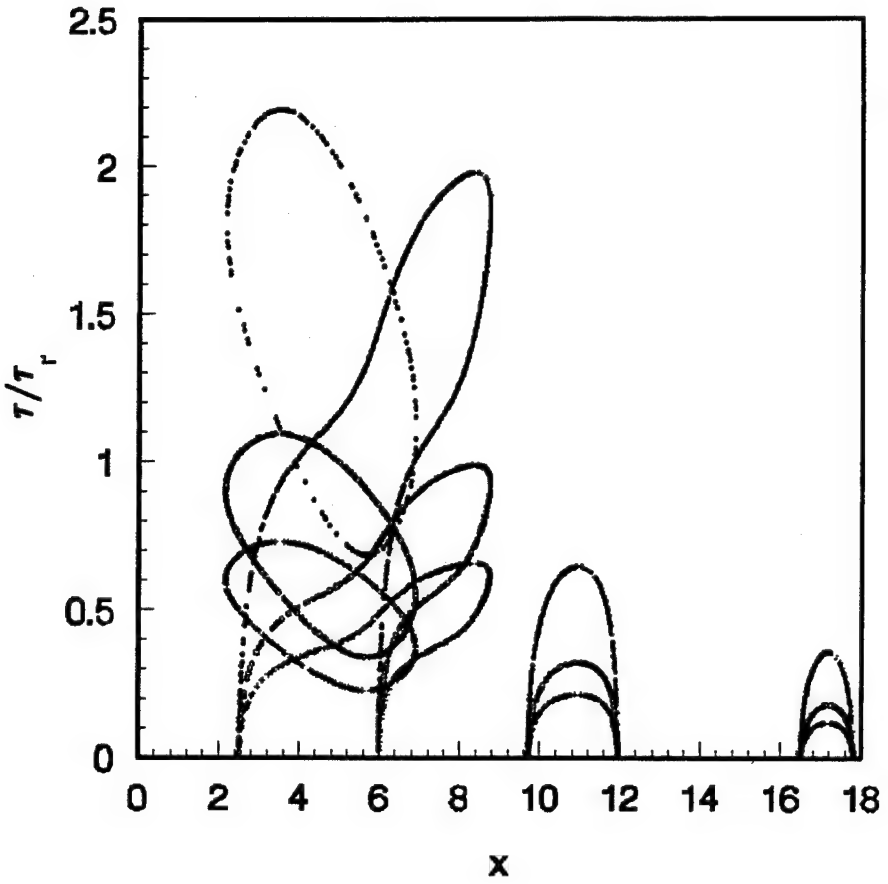

which play no role in the single-mode case, can become important in describing multimode instabilities, and note that they extend beyond the negative-slope branches. For this value of $C\tau$, experimentally feasible with $C = 200$ and $\tau = 0.05$, the resonant cavity will display both J_1-type and J_2-type multimode instability ($n = 2$) in the region just above the first branch of negative slope. The cavity driven between modes ($n = 1,3$) will exhibit instabilities in all three regions shown, provided that the ratio of transit time to round-trip time is within the proper ranges.

In summary, we have extended the instability analysis of transit-multistable ring resonators to the multimode case. Further results and analyses will be given in the paper.

References

[1] F. Casagrande, L. A. Lugiato, W. Lange, and H. Walther, Phys. Rev. A 48, 790 (1993).
[2] A. T. Rosenberger and Jeong-Mee Kim, Opt. Commun. 101, 403 (1993).
[3] Jeong-Mee Kim and A. T. Rosenberger, Opt. Commun., in press.
[4] H. J. Carmichael, Phys. Rev. Lett. 52, 1292 (1984).

Nonlinear Dynamics of Additive Pulse Modelocked Lasers

Gregg Sucha
IMRA America

Sarah R. Bolton, and Daniel S. Chemla
Materials Science Division,
Lawrence Berkeley Laboratory

Nonlinear dynamics have been studied in a number of modelocked laser systems, primarily in actively modelocked systems. However, less attention has been paid to the dynamics of passively modelocked laser systems. With the recent revolutionary advances in femtosecond modelocked laser technology, the understanding of instabilities and dynamics in passively modelocked lasers is an important issue. Here, we present experimental and numerical studies of the dynamics of an additive-pulse modelocked (APM) color-center laser. However, it is important to note that our discussions are more general, and apply to other types of passively modelocked lasers, because we have also observed these dynamics in a self-modelocked Ti:sapphire laser, and in a modelocked Er:fiber laser as well. The APM laser and the other above mentioned lasers are all examples of lasers using a fast saturable absorber (FSA).

We have studied two types of APM lasers; the Fabry-Perot APM[1,2] and the Michelson APM.[3] Both were based on a color-center laser which used NaCl as the gain medium. The Fabry-Perot APM laser consists of a main cavity (containing the NaCl gain crystal) and a control cavity which contains a single-mode fiber to provide the Kerr nonlinearity. These two cavities are coupled end-to-end in the Fabry-Perot configuration. When passively modelocked at a power of P=200 mW, the laser produces pulses of less than 150 fsec duration, at a repetition rate of 76 Mhz, corresponding to a pulse spacing of 13 nsec. At a slightly higher power, (P=240 mW), a period-doubled pulse train is produced (Figure 1[a]), and at even higher power (P>280 mW), a quasiperiodic pulse train is generated (Figure 1[b]). Yet the measured pulse intensity autocorrelations still indicate relatively short pulses (τ~150 fsec).

Numerical simulations of the Fabry-Perot APM laser show that this period-doubling is expected as the nonlinearity is increased. The bifurcation diagram in Figure 2 shows how the laser pulse energy varies as the control cavity nonlinearity is increased. First, the laser goes from CW to modelocking (the "second-threshold"). As the nonlinearity is increased, the pulses get shorter and shorter until the laser goes to period-doubled modelocking. With further increases in n_2 the

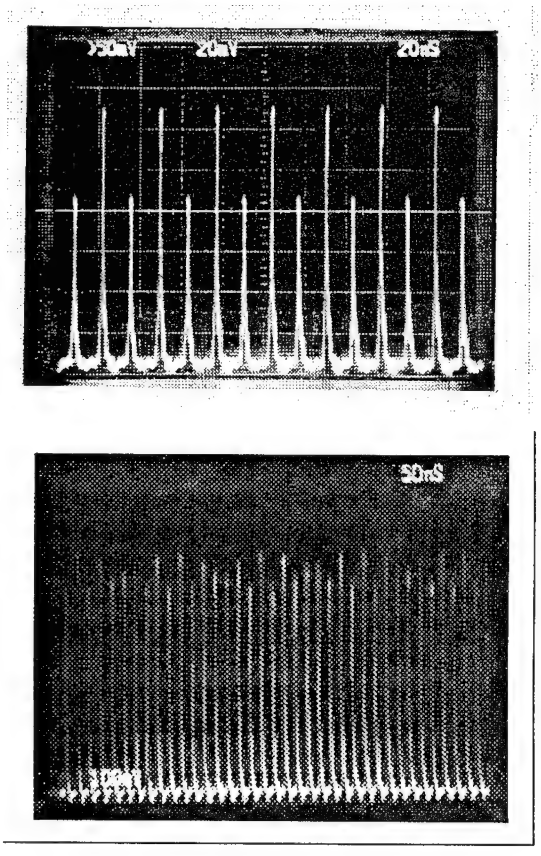

Figure 1. Period-doubled pulse train (a) and quasiperiodic pulse train (b) from APM laser. Note that pulse spacing is 13 nsec in both traces.

laser makes a switching transition to another period-doubled mode, and then a sudden transition to apparent chaos, indicating a crisis.
The figure also shows the pulse solutions at two values of nonlinearity. Note that the pulse solutions for the upper and lower branches have very different intensity profiles.
We have also studied and numerically simulated the Michelson APM laser and have found that it exhibits none of these effects, no matter how large the nonlinearity is made, or how hard the laser is driven. The only instabilities encountered in reality were relaxation oscillations. This agrees with previous observations by Grant[4] who did an experimental comparision between the F-P and Michelson configurations. In the simulations of the Michelson APM, as the nonlinearity is increased beyond the normal bounds, the modelocked pulse becomes distorted, broadened, and develops multi-peaked structure, but no pulse train instabilities were generated. This also agrees with the predictions of Cormier & Piché.[5]
Another type of APM laser cavity is the "figure-8" configuration, which has been used for modelocked Er:fiber lasers. We might expect this to be similar to the Michelson cavity in terms of behavior; however, we have not considered this case yet.
In conclusion, we have studied the nonlinear dynamics of pulse train instabilites and pulse reshaping in APM lasers using two different cavity configurations. These results are important for understanding the general behavior of various types of self-modelocked lasers which use fast-saturable absorber effects.

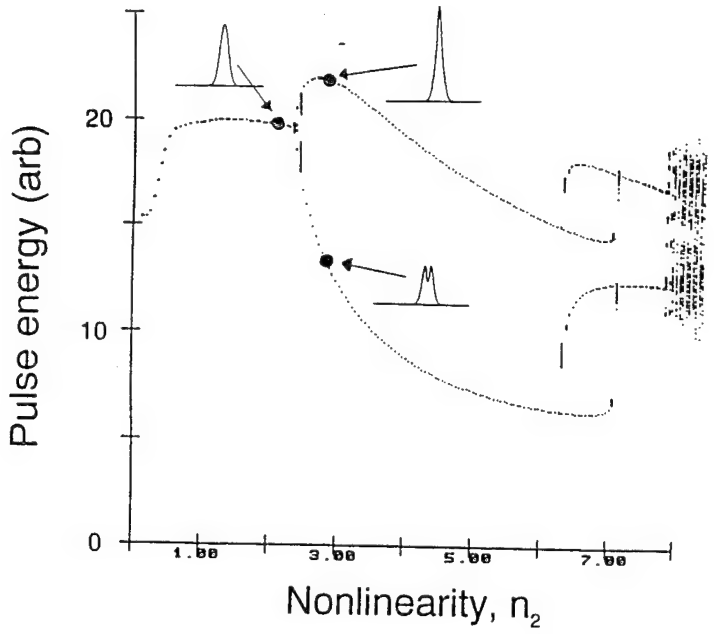

Figure 2. Bifurcation diagram of (simulated) laser pulse energy versus nonlinearity for a Fabry-Perot APM laser. Pulse solutions are shown for two values of nonlinearity: one for normal modelocking ($n_2 = 2.3$) and two for period-doubled modelocking ($n_2 = 2.8$).

This work was supported by the Director, Office of Energy Research, Office of Basic Energy Sciences, Materials Science Division, of the U.S. Department of Energy under Contract No. DE-AC03-76SF00098

References:

1. J. Mark, L. Y. Liu, K. L. Hall, H. A. Haus, and E. P. Ippen, *Opt. Lett.* **14**, 48 (1989).
2. P. N. Kean, X. Zhu, D. W. Crust, R S. Grant, N. Langford, and W. Sibbett, *Opt. Lett.* **14**, 39 (1989).
3. F. Ouellette and M. Piché, *Opt. Comm.* **60**, 99 (1986).
4. R. S. Grant, *et. al. Opt. Comm.* (1991).
5. J. F. Cormier, and M Piché, in "*Nonlinear Dynamics in Optical Systems,*" OSA Tech. Digest **16**, (1992).

Transverse dynamics of a phase-conjugate resonator with phase mismatch.

Dan Korwan and Guy Indebetouw

Physics dept. 0435

Virginia Tech

Blacksburg, VA 24061

Tel.: (703) 231-5896 (Korwan)/(703) 231-8727 (Indebetouw)

E-Mail: Korwandr@vtcc1.cc.vt.edu/Gindebt@vtpcn.phys.vt.edu

Fax: (703) 231-7511

Summary

Phase-conjugate resonators have unique properties which make them potentially attractive for applications in image processing and storage. These applications require some of the following attributes: gain, phase healing and spatial multistability.

We have studied experimentally the spatiotemporal behavior of a linear resonator using an externally pumped photorefractive phase-conjugate mirror in a confocal cavity. This system has gain and a phase healing mechanism, but observations indicate that spatially non uniform solutions are time dependent unless the phase matching condition is precisely satisfied [1].

We analyzed the effect on the spatiotemporal dynamics using a phase or momentum mismatch introduced by an angular tilt of the pump beams. At low Fresnel number ($F<2$) a time independent, spatially uniform solution exists. A phase mismatch reduces the gain until the resonator falls below threshold. For $2<F<3$, the cavity can sustain more than one transverse mode. The motion is periodic consisting of a vortex pair nucleating at the center and vanishing at the boundary, with a trajectory along a line normal to the transverse momentum mismatch. The frequency of the motion increases with the mismatch [fig. 1] and vanishes when phase matching is achieved with exactly counter propagating pumps. The output is then spatially uniform and time independent. The spatial patterns were analyzed using a singular value decomposition revealing the presence of two significant eigenmodes oscillating in phase quadrature [2] [fig. 2].

At higher Fresnel numbers the motion is complex and may become chaotic, involving several pairs of dynamic vortices. The characteristic frequencies are again seen to vanish when approaching phase matching where the output converges to a time independent, spatially non uniform solution (e.g. a doughnut at $F\sim4$).

The paper includes detailed accounts of the experiments and attempts to model the observed behavior.

The work was funded in part by a grant from NASA Langley Research Center (NAG 1363).

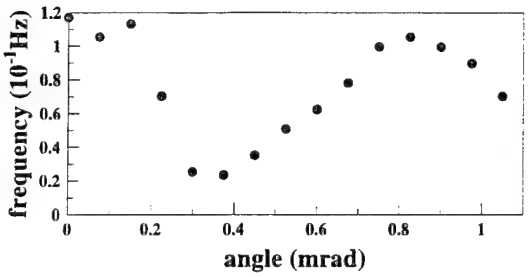

Fig. 1 Frequency of the periodic motion at F=2.5 vs. pump angular position (phase match at ~0.35mrad).

Fig. 2 (below) Singular value decomposition at F=2.5. Two eigenmodes (a) with significant eigenvalues λ (b) and coefficients oscillating in phase qudrature (c). (d) local time series with its power spectrum.

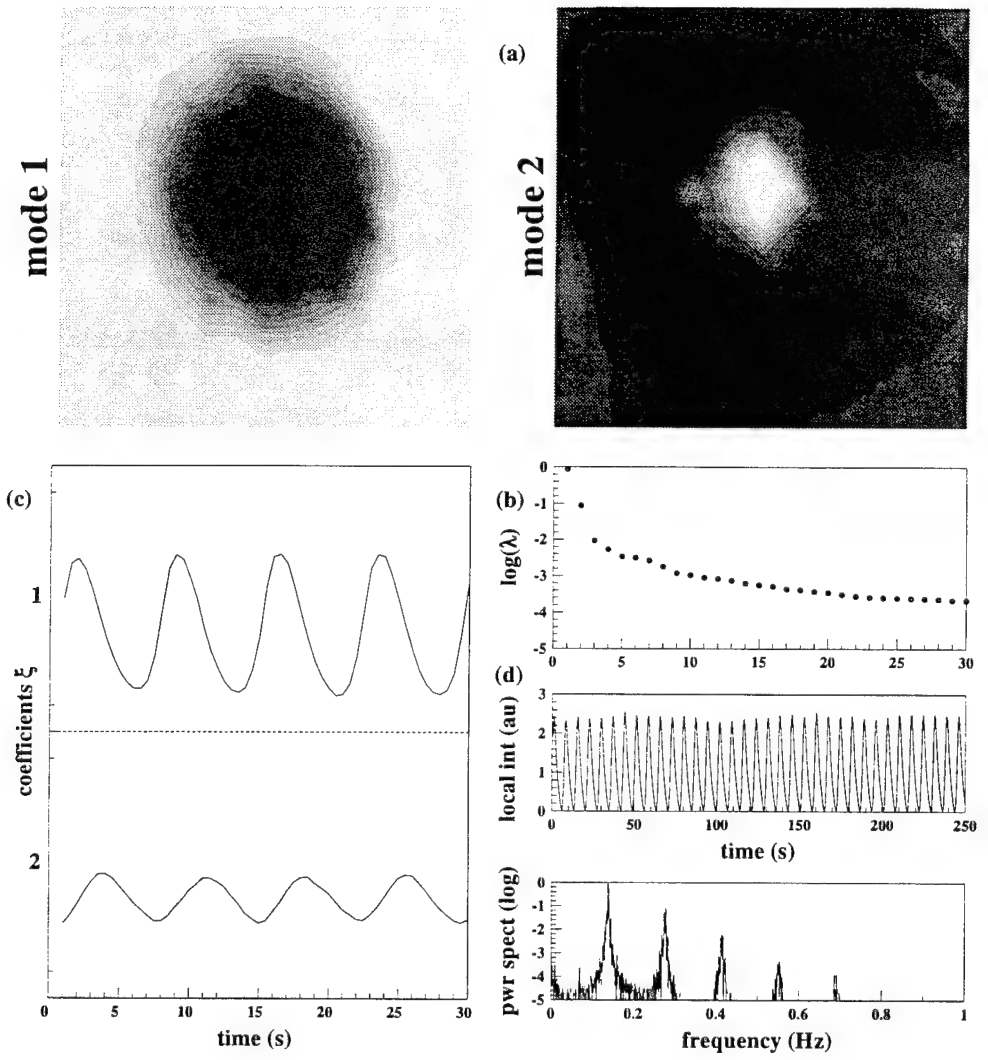

References

[1] S. R. Liu and G. Indebetouw, J. Opt. Soc. Am. B9, 1507 (1992)

[2] G. Indebetouw and D. Korwan, J. Mod. Opt. 41, 941 (1994)

PUMP POLARIZATION MODULATION IN AN OPTICALLY PUMPED LASER

A. Kul'minskii, R. Vilaseca,

Departament de Física i Enginyeria Nuclear, Universitat Politècnica de Catalunya, Colom 11, E-08222 Terrassa, Spain.
Phone: (34)-3-7398137; fax: (34)-3-7398101; e-mail: vilaseca@fen.upc.es

and **R. Corbalán**

Departament de Física, Universitat Autònoma de Barcelona, E-08193 Bellaterra, Spain.
Phone: (34)-3-5811653; fax: (34)-3-5812155; e-mail: ifop0@cc.uab.es

Usually, modulation of a laser system is accomplished by acting on the pump strength (or gain), on cavity parameters such as losses, detuning or anisotropy, or on an applied magnetic field /1-3/. In this work we investigate theoretically a new type of modulation, in which action takes place on the *polarization* state of a pump light beam. This can be performed in an optically pumped laser where a pump beam acts on a $J \rightarrow J'$ transition and the generated laser beam is coupled with an adjacent $J' \rightarrow J''$ transition in a Λ level scheme. Because of the M-degeneracy of the atomic or molecular levels, the system is sensitive to the polarization state of both the pump and laser fileds.

Here we consider specifically the simple case of a Λ level configuration $J=0 \rightarrow J'=1 \rightarrow J''=0$, with a linearly polarized pump beam. Modulation is accomplished by rotating at a constant angular velocity Ω the polarization plane of the pump beam. We have considered two situations. In the first one the cavity losses are assumed to be strongly anisotropic (Brewster-angle-plate type), so that the generated field maintains a linear polarization at a fixed orientation angle. Thus, if θ represents the relative angle between the polarization planes of the pump and laser fields, it varies with time in the form $\theta=\theta_0+\Omega t$.

As θ changes, the interaction between the pump and laser fields through the active medium changes. For instance, it is known that at $\theta=\pi/2$ (orthogonal polarizations) the two-photon (Raman) contribution to pumping is null /4/ and that the population in the $J'=1$ sublevel manifold accumulates in a trap dressed state /5/, facts which do not occur in the case $\theta=0$ (parallel polarization). This makes that the dynamics is very different for different fixed values of θ between 0 and $\pi/2$ /6/.

When θ is increased very slowly with time ($\Omega \ll \gamma$, being γ a typical relaxation time of the system), one could expect the system to follow periodically (with period $\pi/2\Omega$) the

rich sequence of steady or dynamic states that correspond to each successive value of θ, but several new features appear. For small pump-field intensity, *Q-switching-like* behavior occurs, with very large and delayed intensity spikes (see fig. 1). For moderate pump-field intensities, there is *quenching* of the time-dependent (chaotic) behavior expected to occur in a wide domain of values of θ /6/, which leads to stabilization of the unstable stationary solution (the system "follows" that solution as θ varies).

For larger values of Ω (but still verifying $\Omega<\gamma$), the observed features become quite different from those observed in the limit $\Omega\rightarrow 0$. The system's inertia is large enough to prevent following of the sequence of solutions corresponding to the different values of θ. Finally, if Ω is further increased ($\Omega\gtrsim\gamma$), emission disappears, since polarization rotation is equivalent to introducing a frequency difference between the dextro and levo circularly polarized components of the pump field, which puts them out of resonance.

In the second situation we are presently investigating, the cavity is assumed to be isotropic, so that the laser field vector can evolve freely and the dynamics involves both the intensity and polarization of the laser field. Results will be presented at the Conference.

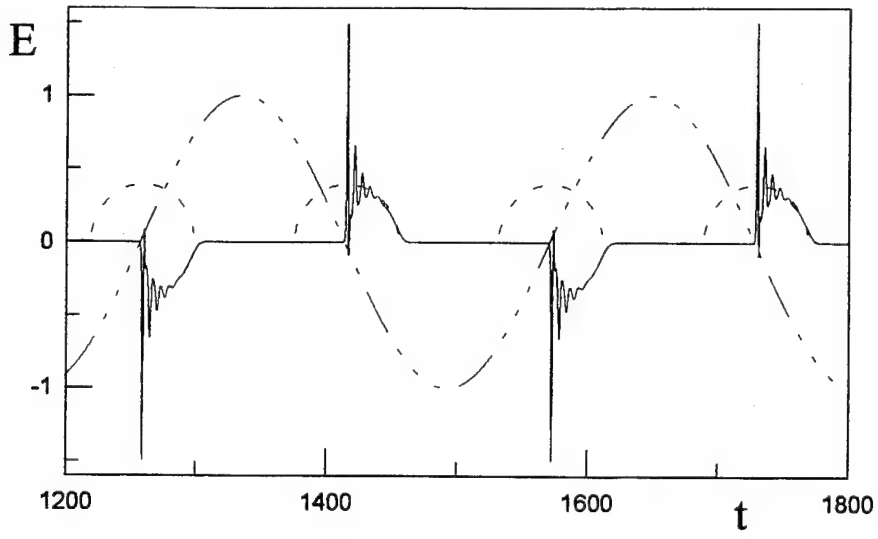

Fig.1.- Laser field amplitude vs. time, in a case of low pump intensity. The dotted-dashed line represents the function $\cos\theta=\cos(\theta_0+\Omega t)$ and the dashed line shows the associated sequence of steady states.

/1/.- C.O. Weiss and R. Vilaseca: *Dynamics of Lasers* (VCH, Weinheim, 1991).

/2/.- J.Ch. Cotteverte, F. Bretenaker, A. Le Floch, P. Glorieux: Phys Rev A **49**, 2868(1994)

/3/.- A.P Voitovich, AM. Kul'minskii, V.N. Severikov: Quantum Electron. **23**, 768(1993).

/4/ R. Corbalán et al.: Phys Rev. A 48, 1483 (1993).

/5/.- E. Roldán, G.J. de Valcárcel, R. Vilaseca, R. Corbalán: Phys Rev. A **49**, 1487(1994).

/6/.- A.M. Kul'minskii, R. Vilaseca, and R. Corbalán: (to be published)

Control of Spatio-temporal Chaos in Neural Networks and Its Application to Associative Memory

Masanori Kushibe, Yun Liu, and Junji Ohtsubo
Faculty of Engineering, Shizuoka University, Johoku 3-5-1, Hamamatsu, 432, Japan
Tel: +81-53-471-1171 Fax: +81-53-478-1251 e-mail: ohtsubo@oeme.shizuoka.ac.jp

Abstract

Spatio-temporal chaos in a discrete-time neural network with continuous state variables is investigated. It is demonstrated that the chaotic behavior can be controlled with the knowledge of only a (random) part of the target information. The application to the associative memory is described and the results show that the target pattern can be successfully associated with the proposed control algorithm.

1 Introduction

Recent researches in physiological science fields revealed the existence of chaotic dyanmics in some biological neural systems.[1] On the other hand, nonlinear dynamics and chaos have been recognized and investigated in a variety of asymmetric neuron models.[2] It becomes a growing attractive topic whether chaos plays functional roles in the information processing of neural systems.

In this paper, we study the spatio-temporal chaos in a neural network and in particular concentrate on the functional roles of chaotic dynamics in the information processing of the neural networks. Using the Lyapunov spectrum and the bifurcation diagram, we analyze the characteristic features of the spatio-temporal chaos. Spatio-temporal chaos is controlled by employing the parameter control technique. We also apply the control algorithm to the memory search and show that the system successfully associates the target pattern by using only a part of the target information.

2 Chaotic Neural Network

We consider a chaotic neural model with discrete-time and continuous states as follows

$$y_i(n+1) = ky_i(n) + \sum_{j=1}^{M} w_{ij}x_i(n) - \alpha x_i(n) + a_i, \quad (1)$$

$$x_i(n+1) = \tanh(y_i(n+1)/\epsilon), \quad (2)$$

where $y_i(n)$ and $x_i(n)$ are the internal state and output of the ith neuron, M is the total number of neurons in the network, k is the memory constant, α is the relative inhibitory constant, w_{ij} is the connection matrix componet, and a_i is the external input of the ith neuron.

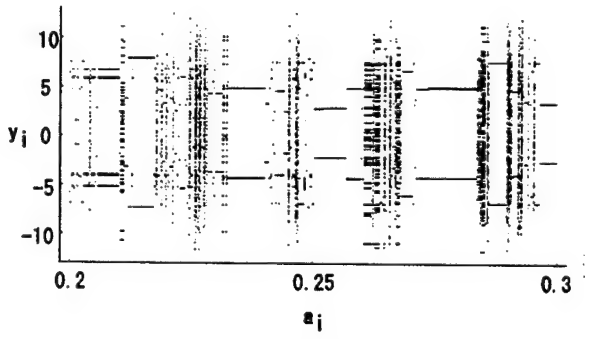

Fig. 1 Bifurcation diagram via the external input of a single neuron in a chaotic neural network. M=36, k=0.1, α=1.0, ε=0.02.

The output of the network appears chaotic for certain parameter regions. Figure 1 displays a bifurcation diagram of the 15th neuron via the external input. Clearly, as a_i is varied, the network transits from periodic state to chaos. Besides the bifurcation diagram, we also employed the Lyapunov spectrum to investigate the network dynamics. The results show that the network behaves chaotically for a wide range of positive values of k, α, and a_i. It is worth noting that for zero values of k, α, and a_i, the connection becomes symmetric and the only attractors are fixed points and period-two limit cycles.[3]

The target patterns can be embedded by defining

the connection matrix as

$$w_{ij} = \frac{1}{L}\sum_{r=1}^{L} e_i^{(r)} e_j^{*(r)}, \tag{3}$$

where $e^{(r)}(r=1,2,\cdots,L)$ is the vector of the embedding pattern and $e^{*(r)}$ is its adjoint vector defined by

$$\sum_{i=1}^{M} e_i^{(r)} e_i^{*(s)} = \delta_{rs}. \tag{4}$$

3 Spatio-temporal Chaos Control and Its Application

In the configuration of the parameter control technique[4], the parameter z ($=k$, α, a_i) is varied as a function of a control signal $\mu^{(\tau)}(n)$

$$z = \left[1 - \mu^{(\tau)}(n)\right] z(0). \tag{5}$$

Here $z(0)$ is the initial value of z and τ represents one of the embedded target patterns. The control signal is generated with following two algorithms.

1. Algorithm I: regular sampling

$$\mu^{(\tau)}(n) = \frac{1}{N}\sum_{i=1}^{M}\left\{\sum_{k=1}^{N}\delta(i-Pk)[g^{(\tau)}(n,i)]\right\}, \tag{6}$$

where P is the spatial sampling density and $N = M/P$.

2. Algorithm II: random sampling

$$\mu^{(\tau)}(n) = \frac{1}{N}\sum_{i=1}^{N} g^{(\tau)}(n, R_i), \tag{7}$$

where $N < M$ is the sampling number and R_i is a number randomly distributed within 1 to M.

g^{τ} is calculated by comparing the current state with the target one as

$$g^{(\tau)}(n,i) = \mathrm{sgn}[x_i(n)\cdot e_i^{(\tau)}]\exp\left\{\left|\frac{x_i(t)}{e_i^{(\tau)}}\right| - 1\right\}. \tag{8}$$

The Numerical simulations have been performed by using a 36 neuron network model. Three characters "A", "T", "E" are embedded in the network as the target patterns. The initial values of k, α, and a_i are set to proper values for which chaos is observed. Figure 2 shows the associative processes for the target pattern "A". Sampling density is 1/3 for both cases. Even starting from a random initial pattern, the memory search succeeds without trapping in local minima.

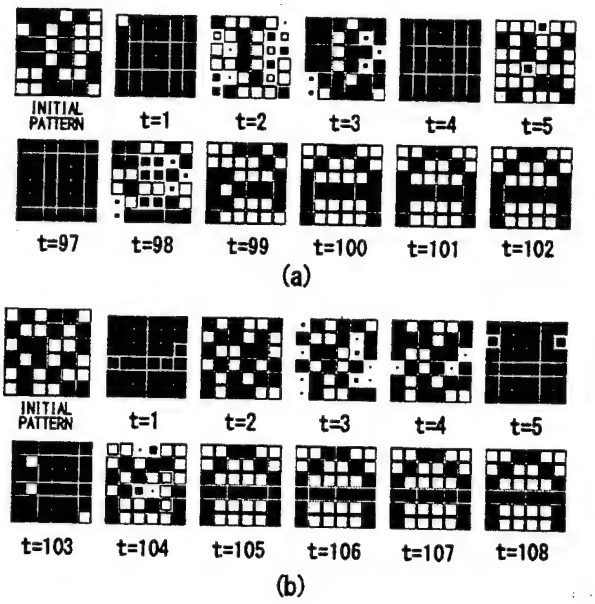

Fig. 2 Associative memory search process with spatio-temporal chaos controlling. M=36, k=0.9, α=0.6, ε=0.02, and a_i=0.25 for all neurons. (a) Algorithm I for P=3; (b) Algorithm II for N=12.

4 Conclusions

We have applied spatio-temporal chaos controlling to associative memory search in a chaotic neural network. The simulations show that the association is successfully performed by using only a part of the target information. Our results imply the possibility of avoiding the local minimum problem by appropriate use of the flexibility of chaotic dynamics. We believe that the current study is helpful in understanding the functional roles of complex dynamics like chaos in neural networks.

References

[1] A. Babloyanz, J. M. Salazar, and C. Nicolis, Phys. Lett., **111A** (1985) 152.

[2] T. Fukai and M. Shiino, Phys. Rev. Lett., **64** (1990) 1465.

[3] C. M. Marcus and R. M. Westervelt, Phys. Rev. A **40** (1989) 501.

[4] K. Nakamura and M. Nakagawa, J. Phys. Soc. Jpn., **62** (1993) 2942.

OPTICAL PATTERNS GENERATED IN THE SINGLE- MIRROR DEVICE WITH POLARIZATION INSTABILITY

by

M. Le BERRE, D. LEDUC, E. RESSAYRE , A. TALLET
Laboratoire de Photophysique Moléculaire du C.N.R.S
Bat.213, Université Paris-Sud, 91405 ORSAY Cedex ,FRANCE
tel (1) 69417392 , Fax (1) 69416777 e-mail: tal@psisun-psud.fr

and

A. MAISTRE
Laboratoire KASTLER-BROSSEL
Université Pierre et Marie Curie, Case 74, 75252 PARIS Cedex, FRANCE

SUMMARY

This theoretical study deals with the spatial instabilities generated in the transverse profile of the light beam transmitted by a gazeous atomic cell that couples the linear cross- polarized components of the electric field. Such a nonlinear medium is typically made of atoms which have a transition with spin momentum $\frac{1}{2}$ like the transition $5S_{1/2}$Æ $5P_{1/2}$ of the isotope 85 of the Rubidium. The input field is linearly polarized and the feedback is realized via a plane mirror located at a variable distance d from the cell. Spatio-temporal instabilities occur in the two cross-polarized field components but we focus on the structures displayed with a polarization orthogonal to the input one.

The analysis of the structures generated in a such a device was primarly motivated by the flower-like patterns observed by Grinberg et al [1]. While these patterns were interpreted in Ref. [1] as a non-Kerr cell effect, they are basically due to a **small aspect ratio,** as shown by the authors in Ref[2]. This circumstance of a small ratio aspect arises from the optical set-up, that favours the diffraction outside the cell along the optical path of length, 2d very large with respect to the cell length, ℓ . It follows

that the aspect ratio is lowered by the amount $\sqrt{\frac{\ell}{2d}}$ with respect to the case without any feedback mirror where diffraction only works in the cell. With such a distributed feedback device, typical patterns like hexagons and rolls were experimentally displayed[3], still with the same Rb transition.

Propagation outside the nonlinear cell provides a threshold instability characterized by a degeneratemulticonical emission, with critical wavenumbers, K_ℓ, $\ell = 1,2,...$ On the focusing side, $K_\ell = \sqrt{1+4\ell}\, K_1$, on the defocusing side, $K_\ell = \sqrt{3+4\ell}\, K_1$. In the very neighbourhood of the threshold intensity, the far-field patterns only display the smallest critical wavenumber and, in the limit of small aspect ratio, flower-like patterns have been numerically reproduced[2]. As the input intensity increases further, the patterns display the influence of the multiconical process through a cubic interaction. That favours the occurrence of square patterns, that actually occur on the focusing side of resonance, in both cases of large and small aspect ratios. Two examples are shown below:

a) See the far-field structure for positive detuning and aspect ratio, $\Re \sim 1$, made of a square pattern of radius K_1 surrounded by twelve spots. Eigth of them are the signature of a cubic interaction in a such a way that the wavenumber built from K_1 is nothing but $K_2 = \sqrt{5}\, K_1$, emphasizing the multiconical emission process.

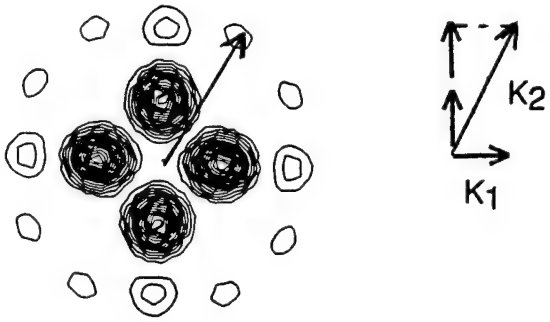

b) On the defocusing side and for large aspect ratio, $\Re \sim 7$ the cubic interaction and the multiconical emission process operate together for building a rectangular structure, with radius equal to K_1 and angle $\phi = 48°$ as a consequence of $K_2 = \sqrt{\frac{7}{3}}\, K_1$. But the K_2 mode amplitudes are very small as compared with the K_1 ones and not visible on this countour line.

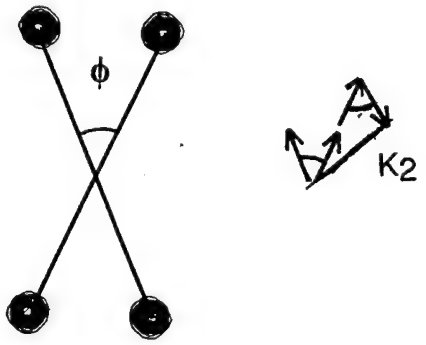

1-G. Grynberg, A. Maitre, A. Petrossian, Phys.Rev.Lett. **72**,2379 (1994)

2-M. Le Berre, *et al* submitted for publication to Opt. Commun.

3-A. Petrossian, M. Pinard, A. Maitre, J.Y. Courtois, G. Grynberg, Europhys. Lett.**18**,689(1992).

Instabilities of a Microcavity Laser with a Weak Optical Injected Signal

Hua Li and T. L. Lucas
Center for High Technology Materials
The University of New Mexico
Albuquerque, NM 87131

John G. McInerney
Department of Physics
National University of Ireland
University College
Cork, Ireland

Summary

The experimental and theoretical study of injection instabilities of a semiconductor laser has been reported before/1-6/. The most theoretical analysis was for a single mode semiconductor laser with monochromatic weak external injection. The corresponding experiments were often performed by using edge-emitting lasers. There was a problem appear quit often: when the laser was driven into unstable regime by external injection, the original lasing mode became unstable and other longitudinal modes appeared, therefore the nonlinear dynamics caused by injection was companied by mode competition instabilities. This limited the experimental observation of injection dynamics only within a narrow parameter range. Here we show our experimental observation of injection dynamics by using an electrically pumped vertical cavity surface emitting laser (VCSEL) as slave laser. Because of extremely short cavity length, VCSEL can only operate with single longitudinal mode. Controlling driving condition guarantees fundamental transverse mode. We can therefore use large detuning and injection power to study dynamics without disturbance of mode competition.

The experimental results will be reported as follows: (1). the measured asymmetric stable locking range implies the linewidth enhancement factor of ~ 2.3; (2).as detuning was settled outside the locking range, uncompleted locking happens often complained by the enhanced relaxation oscillation, its harmonics and subharmonics or beating between slave laser oscillation with injected signal; (3) as detuning was far away from the stable locking range, frequency pushing effect was observed; (4) the resonance effect of injection signal on the transverse modes was also recorded. 4WM signal was expected but not observed because of the limitation of the detection sensitivity.

The corresponding theoretical simulation will be presented. We use two-mode equation based on rate equations calculating transient process and optical spectra under different detuning and injection power. The experimentally observed effects, as described above (1)-(3), were obtained from calculations with good agreement with experiment. 4WM signal was obtained from the theory with a signal level <-30dB which explained why we

did not observe it in our experiment. The experimentally observed resonance influence of injection on the transverse modes needs more sophisticated model which should include polarization dynamics to describe the system in much short time regime of picoseconds range.

In conclusion we show our experimental and theoretical study of injection dynamics. Our results emphasize that the intrinsic relaxation oscillations have important role; the competing of injected signal with original oscillation in slave laser and quenching one by another can be explained mainly through carrier dynamics by rate equations, but more quick process also exits requiring better models.

References:

1. Charles E. Moeller, Peter S. Durkin, Gregory C. Dente, IEEE Journal of Quantum Electron., Vol. **25**, 1603(1989).
2. R. Nietzke, P. Fenz, W. Elsaesser, and O. Goebel. Appl. Phys. Lett., **51**, 1298(1987).
3. D. Boggavarapu, R. Jin, J. Grantham, Y. Z. Hu, F. Brown de Colstoun, C. W. Lowry, G. Khitrova, S. W. Koch, M. Sargent III, and H. M. Gibbs. Optics Letters, Vol. **18**, 1846(1993).
4. J. G. Provost, and R. Frey. Appl. Phys. Lett. **55**, 519(1989).
5. T. B. Simpson, J. M. Liu, A. Gavrielides, V. Kovanis, and P. M. Alsing, Appl. Phys. Lett. , **64** (26), 3539(1994).
6. G. H. M. van Tartwijk and D. Lenstra, SPIE. , Vol. **2099**, 89(1994).

Interaction of Counterpropagating Waves and Self-organizing Distributed Feedback Laser in a Resonant Superfluorescence

I. V. Mel'nikov

General Physics Institute RAS, ul. Vavilova 38, Moscow 117942, Russian Federation

Phone: +7 095 135 0372, Fax: +7 095 135 0270, E-mail: ivm@gpi.ac.ru

Many optical phenomena involve nonlinear coupling of counterpropagating waves. Such devices like laser gyro, correlated emission laser, and microcavity semiconductor laser are well known examples. Following the original work of Schwan et al. [1] attention has been turned to the possibility of the coupling to manage superfluorescent decay (SFD) as a distributed feedback laser. This Report is aimed on the development of such model of the process in which ensemble of evenly distributed atoms can organize itself into a spatially periodic structure.

The model is based on the following argument. When, owing to quantum fluctuations of dipole moment and field, an inverted atom begins to decay it emits independently on the rest of the ensemble, total intensity of radiation from the sample is a sum over all ensemble, and no correlations occurs. The first step toward creation of feedback structure can be achieved through seeding of classical field. This field stems from non-zero polarization of a single atom and is fed by classical fields of surrounding atoms. Then the mechanism of growing of spatial correlations can be viewed as a result of interference between the source and its own field backscattered by the decaying neighbors. Consequently, it prevents reducing consideration to a couple of interacting waves and demands solving a set of Maxwell-Bloch equation beyond traditional slow-envelope approximation.

In order to discuss the process qualitatively the dynamics of the atom in external field can be examoned near the state of inversion. Starting from linearized Bloch equations it is derived such equation for the resonant polarization that comprises effect of the resonant environment as follows,

$$\frac{\partial P(x,\tau)}{\partial \tau} = \frac{1}{L}\int_{-L/2}^{L/2} P(\xi,\tau)\exp(ik_0|x-\xi|)\,d\xi,$$

Although it is only approximate, this equation gives the general trend, and shows in particular that, as the sample length approaches integer number of the half-waves, the output intensity on the left face of the sample reaches its local maximum while it equals to zero in the opposite direction, and vice versa. Violation of this condition leads to symmetrization of SFD, the intensity of the radiation experience monotonous growth in the opposite directions.

To achieve additional insight into the process numerical methods are used, and their results are depicted in Fig. 1. The sample is supposed to be excited by an ultrashort optical pulse coming from the left, and the concentration of the resonant centers is chosen to be equal that of the experiment [1]. It is quite remarkable that for the sample with the length of

10 λ the intensity of the emission to the left is approximately five times greater than to the right, and such switching behavior accomplishes with

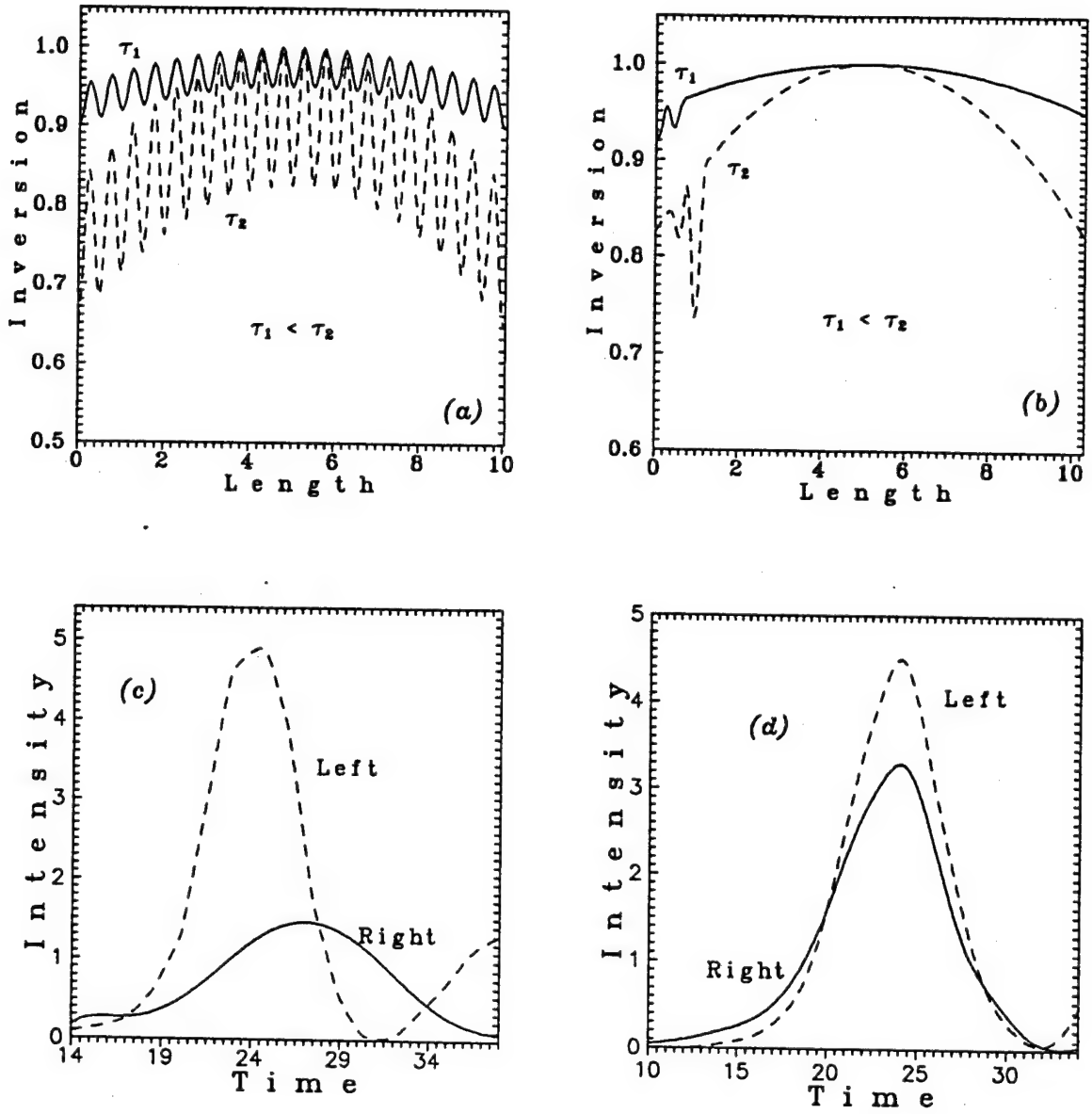

Figure 1 Variance of inversion vs sample length (a), (b) and corresponding intensities

patterning of grating with period λ/2 in the spatial profile of the inversion population [Fig. 1a,c]. Thiny increasing of the sample length up to 10.25 λ [Figs. 1b,d] equalizesthe intensities on the opposite sides of the sample, and does smooth the inversion profile.

Reference

1. L.O.Schwan, R.Florian, and D.Schmid, Phys.Rev. A29, 2709 (1984).

Optical patterns in sodium vapor: Experiment and theory

T. Ackemann, Y. Logvin, A. Heuer and W. Lange

Institute of Applied Physics, University of Münster, Corrensstrasse 2/4, D-48149 Münster, Germany, Tel.: +251-83-3553, Fax: +251-83-3513, E-mail: ackeman@nwz.uni-muenster.de

Because of its simplicity, a system consisting of a nonlinear medium and a single feedback mirror is very attractive for studies of optical patterns [1]. It was demonstrated in a recent experiment that sodium vapor in an external magnetic field provides favorable properties for studying the spontaneous generation of optical patterns and their symmetry [2]. Here we present further experimental results and a theoretical discussion – based on a microscopic model – of the nonlinear optical properties of the system and their role in pattern formation.

Our experimental set-up is a slightly modified version of the one described in [2] with a further improved spatial filtering (by a single-mode fiber) and a shortened heated zone ($L = 15$ mm) to reduce propagation effects inside the medium. The circularly polarized, enlarged ($w_0 = 1.4$ mm being the $1/e^2$ point of intensity) beam of a cw dye laser is injected into a sodium cell (Na particle density of about $10^{14}\mathrm{cm}^{-3}$, nitrogen buffer gas pressure 300 mbar). The transmitted beam is fed back into the cell by a plane mirror ($R = 91.5\%$). An external magnetic field is produced by a system of three pairs of Helmholtz coils. At the red side of the D_1-line highly modulated patterns appear if and only if the magnetic fields are properly adjusted (fig. 1a). As in [2] the appearance of stable patterns with an increasing number of filaments and different global symmetries for increasing beam power is observed and thus shown to be independent of the beam radius. In the region with pattern formation the integral transmission decreases with increasing power of the incoming beam (fig. 1b).

For the theoretical description we adopt the model of Ref. [1] for the propagation of the optical field, but replace their Kerr-like model equations by the one for a two-level spin system [3] (including the thermal diffusion of the sodium atoms in the buffer gas atmosphere), since under our experimental conditions optical pumping between the Zeeman sublevels of the ground state is the relevant nonlinear mechanism. This introduces the qualitatively new features of saturation and a sensitive dependence on - and hence controllability by - external magnetic fields. A plane wave solution and its stability analysis already explain some basics of the experimental findings. The principal shape of the transmission curves (fig. 2a) as well as the location of the instability regions in the parameter subspace spanned by the magnetic field components are rather well reproduced. The theoretical analysis shows in accordance with the experiment that pattern formation is only feasible in a small transverse magnetic field, which suppresses wash-out by diffusion while still allowing significant optical pumping. As reported, the experiment is performed for *red* detuning, which is regarded to be a *self-defocusing* situation. However, in parameter regions favorable for pattern formation, the refractive index n shows a nonmonotonic dependence on the light intensity, as revealed by the transmission curve in fig. 2a. (n is related to the transmission through $\ln T \sim (n-1)$.) In the region with negative slope, where in accordance with the experiment patterning occurs, the medium is *self-focusing*. Hence, also the characteristic length scale is qualitatively the one which is expected for a focusing medium. For higher intensity the medium becomes again self-defocusing and the transmission increases with the possibility of switching effects, shown in fig. 2a. (In the experiment, this increase can be observed for small longitudinal magnetic fields and/or close to resonance. However, for parameters which allow pronounced patterning (e.g. fig. 1), the observation is prevented by the limitation of the available laser power.)

The observed behavior is the manifestation of a *light-shift induced level-crossing*, which occurs if the influence of the light-shift and the external longitudinal field component have opposite sign. A close inspection shows that – depending on whether this level-crossing occurs in the minima or maxima of the intensity grating inside the medium – the spatial modulation of the orientation and the intensity are in or out of phase, corresponding to either a self-defocusing or self-focusing situation. Note, that the action of the magnetic field is not limited to destroy orientation and thus to supply the term modelling relaxation in [1], which would otherwise be negligible in alkali metal vapors. Furthermore, in a spatially modulated optical field the condition for level-crossing varies and thus the rate of the destruction of orientation is modulated and can adopt itself to sustain optimal contrast. This fits nicely to the results of a recent degenerate four-wave mixing experiment in sodium vapor, where the same mechanism was shown to control the contrast of the refractive index grating [4].

Obviously, the situation in a Gaussian beam is more involved than the plane wave case due to the

inhomogeneous intensity distribution, but two-dimensional simulations with a Gaussian input beam (fig.2b) and the experiment show that the general features survive. The transmission characteristics are only somehow smoothed. The numerically calculated patterns turn out to be very similar to the experimental ones (inset in fig. 2b). The theoretical results suggest the possibility of the simultaneous existence of defocusing (e.g. in beam center) and focusing (e.g. in the beam wings) regions in the same beam.

[1] G. D'Alessandro and W. J. Firth, Phys. Rev. A 46, 537 (1992); F. Papoff, G. D'Alessandro, G. L. Oppo and W. J. Firth, Phys. Rev. A 48, 634 (1993).
[2] T. Ackemann and W. Lange, Phys. Rev. A 50 R4468 (1994).
[3] F. Mitschke, R. Deserno, W. Lange and J. Mlynek, Phys. Rev. A 33, 3219 (1986).
[4] M. Schiffer, E. Cruse and W. Lange, Phys. Rev. A 49, R3178 (1994).

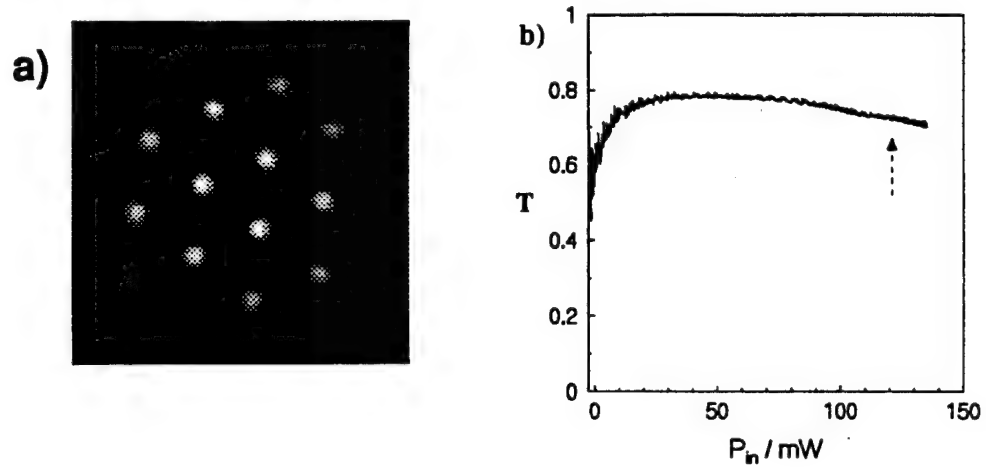

Fig. 1: a) Pattern observed at the exit face of the medium for P =125 mW, $\Delta = -15$ GHz, $B_{trans} = 3.9\mu$T, $B_{long} = -31\mu$T, cell center to mirror distance 76 mm. b) Integral transmission of the cell as a function of incident power. The arrow marks the appearance of the pattern in a).

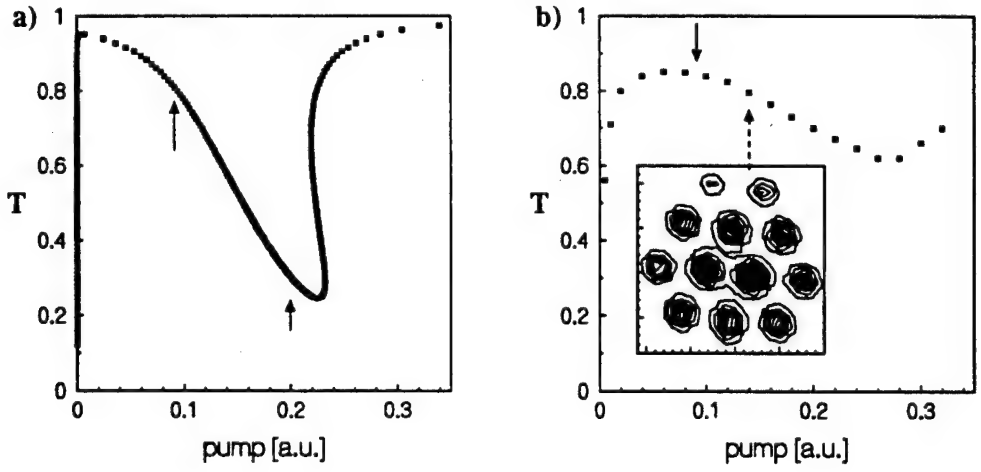

Fig. 2: Transmission coefficient versus external pump power. a) Plane wave analytical theory. The arrows mark the region of instability against transverse perturbations. b) Numerically calculated integral transmission for Gaussian beam input. The inset shows the pattern at the pump power indicated by the dotted arrow. The closed arrow marks the onset of pattern formation. Parameters as in fig. 1.

Polarisation effects on pattern formation in liquid crystal light valves : theory, simulations and experiments.

R. Neubecker, B. Thuering*, T. Tschudi*, and G.-L. Oppo

Department of Physics and Applied Physics, University of Strathclyde
107 Rottenrow, Glasgow, G4 0NG, Scotland, UK
Tel + 44 - 141 - 552 - 4400 (ext. 3761)
Fax + 44 - 141 - 552 - 2891
Email : gianluca @ phys.strath.ac.uk

Pattern formation in nonlinear optics has increasingly attracted attention over recent years and occurs in different types of spatially-extended optical systems often with nonlinear feedback. Single feedback systems are basically formed by a pump beam which traverses a nonlinear medium and gets reflected back into the medium by a single mirror. They have a simple architecture and are easy to model.

Effort is also taken to experimentally realise large-aspect ratio patterns whose the typical length scale is much smaller than the aperture. This is often hard to achieve since high intensities and large beam diameters are needed simultaneously. The Liquid Crystal Light Valve (LCLV), however, has turned out to be an ideal device to investigate large aperture patterns in single feedback setups. While LCLVs had already been used for pattern formation induced by geometrical transformations of the feedback [1], recent experiments [2,3] focused on the realisation of the "single feedback Kerr slice" setup originally proposed by D'Alessandro and Firth [4].

The LCLV is an optically addressable spatial light modulator, which can be regarded as an optical nonlinearity with physically separated interaction light→matter and matter→light. Its main experimental advantages lie in the high modulation sensitivity and the large space-bandwidth product. Being designed for display applications, LCLVs have the ability of modulating the pump beam polarisation in a way similar to an intensity controlled optical retarder plate [5]. Therefore the pure phase modulation used in [2,3] is only a subset of a more general case for which we set up an appropriate theoretical description. We also study the changes between self-defocusing and self-focusing behaviour by virtue of an experimental trick.

Plane wave solutions under the action of polarisation modulation show optical multistability, which in turn generates a rich variety of spatial instabilities. A linear stability analysis is used to determine the thresholds of pattern formation. These thresholds, and the unstable wavenumber in particular, critically depend on an easily accessible operation parameter of the LCLV: its supply voltage.

Extensive numerical simulations confirm the analytical predictions and furthermore show that the type of the pattern depends on the supply voltage as well. By changing this control parameter, the intensity pattern switches between rolls, squares, hexagons, and structures of more complicated geometry (see Figure 1).

An experiment that tests the reliability of our theoretical and numerical predictions has been set up by adding a polariser in the feedback loop of a LCLV. Transitions

between rolls, hexagons and squares have been observed in agreement with the theoretical results. More importantly, for large enough polarisation modulations, the spatial wavelength of the pattern can be consistently modified by changes of the supply voltage. A comparison between experimental results and theoretical predictions is presented in Figure 2. The agreement is simply spectacular. The proposed setup which takes advantage of the polarisation modulation, allows for a simple control of the generated patterns and their scalability.
Support from EPSRC (GR/J/30998) is gratefully acknowledged.

References

[1] S. Akhmanov et al., J. Opt. Soc. Am B **9**, 78 (1992).
[2] B. Thuering, R. Neubecker, and T. Tschudi, Opt. Comm. **102**, 111 (1993).
[3] E. Pampaloni, S. Residori, and F.T. Arecchi, Europhys. Lett. **24**, 647 (1993).
[4] G. D'Alessandro and W. Firth, Phys. Rev. A **46**, 537 (1992).
[5] K. Lu and B. Saleh, Appl. Opt. **30**, 2354 (1991).

(*) Institut fuer Angewandte Physik, Technische Hochschule, Darmstadt, Germany.

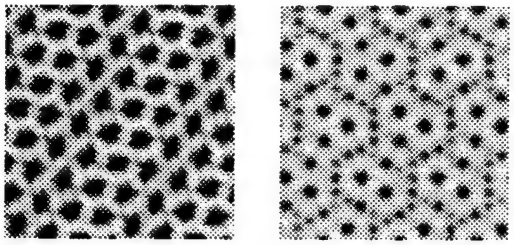

Figure 1: *Typical patterns found numerically for a self-defocusing nonlinearity upon changes of the LCLV supply voltage.*

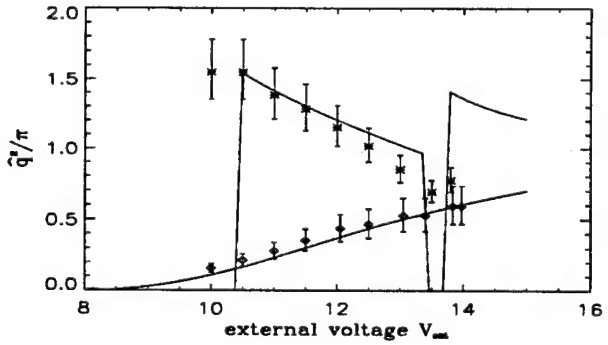

Figure 2: *The pattern wavenumber $\hat{q}$ versus the supply voltage. Solid lines correspond to theoretical predictions while dots refer to experimental measurements for the defocusing (upper curves) and focusing (lower curves) cases.*

Competing spatial instabilities in a coupled LCLV feedback system

B. Thüring, A. Schreiber, M. Kreuzer, T. Tschudi

Institute of Applied Physics, Technische Hochschule Darmstadt,

Hochschulstr.6, 64289 Darmstadt

Tel. +49-6151-16 2379, Fax +49-6151-16 4123,

Email: bernd@gaston.iap.physik.th-darmstadt.de

One of the most interesting problems of selforganized systems showing spontaneous pattern formation is the question how the system *selects* a defined wavenumber or a narrow band of wavenumbers [1]. Do various mechanisms select the same, *preferred* state, or does each participating process produce its own wavenumber? If there are different selected states, it is natural to ask what happens if two mechanisms are operating simultaneously. We discuss this question experimentally and theoretically in a nonlinear optical system with two separate single feedback loops of distinct lengths L_1 and L_2. Each single feedback is able to develop spontaneous transversal patterns with a spatial wavenumber which scales with the feedback length [2]. We realize a dispersive optical nonlinearity by an optical addressed liquid crystal light valve (LCLV), operating as a defocusing (Kerr-) medium [3]. Due to the distinct propagation lengths, each feedback selects a well defined wavenumber, so that we can control the mutual influence of these competing spatial instabilities by changing the ratio of the distinct feedback lengths. We show that such a competition crucially influences the pattern selection process and helps to explain complex spatio temporal dynamics.

First we show how a variation of the ratio $\xi = L_2/L_1$ changes the principal behaviour of the system. In a wide parameter range of ξ, we find stationary, hexagonal ordered patterns (Fig. 1a), with a typical macroscopic structure size, scaling with the ratio ξ. In this case the system selects a pattern with *one* well defined spatial wavenumber. Close to a critical point ξ_c, the pattern becomes non-stationary. In transient states, we find two different coexisting macroscopic scales (fig. 1b), but generally the pattern oscillates irregularly between the attracting wavenumbers, interrupted by sudden *bursts* of disorder. These oscillations are important hints that we observe in this parameter range a real competition of coexisting spatial instabilities with two different wavenumbers involved. For a ratio ξ smaller than ξ_c we find stationary patterns with similar scaling behaviour again, but on a smaller scale than for ratios larger than ξ_c (fig. 1c).

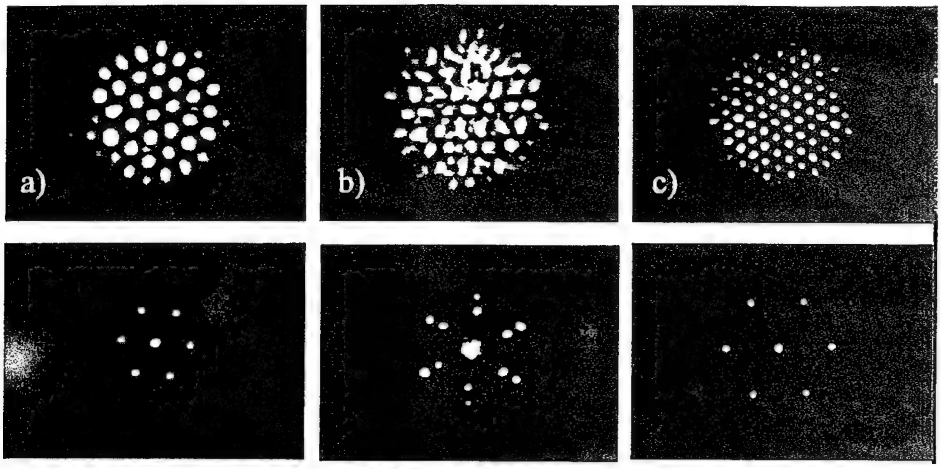

Figure 1: **top:** Experimentally observed output patterns, (a): $\xi = 0.62$ (b): $\xi = \xi_c \simeq 0.54$ (c): $\xi = 0.42$; **bottom:** Corresponding far field patterns, showing the selected wavenumbers

In order to get a closer understanding of the observed complex behaviour, a linear stability analysis is carried out. The results show that depending on the ratio of the two distinct feedback lengths ξ, two most unstable wavenumbers have equal pattern forming threshold intensities for certain values of ξ, leading to a *coexistance* of spatial instabilities. This confirms our assumptions made above, that a competition of coexisting spatial instabilities is the reason of the observed oscillatory behaviour. The numerically derived scaling behaviour of the macroscopic structure size due to the parameter ξ is marked by striking *jumps*, indicating the points where spatial instabilities coexist. Comparing the experimantal results with numerical simulations we find a good qualitative and quantitative agreement.

References

[1] M.C. Cross, P.C. Hohenberg, *Rev. Mod. Phys.*, Vol. 65, No.3,1993

[2] G. D'Alessandro, W.J. Firth, *Phys. Rev. A*, Vol. 46, No.1, p. 537-548, 1992; M.A. Vorontsov, W.J. Firth,*Phys. Rev. A*, Vol. 49, No. 4, p. 2891-2906, 1994

[3] B.Thüring, R.Neubecker, T.Tschudi. *Opt. Commun.*, Vol.102, No.1,2, p. 111-115, 1993; E.Pampoloni, S. Residori, F.T. Arecchi, *Europhys. Lett.*, Vol.24, No.2, p. 647-652, 1993; R.Neubecker, B.Thüring, T.Tschudi, *Chaos, Solitons and Fractals*,Vol.4, Nos.8/9, 1994; R.Neubecker, G.-L. Oppo, B.Thüring, T.Tschudi. submitted to *Phys. Rev. A*, 1994

Transport induced optical instabilities in a nonlinear spatially extended system

P.L. Ramazza, S. Residori, E. Pampaloni and F.T. Arecchi(+)

Istituto Nazionale di Ottica, 50125 Firenze

(+) also Phys. Dept., University of Florence

We describe a new scenario of pattern formation in a system formed by a Liquid Crystal Light Valve with feedback, when a translationally invariant simmetry breaking is introduced in the feedback loop. From a practical point of view this simmetry breaking is obtained by means of angular tilt or translation of the beam that is fed back on the Valve.

The experimental procedure used corresponds to the introduction of a transverse transport term in the wave equation describing the evolution of the optical field [1],[2]. This extra term is responsible for the onset of a drifting roll instability, as theoretically predicted [1],[2] and experimentally demonstrated [3],[4] for the case in which the nonlinear medium is an alkali vapour filled cell.

In our experiments we have investigated both one-dimensional and two-dimensional geometries. In the one-dimensional case, we confirm the existence of a drifting roll instability and discuss the dependence of the roll wavelength and drift frequency on the experimental parameters.

The two-dimensional geometry displays a much richer set of pattern forming

instabilities, some of which (cross-roll instability, zig-zag instability) have been previously observed in hydrodynamical systems. We give a classification of the domains of stability of the various patterns in the experimental parameter space.

References

[1] M. Haelterman and G. Vitrant, J. Opt. Soc. Am. **B 9**, 1563 (1992).

[2] G. Grynberg, Opt. Comm. **109**, 483 (1994).

[3] P. La Penna and G. Giusfredi, Phys. Rev. **A 48**, 1610 (1993).

[4] A. Petrossian, L. Dambly and G. Grynberg, to be published in Europhys. Lett. (1995).

[5] P. Manneville, *Dissipative structures and weak turbulence*, Academic Press, San Diego (1990).

Pattern Formation in a Microfeedback System

W.J.Firth[a], Yu.A.Logvin[b] and B.A.Samson[b]
[a] Department of Physics and Applied Physics, University of Strathclyde, 107 Rottenrow, Glasgow, G4 0NG, Scotland
[b] Institute of Physics, Belarus Academy of Sciences, 70 F.Skaryna Ave., Minsk, 220072, Belarus

The Kerr slice with feedback mirror [1] has proved a very fertile concept for studies of optical pattern formation. For applications and for fundamental reasons it is of interest to consider miniaturising these patterns. This raises the question of the ultimate limitations on the scale of the hexagons, rolls and other structures observed in such feedback experiments. The optical wavelength obviously provides a basic limit, but to even to reach that scale some generalisation is necessary. In particular, envelope and paraxial approximations need to be removed. In this work we investigate these questions, and show that the pattern formation survives, and is indeed enhanced, in the more general model.

The optical scheme consists of the nonlinear layer and flat feedback mirror parallel to the layer at a distance d. The key point is that the layer is assumed to much thinner than the optical wavelength λ, and that d may be comparable to λ. Such a structure could be realised in semiconductors using techniques established for microresonators [2]. A plane wave with the amplitude E_{inc} illuminates the layer normally from one side, the mirror feedback illuminating the layer from other side.

We suppose the nonlinearity of the nonlinear layer to approximate a two-level system, which is a reasonable first approximation to saturable media such as semiconductors. The bulk dynamics of the two- level centers then obeys the Bloch equations

$$R_t = (-1 + i\delta)R + iWE, \qquad W_t = -\gamma(W+1) + i(RE^* - R^*E)/2, \quad (1)$$

where R and W are the polarization envelope amplitude and population difference, γ is the normalized relaxation rate, δ is the detuning of a light frequency from the resonance, E is the amplitude of the total driving field (input plus feedback):

$$E(t, \mathbf{r}_\perp) = 2E_{in}(t, \mathbf{r}_\perp) - i2C(R(t, \mathbf{r}_\perp) + \hat{P}_d R(t, \mathbf{r}_\perp)), \quad (2)$$

The coefficient C is the bistability parameter, proportional to layer thickness, volume density of the centers and their dipole moment (see [3] for discussion of this model, and references). $\hat{P}_d$ is the propagation operator. Both in paraxial

and non- paraxial cases the plane wave $\exp(i\mathbf{k}_\perp\mathbf{r}_\perp)$ is an eigenfunction of $\hat{P}_d$ with eigenvalue $\exp(-i\alpha)$ In the usual paraxial approximation $\alpha = \mathbf{k}_\perp^2 d$.

Performing linear stability analysis around steady-state uniform solutions, considering the intensity $|E_s|^2$ as the threshold parameter, one finds that pattern-forming perturbations with finite $\mathbf{k}_\perp$ normally have lowest threshold.

Multiple-scale expansion in the vicinity of the threshold results in a set of Ginzburg- Landau equations for the amplitudes of hexagon (roll) components. Their analysis shows subcritical bifurcation to negative hexagons at the lower end of the instability interval and to positive hexagons at the upper end, and they can also describe roll-hexagon competition.

There is a symmetry in the system's behaviour with respect to the sign of the detuning δ: $\alpha_{crit}(-\delta) = 2\pi - \alpha_{crit}(\delta)$. This is important for the multiple-scale analysis at small $|\delta|$. In this case we derive the Swift-Hohenberg-like equation:

$$Y_t = \epsilon\sigma_1 Y + (\nu_1\delta^2 + \nu_2\delta\Delta_\perp - \nu_3\Delta_\perp\Delta_\perp)Y + \sigma_2 Y^2 - \sigma_3 Y^3, \qquad (3)$$

where ϵ is the distance from the threshold, and coefficients σ and ν depend on parameters of initial equations (1), (2). This equation also describes the patterns at negative δ.

The numerical simulation of the problem (1),(2) in $1D$ and $2D$ cases is in good agreement with the above linear and nonlinear analysis. We observed spontaneous hexagon, roll, square, rhomboid and stretched hexagon patterns formation, together with creation of defects, hexagon-roll competition, hysteresis caused by subcritical bifurcations, and switching initiated by pattern formation.

We will describe these phenomena, emphasising non-paraxial features of the near- and far-field output, and assess parameter values for implementation of semiconductor microfeedback systems.

References

[1] W. J. Firth, J. Mod. Opt. **37**, 151 (1990): G. D'Alessandro and W. J. Firth, Phys. Rev. Lett. **66** 2597 (1992): G. D'Alessandro and W. J. Firth, Phys. Rev. **A46** 537 (1992).

[2] *Optical Processes in Microcavities*, Y. Yamamoto and R. E. Slusher, *Physics Today*, June 1993, *pp* 66-73, and *op. cit.*

[3] Yu. A. Logvin and A. M. Samson, Sov. Phys. JETP **75** 250 (1992).

Patterns, pattern dynamics, and pattern correlations in a photorefractive bidirectional ring resonator

Z. Chen, D. McGee and N.B. Abraham
Department of Physics, Bryn Mawr College, 101 N. Merion Ave,
Bryn Mawr, PA 19010-2899 USA
nabraham@cc.brynmawr.edu fax: 610-526-7469

We present theoretical and experimental studies of the bidirectional emission of a ring resonator containing a photorefractive medium. Our recent numerical simulations in the transmission grating limit, have revealed intriguing spatiotemporal pattern dynamics in the bidirectional oscillation [1]. We will review the model and the results for pattern formation (depending especially on cavity length and Fresnel number), spontaneous pattern dynamics (pulsation and rotation in the symmetric case), spontaneous pattern alternation when there is astigmatism or misalignment, and the increasing decorrelation of the counterpropagating patterns as the Fresnel number is increased.

Experimentally, using a $BaTiO_3$ crystal as the photorefractive medium and a low-power single-mode and single-frequency HeNe laser for the pump beams, we have measured the formation and evolution of the counterpropagating patterns in a four-mirror ring resonator. Pattern alternation in definite and repeatable sequences (with periodic or chaotic temporal alternation) which we have observed, similar to previous experiments for unidirectional emission based on photorefractive two-beam coupling [2], seems in our case to result from slow thermal drifts in the cavity length as suggested in other two-beam studies [3]. The number of distinct patterns and the complexity of the dynamics depends on the Fresnel number of the resonator. For low Fresnel numbers the counterpropagating patterns are highly correlated, with essentially the same pattern in space and time including tracking of the intensity and orientation of the patterns. For higher Fresnel numbers, as the number of modes involved in the pattern dynamics increases, more complicated spatiotemporal patterns are observed which do not correspond to any transverse modes of the cavity, and these patterns rotate, oscillate and dance besides alternating, with the counterpropagating patterns less correlated, essentially becoming fully decorrelated patterns evolving independently for very large Fresnel number.

The Fresnel number affects the spatial structure of the pattern in both beams dramatically. It controls the number of transverse cavity modes which have relatively low cavity loss. In the following, we will report the results obtained when the Fresnel number is varied as a control parameter (by changing the two apertures) while the pump beam ratio is fixed at 10 to 1.

The output alternated among a small set of nearly pure modal patterns in a fixed sequence with the timing governed by the drifting cavity length when the Fresnel number was not too large. Even when the Fresnel number was small enough to permit only the fundamental TEM_{00} mode to oscillate, there was alternation between a period of emission of this mode and a long period of zero-intensity. For instance, at F=0.8, a single spot winked on and off in both beams synchronously. When F was increased to 2.0, a two-spot pattern or a donut pattern joined the alternation sequence. For low Fresnel numbers, the pattern sequence consists of relatively long residency times with patterns closely equivalent to low-order Gauss-Laguerre (GL) or Gauss-Hermite (GH) modes. As the Fresnel number is increased, the highest order of transverse modal pattern in the alternation sequence increases, the periodic nature of pattern alternation decreases, and the transitions from one relatively stable modal pattern to another involve more transitional intermediate states. For high Fresnel numbers (F=9.1), there is no longer clear modal pattern or alternation sequence, instead, it appears that the patterns are restless with irregular changes in space and time which may have the dynamics termed "spatiotemporal chaos" [4].

Several other distinct features are noticed in the changes in the pattern evolution with increasing Fresnel number. First of all, the bidirectional patterns are well correlated in space and time for low Fresnel numbers in the sense that they both have basically the same modal pattern and they evolve synchronously. This correlation is progressively lost for increasing Fresnel number as the correlation between the counterpropagating emissions breaks down with differences first in the brightness of sections of geometrically similar patterns, and then in both geometrical structure and relative intensity of the patterns. At F=9.1 and F=12.6, the patterns in the two beams cannot be

described by any single cavity mode and they both perform "chaotic dancing" with no evident correlation between them.

Compared to GH modal patterns, GL modal patterns have shorter dwell times. Although modal patterns such as the donut mode at F = 2.0, GL_{02} at F = 4.5, and GL_{04} mode at F = 7.1 are identifiable, they appear as nonstationary intermediate states. On the other hand, a low-order GH modal pattern in the alternation sequence can stay relatively stable indicating GH modes are present when there are fewer overall modes accessible to the system with detuning. Interesting enough, there is sustained rotation during evolution of the Gauss-Laguerre modal pattern, with both beams rotating in synchrony. An example of such rotation was found for F = 4.5. The alternation sequence consists of a TEM_{00} mode, a GL_{02} mode, a GH_{20} mode, a GH_{10} mode and the zero-intensity. But unlike Gauss-Hermite modal patterns which are orientationally stationary during their dwell time, the four-spot GL_{02} modal pattern in both beams rotate azimuthally, like traveling waves. We can understand this since it is likely that there is some breaking of the transverse rotational symmetry (by astigmatism from alignment of the variously angled crystal surfaces, optical elements, or pump beams). This gives a preferred orientation for each nonrotationally symmetric pattern. By contrast, when there is rotational symmetry which might favor GL modes, all rotational orientations may be equally favored. Either the nodes of $\cos(n\theta)$ are fixed by azimuthally localized losses, or perturbations should cause diffusion. Steady rotation of such GL_{0n} [$=\cos(n\theta+\phi)$] patterns correspond to a frequency difference in the $\exp(n\theta)$ and $\exp(-n\theta)$ basis patterns. The bright and dark regions of the patterns seem to vary in the counterpropagating patterns, sometimes a given θ has a bright spot in both beams but of different relative strengths compared to other overlapping bright spots. Sometimes the bright spots in one beam occur at angles at which there are dark spots in the other pattern as if $\cos(n\theta)$ patterns were interleaved in the two beams. Despite changes in the intensity of each section of the pattern, the patterns in both beams retain a geometrically similar structure during rotation. Because we are looking from opposite sides of the crystal, the counterpropagating patterns appear to rotate in opposite directions.

Since we used a slow crystal pumped at low power, the dynamics could be resolved during the transitions between different patterns. Some intermediate patterns during switchings can be clearly interpreted to be the result of two-mode mixing or intermode beating, for instance, between a TEM_{00} and a GL_{01} of different frequencies which causes a rotating dark spot. The radius at which the dark spot is located is determined by the relative strength of the two modes and the rotation rate of the dark spot is determined by the frequency spacing of the two modes. The interaction between a TEM_{00} mode and a GH_{01} mode may cause alternate blinking of two spots. In our case blinking was observed during the transition between a single-spot pattern and a two-spot pattern, first in one direction and then, through a rotation, in other direction, and it repeated several times before the pattern became relatively stationary. Other phenomena involving interaction (rotation, approach, departure, and annihilation) of two dark spots were also observed as part of the intermediate transition between two patterns in an alternation sequence when there was competition among a few excited modes as discussed recently in a related system [4].

We have yet to observe in our experiments, the spontaneous pattern alternation found in our numerical simulations for misaligned (or astigmatic) optical cavities. Nor have we seen the predicted [5] and observed [2,5] spontaneous alternation for symmetric alignments in 2-beam systems.

1. Z. Chen and N.B. Abraham, to appear in Appl. Phys. B (1995).
2. F.T. Arecchi, G. Giacomelli, P.L. Ramazza and S. Residori, Phys. Rev. Lett. **65**, 2531 (1990); Phys. Rev. Lett. **67**, 3749 (1991); F.T. Arecchi, S. Boccaletti, G.P. Puccioni, P.L. Ramazza and S. Residori, Chaos **4**, 491 (1994).
3. D. Hennequin, L. Dambly, D. Dangoisse and P. Glorieux, J. Opt. Soc. Am. B **11**, 676 (1994).
4. G. Indebetouw and D.R. Korwan, J. Mod. Opt. **41**, 941 (1994).
5. K. Staliunas, M.F.H. Tarroja, G. Slekys and C.O.Weiss, preprint 1994.

Polarization Pattern Dynamics in the Laser Vector Complex Ginzburg-Landau Equation

A. Amengual, M. San Miguel, R. Montagne and E. Hernández-García
Departament de Física, Universitat de les Illes Balears
E-07071 Palma de Mallorca, Spain
Tel: 34 (71) 173229 - Fax: 34 (71) 173426 - e-mail: dfsmsm0@ps.uib.es

I. Introduction

Lasers offer a very interesting opportunity for the study of complex spatio-temporal dynamics in systems requiring a vectorial order parameter description. The slowly varying amplitude of the vector electric field $\mathbf{A}$ has a global phase θ and a relative phase ψ. When the laser polarization is fixed, for example by Brewster windows, the phase θ, which gives the time origin of the field oscillation, is the relevant phase and transverse pattern formation is often associated with θ-instabilities (scalar case). For an isotropic laser emitting linearly polarized light the dynamics of ψ, describing the direction of polarization, incorporates a much richer variety of possible states of laser light. We report here a numerical study, for the one-dimensional case, of a recently derived Vector Complex Ginzburg-Landau Equation (VCGLE) for an atomic $J = 1 \rightarrow J = 0$ transition [1,2]. We describe linearly-polarized Travelling Waves (TW), Polarized Standing Waves (SW) and depolarized solutions, as well as dynamical evolution among these states through polarization-phase instabilities. We also show that when the laser radiation grows form spontaneous emission noise it generally reaches complex disordered states. In particular, a vector form of Spatio-Temporal Intermittency is found.

II. Polarization states of the laser VCGLE

For a negative detuning between atomic and cavity frequencies and close to threshold, a one-dimensional amplitude equation description yields a VCGLE for $\mathbf{A}$ (see [2] for the positive detuning case):

$$\begin{aligned}\partial_t \mathbf{A} &= \mu\mathbf{A} + (1+i\alpha)\partial_x^2\mathbf{A} \\ &- (1+i\beta)((\mathbf{A}\cdot\mathbf{A}^*)\mathbf{A} + \delta(\mathbf{A}\cdot\mathbf{A})\mathbf{A}^*)\end{aligned} \quad (1)$$

In this equation μ measures the distance to threshold, α originates from diffraction and β is associated with detuning. The coupling parameter δ is determined by decay rates associated with the coherence and population difference between upper levels with different spin number. The fact that δ is a real number, together with $1+\alpha\beta > 0$, are the two main parameter restrictions for this version of the VCGLE appropriate to describe laser systems.

In terms of the right and left circularly polarized components of $\mathbf{A}$, $A_\pm = (A_x \pm iA_y)/\sqrt{2}$, a family of solutions of the laser VCGLE is

$$A_\pm(x,t) = Q_\pm \exp\left(-ik_\pm x + i\omega_\pm(k_\pm)t + i(\theta_0 \pm \psi_0)\right) \quad (2)$$

We will focus in the case $\delta < 0$ in which the spatially homogeneous ($k_+ = k_- = 0$) solutions stable with respect to zero wavenumber ($q = 0$) perturbations are linearly polarized: $Q_+ = Q_-, A_x \propto \cos\psi_0$, $A_y \propto \sin\psi_0$. We distinguish three classes of polarization pattern solutions:

a)Linearly Polarized Traveling Waves (TW): $k_+ = k_- \equiv K, Q_\pm^2 = (\mu - K^2)/(1+\gamma), \omega_\pm = -\alpha K^2 - \beta(1+\gamma)Q_\pm^2$. These solutions are linearly polarized with an arbitrary direction ψ_0.

b)Polarized Standing Waves (SW): $k_+ = -k_- \equiv K$, $Q_\pm^2 = (\mu - K^2)/(1+\gamma)$, $\omega_\pm = -\alpha K^2 - \beta(1+\gamma)Q_\pm^2$. They can be visualized (Fig.1a) as linearly polarized solutions in which the direction of polarization is periodic in space, with each cartesian component of the field being a standing wave for the intensity of the electric field:

$$A_x \propto \cos(Kx + \psi_0)\ ,\ A_y \propto \sin(Kx + \psi_0) \quad (3)$$

c)Depolarized solutions (DPS): The general solution (2) for $k_+ \neq k_-$ corresponds to spatio-temporal states of the laser field without a simple polarization description (Fig.1b). These solutions can be parametrized by $K = (k_+ + k_-)/2$ and $d = k_+ - k_-$

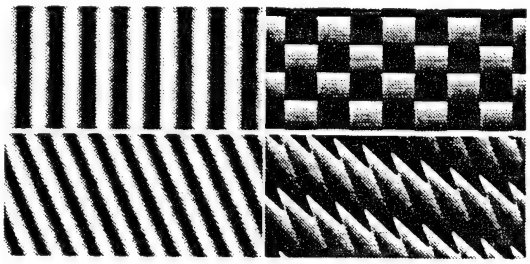

Figure 1: Space-time plot of the modulus (left) and the phase (right) of the amplitude A_x for a standing wave with $K = 0$ and $d = 0.098$ (top) and a depolarized solution $K = 0.074$ and $d = 0.123$ (bottom). The horizontal axis represents space and the vertical axis time. The maximum of the modulus has been scaled to white and the phase ranges from 0 (white) to 2π (black). The parameters are: $\mu = 0.2$, $\alpha = 2.6$, $\beta = 0.2$, $\delta = -0.25$; the system size is 512 and the last plotted time is 300 time units.

III. Dynamics of Polarization-Phase Instabilities

The polarization pattern solutions of the laser VCGLE have a wavenumber-range of stability determined by polarization-phase instabilities [1]: Since $1+\alpha\beta$ is positive, the solution with $k_+ = k_- = 0$ is always marginally stable, and there is no Benjamin-Feir instability in the laser VCGLE. The phase ψ of the TW solutions is linearly unstable for $K^2 > K_p^2 \equiv \frac{\mu(1+\alpha\beta)}{1+\alpha\beta+2\frac{1+\delta}{\delta}(1+\beta^2)}$. The phases ψ and θ of SW solutions are simultaneously linearly unstable for $K^2 > K_s^2 \equiv \frac{\mu\delta(1+\beta\alpha)}{\delta(1+\alpha\beta)-(1+\beta^2)}$. The depolarized solutions have also a region of the (K,d)-plane centered in the origin beyond which they are phase-unstable. Our numerical analysis shows that TW and SW unstable solutions evolves to other solutions of

the same class and smaller wavenumber through transient depolarized states (Fig.2, notice that the difference $Q_+ - Q_-$ measures the degree of depolarization). Unstable depolarized solutions evolve in time to other states, which generically are also depolarized, through a mechanism in which the circularly polarized component of larger wavenumber reduces its wavenumber while the other component remains stable (Fig. 3).

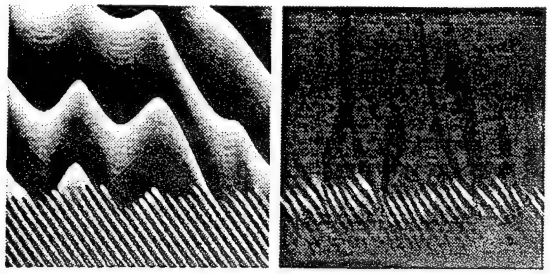

Figure 2: Space-time plot of the phase of A_+ (left) and the difference $Q_+ - Q_-$ (right) for an unstable travelling wave. The initial wave has $K = 0.270$ and $d = 0$, with a small (mean squared amplitude of 0.002) Gaussian-noise perturbation superimposed. Model parameters and system size as in Fig. 1; time running from 0 to 400. Gray levels from white to black: from 0 to 2π for the phase, and from negative to positive differences for the amplitudes (the dominant gray color on the right corresponds to $Q_+ - Q_- = 0$).

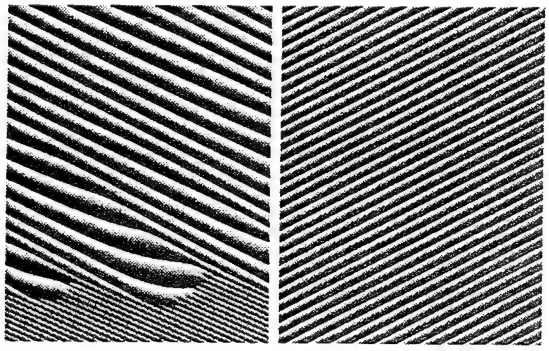

Figure 3: Phases of A_+ (left) and A_- (right) plotted in gray levels, as in Fig. 1, for an unstable depolarized wave. Model parameters and system size as in Fig. 1; The evolution is showed from 500 to 2500 time units. The initial DPS has $K = 0.049$ and $d = 0.393$, with a Gaussian-noise perturbation (mean squared amplitude of 0.002) superimposed.

IV. Growth from noise and SpatioTemporal Intermittency

A numerical solution of the laser VCGLE with random initial conditions mimics the process of laser radiation growth from spontaneous emission noise. For small system size the homogeneous solution dominates, but for a large enough system size local growth and competition of the different stationary solutions discussed above occurs. This leads to complex spatio-temporal dynamics (Fig.4). In addition, exploring various ranges of parameters in (1) one expects to find regimes of Spatio-Temporal Intermittency similar to the ones found for the ordinary CGLE in the Benjamin-Feir *stable* regime [3]. Fig. 5 shows this dynamical state for a weak coupling of the circularly polarized components (close to the scalar case) and a more genuine vectorial form of this dynamical regime.

Figure 4: Space-time plot of the modulus of A_x in gray levels (white=maximum amplitude) from $t = 0$ to $t = 2000$. Model Parameters as in Fig. 1. The system size is 4096 and the initial condition is Gaussian-noise with a mean squared amplitude equal to 0.001.

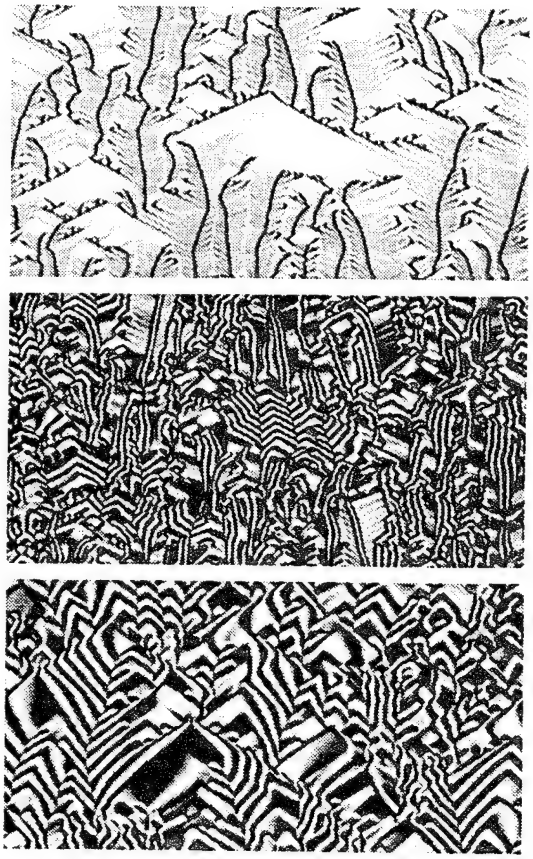

Figure 5: Spatio-temporal intermitency appearing for the model parameters $\mu = 1.0$, $\alpha = 0.2$ and $\beta = 2.0$, showed in gray levels (white=maximum amplitude) between $t = 1000$ and 1500 time units. From top to bottom: A_+ and A_x for $\delta = -0.45$, and A_x for $\delta = -0.25$. The size of the system is 512 and the initial condition is Gaussian-noise of mean squared amplitude 0.001.

[1] M. San Miguel, *Phase instabilities in the Laser Complex Ginzburg Landau Equation*, (unpublished).

[2] Q. Feng, M. San Miguel, J.V. Moloney, and A. Newell in this conference.

[3] H. Chaté, Nonlinearity **7**,185 (1994).

POLARIZATION PATTERN FORMING INSTABILITIES IN LASERS

Q. Feng*[1], M. San Miguel#, J.V. Moloney* and A.C. Newell*

*Department of Mathematics, University of Arizona, Tucson, AZ 85721, USA

#Departament de Física, Universitat de les Illes Balears, E-07071 Palma de Mallorca, Spain

Transverse pattern formation in lasers has attracted much attention in recent years and a rich variety of pattern forming instabilities has been found. Most of studies have concentrated on systems in which the direction of the electric field in the laser cavity is fixed (by, e.g. Brewster windows). In this study we consider the case where the degree of freedom of the electric field polarization is unconstrained. We analyze the stability of solutions corresponding to transverse patterns: linearly polarized traveling waves and polarized standing waves. The interplay between the polarization and transverse effects leads to new instabilities whose natures are identified with amplitide equations. Here we report results for the positive detuning case (results for negative detuning have been reported elsewhere[1, 2]).

The system we considered is a wide aperture, single longitudinal mode, ring cavity laser with transverse flat end reflectors. The basic equations are the vectorial Mawell-Bloch equations[3] governing space-time evolution of the slowly varying complex envelopes of the electric field in the laser cavity, $E_\pm = \frac{1}{\sqrt{2}}(E_x \pm iE_y)$, which are the left- and right-circularly polarized components. For positive detuning, lasing modes with finite transverse wavenumbers lose stability as the pump (r) is increased above threshold (r_c). From the vectorial Maxwell-Bloch equations we derived the amplitude equations which are valid near threshold:

$$\begin{aligned}
\tau(\partial_t + v_g\partial_x)z_1 &= \epsilon z_1 + \xi^2(1+ic_1)\partial_x^2 z_1 - \left[\alpha|z_1|^2 + 2\alpha|z_2|^2 + \beta|z_3|^2 + \beta|z_4|^2\right] z_1 - \beta z_2 z_3^* z_4,\\
\tau(\partial_t - v_g\partial_x)z_2 &= \epsilon z_2 + \xi^2(1+ic_1)\partial_x^2 z_2 - \left[\alpha|z_2|^2 + 2\alpha|z_1|^2 + \beta|z_3|^2 + \beta|z_4|^2\right] z_2 - \beta z_3 z_4^* z_1,\\
\tau(\partial_t - v_g\partial_x)z_3 &= \epsilon z_3 + \xi^2(1+ic_1)\partial_x^2 z_3 - \left[\alpha|z_3|^2 + 2\alpha|z_4|^2 + \beta|z_1|^2 + \beta|z_2|^2\right] z_3 - \beta z_4 z_1^* z_2,\\
\tau(\partial_t + v_g\partial_x)z_4 &= \epsilon z_4 + \xi^2(1+ic_1)\partial_x^2 z_4 - \left[\alpha|z_4|^2 + 2\alpha|z_3|^2 + \beta|z_1|^2 + \beta|z_2|^2\right] z_4 - \beta z_1 z_2^* z_3,
\end{aligned}$$

where z_1 (z_2, z_3 and z_4) is the amplitude of right- (right-, left- and left-) circularly polarized, traveling wave traveling in $+x$ ($-x$, $-x$ and $+x$) direction, respectively. The coefficients α and β are related to the material parameters: $\alpha = b^{-1}$, $\beta = (b^{-1} + c^{-1})/2$, where b is the decay rate of the population inversion between the atomic levels ($J = 1$, $J_z = \pm 1$) and ($J = 0$), c the decay rate of the coherence between the levels ($J = 1$, $J_z = \pm 1$) (they are measured in units of material polarization decay rate). Usually $c > b$ and we will restrict ourself to this case through this study.

The Amplitude equations admit linearly polarized traveling wave solutions,

$$(z_1, z_2, z_3, z_4) = (v, 0, 0, v)e^{i(Qx - \nu t)}.$$

A linear stability analysis determines the stability wavenumber $|Q|$ band (for given $\epsilon = r - r_c$). We found four types of instabilities, each of which sets in at wavenumber $|Q| > |Q_i|$, $i = 1, 2, 3, 4$, respectively, where

$$Q_1^2 = \frac{1}{3}\frac{\epsilon}{\xi^2},\quad Q_2^2 = \frac{c-b}{b+7c}\frac{\epsilon}{\xi^2},\quad Q_3^2 = \frac{1}{2}\frac{\epsilon}{\xi^2},\quad Q_4^2 = \frac{c-b}{4c}\frac{\epsilon}{\xi^2}.$$

The instability occuring at Q_1 is the well-known Eckhaus instability (the typical $\frac{1}{3}$-rule), which is caused here by the long-wavelength perturbation in the sum of the phases of z_1 and z_4, the right- and left-circularly polarized traveling waves (traveling in the same direction). The Q_2-instability is the one due to the long-wavelength perturbation in the phase difference of z_1 and z_4. The Q_3-instability is the amplitude instability due the interaction with a wave, with the same polarization, traveling in the opposite direction[4]. The Q_4-instability is another amplitude instability which is caused by an orthogonally polarized, oppositely traveling wave. Both Q_2 and Q_4 depend on relative magnitudes of the decay rates: $Q_2 \to 0^+$ and $Q_4 \to 0^+$ as $c \to b^+$.

[1]Tel: (602)621-6652 Fax: (602)621-1510 E-mail: feng@math.arizona.edu

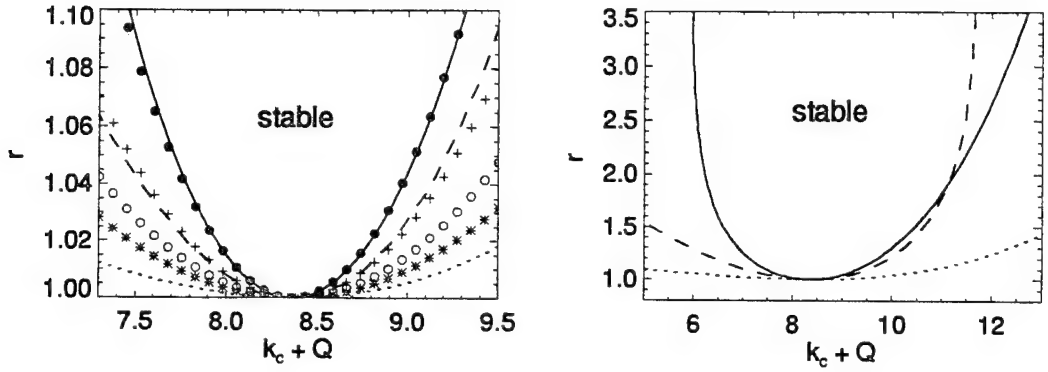

Figure 1: *Stability diagrams for positive detuning. The open circles, filled circles, crosses and asterisks correspond to Q_1, Q_2, Q_4 and Q_3, respectively (see text). The dotted line is the neutral curve. The solid and dashed lines are stability boundaries obtained from direct stability analysis based on the vectorial Maxwell-Bloch equations.*

This means that the stable band disappears as $c \to b^+$. Near threshold the Q_1-instability limits the stability band, while far above threshold it is the amplitude instability originating from the Q_4-instability that limits the stability band (see Fig.1). The instabilities in the far above threshold region are obtained from the numerical stability analysis based on the vectorial Maxwell-Bloch equations.

The amplitude equations have another type of stable solutions, the polarized standing waves,

$$(z_1, z_2, z_3, z_4) = (ve^{i(Qx-\nu t)}, 0, ve^{i(-Qx-\nu t)}, 0),$$

which correspond to standing waves in both x and y components of the electric field. We have also studied the stability of these solutions and found four types of instabilities: two phase instabilities and two amplitude instabilities. Among the two phase instabilities, however, the Eckhaus $\frac{1}{3}$-rule-instability is now caused by the long-wavelength perturbation in the phase difference of z_1 and z_3, while the instability which sets in at Q_2 is caused by the long-wavelength perturbation in the sum of the phases. We have performed a series of numerical simulation on the vectorial Maxwell-Bloch equations with different transverse boundary conditions[5]. The linearly polarized traveling waves tend to be destabilized, while the polarized standing waves could be more robust to survive under realistic boundaries.

References

[1] M. San Miguel, (unpublished).

[2] M. San Miguel, Q. Feng, J.V. Moloney, and A.C. Newell, in *Fluctuation Phenomena: Disorder and Nonlinearity*, edited by L. Vazquez (World Scientific, Singapore, 1995).

[3] G.P. Puccioni, M.V. Tratnik, J.E. Sipe and G.L. Oppo, **Opt. Lett. 12**, 242(1987).

[4] Q. Feng, J.V. Moloney and A.C. Newell, **Phys. Rev. Lett. 71**, 1705(1993).

[5] Q. Feng, M. San Miguel, J.V. Moloney and A.C. Newell, (to be published).

Polarization Switching in Quantum Well Vertical-Cavity Surface Emitting Lasers

J. Martín-Regalado[1], M. San Miguel[1], N. B. Abraham[1,2],F. Prati [3]
[1]Departament de Física, Universitat de les Illes Balears, E-07071 Palma de Mallorca, Spain.
Phone: (34-71) 17 32 34, Fax: (34-71) 17 34 26, e-mail: josep@hp1.uib.es
[2] Permanent address: Physics Department, Bryn Mawr College, 101 N. Merion Ave., Bryn Mawr, PA 19010, USA
[3] Department of Physics, University of Milan, via Celoria 16, 20133 Milan, Italy

Polarization switching in vertical-cavity surface emitting lasers (VCSEL's) has been experimentally observed [1]. The only explanations offered for switchings in the strengths of the differently polarized fields are the combined shifts of the gain and cavity resonances as the device temperature changes with injection current and their impact on the net gain of the frequency-split linearly polarized modes.

An alternative explanation, explored here, is that polarization state switching arises from the coupling of the vector field to the spin dynamics of the carriers in the medium. A model has been recently developed to take account of the coupling of circularly polarized components of the field to different spin sublevels of the conduction and valence bands in surface emitting quantum well semiconductor lasers [2]. The rate equation version of this model appropriate for single-mode gain-guided VCSEL's is

$$\frac{dE_{\pm}}{dt} = \kappa(1+i\alpha)(-1+N\pm n)E_{\pm} - i\gamma_p E_{\mp} - \gamma_a E_{\mp} \quad (1)$$

$$\frac{dN}{dt} = -\gamma(N-\mu) - \gamma(N+n)|E_+|^2 - \gamma(N-n)|E_-|^2 \quad (2)$$

$$\frac{dn}{dt} = -\gamma_s n - \gamma(N+n)|E_+|^2 + \gamma(N-n)|E_-|^2 \quad (3)$$

where $E_{\pm}$ are the slowly varying amplitudes of the optical field left($-$) and right($+$) circularly polarized, N is the total population difference between conduction and valence bands and n is the population differece between the sublevels with opposite value of spin. The physical parameters of these equations are the following: κ is the field decay rate, α is the linewidth enhancement factor, γ_p gives the relative detuning of the linearly polarized modes, γ_a is the strength of the anisotropic losses for the linearly polarized modes, γ is the decay rate of the total carrier population, μ is the normalized injection current which takes the value 1 at the lasing threshold, and γ_s is the decay rate which accounts for the mixing of the populations with opposite value of spin through spin-flip relaxation processes [2]. The spin decay time is known to be of the order of tenths of picoseconds [3]. Previous analyses of gas lasers found that polarization state dynamics depended sensitively on linear phase and loss anisotropies and contributions of the material dynamics to the cross saturation of the orthogonally polarized fields [4]. The VCSEL's have the former characteristics naturally from crystal properties and from geometrical distortions and the latter is gained by the spin-sensitive dynamical model for the carriers.

If anisotropies are not considered, a field linearly polarized in an arbitrary direction is obtained. However, the presence of linear phase anisotropy in a particular direction fixes the polarization emission axis. Then, in absence of linear amplitude anisotropy, the linearly $\hat{x}$ and $\hat{y}$-polarized states are given by

$$E_x = \frac{E_+ + E_-}{\sqrt{2}} = \sqrt{\mu-1}e^{-i\gamma_p t} \; ; \; E_y = \frac{E_+ - E_-}{i\sqrt{2}} = \sqrt{\mu-1}e^{+i\gamma_p t}$$

Other relatively simple solutions are also numerically found, including steady state elliptically polarized solutions and what we call "two frequency solutions" (differently polarized emission at two different optical frequencies, each with nearly constant amplitude). All of these appear to correspond to observed states in experimental measurements of VCSEL characteristics.

The linear stability analysis allow us to determine the stability of the linear polarized solutions in the phase space (μ vs. $\frac{\gamma_p}{\gamma}$) represented in Fig. 1.

In order to see some of the types of switching possible within this model we have scanned the phase space for $\gamma_p = 2\gamma$ (to the left of the dashed line) and $\gamma_p = 10\gamma$ (to the right of the dashed line). The optical field can have complicated time dependence (that can be inferred from the optical power spectra and vector field dynamics), but for comparison with typical experimental results we show first the time averaged power of the $\hat{x}$ and $\hat{y}$-polarized components.

For $\gamma_p = 2\gamma$ (Fig. 2) and increasing μ we can obtain two kinds of transitions since just above threshold (μ=1) two solutions are stable: i) if the system begins because of noise fluctuations near threshold with the

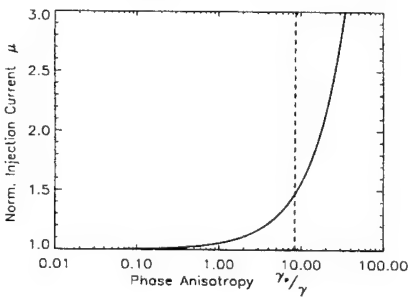

FIG. 1. Stability diagram of the linear polarized solutions for the parameters κ= 300 ns^{-1}, γ= 1 ns^{-1}, γ_s= 50 ns^{-1} and $\alpha = 3$. $\hat{x}$-polarized solution is stable below the solid line, while $\hat{y}$-polarized solution is stable to the left of dashed line.

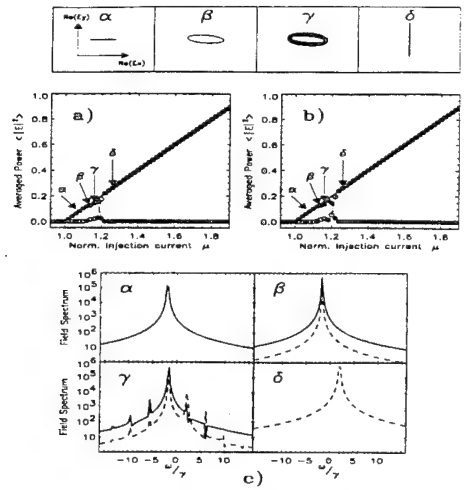

FIG. 2. Time averaged power of the $\hat{x}$-polarized (filled circle) and $\hat{y}$-polarized (empty circle) fields for $\gamma_p = 2\gamma$. Time averages are taken over 20 nsec. Switching in a) absence ($\gamma_a = 0$) and (b) presence ($\gamma_a = -0.1\gamma$) of linear amplitude anisotropy are shown. Trajectories of the real part of the vector field amplitude in space are given above, and optical spectra of indicated operating points are given in c) ($\hat{x}$ and $\hat{y}$-polarized fields indicated by solid and dashed lines, respectively).

$\hat{y}$-polarized solution, it retains this polarization as μ is raised and lowered, or ii) if the system begins with $\hat{x}$-polarized emission, it switches to $\hat{y}$-polarized emission after passing through elliptically polarized light, and more complex time dependent intensity (modulated at the optical beat frequency of order γ_p). In this case if μ is raised enough to give $\hat{y}$-polarized emission, then this polarization state is retained stably when μ is lowered, giving an evident hysteresis signature. Moreover, instead of two different transitions selected randomly by the stochastic noise process, we can force the system to have a unique switching transition by including a small amplitude anisotropy favoring the $\hat{x}$-polarized state ($\gamma_a < \gamma$).

For the case of $\gamma_p = 10\gamma$ (Fig. 3), there is no abrupt switching at low values of the injection current for $\gamma_a = 0$, but a saturation of the intensity of the $\hat{x}$-polarized state is observed at larger values of the injection current. The results for the time averaged power of the $\hat{x}$ and $\hat{y}$-polarized components of the field could be understood as a coexistence of linearly polarized states. However, the system passes through a variety of states of mixed polarization or time dependent oscillations, with examples indicated with arrows in the figure which can be characterized by their spectra shown in Fig. 3c. We can also force an abrupt switching by including a small amplitude anisotropy favoring $\hat{y}$-polarized emission near threshold ($\gamma_a > \gamma$). This case is shown in Fig. 3b, for which the behavior for values of μ above the abrupt switch is nearly the same as in Fig. 3a.

The appearance of so many of the phenomena observed experimentally in a model which includes

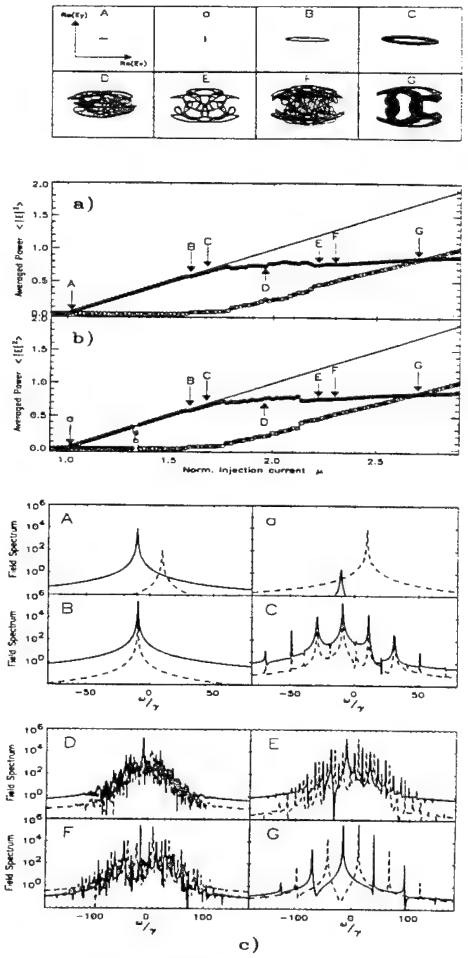

FIG. 3. Time averaged power of the $\hat{x}$-polarized (filled circle) and $\hat{y}$-polarized (empty circle) fields for $\gamma_p = 10\gamma$, in a) absence ($\gamma_a = 0$) and b) presence ($\gamma_a = 0.1\gamma$) of linear amplitude anisotropy. Solid line gives the averaged total intensity. Trajectories of the real part of the vector field amplitude in space are given above and optical power spectra (as in Fig. 2) of indicated operating points are given in c).

realistic values of the parameters and the dynamics of the spin states of the carriers, suggests that these dynamics may be an important part of the explanation.

[1] C.J. Chang-Hasnain, J.P. Harbison, G. Hasain,A.C. Von Lehmen, L.T. Florez and N.G. Stoffel, IEEE J. Quantum Electron. **27**, 1402 (1991); K.D. Choquette and R.E. Leibenguth, IEEE Phot. Tech. Lett. **6**, 40 (1994); K.D. Choquette, D.A. Richie and R.E. Leibenguth, Appl. Phys. Lett. **64**, 2062 (1994).

[2] M. San Miguel, Q. Feng, J.V. Moloney, "Light Polarization Dynamics in QW Semiconductor Lasers", submitted to Phys. Rev. A.

[3] T. C. Damen, L. Vina, J.E. Cunningham, J. Shah and L.J. Sham, Phys. Rev. Lett **67**, 3432 (1991); S. Bar-Ad and I. Bar-Joseph, Phys. Rev. Lett. **68**, 349 (1992).

[4] W. Van Haeringen, Phys. Rev. **158**, 256 (1967); D. Lenstra, Phys. Repts. **59**, 299 (1980).

Transverse and polarization effects in VCSELs

F. Prati, G. Tissoni, L.A. Lugiato
Dipartimento di Fisica dell'Università, via Celoria 16, 20133 Milano, Italy
phone: +39-2-2392264, fax: +39-2-2392712 e-mail: prati@mi.infn.it
J. Martin–Regalado, M. San Miguel and N.B. Abraham[1]
Departament de Fisica, Universitat de les Illes Baleraes, Palma de Mallorca, Spain
[1] Permanent address: Physics Department, Bryn Mawr College, 101 N. Merion Ave., Bryn Mawr, PA 19010, USA

Unlike edge–emitting semiconductor lasers, in vertical cavity surface emitting lasers (VCSELs) the polarization of emitted light can have a random orientation. As the injection current is increased, spontaneous switching between two orthogonal polarizations [1] as well as coexistence of them [2] has been reported. In addition, when higher order transverse modes are excited, they may present different directions of polarization [3].
In this paper we give a description of combined polarization and transverse effects in VCSELs. The starting point is a recently formulated model [4] which takes into account the coupling of circularly polarized components of the field to different spin sublevels of the conduction and valence bands. In the plane wave limit this model has been already used successfully to explain polarization switching [5]. Now we extend it by including transverse modes in the way described in [6]. In particular, we focus on the case in which only Gauss-Hermite modes TEM_{10} and TEM_{01} , or their linear combinations known as doughnut modes, are active. In these conditions, the scalar model [6] predicts that the doughnut modes are stable only in a small domain very close to lasing thresholds, while modes TEM_{10} and TEM_{01} are stable in a wider domain, for larger values of the injected current.
The introduction of polarization effects changes considerably this picture. We first studied the perfectly isotropic case, in which no direction of polarization is privileged. We found that Gauss-Hermite modes are always unstable, because of the competition between modes which are orthogonal both in space and in polarization orientation (e.g. mode TEM_{10} x–polarized and mode TEM_{01} y–polarized). On the contrary, the small stability domain of rectilinearly polarized doughnut modes persists, but now there is a much larger range of values of the injected current for which another kind of solution is stable. This new solution is a superposition of a TEM_{10} mode and a TEM_{01} mode, orthogonally polarized. The electric field is still linearly polarized, but the orientation changes point by point. Depending on the value of the relative phase (0 or π) between the two modes, we found the three different patterns shown in Fig. 1. Using the terminology introduced in [7] the defects shown in Figs. 1a and 1b are called *director* vortex and antivortex $LP(0,\pm 1)$ (the defects of rectilinearly polarized doughnut modes are called *argument* vortex and

antivortex $LP(\pm 1, 0)$). Fig. 1c can be obtained from Fig. 1a simply rotating the electric field by $\pi/2$. Hence, the two patterns are physically distinguishable [8] but topologically equivalent.

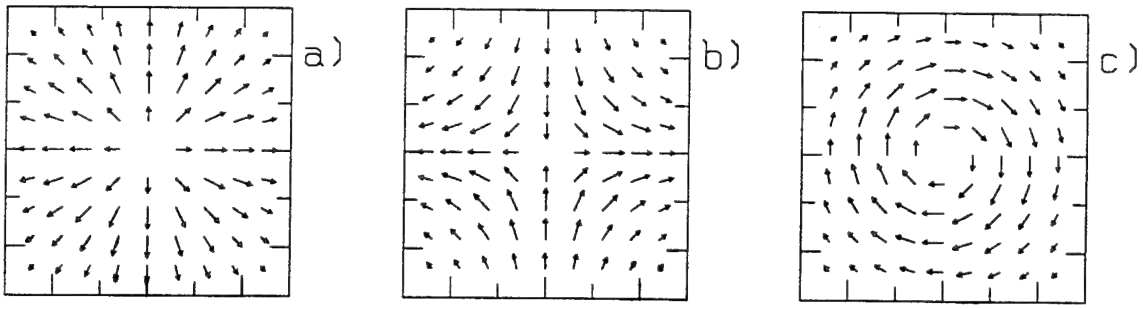

Fig. 1. Behaviour of the electric field vector in the transverse plane for three different modes of emission of the laser.

Next, we introduced in the model some small phase anisotropies to simulate crystal birefringence. This has the consequence of removing the frequency degeneracy between the two states of polarization. As long as the anisotropy parameter is small, the two frequencies are able to lock and we still observe the same patterns of Fig. 1, slightly distorted. For larger anisotropies the two modes TEM_{10} and TEM_{01} start to beat one with the other, giving rise to oscillating patterns [3]. Finally, by introducing loss anisotropies, one polarization is suppressed, and we recover the results of the scalar model [6].

Research partially supported by the ESPRIT Basic Research Project 7118 TONICS.

References

[1] Z.G. Pan et al., Appl. Phys. Lett. **63**, 2999 (1993)

[2] K.D. Choquette et al., Appl. Phys. Lett. **64**, 2062 (1994)

[3] C.J. Chang–Hasnain et al., IEEE JQE **27**, 1402 (1991)

[4] M. San Miguel, Q. Feng and J.V. Moloney, *Light Polarization Dynamics in QW Semiconductor Lasers*, submitted to Phys. Rev. A

[5] J. Martin–Regalado, M. San Miguel, N.B. Abraham and F. Prati, *Polarization Switching in Quantum Well Vertical–Cavity Surface Emitting Lasers* submitted to Appl. Phys. Lett.

[6] F. Prati et al., Chaos, Solitons and Fractals **4**, 1637 (1994)

[7] L.M. Pismen, Physica D **73**, 244 (1994)

[8] D. Pohl, Appl. Phys. Lett. **20**, 266 (1972)

POLARIZATION CHAOS IN A CAVITY-ISOTROPIC OPTICALLY PUMPED LASER

C. Serrat, R. Vilaseca,

Departament de Física i Enginyeria Nuclear, Universitat Politècnica de Catalunya, Colom 11, E-08222 Terrassa, Spain.
Phone: (34)-3-7398137; fax: (34)-3-7398101; e-mail: vilaseca@fen.upc.es

and **R. Corbalán**

Departament de Física, Universitat Autònoma de Barcelona, E-08193 Bellaterra, Spain. Phone: (34)-3-5811653; fax: (34)-3-5812155; e-mail: ifop0@cc.uab.es

Increasing attention is being paid to laser systems in which the dynamics can affect not only the amplitude and phase of the laser field but also its vector character, i.e., the orientation of the laser field vector /1-4/.

In the case of gas lasers, the connection between polarization and dynamics is due to two kinds of factors; namely, to the M-degeneracy of the atomic or molecular levels of the active medium, and to cavity anisotropies or to external agents such as a magnetic field. Focusing on the case of cavity-isotropic lasers, in which the field vector can evolve freely, a theoretical analysis of a homogeneously broadened incoherently pumped $J=1\rightarrow J=0$ laser, for any intensity of the generated field and in the absence of magnetic field, has been performed in /4,5/.

In the present work we extend this kind of analysis to the case when incoherent pumping of the laser transition $J=1\rightarrow J=0$ is substituted by *coherent* pumping, which is accomplished by means of a linearly polarized pump field acting on an adjacent transition in a $J=0\rightarrow J=1\rightarrow J=0$ atomic Λ level scheme. This fact introduces two important changes in the physical system. First, the presence of the pump beam breaks the spatial isotropy with respect to rotations around the cavity axis, leading to *gain anisotropy*. And second, two-photon (Raman) pump processes can be present.

The two new factors lead to a laser behavior very different to that of the incoherently pumped laser. New interesting features appear, specially when an axial magnetic field is applied to the active medium. Among these features, we can mention:

i) Violation of the "*maximum emission principle*" /6/, commonly verified in laser physics. This occurs even in the simplest situation, i.e., in steady-state emission in the absence of magnetic field.

ii) Strong frequency locking of the two circularly polarized components of the generated laser field, which persists up to high values of the magnetic field strength.

iii) Rich dynamics affecting simultaneously the modulus and orientation of the laser field vector, as shown in the examples of Fig. 1. This figure shows the slow evolution of the field-amplitude vector, in cases with: (a) periodic evolution –the parameter ε represents the magnetic field strength–; (b) type-I intermittency; (c) well-developed chaos, and (d) Shilnikov-type chaos. In all the cases the laser field polarization remains linear (assuming pump and laser fields to be on resonance), but the polarization direction changes with time. Uncorrelation between intensity and polarization dynamics is apparent in case (c).

To our knowledge this is the first time polarization chaos (in different forms) is found in laser physics.

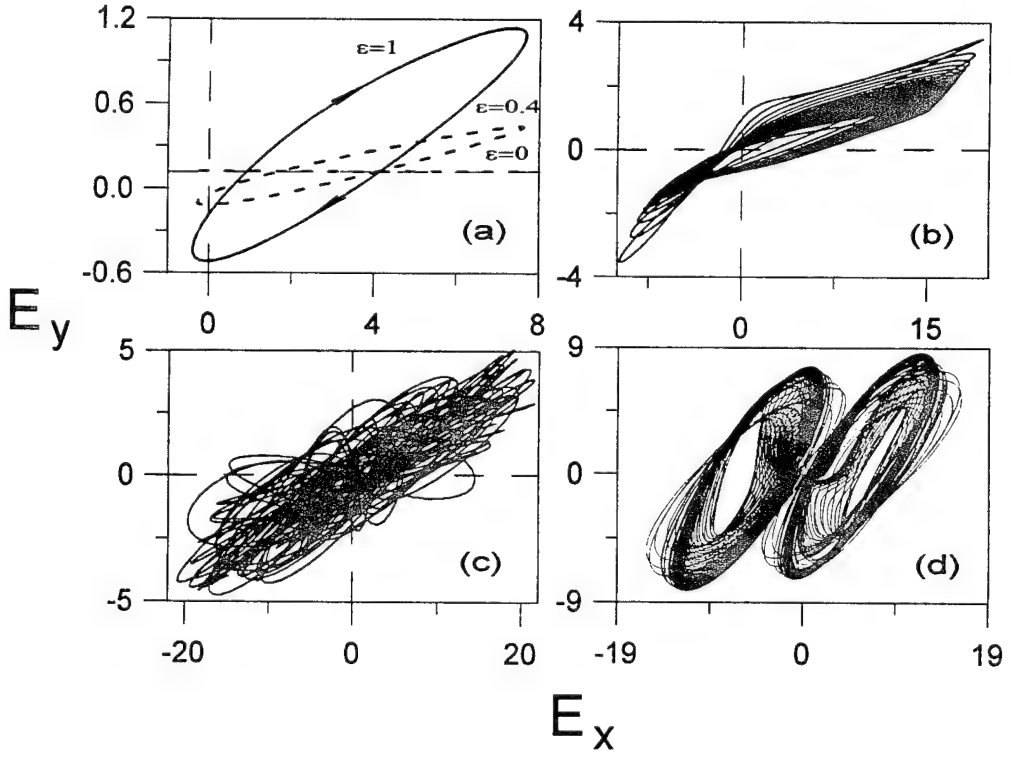

/1/.- J.-Ch. Cotteverte, F. Bretenaker, A. Le Floch, P. Glorieux: Phys. Rev. A **49**, 2868(1994) S. Bielawski, D. Derozier, and P. Glorieux: Phys. Rev. A **46**, 2811 (1992).

/2/.- L.P. Svirina: Opt. Commun. **111**, 370(1994). A.P. Voitovich et al.: ibid, **80**, 435(1991)

/3/.- L. Gil: Phys. Rev. Lett. **70**, 162 (1993); M. San Miguel: to be published.

/4/.- M. Matlin, R. Gioggia, N.B. Abraham, P. Glorieux, T. Crawford: to be published. N.B. Abraham, E. Arimondo, M. San Miguel: to be published.

/5/.- G.P. Puccioni, M.V. Tratnik, J.E. Sipe, G.L. Oppo: Opt. Lett. **12**, 242 (1987).

/6/.- C.L. Tang, H. Statz: Phys. Rev. **128**, 1013 (1962); J. Apll. Phys. **38**, 2963 (1967).

POLARIZATION INSTABILITY IN A ZEEMAN LASER MODEL *VIA* ON-OFF INTERMITTENCY

J. Redondo, E. Roldán, and G.J. de Valcárcel
Departament d'Òptica, Universitat de València, Dr. Moliner 50, 46100-Burjassot, SPAIN
e-mail: qoval@vm.ci.uv.es

Abstract

We predict on-off intermittent behaviour in the polarization of a Zeeman laser with large cavity anisotropy. The intermittency is induced by the chaotic Lorenz dynamics of the field component with less losses, that excites the other component.

The study of polarization dynamics in Zeeman lasers beyond the Lamb theory is a subject of recent attention. Puccioni *et al* [1] proposed a simple Zeeman laser model with a J = 0 lower level and a J = 1 upper level that has been recently revisited by Abraham *et al* [2] and Matlin *et al* [3]. In another paper Abraham *et al* [4] have refined the model of Ref.1 by including more detailed decaying terms and showing the importance of these factors. In these previous works an isotropic cavity is assumed (in Ref.3 a slightly anisotropic cavity is considered but the influence of the anisotropy is not explicitely studied).

In the present work we study the influence of the cavity anisotropy on the stability and dynamical properties in the model of Puccioni *et al*, assuming that all material variables decay with the same relaxation constant γ. We denote by E_x and E_y the two amplitudes of the components of the electric field along two mutually orthogonal directions on the polarization plane, and by κ_x and κ_y the cavity losses associated to each direction, and we assume for definiteness that $\kappa_x < \kappa_y$. Under these conditions the only lasing stationary solution is linearly polarized along the $\hat{x}$ axis. By increasing pump this solution can destabilize through two independent Hopf bifurcations. One of them is the well known Lorenz instability (affecting E_x) and the other one is a polarization instability that gives rise to the self-pulsing amplification of E_y. The precedence of one or the other of these bifurcations strongly depends on the value of the cavity losses.

The dynamic behaviour above the bifurcations is charaterized by transitions between periodic and chaotic pulsations through both quasiperiodic and intermittent scenarios. The intermittent behaviour is particularly rich including a kind of type-II intermittency of a torus. We report here on the on-off intermittency[5] found when the Lorenz instability preceeds the polarization one for large cavity losses and cavity anisotropy.

Since both Hopf bifurcations affect mutually orthogonal manifolds in the phase-space, a very likely skew-product structure of the equations near the bifurcations is achieved. Under these conditions the chaotic behaviour of E_x excites E_y in a random way, giving rise to on-off intermittency. The observed behaviour of E_y exhibits alternancy between very small amplitude oscillations of regular shape (laminar phases) and bursts of irregular appearance when the pump is increased approaching the polarization instability. Fig.1(a) shows an example of this kind of behaviour.

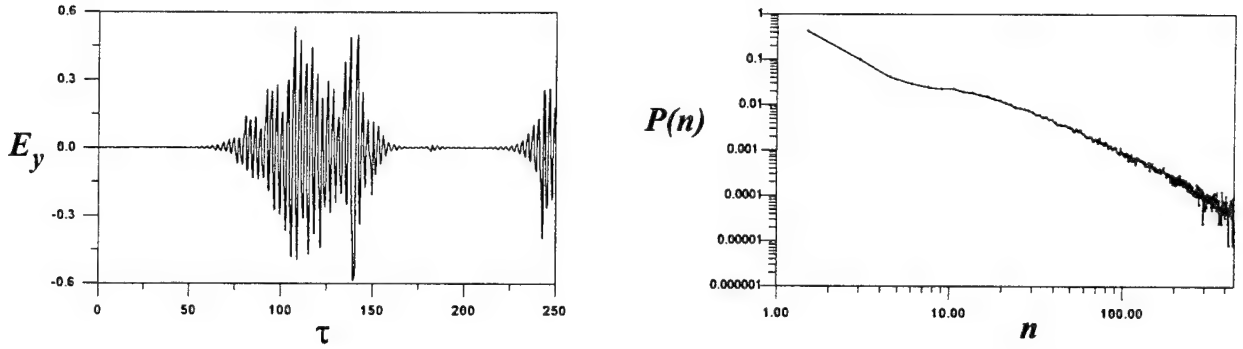

FIG.1. (a) Time trace of the amplitude of the $\hat{y}$-component of the field in on-off intermittency. (b) log-log representation of the histogram of the duration of laminar phases (of which (a) is an example) constructed from 10^5 *ca* laminar phases ($I_0 = 0.01\gamma^2$) (see text). Two linear regions are appreciated, joined with a shoulder. Parameters are: $\kappa_x = 4\gamma$, $\kappa_y = 28\gamma$, and the proportion of Lorenz instability pump, actual pump, and polarization instability pump is 16.00 : 21.00 : 27.77.

In Fig.1(b) we show the probability of finding a laminar phase of length n, $P(n)$. We take n as the number of consecutive intensity maxima of the $\hat{y}$-component, such that none of them be greater than a certain intensity threshold value I_0. On-off intermittency theory predicts the following universal characteristics: (*i*) the duration of the short laminar phases follows the law $P(n) \propto n^{-3/2}$; and (*ii*) for large laminar phases the law is exponential of the form $P(n) \propto e^{-k\,n}$. Contrarily, our preliminary results show a linear dependence for large phases and the slope corresponding to the linear region for small n is clearly smaller than $-3/2$. We have checked that the statistical results are quite independent of I_0.

We gratefully acknowkedge N.B. Abraham for sharing with us Refs.[2-4] prior to publication. This work has been supported by the DGICYT (Spain), Project No. PB92-0600-C03.

[1] G.P. Puccioni, M.V. Tratnik, E.P. Sipe, and G.L. Oppo, Opt. Lett. **12**, 242 (1987)

[2] N.B. Abraham, M. Matlin, and R. Gioggia (to be published, 1995)

[3] M. Matlin, R. Gioggia, N.B. Abraham, P. Glorieux, and T. Crawford (to be published, 1995)

[4] N.B. Abraham, E. Arimondo, and M. San Miguel (to be published, 1995)

[5] N. Platt, E.A. Spiegel, and C. Tresses, Phys.Rev.Lett. **70**, 279 (1993)

Ultrashort Pulse Propagation in the Spatio-Temporal Regime

Govind P. Agrawal and Andrew T. Ryan
The Institute of Optics, University of Rochester, Rochester, NY 14627
Tel: (716)275-4846; E-mail: gpa@optics.rochester.edu

Virtually all materials exhibit some optical nonlinearities at high power levels. An important manifestation of such nonlinearities is to render the index of refraction intensity dependent such that $n(\omega,I) = n_0(\omega) + n_2 I$, where the frequency dependence of the linear part of the index $n_0(\omega)$ stems from chromatic dispersion and the nonlinear-index coefficient n_2 governs the intensity induced change in the index.[1] The changing index affects both the time-dependent and space-dependent behavior of the field. In the plane-wave limit (as in optical fibers or for broad beams) diffractive effects can be neglected, and the nonlinear medium will support temporal solitons. By contrast, in the cw or quasi-cw limit (as for pulses much longer than 10 ps) the effects of medium dispersion can be ignored. Both approximations are similar to that made for a highly elliptical beam where diffraction along the long axis is neglected compared to diffraction along the narrow axis since its effects occur on a much longer distance scale.

When an elliptical beam of ultrashort optical pulses is launched into a nonlinear medium in the spatio-temporal regime group-velocity dispersion (GVD) must be considered together with diffraction and the nonlinear modal index. Pulse propagation this regime is adequately described by a multidimensional nonlinear Schrödinger equation whose normalized form is

$$i\frac{\partial u}{\partial \zeta} + \frac{1}{2}\frac{\partial^2 u}{\partial \xi^2} - \frac{s}{2}\frac{\partial^2 u}{\partial \tau^2} + \mathrm{sgn}(n_2)N^2|u|^2u = 0. \qquad (1)$$

Here $u(\zeta,\xi,\tau)$ is the amplitude of the pulse envelope, $\zeta = z/L_d$, $\xi = x/\sigma$, $\tau = (t - z/v_g)/T_0$, σ is the input spot size in the x-direction, T_0 is the input pulse width, and $L_d = (2\pi/\lambda)\sigma^2$ is the diffraction length (also known as the Rayleigh range). The parameter $s = (2\pi/\lambda)\sigma^2\beta_2/T_0^2$ includes the dispersive effects through the GVD parameter β_2 and the parameter $N = (2\pi\sigma/\lambda)\sqrt{n_0|n_2|I_0}$ represents the medium nonlinearity where I_0 is the peak intensity of the pulse. This equation also describes ultrashort pulse propagation in nonlinear planar waveguides.

In the absence of dispersion ($s = 0$), Eq.(1) can be solved by the inverse scattering method and indicates that planar waveguides support spatial solitons in the case of a self-focusing nonlinearity. However, for picosecond and especially femtosecond optical pulses dispersive effects cannot be neglected and the s-dependent term must be retained in Eq.(1). Such pulses experience diffraction in space and dispersion in time simultaneously.

Moreover, the Kerr nonlinearity governed by the parameter N couples the two effects and introduces spatial-temporal coupling. We solve Eq.(1) numerically to explore the novel features introduced by such spatio-temporal coupling. We consider the four cases corresponding to media with positive or negative GVD and positive or negative nonlinearity separately and discuss the interesting features in each case. As an example, the figure below compares the propagation of an input pulse (with Gaussian spatial and temporal profiles and a peak intensity such that N = 3) in (a) the plane-wave approximation and (b) the spatio-temporal regime for the case of positive GVD ($\beta_2 > 0$) and positive nonlinearity ($n_2 > 0$). In the plane-wave limit, the pulse spreads as expected. By contrast, in the spatio-temporal regime, the input pulse experiences compression. Such pulse compression is attributed to spatio-temporal coupling induced by the medium nonlinearity.[2]

1. G. P. Agrawal, *Nonlinear Fiber Optics*, 2nd ed. (Academic Press, Boston, 1995)
2. A. T. Ryan and G. P. Agrawal, Opt. Lett., **20**, Feb. (1995)

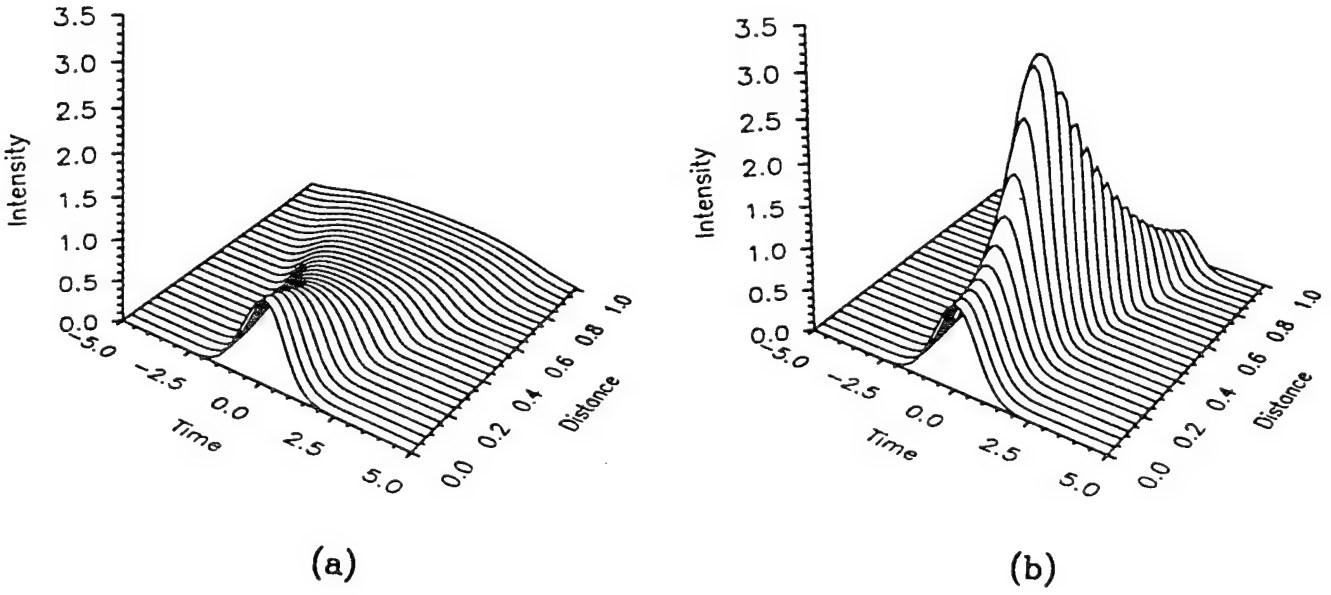

Evolution of a Gaussian input pulse in a normally dispersive nonlinear medium for N = 3 in (a) the plane-wave limit and (b) the spatio-temporal regime such that s = 0.5 in equation(1).

Chaotic Pulse Dynamics in Fiber Arrays

Gregory G. Luther and Alejandro B. Aceves

Department of Mathematics and Statistics
University of New Mexico
Albuquerque, New Mexico 87131
(505) 277-3332, Fax: (505) 277-5505
luther@math.unm.edu, aceves@math.unm.edu

Numerical simulations show that for suitable initial conditions, behavior reminiscent of spatiotemporal chaos develops in the optical fiber array. This behavior is studied and contrasted with the 1 + 1 continuous and discrete nonlinear Schrödinger systems.

The nonlinear Schrödinger lattice (NLSL) equations are obtained from a standard coupled mode expansion of the nonlinear fiber array. They are written,

$$i\frac{\partial A_j}{\partial z} - \beta_2\frac{\partial^2 A_j}{\partial t^2} + 2\gamma|A_j|^2 A_j - \delta(A_{j+1} + A_{j-1} - 2A_j) = 0, \quad (1)$$

where $j = 1, 2, ..., N$ is the fiber index, $t = (T - Z/v_g)$ is the retarded time, $\delta(\mathrm{km}^{-1})$ is the linear coupling, $\beta_2(\mathrm{ps}^2\mathrm{km}^{-1})$ is the group velocity dispersion coefficient, and $\gamma(\mathrm{W}^{-1}\mathrm{km}^{-1})$ is the nonlinear coefficient. As shown in Fig. 1, we take the fiber array to be periodic in j.

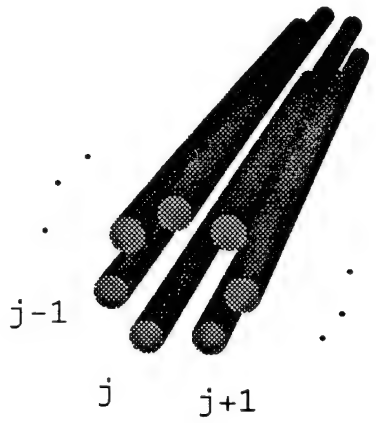

FIG. 1. The periodic fiber array is modeled using the nonlinear Schrödinger lattice.

For certain classes of initial data, the field governed by the NLSL undergoes a modulational instability that seeds a localization process called quasi-collapse and is closely related to wave collapse in the 2D nonlinear Schrödinger equation (NLS). In recent work [1,2] this dynamics has been shown to be very stable, where the attractor for a large class of initial conditions consists of localized states along the fiber that have *sech* like temporal profiles. This process suggests that the nonlinear fiber array can be used as an effective optical pulse compression device [2].

The NLSL also exhibits highly irregular behavior. We have observed several manifestations of this behavior numerically. Such behavior should not be surprising in the NLSL since homoclinic chaos has been shown to exist both in discrete NLS ($\beta_2 = 0$ in the NLSL) [3,4] and in the perturbed NLS [5]. In the NLSL we have observed that the field may localize in j, the discrete dimension, and form a regular pulse train in t, the continuous dimension, yet evolve irregularly in the evolution variable, z. This dynamics is clearly reminiscent of the spatiotemporal chaos that arises in ring cavities, where the regular structures are spatial rings [5] which emerge or disappear in a chaotic fashion as a function of the map describing the round-trip along the cavity. It should also be closely related to the dynamics studied in [3,4] and in their later works.

The temporal profiles that we observe are similar to what is reported in [1]. The NLSL admits a highly localized solution, where $|A_j| >> 1 >> |A_{j\pm1}| >> |A_{j\pm2}| >>$ .... To first approximation with this ordering, the envelope A_j satisfies the NLS equation. Pulse train solutions are then obtained for A_j. Wave forms of this type appear to persist in spite of the irregular evolution of the amplitudes in z.

In Fig. 2 the characteristics of the evolution of the field in one node of the NLSL are illustrated. Here we have numerically integrated (1). This solution was initiated with $A_j(z = 0, t) = 0.8\,\mathrm{sin}(4\pi t)[1.0 + 0.25 * \mathrm{cos}(\pi j/N)]$, where $\beta_2 = -1$, $\gamma = 1$, $\delta = -1$, and $N = 8$. The figure shows the evolution of the temporal profile at $j = 2$. Wave energy was localized in this node through the quasi-collapse dynamics. The wave form remains regular or coherent in t and localized in j as it varies irregularly in z. Note that the number of pulses in the train varies as a function of z indicating a competition among several temporal modes. To our knowledge this is the first report of such behav-

ior in a lattice composed of one of the class of universal nonlinear evolution equations. In addition, the interaction of a modulational instability and quasi-collapse to access a localised coherent state that undergoes chaotic amplitude evolution appears to be novel.

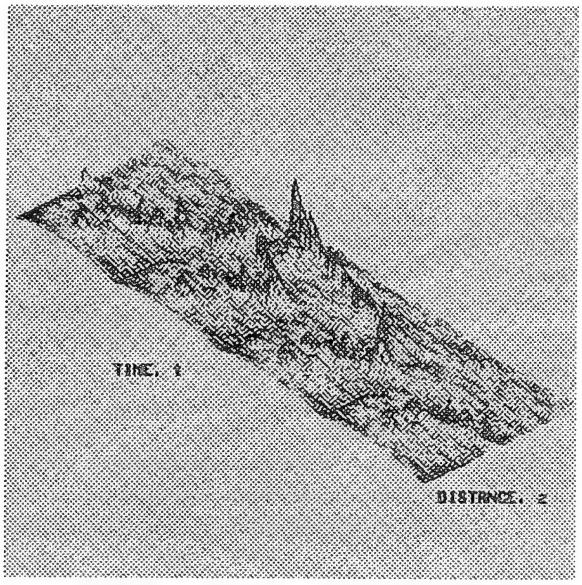

FIG. 2. Evolution of $|A_2(z,t)|$ of the nonlinear Schrödinger lattice.

The authors wish to thank the Air Force Office of Scientific Research (AFOSR) for their supported of this work under contract F49620-94-1-0007.

---

[1] A.B. Aceves, C. De Angelis, A.M. Rubenchik, and S.K. Turitsyn, "Multidimensional Solitons in Fiber Arrays," *Opt. Lett.* **19**, 329 (1994)

[2] A.B Aceves, C. De Angelis, G. G. Luther, and A. Rubenchik, "Modulational Instability of Continuous Waves and One-Dimensional Temporal Solitons in Fiber Arrays," *Opt. Lett.* **19**, 1186 (1994).

[3] M. J. Ablowitz and B. M. Herbst, "On Homoclinic Structure and Numerically Induced Chaos for the Nonlinear Schrödinger Equation," *SIAM J. Appl. Math* **50**, 339 (1990).

[4] D. W. McLaughlin and C. M. Schober, "Chaotic and Homoclinic Behavior for Numerical Discretisations of the Nonlinear Schrödinger Equation," *Physica D* **57**, 447 (1992).

[5] D.W. McLaughlin, J.V. Moloney, and A.C. Newell, "Solitary Waves as Fixed Points of Infinite-Dimensional Maps in an Optical Bistable Ring Cavity," *Phys. Rev. Lett.* **51**, 75 (1983).

Femtosecond Nonlinear Dynamics of Periodic Structures through Direct Integration of Maxwell's Equations

Stojan Radic, Nicholas George and Govind P. Agrawal

The Institute of Optics, University of Rochester, Rochester, NY 14627

A rigorous solution that describes the propagation of an optical field in linear, dispersive, inhomogeneous media represents one of the most challenging problems in computational electromagnetics today.[1] If an optical medium exhibits instantaneous or dispersive nonlinearity, the propagation problem becomes even more complicated, and exact solutions exist only in a few special cases.[2] With renewed interest in nonuniform, nonlinear periodic structures[3,4] for optical switching, this class of propagation problems is becoming increasingly more important.

The generalized finite-difference time-domain (GFDTD) method[2] offers a unique capability of exactly solving Maxwell's equations, for arbitrary interaction geometries, while fully accounting for the dispersive and nonlinear nature of the material response. The arbitrary-order linear dispersion and higher-order material nonlinearities are built into the constitutive relation that connects the dielectric displacement (**D**) to the electric field (**E**) within the optical media. None of the familiar assumptions found in various approximate methods (e.g. coupled-mode equations, nonlinear Schrodinger equation) such as a finite number of coupled modes, slowly-varying field envelope, or weak media perturbation is used in GFDTD. Moreover, both forward and backward propagating waves are automatically included.

We have recently demonstrated a full GFDTD treatment of a linear, dispersive and uniform periodic structure.[5] In this paper we further extend the use of GFDTD method by analyzing uniform and nonuniform nonlinear periodic structures and their response to subpicosecond optical pulses. We model the linear material response by first- (Debye) and second-order (Lorentz) dispersion and its nonlinear response by the instantaneous Kerr and dispersive Raman responses that remain spatially uniform along the propagation length. The method is demonstrated by transmitting a 65-s optical pulse through 40-μm long linear (Fig. 1a) and nonlinear (Fig. 1b) DFB structures. The center frequency of the incident pulse is tuned near the upper edge of the Bragg stop-band. In the nonlinear case the incident optical intensity is sufficient to cause a shift in the photonics band, resulting in a higher transmission (Fig. 1b). Even more interesting is the transmission through a λ/4-shifted nonlinear periodic structure, shown in Fig. 2. The spectrum of a 1-ps incident pulse fits within the central transmissive peak of the λ/4-shifted structure, thus allowing for full transmission in the linear case. However, in the nonlinear case the photonics band is significantly changed even for modest input intensities of $I \sim 0.01 I_{crit}$, resulting in all-optical limiting behavior, as shown in Fig. 2. We discuss the limitations and advantages of the GFDTD technique, and compare its performance to conventional coupled-mode techniques.

References:

1. K. E. Oughstun and G. C. Sherman, J. Opt. Soc. Am. **A6** 1394 (1989).
2. P. M. Goorjian, A. Taflove, R. M. Joseph and S. H. Hagness, IEEE J. Quantum Electron. **28**, 2416 (1992).
3. C. M. de Sterke and J. E. Sipe, Phys. Rev. **A42**, 550 (1990).
4. S. Radic, N. George and G. P. Agrawal, Opt. Lett. **19**, 1789 (1994).
5. S. Radic and N. George, Opt. Lett. **19**, 1064 (1994).

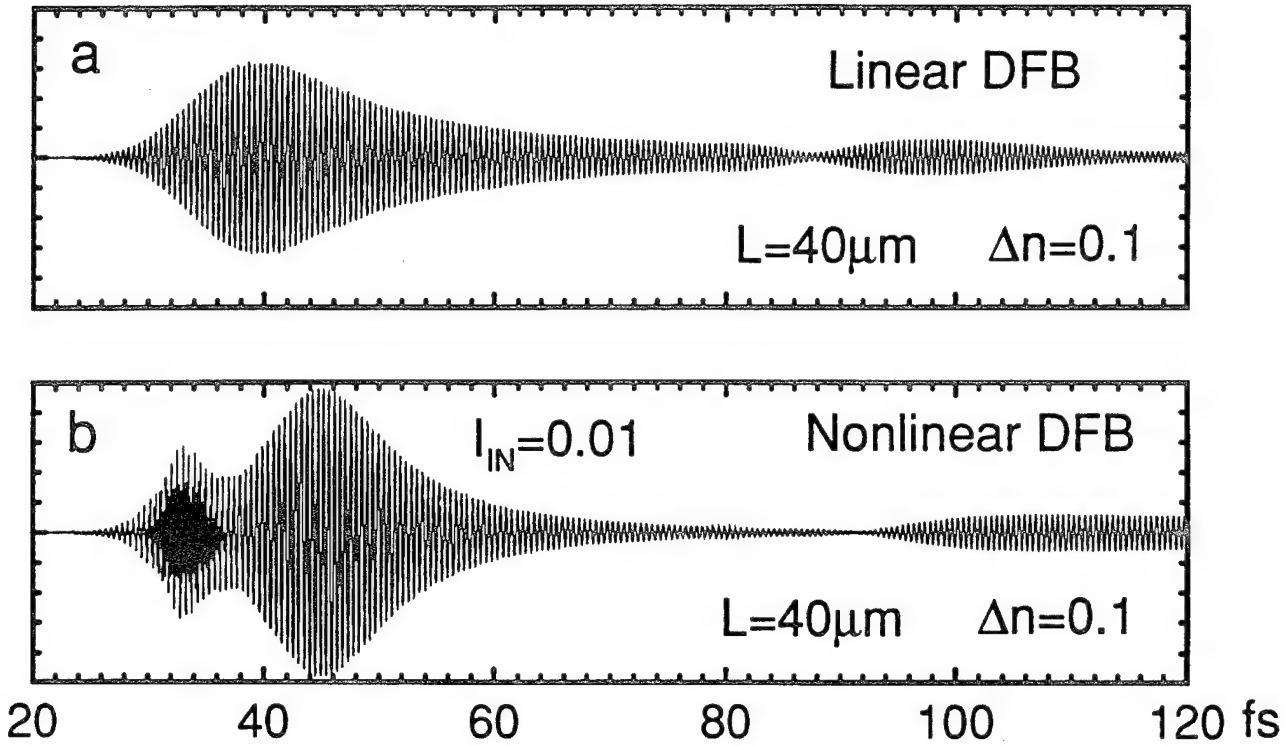

Fig. 1 Transmitted pulse for a) linear DFB structure and b) nonlinear DFB structure. In both cases, the input pulse is 65 fs long and is tuned close to a stop-band edge.

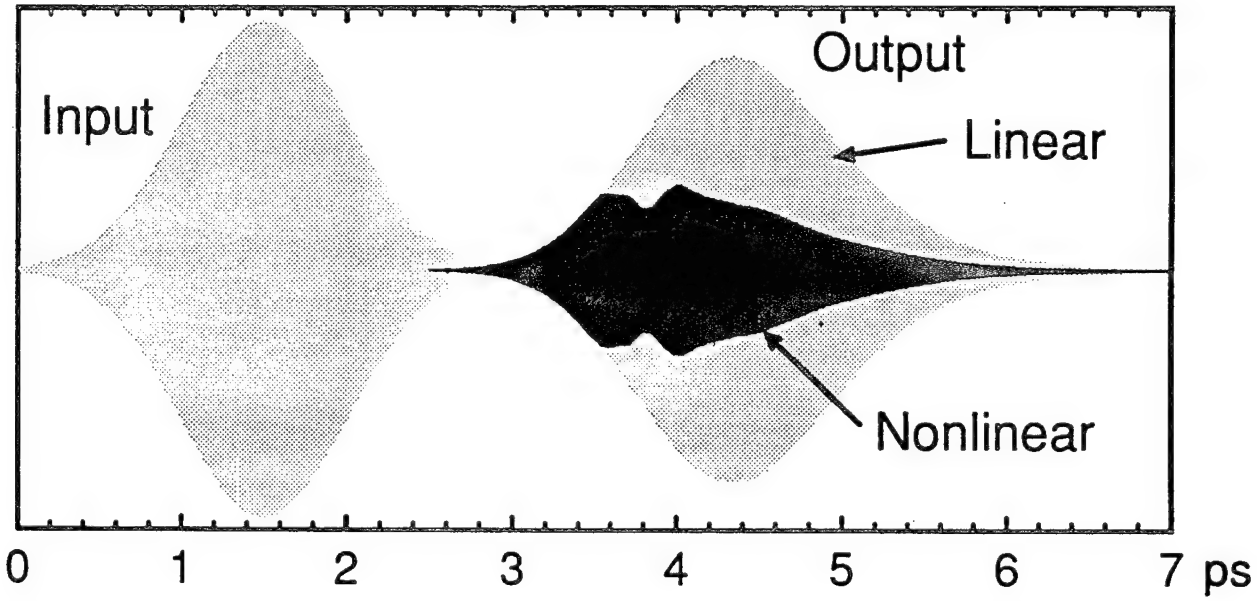

Fig. 2 Input and ouput pulses for a 20-μm long λ/4-shifted nonlinear DFB structure.

Self-Induced Transparency in Bragg Reflectors: Gap Solitons Near Absorption Resonances

Alexander Kozhekin and Gershon Kurizki
Chemical Physics Department, Weizmann Institute of Science, Rehovot 76100, Israel
Tel.: (972)-834-2365
Fax.: (972)-834-4123
E-mail: CFKURIZK@WEIZMANN.WEIZMANN.AC.IL

Pulse propagation in a non-uniform resonant medium, e.g., a periodic array of resonant films, can destroy self-induced transparency (SIT) [1], because the pulse area is then split between the forward and backward (reflected) coupled waves, and is no longer conserved [2]. Should we then anticipate severely hampered transmission through a medium whose resonance lies in a reflective spectral domain (photonic band gap) of a periodically-layered structure (a Bragg reflector)? We have shown analytically that it is possible for the pulse to overcome the band-gap reflection and produce SIT in a near-resonant medium embedded in a Bragg reflector. The predicted SIT propagation is a *principally new type of a gap soliton*, which does not obey any of the familiar soliton equations, such as the non-linear Schrödinger equation (NLSE) or the sine-Gordon equation. Its spatio-temporal form and intensity dependence are shown here to be distinct from the extensively – studied gap solitons in Kerr–non-linear Bragg reflectors [3], which are described by the NLSE.

In treatments of bidirectional field propagation in media with arbitrary spatial distribution of near-resonant atoms [4], the Bloch equations for the population inversion and polarization are entangled in a fashion which leads to an infinite hierarchy of equations for successive spatial harmonics. Here we avoid this complication by confining the near-resonant two-level systems (TLS) to layers much thinner than the resonant wavelength, with the same periodicity as the dielectric structure.

Our main idea has been to try the following phase-modulated 2π–soliton SIT solution for the envelope of the forward (F) and backward (B) field

$$E_{F(B)} = \frac{\hbar}{2\mu\tau_c}\left(1 \pm \frac{1}{u}\right) A_0 \frac{\exp\left[i(\alpha n_0 z/c\tau_c - \Delta t)\right]}{\cosh\left[\beta(z/\tau_c cu - t)\right]} \tag{1}$$

where μ is the transition dipole moment, τ_c is the cooperative (resonant) absorption time, A_0 is the amplitude of the solitary pulse, u is the velocity (normalized to c), n_0 is the mean refractive index and Δ is the field detuning from the gap center.

We focus here on the most illustrative case, when the TLS resonance is exactly at the center of the optical gap. Then the phase modulation α, the pulse inverse-width $\beta = A_0/2$ and the detuning Δ are analytically obtainable as a function of the group velocity cu. We find that the condition for SIT is that the cooperative *absorption length* $c\tau_c/n_0$ should be *shorter than the reflection* (attenuation) *length* at the gap $1/\kappa$, i.e., that the incident light should be absorbed by the TLS before it is reflected by the Bragg structure. SIT is found to exist only on one side of the band-gap center, depending on whether the TLS are embedded in the region of higher or lower linear refractive index in the Bragg structure. This result may be understood as the addition of a near-resonant non-linear refractive index to the modulated index of refraction of the Bragg structure. When this addition compensates the linear modulation, then there is no band gap and soliton propagation is possible. The soliton amplitude dependence on frequency detuning from the gap center (which coincides with the TLS resonance) is shown in Fig.1. The parameters obtained from our analytical solutions fully agree with those which yield both forward and backward soliton-like pulses in a numerical simulation of Maxwell-Bloch equations (Fig.2).

An adequate system for experimental observation of this effect appears to be a periodic array of 12-nm–thick GaAs quantum wells ($\lambda = 806$nm) separated by $\lambda/2$ non-resonant Al-GaAs layers. Area density concentration $\sigma \sim 10^8$–10^9 cm^{-2} of the quantum-well excitons yields $\tau_c \simeq 10^{-13}$–10^{-14}s. A solitary pulse of $\lesssim 1$ps, i.e., much shorter then the dephasing time $T_2 \sim 10$ps (at 2^0K) in this structure requires band-gap reflection length $1/\kappa \gtrsim 100\ \lambda$.

The salient advantage of the predicted near-resonant gap soliton is stability with respect to absorption. By contrast, strong absorption is a severe problem associated with a large Kerr coefficient required for NLSE gap solitons [3].

[1] S. L. McCall and E. L. Hahn *Phys.Rev* **183**, 457 (1969); A. I. Maimistov et al. *Phys.Rep.* **191**, 2 (1990)
[2] B. I. Mantsyzov and R. N. Kuz'min *Sov. Phys. JETP* **64**, 37 (1986); T. I. Lakoba *Phys. Lett. A* **196**, 55 (1994)
[3] W. Chen and D. L. Mills *Phys.Rev.Lett* **58**, 160 (1987); C. M. de Sterke and J. E. Sipe *Phys.Rev. A* **38**, 5149 (1988); M. J. Steel and C. M. de Sterke *Phys.Rev. A* **48**, 1625 (1993)
[4] M. I. Shaw and B. W. Shore *JOSA B* **8**, 1127 (1991); R. Inguva and C. M. Bowden *Phys.Rev.A* **41** , 1670 (1990)

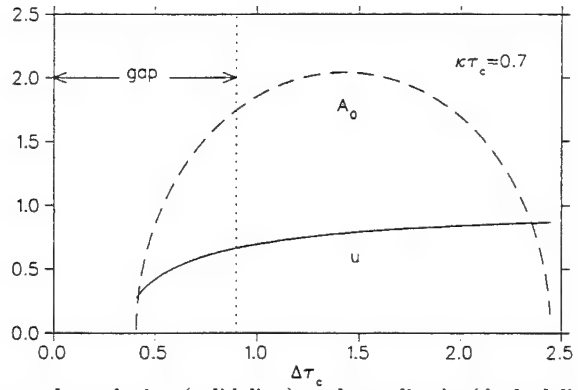

FIG. 1. Dependence of the solitary pulse velocity (solid line) and amplitude (dashed line) on frequency detuning from the center of band gap. At the gap edge (dotted line) $u = 1/\sqrt{3}$.

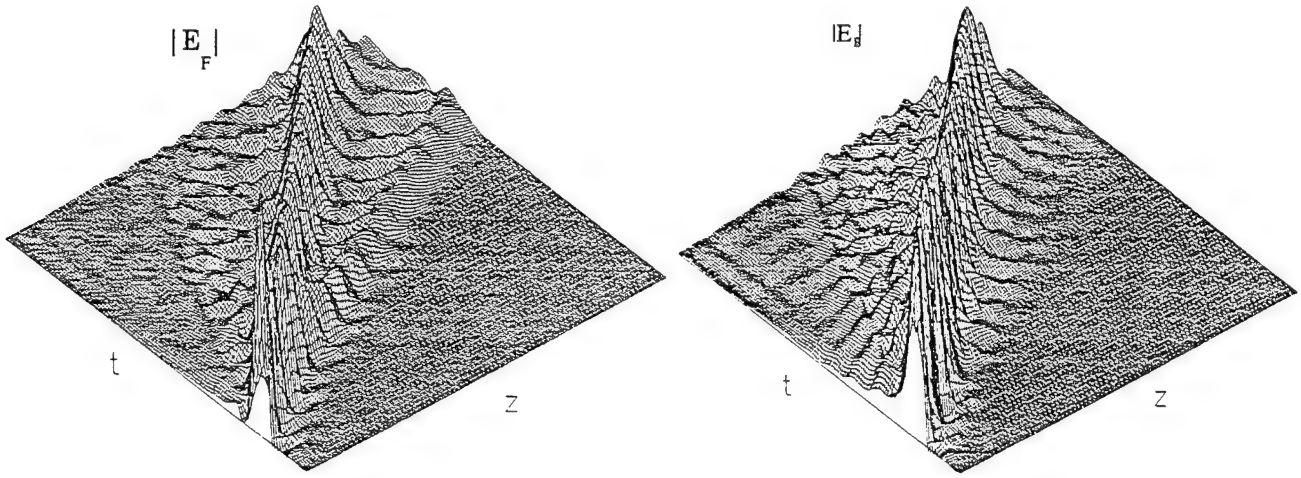

(a) (b)

FIG. 2. Numerical simulations of the intensities of (a) "Forward" and (b) "Backward" waves ($\kappa\tau_c = 0.7$, group velocity $u \simeq 1/\sqrt{3}$).

Picosecond soliton dynamics beyond the guiding-center-soliton regime

René-Jean Essiambre and Govind P. Agrawal
The Institute of Optics, University of Rochester, NY 14627

Abstract

We numerically demonstrate stable transmission of picosecond solitons ($T_p \simeq 1$ ps) in periodically amplified optical communication systems having amplifier spacings much larger than the soliton period. Intrapulse Raman effect is included in the model but soliton self-frequency shift is suppressed through a proper design of the transmission line. Such solitons can be used for data transmission at bit rates as high as 100 Gb/s with amplifier spacing up to 20 km.

1. Introduction

The transmission of solitons over long distances is attracting increasing attention because of its impact on future communication systems. There has been mainly two approaches for soliton-based communication systems. The first one makes use of long active fibers to continuously compensate for fiber losses. This can be accomplished by using the Raman-gain window in a non-doped fiber[1] or the gain window centered near 1.55 μm in an erbium-doped fiber.[2] But, up to now, the distributed amplification scheme has not become practical. The other approach uses a periodic amplification scheme where small lengths ($\sim$ 10 m) of fiber amplifiers (discrete amplification) are periodically inserted between long passive fibers. It has been demonstrated that when the amplifier spacing is a small fraction of the soliton period, the periodically perturbed, lossy, nonlinear Schrödinger equation (NLSE) can be well approximated by a new NLSE accurate to second order in the ratio of the amplifier spacing to the soliton period. The solitary-wave solutions of this new NLSE are called 'guiding-center soliton' (GCS)[3] or 'average soliton'.[4] Unfortunately, for practical amplifier spacings ($\sim$ 20–30 km) the pulse width of such solitons should exceed 10 ps to ensure that the amplifier spacing is well below the soliton period. As a result, the bit rate is typically limited to 10 Gb/s when GCSs are used for signal transmission. One can make use of pulses of higher peak powers than those needed by the GCS regime to increase the amplifier spacing up to a soliton period, but not more than that. The soliton duration is still on the order of 10 ps.[5]

2. Model

We present here the operation of a soliton communication system with periodic amplifiers where solitons of about 1 ps or less are transmitted over hundreds of kilometers in a dispersion-shifted fiber. The amplifier spacing is much longer than the soliton period. The concept of GCS is no longer valid for this regime, but long-term stability is possible. Significant pulse evolution occurs between each amplifier.[6]

Recently, Smith and Blow[7] also considered amplifier spacings much larger than the soliton period in the context of fiber-loop mirrors acting as optical filters. However, it is not clear whether the Raman effect important for solitons of small duration has been taken into account.

The basic principle underlying the proposed scheme is the following. If one provides the energy in a proper way to a soliton and lets it evolve over many soliton periods, a new soliton will eventually form with a small part of the energy (typically around 3%) shed as dispersives waves.[8] These dispersives waves become well separated (in the time domain) from the soliton during propagation between amplifiers and can thus be easily filtered, reducing instabilities associated with the interaction of dispersives waves and the soliton.[9] We use a simple model of fast saturable absorber which removes 99% of the energy at low power and is transparent at high powers exceeding 1/10 of the soliton peak power. Within lossy fibers, most of the energy provided to a soliton is used to compensate fiber losses. Since the soliton experience significant losses between amplifiers, the soliton duration will generally increase significantly between two amplifiers in the adiabatic soliton regime.[10] However, nonlinear compression can act as a mechanism to reduce the soliton broadening. An important issue in a regime where a pulse evolves over many soliton periods before to be amplified is the way the gain medium is reshaping the pulse spectrum at each amplification. The gain lineshape is chosen to be Lorentzian with a bandwidth on the order of the soliton spectral bandwidth so that it does not provide too strong frequency reshaping as a bandpass filter of bandwidth of the order of the soliton spectrum width would do.

Another important issue when dealing with solitons of small durations is higher-order nonlinear effects. It is well known that the intrapulse Raman effect for soliton which produces the soliton self-

frequency shift (SSFS) is the most important of these effects.[11] We used a Raman time constant T_R of 6 fs in our simulations. The mechanism here to control this effect is a periodic upward frequency pulling combined with high-frequencies losses induced through frequency-independent insertion losses properly compensated for at central frequencies by a higher gain. In our model, this is accomplished by the bandwidth-limited Lorentzian gain in combination with 50% insertion losses.

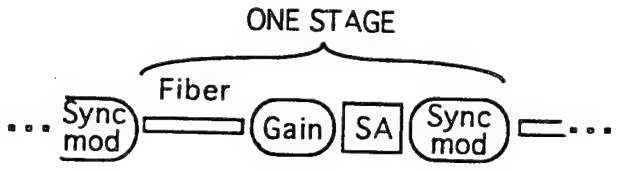

Fig.1. The elements forming one stage of the transmission line (SA: saturable absorber). The synchronous modulator helps to control the timing jitter.

The Raman term introduced in the NLSE makes the group velocity of solitons to depend on the power. A power-dependent group velocity can lead to additional timing jitter on top of the timing jitter introduced by the amplifier noise (the Gordon-Haus effect[12]). To reduce such timing-jitter effects we include a synchronous modulator[13] which not only acts as an active control of the soliton position within the time slot but also stabilizes the soliton peak power. Due to the power-dependent group velocity induced through the Raman term, special care must be given to the choice of the frequency of the synchronous modulation. Figure 1 shows one stage of such a transmission line.

3. Results

We present in Fig. 2 the propagation of a soliton over 50 stages of amplification. We have considered the effect of the SSFS, saturable absorber, synchronous modulation and amplifier noise. A steady-state soliton appears within 25 stages. The amplification spacing is 10 km and the soliton duration (full width at half maximum) varies from 850 fs to 1.34 ps between two amplifiers. No degradation of the pulse is observed suggesting that much longer distances of propagation are possible. Since the soliton remains well confined to the time slot, the sensitivity to power fluctuations of the input pulse is expected to be low.

Our preliminary results have shown that a stable propagation of solitons of much shorter duration than those used in the average soliton regime is possible within a realistic model. We are in the process of studying this scheme. Detailed results will be presented at the meeting.

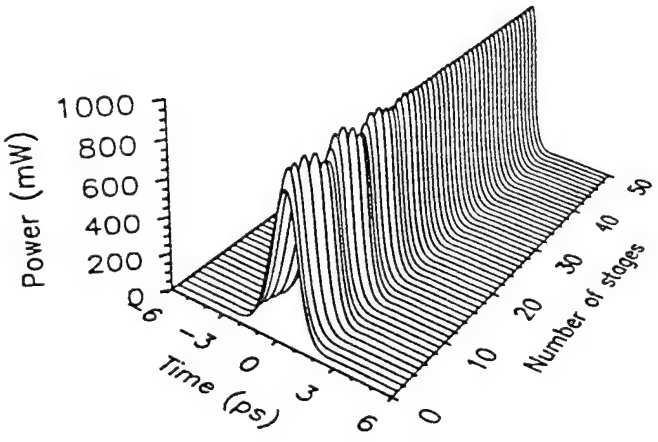

Fig.2. Propagation of a picosecond soliton in the transmission line over 500 km.

4. References

1. L.F. Mollenauer, R.H. Stolen, and M.N. Islam, Opt. Lett. 10, 229 (1985).
2. K. Kurokawa and M. Nakazawa, IEEE J.Quant.-Electron. 28, 1922 (1992).
3. A. Hasegawa and Y. Kodama, Opt. Lett. 15, 1443 (1990).
4. K.J. Blow and N.J. Wood, IEEE Photon.Technol.-Lett. 3, 369 (1991).
5. K. Tang and P. Ye, Fiber and Integrated Optics 13, 261 (1994).
6. R. Vallée and R.-J. Essiambre, Optics Lett. 19, 2095 (1994).
7. N.J. Smith and N.J. Doran, Electron. Lett. 30, 1084 (1994).
8. M. W. Chbat, P. R. Prucnal, M. N. Islam, C. E. Soccolich, and J. P. Gordon, J.Opt.Soc.Am. B 10, 1386 (1993).
9. S.M.J. Kelly, Electron. Lett. 28, 806 (1992).
10. G. P. Agrawal, *Fiber-Optic Communication Systems* (Wiley, New-York, NY, 1992).
11. G. P. Agrawal, *Nonlinear Fiber Optics* (Academic Press, Boston, Mass., 1989).
12. J.P. Gordon and H.A. Haus, Opt. Lett. 11, 665 (1986).
13. M. Nakazawa, H. Kubota, E. Yamada, and K. Suzuki, Electron. Lett. 28, 1099 (1992).

Transmission of Solitons Generated by Modulation of Laser Diodes Using TDM and In-line Phase Conjugation

Claudio R. Mirasso[1] and Luis Pesquera[2]

1- Instituto de Estructura de la Materia, CSIC, Serrano 123, E-28006 Madrid, Spain.
2- Departamento de Física Moderna, Universidad de Cantabria, Avda. Los Castros s/n, E-39005 Santander, Spain

Phone 34-1-585-5383, Fax: 34-1-585 5184, e-mail: emclaudio@iem.csic.es

It has been recently pointed out that pseudorandom sequences of solitons can be generated and transmitted at GHz rates by direct modulation of laser diodes (LD) when biasing slightly below threshold[1]. Using this bias current the response of the gain-switched laser to a bit "1" is independent of the previous input bits. A large jitter has been observed after transmission over transoceanic distances[2] of solitons generated by gain-switched LD. We have shown that this is due to the pulse-to-pulse frequency jitter originated in the LD[3] and that this jitter can be reduced by mid-span optical phase conjugation[4] (OPC). Other important effects at high bit rates are soliton interaction and Gordon-Haus jitter. When perfect solitons are used as input OPC can compensate these soliton effects[5].

In this work we study the transmission of pseudorandom sequences of solitons at 15 GHz rate obtained by time division multiplexing (TDM) of three 1.55 μm LD modulated at 5GHz and biased slightly below threshold[1]. A narrowband optical filter is used to limit the large bandwidth of the signal produced by the chirping. Due to the high transmission rate it is expected that soliton interaction plays an important role. In Fig. 1 (left panel) we show the propagation of the 16 bits sequence "1 0 1 0 0 1 1 1 0 0 0 1 0 0 1 1" until z=10000 km. Soliton interaction can be clearly seen in the set "11" at the end of the sequence. From z=0 until z $\approx$ 2000 km the pulses collapse and then they begin to separate as the transmission distance increases. On the contrary in the set "111" the pulses start to separate at z=0. As it can be clearly seen at 10000 km the interaction leads to errors since it seems that two or more "0" bits are placed between the "1" bits of these sequences.

Midsystem OPC has been proposed to recover at the end of the transmission line the original signal when soliton interaction is present. This has been demonstrated when the input sequence is composed by perfect soliton pulses[5]. When the pulses are generated by the LD their shape change until they reach a soliton-like shape at z $\approx$ 2000 km. In our case it seems to be more appropriate to perform the OPC at a distance greater than the mid-point. In Fig. 1 (right panel) we show the behavior of the sequence of pulses with OPC placed at $\sim$ 6000 km. It is clearly seen that the soliton interaction has been almost compensated and the sequence at the output of the fiber is close similar to the one at the input.

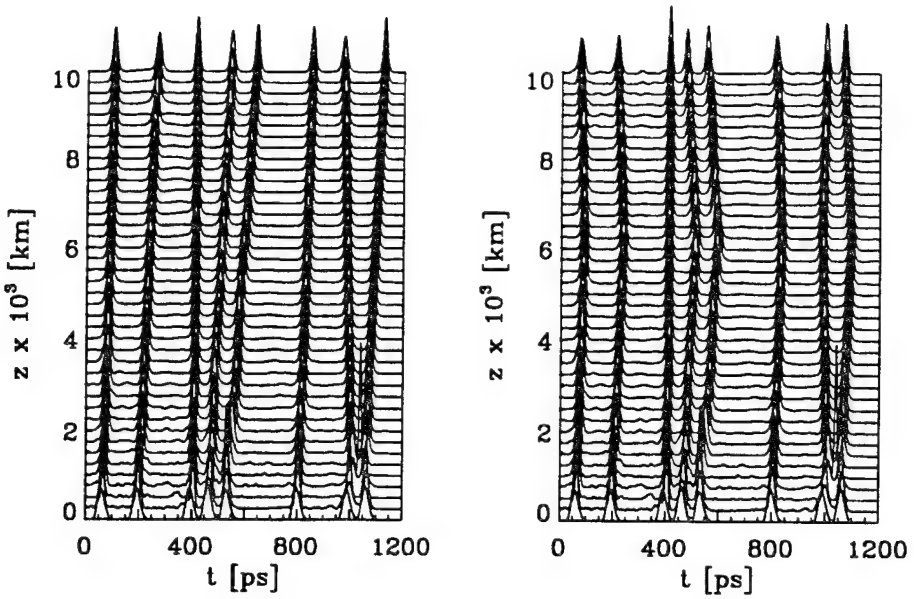

Fig. 1. Transmission of a 16 bit sequence at 15 GHz until 10000 Km. Left side without OPC. Right side with OPC at 6000 Km.

In summary, we have shown that OPC is a very efficient mechanism to reduce soliton interaction in a 15 GHz TDM transmission sequence, even when the pulses at the beginning of the fiber are not perfect solitons, as it is the case for the pulses generated by gain-switching laser diodes.

References

[1] C. R. Mirasso and L. Pesquera, IEEE Photon. Tech. Lett., April 1995.

[2] L. F. Mollenauer, B. M. Nyman, M. J. Neubelt, G. Raybon and S. G. Evangelides, Electron. Lett., vol. 27, pp. 178-179, 1991.

[3] C. R. Mirasso, L. Pesquera and A. Mecozzi, IEEE Photon. Tech. Lett., vol. 5, pp. 1455-1458, 1993.

[4] C. R. Mirasso and L. Pesquera, "Non-Linear Guided Waves", Dana Point, USA, 1995, paper NFA10.

[5] N. J. Doran, W. Forysiak, CLEO'94, Anaheim, USA, paper CThN2.

SELF-PULSING IN A MESOMASER

C.Balconi, F.Casagrande, L.A.Lugiato
Dipartimento di Fisica dell'Università
Via Celoria 16, I–20133 Milano, Italy
Tel.: ++39(2)2392708
Fax : ++39(2)2392712

W.Lange†, H.Walther
Max–Planck–Institut für Quantenoptik
D–85748 Garching bei München, Germany
Tel.: ++49(89)32905704
Fax : ++49(89)32905200

Multistable behavior and temporal instabilities were recently predicted to occur in the resonant interaction of two-level Rydberg atoms with a coherently driven mode of a microwave cavity [1]. The physical system considered is similar to the micromaser [2], but differs due to the presence of the injected field and a larger number of atoms N in the cavity, which ranges from a few tens to a few hundreds. As the regime covered is intermediate between the micromaser ($N < 1$) and ordinary masers ($N \gg 1$), the system may be termed *mesomaser*. In this report, the atoms are assumed to enter the cavity in the lower state, acting as a nonlinear absorber.

The mesomaser may be employed to explore a parameter range of particular interest, where the atom-field coupling constant and the cavity mode linewidth have the same order of magnitude. For a sufficiently weak driving field, the dynamics in this case is governed by atomic cooperation, leading to nonlinear and collective phenomena. Assuming a saturation photon number well above that of the micromaser, the system dynamics can be described semiclassically by Maxwell-Bloch equations, propagation effects being taken into acount[1]. For Rydberg transitions, atomic relaxation can be neglected so that the main contribution to the atomic line width is transit broadening due to the finite time-of-flight through the cavity. This leads to remarkable differences compared with the corresponding optical system. As in optical bistability, more than one stable state is predicted. However, for Rydberg atoms the rotation of the Bloch vector is not affected by atomic relaxation processes, which leads to phenomena distinct from the optical domain. Examples are the occurrence of *multistability*, i.e., the appearance of more than one hysteresis loop, and *instabilities* in the upper-branch of the hysteresis curve [1]. Neither effect can occur in absorptive single-mode bistability in the optical range [3, 4]. Multistable behavior of Rydberg atoms in a cavity is presently under experimental investigation at the Max-Planck-Institut für Quantenoptik in Munich.

---

† Present address: *California Institute of Technology, Pasadena, California 91125, USA.*
Tel.: (818)3958346, Fax : (818)7939506, E-mail : wlange@cco.caltech.edu

Here, theoretical results concerning the nonlinear *dynamics* of the system are reported, obtained by numerically integrating the Maxwell-Bloch equations [5]. To this end, a method developed by Risken and Nummedal for the analysis of laser dynamics [6] is adapted. The central result of these calculations is the appearance of spontaneous, undamped oscillations in the evolution of the system variables (*self-pulsing*), which bifurcate from the unstable sections of the upper hysteresis branches. If the amplitude of the oscillations is large enough, the system may even precipitate from an oscillating state to a stable one. Self-pulsing behavior is described in the time and frequency domains, and the conditions for its occurrence are discussed in detail. The numerical results yield the envelopes and the frequencies of the oscillations. The values of these frequencies at the instability boundaries can be compared with the predictions of the linear stability analysis in Ref. [1]. They turn out to be in excellent agreement. Self-pulsing oscillations occur in the cavity field amplitude as well as the atomic population, monitored at the cavity exit. In the phase space spanned by these variables, the system dynamics is governed by a limit cycle.

The self-pulsing effect is shown to originate from cooperative behavior of the mesoscopic atomic system, which leads to an exchange of energy between atoms and cavity field at a rate larger than the inverse atomic transit time, i.e., the transit broadening. In this case, the system can self-organize and develop periodic undamped oscillations at frequencies which are smaller than, or comparable with the inverse time-of-flight.

Finally, we present the first results on the extension of the investigation to the case of nonresonant interaction. The linear stability analysis has been carried out with atomic detuning included. In this case, the number of degrees of freedom of the system increases from two to four, which opens the possibility of the system entering the chaotic regime.

References

[1] F. Casagrande, L. A. Lugiato, W. Lange, and H. Walther, Phys. Rev. A **48**, 790 (1993).

[2] D. Meschede, H. Walther, and G. Müller, Phys. Rev. Lett. **54**, 551 (1985).

[3] L. A. Lugiato, in *Progress in Optics*, edited by E. Wolf (North-Holland, Amsterdam, 1984), Vol. XXI, Chap. II: Theory of Optical Bistability, pp. 69–217.

[4] G. Rempe, R. J. Thompson, R. J. Brecha, W. D. Lee, and H. J. Kimble, Phys. Rev. Lett. **67**, 1727 (1991).

[5] C. Balconi, F. Casagrande, L. A. Lugiato, W. Lange, and H. Walther (to appear in Optics Communications).

[6] H. Risken and K. Nummedal, J. Appl. Phys. **39**, 4662 (1968).

Spatio-Temporal Dynamics in a Broad Area Laser Diode

I.Fischer[1], O.Hess[2], and W.Elsäßer[1]

[1] *Fachbereich Physik and Material Science Center,*
Philipps-Universität Marburg, Renthof 5, D-35032 Marburg, Germany
e-mail: fischer@ax1305.physik.uni-marburg.de
Phone: [49] 6421/28-2401, Fax:[49] 6421/28-7036

[2] *Institut für Technische Physik, DLR*
Pfaffenwaldring 38-40, D-70569 Stuttgart, Germany

The study of spatio-temporal complexity in nonlinear optical media has gained considerable interest within the last years. The systems under investigation can be classified with respect to the number of relevant spatial degrees of freedom and by the criterium if the medium is passive or active. An interesting active system with one spatial degree of freedom is the broad area laser. Its active region is smaller than the lasing wavelength in one transverse direction and much larger in the other one. It has been designed to achieve high output power from a semiconductor laser. Here, we present results obtained from numerical modelling and, for the first time, experimental measurements of the near-field, giving evidence for the spatio-temporal dynamics of these lasers.

We study the turn-on dynamics of a 100 μm wide GaAs/GaAlAs broad area laser, emitting at $\lambda = 810nm$. The modelling is based on the semi-classical Maxwell-Bloch equations for the complex field, the polarization and the electron and hole density. It predicts for the dynamical behavior spontaneous creation of filaments some ns after the first relaxation oscillation which propagate in space and time [1,2]. Figure 1 a) shows the result of the numerical modelling 8 ns after the first relaxation oscillation for a time interval of 1.5 ns with an injection current roughly twice the threshold current. Irregular pulsing combined with diagonally propagating filaments are the most striking phenomena in this regime. This effect can be attributed to the interplay of the self-focussing properties of the semiconductor medium, the charge carrier diffusion and the gain of the medium.

The corresponding experimental measurements have been performed using a single-shot streak-camera. The current to the broad area laser has been supplied by a signal generator, providing rectangular pulses that pump the broad area laser for 25ns with an injection current that is twice its treshold current. In Figure 1 b) we have depicted one example of a single shot streak-camera time trace for the same time interval as in the modelling. With these measurements we can for the first time clearly demonstrate propagating filaments in the active region of the laser which even show roughly the same propagation velocity as

in the calculated time trace. However, there are still differences between experiment and modelling, e.g. in the modulation depth of the light intensity between the irregular pulses. In conclusion, this is the first direct experimental evidence for the spatio-temporal dynamics in broad area lasers. Combining modelling and experiments this laser promises to become a model system for the investigation of spatio-temporal complexity.

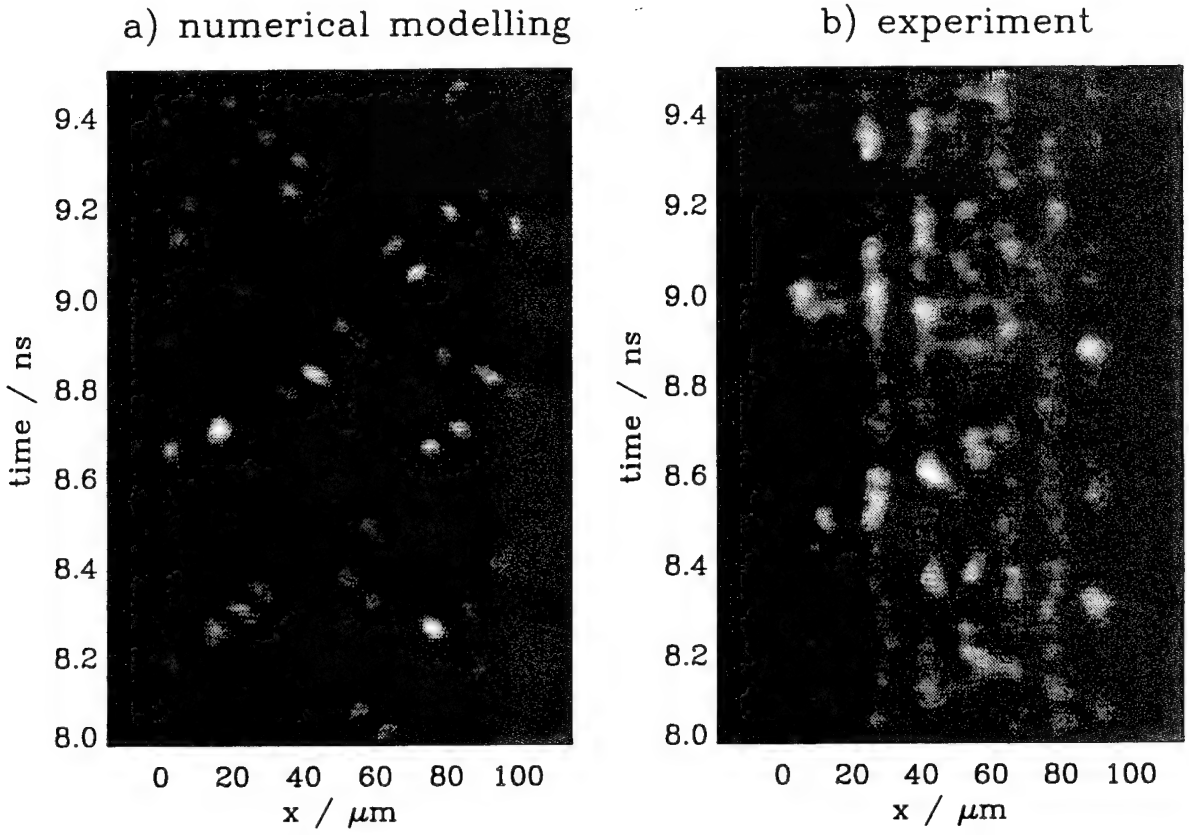

FIG. 1. Spatio-temporal dynamics in the near-field of a broad area laser showing the grey-scaled light intensity in the active region versus the time, 8ns after the turn-on of the laser. a) numerical modelling based on the semi-classical Maxwell-Bloch equations b) experimental single-shot streak-camera measurement

---

[1] H.Adachihara, O.Hess, E.Abraham, P.Ru, and J.V.Moloney. Spatio-temporal Chaos in Broad-Area Semiconductor Lasers. *J. Opt. Soc. Am.*, **B4**,658 (1993).

[2] O.Hess. Spatio-temporal complexity in multi-stripe and broad-area semiconductor lasers. *Chaos,Solitons & Fractals*, **4**,1597 (1994).

Nonlinear Dynamics in Lasers With Phase-Conjugate Optical Feedback

George R. Gray, David H. DeTienne
Electrical Engineering Department, University of Utah
Salt Lake City, Utah 84112
email: gray@ee.utah.edu

Govind P. Agrawal
The Institute of Optics, University of Rochester
Rochester, New York 14627
email: gpa@optics.rochester.edu

Lasers operating with phase-conjugate feedback (PCF) display dyanmical behavior which is often richer than that obtained with ordinary optical feedback arising from a conventional reflector.[1-4] The light fed back from a phase-conjugate mirror is not only delayed by the external round-trip time but also may be shifted to a new frequency, if the PCF is generated by using a non-degenerate four-wave mixing mechanism. The influence of PCF, therefore, can be considered to be a combination of ordinary feedback, since the feedback is delayed by the external roundtrip time, and optical injection, since there is the possibility of detuning. When the solitary laser operates in multiple longitudinal modes, the PCF provides a novel mode-coupling mechanism which can even lead to mode-locking behavior and to the generation of ultrashort optical pulses.

This paper investigates through computer simulations the dynamical behavior of lasers in the presence of PCF. In general, the laser displays rich and complicated behavior which depends on the strength of the feedback, the external cavity length, as well as the operating point of the laser. Bifurcation diagrams are constructed which show at a glance for what values of PCF the laser operates stably, periodically, or chaotically. As an example, Fig. 1 shows a bifurcation diagram of the total output power versus PCF strength for a semiconductor laser operating with four longitudinal modes and 40% above threshold. The bifurcation diagram is constructed with spontaneous-emission fluctuations neglected so that the dynamical behavior represents true deterministic effects. Also shown in Fig. 1 is the total standard deviation of the net (reduced) phases, both with and without the effect of spontaneous emission noise. The net phases are defined in the usual way as $\Psi_j = (2\omega_j - \omega_{j-1} - \omega_{j+1})t + (2\phi_j - \phi_{j-1} - \phi_{j+1})$, where ω_j and ϕ_j are the frequency and the phase of longitudinal mode j. Mode locking occurs when all the Ψ_j become constant, so monitoring the sum of the standard deviations of each Ψ_j is an effective way to judge mode locking. An investigation of Fig. 1 shows that the output power experiences several different types of nonlinear dynamical behavior, depending on the feedback strength. In addition, we find that PCF causes the laser to mode lock over a fairly wide range of feedback strengths, even though the individual mode powers might display complicated behavior (*e.g.* at $\kappa\tau = 1.5$

where the modes undergo period-4 quasi-periodic behavior). The mode-locking behavior is maintained even when the spontaneous emission is turned on, indicating that the mode locking is robust.

The paper will present the detailed nonlinear dynamics of semiconductor lasers induced by PCF under a variety of conditions. Both single-mode and multi-mode dynamics will be considered. Mode-locking behavior as well as FM laser operation will be shown.

1. G. P. Agrawal and J. T. Klaus, Opt. Lett. **16**, 1325 (1991).
2. G. H. M. van Tartwijk, H. J. C. van der Linden, and D. Lenstra, Opt. Lett. **17**, 1590 (1992).
3. G. P. Agrawal and G. R. Gray, Phys. Rev. A **46**, 5891 (1992).
4. G. R. Gray, D. Huang, and G. P. Agrawal, Phys. Rev. A **49**, 2096 (1994).

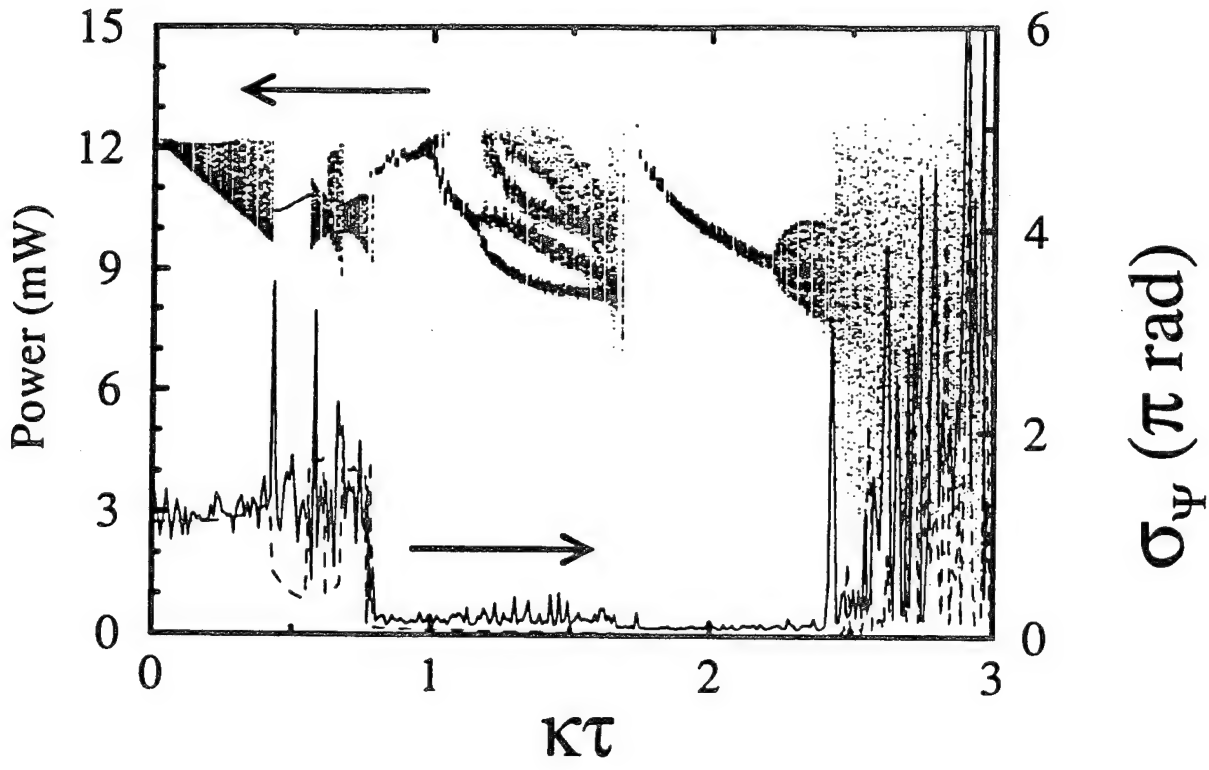

Figure 1. Bifurcation diagram of total power vs. PCF strength $\kappa\tau$ for I/I_{th} = 1.4 for a semiconductor laser with four longitudinal modes. The total standard deviation of the reduced phases of the modes is also shown without (dashed line) and with (solid line) spontaneous-emission noise.

STRONGLY PULSATING OSCILLATIONS IN LASERS SUBJECT TO CONTINUOUS DELAYED FEEDBACK

D. Pieroux and T. Erneux

Université Libre de Bruxelles, Optique Nonlinéaire Théorique,
Campus Plaine, C.P. 231, 1050 Bruxelles, Belgium
Fax:+ 32 2 650 5824 email(PIEROUX,TERNEUX@ULB.AC.BE)

ABSTRACT

Many lasers subject to optical or optoelectronic delayed feedback exhibits strongly pulsating oscillations. A typical time evolution of the intensity consits of successive high pulses separated by relatively long intervals of time with almost zero intensity. Pulsating oscillations have been predicted for semiconductor lasers subject to optoelectronic feedback [1,2] and for semiconductor lasers subject to optical feedback [3,4]. Moreover a continuous delayed feedback is used for the control of unstable orbits of a periodically modulated laser [5]. Until recently, pulsating oscillations were investigated by computer simulations only.

Analytical theories consiting on separate approximations for the active pulses and the long recovery intervals have been initiated in [1,2]. In [6], we formulate equations for a class of lasers subject to a delayed feedback of the form

$$\frac{dx}{d\tau} = - y - \gamma y(\tau - \theta) - \beta x F(y, y(\tau-\theta), \gamma), \qquad (1)$$

$$\frac{dy}{d\tau} = x(1 + y). \qquad (2)$$

where $F(y,\gamma)$ is a linear, positive function of y and $y(\tau - \theta)$. These equations are motivated by two laser problems which have been studied independently [1,3]. The variables x and y are deviations of the inversion of population and the intensity of the laser field from their steady state values, respectively. The parameters γ and θ denote the amplitude and the delay of the feedback, respectively. β is proportional to a ratio of two time constants and is typicall an $O(10^{-2}\text{-}10^{-3})$ small quantity.

We investigate Eqs. (1) and (2) in the limit

$$\gamma \to 0 \text{ and } \beta \to 0 \qquad (3)$$

and use averaging methods to derive a one dimensional map for the amplitude of the oscillations. We analyze the equation for the map in term of θ. We predict several cases depending on the relative value of θ with respect to the period of the oscillations. As a result, we find different time evolutions for the intensity which correspond to different features of the bifurcation diagram. We have compared numerical and analytical solutions of Eqs. (1) and (2) using $F = w + s(y + \gamma y(\tau - \theta))$ ax in [3,4] ($w = 1.1$, $\gamma = 1.5\text{x}10^{-3}$ and $s = (w-1)/(\gamma+1)$). We show that a Hopf bifurcation appears at

$$\theta_H = \beta w/\gamma \ll 1 \qquad (4)$$

but harmonic oscillations are observed only in the vicinity of θ_H (θ = 0.06). They become strongly pulsating for a sligthly larger value of θ (θ = 0.07). For $0.07 < \theta < 10$, the amplitude of the pulsating solutions remains almost constant. We find that (see Figure 1)

$$\max(x) \approx 3\gamma/\beta w >> 1 \tag{5}$$

Period doubling bifurcation appears for larger values of θ and corresponds to a secondary bifurcation from a θ-periodic to a 2θ-periodic state. We derive a different map and find that the first period doubling bifurcation of a cascade is given by

$$\theta_{PD} \approx (6/\gamma)^{1/2} >> 1. \tag{6}$$

We have found excellent agreement between (6) and the exact numerical solutions as soon as $\gamma < 0.1$. The asymptotic solution is particularly useful for $\gamma << 0.1$ because an accurate numerical solution is difficult to obtain.

REFERENCES

1. N.A. Loiko and A.M. Samson, Opt. Comm. 93, 66-72 (1992)
2. E.V. Grigorieva and S.A. Kashchenko, Opt. Comm. 102, 183-192 (1993)
3. K. Otsuka and J.-L. Chern, Opt. Lett. 16, 1759-1761 (1991).
4. J.-L. Chern, K. Otsuka and F. Ishiyama, Opt. Comm. 96, 259-266 (1993)
5. S. Bielawski, D. Derozier, and P. Glorieux, Phys. Rev. E49, R971 (1994).
6. D. Pieroux, T. Erneux and K. Otsuka, Phys. Rev. A 50, 1822-1829 (1994)

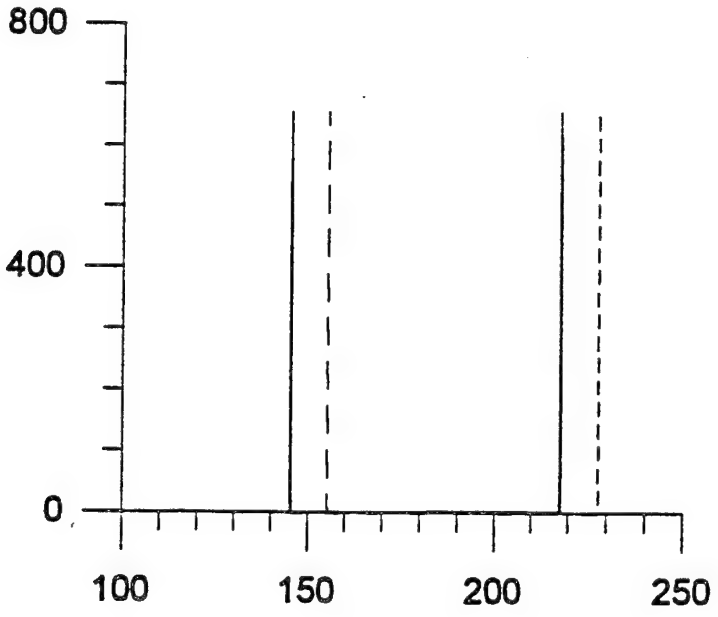

Figure 1. Pulsating solution for w = 1.1, θ = 10, $\gamma = 1.5\text{x}10^{-3}$, $\beta = 0.06\gamma/w$. Full and dotted lines correspond to $y(\tau)$ and $y(\tau - \theta)$, respectively.

Relaxation oscillation in an injection-locked semiconductor laser

Piet C. De Jagher

Dept. of Physics, Eindhoven University of Technology, POB 513,
5600 MB Eindhoven, NL

Daan Lenstra

Department of Physics and Astronomy, Free University
De Boelelaan 1081, 1081 HV Amsterdam, NL

Tel: +31 20 444 7855; Fax: +31 20 444 7899; Email: lenstra@nat.vu.nl

The dynamical behavior of semiconductor lasers is an extensively studied topic. The stability of the dynamics of these lasers is greatly influenced by the value of the phase-amplitude coupling parameter α. The associated chirping effect severely alters the dynamics and stability of the laser compared to $\alpha=0$ type lasers. In fact, the dynamics becomes so complicated that simple models are needed for better understanding of the various types of behavior. An example of such a simple model is the Adler locking model and associated potential model [1] in case of weak injection near the locking edge. At larger injection rates, a Hopf-bifurcation takes place causing undamped relaxation oscillations within the locking wedge and the above-mentioned model is no longer adequate due to oscillations in amplitude and phase.

We have studied the relaxation oscillation (RO) in a single-mode semiconductor laser subject to external optical monochromatic injection. A two-variable scalar function W is constructed from which the slow transient dynamics of the RO can be derived as well as the above-mentioned potential model as an asymptotic case. The function W is used to study a Poincaré-mapping to obtain a description of the RO-dynamics in the locking region. This allows us to investigate when the RO gets excited and when the excited RO becomes unstable.

First, we transform the rate equations into a form in which the relevant orders of magnitude appear as separate parameters. Since the RO is the fastest motion present, we can use an averaging procedure to analyse the evolution on a slower timescale. Thus we derive the slow-timescale set of 2 coupled equations for the time-averaged amplitude of the RO and phase (with respect to the injection phase) . We then show that these equations can be related to a single function W. The average flow has the form $x_t=W_x$, $y_t=-W_y$, so that steady-state undamped RO's correspond to the saddle points of W. Alternatively, we show that a Poincaré-mapping of the flow can be defined which leads to a dynamical system which is nearly the same as the above-mentioned average flow. This mapping appears to be very suitable for studying the stability of periodic orbits.

We retrieve the known locking region [2,3] and the region where a constant locked laser field can be produced. We find that, upon increasing the power of the injected field, *locked* solutions with undamped RO exist; these become unstable when the injected power exceeds a certain value, at which point a period-doubling bifurcation occurs. Furthermore,

we find a bistability for not too small values of α (i.e. above a certain value between 1 and 2): parameter values exist for which two distinct undamped RO's are stable. A similar bistability was reported in [4]. The location of the Hopf and the period-doubling bifurcations are found in good, respectively fair agreement with numerical simulations on the full equations.

references

[1] D. Lenstra, G.H.M. van Tartwijk, W.A. van der Graaf, P.C. De Jagher, Chaos in optics, SPIE 2039 (1993) 11

[2] F. Mogensen, H. Olesen, G. Jacobsen, IEEE J. Quantum Electron. 21 (1985) 784

[3] I. Petitbon, P. Gallion, IEEE J. Quantum Electron. 23 (1988) 148

[4] E.-K. Lee, H.-S. Pang, J.-D. Park, H. Lee, Phys. Rev. A47 (1993) 736

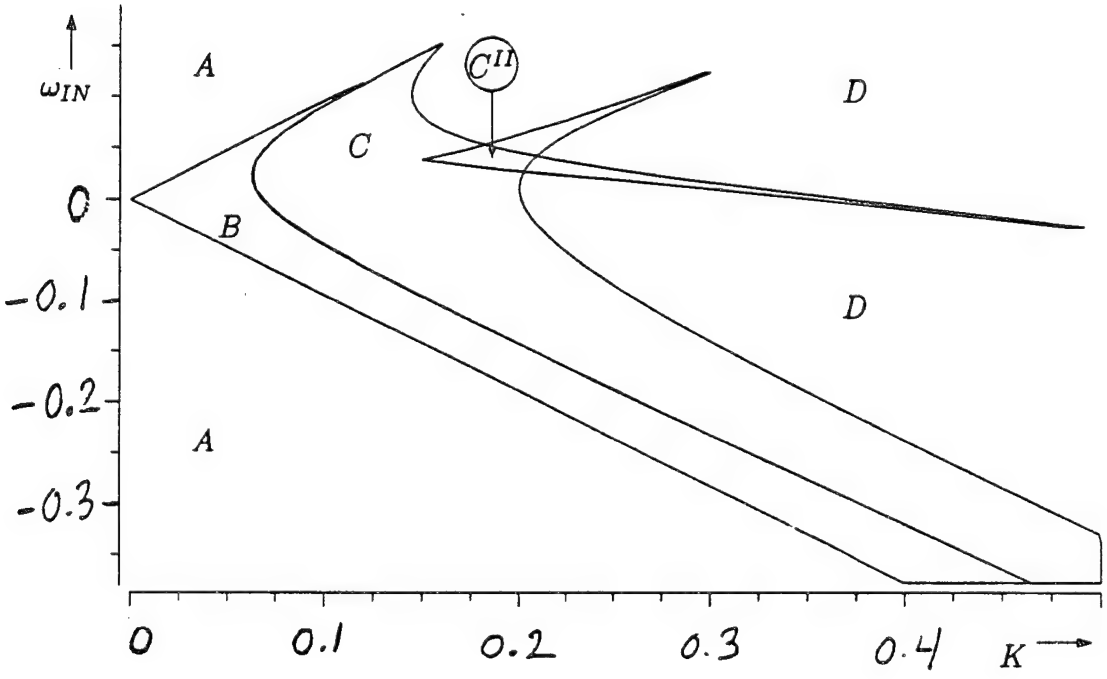

Stability diagram obtained with the *W*-function approximation indicating the Hopf, period-doubling, and other bifurcations. *K* and ω_{IN} are the scaled injection amplitude and detuning frequency. Region A is outside the locking range; in region B locked solutions exist with time-independent amplitude; in C locked solutions with excited RO exist, in C^{II} a bistability is found; in D the RO is not stable. The boundary between C and D indicates the start of a period-doubling tree.

Travelling Wave Model for the Multimode Behavior of a Fabry-Pérot Laser

M. Homar[1,2], J. V. Moloney[1] and M. San Miguel[1,2]
[1] Arizona Center for Mathematical Sciences, University of Arizona
[2] Departament de Física, Universitat de les Illes Balears
E-07071 Palma de Mallorca, Spain
Tel: 34 (71) 173229 - Fax: 34 (71) 173426 - e-mail: dfsmsm0@ps.uib.es

I. Introduction

Longitudinal multi-mode emission is important in dye, solid-state and semiconductor lasers [1 – 3]. The theoretical description of this phenomena is usually done through multimode rate equations. The shortcomings of this approach are well known: The number of modes considered is fixed a priori, a whole set of parameters for the gain of the different modes has to be introduced, Spatial Hole Burning (SHB) is not easily taken into account and phase sensitive interactions are often neglected. An alternative more complete modeling is given by a Travelling Wave (TW) approach for the field in the laser cavity, but TW models in which the dipole polarization variable is eliminated are intrinsicaly unstable at large wave numbers. We report here the results of a numerical study of a TW model of a Fabry-Pérot (FP) laser based on the complete set of Maxwell-Bloch equations for a homogeneously broadened two-level medium. Our TW approach is trivially extended to include optical feedback from an external mirror. We elucidate the competing role of spontaneous emission noise, SHB and diffusion in multimode emission. We also characterize intracavity mode selection by optical feedback in external cavities of various lengths.

II. Model

A slowly varying envelope approximation and a Fourier expansion for the material variables, leads to equations for the counterpropagating electric field amplitudes in the FP cavity $E^{\pm}(z,t)$, and for the Fourier components of polarization $P^{\pm}_{(p)}$ and population inversion $N_{(p)}$ [4, 5]

$$\frac{\partial E^{\pm}}{\partial t} \pm \frac{\partial E^{\pm}}{\partial z} = -P^{\pm}_{(0)}$$

$$\frac{\partial P^{+}_{(p)}}{\partial t} = -\gamma_{\perp}\left[\left(1+i\frac{\delta}{\gamma_{\perp}}\right)P^{+}_{(p)} + \left(N_{(p)}E^{+} + N_{(p+1)}E^{-}\right)\right]$$

$$\frac{\partial P^{-}_{(p)}}{\partial t} = -\gamma_{\perp}\left[\left(1+i\frac{\delta}{\gamma_{\perp}}\right)P^{-}_{(p)} + \left(N^{*}_{(p)}E^{-} + N^{*}_{(p+1)}E^{+}\right)\right]$$

$$\frac{\partial N_{(p)}}{\partial t} = -\gamma_{\parallel}\left[(1+\delta(p-1)\frac{4Dk^2}{\gamma_{\parallel}})N_{(p)}\right.$$

$$\left. + \left(E^{-*}P^{+}_{(p-1)} + E^{+}P^{-*}_{(p-1)} + E^{+*}P^{+}_{(p+1)} + E^{-}P^{-*}_{(p+1)}\right)\right]$$

$$\frac{\partial N_{(0)}}{\partial t} = D\nabla^2 N_{(0)} + J$$

$$-\gamma_{\parallel}\left[N_{(0)} + E^{+}P^{+*}_{(0)} + E^{-}P^{-*}_{(0)} + (*)\right]$$

In these equations δ is the detuning parameter, $\gamma_{\perp}$ is the decay rate for the polarization, $\gamma_{\parallel}$ the decay rate for population inversion, J is the pumping, D is a diffusion coeficient and k is the carrier wavenumber. Spontaneous emission is introduced by Langevin Gaussian white noise sources in the equations for $P^{\pm}_{(p)}$. The grating terms ($p > 0$) in the equations for the material variables describe effects of Spatial Hole Burning (SHB). In our numerical solution we truncate the Fourier expansion at $p = 1$. This model must be solved in conjunction with boundary conditions imposed by cavity mirrors at $z = 0$ and $z = L$ with field reflectivities r_1 and r_2. Optical feedback is introduced by free propagation of counterpropagating fields between $z = L$ and $z = L + L_{ext}$ and an external mirror field reflectivity r_3.

We have solved this model with a semi-implicit finite-difference numerical integration scheme [4]. In our study we have kept fixed the following parameter values which reflect typical time scales of a semiconductor laser: $\gamma_{\perp} = 1 \times 10^{13} s^{-1}$, $\gamma_{\parallel} = 2 \times 10^{8} s^{-1}$, $L = 250\mu m$, $r_1 = 99.5\%$, $r_2 = 56.6\%$. Our results also give expected qualitative behavior for some dye and solid-state lasers in different time scales. The AM/FM coupling is here introduced through the detuning δ which models a small linewidth-enhancement factor for semiconductor lasers.

III. Factors influencing Multimode Behavior of a FP laser

If SHB is neglected (setting to zero the grating terms) and spontaneous emission noise is also neglected, the FP laser shows single mode behavior at any pumping level above threshold. This behavior is modified by the following dynamical ingredients which we consider separately:

a) Spatial hole burning: Neglecting spontaneous emission noise and carrier diffusion, the number of lasing modes grows with pumping level, becoming constant far above threshold, as seen in the Field Power Spectra (FPS) of Fig.1 (left column).

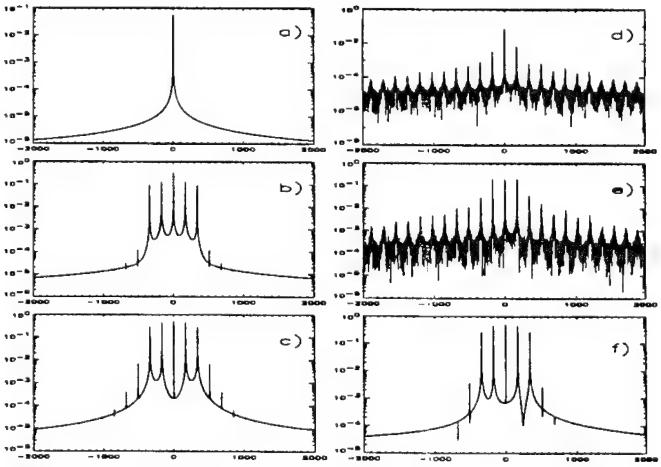

Figure 1 FPS (log scale, frequency in GHz). Pump values: $(J/J_{th}) = 1.02(a,d), 1.7(b,e), 3.5(c,f)$. Spontaneous emission noise: $\beta = 0$ (left column: a,b,c), $\beta = 10^{-4} s^{-1}$ (right column: d,e,f). $\delta = 0$, $D = 0$.

b) Spontaneous Emission Noise: Close to threshold, spontaneous emission noise excites a number of cavity modes (Fig.1 right column) at pump levels for which SHB alone does not destroy single mode emission. Neglecting SHB, the modes excited by spontaneous emission alone have a Side Mode Suppresion Ratio (SMSR) above 20dB for pump values above $J = 1.8J_{th}$. In general both spontaneous emission noise and SHB contribute to multimode emission (see also Fig.4a). For large enough pumping there is a saturation in the number of lasing modes as typically observed in solid-state lasers.

c) Carrier Diffusion: Carrier diffusion plays a crucial role in semiconductor lasers (Fig.2). It competes with SHB and damps side modes. Restoration of single-mode emission for large enough pumping levels is shown, but smaller diffusion coefficients lead to multimode-emission far above threshold. For intermediate pump levels we have observed simultaneous operation of a few modes, but we have not observed mode hopping.

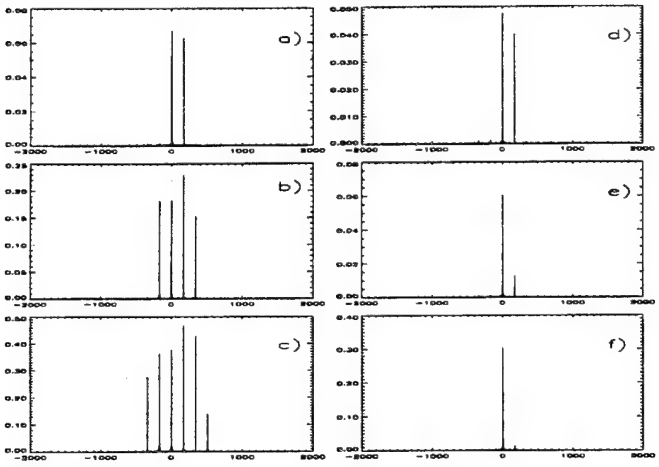

Figure 2 FPS (linear scale, frequency in GHz).Pump values: $(J/J_{th}) = 1.05(a,d), 1.5(b,e), 2.5(c,f)$. Carrier diffusion: $D = 0m^2s^{-1}$ (left column: a,b,c), $D = 4 \times 10^{-4}m^2s^{-1}$ (right column: d,e,f). $\delta = 70GHz$, $\beta = 10^{-4}s^{-1}$.

IV. Feedback and mode selection

Optical feedback from an external mirror combines with intracavity fields and can lead to mode selection depending on feedback level and external cavity length. We first consider weak feedback levels to avoid instabilities of the output intensity. We analyze three cases with different external cavity lengths L_{ext} and an intermediate value of carrier diffusion for which multimode emission occurs in a large range of pump values. For $L_{ext} = 75$ μm external cavity modes are separated $2000GHz$, while the laser cavity modes have an intermode spacing of $171GHz$. The laser cavity mode closest to the maximum of the gain curve which resonates with one of the external modes is selected. Single-mode emission with a SMSR of 20dB is obtained for an external mirror field reflectivity r_3 of just 1%. By a $\lambda/2$-shift of the external mirror different intracavity modes can be selected. For an external cavity of 450 μm, the external cavity mode spacing coincides with twice the internal one, so that the laser might be forced to reduce its multimode emission to lasing in two modes. Such two mode selection with a SMSR of 20dB for $r_3 = 2\%$ is shown in Fig.3.

For longer external cavities mode selection is not found; instead weak feedback leaves many intracavity modes excited in a many-mode spectrum as shown in Fig. 4.

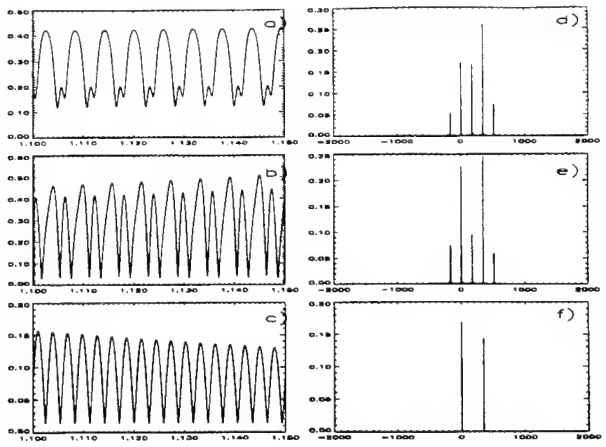

Figure 3 Left colum: Light intensity vs time (ns). Right colum: FSP (linear scale, frequency in GHz). External field reflectivity: $r_3 = 0\%$ (a,d), 0.5% (b,e), and 2% (c,f). $J/J_{th} = 1.3$, $L_{ext} = 450\mu m$, $\delta = 70GHz$, $\beta = 10^{-4}s^{-1}$, $D = 10^{-4}m^2s^{-1}$.

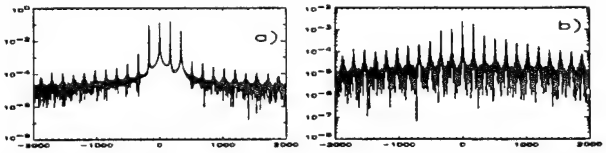

Figure 4 FPS (log scale, frequency in GHz). External field reflectivity: $r_3 = 0\%$ (a), 2% (b). $J/J_{th} = 1.4$. $L_{ext} = 1cm$, $\delta = 70GHz$, $\beta = 10^{-4}s^{-1}$, $D = 10^{-4}m^2s^{-1}$.

Finally, we have considered the possibility of mode selection through moderate or strong feedback. We note that within our numerical scheme multiple external reflections are included. For the shortest external cavity ($L_{ext} = 75$ μm), for which single-mode emission occurs for $r_3 = 1\%$, the laser output becomes unstable with broad FPS at moderate feedback levels (Fig. 5a). However, for strong feedback, two groups of intracavity modes are selected, so that a few-mode emission is recovered. The spacing between these groups is given by the separation of the broad external cavity resonances (Fig. 5b).

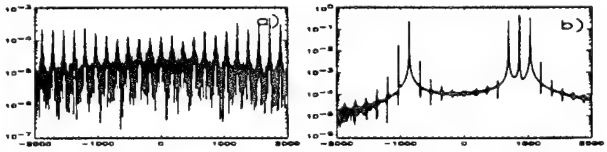

Figure 5FPS (log scale, frequency in GHz). External field reflectivity: $r_3 = 10\%$ (a), 40% (b). $J/J_{th} = 1.5$. $L_{ext} = 75\mu m$, $\delta = 70GHz$, $\beta = 10^{-4}s^{-1}$, $D = 10^{-4}m^2s^{-1}$.

Acknowlegments This work has been supported by AFOSR contract F49620-94-1-0144DEF. M.S.M. and M.H. also acknowledge CICYT (Spain) project TIC93-0744.

[1] M. Munroe et al., Opt. Lett., **19**, 105 (1994).

[2] T. Baer, J. Opt. Soc. Am. B, **3**, 1175 (1986).

[3] Tien-Pei Lee et al., IEEE J. Quantum Electron., **QE-18**, 1397 (1982).

[4] J. A. Fleck, Jr., Phys. Rev. B, **1**, 84 (1971).

[5] Alan C. Newell and J. V. Moloney, *Nonlinear Optics*, Addison-Wesley Publishing Company (1991).

Tuneable Polarisation Modulation Instability in Weakly Birefringent Fibres

S. G. Murdoch, R. Leonhardt , D.A. Wardle and J. D. Harvey
Physics Department, University of Auckland
Private Bag 92019
Auckland, New Zealand
Ph +64-9-373-7599 Ext 8831
Fax +64-9-373-7445

In the scalar description of wave propagation in optical fibres governed by the nonlinear Schrödinger equation (NLSE), modulation instability can occur only in the anomalous dispersion regime, and this was the first form of MI to be observed [1]. The coherent interaction of two different circularly polarised waves of the same frequency propagating in a birefringent fibre has also been predicted to give rise to modulation instability in both the normal and the anomalous dispersion regimes [2]. Modulation instability has however, only been observed in the normal dispersion regime by pumping highly birefringent fibres with intense red or green pulses [3,4]. This form of MI arises from the incoherent interaction of two linearly polarised pulses. We have recently observed "polarization modulation instability" PMI in the normal dispersion regime[5]. When pumping on the slow axis of the fibre, there is no low power threshold for the instability and the peak gain is always at a finite detuning from the pump.

In these experiments, the pump laser used was a mode locked cavity dumped Krypton ion laser, operating at 647nm, which can produce 60ps pulses with a peak power of in excess of 1kW at a repetition rate of 1.2MHz. PMI has been observed at frequencies up to 20THz using a standard low birefringence HeNe single mode fibre whose birefringence could be altered by changing the radius of the spool on which it was wound. In addition, PMI has been observed using a fibre having a birefringence intermediate between that of a "High" and that of a "Low" Birefringence fibre which has enabled us to generated amplitude modulated light at a frequency of 48THz (see Figure 1) .

The fact that the sidebands appear on the orthogonal axis to that of the pump in PMI has important implications for squeezing experiements[6]. The ability to observe the PMI sidebands in a short length of fibre (where the pump remains strongly polarised along the desired axis) ensures that the downshifted sideband does not experience parallel raman gain, although some interference from orthogonal raman gain was still experienced, in spite of the large frequency shift of the MI sidebands (in the Figure, the peak at 667nm is from stimulated raman scattering).

The dependence of PMI gain on the induced birefringence has been used to construct a ring laser using a fibre wound on a conical spool. This laser has gain for a range of different modulation frequencies, and can be used to generate modulated pulses with tuneability over 1-2 Terahertz utilising the different round trip times of the induced sidebands in the cavity. Tuneability has also been achieved by altering the stress on a spooled fibre[7]

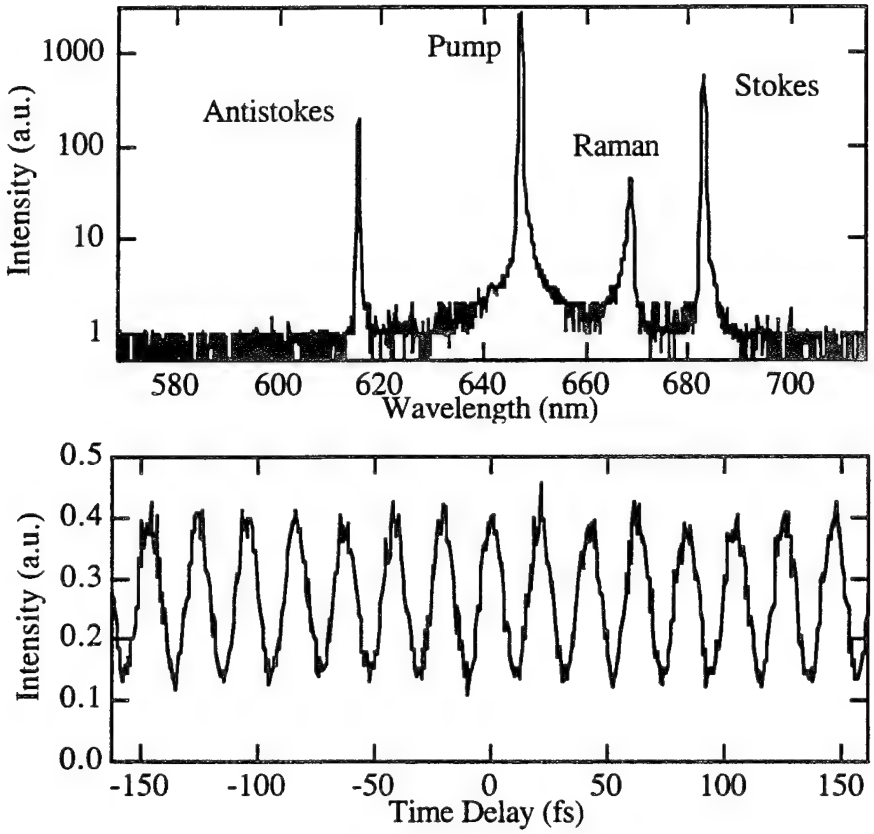

Figure 1: Spectrum and autocorrelation function of PMI in 4m of Stolen fibre, P_{in}=700W, λ_{stokes}=682.8nm, $\lambda_{antistokes}$=615.4nm ($\delta\omega$=48.1THz) Modulation period 21fs (47.6THz)

References.

[1] K.Tai, A.Hasegawa, A.Tomita, Phy.Rev.Lett **56** 135 (1986)

[2] S.Wabnitz, Phy.Rev.A **38** 2018 (1988)

[3] P.Drummond, T.A.B.Kennedy, J.M.Dudley, R.Leonhardt, J.D.Harvey, Opt.Comm **78** 137 (1990)

[4] J.E.Rothenberg, Phy.Rev.A **42** 682 (1990)

[5] S.G.Murdoch,R.Leonhardt and J.D.Harvey , Optics Lett. in press (1995)

[6] T.A.B. Kennedy & S. Wabnitz, Phys. Rev. A, **38** 563 (1988)

[7] K. Bløtekjær Optics Lett **18**, 1059 (1993).

Critical Phenomenon in a Hybrid Optical Bistable System

Jian-Hua Dai, Hua-Wei Yin, Hong-Jun Zhang

Institute of Physics, Chinese Academy of Sciences, P. O. Box 603, Beijing 100080, China

FAX: 86-1-2562605, E-Mail: user307@aphy01.iphy.ac.cn

The time evolution of the output of a hybrid optical bistable device is well described by the following delayed differential difference equation[1-2]:

$$\tau\frac{dx}{dt} = -x + A\sin^2(x(t-t_R) - x_b), \tag{1}$$

where x and A are proportional to the output and input intensity, respectively, x_b is the bias voltage, τ the relaxation time of the system, and t_R the delay time of the feedback loop. The device is an infinite-dimensional dynamical system[3] which can be solved numerically with a forth-order Runge-Kuntta algorithm . We have solved Eq.(1) with the parameters x_b, τ and t_R fixed at 3.0,1.0 and 10.0, respectively. Increasing A from 1.0 to 5.0, we have traced out the bifurcation by selecting as the starting point of a given equation the final condition corresponding to the previous values of A. The system has been shown to exhibit complicated dynamical behavior including Hopf bifurcation, period adding, intermittency, phase locking, quasiperiodicity, hyperchaos, crisis, long-lived chaotic transients, *etc*. In this paper, with the help of the Lyapunov exponents, Poincare sections, power spectrum and phase portraits, Fig.1(a) shows the spectrum of the first ten Lyapunov exponents($\lambda_1 \geq \lambda_2 \geq ... \geq \lambda_{10}$) as the parameter A is varied from 2.0 to 4.0 by step 0.05. As an example, we discuss in detail the crisis occurring at critical point Ac=3.69997092 in the second periodicity windows. Fig.1(b) is the blow-up of the range of A from 3.69993 to 3.702. Before crisis the attractor is a hyperchaos with five positive Lyapunov exponents. After crisis the largest two Lyapunov exponents are zero, indicate that the system behavior is quasiperiodic. Increasing A ($3.86 > A > 3.701$), we find many pairs of equal negative Lyapunov exponents, for example, $\lambda_2=\lambda_3$, $\lambda_4=\lambda_5$, $\lambda_7=\lambda_8$ *etc*. This means that the quasiperiodicity evolves into limit cycle through frequency locking. These are verified by the power spectrum and Poincare section. At the same time, we observe the very long-lived chaotic transient. For example, at A=3.71, the average chaotic transient lifetime $\langle\tau\rangle = 2.6\times10^5$. A crisis[4] from hyperchaos to quasiperiodicity happens at Ac for which we calculate the critical exponent $\gamma \approx 1.75$ (Fig. 2). This critical exponent is different from that (γ=1.0) of intermittency corresponding to the type of Hopf bifurcation.

References

[1] H. M. Gibbs, F. A. Hopf, D. L. Kaplan, and R. L. Shoemaker, Phys. Rev. Lett. **46**, 474 (1981).

[2] Hong-Jun Zhang, Jian-Hua Dai, Peng-Ye Wang, and Chao-Ding Jin, J. O. S. A. **B3**, 231 (1986).

[3] J. Doyne Farmer, Physica 4D, 366 (1982).

[4] C.Grebogi, E. Ott, F. Romeiras, J. A. Yorke, Phys. Rev. A, **36**, 5365 (1987).

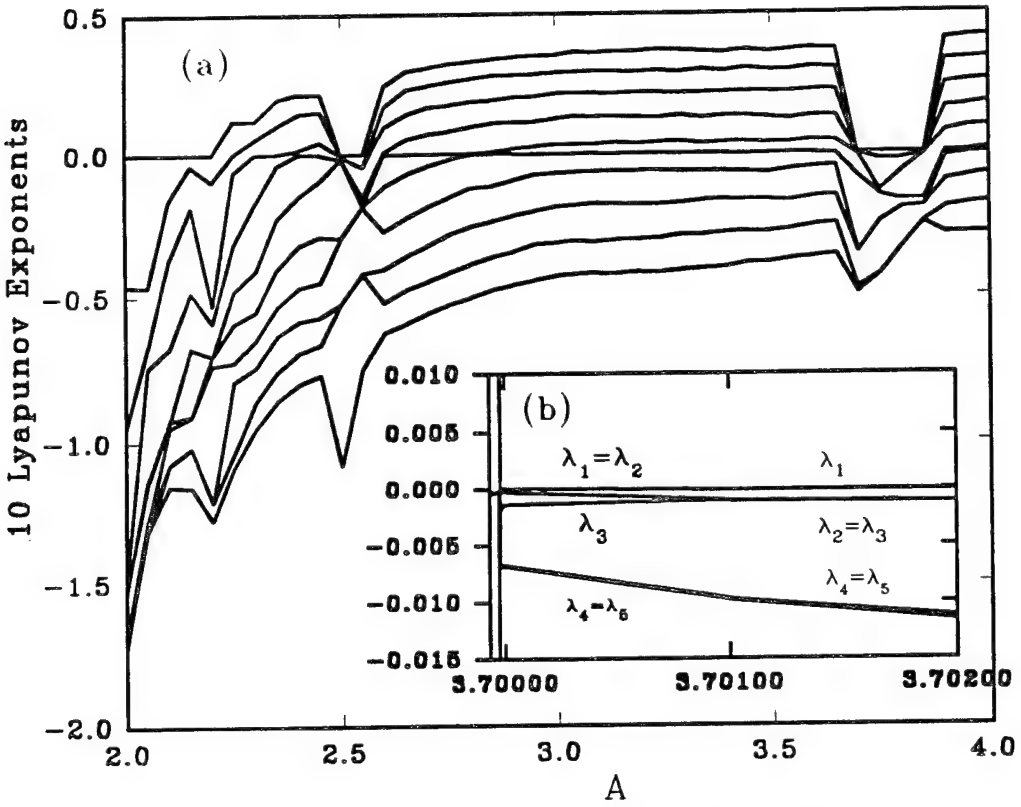

Figures 1 Lyapunov spectra

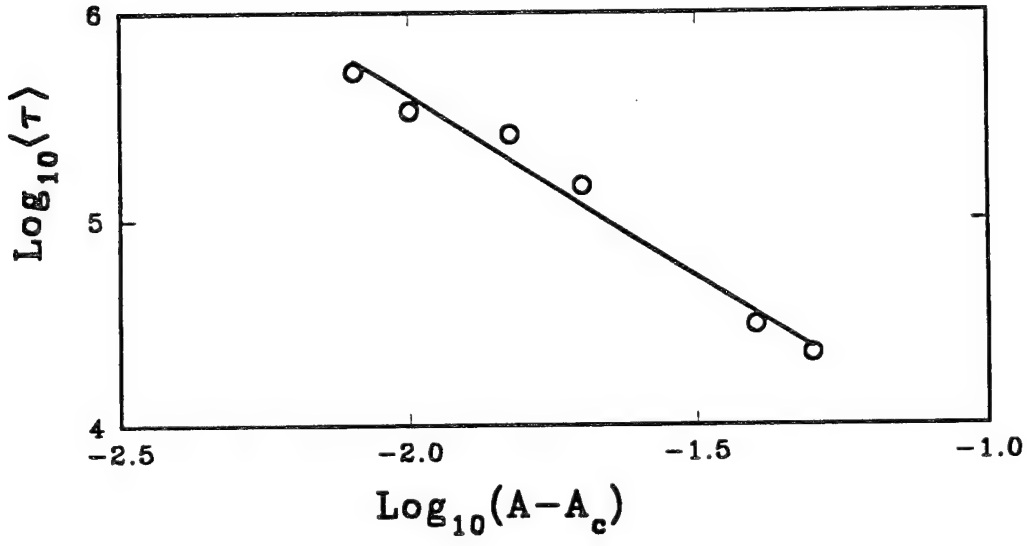

Figure 2 Critical exponent $\gamma=\log_{10}<\tau>/\log_{10}(A-A_c)$

BISTABILITY AND RECTANGULAR PULSES UNDER SECOND HARMONIC GENERATION

A.V.Ghiner, G.I.Surdutovich+ and N.P.Konopleva++
Universidade Federal do Ceara, C.P.6030, CEP 60450-970, Fortaleza, Brazil
+Instituto de Fisica de Sao Carlos/USP, C.P.369, CEP13560-970,Sao Carlos,Brazil
fax 55(162)713616, e-mail surdutovich@ifqsc.sc.usp.br
++Novosibirsk State University, 630090, Novosibirsk,Russia

A simple model of the second harmonic (SH) generation in a passive resonant ring cavity with nonlinear medium of the length l is studied. Such a system has bistable and multistable stationary solutions. The bistability springs up only for sufficiently large, more than critical, value of the parameter $\frac{l}{L}$: $\frac{l}{L} > 4$, where $L = 1/\sigma a_p$ is the transformation length, σ is the nonlinear coupling constant of the waves , and a_p is the pump amplitude. This limitation is connected with the fact that increase of the SH intensity due to the resonator effect for high-quality cavities does not cause a sufficient change of the nonlinear phase to enable appearance of additional solution.

The ruin of stability means arise of two "álternative" states while each of them reproduces itself through an even number of resonator round-trips. Formally such a solution cannot be "inserted" into the cavity. In fact between these alternative states arises switching front "inserted" into the resonator, which travels into the cavity with a phase velocity (Fig.1). For dispersionless system switching front turns into steep-like one and so pulses acquire the rectangular form. As a result system starts generate a repetitive succession of rectangular pulses with the duration and relative duration equal to the round-trip time of the cavity (Fig.2).

With increasing of the resonator quality 2τ-periodical solutions become unstable so that bifurcation (doubling of the period) takes place and the amplitude oscillates between not *two* but *four* points. Such mode instability is of the Ikeda's type in a new physical situation We emphasize that in our case the system can demonstrate not only bistability of stationary states but "bistability of regimes" as well. For a fixed set of the parameters there are stable stationary and periodic solutions depending on the initial conditions.

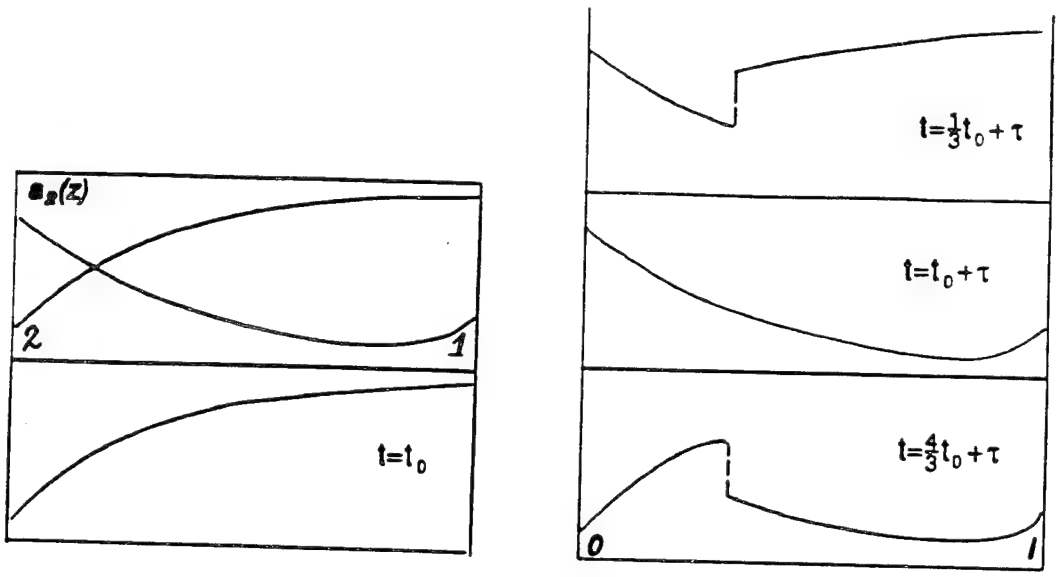

Fig.1.a) SH amplitude dependence on the distance for two different initial conditions(stationary solutions 1 and 2). b) Instantaneous field distributions inside the cavity at different moments of time under doubleperiodic mode.

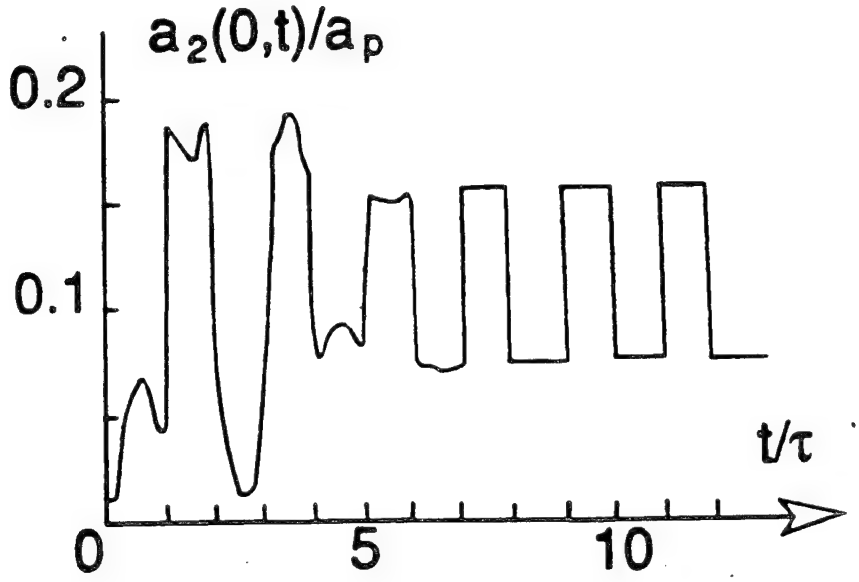

Fig.2. Temporal change of the SH amplitude $a_2(0,t)$ inside the cavity (normalized to the pump amplitude a_p).

Nonlinear Dynamics of Chirped Solitons in Doped Fibers

L. W. Liou and Govind P. Agrawal
The Institute of Optics, University of Rochester
Rochester, New York 14620
Tel: (716) 275-6195
Fax: (716) 244-4936
E-mail: liou@optics.rochester.edu

The spectrum of pulses emitted from mode-locked fiber lasers often characteristically exhibits sharp, unequally spaced sidebands. The origin of these sidebands is well understood. They result from the constructive interference between the soliton and the dispersive waves that are shed from the pulse due to perturbations in the cavity loss, gain, dispersion, or nonlinearities.[1] Spectral sidebands correspond to frequencies of dispersive waves for which the relative phase difference is a multiple of 2π.

In previous work,[2] the sideband frequencies were determined by assuming a chirp-free soliton as in the case of passive, undoped fibers. By using the phase-matching criterion between the soliton and dispersive waves, an expression for the sideband frequencies was derived. However in active fibers, the gain dispersion results in pulses of the form $(\mathrm{sech}\tau)^{(1+iq)}$, where the parameter q governs the amount of chirp in the pulse.[3] This chirp is responsible for modifying the interference condition between the soliton and dispersive waves and consequently, the frequency of the sidemodes generated through the dispersive wave resonances. We have obtained a new expression for the sideband frequencies in the anomalous dispersion regime which is given by:

$$\delta\nu_m = \frac{0.28}{T_s}\left[\frac{8mz_0}{L} - (1 - q^2 - 2qd)\right]^{1/2}, \qquad (1)$$

where $\delta\nu_m$ is the frequency offset of the sideband from the center frequency of the soliton, m is the order of the sideband, T_s is the soliton width (full width at half maximum), z_0 is the dispersion length, L is the length of the laser cavity, and d is the gain dispersion parameter. This expression

reduces to the previously obtained result for unchirped solitons by setting q = 0. However, in general, q is not zero, and the pulses formed inside a fiber laser are chirped solitons.

The chirp of the emitted soliton is highly dependent on the gain experienced by the pulse in a round-trip of the laser cavity. This is shown in Fig. 1 where the chirp parameter is plotted as a function of the round-trip gain. The solid and dashed curves correspond to the anomalous and normal dispersion regimes, respectively. Since the round-trip gain must equal the total cavity losses, there is a direct connection between the amount of loss in the cavity and the sideband frequencies observed in the pulse spectra. We show how the positions of the soliton sideband spectra are dependent not only on the net dispersion of the cavity as previously thought[4] but also on the total cavity losses.

[1] J. P. Gordon, J. Opt. Soc. Am. B **9**, 91 (1992).

[2] S. M. J. Kelly, Electron. Lett. **28**, 806 (1992).

[3] P. A. Belanger, L. Gagnon, C. Pare, Opt. Lett. **14**, 943 (1989)

[4] M. L. Dennis and I. N. Duling III, IEEE J. Quant. Electron. **30**, 1469 (1994).

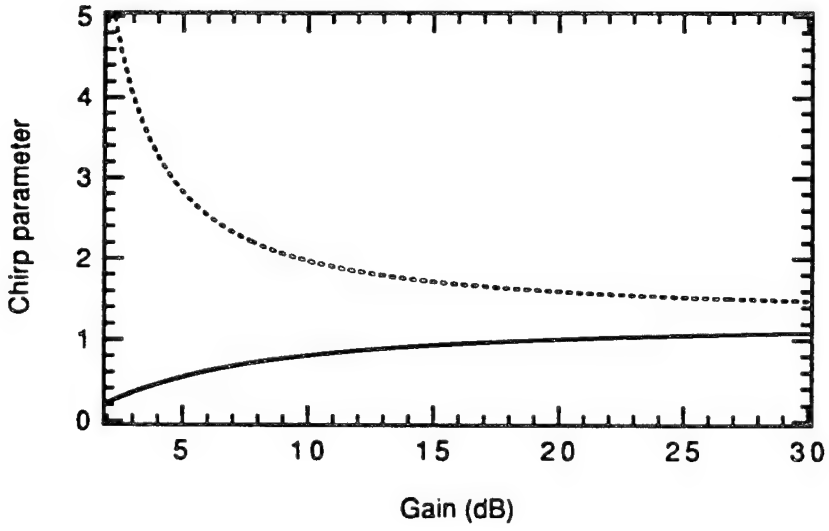

Fig. 1

Fig. 1. Chirp parameter q of the output pulse as a function of the round-trip intra-cavity gain. The solid and dashed curves correspond to the anomalous and normal dispersion regimes, respectively.

Noise and Chaos in a Multimode Solid State Laser

Clif Liu[1], Henry D. Abarbanel[1,2], Zelda Gills[3], and Rajarshi Roy[3]

[1] Department of Physics and Institute for Nonlinear Science, University of California, San Diego, La Jolla, CA 92093; phone: (619)534-5810; fax: (619)534-7664; email: clif@rutherford.uscd.edu

[2] Marine Physical Laboratory, Scripps Institution of Oceanography, University of California, San Diego, CA 92093; phone: (619)534-5590; fax: (619)534-7664; email: hdia@hamilton.ucsd.edu

[3] School of Physics, Georgia Institute of Technology, Atlanta, GA 30032; phone: (404)894-5265; fax: (404)853-9958; email: ph276rr@gitvm1.gatech.edu

The solid state Nd:YAG (neodymium doped yttrium aluminum garnet) laser with an intracavity frequency doubling KTP (potassium titanyl phosphate) crystal [1] can show chaotic intensity fluctuations when operated with at least three longitudinal infrared modes. The source of chaotic behavior is the coupling of the infrared modes through the process of sum-frequency generation in the KTP crystal. This process destabilizes the relaxation oscillations which are normally heavily damped in the system without the intracavity crystal. We show that the laser can be operated both in a low dimensional chaotic regime and in a regime where intrinsic noise significantly influences the deterministic dynamics.

The laser system was prepared so that it was clearly chaotic in operation with two distinct polarization configurations of the three lasing fundamental modes. In Figure 1(a) we show a time trace of the total infrared intensity I(t) when all three modes are parallel polarized ("type I" chaos). In Figure 1(b) we show I(t) with one mode polarized perpendicular to the other two ("type II" chaos). Type I chaos consists of long "bursts" of relaxation oscillations, while type II appears far more irregular. Very little green light is generated for Type I behavior--which consists of low dimensional chaos that is controllable by the method of occasional proportional feedback (OPF) [2,3]. Type II chaos is accompanied by the generation of a substantial amount of green light and the presence of high dimensional intrinsic noise. Typically, type II chaos can not be controlled using OPF.

We report results of nonlinear time series analysis [4] for quantitative distinction between chaotic behavior where the noise level is very low (type I) and chaotic behavior where the noise level is substantial (type II). Our analysis uses average mutual information [5] and percentage of false nearest neighbors [6], as shown in Fig. 2, to reconstruct the system dynamics by time delay embedding. We also evaluate the Lyapunov spectrum of the system to firmly establish that the motion is chaotic and to estimate the overall dissipation of the system. Large noise fluctuations are associated with the substantially larger dissipative type II chaos. We suspect that the origin of this noise is in the microscopic fluctuations of the photon fields arising during the conversion of pairs of infrared (1.064 mm) photons to green light (0.532 mm).

References:

1. C. Bracikowski and R. Roy, Chaos **1**, 49 (1991).
2. R. Roy *et. al.*, Phys. Rev. Lett. **68**, 1259 (1992).
3. Z. Gills *et. al.*, Phys. Rev. Lett. **69**, 3169 (1992).
4. H. Abarbanel *et. al.*, Reviews of Modern Physics **65**, 1331 (1993).
5. A. Fraser and H. Swinney, Phys. Rev. A **33**, 1134 (1986); A. Fraser, IEEE Trans. on Info. Theory **35**, 245 (1989).
6. M. Kennel *et. al.*, Phys. Rev. A **45**, 3403 (1992).

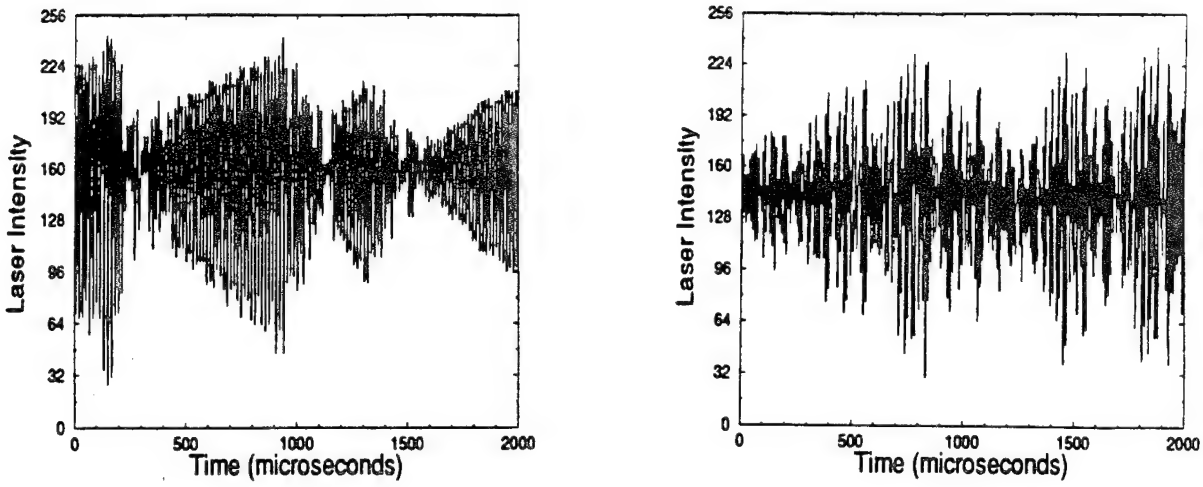

Figure 1. (a) Fluctuations of the total infrared intensity for three mode Nd:YAG laser operation with all modes polarized parallel to each other. Relaxation oscillations of period ≈ 16 μsec are evident within a modulating envelop, typical of type I dynamics. (b) Fluctuations of the total infrared intensity for three mode Nd:YAG laser operation with one mode polarized perpendicular to the other two (type II). The relaxation oscillations are still visible.

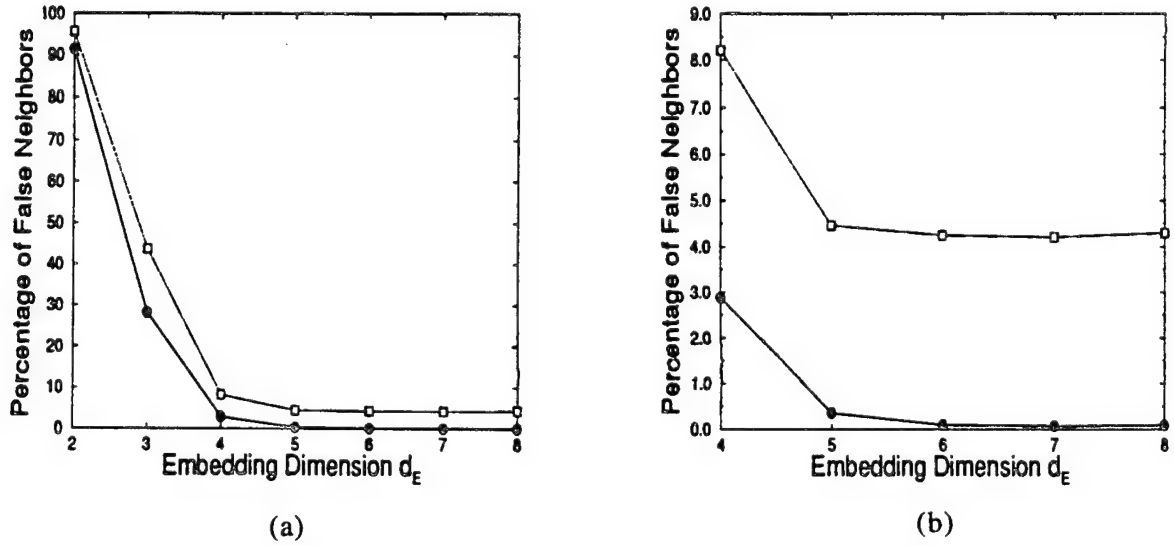

Figure 2. (a) Percentage of false nearest neighbors (FNN) versus the embedding dimension d_E for type I (solid symbols) and type II (open symbols) chaotic data sets. These are averages over the collection of type I and type II data collected. (b) Enlargement of Fig. 2(a) showing that the percentage of Type I FNN drops to 0.1 percent and stays there as d_E increases but the percentage of type II FNN does not drop below 4 percent. Both operating conditions show intrinsic noise; but, the much higher level of residual false neighbors in type II chaos is the signature of a system where noise is appreciable enough to influence the deterministic dynamics.

Suppression of Chaos in External Cavity Semiconductor Laser

Yun Liu and Junji Ohtsubo
Faculty of Engineering, Shizuoka University, Johoku 3-5-1, Hamamatsu, 432, Japan
Tel: +81-53-471-1171 Fax: +81-53-475-1764 e-mail: y-liu@seibu2.shizuoka.ac.jp

Abstract

In chaotic dynamics of a semiconductor laser with external optical feedback, we describe a method that controls or suppresses chaos into regular state by means of a coherent second external feedback. The potential applicability of the control algorithm to the intensity noise reduction has also been discussed.

1 Introduction

Semiconductor lasers with external optical feedback provide one of the best physical systems for studying nonlinear dynamic phenomena. A rich variety of behavior has been observed in these systems, including periodic, quasi-periodic oscillations, and chaos.[1] In some applications, feedback induced chaos can be harmful to the performance of semiconductor lasers because it enhances the intensity noise.[2] Therefore one wishes to reduce or suppress undesired chaotic instabilities. This is the task of so called chaos-controlling.

In this paper, we introduce the second external feedback (see Fig. 1) loop to suppress chaotic dynamics of external cavity semiconductor laser. The configuration has been studied as a high-dimensional chaos model.[3] Here we lay emphasis on the control of the chaotic dynamics by adjusting the parameters of the second feedback loop. We show that chaos can be effectively suppressed by setting the ratios L_2/L_1 and R_2/R_1 to appropriate ranges. Moreover, by calculating the RIN (relative intensity noise) levels for different states, we demonstrate that the proposed algorithm can be used for the noise reduction in some applications of semiconductor lasers.

2 Results and Discussions

The shematic of the laser diode with doulbe external feedbacks is shown in Fig. 1. The light source is a CSP

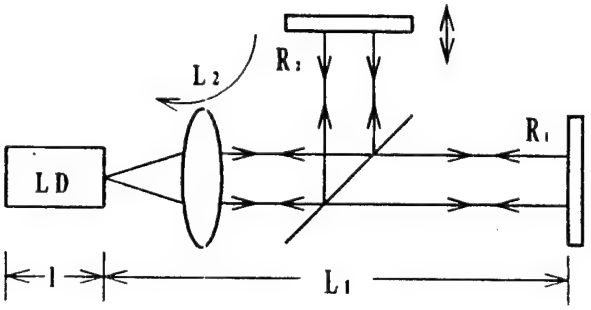

Fig. 1 Experimental setup. L_1, L_2: distances of two external mirrors from the front facet of the laser, R_1, R_2: amplitude reflectivities of two mirrors.

AlGaAs semiconductor laser with the cavity length l, the refractive index η, and the amplitude reflectivity of two facets r_0.

For a weak to moderate feedback level, one has the following rate equations

$$\begin{aligned}\dot{E}(t) &= \{j\omega(N) + \frac{1}{2}G_N[N(t) - N_{th}]\}E(t) \\ &+ \frac{\kappa_1}{\tau_{in}}E(t-\tau_1) + \frac{\kappa_2}{\tau_{in}}E(t-\tau_2) + F_E(t), \quad (1) \\ \dot{N}(t) &= J - \frac{N(t)}{\tau_s} \\ &- G_N[N(t) - N_0]|E(t)|^2 + F_N(t). \quad (2)\end{aligned}$$

Here, $E(t)$ the complex eletric field at the front facet, $N(t)$ is the average carrier density in the active region, ω_N is the angular optical frequency of the laser, G_N is the modal gain coefficient, N_{th} is the threshold carrier density for the solitary laser, $\kappa_{1,2} = (1-r_0^2) \times R_{1,2}/r_0$ is the feedback coefficient, F_E and F_N are Langevin noise terms. Also, τ_{in} is the optical round trip time in the laser diode cavity, τ_s is the carrier life time, $\tau_{1,2} = 2L_{1,2}/c$ is the external cavity round trip time, and J is the injection current density.

We have numerically calculated Eqs. (1) through (3) by employing a fourth order Runge-Kutta algorithm and verified various phase transitions among fixed points, periodic states, and chaos. The emphasis is put on the variations of the dynamics with respect to the ratio of optical length or the reflectivity be-

tween two external feedback loops. Figure 2 shows a typical example of such variations. In the case of the single feedback, the result (broken line) demonstrates chaotic behavior. With the second feedback, the chaotic output is reduced to a periodic oscillation (solid line) or even a fixed fixed (dotted line). In the calculation, the chaos suppression occurs for various set of parameters. Especially for $L_2/L_1 = 0.85 \sim 0.99$, there exist dramatical changes of dynamics due to the variation of parameters. Figure 3 summarizes a bifurcation for a certain condition: J=1.07 J_{th}, L_1=30 cm, and R_1=1.5%.

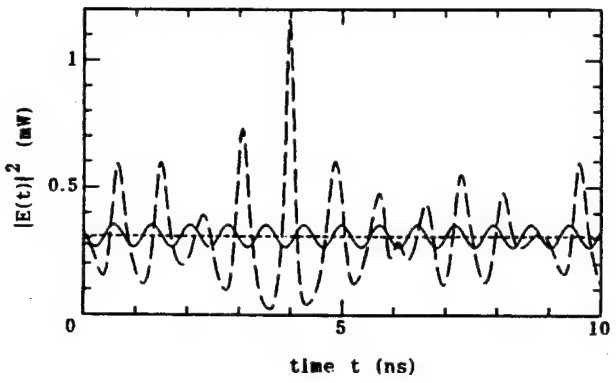

Fig. 2 Numerical results for J=1.07 J_{th}, L_1=30 cm, and R_1=1.5%. Broken line: single feedback; Dotted line: L_2/L_1=0.925, R_2/R_1=1/3; Solid line: L_2/L_1=0.925, R_2/R_1=2/3.

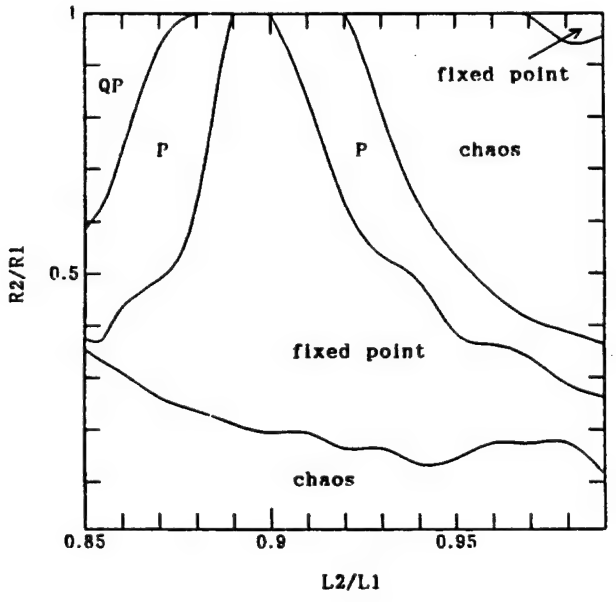

Fig. 3 Bifurcation diagram for J=1.07 J_{th}, L_1=30 cm, and R_1=1.5%.

The reason why chaos is suppressed with the second coherent light feedback can be considered as follows. In the case of double external cavities, the laser couples with an interference signal formed by two coherent feedbacks. Under certain proper parameter conditions, the interference signal becomes a periodic beat signal. The feedback of such beat signal yields the coherence of the phase and finally the periodicity of the laser dynamics.

Optical feedback may cause the intensity noise enhancement which drametically deteriorates the performance of semiconductor lasers. We consider that the feedback induced deterministic instabilities are responsible for the intensity noise enhancement.[4] As the double external cavities can be introduced in the practical case, the chaos suppression of the current configuration might be applied to the noise reduction. To verify this property, we generate the Langevin noises in Eqs. (1) through (3) and calculate the RIN levels for the cases with or without the control. As an example, the average RIN corresponding to Fig. 2 reads -71.5, -101.0, and 91.3 dB/Hz for the broken, solid, and dotted lines, respectively. In general, the RIN level can be reduced 20 dB/Hz or more provided chaos is suppressed to periodic or fixed states. This suggests that the control algorithm is very promising in reducing the feedback induced noise.

3 Summary

We have introduced and tested an algorithm that applies to the suppression of chaos in the semiconductor laser with external optical feedback. The nolvelty of the proposed procedure lies in the fact that it employs only the external feedback itself to achieve the control. It has been confirmed that the method is suitable for the reduction of the feedback induced intensity noise.

References

[1] see for example, J. Mørk, B. Tromborg, and J. Mark, IEEE J. Quantum Electron., **QE28** (1992) 93.

[2] T. Kanada, Trans. IEICE Jpn., **68** (1985) 180.

[3] I. Fischer, O. Hess, W. Elsäßer, and E. Göbel, Phys. Rev. Lett., **73** (1994) 2188.

[4] Y. Liu, N. Kikuchi, and J. Ohtsubo, Phys. Rev. E, submitted.

CHAOS CONTROL IN A MODULATED CLASS-B LASER

N.A.Loiko, A.V.Naumenko, and S.I.Turovets.

Institute of Physics of Academy of Sciences of Belarus
70 F.Skaryna Prosp., Minsk 220072, Belarus
Phone: 7(0172)395521, fax: 7(0172)393131
E-mail: ifanbel%bas03.basnet.minsk.by@demos.su

Since the original method of chaos control by Ott, Grebogi, and Yorke (OGY) was presented [1] a number of successful applications of this method for taming chaotic dynamics in experiments including lasers has been reported. In particular, Roy et. al. have resolved the problem of multimode instability (so-called "green" problem) in the Nd:YAG laser with intracavity frequency doubling on the KTP crystal[2], Glorieux and coworkers have stabilized a chaotic output of selfpulsing fiber and modulated CO_2 lasers [3 and references therein].

At the same time, the OGY method itself and its modifications have some drawbacks which are essential for widespread applications in practical devices. The main of these are usually a priori unknown parameters of control, so the adjustments to correct values may become quite tedious, the extremely high sampling frequencies in very fast systems, and sometimes absence of robustness to noise.

In this paper we analyze theoretically possibilities of improving these techniques using as a paradigmatic example the rate equations model for a modulated class-B laser.

First, we have considered delayed impulsive feedback (DIF) techniques. The consideration covers the cases when one or two of the following control parameters are accessible : the losses of cavity, the pump parameter and the energy of injected pulse from a master laser. The key point here is existence of an optimal phase of applying impulsive correction signals. In particular, in a modulated laser with control on cavity losses this phase corresponds to the vertical orientation of an unstable manifold of a saddle nT-periodic cycle to be stabilized and coincides with an optimal phase of amplification near a threshold of an instability which, in its turn, can be readily identified theoretically and experimentally [4]. More than that, there is also an optimal strength of the feedback kicks. It also can be expressed analytically through the parameters of characterization of the unstable orbits. In Fig.1 we present the theoretical results illustrating this optimal control technique applied to the model of a modulated CO_2 laser with losses controlled by an additional spiking laser [4]. It can be easily seen, that in a parameter space of the control scheme there is a domain of achieving control with an optimum in the centres of contour plots. The external boundaries of this domain are

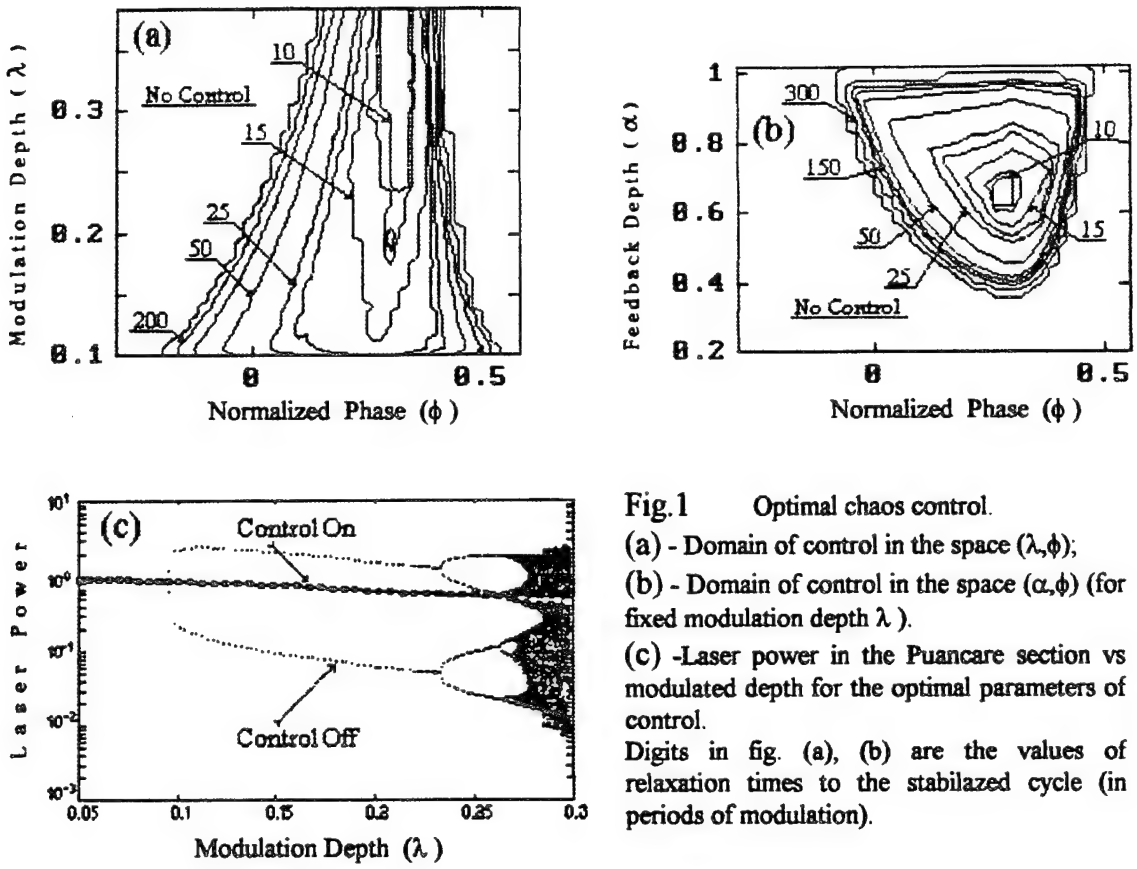

Fig.1 Optimal chaos control.
(a) - Domain of control in the space (λ,ϕ);
(b) - Domain of control in the space (α,ϕ) (for fixed modulation depth λ).
(c) -Laser power in the Puancare section vs modulated depth for the optimal parameters of control.
Digits in fig. (a), (b) are the values of relaxation times to the stabilazed cycle (in periods of modulation).

found analytically from the condition that Floquet multipliers of the resulting system are in the unit circle. It is also seen that stabilization of the unstable orbits is traced to the chaotic region without any readjusting of the control scheme parameters.

We have also performed a linear stability analysis for a delayed continuous feedback techniques (DCF) in a modulated laser, which has a number advantages in applications [3]. As a result using the Stokes generalization of the Floquet theory for functional equations, we derived a generalized bifurcation condition which contains as particular cases subgarmonic, saddle-node and Hopf instabilities. It has been shown that DCF control does not change the saddle-node bifurcations in the original systems and suppresses period doubling bifurcations. These results are in good agreement with the recent experiments on controlling unstable orbits in a CO_2 laser by DCF [3].

[1]. E.Ott, C.Grebogi, and J.A. Yorke, Phys.Rev.Lett 64,1196 (1990).
[2]. R.Roy et. al., Phys.Rev.Lett 68,1259 (1992).
[3]. S. Bielawski, D. Derozier, and P. Glorieux, Phys.Rev E 49, R971(1994).
[4]. V.N. Chizhevsky and S.I. Turovets, Opt. Commun. 102, 175 (1993).

BIFURCATION TO ANTIPHASE PERIODIC SOLUTIONS IN A MODULATED SOLID-STATE FABRY-PEROT LASER

Paul Mandel and T. Erneux

Université Libre de Bruxelles, Optique Nonlinéaire Théorique,
Campus Plaine, C.P. 231, 1050 Bruxelles, Belgium
Fax: +32 2 650 5824 Email: PMANDEL(TERNEUX)@ULB.AC.BE

The antiphase state denotes a simple periodic, multiperiodic or chaotic state that was observed recently in multimode lasers experiments [1-5]. The simplest type of antiphase state is characterized by the fact that the intensity of each mode oscillates with a similar waveform but not with the same phase. Antiphase states appear with high multiplicity because there is no preferential mode if all modes are equally coupled. Furthermore, these antiphase states are competing with the in-phase state (all modes are in phase). It is thus of particular interest to determine the bifurcation diagram of the antiphase states.

Specifically, we consider the Tang, Statz and deMars equations modeling a solid-state Fabry-Perot laser [6] with a periodic pump modulation [7]. Each of the N modes is characterized by the ratio κ_p of the field decay rate to the population inversion decay rate and by its gain γ_p. The laser pump rate is w. Assuming $\kappa_p \equiv \kappa$, we have determined an asymptotic approximation of the laser equations in the limit $\kappa \gg 1$ and $\gamma_p = \gamma + O(1/\sqrt{\kappa})$. To dominant order in κ, the laser is characterized by only two frequencies, $\Omega_1\sqrt{\gamma_\parallel \kappa}$ and $\Omega_2\sqrt{\gamma_\parallel \kappa}$, where Ω_2 is N - 1 degenerate. Using the expressions given in [8] we find the following limits for w close to 1, w large and N large, respectively:

1/ $w = 1 + \varepsilon$, $N = O(1)$:
$\Omega_1^2 = \varepsilon + O(\varepsilon^2)$, $\Omega_2^2 = \varepsilon/(2N + 1) + O(\varepsilon^2)$,

2/ $w \gg 1$, $N = O(1)$:
$\Omega_1^2 = w + O(1)$, $\Omega_2^2 = w/(2N - 1) + O(1)$,

3/ $N \gg 1$, $w = O(1)$:
$\Omega_1^2 = w - 1 + O(1/N)$, $\Omega_2^2 = (w - 1)/2N + O(1/N^2)$.

In particular, for N = 2, we find $3 < (\Omega_1/\Omega_2)^2 < 5$ and $\Omega_1/\Omega_2 = 2$ for $w = 15/7$. Scaling the time so that the degenerate frequency equals 1, the leading order approximation is

$$dx_p/dt = - y_p - M\cos(\sigma t) - \lambda \sum_j^N y_j \,, \tag{1}$$

$$dy_p/dt = x_p(1 + y_p) \,, \tag{2}$$

where p = 1,2,... N. In these equations x_p and y_p are proportional to the deviation of the population inversion and the intensity from their steady state values, respectively. M and σ are proportional to the amplitude and the frequency of the modulation. λ depends on the pump parameter w. If M = 0, Eqs. (1) and (2) form a conservative problem that admits antiphase periodic solutions [9]. The fact that when N = 2 there is a significant domain of parameters for which $\Omega_1/\Omega_2 \simeq 2$ suggests a near resonance phenomenon between the two periodic solutions of the linearized theory. We investigate this problem by determining the bifurcation diagram of the periodic solutions of Eqs. (1) and (2). For N = 2, we find that the leading approximation of the solution for y(t) is given by

$$y_{p1} = [\,(-)^p B e^{it} + c.c.] + [\,A e^{2it} + c.c.], \quad p = 1,\ 2. \tag{3}$$

If B = 0 and A ≠ 0, the solution is a pure in-phase periodic solution. If B ≠ 0, the solution corresponds to an antiphase periodic solution whatever the value of A. We derive amplitude equations for A and B by formulating solvability conditions for the two possible cases of resonance (σ = 1 and σ = 2). If σ = 1, we find that an antiphase periodic solution is the only possible solution. If σ = 2, both antiphase and in-phase solutions are possible.

REFERENCES

1. K.Wiesenfeld, C.Bracikowski, G.James and R.Roy, Phys. Rev. Lett. 65, 1749 (1990); G.E. James, E.M. Harrell, and R. Roy, Phys. Rev. A 41, 2778 (1990).
2. K.Otsuka, P.Mandel, S.Bielawski, D.Derozier and P.Glorieux, Phys. Rev. A 46, 1692 (1992).
3. S.Bielawski, D.Derozier and P.Glorieux, Phys. Rev. A 46, 2811 (1992)
4. K.Otsuka, M.Georgiou and P.Mandel, Jpn. J. Appl. Phys. 31 L1250- L1252 (1992).
5. K.Otsuka, P.Mandel, M.Georgiou, and C.Etrich, Jpn. J. Appl. Phys. 32, L318-L321 (1993).
6. C.L.Tang, H.Statz, and G.deMars, J. Appl. Phys. 34, 2289 (1963).
7. P.Mandel, M.Georgiou, K.Otsuka and D.Pieroux, Opt. Comm. 100, 341 (1993).
8. D.Pieroux and P.Mandel, Opt. Commun. 107, 245 (1994).
9. T.Erneux and P.Mandel, submitted (1995)

Spatio-temporal dynamics of gain-guided semiconductor laser array

J. Martín-Regalado, S. Balle and N. B. Abraham*
Departament de Física, Universitat de les Illes Balears, E-07071 Palma de Mallorca, Spain.
Phone: (34-71) 17 32 34, Fax: (34-71) 17 34 26, e-mail: josep@hp1.uib.es
* *Permanent address: Physics Department, Bryn Mawr College, 101 N. Merion Ave., Bryn Mawr, PA 19010, USA*

I. INTRODUCTION

Complex spatio-temporal behavior is a general property of semiconductor laser arrays. Many experimental [1] and numerical [2-4] studies have shown that index/gain guided laser arrays exhibit strong spatio-temporal pulsations which are usually related to the presence of amplitude-phase coupling through the α-parameter [3] and multilateral mode operation [4]. With such a complicated dynamics well documented, a better understanding of the causes of the complex dynamics characteristic of semiconductor laser arrays is required. To distinguish between cause and effects, theoretical modeling of such devices is a key step.

II. LASER MODEL

In order to avoid the unphysical high-wave-number instabilities that appear in Rate Equation models when spatial effects are explicitely included [5], we modify the semiclassical Maxwell-Bloch model for a two level homogeneously broadened medium to capture appropriately more of the semiconductor laser physics [6]. Assuming that the optical field can be decomposed as

$$\hat{E}(x,y,z;t) = \hat{x}Re[E(x;t)\phi(y)\Psi(z)exp(-iwt)]$$

where $\phi(y)$ ($\Psi(z)$) is the transverse (longitudinal) field distribution of the fundamental transverse (longitudinal) mode, $E(x;t)$ the slowly varying lateral field distribution parallel to the juncion plain whose amplitude may depend on time, and w is the carrier frequency, we can write these equations as

$$\frac{\partial E}{\partial t} = -\frac{\gamma}{2}(1+i\alpha)E + \frac{ic^2}{2\omega\eta^2}\frac{\partial^2 E}{\partial x^2} + \frac{P}{2} \quad (1)$$

$$\frac{\partial P}{\partial t} = -\gamma_p\left[1 - i\alpha\left(1 - \frac{\gamma}{2\gamma_p}\right)\right]P + \gamma_p(1+\alpha^2)a(N-N_0)E \quad (2)$$

$$\frac{\partial N}{\partial t} = \frac{C(x)}{ql} - \gamma_e N + D\frac{\partial^2 N}{\partial x^2} - \frac{1}{2}[EP^* + E^*P] \quad (3)$$

where $P(x;t)$ is the slowly varying enveloppe of the material polarization for a carrier frequency ω, and N the carrier density. Spontaneous emission and thermal noise are modeled by Gaussian white noise sources in the equations for P and N.

The main physical parameters of these equations are: distributed loss γ=0.723 ps^{-1}, linewidth enhancement factor α=3, reference frequency ω=2.2987 10^{14} s^{-1}, index of the active layer η=3.5, polarization decay rate γ_p=10^{13} s^{-1}, differential gain a=2 10^{-6} μm^3 ps^{-1}, carrier density at transparency N_0 =1.3 10^6 μm^{-3} , carrier decay rate γ_e=3.3 10^8 s^{-1}, active layer thickness l=0.2 μm, c is the velocity of light, D is the diffusion coeficient and q is the electron charge.

The dependence of the current density profile, $C(x)$, on the lateral direction allows us to have narrow stripe, broad-area or multi-stripe configurations. Current spreading is also taken into account by a layered approximation in which the current density is almost uniform across the stripes (C_{max}) and the interstripe regions, and the relationship between both values is a fixed ratio r [4].

A four-stripe gain-guided semiconductor laser array has been modeled where the width of the stripes is maintained constant (5 μm). In all the simulations, the device is switched-on by abruptely changing the injection current from transparency to a certain level above threshold which is kept constant for the whole time interval of integration.

III. DYNAMICS OF THE ARRAY

In gain-guided devices, the carrier distribution provides not only gain, but also field confinement. Hence the system is by far more sensitive to any mechanism which changes the carrier profile, thus leading to a decreased stability of phase-locked states. The influence of different mechanism on the array dynamics is considered.

a) Carrier Diffusion: Carrier diffusion mainly affects the effective current injection and the field confinement within the stripes. The first one can cause a different emission frequency for each stripe, and also can lead to the discrimination of the outer stripes [7] as shown in Fig. 1. The second one will influence the coupling between neighbouring stripes through the evanescent fields, thus favouring the arousal of dynamical instabilities.

b) Interstripe Distance: The distance between stripes strongly determines the coupling strength between neighbouring stripes. We have explored the effect of varying the interstripe distance, adjusting the injection current for each value of the interstripe separation to satisfy that the current density profile is the same in all the cases,

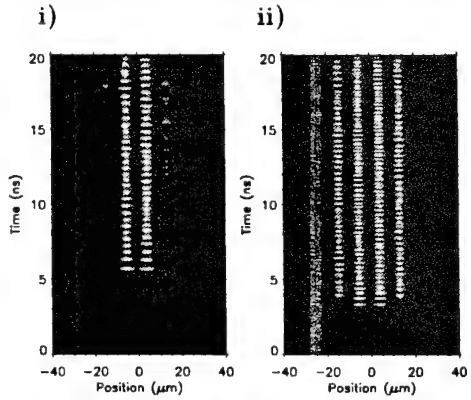

FIG. 1. Effects of carrier diffusion. Near field plot for L_D = 3μm , r = 0.05, s = 4μm and i) I = 180mA, ii) I = 200mA.

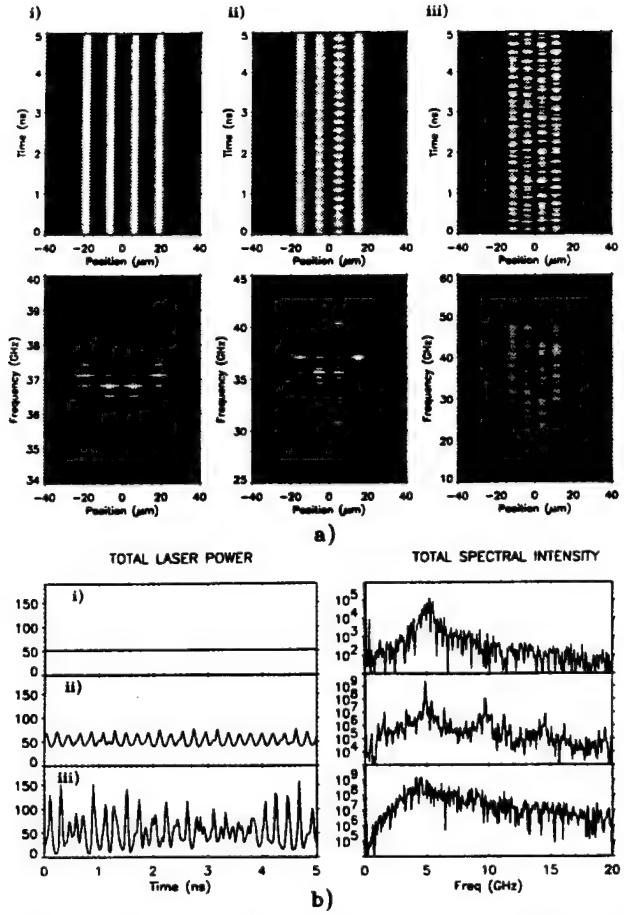

FIG. 2. Influence of the interstripe distance: a) Near field and (x,ω) plots for $L_D = 2\mu$m, $r = 0.33$ and $C_{max} \sim 2\ C_{th}$; and b) Time series and spectra of the total intensity emited by the array, for i) $s = 8\mu$m and I=350 mA, ii) $s = 6\mu$m and I=300 mA, and iii) $s = 4\mu$m and I=250 mA

in order to obtain approximately the same mean output power. Fig. 2 shows the near field plot and the corresponding (x,ω) plot for three different interstripe separations.

For large interstripe distances (s=8 μm) the stripes are almost isolated and each one behaves as a single laser having its own lateral fundamental mode ('local' mode), and the 'array' modes can be described as combination of such 'local' modes. However, the weak coupling of neigbouring stripes breaks the frequency degeneracy between fields of different stripes, and small beating between such 'array' modes is expected ($\sim$ 0.3GHz). When the interstripe distance is decreased (s=6 μm), the relaxation oscilations frequency (f_r) is close to a harmonic of the beat note (frequency difference between 'local' modes), yielding strong spiking of the intensity in each stripe. A futher decrease to s=4 μm leads a strong drop of the laser coherence, the spectral power being distributed over $\sim$ 50 GHz. Moreover, these dynamics and characteristic frequencies are also observed in the total laser power and spectra plots.

c) Current Injection: Increasing the injection current leads to the same dynamics as previously described: the device passes through stable, quasi-periodic and chaotic outputs as the current is increased. For low injection currents, the array dynamics can be depicted as the result of the interaction among a few "array modes" defined as combinations of "local" modes defined within each stripe, thus reminding of Coupled-Mode Models. As the current injection is increased, more and more of these "array modes" are required in order to describe the resulting dynamics.

IV. STRONG COUPLING LIMIT

A completely different behavior is obtained when the stripes are so close and coupled that they behave almost as a single broad stripe (see Fig. 3). Opposite to the cases discused in the previous section, the space-resolved spectrum shows well defined peaks with defined lobes (similar to the one observed for broad area lasers [8]). It must be emphasized that these "supermodes" cannot be constructed as combinations of the different "local" modes, thus breaking the validity of a Coupled-Mode approach.

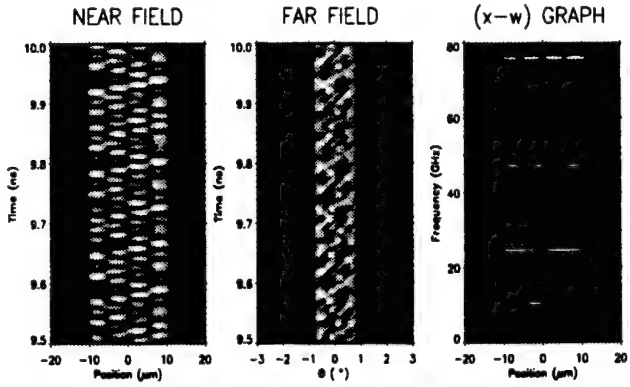

FIG. 3. Broad Area behavior: a) Near field, far field and (x,ω) plots for $L_D = 2\mu$m, $r = 0.33$, $s = 0.5\mu$m and I=203 mA ($C_{max} \sim 2\ C_{th}$).

The authors wish to thank Prof. M. San Miguel for helpful discussions and comments. Financial support from the Comisión Interministerial de Ciencia y Tecnología, Project No. TIC93/0744 is also acknowledged.

[1] R. A. Elliott et al.,*IEEE J. Quantum Electron.*, vol. QE-21, pp. 598-602, 1985.; N. Yu et al., *Electron. Lett.*, vol. 24, pp. 113-115, 1988.; R. K. DeFreez et al.,*Appl. Phys. Lett.*, vol. 53, pp. 2380-2382, 1988.

[2] H. G. Winful, and S. S. Wang,*Appl. Phys. Lett.*, vol. 53, pp. 1894-1896, 1988.; H. Adachihara et al.,*J. Opt. Soc. Am. B*, vol. 10, pp. 496-506, 1993.

[3] L. Rahman, and H. G. Winful,*Opt. Lett.*, vol. 28, pp. 128-130, 1993.; P. Ru et al.,*J. Opt. Soc. Am. B*, vol. 10, pp. 507-515, 1993.

[4] S. Fernandez-Casares et al.,*IEEE J. Quantum Electron.*, vol. QE-30, pp. 2449-2457, 1994.

[5] P. K. Jakobsen et al.,*Phys. Rev. A.*, vol. 45, pp. 8129-8137, 1992.

[6] A. Yariv, *Quantum Electronics.*, Wiley, New York, 1989.

[7] D.R. Scifres et al., *App. Phys. Lett.*, vol. 33 (12), pp. 1015-1017, 1978.

[8] C. J. Chang-Hasnain et al.,*Appl. Phys. Lett..*, vol. 54, pp. 205-207, 1989; C. J. Chang-Hasnain et al., *IEEE J. Quantum Electron.*, vol. QE-27, pp. 1402-1409, 1991.; N. Yu et al., *Appl. Opt.*, vol. 30, pp. 2503, 1991

Nonlinear Dynamics and Chaos in a Periodically Driven SBS Oscillator: Experiment and Theory

Weiping Lu, Paul M. Ripley and Robert G. Harrison
Department of Physics, Heriot-Watt University, Edinburgh, EH14 4AS, UK
Tel: 0131-4513047 Fax: 0131-4513136; E-mail: phywl@phy.hw.ac.uk

In this paper we report nonlinear dynamics and weak chaos in a periodically driven *spatially extended* nonlinear optical oscillator, namely, stimulated Brillouin scattering in single mode fibre with external feedback and under periodical excitation. Driven nonlinear oscillators have historically played a key role in the study of bifurcation theory and universality laws of nonlinear dynamics and chaos and, through the connection of coupled oscillators to the Ginzburg-Landau equation, they have more recently attracted attention in pattern formation and spatio-temporal chaos. The focus of our attention here is on experimental and theoretical investigations of how complex bifurcations can be induced, through periodic pump excitations of different frequencies and depths of modulation in a *spatially extended* Brillouin oscillator. We have quantified the dynamical features we observe, including a quasiperiodic route to weak chaotic states. The theoretical findings are found to be in good accord with experimental observation, providing physical insight into this dynamical system.

Experiment: The SBS emission was generated in a single mode fibre pumped by the emission from a stablized single mode cw Nd:YAG laser operating at 1.06 μm. The experimental set up, as detailed earlier [1], now includes an acousto-optical modulator (AOM) to modulate the pump source, providing at the entrance of the fibre (120m length) a modulated excitation $P = I_0(1 - \alpha sin^2(\omega t/2))$, where I_0 is the laser output intensity, α and ω are repectively the depth and frequency of the modulation. In the absence of the modulation the SBS emission was set, by pump level, to provide periodic dynamics [1], sustained by the natural reflectivity of the fibre. In the presence of the modulation the SBS emission was found to be periodic, quasiperiodic and weakly chaotic, dependent on the two main control parameters ω and α, when the average incident power in the fibre was held constant. Periodic emission was observed only when the frequency of the AOM was located in the vicinity of the fundamental frequency of the oscillator, $1/2T_r$, or its harmonics, where T_r is the trip time of light traveling in the fibre. Quasiperiodic bands were observed in other frequency regions, total range investigated being $1/4T_r - 1/T_r$, within which the temporal wave forms were quite diverse though all arising from the combination of these two frequencies. Chaotic emission was experimentally found to emerge in two small domains in this range through a quasiperiodic route on increasing the modulation depth to 25$\sim$ 30%, as shown in Fig.1, the maximum depth being limited at 30$\sim$ 35% in the experiment due to excessive heating effect. The weakly chaotic behaviour in Fig.1(c) was manifested by the emergence of a third frequency component in the power spectrum and confirmed by the convergence of the correlation dimensions of this data set

on increasing the embedding dimensions. Its value was measured to be ~ 2.9

Theory: The theoretical model description of this dynamical system involves a three wave interaction of the pump, Stokes and acoustic waves, initially driven by spontaneous Brillouin noise and accounts for nonlinear refractive effects and the boundary conditions of the fibre system (see Eq.(1)-(6) in Ref.[2]). The pump amplitude, now modulated, is written as A(z=0)= $\sqrt{P}$ since the AOM does not induce any effective phase information to the system. The physical parameters used are those corresponding to the polarisation scrambled single mode fibre we use in the experiment and the normalised pump parameter is fixed at $g = 5.9$, well within the periodic operating region obtained in the absence of the pump modulation. The dynamics of Stokes emission were found to be in good qualitative accord with the experimental findings on change of the two parameters, in particular the quasiperiodic route to chaos, on increasing modulation depth for fixed values of the modulation frequency as in experiment. Theoretical results further show an evolution of weak chaos to full chaos with further increase of the modulation depth to 100%. While the calculated correlation dimensions for the parameters in Fig.1(c) show a quicker convergence than that of the experiment they nevertheless give a pleasing agreement on their converged values as shown in Fig.2, indictive of similar behaviour of the both attractors. In general, our findings establish that many aspects of the universal dynamical features of driven nonlinear system described by ODE's are preserved in this spatially extended driven system.

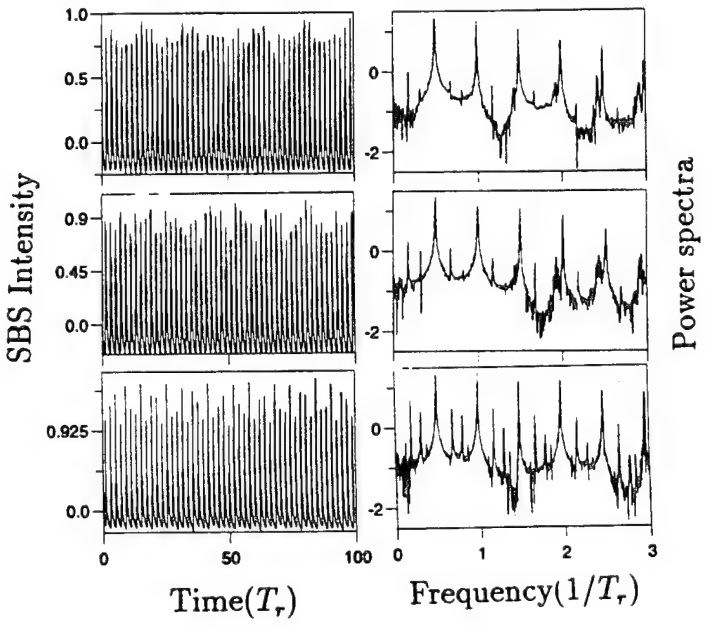

Fig.1. A quasiperiodic route to weak chaos on increasing modulation depth, 5,20,30 % (from top to bottom), for a fixed frequency at $0.7/2T_r$.

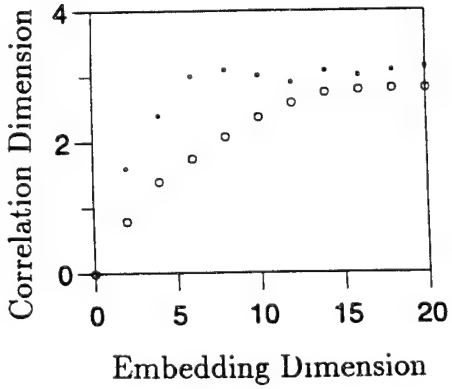

Fig.2. Corr. dim. vs embed. dim: open circles for the data set in the bottom of Fig.1; closed circles for the corresponding theoretical data.

References

1. R. G. Harrison, P. M. Ripley and Weiping Lu, Phys. Rev. **A** 49, 24 (1994).
2. Dejin Yu, Weiping Lu and Robert G. Harrison, Phys. Rev. **A** The 1st issue of 1995.

Coherent Effects on Ultrashort Pulse Interaction in a Doped Fiber

I. V. Mel'nikov and A. V. Luchnikov

General Physics Institute, ul. Vavilova 38, Moscow 117942, Russian Federation

Phone: +7 095 135 0372, Fax: +7 095 135 0270, E-mail: ivm@gpi.ac.ru

In fiber soliton communication systems one of the main constraints on the single-channel bit rate is the interaction between adjacent pulses. It has been shown that spectral limited amplification is effective tool of suppression of this source of timing jitter. However the results on spectral limited amplification have been thus far obtained for the case of pulse duration larger than the time of polarization relaxation. For a pulse which duration is comparable with or less than the relaxation time this approximation loses its justification, the interaction of the optical pulse with amplifying medium becomes coherent, and the response of the active medium depends nonlinearly on the preceding history of the pulse.

Recently it has been shown by us that coherent effects might develop trailing substructure of the amplifying soliton [1]. The every subpulse has phase opposite to that of the subsequent one, and the situation can be thought when the adjacent solitons are placed at opposite extrema of the trailing substructure which thus might act as a phase modulator, breaking interaction between them. In this Report we consider the features of the interaction of the sub-picosecond solitons in Er-doped fiber. The dynamics of the soliton pair is described by nonlinear Schrödinger equation (NSE) modified by the appropriative inclusion of the resonant polarization which, in turn, obeys the set of Bloch equation [1]. We do not take into account stimulated Raman scattering here because our purpos is to study the process of soliton interaction ina two-level medium in the presence of dispersion and Kerr-like self-phase modulation.

The governing set of equations was solved numerically. As an initial value we used isolated pair of NSE solitons having pulse width 0.15 ps, the relaxation time was supposed to be equal to 0.3 ps, and the dopant concentration 1 ppm was used to satisfy the condition of adiabatic following. In Figs. 1,2 the propagation of the pair of the off phase solitons in pumped erbium fiber is depicted. We note the following features.

In Fig. 1 the dynamics of the interaction between two off-phase solitons of 0.15 ps pulse width and 0.9 ps pulse separation is shown. Since solitons are off-phase and close enough the soliton interaction can be suppressed. However the development of trailing substructure leads to their repulsion. Eventully, soliton prolifiration occurs.

The phenomenon of soliton annihilation in interacting of two identical solitons with different phases is shown in Fig. 2. In this case the scale of developing of the trail of the leading soliton equals to the interpulse separation. The attraction between the training substructure and second soliton does pull them closer and makes them overlap significally. This produces a chance for the leading soliton to pump the triling one that can lead a single amplified and compressed soliton emerges from the bandwidth limited fiber amplifier.

Reference

1. I.V.Mel'nikov, R.F.Nabiev, and A.V.Nazarkin, Optics Lett. 15, 1348 (1990).

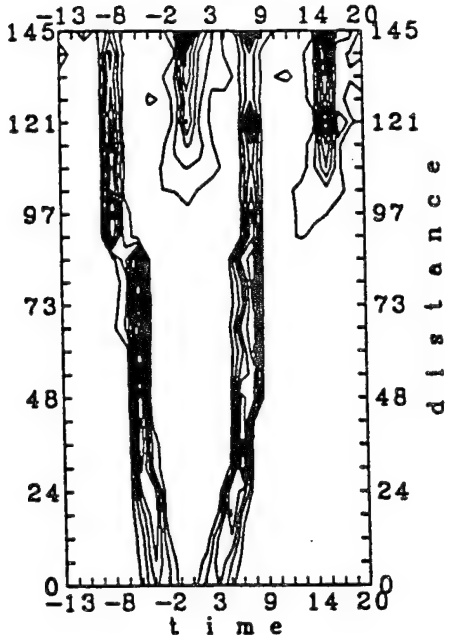

Fig. 1 Interaction between two identical out off phase solitons; interpulse separation 0.9 ps.

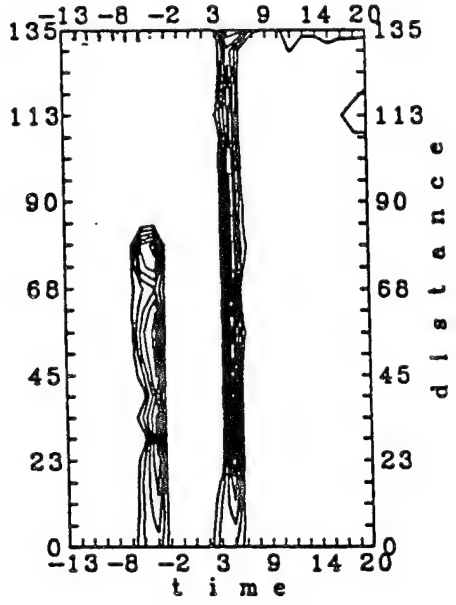

Fig. 2 Same as Fig.1, except with interpulse separation of 1.2 ps

Spectral Features of a Short Pulse Self-Action in a Resonant Medium

Leonid A.Melnikov, Andrey I.Konukhov, Irina V.Veshneva

Department of Optics, Chernyshevsky State University, 83 Astrakhanskaya str., Saratov 410071, Russia
phone: (845-2)51-51-95, e-mail: melnikov@scnit.saratov.su, melnikov@ire.saratov.su

It was found experimentally in a study of self-induced transparency that a short high-intensity laser pulse have anomalously long distance of propagation in a resonant medium [1]. Besides that the central frequency of a pulse was shifted to the red side of the transition line. As was mentioned in [1] appearance of the shift leads to a weakening of pulse absorption.

In these experiments above mentioned phenomena were observed only when the light beam was focused on the rear plane of a gas cell using a lens. Moreover, the self-focusing occurred, so the transverse pattern effects must be included into consideration. Approximate analysis of the experiments based on the concept of space-temporal soliton was presented in [2], [3]. In this paper we discuss the results of numerical simulation of a coherent pulse propagation in the optically dense longitudinally extended resonant absorbing two-level medium.

Our model includes the Maxwell-Bloch equations:

$$\partial P(z,\vec{r},t)/\partial t = -(\Gamma + i\Delta)P + (iE/2)(N_b - N_a)\Gamma,$$

$$\partial N_a(z,\vec{r},t)/\partial t = -\gamma_a N_a - (i/2)(E^*P - P^*E)2\gamma_a\gamma_b/(\gamma_a + \gamma_b),$$

$$\partial N_b(z,\vec{r},t)/\partial t = -\gamma_b(N_b - 1) + (i/2)(E^*P - P^*E)2\gamma_a\gamma_b/(\gamma_a + \gamma_b),$$

$$2i\partial E(z,\vec{r},t)/\partial z + \nabla_\perp^2 E(z,\vec{r},t) = -igP(z.\vec{r},t),$$

where $P(z,\vec{r},t), E(z,\vec{r},t)$ are the slow varying amplitudes of the electric field and medium polarization, $t \rightarrow t - z/c$ is the local time of the pulse, N_a, N_b are the populations of upper (a) and lower (b) levels, respectively, normalized on the unsaturated value of N_b, Δ is the pulse carrier frequency detuning, $\Gamma, \gamma_a, \gamma_b$ are the relaxation rates of the polarization and populations, respectively.

For the numerical simulation we use the field representation on the grid in transverse plane defined by coordinates lines $\varphi = const$ and $r = const$ in cylindrical coordinate system. Then for every knot of this grid the equations for $P(t), N_a(t)$ and $N_b(t)$ were solved numerically, supposing that $E(z,\vec{r},t)$ is a given function of t. So we obtain the temporal evolution of medium polarization. In the solution of the paraxial wave equation we use the step-splitting method. At the diffraction step it is convenient to exploit the simple algebraic relations describing the transformation of empty-space modal amplitudes. At the nonlinear step it is easy to solve density matrix equations at grid knots.

The initial pulse at the input plane had gaussian profile both in time and in space. The initial condition for the medium were $P(z,\vec{r},0) = 0$, $N_a(z,\vec{r},0) = 0$, $N_b(z,\vec{r},0) = 1$. The used algorithm allows to obtain temporal evolution of the field in any point of transverse plane, temporal dependence of modal amplitudes, and correspondent snapshot of a transverse pattern at any given moment. The carrier frequency shift was determined as an average value of chirp ($\delta\nu = -d\phi/dt$, where ϕ is the phase of the field) along the pulse at longitudinal axis or space-time average value of chirp.

The results of the simulations are summarized as follows:

- The pulse spectrum variations occurs due to self-phase modulation of special kind: the beam diameter variation occurring due to self-action of light beam leads to phase modulation;

- The magnitude and sign of spectral shift depends essentially from input pulse power, pulse duration, and optical thickness of absorber;
- The carrier frequency can be shifted both to the red and to the blue in the case of very short pulse with pulse width less than Γ^{-1};
- More long pulses with the pulse width greater than Γ^{-1} have the red shift up to 1/4 of the transition linewidth.

For the qualitative explanation we have used the results of the simulations of the evolution of the phase on the axis in the case of stationary self-action [4], shown in Fig. at different values of input intensity. Here z is the longitudinal coordinate, normalized to diffraction length, initial beamwaist was π. In Fig. the phase evolution along longitudinal axis was shown vs different initial axial intensity of the beam. It is easy to see, that for the varying initial intensity chirp will occur, corresponded to the blue shift at the leading edge and to the red at the trailing edge. In absorbing media the leading edge is absorbed considerably while trailing edge propagate in saturated medium. Thus the average shift will be red.

This work was supported by the Commission of the European Communities under ESPRIT Contract P9282-ACTCS, EU-Russia Collaboration, and ISF grant NS4000.

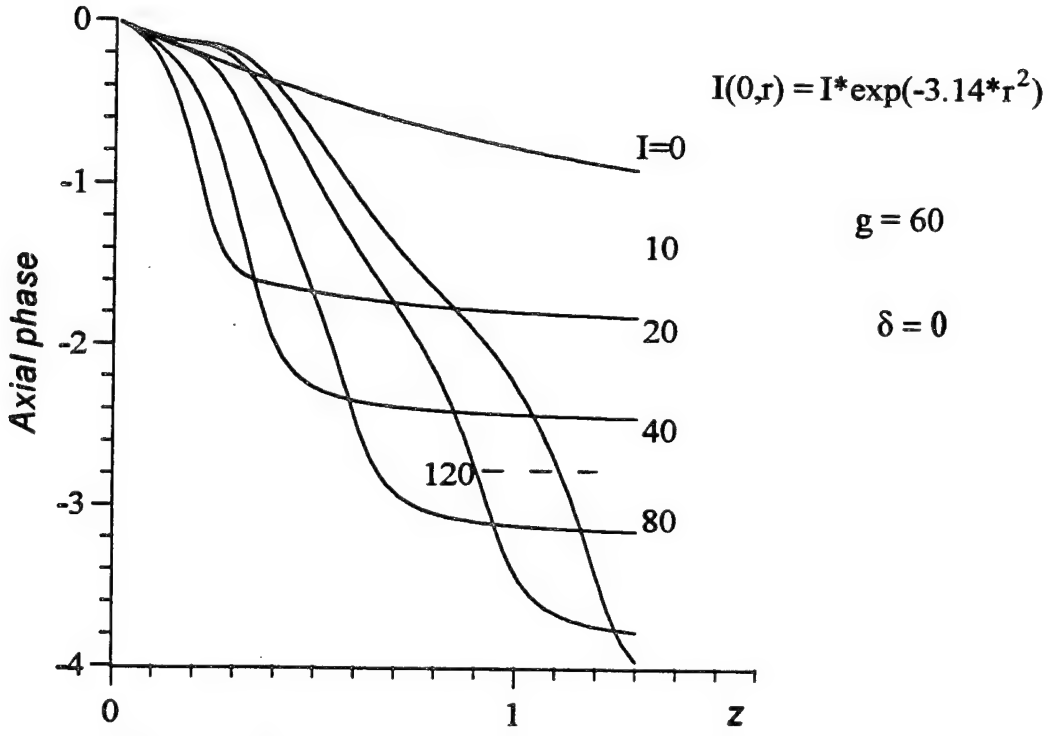

[1] Egorov V.S., Reutova N.M. *Optika i spektr.***67**, 1231(1989)
[2] Egorov V.S., Kozlov V.V., Reutova N.M., Fradkin E.E. *Optika i spektr.* **72**, 636(1992)
[3] Kozlov V.V., Fradkin E.E. *J. Exp. Theor. Phys.* **103**, 1902(1993)
[4] Derbov V.L., Melnikov L.A., Novikov A.D., Potapov S.K. *J.Opt.Soc.Amer.* **7**,1079(1990)

CHAOS AND CONTROL IN SEMICONDUCTOR LASERS

Govind P. Agrawal
University of Rochester, Rochester, NY 14627

Charles M. Bowden and Shawn D. Pethel
Weapons Sciences Directorate, AMSMI-RD-WS-ST
U. S. Army Missile Command, Redstone Arsenal, AL 35898-5248
Phone: 205-876-2650 FAX: 205-955-7216

A generalized Maxwell-Bloch formulation for laser-field-coupled semiconductors was derived from a two-band model which includes the direct Coulomb interactions as well as the effects of the density of states distribution. The resulting system is composed of a self-consistent set of coupled equations in four dynamical variables for the semiconductor medium, together with the electric field amplitude coupled through the Maxwell wave equation in semiclassical approximation and are obtained to lowest order in the Coulomb exchange interaction and the density of states distribution [1]. The temporal evolution of these equations in the spacial mean field limit forms the basis for the dynamical system in our analysis.

It is shown that dynamical instabilities and chaos are intrinsic with respect to the parameter space of this model, Fig. 1. A novel and sensitive method [2] is used to characterize the chaotic system and it is shown also that the new method is particularly applicable to distinguish deterministic from stochastic components when stochastic fluctuations are introduced. It is shown that in general, the coherent Coulomb exchange interaction lowers the chaotic threshold [3].

Several distinct control schemes are applied to achieve selective decomposition of the chaotic attractor into unstable periodic orbits, and the effects of the control schemes are analyzed. The method of Occasional Proportional Feedback (OPF) [4] is applied using the gain (injection current) as control parameter. Also, the method of Continuous Delayed Proportional Feedback (CDPFB) was applied with measured success [5]. The effects and stability of the two procedures are compared. The latter procedure appears more practical for semiconductors since it can be implemented optically. Shown in Fig. 2 is the result of applying OPF to the system under the identical conditions corresponding to the chaotic dynamics represented in Fig. 1.

Currently, we are formulating a novel control scheme using fast training neural network algorithms [2] to achieve global, nonlinear adaptive control using several control parameters simultaneously. This method is distinct from existing local linear methods [4,5] and is anticipated to be robust for higher dimensional systems.

REFERENCES

1. C. M. Bowden and G. P. Agrawal, "Generalized Bloch-Maxwell Formulation for Semiconductor Lasers," Phys. Rev. A, in press.

2. S. D. Pethel and C. M. Bowden, "Characterization of Chaotic Signals Using Fast Learning Neural Networks," invited contribution in *Handbook of Neural Computation* (Institute of Physics, Oxford University Press, NY, 1995), in press.

3. C. M. Bowden, S. Singh, and G. P. Agrawal, "Laser Instabilities and Chaos in Inhomogeneously Broadened Dense Media," J. Mod. Opt., to be published.

4. E. Ott, C. Grebogi, and J. A. Yorke, Phys. Rev. Lett. **64**, 1196 (1990).

5. J. E. S. Socolar and D. J. Gauthier, private communication.

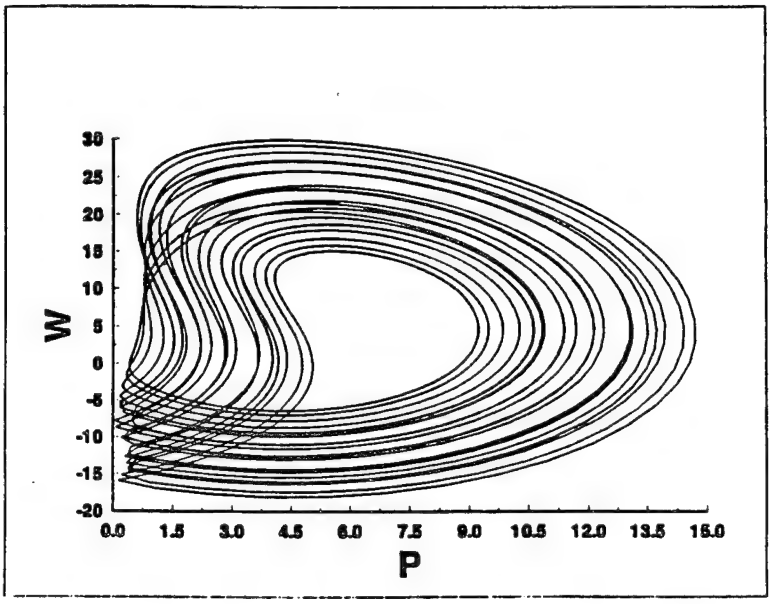

Figure 1. Polarization |P| versus carrier density W, no control

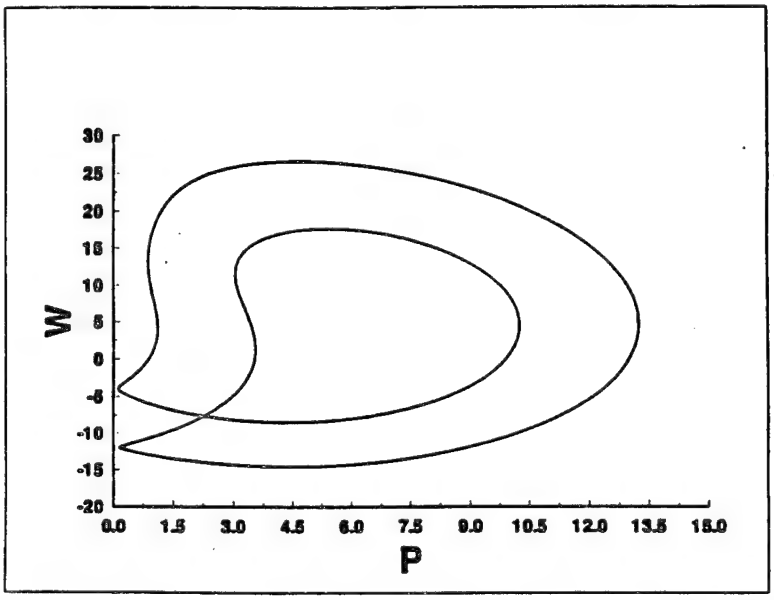

Figure 2. Polarization |P| versus carrier density W, with COPFB control

Three-order nonlinearities as mechanism of the mode-locking

V.P.Mikhailov, V. L. Kalashnikov, V.P.Kalosha and I.G.Poloyko

International Laser Center of Belarus State University, 7 Kurchatov Str., Minsk, 220064, Belarus, Tel/fax.: (7-0172)78-57-26, E-mail:user3@mikhai.bsu.minsk.by

The soliton-like states in the lasers are formed by a nonlinear interaction between the transverse resonators modes. This process requires a dynamical balance between the gain saturation and nonlinear losses which depend on the intracavity field intensity. Traditionally, this dependence is provided by modulators based on the saturable absorbers [1]. The possibilities of these modulators, however, are limited by inertial nature of the resonant nonlinearity.

Recently considerable progress has been made in the development of the mode-locked lasers. Apart from methods of the soliton formation involving the use of the saturable absorbers, new methods use the instantaneous nonresonant nonlinearities. It is very attractive method for the generation of the high intensity pulses shorter than 100 fs [2].

In this connection the purpose of the present paper is to perform a complex method of the generation dynamics analysis for the mode-locked solid-state lasers with the three-order nonlinearities producing self-phase modulation (SPM) and Kerr self-focusing (KSF).

We have developed the general approach to the mode-locking analysis. This approach combines the investigation of the critical points of the laser evolution operator (its first and second derivatives) and its structural stability, the self-consistent field theory and the numerical simulation of the generation dynamics.

The possibilities of this approach have been demonstrated for the research of the lasers mode-locked by nonlinear Fabri-Perót interferometer (an additive-pulse mode-locking), by antiresonant loop with SPM and by KSF. The key point in the utilization of the three-order nonlinearities in these systems is a transformation of the nonlinear phase perturbations to intensity-dependent losses. This transformation is performed by interference of the splitting laser beams in the Fabri-Perót interferometer and antiresonant loop or by aperturing of the self-focused beams.

We are shown that the zones of the effective mode-locking have a point structure and the mode-locking regime develops from this "seeding" points. The perturbations of the laser parameters destroys the mode-locking zone, but the point structure is the stable (see fig.). We have found that the "seeding" point set corresponds to the parameters of the stable soliton propagation and the nonefficient mode-locking regime corresponds to the periodical cycles appearance.

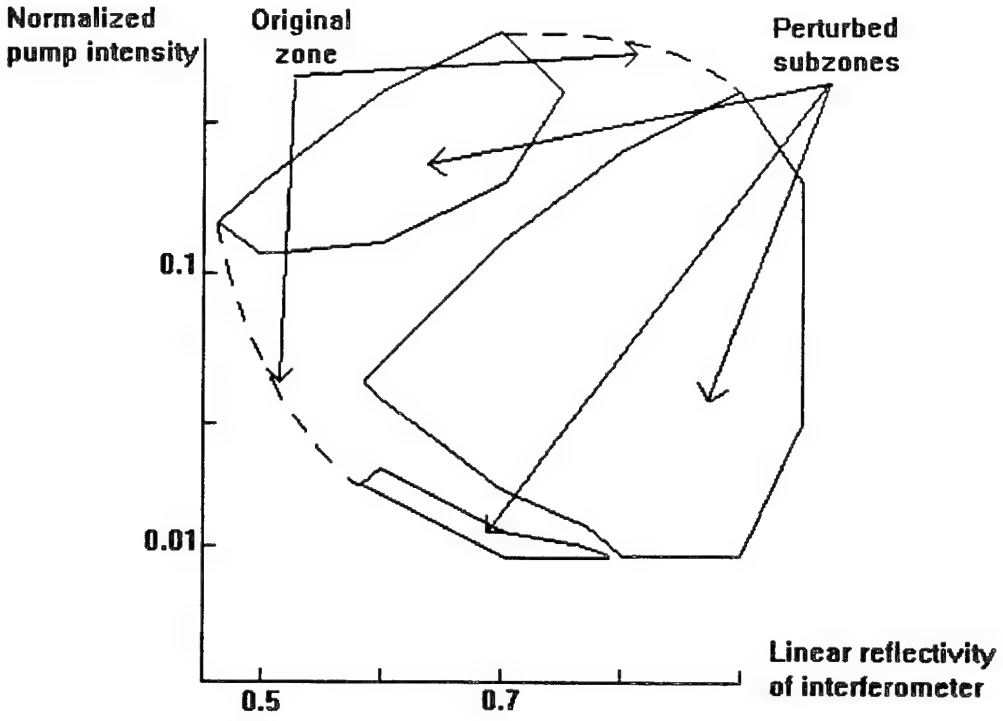

The investigation of the Kerr-lens mode-locking technique allows to find the criteria for the creation of the mode-locking regimes with the highest efficiency. The analysis of the generation dynamics establishes the wide set of the oscillation and chaotic effects in this systems.

We believe that the complex analysis of the laser systems mode-locked by three-order optical nonlinearities allows to open the simplest way for the design of the compact and stable femtosecond lasers.

REFERENCES:

1. J.Herrmann, B.Wilhelmi. *Laser fur Ultrakurze Lichtimpulse*, Berlin (1984).

2. H.A.Haus, J.G.Fujimoto, and E.P.Ippen. *IEEE J. Quant. Electron.* 28 (1992) 2086.

Transmission of Laser Diode Pulses in Standard Optical Fibers: Different Compensation Techniques

Claudio R. Mirasso, P. García-Fernández and C. Lozano
Instituto de Estructura de la Materia, CSIC
Serrano 123, E-28006 Madrid, Spain.

Phone 34-1-585-5383, Fax: 34-1-585 5184, e-mail: emclaudio@iem.csic.es

The effect of Group Velocity Dispersion (GVD) and Self Phase Modulation (SPM) has been considered by several authors to study the propagation of optical pulses in optical fibers. Most of them used Gaussian [1] or Supergaussian models to describe the optical pulses [1]-[3]. To our knowledge, one of the few works that uses the rate equations of the laser diode to generate the optical pulses is the one of Suzuki and Takeshi [4]. They studied the effect of GVD and SPM in dispersion shifted fibers.

In our work, the eye opening degradation due to GVD and SPM is analyzed by studying the propagation of optical pulses generated by a single mode semiconductor laser (SMSL) in standard single mode fibers, similar to the ones already installed. We study different techniques that allow partial recover of the eye degradation or allow for longer distance transmissions: pre-compensation and post-compensation using dispersion shifted fibers and in-system phase conjugation.

We start our study by solving numerically the noise driven rate equations for the SMSL [5]. The wavelength of the laser is 1.55 μm and most of the other parameters characterizing the laser are fixed but we allow for different values of the linewidth enhancement factor α which plays an important role during the propagation of pulses in highly dispersive fibers. The SMSL is directly modulated by a square wave electrical current as in ref. [5], with a maximum current of 33.7 mA and a bias current of 13.12 mA (the threshold current is 13.25 mA). We consider two modulation frequencies: 5 Ghz in the RZ scheme and 10 Ghz in the NRZ scheme. The optical pulses so obtained are then coupled to the optical fiber. To study the propagation we numerically solve the non-linear Schrödinger equation by the Split Step Fourier Method [1]. The dispersion parameter of the fiber is $\beta_2 = -17$ ps^2/km and the non-linear parameter $\gamma = 0.002$ mW^{-1} km^{-1}.

In figure 1 a) and b) we show, as an example, the result of the propagation of the 2^7 pulses from a pseudorandom sequence with and without pre-compensation for a value of $\alpha = 4$, in the RZ scheme. In panel a) we show the eye diagram at z=15 km without pre-compensation and in b) the eye diagram at z=25 km with pre-compensation in a 3 km fiber of $\beta_2 = 45$ ps^2/km. 3 km is the distance at which maximum compression is obtained in the pre-compensation for the parameters used in the simulations. By comparing both eye diagrams it can be seen that they have almost the same degradation, i.e. with pre-compensation one can achieve 10 km more. In both cases the degradation of the eye diagram is noticeable. This degradation is due to several mechanisms: timing jitter in the SMSL, pattern effects due to the input sequence of random bits [4], fluctuations in the frequency chirp, fiber dispersion and also, due to the large modulation frequency of the laser current, to a pulse-pulse interaction during the propagation. This effect gives rise to the large oscillations in the tails of the pulses and in some cases, where two or more "1" bits appear

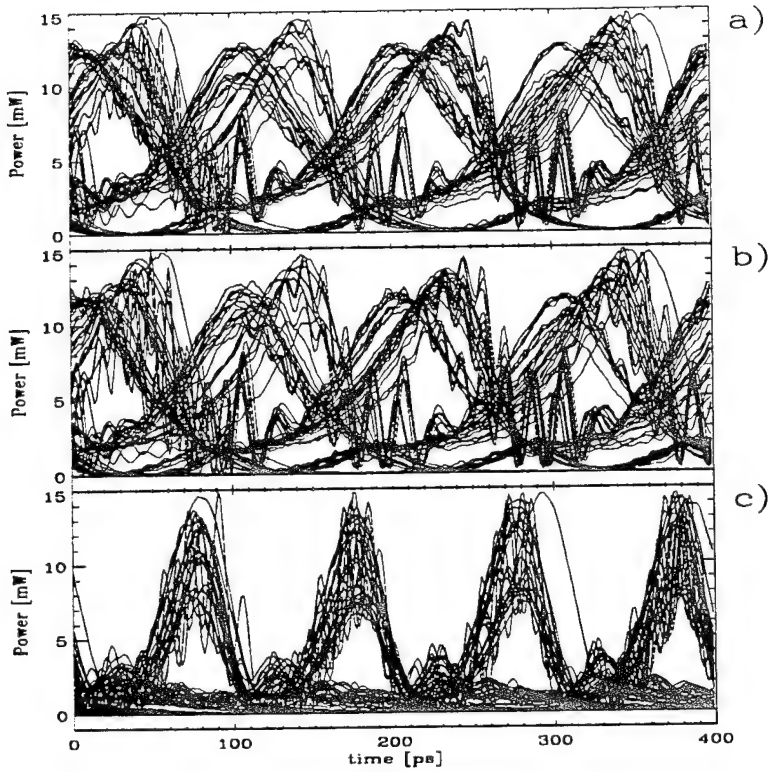

Fig. 1 Eye diagram at the output of the fiber: a) 15 Km. b) 25 Km using pre-compensation. c) 35 Km using optical phase conjugation

In panel c) we plot the eye diagram at 35 km distance when an optical phase conjugation is performed at the output of the laser (which in this case also coincides with the origin of the fiber). Due to the sign of the frequency chirp of the SMSL and the parameter β_2 of the standard fiber, GVD has the effect of broadening the optical pulses. Phase conjugation basically inverts the chirp sign at the output of the laser leading to a narrowing of the pulses during the first kilometers of the propagation and so allowing a larger distance for the transmission. As can be see in the figure the result in this case is better than when using pre-compensation.

The effect of post-compensation, different α values of the laser and the NRZ scheme will be also discussed during the talk.

References

[1] G. P. Agrawal, *Nonlinear Fiber Optics*. San Diego: Academic Press, 1989.

[2] A. Naka and S. Saito, Electron. Lett., **28**, pp. 2221-2223, 1992.

[3] M. Schiess, Proc. ECOC, Montreux 1993, We 18, vol. 2, pp. 482-484.

[4] N. Suzuki and T. Oseki, J. Lightwave Tech. **11**, pp. 1486-1494, 1993.

[5] C. R. Mirasso, P. Colet and M. San Miguel, IEEE J. Quantum Electron., **29**, pp. 23-32, 1993.

Reflection of a Gaussian Beam from a Saturable Absorber: Experimental Results

D. V. Petrov, A. S. L. Gomes, and Cid B. de Araújo
Departamento de Física, Universidade Federal de Pernambuco,
50670-910, Recife , PE, Brazil
phone: (055)-(081)-271-01-11,
fax: (055)-(081)-271-03-59
e:mail: 10CBA@NPD1.UFPE.BR

A laser beam incident on the surface of a nonlinear medium can display characteristic features such as self-focusing and self-induced transparency. If nonlinear effects are strong enough the intensity profile of the reflected wave may exhibit drastic spatial modifications due to the refractive index modulation in the longitudinal direction in the bulk [1-3]. In this paper we present experimental results on the modification of a Gaussian beam profile caused by the electronic contribution for optical properties of a surface.

Recently we introduced the reflection Z-scan technique (RZ-scan) to investigate the spatial modification of a Gaussian beam by reflection on a surface [4]. As in the conventional Z-scan [5] the beam profile modification is monitored through an aperture placed in the far-field region. Hence, the phase distortion produced in the reflected beam is transformed to amplitude distortion which is easily detected by a simple photodiode.

The experiments were performed with samples of semiconductor doped glass (Scott glass RG695). Two slabs of different thickness (sample A with $0.013cm$ and sample B with $0.2cm$) were used. For the wavelength used in the experiments ($\lambda_o = 532nm$) the linear absorption coefficient was $200cm^{-1}$. The second harmonic of a $Q-$switch and mode-locked $Nd:YAG$ laser was used as a light source. Each Q-switch burst consists of about 20 pulses of $80ps$ duration separated by $10ns$. The low repetition rate of the Q-switch ($5Hz$) was chosen in order to avoid cumulative thermal index of refraction and absorption changes. The beam was focused on the sample's surface by a $15cm$ focal distance lens and the intensity was changed by a combination of half-wave plate and polarizer.

A plot of the far-field reflectance as a function of the sample's position relative to the beam's focus is shown in Fig.1. From this plot it is possible to calculate the nonlinear absorption parameter κ_2. (We define the complex refractive index $\widehat{n} = n_0 + n_2 I + i(\kappa_0 + \kappa_2 I)$, where n_0 and κ_0 are the linear refractive index and extinction coefficient, n_2 and κ_2 are the nonlinear refractive index and extinction coefficient, I is the intensity of laser beam). On the other hand the reflectance measured without aperture do not show any changes as a function of the sample's position.

These results were explained using a model for the reflection of a Gaussian beam from a surface which suffers nonlinear refraction and absorption.

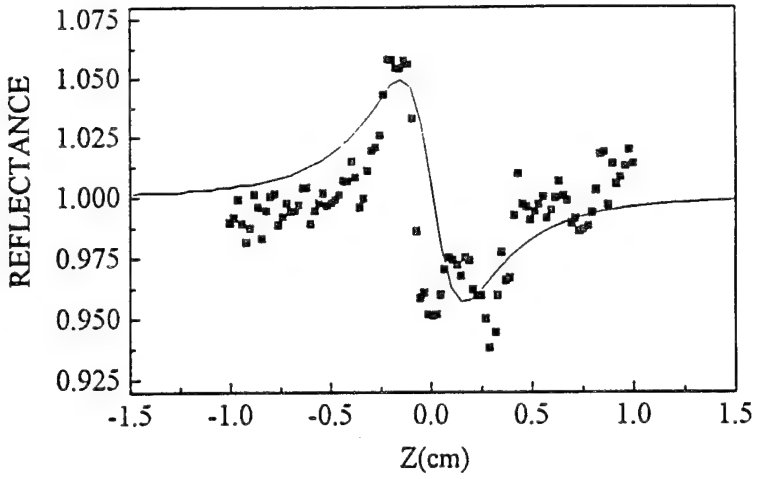

The value of $\kappa_2 = -3 \times 10^{-8} cm^2/W$ deduced from this experiment is about 75 times larger than the value obtained for the sample using the conventional Z-scan technique. It can be explained by the fact, that the Z-scan measurements give information on the nonlinear bulk properties, averaged on the effective propagation length. By reflection the spatial modification of a reflected beam is due the nonlinear properties of a thin layer near the surface and several nonlinear mechanisms inherent to the interface may contribute.

This work was supported by the Brazilian Agencies Conselho Nacional de Desenvolvimento Científico e Tecnológico (CNPq) and Financiadora de Estudos e Projetos (FINEP).

References

1. L. Roso-Franco, Phys. Rev. Lett., **55**, 2149 (1985).

2. S. R. Hartmann and J. T. Manassah, Opt. Lett., **16**, 1349 (1991).

3. S. D. Kunitsin, A. P. Sukhorukov, and V. A. Trofimov, Bull. Rus. Acad. Sci., **56**, 2007 (1992).

4. D. V. Petrov, A. S. L. Gomes, and Cid B. de Araújo, Appl. Phys. Lett., **65**, 1067 (1994).

5. M. Sheik_Bahae, A. A. Said, T.- H. Wei, D. J. Hagan, and E. W. Van Stryland, IEEE J. Quantum Electron., **QE-26**, 760 (1991).

Multistability in a thin layer laser with inclined external cavity

I.E. Protensko, A.N. Oraevsky
P.N. Lebedev Physics Institute, Russian Academy of Sciences, 53 Lenin Prospect, 117924
Moscow, Russia, Tel. 132-1529, F. 336-0901, E. oraevsky@sci.fian.msk.su

J.D. Graham, R.T. Edmonson, D.K. Bandy
Physics Department and Center for Laser Research
Oklahoma State University, Stillwater, Oklahoma 74078,
Tel.405-744-7488, F. 744-6406, E. physdkb@osu.ucc.okstate.edu

Two lasing regimes are possible when a thin layer semiconductor laser operates with an inclined external cavity. In the regime of total internal reflection we find multistability and more than one operational threshold.

Summary

Progress in modern optics, particularly in networking and information processing, demands the development of new solid-state lasers of small dimensions - on the order of an optical wavelength or less. An extensive search continues for passive optical bistable devices that can provide high contrast multistability and short switching times [1]. A few miniature lasers have been studied experimentally, for example, Ref. [2]. These finding encourage theoretical investigation of thin layer semiconductor lasers (TLL) which can lase in the direction perpendicular to the active layer.

In our paper we investigate thin layer semiconductor lasers considering the specific case when the active layer is positioned inside an external cavity and inclined with respect to its axes. (See Figs. 1.) In general, the external cavity leads to the stabilization of semiconductor laser generation [3] which is obviously important for practical applications. Similarly, one expects to stabilize the TLL, but in this case the external cavity brings even more.

We discuss two different regimes of generation: the normal reflection (NR) regime and a regime of total internal reflection (TIR). The NR regime (Fig. 1a) occurs when the output radiation leaves the external cavity due to reflection from the layer. One attractive feature of NR regime is that the layer can be inclined with respect to the axes of external cavity under an almost arbitrary

angle θ. It provides flexibility in the choice of output radiation direction. In particular it lets us organize TLL's in a compact vertical array or other spatial configurations.

The TIR regime (Fig. 1b) can take place, when the index of refraction of the cavity medium is greater than the index of refraction of the semiconductor layer. Unlike the NR case the laser generation is possible only when $\theta = \theta_{TIR}$, the total internal reflection angle. However, much more volume of active medium is involved, which leads to a noticeable increase in the amplification coefficient. TIR regime is accompanied by multistability caused by the local field correction and some interesting dynamical features.

Despite the different experimental setups necessary for NR and TIR, they can be described (to a first approximation) by the same set of nonlinear differential equations. Mathematical description of the problem is based on the assumption that the cavity mode field is much stronger than any other field interacting with the layer.

Acknowledgment: This work was done with the financial support of NSF Grant ECS-9215852, Soros ISF, Russian Foundation for Fundamental Research 93-02-3563 and NATO Grant #921019.

References:

1. H. M. Gibbs, Optical Bistability: Controlling Light with Light (Acad.Press, New York, 1985).

2. K.Iga et al. *Electron.Letts.* **23**, 134 (1987). C.Lee, T.G.Rogers, D.G.Deppe, B.G.Streetman. *Appl. Phys.Letts.* **58**, 1122 (1991).

3. V.L. Velichansky, A.S. Zibov, V.S. Kargopol'tsev, V.I. Molochev, V.V. Nikitin, V.A. Sautenkov, G.G.Kharisov, and B.A.Tyurikov, *Sov.Tech.Phys.Lett.* **4**, 438(1978).

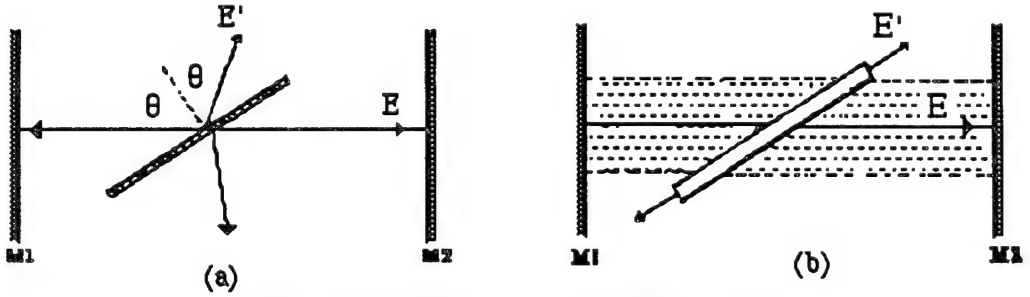

Figure 1 (a) NR regime, (b) TIR regime

NONLINEAR DYNAMICS OF A CO_2 LASER WITH EXTERNALLY MODULATED AND RE-INJECTED OPTICAL SIGNAL

E.M.Rabinovich[1], J.M. Kowalski[2] , M.A.Safonova[3], and C.L..Littler[2]

1) Advanced Isotope Technologies, Incorporated, P.O. Box 5073, Denton, Texas 76203-5073, e-mail : 76341.1040@compuserve.com
2) Department of Physics, University of North Texas, Denton, Texas, 76203, telephone : (817) 565-4291, fax : (817) 565-4160 ; e-mail : fd23@vaxb. acs.unt.edu ,
3) Courant Institute of Mathematical Science, New York University ,251 Mercer Street, New York, NY 10012, e-mail : safonova@acf4.nyu.edu

CO_2 lasers are very sensitive to back-reflected radiation and can be driven into a large variety of dynamical states by an external modulation of the feedback parameters. We report on the experimental and theoretical results concerning instabilities in CO_2 lasers induced by an optical phase modulation of the reflected back signal. The mentioned above phase modulation was carried out by periodically varying either a geometrical length of a feedback (by means of a piezo-ceramic driver) or an optical length of feedback (by means of an electro-optical modulator EOM). Experimental results show the presence of stable periodic orbits of different periods, bistability of periodic orbits and chaotic attractors with complex transition scenarios.

This new experimental method generating chaos in carbon-dioxide lasers, where an external modulation of optical feedback parameters is applied, is much simpler then more sophisticated intercavity losses modulation technique which has been widely used in previous investigations (see, for example , [1].)

The experimental setup is shown in Fig.1. In this scheme an axial-flow gas CO_2 laser operating at a wave length of λ = 10.6 μm was used. This laser has the resonant cavity 2.5m long, the diameter of the discharge tube is 6 mm, and the pressure of the conventional gas mixture varies from 15 to 20 mmHg. An additional mirror, placed on the piezoceramic driver, provides the radiation feedback into the active region. This mirror is mounted on a piezoelectric ceramic drive allowing static tuning and/or periodic modulation of the optical feedback length .

The length of the optical feedback does not exceed 30 cm. The laser intensity is measured by a HgCdTe photodetector monitoring part of the radiation reflected from a diffraction grating. The intensity signal from the detector and its time-delayed copy are fed into an oscilloscope , operating in the x-y mode. The electrical signal delay line has a constant delay of 2.5 μs. This simple scheme allows real time observations of the two-dimensional projections of the system trajectories in the space of delayed signals. A spectrum analyzer of bandwidth 20 Hz - 40 MHz simultaneously displays the power spectra. The electronics allows one to "freeze" at any instant the phase portrait and power spectra, and digitize the signal using a digitizer with variable sampling frequencies and store the data.

The optical feedback system was modulated by using an electro-optical modulator (EOM) with a quarter wave voltage of 2.2 KV. The EOM was a Cd-Te crystal having an active length of 48 mm, and an aperture diameter of 3 mm. The voltage applied to the EOM had a DC component

of 1.5 KV and the amplitude and frequency of the modulated signal varied within 100-900V and 50-85 KHz, respectively. In the second series of experiments phase of the feedback radiation was modulated by the induced oscillations of the feedback providing mirror mounted on a

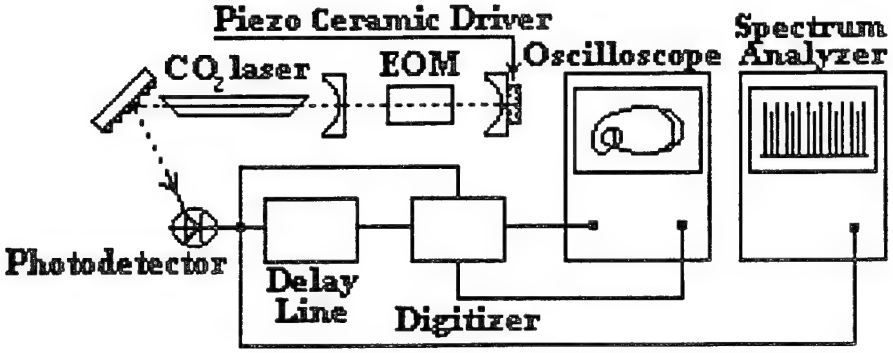

Fig.1 Experimental Setup for Nonlinear Dynamical Phenomena Investigation in CO_2 Laser

piezoelectric drive. The driving frequencies varied from 30 KHz to 60 KHz

The theoretical analysis of the single-mode laser with an optical feedback is based upon consideration of two equations which are extensions of Lang-Koboyashi equations [2] for harmonically modulated time of delay.

Literature

[1] F.T.Arecchi, R.Meucci, G. Puccioni, and J.Tredicce, Experimental Evidence of Subharmonic Bifurcations, Multistability, and Turbulence in a Q-Switched Gas Laser, Physics Review Letters, **49**, pp.1217-23, (1982)

[2] R.Lang and K.Koboyashi, External Optical Feedback Effects on Semiconductor Injection Laser Properties, IEEE J. Quantum Electron., **QE-16**,pp.347-355,(1980).

POPULATION INVERSION WITHOUT AMPLIFICATION VIA FIELD-DEPENDENT RELAXATION

Yevgeny V. Radeonychev
Institute of Applied Physics, Russian Academy of Science, 46 Ulyanov St., 603600 Nizhny Novgorod, Russia
fax: 7-8312-363792, e-mail: radion@appl.nnov.su

Recent researches into atomic coherence effects essentially modified many traditional concepts in quantum optics. In particular, lasing without inversion and inversion without lasing (which are based on the phenomenon of the atomic interference) were predicted and attracted much attention [1].

We show that strong monochromatic field can produce steady-state population inversion at the resonant transition. Hence one more commonly believed conclusion about impossibility of such process does not hold in general. This effect is due to modification of the atomic relaxation rates caused by strong field and appears when intensity of the field becomes high enough. However such population inversion does not lead to amplification of this field. On the contrary it provides even more effective transfer of energy from the electromagnetic field to the medium.

Our analysis is based on the set of generalized master equations [2] which takes into account dependence of the relaxation rates on the frequencies of the dressed transitions. Such dependence introduces specific asymmetry between the relaxation rates at the dressed transitions. This asymmetry

results in turn in a redistribution of both dressed and bare states populations. In case of sufficiently strong field it makes possible a population inversion in the finite domain of the detunings.

In two-level system such frequency detunings can essentially exceed the natural linewidth but the magnitude of population inversion remains relatively small.

In three-level system almost full inversion (i.e. transfer most of atoms to the upper level) is achievable. The last phenomenon occurs when one of two Stark sublevels crosses the third neighboring atomic state what is accompanied by the reversal of the relaxation direction between the crossing levels.

Finally field-dependent relaxation makes possible a steady-state population inversion at the resonant transition under the action of the strong field and provides one more mechanism for population inversion without amplification.

Placing two-level atoms inside optical cavity and three-level atoms into high Q micro-wave cavity and tuning of these cavities accordingly to the Rabi-sidebands and to the Rabi frequency allows to vary both the domain of the detunings providing population inversion and the magnitude of this inversion.

This research was supported by Russian Foundation for Fundamental Researches (93-02-3647).

1. O.Kocharovskaya, Phys. Rep. 219 (1992) 175.

2. O.Kocharovskaya, M.O.Scully, S.-Y.Zhu, P.Mandel and Y.V.Radeonychev, Phys. Rev. A 49 (1994) 4928.

Spatio-Temporal Coupling Implications for Z-Scan Measurements

Andrew T. Ryan and Govind P. Agrawal
The Institute of Optics, University of Rochester, Rochester, NY 14627
Tel: (716)275-4846; E-mail: ryan@optics.rochester.edu

Frequently, ultrashort pulses are employed as the most practical method for achieving the high powers required for the observation of spatial effects due to fast optical nonlinearities. In particular, the Z-scan method[1] of measuring the nonlinear index, n_2, of a material relies on the nonlinearity of the test material to alter the spatial phase distribution of the field and thus its intensity distribution in the far field. A drawback of this method is that the temporal behavior of the field is also affected by the nonlinearity. For example, the same material that supports spatial solitons can, under the proper conditions, support temporal solitons. Moreover, the nonlinearity couples the two behaviors together so that the magnitude of the spatial effect may become dependent on the width of the pulse. This spatio-temporal coupling can be shown to lead to pulse compression in the normal dispersion regime[2] and spatial narrowing in a self-defocusing medium. The work presented here is a result of numerical simulations which demonstrate how spatio-temporal coupling can lead to erroneous n_2 measurements in Z-scan experiments employing ultrashort pulses.

We use an algorithm based on the split-step Fourier method to model the evolution of spatially one-dimensional (corresponding to an elliptical beam) pulses in a Z-scan apparatus. The behavior of ultrashort pulses propagating in nonlinear dispersive Kerr media is described by the multidimensional nonlinear Schrödinger equation (NSE),

$$i\frac{\partial u}{\partial \zeta} + \frac{1}{2}\frac{\partial^2 u}{\partial \xi^2} - \frac{s}{2}\frac{\partial^2 u}{\partial \tau^2} + \mathrm{sgn}(n_2)N^2|u|^2u = 0. \qquad (1)$$

Here $u(\zeta,\xi,\tau)$ is the amplitude of the pulse envelope, $\zeta = z/L_d$, $\xi = x/\sigma$, $\tau = (t - z/v_g)/T_0$, σ is the input spot size in the x-direction, T_0 is the input pulse width, and $L_d = (2\pi/\lambda)\sigma^2$ is the diffraction length (also known as the Rayleigh range). The parameter $s = (2\pi/\lambda)\sigma^2\beta_2/T_0^2$ includes dispersive effects through the group velocity dispersion parameter β_2 and the parameter $N = (2\pi\sigma/\lambda)\sqrt{n_0 n_2 I_0}$ represents the medium nonlinearity where I_0 is the peak intensity of the incident pulse. The normalized units not only simplify the problem, they also broaden the applicability of the results discussed below.

Plotted in figure (1) are the time-integrated far-field intensity distributions resulting from the propagation of an input field of the form $u(0,\xi,\tau) = \exp[-\xi^2/2 - (1 + iC)\tau^2/2]$

travelling through a Z-scan apparatus for three separate dispersion conditions. For these simulations $N^2 = 12$, $s = \pm 2$, and $C = 0$ or 2 in equation (1). The plots correspond to a sample placed at the point of the trough in the Z-scan. To get the actual value of the Z-scan at that one point it would be necessary to integrate over a small central section of the plots below. The upper (dashed) curve is the far-field for the normal-dispersion case with the strength of the dispersion chosen such that $s = 2$ in equation (1). The middle (solid) curve is for the anomalous dispersion case with $s = -2$. In the absence of dispersion ($s = 0$) the curve would fall between the upper two curves. The error in the measurements of the nonlinearity in these cases would be small but measurable. The lower (dotted) curve is for a chirped pulse ($C = 2$) in an anomalously dispersive ($s = -2$) medium The lower curve points to the significant effect that a chirped pulse can have on the Z-scan measurement. In all cases, the error results from the spatio-temporal coupling induced by the nonlinearity. We will present a comprehensive analysis of the roles dispersion and chirp play on the spatio-temporal coupling and on the Z-scan measurements.

1. M. Sheik-Bahae, A. A. Said, T.-H. Wei, D. J. Hagan and E. W. Van Stryland, IEEE J. of Quantum Electron., **26**,760(1990)
2. A. T. Ryan and G. P. Agrawal, Opt. Lett., **20**, Feb. (1995)

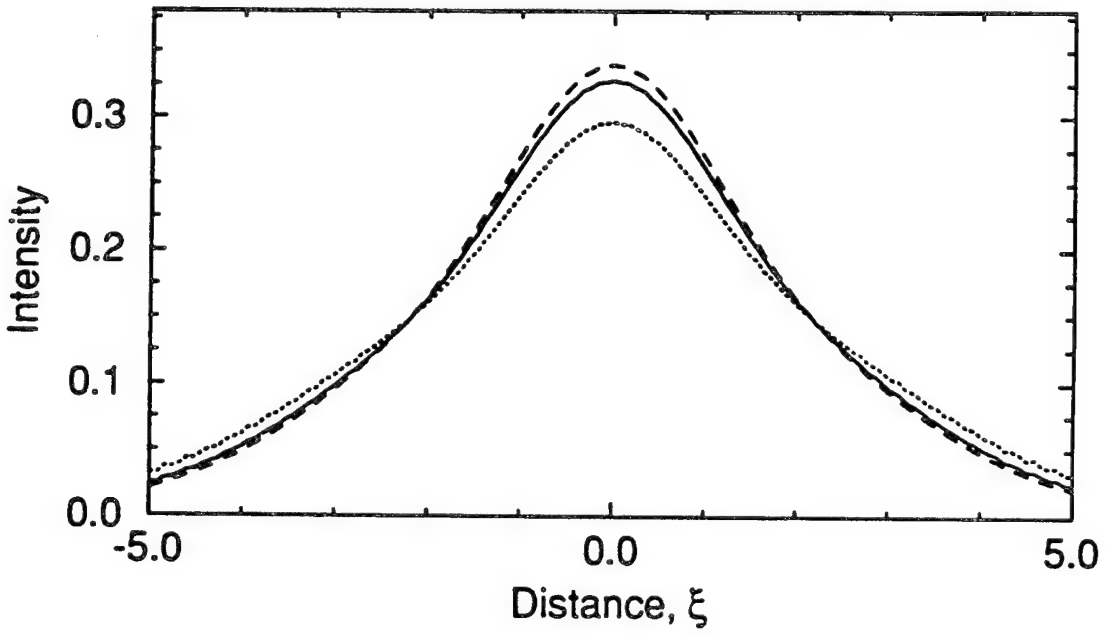

Figure 1. Time integrated far-field intensity distribution of Gaussian input pulses after propagation through a Z-scan apparatus. Dashed curve: normal dispersion with $s = 2$ in eqn.(1). Solid curve: anomalous dispersion with $s = -2$. Dotted curve: anomalous dispersion, $s = -2$, with chirp $C = 2$.

Pulsations of transverse drift modes in misaligned linear and ring cavities

Mark Saffman

Department of Optics and Fluid Dynamics,
Risø National Laboratory, DK-4000 Roskilde, Denmark

tel: +45 46 77 45 03
fax: +45 46 75 40 64
e-mail: saffman@risoe.dk

Misalignment induced drift instabilities have been considered in the context of Fabry-Perot [1,2] and thin slice with feedback mirror geometries [3,4]. Related drift instabilities of localized modes in misaligned ring resonators have also been observed [5]. We report here on analytical and numerical studies of drift wave thresholds and dynamics in misaligned linear and ring resonator geometries.

Transverse mode drift may be due to either misalignment of the optical cavity [4,5], or nonnormal incidence of the pump beam on a well aligned cavity [1,2,3]. In the case of a roll instability in the near field the twin beams in the far field will be frequency shifted by $\pm\Omega$ from the pump beam. This frequency shift corresponds to a transverse drift of the roll pattern with velocity $\lambda 2\Omega/\theta$, where the twin beams are separated by an angle 2θ. Note that media with a complex (mixed absorptive-dispersive) nonlinearity may give rise to frequency shifted dynamic instabilities, and hence near field drift motion, even in the case of normal incidence on perfectly aligned cavities[6,7,8].

When attention is restricted to small misalignments, such that the transverse displacement $\Delta x = \alpha L$ (α is a tilt angle and L is the effective cavity length), is small compared to the width of the incident beam a plane wave analysis is appropriate. Within such a framework we calculate the dispersion relations for drift waves in the linear and ring geometries shown in Fig. 1. assuming a Kerr type nonlinearity of the form

$$n = n_0' + in_0'' + \left(n_2' + in_2''\right)\frac{I}{1 - i\Omega\tau}.$$

Here we allow for a complex n_2, I is the intensity, and τ is the material response time. We carry out the analysis for the case of thin nonlinear media [9]. The resulting dispersion relations extend the results of Grynberg [3], who considered a polarization instability, to the case of Kerr media.

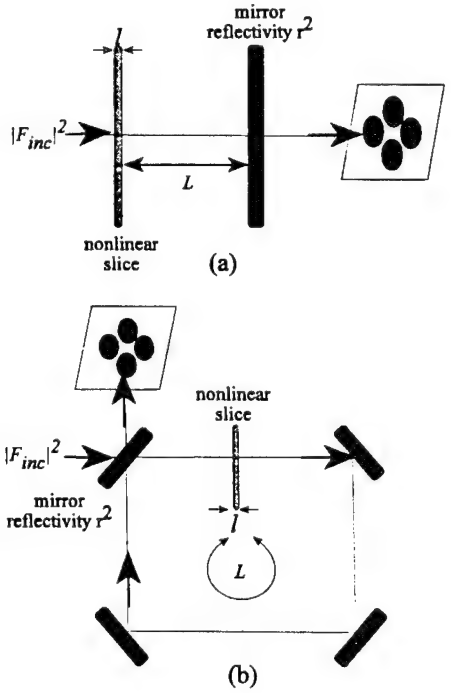

Figure 1. Linear (a) and ring(b) geometries for pattern formation.

When the misalignment is increased such that the displacement Δx is comparable to the beam width the instability thresholds rise dramatically, and the dynamics change character. Instead of a continuous frequency shifted oscillation, the instability grows, drifts towards the edge of the finite sized pumping region, disappears, and starts over. This type of scenario has been observed experimentally in photorefractive ring resonators[5]. In this regime the plane wave description breaks down and we have used direct numerical simulations to study the dynamics, including the transition from a continuous to a pulsed scenario.

This work was supported by a grant from the Danish Natural Science Research Council.

References

1. M. Haelterman and G. Vitrant, J. Opt. Soc. Am. B **9**, 1563 (1992).

2. P. LaPenna and G. Giusfredi, Phys. Rev. A **48**, 2299 (1993).

3. G. Grynberg, Opt. Commun. **109**, 483 (1994).

4. A. Petrossian, L. Dambly, and G. Grynberg, Europhys. Lett. **29**, 209 (1994).

5. M. Saffman, D. Montgomery, and D.Z. Anderson, Opt. Lett. **19**, 518 (1994).

6. M. Saffman, D. Montgomery, A.A. Zozulya, K.Kuroda, and D.Z. Anderson, Phys. Rev. A **48**, 3209 (1993).

7. M. Saffman, A.A. Zozulya, and D.Z. Anderson, J. Opt. Soc. Am B **11**, 1409 (1994).

8. J. Glückstad and M. Saffman, to appear Opt. Lett., 1995.

9. W.J. Firth, J. Mod. Opt. **37**, 151 (1990).

Self-induced gain and stratification in counter-propagation of resonant light beams in dense media

B.A.Samson and W.Gawlik

Institute of Physics, Jagellonian University, ul.Reymonta 4, Krakow 30-059, Poland.
Fax: (48-12) 33-70-86, e-mail: bsamson@castor.if.uj.edu.pl

Phenomena caused by the local fields in optically dense atomic media are of a growing interest because of their possible applications in optoelectronics and physics of atomic traps. The principal mathematical manifestation of this effect is the appearence of non-linear terms in the Bloch equations for atomic dynamics in a light field. Such terms were shown to be responsible for the feedbackless, intrinsic optical bistability (IOB) [1].

In this work we study the consequences of the IOB for the dynamics of counter-propagating light beams in homogeneously absorbing dense media. We demonstrate the possibility of unidirectional energy exchange between the counter-propagating light beams resulting in an amplification of one of them. It occurs for certain values of the beam intensities, which leads to a self-induced stratification along the propagation direction.

The equations for the dynamics of population difference n and polarization amplitude p of a two-level atom in the external field of amplitude Ω can be written in the following form:

$$\dot{p} = [-1 + i(\delta - \sigma n)]p + in\Omega/2, \qquad \dot{n} = -\eta(n-1) + i(p\Omega^* - p^*\Omega), \tag{1}$$

where η is the ratio between longitudinal T_1 and transverse T_2 relaxation rates, δ is the detuning of the light frequency from the resonance, and σ is the dimensionless local-field parameter [1].

We suppose Ω to be a sum of two counter-propagating waves with slightly different frequencies:

$$\Omega = \Omega_+ e^{ikz + i\epsilon t} + \Omega_- e^{-ikz}, \tag{2}$$

where k is the linear wavenumber. The small relative frequency shift $\epsilon \ll T_2^{-1}$ is introduced to produce a moving grating in order to eliminate an uncertainity in a spatial distribution of the atomic variables, which dependence on the light intensity is bistable. This purpose can be achieved also by assuming a slow motion of the medium in a z direction.

Under such conditions the polarization and population difference spatial distributions could be expanded in series of elementary gratings with the basic scale given by the light interference pattern $|\Omega|^2 = s_0 + s_1 \cos(2kz + \Psi_+ - \Psi_-)$ ($\Psi_\pm$ are the phases of the fields $\Omega_\pm$):

$$p(z) = \Omega[d_0 + d_c \cos(2kz + \Psi_+ - \Psi_-) + d_s \sin(2kz + \Psi_+ - \Psi_-) + ...]. \tag{3}$$

The main consequence of the IOB in expansion (3) is the appearence of the *sin*-term, which is absent at $\sigma = 0$. Physically it produces a nonlinear gain for the wave Ω_+ and additional absorption for Ω_- after extracting in $p(z)$ resonant with the interacting beams terms. This unidirectional energy flow can result in an amplification of Ω_+, which takes

place for certain beam intensities $I_\pm = |\Omega_\pm|^2$, as shown in Fig.1.

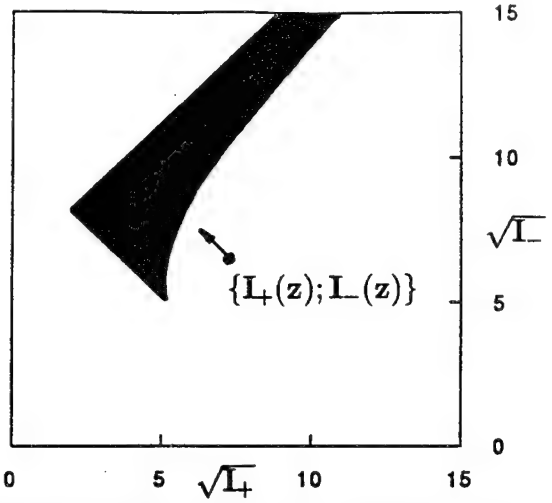

Fig.1. Diagram displaying the region of the self-induced amplification of the wave Ω_+ (shaded area) at $\delta = 0$ and $\sigma = 20$.

The point $\{I_+(z); I_-(z)\}$ for specific boundary conditions enters the region of Ω_+-amplification producing hence a number of spatial first-order phase transitions "gain-absorption". The typical spatial intensity distribution illustrating such self-induced stratification is shown in Fig.2.

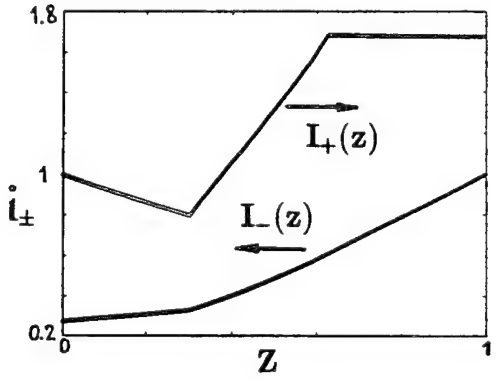

Fig.2. Longitudinal distribution of normalized field intensities $i_+ = I_+/I_+(z=0)$ and $i_- = I_-/I_-(z=L)$ in a medium at $\delta = 0, \sigma = 20, I_+(z=0) = 9, I_-(z=L) = 169$.

Inversion of the sign of ϵ, or of the medium motion direction, changes the direction of the energy flow, creating a region of Ω_--amplification. This effect could find an application in sensitive motion detectors.

Another important consequence of the described energy transfer could be a new, stimulated optical force which acts at sufficiently high medium density. It would be very interesting to check whether this local-field-induced force could overcome the repulsive force due to radiation trapping in optical atomic molassis [2] and thereby the density limit on a way toward the Bose-Einstein condensation.

The work is supported by the Polish Committee for Scientific Research (grant 2P30205205).

[1] Y.Ben-Aryeh, C.M.Bowden, and J.C.Englund, Phys.Rev.**A 34**, (1986) 3917.
[2] T.Walker, D.Sesko, and C.Wieman, Phys.Rev.Letts **64**, (1990) 408.

Dye laser with polarized pumping dynamics

S.V.Sergeyev, S.K.Gorbatsevich, S.A.Sakharuk
Department of Physics, Belarus State University,
4 Skorina Ave.,Minsk 220050, Republic of Belarus
e-mail: root@mfp.bsu.minsk.by
fax: (007-0172) 26-59-40

There a lot of papers dealing with coupled-oscillators dynamics and its' application to biology and chemistry. The problem can be represented in the following form:

$$\begin{aligned} d\mathbf{X_1}/dt &= F_1(\mathbf{X_1}) + D_1(\mathbf{X_2} - \mathbf{X_1}), \\ d\mathbf{X_2}/dt &= F_2(\mathbf{X_2}) + D_2(\mathbf{X_1} - \mathbf{X_2}), \\ \mathbf{X_1}, \mathbf{X_2} &\in R^n, \end{aligned} \tag{1}$$

The results obtained can be summarized as following: (i) if oscillators (F_1, F_2) in (1) are sufficiently different than coupling suppress the auto-oscillations and system goes to steady-state (Bar-Eli effect); (ii) if oscillators in (1) are identical $(F_1 = F_2)$ than phase-drift and phase-locked solutions, various tori, multiple oscillations, period doubling and chaos for large enough coupling can occur.

For the anisotropic lasers polarizations modes play role of coupled oscillators that gives opportunity to use results of theory mentioned above. It can be illustrated by means of semi-classical model of the ring cavity cw dye laser with polarized pumping and Orientational Relaxation Processes (Brownian Rotation of molecules or Radiationless Energy Transfer) in the active medium:

$$\begin{aligned} \frac{dE_i}{dt} &= -k_i(E_i - \int P(g)(\mathbf{m_e e_i})dg), \\ \frac{dP}{dt} &= -(1 + i\Delta)P - \sum_{j=x,z} \psi_j D(\mathbf{m_e e_j})E_j, \\ \frac{dD}{dt} &= \gamma(d_0(\mathbf{m_a e_p})^2 - (1 + \hat{\mathcal{L}})D - \frac{1}{2}\sum_j (P^* E_i + P E_i^*)(\mathbf{m_e e_j})), \end{aligned} \tag{2}$$

where E_i, $(i = z, x)$ are polarization modes of ring cavity dye laser, Δ is detuning of the laser cavity with respect to the maximum of emission spectrum of dye molecules. g are

the Euler's angles; $\mathbf{e}_p$,$\mathbf{e}_i$ are unit vectors of polarization of excitation and emission for the i-th mode; $\mathbf{m}_a$, is unit vector oriented along dipole moment of the optical transition with absorption, vector $\mathbf{m}_e$ is a vector oriented along dipole moment of the optical transition with emission, $\hat{\mathcal{L}}$ are operators of Orientational Relaxation (Brownian Rotation and Radiationless Energy Transfer).

It has been found by means of nonliner analysis that for the case when pumping is polarized along the cavity neutrally stable circular polarized waves can appear above the first threshold. Numerical solution of equations (2) confirms the results of analytical consideration and gives opportunity to find phase-drift solution and polarization chaos (fig.1.) that means chaotic modulation of phase difference between polarization modes $\Delta\varphi$.

Phase correlation between polarization modes decreases when rate of ORP increases. In the limit of infinitely high rate of ORP the is no any correlation and anisotropic dye laser looks like isotropic one (Lorenz-Haken model). Polarization chaos displayed is located more close to the first laser threshold than chaotic attractor in Lorenz-Haken model.

The dynamics displayed looks like the identical coupled oscillators dynamics with phase-drift and chaotic operations. By means of rotating pumping polarization plane the case of different coupled oscillators has been realized.

fig.1. $k_i = 0.1, \quad \Delta = 0.2$

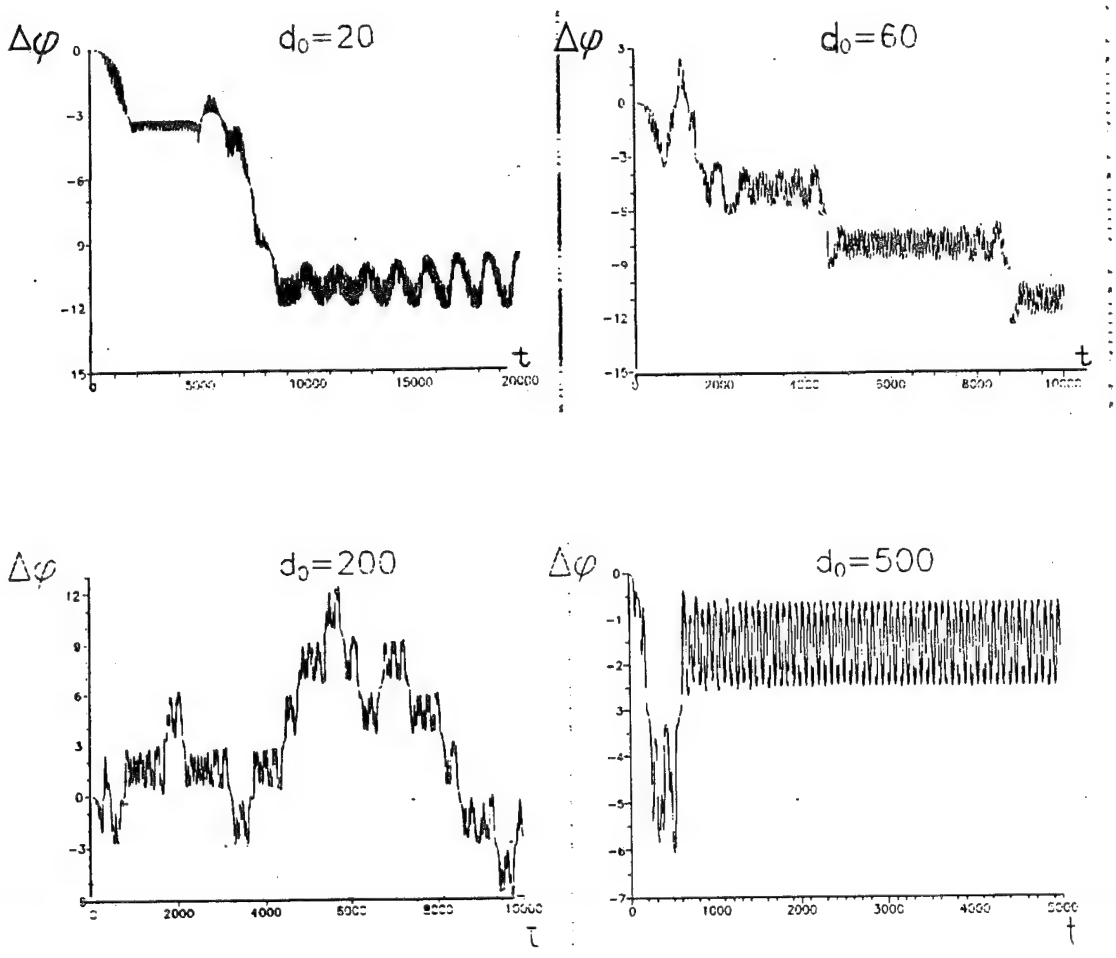

Role Of The "Cascading Effect " In A Ring Cavity Filled With A Quadratic Nonlinear Medium

C.Sibilia, A.Re, E.Fazio, M.Bertolotti

Dipartimento di Energetica -Univ.Roma "La Sapienza"

Via Scarpa 16, 00161 Roma, ITALY ,

GNEQP of CNR and INFM

Tel 39 6 49916524, Fax 39 6 44240183
BERTOL88@ITCASPUR.CASPUR.IT

In the last few years the interest for the spatial and/or temporal evolution of optical fields in nonlinear systems has particularly increased. The conditions to have constant or periodic solutions or period doubling route to chaos (see [1] and references inside) have been studied in the case of a cavity filled with second order nonlinear material. Instabilities in a Fabry-Perot resonator filled with a medium with a second order nonlinearity, having a pulsed input, have been studied in ref.[2], considering pulses short with respect to the transit time in the medium. In this case no backward field is present , and no additional effects associated to the nonlinear phase shift are present.

Here a quasi c.w. operation is considered in a ring cavity filled with a second order nonlinear medium, working in conditions to produce a nonlinear phase-shift (mismatching conditions between pump and generated fields are used) . We study the case of second harmonic generation (SHG), when at the initial time , at the input mirror, only the pulse at fundamental frequency is present . It can be proved that the nonlinear harmonic generation process is strongly influenced, by the phase mismatching Δk between the two beams [3,4] and by the difference ΔE of the amplitudes of the fields at the input of the nonlinear medium[3,4]. Because these two parameters are independent one from the other, we can

consider, for instance the generation process inside the cavity for $\Delta k=0$, at fixed cavity detuning , and study what happens by varying ΔE. The difference ΔE automatically varies if we adjust the input pulse repetition rate and the cavity length , so that at the entry of the nonlinear medium there are, at the same time , the input pulse and the two pulses circulating inside the cavity (synchronous configuration) . This is sufficient to produce a third - order- like nonlinear phase shift into the pump beam, which behaves as a nonlinear cavity detuning . Owing to the nonlinearity, the output pulses will in general be different from the input one both in modulus and phase. In other words the output and, consequently, the input may vary in time, in spite of the lack of variation of the input at the entrance of the cavity, yielding a continuous modification of ΔE. This behavior, by means of the feedback, can show, for suitable values

of the input power and fixed linear cavity detuning , a periodic, constant or intermittent behavior of the output.

In our analysis we consider the evolution of the moduli and phases of the output pulses as a function of the modulus of the input .

It is also useful to make an analysis in similar conditions by varying Δk (detuning for the generation process) and maintaining constant the input power at fundamental frequency.

A stability analysis of the system descrining the interaction inside the cavity is presented and discussed : it gives a direct connection between the instable behaviour and the nonlinear phase shift of the pump beam.

References

[1] Hao Bai Lin: "Chaos". 1984, World Scientific ed..

[2] H.J.Bakker *et al.* , "Phase modulation in second-Order nonlinear-optical processes" Phys. Rev. A **42**, 7 (1990)

[3] A.Re, C.Sibilia and M.Bertolotti: to be published

[4] R.DeSalvo *et al.*: "Self-focusing and self-defocusing by cascaded second-order effects in KTP". Optics Letters **17**,28(1992)

Dynamic transverse patterns in a two-mode laser.

D.V.Skryabin, A.G.Vladimirov, and A.M.Radin
Dept. of Quantum Electronics, Institute of Physics, St.Petersburg State University,
1 Ulianovskaya st., Petrodvorets,St.Petersburg, 198904, Russia
fax: +7 (812) 4287240; e-mail: bell@dc1.phys.samson.spb.su

Investigation of nonlinearity influence on transverse configuration of electromagnetic field in lasers and passive optical systems now attracts considerable attention. In the present work we study nonlinear interaction of two Gauss-Laguerre modes with opposite angular momenta. These modes are characterized by the radial index $p = 0$ and angular indices $l = \pm 1$. As it was shown earlier [1,2], the interaction of these modes can lead to regimes with stationary or time-dependent intensity patterns. Here we show that class-A laser (e.g. Na_2, He-Ne, He-Xe) operating in two modes with opposite angular momenta may exhibit three different kinds of time-dependent transverse patterns. Let us neglect the dependence of laser field intensity I on the coordinate along the optical axis. Then, for a bimode laser under consideration, it can be written as

$$I \propto \rho^2 \exp(-\rho^2)(E_+^2 + E_-^2 + 2E_+E_- \cos(2\phi + \mu_+ - \mu_-). \qquad (1)$$

Here $E_\pm$ and $\mu_\pm$ are the slowly varying amplitudes and phases of the modes. ρ is the normalized distance from the optical axis in the transverse direction, ϕ is the polar angle. The complex mode amplitudes $\tilde{E}_\pm = E_\pm \exp(i\mu_\pm)$ obey the equations

$$\partial_t \tilde{E}_\pm = (A - \beta(\delta)|\tilde{E}_\pm|^2 - \vartheta(\delta)|\tilde{E}_\mp|^2)\tilde{E}_\pm + iR\tilde{E}_\mp \exp(i\psi), \qquad (2)$$

where A is the pump parameter. β and ϑ are the complex coefficients depending on the detuning δ, inhomogeneous and/or homogeneous linewidths, and the inversion relaxation time of an active medium. R and ψ are the amplitude and the phase of the coefficient of linear coupling between the modes. This coupling results from the axial symmetry breaking in the laser cavity and strongly affects laser dynamics [2].

Eqs.(2) have a pair of solutions of a "standing-wave" type: $E_+ = E_-$ and $\mu_+ - \mu_- = 0, \pi$. These solutions are the usual Gauss-Hermite modes TEM_{10} and TEM_{01}. The "pure-mode" solutions $E_+ \neq 0$, $E_- = 0$ and $E_+ = 0$, $E_- \neq 0$ exist only for $R = 0$. In the presence of linear coupling they are transformed into a pair of "travelling-wave" solutions with $E_\pm \neq 0$. For one of this solutions $E_+ > E_-$ and for another one $E_+ < E_-$. Under the transformation $(\tilde{E}_+, \tilde{E}_-) \rightarrow (\tilde{E}_-, \tilde{E}_+)$ Eqs.(2) remain invariant and the "travelling-wave" solutions are converted into one another.

We have performed a detailed bifurcation analysis of the steady-state and time-dependent solutions of eqs.(2). Let δ be the bifurcation parameter. Then a typical bifurcation sequence can be outlined as follows. The mode TEM_{10} is stable in a certain interval of detunings $\delta_1 < \delta < \delta_2$. At $\delta = \delta_2$ it undergoes a supercritical Hopf bifurcation, and stable limit cycle LC1 arises. These limit cycle LC1 disappears in the homoclinic figure-eight at $\delta = \delta_3$. This homoclinic bifurcation generates a pair of stable limit cycles LC2 and LC3. They disappear at the point $\delta = \delta_4$ where a supercritical Hopf bifurcations on the "travelling-wave" solutions occur.

The limit cycles LC1, LC2 and LC3 correspond to three different kinds of time-dependent transverse patterns. Note, that laser intensity (1) has a minimum at $\phi = (\mu_- - \mu_+ \pm \pi)/2$. Since the phase difference of the modes $\mu_- - \mu_+$ is time-dependent for periodic solutions, the intensity minimum rotates around the optical axis. The time dependencies of the angular velocities of the rotating patterns are shown in Fig.1. The mean value of the angular velocity is equal to zero for a laser operating in LC1 regime. This means that the intensity minimum oscillates back and forth within a finite interval of angles. The angular velocity of the pattern is positive (negative) for a laser operating in LC2 (LC3) regime. Hence, the intensity minimum rotates in the clockwise direction for LC2 in the counterclockwise direction for LC3. Unlike the limit cycle LC1 corresponding to zero frequency splitting of the transverse modes $\Delta\omega = 0$, the limit cycles LC2 and LC3 correspond to nonzero and opposite values of $\Delta\omega$. This may be interpreted as spontaneous phase symmetry breaking of the modes caused by their nonlinear interaction.

References

[1] M.Brambilla et al, Phys. Rev. A 49 (1994) 1427; A.R.Coates et al, Phys. Rev. A 49 (1994) 1452.

[2] R.López-Ruiz, et al, Phys. Rev. A 49 (1994) 4916.

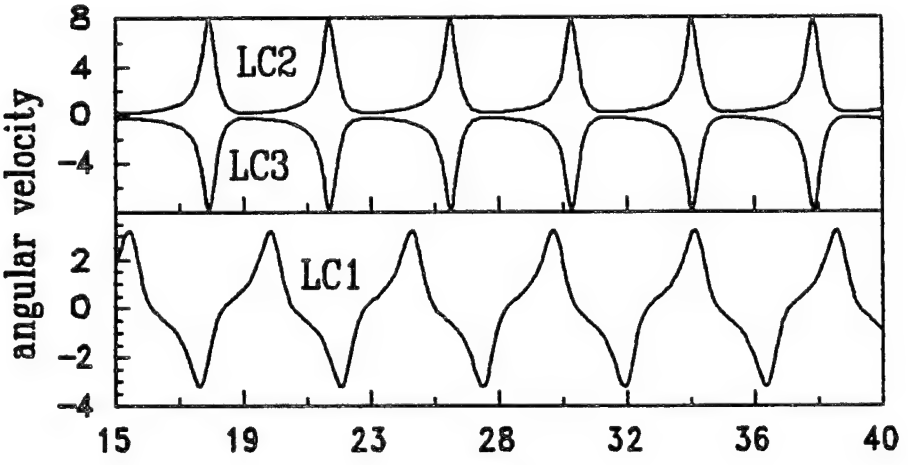

Figure 1.

Spatial Instabilities in DH Stripe Semiconductor Injection Lasers: Effects of Thermal Nonlinearity

G.A.Smolyakov, L.A.Melnikov, S.V.Ovchinnikov,

Department of Optics, Chernyshevsky State University
Saratov, 410071, Astrakhanskaya 83, Russia
phone: (845-2)51-51-95, e-mail: melnikov@scnit.saratov.su

and

E.M.Rabinovich

North Texas Research & Development Corp., University of North Texas
phone: (817) 565-4990, e-mail: fc21@vaxb.acs.unt.edu

Until the present time a variety of models of semiconductor injection lasers have appeared that allowed for a greater or lesser degree of self-consistency. Although the inclusion of such selfconsistent effects as gain saturation and index antiguiding is what all these models have in common, very few of them take into account thermal effects in the same rigorous manner. But as has been shown by Hadley et.al.[1] for diode arrays and broad-area devices the lasing transverse modes are highly sensitive to variations in the lateral temperature distributions. Thermal nonlinearity of the active medium is of primary importance in determining the mode selectivity and on no account can be neglected.

From this point of view we revised the results of our previous experiments with $Ga_{1-x}Al_xAs$ DH stripe injection lasers [2], where we had reported the modulation instabilities of the lasers far field and rather intricate behavior of the phase of intensity modulation across the laser beam. Using in our thermal model the analytical expression for lateral current spreading first proposed by Tsang [3] we showed that in stripe geometry lasers a very specific waveguiding profile of $Re\epsilon(y)$ can occur owing to the fact that lateral temperature distribution is always wider than corresponding carrier distribution. We subjected the waveguiding properties of this specific waveguide to intense scrutiny by solving one-dimensional waveguiding problem:

$$\frac{d^2\psi(y)}{dy^2} + (k_0^2\epsilon_{ef}(y) - \beta^2)\psi(y) = 0, \tag{1}$$

where $\epsilon_{ef}(y) = b\epsilon_1' + (1-b)\epsilon_2' + \Gamma(i\epsilon_1'' + \epsilon'(y) + i\epsilon''(y)) + i(1-\Gamma)\epsilon_2''$; b and Γ are the normalized propagation constant and optical confinement factor, describing the real symmetrical three-layer waveguide in transverse direction and quantities $\epsilon_1 = \epsilon_1' + i\epsilon_1''; \epsilon_2 = \epsilon_2' + i\epsilon_2''$ are the parameters of this waiveguide. The lateral dependence

of the complex permittivity $\epsilon(y) = \epsilon'(y) + i\epsilon''(y)$ was treated as perturbation of the background dielectric constant ϵ_1 of the central layer due to carrier injection. Thermal and carrier contributions to the $\epsilon(y)$ were taken in the form of Epstein profiles [2] of appropriate widths and heights so that their resulting superposition was consistent with the findings of our thermal model. Having solved equation (1) numerically by 'shooting' method for near-field patterns and propagation constants $\beta_m = \beta'_m + i\beta''_m$ of three lowest-order lateral modes we found that in situations of high thermal gradients and relatively wide temperature distribution (high injection currents) the second-order lateral mode can compete with the fundamental one for common gain. The near-field and far-field patterns of each individual mode (rather stable for low injection currents) become enormously sensitive to the temperature variations. This fact is in good agreement with our experiments and supports the primary role the thermal processes play in pattern formation together with such processes as gain saturation and self-focusing. In order to treat mode competition correctly and to account for mutual effect of thermal and optical nonlinearities on pattern formation and spatial instabilities we solved beam-propagation problem:

$$2i\beta\frac{\partial\psi(y,z)}{\partial z} + \frac{\partial^2\psi(y,z)}{\partial y^2} + (k_0^2\epsilon_{ef}(y,|\psi(y,z)|^2) - \beta^2)\psi(y,z) = 0, \qquad (2)$$

where we introduced optical nonlinearity.

References

[1] G.R.Hadley, J.P.Hohimer, A.Owyoung, *IEEE J.Quant. Electron.*, **QE-24**, 2138 (1988).

[2] E.M.Rabinovich, G.A.Smolyakov, V.V.Tuchin, *OSA Proceedings on Nonlinear Dynamics in Optical Systems* (Optical Society of America, Washington, D.C., 1991), **7**, 96 (1991).

[3] Tsang W.T. *Journ. Appl. Phys.*, **49**, 1031 (1978).

QUASISOLITON INSIDE A DISSIPATIVE BISTABLE OPTICAL SYSTEM

G.I.Surdutovich and A.V.Ghiner*

Instituto de Fisica de Sao Carlos/USP,C.P.369,CEP 13560-970,Sao Carlos,SP,Brazil
fax 55(162)713616, e-mail surdutovich@ifqsc.sc.usp.br
*Universidade de Federal do Ceara',C.P.6030, CEP 60450-970, Fortaleza, Brazil

Earlier for a broad class of passive bistable distributed ,i.e.,spatially extended, systems of an arbitrary nature with cw external signal a new type of stationary/quasistationary states was predicted [1]. Later this regime was realized in optical and acoustoelectronic set-ups [2]. A concept of the effect is evident from the Fig.1. In shown at Fig.1 bistable ring system any δ - like pulse on the background of a constant input signal E_0 will be attenuated (a) or amplified (b) depending on its initial height (below or above) of a certain threshold value ΔE_c. A real "seed pulse" of an arbitrary shape and with duration not more than the round trip time T of the cavity turns into a mode of repetitive pulses of definite shape, which are stationary or quasistationary with exponentially small instability increment (solitons or quasisolitons). Here we discuss the characteristics properties and stability of the quasisoliton regime under different models of dispersion..

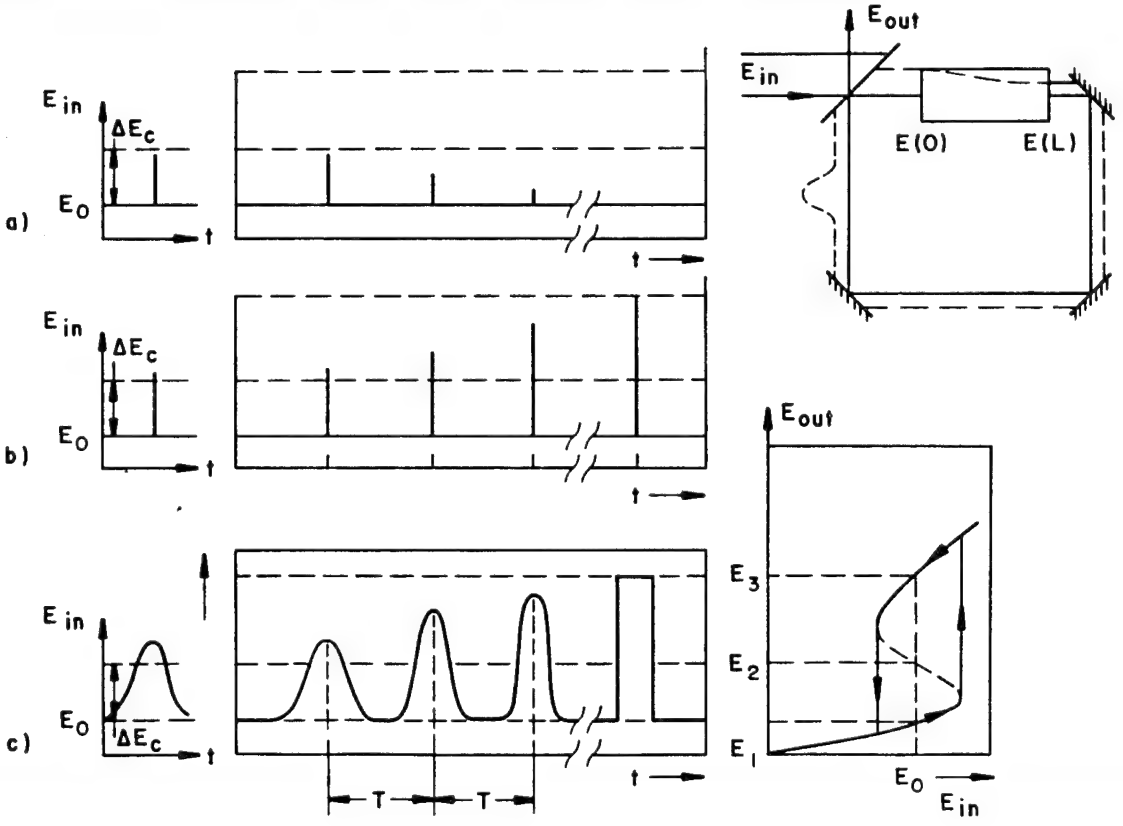

In a simple model of a linear dispersion, when amplitude attenuation coefficient k_r is minimal at the pump frequency ω_0 ($k_r = k_0 - \sigma(\omega - \omega_0)^2$, $\sigma > 0$), we obtain for a pulse amplitude $E(t,\tau)$ equation

$$\frac{\partial E}{\partial t} = E(t,\tau)\frac{k_r(E(t,\tau))-1}{T} + \frac{E_0}{T} + \frac{\sigma}{T}\frac{\partial^2 E}{\partial \tau^2}, \quad E(t+T,\tau) \equiv E(t,\tau+T) \qquad (1)$$

Here $t = nT$, n is the index number of the cavity round-trip passage. Eq.(1) give all the steady states: both steady-state regimes E_1, E_2, E_3 *under* $\frac{\partial E}{\partial \tau} = 0$ and the regimes of steady pulses, whose shapes are given by the solutions of Eq.(1) under $\frac{\partial E}{\partial t} = 0$. Such solutions correspond to motion of a classical particle in a potential well $W(E) = \int \frac{E_0 + E(k_r - 1)}{T} dE$, when amplitude E plays the role of coordinate of the particle. The relative values of the rear and forward fronts velocities $V(E_3 \to E_1)$ *and* $V(E_1 \to E_3)$, i.e., squeezing or broadening of the pulse, depend on the ratio of the potential hills $W(E_1)$ *and* $W(E_3)$ (Fig.2). This ratio is determined by the magnitude of the cw signal E_0 relatively to a certain amplitude E_M, which plays the same role as the known Maxwell curve in the theory of the first order phase transitions. Stability analysis for two models of dispersion is performed.

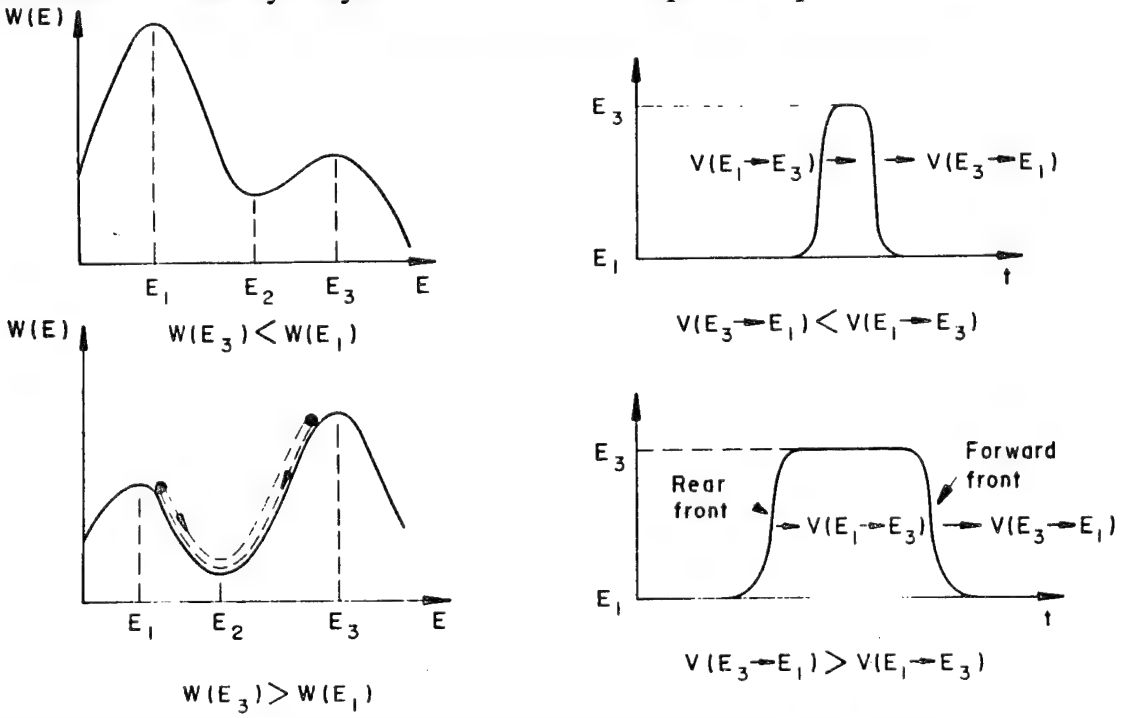

1.A.V.Ghiner and G.I.Surdutovich, Kvant.Electron.(Moscow),15, 975 (1988)
2.V.L.Velichansky, A.V.Ghiner et al, Phys.Stat.Sol.(b),150,605 (1988)

Polariton solitons as asymptotic solutions of coherent semiconductor Maxwell-Bloch equations in the low-density regime

I. Talanina

Abteilung Theoretische Physik, Universität Ulm, 89069 Ulm, Germany

Phone: 49-731-502-2916, FAX: 49-731-502-2924, Email: talanina@physik.uni-ulm.de

A. Knorr and S.W. Koch

Fachbereich Physik und Zentrum für Materialwissenschaften,

Philipps-Universität, Renthof 5, D-35032 Marburg, Germany

Phone: 49- 6421-28-6552, FAX: 49-6421-28-7079, Email:knorr@mv13a.physik.uni-marburg.de

The possibility to form polariton solitons in bulk semiconductors has been recently studied using the theory of excitons [1,2]. It has been shown that sech-shaped polariton pulses can be formed under certain conditions. In particular, it has been found that the pulse duration must be larger than a certain critical value.

This phenomenon of form-invariant polariton pulse propagation should be observable at moderate input light intensities, but no quantitative estimations of the required laser power and pulse duration have been ever performed. Perhaps, for this reason, no efforts to observe the steady-state polariton pulses have been made yet.

Here, we present new analytical results on polariton soliton dynamics in semiconductor media obtained using the semiconductor Maxwell-Bloch equations (SMBE). We compare these results with those obtained recently using the theory of excitons and show that, in the limit of low electron-hole density, both approaches allow analytical steady-state pulse solutions corresponding to polariton solitons.

It should be emphasized that the solitons considered here are different from the self-induced transparency (SIT) solutions which can also be derived from SMBE under certain assumptions. The polariton solitons represent a class of asymptotic solutions of SMBE, but have a different nature in comparisson with SIT solitons: The polariton solitons form when nonlinear effects compensate the dispersive spreading of polariton pulses. In this regard, they resemble the solitons in optical fibers.

We estimate the laser power required to form the steady-state polariton pulses in CuCl and CdS crystals and describe explicitely the conditions which have to be satisfied in experiments to allow a reliable observation of the phenomenon. We believe that experimental studies of the soliton dynamics in semiconductors would have not only basic interest, but could also prove useful for device applications in soliton based all-optical communication lines.

[1] I. B. Talanina, M. A. Collins, and V. M. Agranovich, Solid State Commun. **88**, 541 (1993).

[2] I. B. Talanina, M. A. Collins, and V. M. Agranovich Phys. Rev. B **49**, 1517 (1994).

Simulation of femtosecond pulse propagation in an unpumped Er-doped optical fiber

Xiaonong Zhu and Michel Piché

Département de Physique, COPL, Université Laval,
Cité Universitaire, Québec, Canada, G1K 7P4
Tel: (481) 656-2659; Fax: (418) 656-2623; E-mail: xzhu@phy.ulaval.ca

Summary

In the last few years, experimental measurements of the dispersion in Er-doped optical fibers have been reported by several research groups. It was shown that the extra dispersion due to absorption/amplification in Er-doped fibers can be either comparable to [1] or even much larger [2] than the corresponding background fiber dispersion. In this presentation, we shall show the results of our numerical simulations of a single femtosecond pulse propagating along an unpumped Er-doped fiber. In particular, we examine the influence of erbium absorption on a femtosecond propagating pulse.

We use the standard split-step method to solve an extended nonlinear Schrödinger equation that includes a term representing erbium absorption. For simplicity, the erbium absorption is mimicked by a complex Lorenzian function with its real part standing for the spectrally varying attenuation and the imaginary part representing the corresponding phase distortion. For the parameters we selected, such as peak absorption α_0=1.0/m at 1532 nm, absorption bandwidth $\Delta\lambda_a$ = 30 nm, fiber background dispersion of D = 1.0 ps/nm/km, fiber length L = 0.6 m, the actual fiber dispersion over a spectral region on the short wavelength side of absorption center is turned from normal to anomalous due to the presence of absorption. We then select incident pulses centered at different wavelengths relative to the absorption center. The typical results are shown in Fig. 1, where the dashed lines are associated with the same incident pulse (200 fs, 0.29 nJ, $sech^2$ and bandwidth limited) tuned at three different launching wavelengths. From Fig. 1, we can see that during propagation the pulse launched at 1515 nm is temporally broadened [Fig. 1(a)], whereas those launched at 1532 nm and 1550 nm are compressed [Figs. 1(c), 1(e)]. The spectra of the exiting pulses, however, are broader than those of the input pulses in all the three situations [see Fig. 1(b), 1(d), 1(f)]. Further studies show that the exiting pulses in Figs. 1(c) and 1(e) are actually shorter than those obtained without considering the absorption effect. It is thus evidenced that pulse compression is suppressed/enhanced for the incident pulse launched on shorter/longer wavelength side of the center of absorption spectrum.

To further examine which effect, the amplitude attenuation or the phase distortion due to absorption, dominates the reshaping of the propagating pulses, we also made simulations of the cases where only the real or the imaginary part of the complex absorption was taken into account at the launching wavelength λ_0 = 1515 nm. With only the phase distortion effect considered the exiting pulse has a duration of ~207 fs and so being still broader than the incident one, whereas with pure amplitude effect we observe pulse compression down to about 175 fs. We thus know that it is indeed the phase distortion due to erbium absorption that is responsible for making the propagating pulse out of the solitonic regime.

In conclusion, when the fiber background dispersion is relatively small compared to the dispersion due to absorption, the propagating pulses inside an unpumped Er-doped fiber can be either compressed or broadened, depending on whether the spectrum of the launched pulse is centered on the longer or shorter wavelength side of the absorption center. A switching of the sign of the actual fiber dispersion on one side of the absorption center can lead to a change of pulse propagation pattern from otherwise a solitonic regime into a non-solitonic regime.

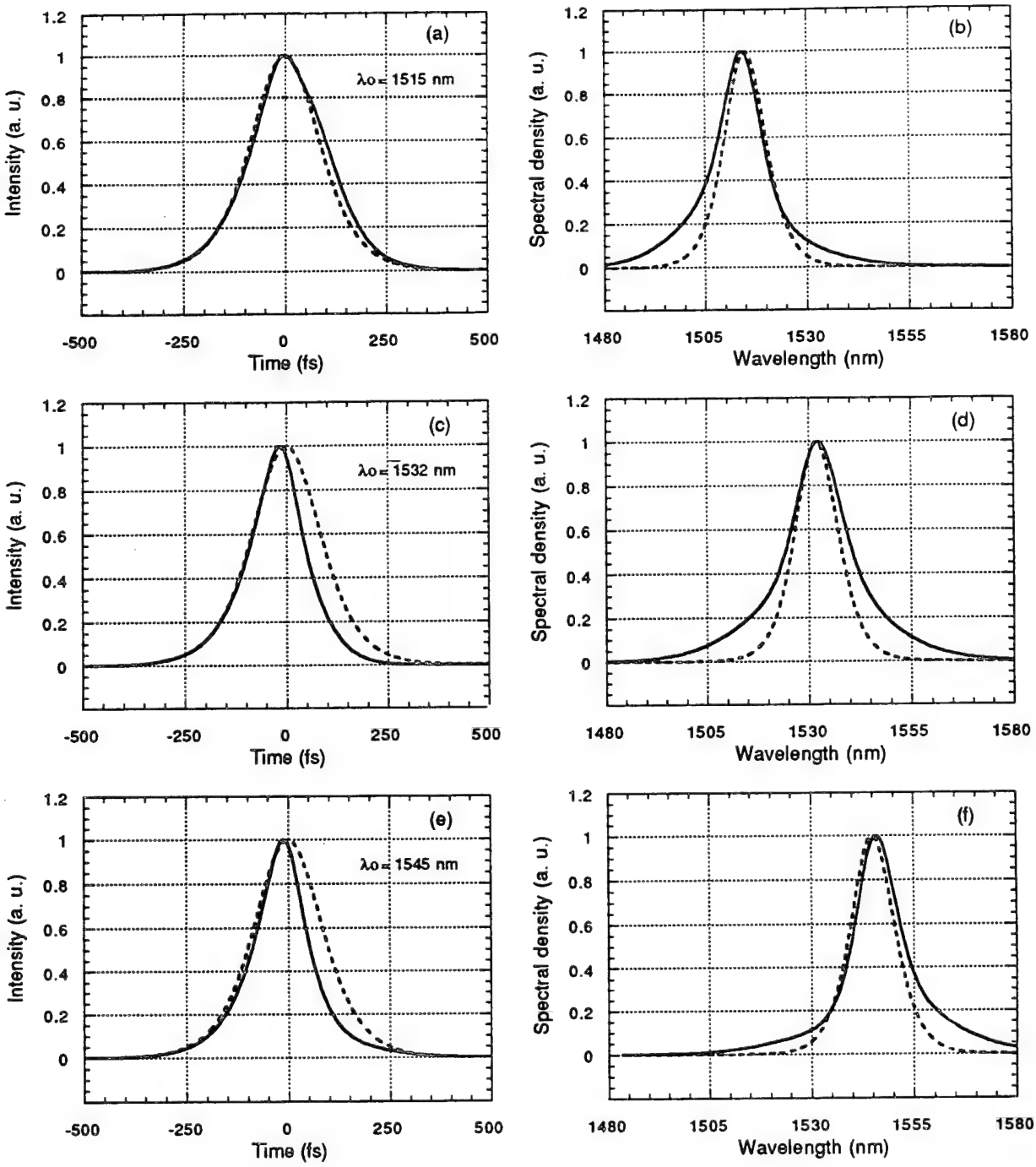

Fig. 1. Temporal profiles and spectra of the pulses incident into (dashed lines) and exiting from (solid lines) a 60-cm-long Er-doped fiber at three indicated launching wavelengths. (The label a. u. stands for arbitrary units).

References:

[1] F. Matera, M. Romagnoli, M. Settembre, M.Tamburrini, and M. Peroni, *Electron. Lett.* vol. 27, 1867, (1991).

[2] C. Thirstrup, Y. Shi, O. Poulsen, B. Palsdottir, *Proc. 5th European Quantum Electronics Conference* 1994, Paper QThF2 1115.

Geometric structure of laser models

Vladislav Yu.Toronov and Vladimir L.Derbov

Department of Physics, Saratov State University,

83 Astrakhanskaya str., Saratov 410071, Russia,

phone: (845-2)51-51-95, FAX: (845-2)24-04-46, e-mail: toronov@scnit.saratov.su

January 10, 1995

In recent years a remarkable similarity was noticed between the laser semiclassical equations and the Schrödinger equation, which results, in particular, in "geometric" properties of the phase of laser field [1,2]. The goals of the present paper are to realize the origin of this analogy basing on differential geometry and to reveal some new physical outcomes of the geometric structure of laser models.

The common feature of the wave function of a quantum system and the complex amplitude of an optical field is the non-sensitivity of the physical state of the system described by these functions to arbitrary perturbations of the total phase. For a laser system such an ambiguity of the point in the phase space $\mathcal{N}$ corresponding to a given physical state may be formally expressed in terms of the fiber bundle formed by the triplet $(\mathcal{N}, \mathcal{P}, \Pi)$, where $\mathcal{P}$ is the space of physical states and Π is the map $\mathcal{N} \to \mathcal{P}$; The fiber bundle $(\mathcal{N}, \mathcal{P}, \Pi)$ is the counterpart of the principal one [3]. We show that if the evolution of a system is represented in $\mathcal{P}$ by the trajectory connecting the points P_1 and P_2, the geometric part of the phase acquired by the field may be expressed as

$$\gamma = \int \frac{Im[(\phi(s), d\phi/ds)]}{(\phi(s), \phi(s))} ds, \qquad (1)$$

where $\phi(s)$ is the lift in $\mathcal{N}$ of the geodesic curve connecting P_1 and P_2. Eq.(1) provides the generalization of the geometric phase setting, given in [1], for the case of noncyclic evolution of a laser system.

The reasonable question is whether these geometric ideas are useful for obtaining the physical knowledge about the laser. We try to answer this question considering two systems, the models of unidirectional and bidirectional ring lasers. The first one, being isomorphic to complex Lorenz equations (CLE) [1], has the five-dimensional phase space associated with the complex amplitudes of the field x and polarization y, and the inversion z. It is a notable fact, which has never been found before, that the map

$$\Pi : u = (|x|^2 - |y|^2)/2, \quad v + iw = x^* y, z \to z$$

provides the non-singular representation of CLE in the four-dimensional space of physical states, where u, v, w and z are the Cartesian coordinates. This representation is:

$$\begin{aligned} \dot{u} &= -(\sigma+1)u + (\sigma - r + z)v - (\sigma - 1)R, \\ \dot{v} &= -(\sigma+1)v - ew - (\sigma - r + z)u + (\sigma + r - z)R, \\ \dot{w} &= -(\sigma+1)w + ev, \\ \dot{z} &= -bz + v; \end{aligned} \tag{2}$$

where $R = (u^2 + v^2 + w^2)^{1/2} = (|x|^2 + |y|^2)/2$. The analysis of laser dynamics using eqs.(2) appears to be rather fruitful. We show that all physical information about the system, including the phase dynamics, Lyapunov exponents and capacity of attractor, may be obtained from equations (2) in a very clear way. Studying these equations we have found some peculiarities of phase dynamics, which can be interpreted as geometric phase manifestations. Apart from that, eqs. (2) provide an effective approach to the investigation of bifurcation phenomena in lasers, as we prove representing a number of new results on bifurcations in a detuned laser.

Using the unidirectional single-mode laser model, the possibility of Berry's phase observation in a steady state laser has been shown , which is due to the adiabatic roundtrip in the parameter space [2]. However, in this case the typical range of the laser parameters allows only very small geometric phase accumulation which in real experiments may be entirely masked by the noise. We have found that the effect can be more substantial in a multimode system. To demonstrate this we consider the equations of motion for the class A bidirectional ring laser [4]:

$$\dot{E}_{\pm} + \frac{\nu}{Q_{\pm}} E_{\pm} + g_{\pm} E_{\mp} = \chi_{\pm} E_{\pm},$$

where $Q_{\pm}$ and $\chi_{\pm}$ are the cavity Q and the nonlinear susceptibilities for two counterpropagating waves, whose amplitudes are $E_{\pm}$, and the complex parameters $g_{\pm}$ are responsible for the mode coupling due to the localized losses. We show that in this system the substantial geometric phase can be induced by switching the Q's and changing the location of the loss sources.

This work was supported by the Committee for High School of Russia (grant 94-2.7-1097).

REFERENCES

1.C.Z.Ning and H.Haken, Phys. Rev. Lett. 68, 2109 (1992).

2.V.Toronov and V.Derbov, Phys. Rev. A 49, 1392 (1994)

3.S.Kobayashi and K.Nomizu, *Foundations of differential geometry* (Interscience, N.Y., 1969)

4.M.Sargent III, M.O.Scully, and W.E. Lamb, Jr., *Laser Physics.* London: Addison-Wesley, 1974.

NONLINEAR DYNAMICS OF A TWO-PHOTON LASER WITH INJECTED SIGNAL IN THE HIGH-Q CAVITY LIMIT

J.F. Urchueguía[1], V. Espinosa[1], G.J. de Valcárcel[1,2], and E. Roldán[2]

[1] Departament de Física Aplicada, Universitat Politècnica de València,
Camí de Vera s/n, 46071-València, SPAIN

[2] Departament d'Òptica, Universitat de València, Dr. Moliner 50, 46100-Burjassot, SPAIN

e-mail: qoval@vm.ci.uv.es

Abstract

The dynamics of a class-A two-photon laser with injected signal is investigated. The possible mustistable configurations are determined. The stability of the steady state as well as that of the Hopf orbits is characterized.

In this work we present a model for a two-photon laser with injected signal (TPLIS) in the high-Q cavity limit, i.e., a class-A TPLIS. In this limit one can adiabatically eliminate the material variables. When the injected signal is resonant with half the two-photon atomic transition frequency the dynamics of the system is described by the single complex equation

$$\frac{d}{d\tau}x = A + \left[R\, g(I) - 1 + i\theta\right]x, \qquad g(I) = \frac{I}{1+I^2}, \tag{1}$$

where x and A represent the complex electric field and injected signal amplitudes, $I = xx^*$ represents the laser intensity, R is the incoherent pump parameter and θ is proportional to the mistuning between half the atomic transition and the cavity frequency. τ is the time normalized to the cavity damping rate. This model is similar to that recently studied by Zeghlache and Zehnlé for a one-photon LIS [1], the difference between both models arising from the function $g(I)$ in Eq.(1), which in the class-A LIS model reads $g(I) = 1/(1 + I)$.

We have found mono-, bi-, and tristable behaviours, and delimited the regions in the parameter plane (R, θ) where these configurations can exist. For large enough detunings only monostable behaviour is found, as in Ref.1, and bi- and tristable solutions appear as resonance is approached. Nevertheless the tristable behaviour cannot exist on resonance.

The linear stability analysis of the stationary solution of Eq.(1) reveals the existence of two independent Hopf bifurcations (HB) for $R > R_{thr} = 8/\sqrt{27}$. One of the HB's is associated with low intensity stationary solutions, and the other one with larger intensities, existing a gap between both. We have identified the regions in the parameter plane where none, one, and two HB's exist. A general feature is that detuning is essential for the existence of self-pulsing

instabilities, as it occurs in the class-A LIS. A difference between both models is that the pump required for the existence of Hopfs in the class-A TPLIS (R_{thr}) is smaller than the free-running two-photon laser emission threshold ($R = 2$). Another difference is the behaviour of the system when the injection A is increased from zero. In the class-A LIS the stationary solution is born unstable and gains stability either through a tangent bifurcation or through the (unique) HB of the system. In the class-A TPLIS the stationary solution is born stable, and loses stability through the low intensity HB, or through a tangent bifurcation. Since the higher intensity HB has a stabilizing effect, the stationary solutions with large enough intensity are stable in both models.

Finally we have studied the stability of the Hopf orbits near the HB's following the criterion of [2], and determined the regions in the parameter plane where the orbits are stable or unstable. Apart from these solutions there exist other (large amplitude) periodic solutions that have their origin at the free-running laser limit ($A = 0$), as in the LIS case. The existence of two of such solutions in the TPLIS (only one in the LIS) combined with the presence of up to two HB's makes the dynamic behaviour of the class-A TPLIS much more complicated, as is illustrated in Fig.1, which has been computed with the aid of program AUTO [3].

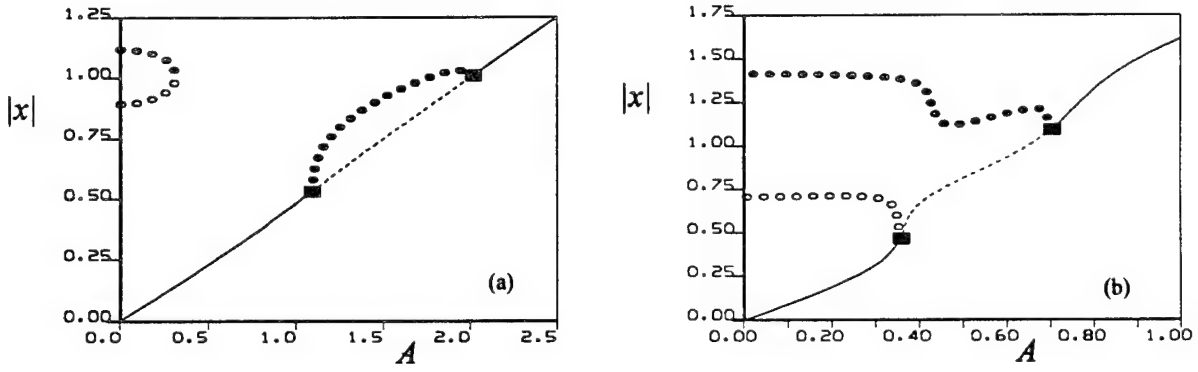

FIG.1. Modulus of the laser amplitude *vs* injected signal amplitude showing two of the possible bifurcation diagrams of the class-A TPLIS. The continuous (dashed) lines, and filled (open) circles, denote stable (unstable) stationary solutions an periodic orbits, respectively. The filled squares denote HB's. In both figures the two HB's are present. In (a) ($R = 2.05$, $\theta = 2.00$) there exists a branch of periodic solutions that connects both HB's, whilst the large amplitude periodic solutions form an isola. In (b) ($R = 2.50$, $\theta = 0.60$) these solutions connect with the HB's.

This work has been supported by the DGICYT (Spain) through Project No. PB92-0600-C03.

[1] H. Zeghlache and V. Zehnlé, Phys. Rev. A **46**, 6015 (1992)

[2] G.J. de Valcárcel, E. Roldán, and R. Vilaseca, Phys. Rev. A **49**, 1243 (1994)

[3] E.J. Doedel, AUTO: *Program for Continuation and Bifurcation Problems in Ordinary Differential Equations (AUTO 86)*, (1986)

Determinism and Stochasticity of Power Dropout Events in Semiconductor Laser Systems with External Feedback

H.J.C. van der Linden, A. Hohl, and R. Roy
School of Physics
Georgia Institute of Technology
Atlanta, GA 30306-0430
Tel: (404) 853-0027; Fax: (404) 853-9957
email: paul@socrates.physics.gatech.edu

Semiconductor lasers are extremely sensitive to external feedback, which can have dramatic effects on its operating characteristics. Power dropout events are one of these effects. During a power dropout, the laser intensity suddenly drops drastically, after which it slowly increases, reaches a metastable state, and then drops again, at irregular intervals. Explanations of the origin of power dropouts have tended to be exclusively deterministic [1] or stochastic [2].

We have included both deterministic and stochastic mechanisms in order to provide a comprehensive modelling of the dropout events. They occur when the laser is pumped around its solitary threshold; a laser undergoes a phase transition at this point. Near this phase transition stochastic fluctuations typically have a large influence on the operation of the system. We focus on the influence of these fluctuations on the dynamics of power dropout events. Numerical and experimental results indicate that noise plays a significant role in the characteristics of the dropout events.

Fig. 1(a) shows the time trace of laser intensity for an injection current slightly below the solitary laser threshold, computed from a model that is entirely deterministic. The results of the computation have been digitally filtered with a cut off frequency of 500 MHz so as to model the bandwidth limitations of the detection instrumentation. In Fig. 1(b) we have included appropriate noise sources in the computation, which is done with exactly the same initial conditions and parameters as in the previous case. The dramatic influence of the noise on the dropout dynamics is obvious. An experimentally measured time trace for operation slightly below the solitary laser threshold is shown in Fig. 2. The qualitative characteristics of the dynamics are in excellent agreement with the results from the model including noise.

Results on the statistics of the dropout events, and a detailed dynamical analysis of reflection instabilites will be presented.

References:

[1] K. Otsuka and H. Iwamura, Phys. Rev. A 28, 3153 (1983); T. Sano, Phys. Rev. A 50, 2719 (1994); G.H.M. van Tartwijk et al., submitted to IEEE J. Quantum Electron.; J. Mork et al., IEEE J. Quantum Electron. QE-28, 93 (1992); J. Sacher et al., Phys. Rev. A 45, 1893 (1992).

[2] C.H. Henry and R.F. Kazarinov, IEEE J. Quantum Electron., QE-22, 294 (1986)

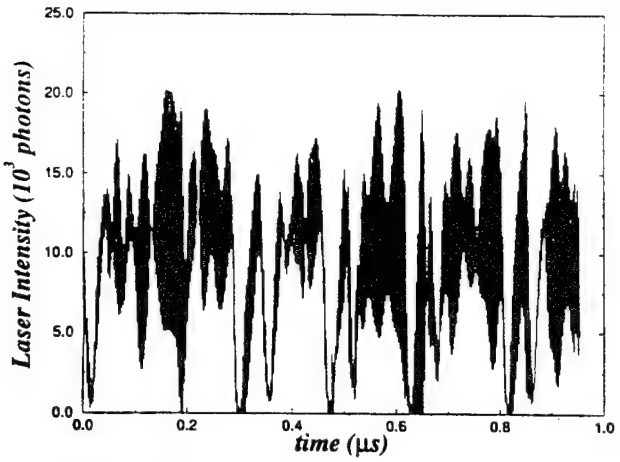

Fig. 1(a) Time trace of the laser intensity from the deterministic model, I/I_{th} = 0.99.

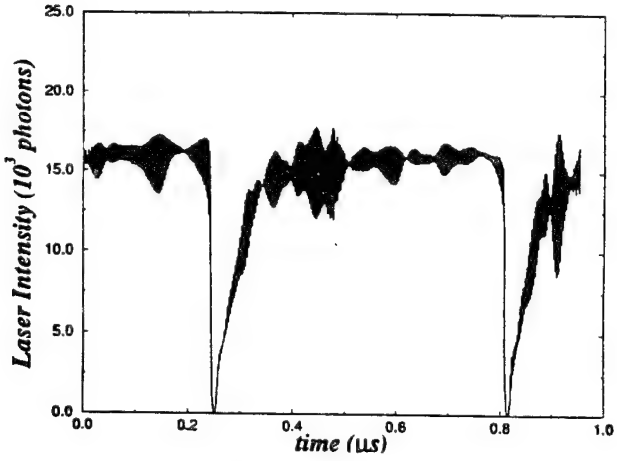

Fig. 1(b) Time trace of the laser intensity from the model with spontaneous emission noise; all other parameters the same as for Fig. 1(a).

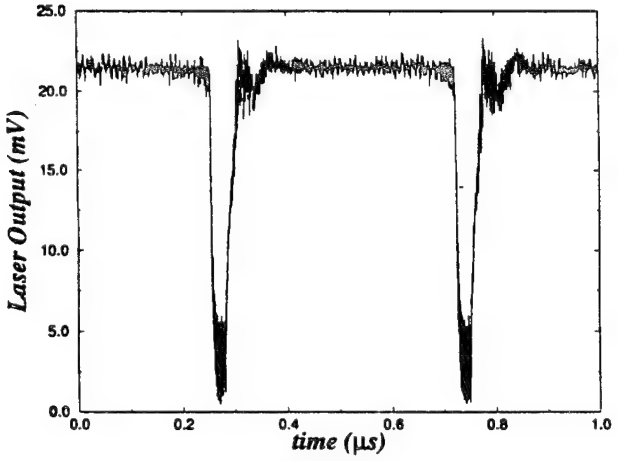

Fig. 2 Experimentally measured time trace for a laser with external reflection, I/I_{th} = 0.97.

Saddle Antiphase Dynamics of a Multimode Laser

E. A. Viktorov,
Institute for Laser Physics, Research Center, S. I. Vavilov State Optical Institute,
199034 St. Petersburg, RUSSIA
Phone: (812) 2189982 Fax: (812) 2181093 E-mail: vikt@ilph.spb.su

D. R. Klemer,
Spectra-Physics Laserplane,
5475 Kellenburger Road, Dayton, Ohio 45424
Phone: (513) 233-8921 Fax: (513) 233-7511 E-mail: klemer@me2.splp.com

M. A. Karim
University of Dayton, Center for Electro-Optics,
300 College Park, Dayton, Ohio 45459-0227
Phone: (513) 229-3611 Fax: (513) 229-2471

ABSTRACT

We have demonstrated, experimentally and theoretically, that for certain conditions of multimode lasing, saddle features of phase-space stationary states give rise to novel antiphase oscillations based on Shil'nikov dynamics and provide a hierarchy of the antiphase states in a miniature multimode solid-state lithium-neodymium-tetraphosphate (LNP) laser operating in three longitudinal modes with intracavity frequency doubling.

Antiphase oscillations exhibited by individual laser modes in a multimode solid-state laser with intracavity second-harmonic generation (SHG) were first observed experimentally by Wiesenfeld, et. al. [1], and the phenomenon of antiphase states is still a very active topic of research in nonlinear laser dynamics [2,3]. In our previous work [4], we described a special case of antiphase dynamics -- generation of homoclinic chaos in a multimode solid-state laser with intracavity SHG, exhibited when the laser is operating with a sparsely-active mode spectrum and phase-space trajectories are influenced by corresponding saddle features in the vicinity of stationary points. In the present work, we present the results of a comprehensive analysis of the influence of such saddle points on the antiphase dynamic behavior of a solid-state laser with intracavity SHG.

Our theoretical model is based on the multimode operation of a LiNd(PO3)4 (LNP) laser with homogeneous gain and an intracavity KTP doubler. We treat the case of three-mode generation under the condition that the central mode is polarized orthogonal to the side modes. For our model, the dynamic regime of interest corresponds to unstable points in phase space, some of which are saddle foci which satisfy the conditions of Shil'nikov's theorem in some region of the control parameter space [5]. Our saddle foci are unique stationary points for which one mode has zero intensity, locally causing the system to exhibit essentially two-mode dynamic behavior with the two nonzero modes having nearly similar magnitude. There are three possible situations which can occur in this case. For the first situation, the central mode has zero intensity and an antiphase process exists between the central mode and the two in-phase side modes. The central mode first exhibits ordinary decaying relaxation pulsations on an unstable phase-space manifold while the side modes remain quiescent; the central mode then itself becomes quiescent as the system transitions to a stable manifold, exhibiting relaxation pulsations of the side modes as the system moves toward a saddle focus point (fig. 1a).

For the second situation, we have two symmetrical saddle foci corresponding to one zero-intensity side mode. There are actually two different antiphase processes for this case: there is an energy exchange between the two nonzero modes at any instant, and there is a second exchange between two coupling groups, the first one formed of the central and one side mode, and the second formed of the central and the opposite side mode. It is important to note that for this situation, unlike the first, the imaginary parts of the eigenvalues for the linearized equations for the system correspond closely to a value of half the relaxation oscillation frequency (ROF), and energy exchange between the two nonzero modes can thus be observed to occur with a frequency of approximately ROF/2 (fig.1b).

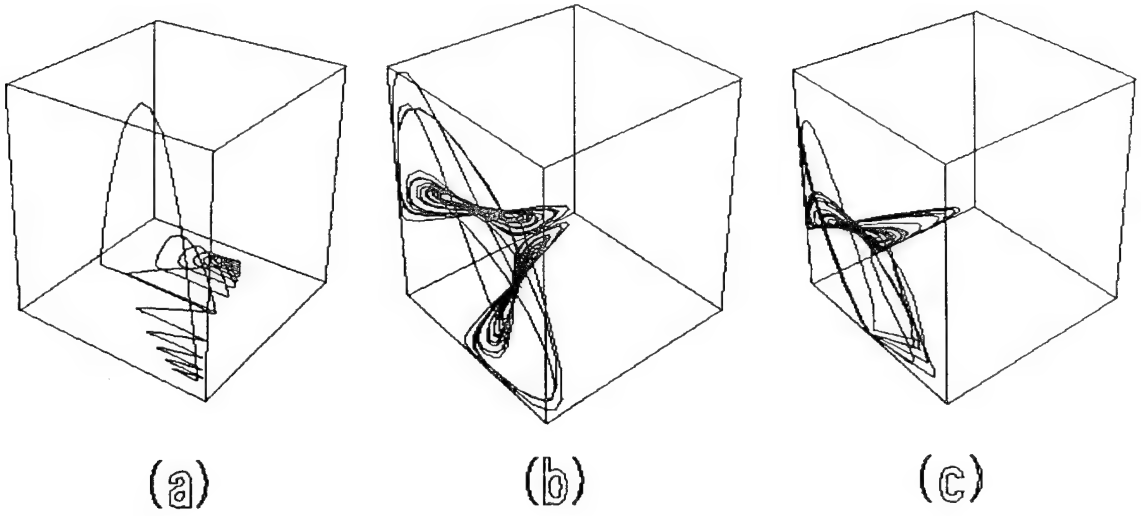

Figure 1. Phase-space attractors for the cases of (a) symmetrical spectrum with zero central-mode intensity saddle-focus, (b) symmetrical spectrum, zero side-mode intensity saddle-focus, and (c) sparse-spectrum.

The same situation occurs for a sparse mode structure, characterized by unequal longitudinal mode spacing arising from etalon and thin-gain-section effects within the cavity [4]. Sparse mode activity creates only a single saddle focus, and energy exchange occurs between the central mode and only one of the side modes. It is particularly interesting to examine the nature of saddle antiphase energy exchange. For normal three-mode antiphase dynamics, energy is transferred sequentially from one mode to the next [1-3]. For saddle antiphase operation, however, there appear to be two coactive antiphase processes, in the first of which, energy is transferred between two modes of nearly-equal intensity, while the third side mode is inactive. The second antiphase process involves a transfer of energy from the first two modes as they converge to the focus in phase space, and either (1) into the third side mode as the flow moves outward along a path tangent to the focus, whereupon the first two modes become quiescent, or (2) into a complementary antiphase process between the third side mode and the central one (fig.3c).

An additional saddle process occurs as saddle bifurcation of the symmetrical limit cycle into antiphase asymmetrical cycles (after Hopf bifurcation in the stationary regime). For every asymmetrical cycle, we have a process of period-doubling and two asymmetrical strange attractors arise with intermittency between them, and later coalesce into a single symmetrical strange attractor.

Experimental investigation was carried out using a diode-pumped LNP laser and a KTP doubler in a 10 mm hemispherical cavity. Linear losses in the cavity were around 1% per round-trip, and SH conversion imposed approximately 0.005% nonlinear loss. The laser was pumped in a range 35-45 times threshold. Various behavior ranging from stable to chaotic could be induced through cavity adjustment and adjustment of relative crystal orientation. Limit cycle creation, periodic pulsation and pure chaos were observed, as well as antiphase pulsations in individual mode portraits. Shil'nikov chaos with antiphase features was exhibited by the system, and dynamic behavior was in excellent agreement with the theoretical prediction.

REFERENCES

1. K. Wiesenfeld, C. Bracikowski, G. James, R. Roy, *Phys Rev Lett* **65** (1990), 1749.
2. K. Otsuka, P. Mandel, J. Wang, *OptComm* **112** (1995), 71-74
3. K. Otsuka, P. Mandel, S. Bielawsky, D. Derozier, P. Glorieux, *Phys Rev A* **46** (1992), 1692
4. E. A. Viktorov, D. R. Klemer, M. A. Karim, *Opt Comm* **113** (1995), 441-448.
5. I. M. Ovsyannikov, L. P. Shil'nikov, *Math USSR Sbornik* **58** (1987), 557.

Nonlinear interaction of transverse modes in a class-B laser

A.G.Vladimirov and D.V.Skryabin
Dept. of Quantum Electronics, Institute of Physics, St.Petersburg State University,
1 Ulianovskaya st., Petrodvorets,St.Petersburg, 198904, Russia
fax: +7 (812) 4287240; e-mail: andrei@dc1.phys.samson.spb.su

The dynamics of transverse modes in lasers has attracted considerable attention of researchers in the recent years. An experimental study of interaction of several transverse modes in CO_2 and Na_2 lasers was described in Ref.1. The results of numerical integration of the Maxwell-Bloch equations for the parameter values typical of these lasers and a solid-state laser were presented in Ref.2. However, bifurcation mechanisms responsible for the appearance of periodic and chaotic behavior of the mode amplitudes in class-B laser still remain rather unclear. Here we propose the simplest mathematical model to describe these mechanisms in a class-B laser operating in tree transverse modes. Basing upon analytical and numerical analyses of this model we study bifurcations of different periodic, quasiperiodic, and chaotic regimes.

We consider a class-B laser operating in three Gauss-Laguerre modes that belong to the families $q = 0$ and $q = 1$. Here $q = 2p + |l|$, where p (l) is the radial (angular) index. They are the fundamental mode ($p = 0, l = 0$) and the two doughnut ones ($p = 0, l = \pm 1$). We assume that (i) laser operates near the linear threshold; (ii) the detunings between the mode frequencies and the atomic resonance frequency are much smaller than the homogeneous linewidth, $(\delta\omega_0/\gamma_\perp)^2, (\delta\omega_\pm/\gamma_\perp)^2 \ll 1$; (iii) the characteristic time scale of mode amplitudes evolution τ is much larger than the time scale associated with the frequency separation of the families $q = 0$ and $q = 1$, $\tau \gg 2\pi/|\delta\omega_0 - \delta\omega_\pm|$. Then the mode amplitudes obey the equations

$$
\begin{aligned}
\partial_t I_0 &= 2I_0(\epsilon + M_0),\\
\partial_t M_0 &= -\gamma(M_0 + I_0 + (|Z_+|^2 + |Z_-|^2)/2),\\
\partial_t Z_+ &= Z_+ + RZ_- + (1 + i\Delta)(Z_+N_0 + Z_-N_2),\\
\partial_t Z_- &= Z_- + RZ_+ + (1 + i\Delta)(Z_-N_0 + Z_+N_2^*),\\
\partial_t N_0 &= -\gamma(N_0 + I_0 + |Z_+|^2 + |Z_-|^2),\\
\partial_t N_2 &= -\gamma(N_2 + Z_+Z_-^*).
\end{aligned}
\qquad (1)
$$

Here I_0 is the normalized intensity of the fundamental transverse mode and $Z_\pm$ are the normalized complex amplitudes of the doughnut modes. M_0, N_0 and N_2 are the spatial harmonics of the inversion. The parameter $\epsilon = \eta_0/\eta$, where $\eta_0(\eta)$ is the dimensionless pump parameter of the fundamental (doughnut) mode. $\Delta = \delta\omega_\pm/\gamma_\perp$, $\gamma = \gamma_\parallel/(\gamma_c\eta)$, where $\gamma_\parallel$ (γ_c) is the inversion (cavity) relaxation rate. R is the complex coefficient of the linear coupling between the doughnut modes. $R \neq 0$ when the cylindrical symmetry of laser cavity is broken [3]. Note, that for $I_0 = 0$ the equations governing the evolution of Z_+, Z_-, N_0, and N_2 are similar to those describing the interaction of the counterpropagating waves in a ring class-B laser [4].

We have performed a detailed bifurcation analysis of steady-state and time-dependent solutions of eqs.(1). Homoclinic loops responsible for appearance of antiphase pulsations of doughnut modes similar to the pulsations observed in experiment of Ref.5, and bifurcation mechanisms leading to quasiperiodic oscillations and their break-up have been investigated. It has been shown that for certain parameter values even a small linear coupling between the modes caused by axial symmetry breaking of the laser cavity can lead to the transition from regular to chaotic laser operation.

Eqs.(1) are invariant under the transformation $(Z_+, Z_-) \rightarrow (Z_-, Z_+)$. Nevertheless, we have found new type of periodic and chaotic solutions characterized by nonzero frequency splitting of the doughnuts. They arise due to spontaneous symmetry breaking caused by the nonlinear interaction of the modes. Presumably, this effect may be observed in experiment. In a bidirectional ring laser it manifests itself as a nonzero frequency splitting of the counterpropagating waves that can exist even if the counterpropagating directions are equivalent.

References

[1] A.B.Coates et al, Phys. Rev. A 49 (1994) 1452.

[2] M.Brambilla et al, Phys. Rev. A 49 (1994) 1427.

[3] R.López-Ruiz, G.B.Mindlin, C.Péres-Garcia, J.R.Tredicce, Phys. Rev. A 49 (1994) 4916.

[4] P.A.Khandokhin and Ya.I.Khanin, J.Opt.Soc.Am. B2 (1985) 225; A.G.Vladimirov, to be puplished.

[5] .H.Hennequin, D.Dangoisse, and P.Glorieux, Opt. Commun. 79 (1990) 200.

Correlation Dimension Analysis of Heterodyne Detection of High-Frequency Chaotic Oscillations from a Laser Diode with Optical Feedback

Nobuyuki Watanabe and Koichi Karaki
Basic Res. Dept., Olympus Optical Co., Ltd., 2-3 Kuboyama-cho, Hachiôji, Tokyo 192, Japan
Tel 81-426-91-8071 Fax 81-426-91-5709
e-mail (N.W.) peterson@ilab.olympus.co.jp (K.K.) karaki-k@rnet.olympus.co.jp

High frequency chaotic fluctuations of compound-cavity LD's output range 1~10 GHz. Since the direct detection of such high-frequency fluctuation cannot be accomplished by using currently available digital equipment, down-conversion of the signal by the RF-heterodyne technique is required. We analyzed numerically the relationship between the frequency gain response of band-pass filter (BPF) for IF signal and the behavior of the correlation dimension (CD) of the IF signal passing through the BPF and compared the CD of such IF signal and that the LD output (RF) signal.

Our numerical model consists of three parts: 1) a compound-cavity LD, 2) a local oscillator and 3) a band-pass filter, as shown in Fig.1. The first part of the model is the dynamics of the compound-cavity LD. The feedback coefficient of the external cavity κ through facet which face to external cavity is defined as $(1 - r_2^2)r_3/r_2$ for a Fabry-Perot-type laser diode, where r_2 is the amplitude reflection of the laser facet and r_3 is that of the external mirror. Here, we consider a weak feedback condition $\kappa \ll 1$ and neglected multiple reflections. The dynamics of the complex electric field $E_0(t)\exp\{j(\omega_0 t + \phi(t)\}$ and the carrier density $N(t)$ are governed by the *Van der Pol* equations[1] .

The second component of the model is a free running local oscillator. The rate equations for the local oscillator L_i which generates a sinusoidal wave are

$$\frac{dL_1(t)}{dt} = \omega_{L.O.} L_2(t), \tag{1}$$

$$\frac{dL_2(t)}{dt} = -\omega_{L.O.} L_1(t). \tag{2}$$

Here, $\omega_{L.O.}=2\pi f_{L.O.}$ is the angular frequency of the local oscillator.

The transfer function of the second order normalized band-pass filter is

$$T(s) = \frac{Y(s)}{U(s)} = \frac{\omega_d s^2}{s^4 + 2\xi\omega_d s^3 + \left(2\omega_c^2 + \omega_d^2\right)s^2 + 2\xi\omega_c^2\omega_d s + \omega_c^4}. \tag{3}$$

Here, $U(s)$ and $Y(s)$ are the Laplace transforms of the input and output signals of BPF respectively, $\omega_c = 2\pi f_c$ is the center angular frequency of the BPF, and $\omega_d = 2\pi f_d$ is the angular frequency that defines bandwidth and ξ is the damping coefficient. The rate equations of the band-pass filter derived from Eq.(3) are expressed with four integrands $Z_i(t)$ (i =1,...,4) as follows.

$$\frac{dZ_1(t)}{dt} = -\omega_c^4 Z_4(t) , \tag{4}$$

$$\frac{dZ_2(t)}{dt} = -2\xi\omega_c^2\omega_d Z_4(t) + Z_1(t) \tag{5}$$

$$\frac{dZ_3(t)}{dt} = -\left(2\omega_c^2 + \omega_d^2\right)Z_4(t) + Z_2(t) + \left(\frac{|E_0(t)|^2}{|E_{sol}(t)|^2} - 1\right)\cdot L_1(t), \tag{6}$$

$$\frac{dZ_4(t)}{dt} = -2\xi\omega_d Z_4(t) + Z_3(t) . \tag{7}$$

Here, $Z_4(t)$ is the IF output signal of the heterodyne detection.

In Eq.(6) the output light intensity of the compound cavity LD was normalized by the light intensity of solitary LD $|E_{sol}|^2$.

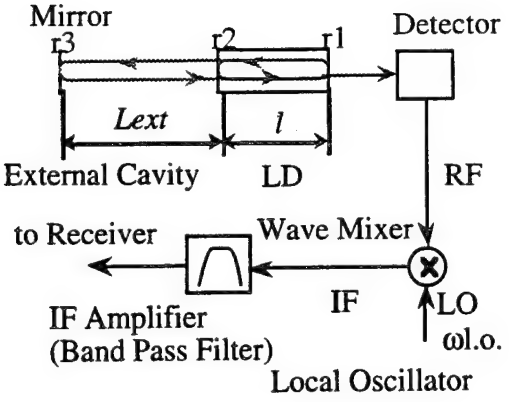

Fig.1 Heterodyne Detection Model

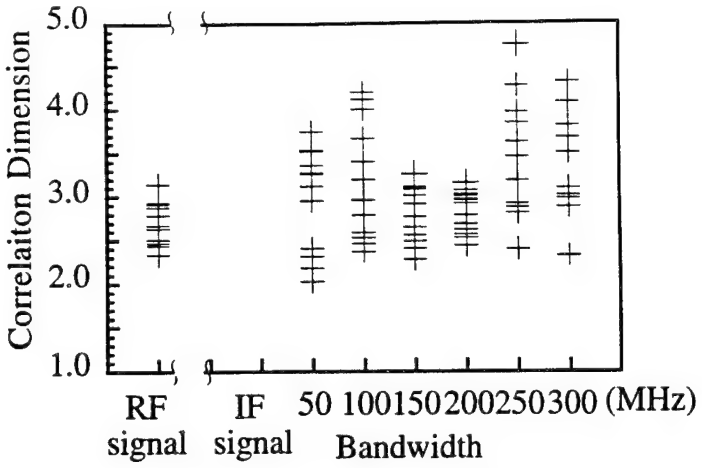

Fig2. Distribution of correlation dimension of RF signal and IF signal

The correlation dimension for the given time series is determined by examining the correlation integral[2]

$$C(r)=\frac{1}{N^2}\sum_{i\neq j}^{N}\Theta\left(r-\left|X_i-X_j\right|\right). \qquad (8)$$

Here, Θ is the Heaviside function which is equal to zero for a negative argument and one otherwise, N is the total number of sampling points, and $\|\ \|$ is the Euclidean norm. The reconstructed vectors X_i and X_j are obtained from the delay coordinate of the time series of the signals $(x_1,x_2,\ldots,x_L)$ as $X_i=(x_i, x_{i+\Delta\tau}, x_{i+2\Delta\tau},\ldots,x_{i+(m-1)\Delta\tau})$, where m is the embedding dimension and $\Delta\tau$ is the time delay. The correlation dimension is determined from the slope of the correlation integral $D = d\log C(r)/d\log r$ as a function of the embedding dimension m, where r corresponds to the radius of hyper-sphere that is centered at X_i in e m-dimensional space.

Figure2 shows the distribution of correlation dimension of the RF signal and IF signal passing through BPF of several bandwidth. By changing $\Delta\tau$, CD's values change, it suggest that the CD depend on the delay time, for finite number of time series which have finite time resolution.[3] The main peak frequency of RF fluctuation is 2.9GHz, and the sampling resolution is 0.02 ns. The delay time $\Delta\tau$ is varied from 5 to 30 times of the resolution (roughly equal to 0.3~1.74 times of the recurrent time). The CD values at m=12 are 2.64(RMS) ± 0.25(SD). For the heterodyne detection, $f_{L.O}$ and f_C were set to 2.8GHz, and 100MHz respectively. The resolution of time series was 0.1 ns (10GHz). The delay times $\Delta\tau$ were varied from 5 to 50 times of the resolution (roughly equal to 0.05~0.5 times of the recurrent time). By changing the bandwidth of BPF, the distribution of the CD values changes. The distribution of the CD of IF signal passing through proper bandwidth BPF (f_d = 150, 200MHz) are very similar to those of RF signal (2.64 ± 0.50 and 2.67 ± 0.41 respectively), whereas the distributions of CD of the IF signal passing through the narrower and the wider BPF are broader than that of RF signal (CD = 2.73 ± 0.82 for f_d = 50MHz, 2.96 ± 0.86 for f_d = 50MHz, 3.17 ± 0.95 for f_d = 250MHz, 3.05 ± 0.90 for f_d = 300MHz)

The fractal (scaling) nature of RF signal could maintain through the down conversion, if we choose the conditions of BPF. The RF heterodyne procedure may be analogous to the self-similar (Affine) transformation when the BPF and frequency of local oscillator satisfy the conditions that preserves the fractal nature of RF signal.

References

1. J. Mørk, B. Tromborg, and J. Mark, IEEE J. Quantum Electron. **QE-28**, 93 (1992)
2. P. Grassberger and I. Procaccia, Physica **9D**, 189 (1983)
3. T.Buzug and G. Pfister, Physica **58D**, 127 (1992)

Fast dynamics of an Er^{3+}-doped fiber ring laser

Quinton L. Williams and Rajarshi Roy
School of Physics
Georgia Institute of Technology
Atlanta, GA 30332-0430
(404)-853-9465 (phone) (404)-853-9958 (fax)
e-mail: gt4010a@prism.gatech.edu

January 30, 1995

Erbium-doped fiber lasers (EDFL) have been developed for femtosecond pulse generation and their use as a source of solitons [1]. Several groups have observed slow, irregular pulsations of the output intensity under conditions of c.w. pumping, and a number of studies of the dynamics have thus focused primarily on long time scales (~ microseconds to milliseconds) [2]. Here, we focus on some very interesting experimentally observed characteristics of an erbium-doped fiber ring laser, pumped at 980 nm, whose output was sampled on a nanosecond time scale.

In our investigations, we have studied the standard deviation of the intensity fluctuations as a function of pump power above threshold, as shown in Fig. 1. We have found that the intensity fluctuations grow rapidly with increasing mean output intensity, in contrast to the previously observed behavior of many other laser systems [3].

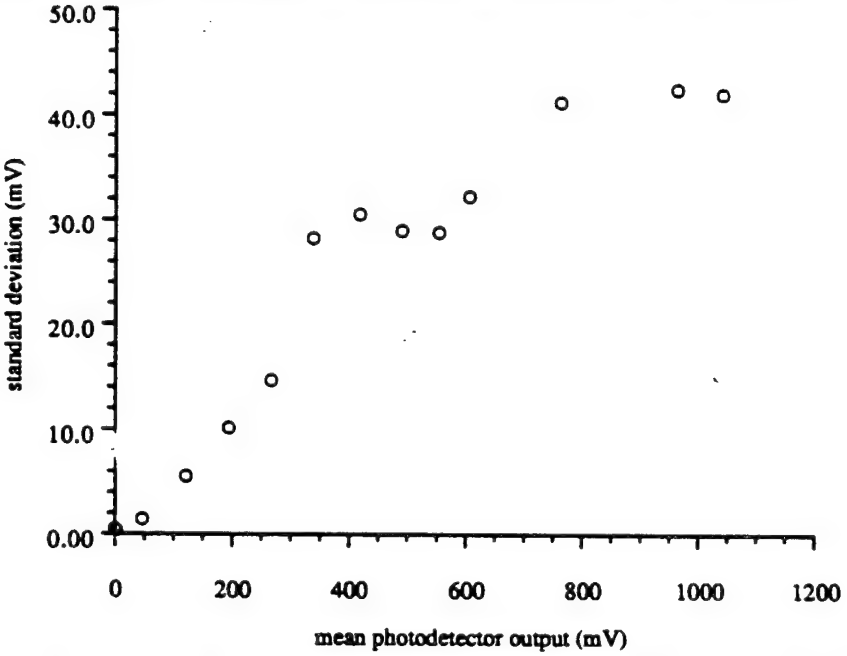

Fig. 1: Plot of the standard deviation vs. mean photodetector output averaged over three different time scales.

From measurements of the optical spectrum of the output intensity at many different pump powers (Fig. 2) we have calculated that over 2000 modes circulate within the full width at half maximum. Figure 3 shows two typical digital oscilloscope time traces of the output intensity, taken at delayed times with a Gigahertz sampling rate. We note that the waveforms between the large peaks are quasiperiodic. The waveforms are found to vary from trace to trace, displaying an enormous range of complex patterns.

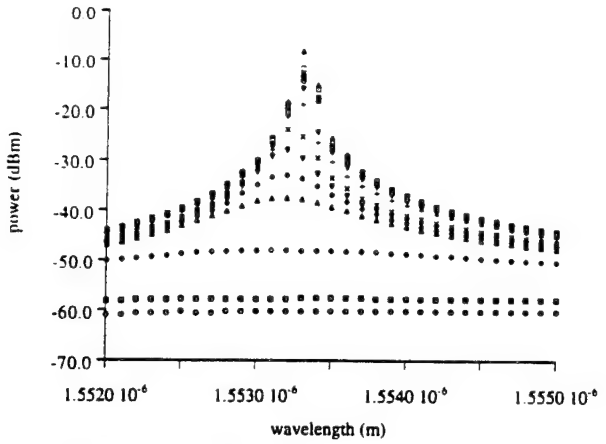

Fig. 2: Spectral plots of laser output from below to above laser threshold with increasing pump power.

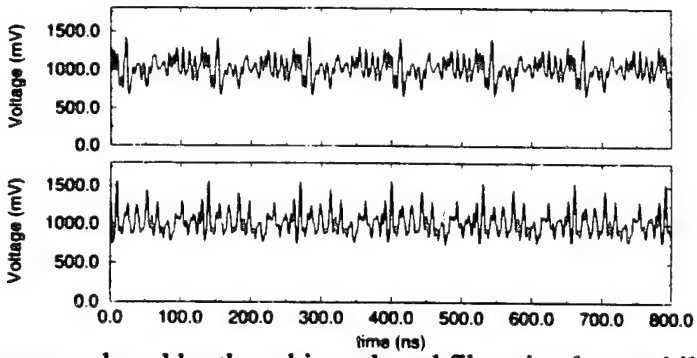

Fig. 3: Waveforms produced by the erbium-doped fiber ring laser while being c.w. pumped ~ 1.5 times above threshold. Sampling rate = 1 Gigahertz.

A model for the observed behavior is proposed, in which mode-mode coupling gives rise to phase-locking between some active modes, while others continue to oscillate with random phases. The result is an output intensity with large peaks separated by the fundamental cavity round trip time; in between there is a complex waveform produced by the modes that are not phase-locked. The long time scale (tens to hundreds of cavity round trips) over which the quasiperiodic temporal pattern is observed suggests that the modes with random phases preserve those specific phase relationships for many microseconds. Eventually, the phases are perturbed, and a new pattern is observed when the scope is next triggered. The experimental measurments will be compared with predictions of the simple model outlined above.

References

[1] E. Desurvire editor, *Selected Papers on Rare-Earth-Doped Fiber Laser, Sources and Amplifiers*, SPIE Milestone Series vol. MS 37, (SPIE, Bellingham, 1992).

[2] (a) P. Le Boudec, M. Le Flohic, P. L. Francois, F. Sanchez and G. Stephan, Opt. Quantum Electron. **25**, 359 (1993). (b) F. Sanchez, P. Le Boudec, P. L. Francois, and G. Stephan, Phys. Review A, vol **48**, no 3, 2220 (1993). (c) E. Lacot, F. Stoeckel and M. Chenevier, Phys. Review A, vol **49**, no 5, 3997 (1994).

[3] A. Yariv, *Quantum Electronics*, third edition,John Wiley and Sons, New York, (1967).

Transverse spatial modulation of a Gaussian beam in $BaTiO_3$:Ce

Ping Xie, Jian-Hua Dai, Peng-Ye Wang and Hong-Jun Zhang
Institute of Physics, Chinese Academy of Sciences, P. O. Box 603, Beijing, 100080, China
FAX: 86-1-2562605, E-Mail: user307@aphy01.iphy.ac.cn

We report the results of our numerical analysis of the transverse spatial modulation of a Gaussian laser beam after passing through a 45°−cut $BaTiO_3:Ce$ crystal. Our results show that an extraordinary Gaussian beam, after passing through the crystal, shows transverse spatial modulation and self-focusing[1] due to the refractive index change modulated by the beam itself. When the refractive index change has been induced by one beam (the first beam), another incoherent weaker beam with a wider beam width than the first (the second beam) shows much stronger transverse modulation after passing through the crystal.

Consider an extraordinary polarized Gaussian beam input into a 45°−cut $BaTiO_3:Ce$ crystal of thickness L, to which an electric field is externally applied. Since the photorefractive effect is strong only in the plane of extraordinary polarization, we restrict our consideration to two dimensions (transverse x and longitudinal z). The electric field amplitude $A(x,z)$ of the beam polarized along the x direction and propagating primarily along the z direction obeys the following paraxial nonlinear wave equation

$$\frac{\partial}{\partial z}A(x,z)-\frac{i}{2k}\frac{\partial^2}{\partial x^2}A(x,z)=\frac{ik}{n_e}\Delta n(x,z)A(x,z), \qquad (1)$$

where the refractive index change $\Delta n(x,z)$ can be obtained by consideration of the wave-mixings between different Fourier components of the amplitude $A(x,z)$,[2] i.e.,

$$\Delta n(x,z)=\frac{1}{|A(x,z)|^2}\iint dq_1dq_2f(q_1,z)f^*(q_2,z)e^{i(q_1-q_2)x}\exp[i(\beta_{q_1}-\beta_{q_2})z]\delta n(q_1,q_2). \qquad (2)$$

Here $f(q_1,z)$ is the spatial frequency distribution of the amplitude $A(x,z)$ and $\delta n(q_1,q_2)$ is the coupling coefficient between two components. We have numerically integrated Eq.(1) for the input Gaussian beam $A(x,z)=A_0\exp(-x^2/w_0^2)$. The numerical calculation is based on the difference method combined with the fast-Fourier-transform: At a given longitudinal z, we decompose the amplitude $A(x,z)$ into its Fourier components by the fast-Fourier-transform and then use Eq.(2) to calculate the refractive index change $\Delta n(x,z)$. Substituting $\Delta n(x,z)$ into Eq.(1) and integrating it by the difference method we obtain the $A(x,z)$ at the next z.

Fig.1(a) and (b) show, respectively, the refractive index change inside a crystal of thickness L=1 *mm* without and with the externally applied electric field of $E_0=120V/mm$ for an input beam waist of $w_0=40\mu m$. For no electric field the near antisymmetrical feature of $\Delta n(x,z)$ about the z axis will lead to the light intensity transferring from the left to the right side of the beam. The externally applied electric field mainly causes the in phase component of the refractive index change relative to the light irradiance. This leads to phase couplings between different plane components and the resulted refractive index change will be symmetrical about the z axis. The fact that the $\Delta n(x,z)$ is slightly larger at $+x$ than at $-x$ is caused by the $\pi/2$ out of phase component

of the refractive index change relative to the light irradiance. Fig.2 gives the transverse intensity distribution of the beam for the case with externally applied electric field. It can be seen that, after passing through the crystal, the beam shows spatial modulation and self-focusing effects. In addition, the amplitude maximum of the beam shifts towards the right.

From Fig.1(b) we see that the transverse range of the refractive index change is wider than that of the input beam intensity. It is thus anticipated that, if a weak second beam has a wider beam width than the first, the former will exhibit stronger transverse spatial modulation than the latter due to the refractive index change caused by the latter. This case is given in Fig.3 for the second beam width of $w_0 = 80\,\mu m$. It is seen that the transverse modulation and focusing effect are much stronger than those given in Fig.2.

The experimental data to verify the above results will be reported.

1. D.N.Christodoulides and M.I.Carvalho, Opt. Lett. **19**, (1994) 1714.
2. M.Segev, B.Crosignani, A.Yariv and B.Fischer, Phys. Rev. Lett. **15**, (1992) 471.

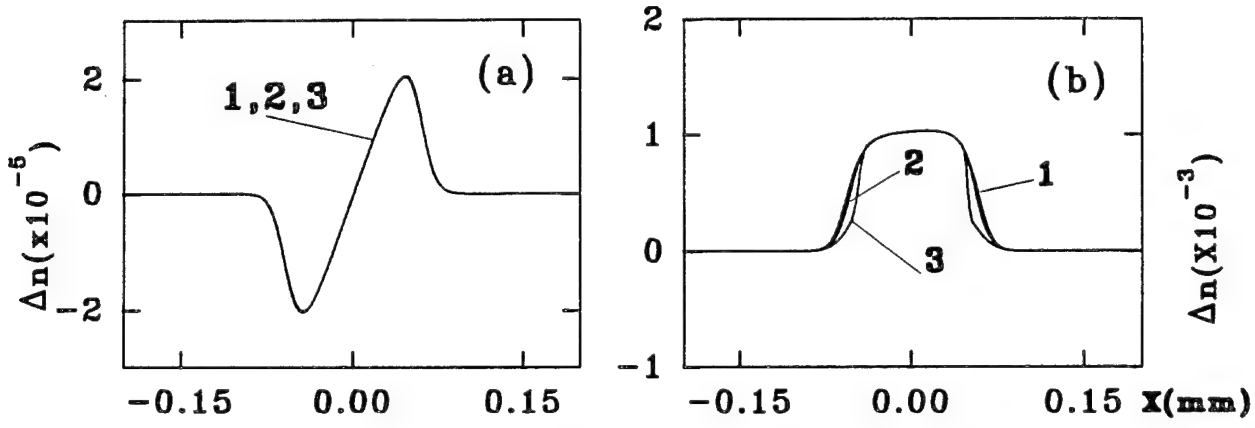

Fig.1. Refractive index change inside the crystal (a) with no externally applied electric field and (b) with the external field. Curves 1, 2 and 3 are for $\Delta n(x,z)$ vs. x at 0mm, 0.5mm and 1mm from the input face.

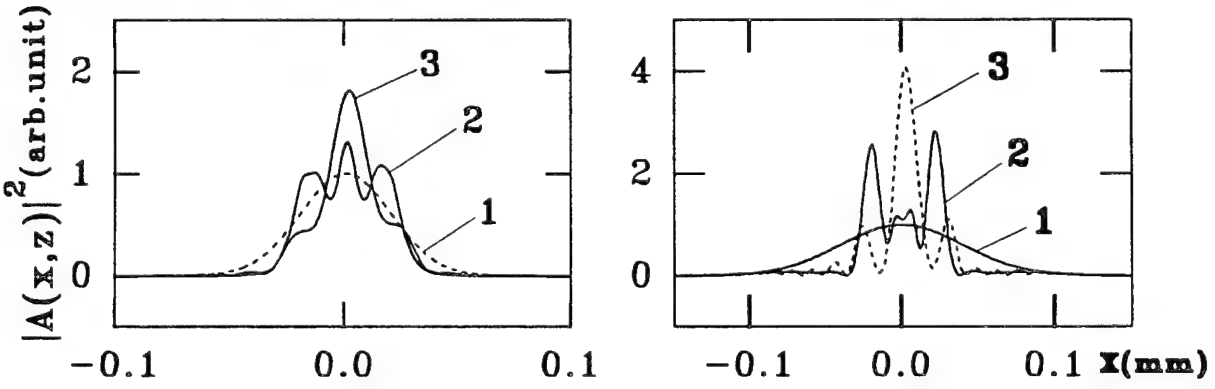

Fig.2. Transverse intensity distribution of the beam at input face(curve 1), and at z=1mm (curve 2) and z=2.5mm (curve 3) from the exit face of the crystal.

Fig.3. Transverse intensity distribution of the second beam at the input face (curve 1), and at z=1mm (curve 2) and z=3mm (curve 3) from the exit face of the crystal.

Exciton Interaction Effects in Optical Transient Grating

V.I. Yudson[1,2], Th. Neidlinger[1] and P. Reineker[1]

[1]Abteilung für Theoretische Physik, Universität Ulm, 89069 Ulm, Germany
[2]Institute of Spectroscopy, Russian Academy of Sciences, Troitzk, Moscow reg. 142092, Russia

Tel.: +49 (731) 502-2914; Fax: +49 (731) 502-2924; E-Mail: yud@theophys.physik.uni-ulm.de

There is a growing interest in nonlinear transient optical phenomena in dense media where the interaction of excitations is important. Most of research is devoted to systems with Frenkel or Wannier-Mott excitons which are electrically neutral complexes with zero static dipole moments. Here we study nonlinear optical response of a system of optically created charge transfer excitons (CTEs) [1]) with nonzero static dipole moments. Recently, the possibility of intrinsic optical bistability due to CTE-phonon interaction was theoretically predicted [2]. A phase transition of a high density CTE system into a metal state was discussed in a later work [3]. However, as estimated in [2, 3], the necessary CTE concentration is so high ($\sim 10\%$) that the problem of the stability of materials arises which may impede realization of the proposed phenomena.

Here we demonstrate that the effects of dipole-dipole interaction of CTEs may manifest in the "transient grating" optical response even at a relatively low CTE concentration. In this pump-probe process, the created excitonic density $n(\mathbf{r}) = n_0 + n_1 \cos(\mathbf{Q}\mathbf{r})$ is spatially modulated in accordance with the spatial modulation of the pump field; $\mathbf{Q}$ is the difference of the wavevectors of the two pump waves. A time delayed probe optical pulse is scattered by the grating in directions determined by the transfer of the grating wavevector $\mathbf{Q}$. The transient grating technique is used to measure the diffusion coefficient D of excitons. With an increase of the pump intensity and thus the density of excitons, the dipole-dipole interaction of CTEs cannot be ignored.

We present a quantative description of the CTE system in a thin layer; a static dipole moment μ of CTEs is chosen perpendicular to the layer. We study the range of temperatures $\mu^2/(\epsilon l^3) \ll T$ where l is the mean distance between CTEs on a layer and ϵ is an effective dielectric constant. We obtain the following nonlinear equation for the two-dimensional macroscopic density $n(\mathbf{r}, t)$ of CTEs:

$$\frac{\partial n(\mathbf{r},t)}{\partial t} = \nabla \left[D \left(1 + 2.8 l_T^2 n \right) \nabla n \right] - \gamma n, \qquad (1)$$

where γ is the decay rate of CTEs, and $l_T = (\mu^2/(\epsilon T))^{1/3}$. ¿From Eq.(1), we find the amplitude of the grating $n_1(t) = n_1(0)\exp(-\gamma_1 t)$, where $\gamma_1 = D_{\rm eff}Q^2 + \gamma$, and the effective diffusion coefficient $D_{\rm eff} = (1 + 2.4 l_T^2 n_0)\, D$. For reasonable values of CTE parameters we estimate the renormalization parameter $\zeta \equiv 2.4 l_T^2 n_0 \approx 0.2 \times [300\,{\rm K}/T]^{2/3}\,[n_0 \cdot 10^{-12} cm^2]$. Even at a room temperature, the influence of the interaction of CTEs becomes appreciable already at a rather moderate CTE density $\sim 10^{12} cm^{-2}$, i.e. at the concentration of excited molecules smaller than 0.05%.

In addition to the renormalization of the diffusion coefficient and of the grating decay rate, the interaction of CTEs manifests also via the generation of higher spatial harmonics ($n_2 \cos(2\mathbf{Q}\mathbf{r})$, etc.) of the initially excited grating. ¿From Eq.(1) we obtain the amplitude of the second harmonic

$$n_2(t) = -\frac{\zeta n_1^2}{2(1+\zeta)n_0}\left[\exp(-2\gamma_1 t) - \exp(-\gamma_2 t)\right], \qquad (2)$$

where $\gamma_2 \approx 4 D_{\rm eff} Q^2$. The appearance of the second spatial harmonic would result in a new peak of the scattered probe wave in the direction which corresponds to the transfer of the momentum $2\mathbf{Q}$ in the layer plane. Higher spatial harmonics may be generated too. It is important that both the renormalization of the diffusion coefficient and the generation of higher spatial harmonics may be appreciable even at a relatively small density of CTEs, thus one can avoid the problem of stability of organic materials at high pumping. This might be especially interesting in connection with possible applications in photonics.

References

[1] See, e.g., D.Haarer and M.Philpott, in: *Spectroscopy and Excitation Dynamics of Condensed Molecular Systems*, ed. by V.M.Agranovich and R.M.Hochstrasser (North -Holland, Amsterdam, 1983) p. 27.

[2] J.F.Lam, S.R. Forrest, and G.L.Tangonan, Phys.Lett.**66**, 1614 (1991).

[3] V.M.Agranovich and K.N.Ilinski, Phys.Lett. A**191**, 309 (1994).

Laser cooling

Physical mechanisms and ultimate limits

*****

Claude Cohen-Tannoudji

Collège de France and Laboratoire Kastler Brossel
24 rue Lhomond, 75231 Paris Cedex 05, France

*****

A review will be presented of various physical mechanisms allowing one to reduce the momentum spread δp of an ensemble of atoms to the lowest possible value. Emphasis will be put on recent developments which have led, in one, two and three dimensions, to values of δp well below the single photon momentum $\hbar k$. New theoretical approaches giving physical insight into the long time limit of these subrecoil cooling methods will be also described.

Controlling Chaotic Lasers

Rajarshi Roy
School of Physics
Georgia Tech
Atlanta GA 30332

Abstract

Over the past decade it has become clear that many different types of lasers exhibit chaotic fluctuations of intensity under a variety of operating conditions. These include exotic systems, such as the far infrared ammonia laser, as well as commonly used semiconductor lasers. Signatures of chaotic fluctuations in laser light and the comparison of experimental observations with predictions of numerical models will be reviewed. An important issue here is the development of measures that can separate noisy and deterministic components of dynamical behavior and provide information relevant for application of dynamical control techniques. While earlier work consisted of efforts to identify and classify chaotic behavior, the emphasis today is on the control of chaotic lasers, and possible applications.

Recent efforts to control chaotic systems have been remarkably successful in many different areas of science and technology. Dynamical techniques for the control of chaos allow a wide variety of waveforms to be stabilized and provide a completely new approach to the control of chaotic intensity fluctuations. Recent experiments require only small perturbations of parameters (about the ambient values). It has also been demonstrated that the stability regime of a laser system can be significantly extended through control and tracking of the unstable steady state. These results indicate the possibility of practical applications of nonlinear dynamics and show that it is possible to orchestrate the emission of light by large ensembles of atoms into complex or simple temporal patterns with rather small but judiciously chosen perturbations.

Several open questions have emerged from these studies. Can we control systems that have more than one positive Lyapunov exponent, i.e., more than one direction of instability in phase space? Second, how does intrinsic noise influence the dynamical behavior and controllability of chaotic systems? These questions will directly impact the control of spatio-temporal systems such as arrays of coupled lasers, or fiber laser systems. Can chaotic systems can be used to our advantage? The possibility of encoding information in a chaotic background and then decoding it in real time with a synchronized chaotic system will be reviewed. Experiments on synchronization of chaotic lasers will be described. The direct relevance of fundamental science to technological applications is clearly illustrated in this field.

QUANTUM ASPECTS OF OPTICAL PATTERN FORMATION

Luigi A.Lugiato

Dipartimento di Fisica dell'Università, Via Celoria 16, 20133 Milano , Italy
Phone +39-2-2392264
Fax +39-2-2392712
E-mail Lugiato@MILANO.INFN.IT

Abstract

The recent years have witnessed a growing interest in the phenomena of spontaneous pattern formation and transformation , which arise in nonlinear optical syatems. With respect to other systems (think, for example, of hydrodynamics, or nonlinear chemical reactions) which are more traditional in the study of structure formation , optical systems present the special feature of displaying interesting quantum effects, even at room temperature. In this paper we focus on the case of the degenerate optical parametric oscillator (OPO) . The parametric conditions are selected in such a way that , above threshold , the OPO emits a signal field with a stripe pattern configuration.
Above threshold, the quantum description reveals relevant quantum effects both in the far and in the near field ; these phenomena are related by a complementarity picture, which is in turn related to the wave and particle aspects of the e.m. radiation. The discussion will focus on the novel concept of **quantum images** , i.e. noisy images whose intensity and phase configuration is entirely uniform on average, but which display a regular spatial structure in the correlation function. It will be shown that the OPO can generate spontaneously quantum images both below and above threshold.
The analysis of quantum fluctuations below threshold completes the classic analogy with second order phase transitions , adding the necessary spatial aspects which were missing in the previous treatments.
With the help of appropriate stochastic realizations of the noisy dynamics of the system, we illustrate how a quantum image appears when it is observed via high frequency detection; the results will be displayed also by a video.

1) L.A.Lugiato and G.Grynberg, Europhys.Lett. **29** , 675 (1995)
2) A.Gatti and L.A.Lugiato, Phys. Rev. A , submitted

Chaos in Semiconductor Lasers with Optical Injection

A. Gavrielides

Nonlinear Optics Center, Phillips Laboratory,
3350 Aberdeen Avenue SE, Kirtland AFB, NM 87117-5776

We have experimentally obtained and theoretically analyzed a systematic map of the various instabilities in a master-slave pair of semiconductor lasers as the amount of optical injection power and degree of detuning is varied. Two distinct islands of chaos have been identified. They are separated by limit cycles, period doubling and transitions into and out of chaos. The period doubling mechanism is investigated analytically based on a new third order pendulum equation.

Here we report on experimental measurements and theoretical calculations based on a single mode rate equation model of a quantum well laser subject to strong external optical injection. Semiconductor laser diodes provide a technologically important system to investigate both high-speed nonlinear dynamics and noise processes in lasers. However, because of the very short time scales (subnanosecond) on which the dynamics occur, it is difficult to measure the time dependent behavior directly. Hence, fourier domain measurements must be combined with model calculations in order to extract detailed information about the nature of the dynamics. We have found a number of very interesting instabilities as the amount of injected power and the degree of detuning between the master and the slave laser is varied. For example the laser diode exhibits chaos over a bounded range of injection levels. As the chaotic regime is approached from either the lower or higher injection levels, it follows a *period-doubling* route *into* and *out* of chaos [1,2], though the route is largely obscured by spontaneous emission noise. Additionally, a new regime of period doubling occurs for injection levels well above the region of chaos.

In Figure 1 we see a systematic experimental characterization of the various dynamic behaviors encountered as we vary the amount of injected power and detuning between the master and the slave semiconductor laser. We identify the following regimes: (S)-stable injection locking, (4)-four wave mixing, (P1)-limit cycle dynamics, (P2)-Period-doubling transitions into and out of chaos, two distinct islands of chaos and (M1)-Multiwave mixing in several longitutinal modes. The identification of these regions was performed by carefully observing the optical power spectra. Refer to Figure 3 for a set of spectra demonstarting the above characteristics.

In order to gain a clear understanding of the nature of the various instabilities we have performed numerical simulations with a single mode rate equation model. The equations are cast in a form that emphasizes key dynamical parameters [3]:

$$\frac{dE}{d\tau} = GE + \xi cos\Psi + \zeta F', \tag{1}$$

$$\frac{d\Psi}{d\tau} = -\Omega - bG - \frac{\xi}{E} sin\Psi - \zeta F''/E, \tag{2}$$

$$T\frac{dN}{d\tau} = P - N - P(1+2G)E^2, \tag{3}$$

$$G = \frac{1}{2}[XN - Y(E^2 - 1)]. \tag{4}$$

Simulations were performed both with and without the noise sources present. The main effect of noise is to obscure the route to chaos. However there is an excellent qualitative and good quantitative agreement between our experimental data and the numerical calculations. There is very strong evidence that single mode rate equations capture the essential physics of a semiconductor laser subject to external optical injection.

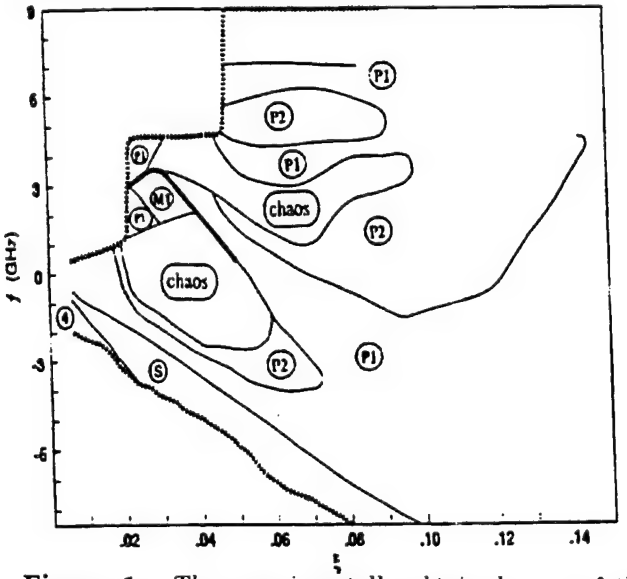

Figure 1. *The experimentally obtained map of the various instabilities for detuning versus injection.*

For example, the full nonlinear coupled equations are first solved with the noise source terms set to zero. Figure 2 depicts the numerically obtained bifurcation diagram of the the extrema of the amplitude, E, versus the detuning parameter, Ω. As the detuning level is varied from negative to positive, the steady state

is destabilized, the relaxation frequency becomes undamped, and a limit cycle is born. Further increasing the detuning, results in a period-doubling route to chaos followed by an abrupt transition to a limit cycle. With a further increase of detuning another period doubling is observed leading to chaos. This bifurcation diagram should be compared with the six observed optical power spectra in Figure 3. Very good agreement is obtained between theory and experiment.

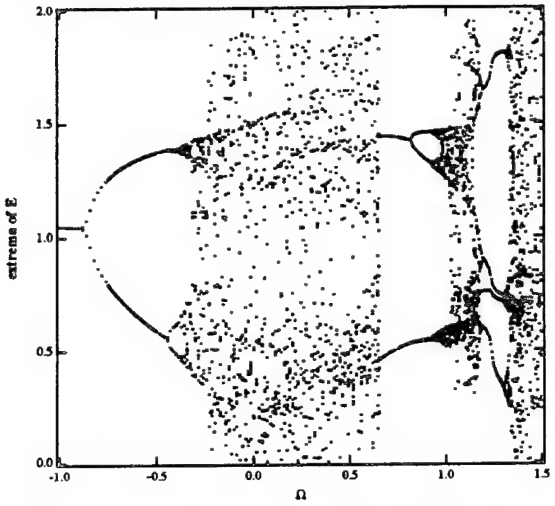

Figure 2. *Numerically obtained bifurcation diagram of the extrema of the normalized optical field amplitude, E, versus the detuning level, Ω. The injection is $\xi = 0.026$. Labeled detuning levels are for comparison with Figure. 3.*

The success of this model motivated us to look for an analytic understanding of the various instabilities. We take advantage of the typical values of the semiconductor laser parameters, in particular the ratio of the photon and the carrier lifetimes, in order to reduce the optical injection model asymptotically to an equation of a harmonic oscillator driven periodically by the phase of the laser field. The mechanism [5] for cascading period doubling instabilities then corresponds to successive subharmonic resonances. The reduced problem can be analyzed in terms of the phase only which satisfies a third order pendulum equation of the form:

$$\frac{d^3\Psi}{dt^3} + \frac{d\Psi}{dt} = \Lambda cos(\Psi) \qquad (5)$$

where $\Lambda = b\xi/\Omega_r$ and $\Omega_r = \sqrt{2P/T}$. This equation captures several aspects of the numerical bifurcation diagram, namely the fixed amplitude of the Period 1 solution and the period doubling bifurcation. This provides a powerful tool for investigating the dynamics of large arrays of semiconductor lasers.

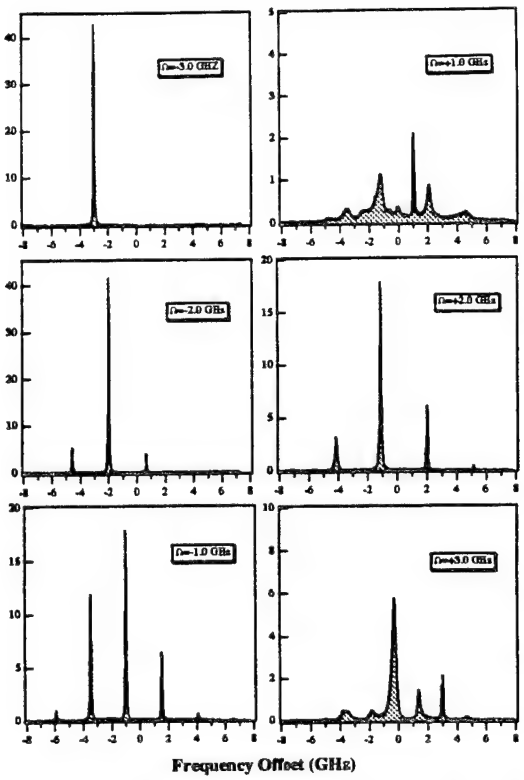

Figure 3. *Measured power optical spectra of the quantum well laser laser at an injection level $\xi = 0.026$ at six levels of detuning Ω (a) at $\Omega = -3GHz$ the laser is injection locked, (b) limit cycle at $\Omega = -2GHz$, (c) period doubling at $\Omega = -1GHz$ (d) chaos at $\Omega = +1GHz$, (e) abrupt transition to at limit cycle at $\Omega = 2GHz$, and (f) transition back to chaos at $\Omega = 3GHz$.*

Finally we will present possible applications of injection locking to improve the broadband modulation characteristics of semiconductor lasers. By adjusting the frequency offset between the master and the slave laser, improved modulation bandwidth and flatness of the modulation response can be achieved.

[1] T.B. Simpson, J.M. Liu, A. Gavrielides, V. Kovanis, and P.M. Alsing To appear in Physical Review A 1 April (1995).

[2] T.B. Simpson, J.M. Liu, A. Gavrielides, V. Kovanis, and P.M. Alsing, Appl. Phys. Lett. **64**, 3539 (1994).

[3] T. B. Simpson and J. M. Liu, J. Appl. Phys. **73**, 2587 (1993).

[4] J. M. Liu and T. B. Simpson, IEEE J. Quantum Electron.**30**, 957 (1994).

[5] T. Erneux, V. Kovanis, A. Gavrielides, and P. M. Alsing, To appear Physical Review A June (1995).

Nonlinear Optical Properties of Quasi-One Dimensional Magneto-Excitons

Daniel S. Chemla
Department of Physics, University of California at Berkeley
Materials Sciences Division, Lawrence Berkeley Laboratory

1 Cyclotron Road
Berkeley, CA 94720

Tel 510-486-4999
Fax 510-486-7768
email: DSChemla@lbl.gov

SUMMARY

Application of a strong magnetic field to a bulk semiconductor reduces the dimensionality of the electronic excitations from 3D to 1D. This gives the opportunity to explore the nonlinear optical properties of one dimensional systems in high quality material, without size fluctuation while avoiding the fabrication of delicate samples.

In this talk we report the first investigations of ultrafast nonlinear optical spectroscopy of GaAs under magnetic field up to 12 Tesla.

We find that even the linear absorption is strongly modified by application of a magnetic field. The lowest energy magneto-excitons remain Lorentzian under magnetic field. However, the high energy magneto-excitons that appear at the onset of the Landau level transitions, become Fano-resonances due to quantum interference with the underlying 1D continua.

The nonlinear optical properties of the two species of excitons were investigated by ultrafast four wave mixing (FWM). The Time resolved amplitude (TR-FWM) and power spectra (PS) were measured as well as the time integrated amplitude (TI-FWM). It was found that the two types of excitons exhibit very contrasted nonlinear optical properties.

For the Lorentzian excitons, the magnetic field enables us to tune the strength of Pauli Blocking relative to that of Coulomb interaction. Signature of exciton-exciton interaction as well as quantum beats were observed. Surprisingly the spectrally resolved FWM exhibit extra resonances that are not seen in the linear spectra. They may be related to excited states of the excitons that, in the linear absorption spectra, are masked by broadening in the absorption edge.

The Fano resonances exhibit the most unusual temporal behavior either in coherent wave mixing or in their quantum beats with the Lorentzian excitons. While the TR-FWM and PS correspond to the same dephasing time, the TI-FWM is instantaneous! This reveals a new type of quantum interference which most likely originates from the fact that Coulomb interaction governs both the appearance of Fano resonance and their nonlinear response. This behavior has even more striking consequences on the quantum beats between Lorentzian and Fano magneto-excitons. Just a few percent of contribution associated with the latter can quench most of the emission of the former! These experimental results are new and so far not explained.

PHASE-CONTROLLED PHOTOCURRENTS IN SEMICONDUCTORS

E. Dupont, P.B. Corkum
Steacie Institute for Molecular Sciences, National Research Council,Ottawa, Ontario K1A 0R6, Canada

H.C. Liu
Institute for Microstructural Sciences, National Research Council, Ottawa, Ontario K1A 0R6, Canada

We experimentally show that all-optical control of the photoresponse of GaAlAs quantum well detector can be achieved using quantum interference in the continuum between free electronic waves which are excited by two different pathways.

Initially, this effect of interference between different quantum pathways was first demonstrated in Xenon photo-ionization experiments[1,2]. Taking profit of the quantum interference phenomena between optical transitions in rubidium, Yin *et al.*[3] could control the angular distribution of photoelectrons. These experiments prove that, in some cases, the phase of a quantum state is as important a variable as frequency. The importance of phase is equally true in single atoms or in semiconductors. For instance, it was recently observed that quantum beats in coupled quantum wells excited with two consecutive laser pulses depended on the relative phase difference between the two pulses[4].

The idea to extend the general concept of phase-controlled photo-ionization to semiconductor devices was theoretically discussed by Kurizki *et al.*[5]. Here, we experimentally show that this concept of coherent control is not confined to atomic quantum systems ; it can also be applied to more complicated materials like solid-state devices. Indeed, we report here all-optical modulation of photocurrent, including *its sign*, in standard mid-infrared GaAs/GaAlAs quantum well (QW) detectors by controlling the quantum interference between two degenerate states in the continuum. Two independent quantum paths were used to "populate" these continuum states (see Fig1). The two paths were (1) a two-photon non-resonant electron intersubband transitions[6] at 10.6μm to excite electrons from the ground level to the symmetric state |E,S> and (2) a linear absorption at 5.3μm to excite electrons to the antisymmetric wave |E,A>. These simultaneously excited states interfere and, depending on the phase ($\varphi_{10.6}$,$\varphi_{5.3}$) and the intensity of each beam, the electron can be partially or completely described by a positive or negative progressive wave. One can estimate the current density j resulting from the interference:

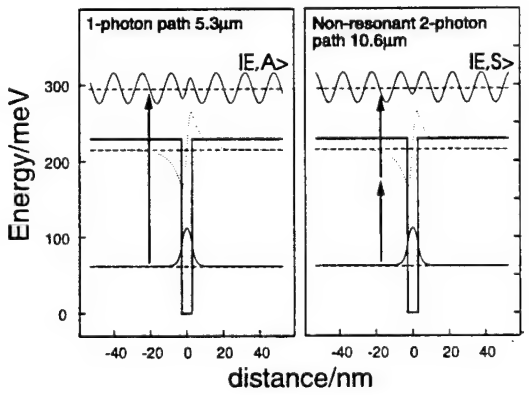

Fig. 1 The two quantum pathways from the ground state to the energy level |E> in the continuum.

$$j = q\frac{n_s}{L}\frac{2\pi}{\hbar}\mu^{(2)}\mu^{(1)}E_\omega{}^2E_{2\omega}D_{1D}^*(E)\tau\frac{\hbar k'\sin\left(2\varphi_{10.6}-\varphi_{5.3}\right)}{m'\sqrt{1+\left(\left(m'k/mk'-mk'/m'k\right)/2\right)^2\sin^2(kd)}} \qquad (1)$$

where m and m' stand for the effective mass in the well and the barrier; k, k' represent the longitudinal free electron momentum in the well and the barrier with an energy E; $\mu^{(2)}$ and $\mu^{(1)}$ are the dipole moments of the linear and quadratic absorption; E_ω and $E_{2\omega}$ are the amplitude of the fundamental and the second harmonic field; D_{1D}^* is the one-dimensional density of state; L is the superperiod of the structure; n_s is the electron concentration in the QWs; τ is the free electron collisional relaxation time. Practically, the sin function in this expression implies that by adjusting the phase difference $\Delta\varphi = 2\varphi_{10.6} - \varphi_{5.3}$ the electron can

be directed to the right or to the left of the quantum well. The expresion within the square root describes the energy dependence of the dipole moment between the symmetric and antisymmetric states, and therefore the strength of interference.

In our experiment, the 5.3μm photons come from the second harmonic of a 10.6μm CO_2 hybrid TEA laser. The relative phase of the co-linear 5.3 and 10.6μm beams is varied by passing the two beams through a 1" NaCl crystal mounted on a rotating stage (see Fig. 2). After amplification, the signal are recorded on a digital scope and gated integrators. The figure 3 shows a scan of the photoresponse of a detector when one rotates the salt crystal. The sign of the photocurrent can be inverted by a rotation of the salt crystal of few tenths of degrees. From the period of the fringes the deduced dispersion $n_{2\omega} - n_{\omega}$ of our NaCl window is 2.54×10^{-2}, which is 7% lower than the data book value. As described above by Eq.1, the amplitude of oscillations varies linearly with the 10.6μm intensity. We checked that this signal is strongly sensitive on the polarization, which is expected for intersubband excitation in n-doped GaAs/GaAlAs QWs. Other coherent-control experiments using bound-to-bound transitions in asymmetric InGaAs/GaAlAs quantum wells and free-to-free transitions in bulk photodetectors[7] will also be presented.

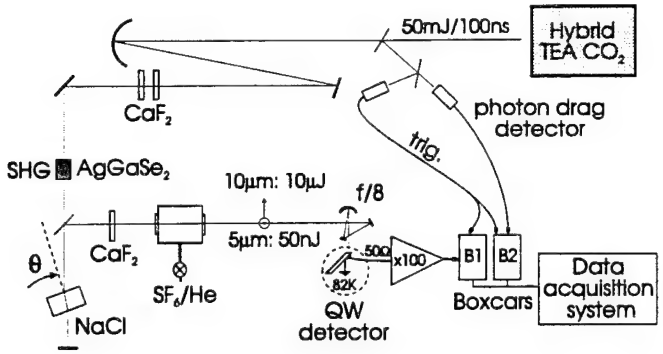

Fig.2 Experimental set-up of the coherent-control experiments

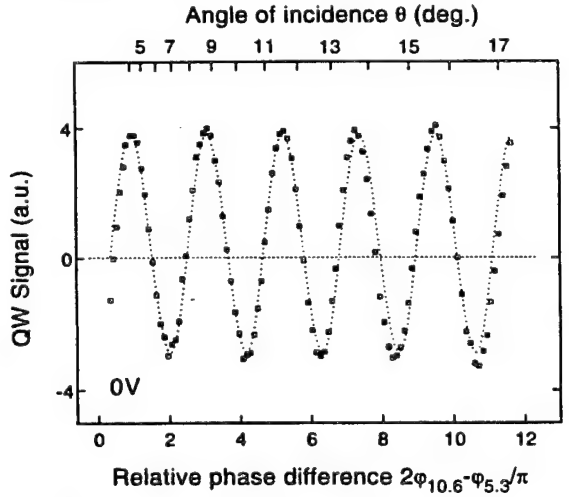

Fig.3 Photoresponse of a 8μm QW detector vs. the relative phase shift between the 5.3 and 10.6μm beams.

References:

[1] J.C. Miller, R.N. Compton, M.G. Payne, W.W. Garret, *Phys. Rev. Lett.* **45**, 114, (1980).

[2] D.J. Jackson, J.J. Wynne, P.H. Kes, *Phys. Rev. A* **28**, 781, (1983).

[3] Y. Yin, C. Chen, D.S. Elliot, *Phys. Rev. Lett.* **69**, 2353, (1992).

[4] P.C.M. Planken, I. Brener, M.C. Nuss, *Phys. Rev. B* **48**, 4903, (1993).

[5] G. Kurizki, M. Shapiro, P. Brumer, *Phys. Rev. B* **39**, 3435, (1989).

[6] E. Dupont, P. Corkum, H.C. Liu, P. Wilson, M. Buchanan, Z. Wasilewski, *Appl. Phys.Lett.* **65**, 1560, (1994).

[7] J.B. Khurgin, *Int. J. of Nonl. Opt. Phys.* (to be published).

Spatial Solitons in Wide-Aperture Nonlinear-Optical Systems

N. N. Rosanov

Institute of Laser Physics
Research Center "S.I.Vavilov State Optical Institute"
199034, St.Petersburg, Russia
Phone (812) 5601874, Fax (812) 2181093, E-mail rosanov@ilph.spb.su

The spatial (or spatio-temporal) solitons present localized patterns in wide-aperture nonlinear-optical systems. Their global features, as well as character of their interaction, vary significantly in different systems. In the present paper I describe and compare the features of spatial solitons in a number of coherent passive and active wide-aperture optical systems with fast nonlinearity.

1. Spatial solitons in transparent medium with saturable self-focusing.

In such a medium light power is conserved; for a wide beam a transverse instability (filamentation) takes place. There is a family of stable spatial solitons with continuous variation of their characteristics (i.e., the soliton maximum intensity). Stationary distributions with nonzero topological index (vortices) are metastable. Interaction of two spatial solitons is ***weak*** if the longitudinal size of zone of their strong overlapping is small enough. Then the perturbation theory gives only small changes of their parameters. In the opposite case of ***strong*** interaction, numerical simulations predict different types of inelastic collision, including formation of new solitons.

2. Laser autosolitons.

Such stable localized dissipative structures exist in wide-aperture laser with nonlinear losses (hard excitation of lasing) even without the modulation instability. The maximum intensity of a single laser autosoliton is definite. Its transverse velocity is arbitrary (in a laser with infinite aperture) or definite (in a laser with spatial filtration). Laser autosolitons with different topological indices (including vortices) are stable. Interaction of two laser autosolitons may also be either weak or strong. In the latter case the number of autosolitons does not conserve. Coupled states of two autosolitons are stable. There are autosoliton structures rotating with constant angular velocity ("planetary systems"). Reflection of laser autosoliton from the mirror edge may result in cardinal changes of its type.

3. Diffractive autosolitons in driven nonlinear interferometers.

For their existence the filamentation is not necessary. In absence of filamentation there is a graphical interpretation of diffractive autosoliton as a coupled state of switching waves. These localized dissipative structures have definite maximum intensity and discrete spectrum of their width. Transverse velocity of a single diffractive autosoliton is zero or nonzero constant in the interferometer without or with spatial filtration, respectively. There are coupled diffractive autosolitons, both transversely motionless (symmetric pairs) and moving (asymmetric structures).

SELF-CONSISTENT MODELS OF LASING WITHOUT INVERSION: PROBLEMS AND PROSPECTS

Olga Kocharovskaya
Institute of Applied Physics Russian Academy of Science,
46 Ulyanov Street, 603600 Nizhny Novgorod, Russia,
fax: 7-831-2-363792, e-mail: kochar@appl.nnov.su
and
Universite Libre de Bruxelles, Campus Plaine, Code Postal 231,
1050 Bruxelles, Belgium,
fax: 32-2-6505824, e-mail: kochar@ulb.ac.be

We review the recent progress both in the theory and experiment on amplification without inversion (AWI) and discuss the prospects for the further development of this rapidly extending domain of investigations.

We concentrate mainly on the analysis of those models which predict a possibility of amplification without "hidden" inversion in any atomic states basis. The major attention is paid to the problem of self-consistency of such models.

Their analysis until now was traditionally based on the Maxwell-Bloch equations, where either incoherent or coherent pumping were incorporated into the set of equations, phenomenologically. In order to be sure that amplification without "hidden" inversion is a real observable process one needs to turn to the self-consistent analysis.

We concentrate mainly on two simplest closed three-level schemes:(i) scheme with both radiative pumping and radiative decay to a common level involving no coherent pumping (ii) so-called P-scheme with a microwave coherent pumping. Our analysis is based on the self-consistent master equations derived for the schemes under consideration from the first principles [1,2].

In the distinction from the phenomenological treatment such self-consistent analysis verifies impossibility of

amplification without inversion in the closed three-level system involving no coherent pumping. It shows also a modification of the inversionless amplification conditions in P-scheme caused by field-dependent spontaneous relaxation.

Both a character and a magnitude of these modifications depend essentially on the position of the adjacent level 2 with respect to the operating levels 1 and 2. The most drastic changes correspond to the crossing between the ground state 1 and the lower dynamic Stark level. Such crossing results in the reverse of the spontaneous emission direction between these two levels. It may provide a new mechanism of inversionless amplification based on the depletion of the ground state and population trapping of atoms into the dynamic Stark level.

We discuss also the applicability of the above results to the nuclear transitions as well as the advantageous of different schemes of inversionless amplification for a realization of the gamma-ray laser which is one of the most attractive goals. We show that a choice of the appropriate scheme depends essentially on the relaxation time of population of the upper operating level T_1. In case of the short-lived isomers ($T_1 < 10^4$ s) a double Λ scheme is the most appropriate while in case of the long lived isomers ($T_1 > 10^4$ s) one should turn to a three-level scheme with a coherent pumping. The estimates show that a requirement for an incoherent pump rate may be essentially weakened in the inversionless amplification schemes. However the weakness of the nuclear transitions results in a hard requirement on the intensity of the coherent pumping.

This research was partially supported by Russian Foundation for Fundamental Researches (grant 93-02-3647).

References

1. O.Kocharovskaya, *et al.*, Phys. Rev. **A 49** (1994) 4928.
2. O.Kocharovskaya and P.Mandel, Quant.Optics **6** (1994), 217.

Ball Bistability

A.N. Oraevsky
P.N. Lebedev Physics Institute, Russian Academy of Sciences, 53 Lenin Prospect, 117924
Moscow, Russia, Tel. 132-1529, F. 336-0901, E. oraevsky@sci.fian.msk.su

D.K. Bandy
Physics Department and Center for Laser Research
Oklahoma State University, Stillwater, Oklahoma 74078,
Tel.405-744-7488, F. 744-6406, E. physdkb@osu.ucc.okstate.edu

Solid-state microballs are proposed as small-size optical bistable elements. The bistability condition for a semiconductor material is derived. It is shown that the bistability condition can be fulfilled for microballs as small as 10 micrometers in diameter.

Summary

Optical bistability is a topic of research pursued for more than thirty years [1], since the origin of optical computers and their association with small optical bistable elements. The classical model for optical bistable elements called for a resonant absorbing medium inserted in a cavity. Important theoretical and experimental results were obtained using this model, but technological difficulties prohibited realistic engineering. Thus, the search for a realistic optical bistable element continues.

A possible way to solve the problems associated with the development of realistic bistable optical elements is by using solid microballs. If the microballs are made of a sufficiently large dielectric susceptibility, we can obtain the necessary associated high-Q electromagnetic field modes, commonly called the whispering-gallery modes, inside this ball. An experiment [2] shows that the Q of the quartz balls of diameter of 140 μm reaches 10^9. It decreases as the ball diameter decreasing but is significant (10^5) even for the diameter of just 14 μm. Recently, quartz microballs were used as an external cavity for frequency stabilization and linewidth narrowing of semiconductor laser radiation [3].

Pure quartz is not a suitable material for optical bistable microball elements because a resonant, well-structured absorption line is required for existence of optical bistability. The bistable microball can be made of different solid substances which are widely used as laser

materials. In particular semiconductor materials appear very attractive. Semiconductors are good materials for a high-Q microball cavitiy because it has a large refractive index. GaAs, for example, has an index of 3.6. Therefore, it is possible to expect that the Q-factor of a cavity made of semiconductor will decrease less as its diameter decreases than the decrease of the Q-factor of the quartz ball when its dameter decreases.

It will be shown in our paper that the bistability condition for semiconductor materials has the form

$$\sigma n_t \tau_c \frac{\alpha}{c} > 3\sqrt{3} \qquad (1)$$

Here σ is a crossection of the band-band transition; n_t is a carrier concentration in a carrier band corresponding to the transparency condition; α is a line width enhancement factor; τ_c is the photon lifetime in the cavity; c is the speed of light in the material. Using standard values for semiconductor parameters we show that condition (1) can be satisfied for microballs as small as 10 micrometers in diameter.

Acknowledgment: This work was done with the financial support of NSF Grant ECS-9215852, Soros ISF, Russian Foundation for Fundamental Research 93-02-3563 and NATO Grant #921019.

References:

1. H.M. Gibbs, P. Mandel, N. Peyghambarian, and S.D. Smith, eds., Optical Bistability, (Springer Verlag, Berlin, 1986).
2. V.B. Braginsky, M.L. Gordetsky, F.S. Il'chenko, Appl Phys. Lett. A137, 393(1989).
3. V.V. Vasil'ev, V.L. Vlichan sky, M.L. Gorodetsky, V.S. Il'chenko, L. Hollberg, Opt. Commun. (to be published).

Modelocking of a Titanium-Sapphire Laser Induced by Intracavity Frequency Shift

Gerd Bonnet, Stefan Balle, and Klaas Bergmann
Fachbereich Physik der Universität, Postfach 3049, D - 67653 Kaiserslautern, Germany
phone: (49) - 631 - 205 - 2671, fax: (49) - 631 - 205 - 3903
e-mail: bergmann@ sun.rhrk.uni-kl.de

Intracavity frequency shift by a highly efficient acousto-optic Bragg diffraction element modifies emission properties of the laser as has been demonstrated for dye-lasers /1 - 5/ and diode lasers /6/. Here, we investigate the response of a Titanium-Sapphire laser to such manipulation. We show that the interplay between intracavity frequency shift, frequency selective elements, self-phasemodulation in the gain medium and gain dynamics, leads to a very robust novel type of selfstarting modelocking.

The variation of the output power vs pump power, shown in Fig.1, exhibits several characteristically different regimes of operation and shows a pronounced hysteresis. Above threshold, region 1, pulsation of the laser is observed, which is best described as sustained spiking. The repetition rate R of the pulses increase with pump power P from 310 to 490 kHz while the spectral envelope shifts towards lower frequencies (the frequency shift induced by the Bragg diffraction element is to higher frequencies, away from the transmission profile of the 200 GHz free spectral range etalon). At about P = 8.5 W the slope efficiency changes suddenly as does R which reaches values near 800 kHz while the spectral envelope settles again at higher frequencies. When P increases further irregular fluctuations around a growing continuous emission level, underlying the gradually dissappearing pulsation, becomes more prominent (region 2). At a well defined value of P = 17 W selfstarting modelocking is observed accompanied by a shift of the center of the spectral envelope to lower frequencies to a value near the transmission maximum of the etalon. The pulse length is about 50 ps. Modelocking is maintained when P decreases (region 3) to values as low as 8 W where the character of the emission changes again to sustained spiking.

Model calculations reproduce the observed features well. Analysis of the results of such calculation reveals that the modelocking derives from the competition of the frequency shift induced by the acousto-optic modulator, which is to higher frequencies away from the transmission maximum of the etalon, and a frequency shift induced by the transmission properties of the etalon. At a high pump power broadening of the spectral envelope due to the nonlinear response of the gain medium (pulse shortening) become relevant and enhances the shift related to the etalon. The latter shift is towards the transmission maximum of the etalon. When it exceeds the acousto-optically induced shift to higher frequencies losses become smaller, the peak power of the pulse increases and the spectral broadening is further enhanced. As a result the center of the spectral envelope is driven to the transmission maximum, a distinct increase in output power is observed and robust modelocking is established. Further analysis of these results indicates that this concept may lead to modelocked ps-pulses of controllable variable pulse length.

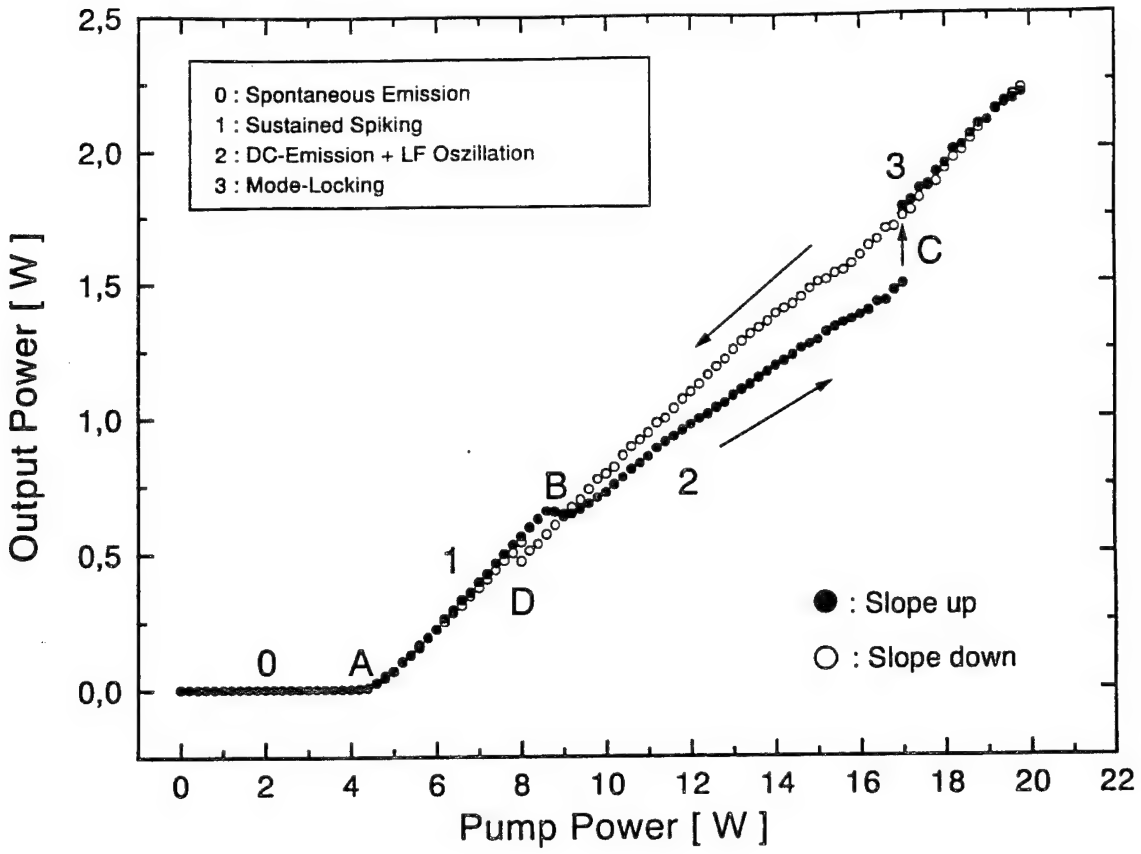

Fig.1: Variation of the output power with pump power P of a Titanium-Sapphire Laser with intracavity frequency shift. Regions with distinctly different emission character, as described in the text, can be identified. Selfstarting modelocking occurs at P = 17 W and is maintained when P is subsequently decreased to 8 W.

/1/ F.V.Kowalski, P.D.Hale, and S.J.Shattil, Opt.Lett. 13, 622 (1988)
/2/ I.Littler, S.Balle, and K.Bergmann, J.Opt.Soc.Am. B8, 1412 (1991)
/3/ I.Littler, S.Balle, and K.Bergmann, Opt.Commun. 88, 514 (1992)
/4/ S.Balle, I.C.M.Littler, K.Bergmann, and F.V.Kowalski,
Opt.Commun. 102, 166 (1993)
/5/ S.Balle and K. Bergmann Opt.Commun (in print)
/6/ J.Martin, Y.Zhao, S.Balle, M.P.Fewell, and K.Bergmann
Opt.Commun. 112, 109 (1994)

Nonlinear coupling in self-mode-locked lasers

Robert E. Bridges, Robert W. Boyd, and Govind P. Agrawal
The Institute of Optics, University of Rochester, Rochester, New York 14627, 716-275-5030, 716-275-4936 (fax)

I. INTRODUCTION

Since its discovery in 1990,[1] the self-mode-locked (Kerr-lens mode-locked) laser has developed rapidly. Today, with Ti:sapphire as the active medium, such lasers have produced pulses of less than 10 fs.[2]

The spatial evolution of the beam in the cavity of a self-mode-locked laser has been studied by accounting for physical effects such as Kerr nonlinearity,[3,4] gain,[5] and thermal lensing.[6] An important effect that has not been included in these studies, however, is that of nonlinear coupling among the beam parameters in the x and y dimensions. This effect is important in self-mode-locked lasers that use Z- or X-shaped cavities because the beams in such lasers are elliptical rather than circular. This ellipticity affects the intensity-dependent nonlinearities such as Kerr, thermal, and gain nonlinearities and results in a coupling among the x and y beam parameters. Previously, we reported a method for including nonlinear coupling and showed that such coupling can dramatically alter laser behavior.[7]

The temporal evolution of the pulse in a self-mode-locked laser has also been studied,[8,9] but without fully accounting for the nonlinear coupling among the beam (pulse) parameters in the x, y, and t dimensions. This coupling comes about because the intensity-dependent nonlinearities are affected by the pulse width in t as well as the beam widths in x and y.

In this paper, we present two new techniques to account for the effects of nonlinear coupling among beam (pulse) parameters in the x, y, and t dimensions. We find that, under conditions typical of a self-mode-locked laser, these two techniques give errors that are relatively small. By comparison, techniques that neglect nonlinear coupling give errors that are much larger. To demonstrate the importance of nonlinear coupling in cavity calculations, we apply these techniques to a specific Ti:sapphire laser and show that nonlinear coupling can cause large qualitative changes in laser behavior.

II. GENERAL FORMULATION

Calculations for a self-mode-locked laser cavity can be carried out accurately using the beam-propagation method (BPM)[10] with three-dimensional fast Fourier transforms (3D-FFTs). Such a technique has not been applied to a thorough treatment of self-mode-locked lasers, however, because of the vast computing resources that would be required.

To derive the new techniques, we write the electric field E in terms of the electric field amplitude A,

$$E(\mathbf{r},T) = A(\mathbf{r},T)\exp(i\beta_0 z - i\omega_0 T)/2 + \text{c.c.}, \qquad (1)$$

where $\beta_0 = n_0\omega_0/c$ is the propagation constant and T is time in the laboratory frame of reference. We let t be the time with respect to the center of the pulse and define the normalized amplitude as $u(x,y,t;z) = A(x,y,t;z)/\sqrt{M(z)}$, where $M(z) = \iiint_{-\infty}^{\infty} \mathrm{d}x\,\mathrm{d}y\,\mathrm{d}t\,|A(x,y,t;z)|^2$.

We can obtain a computational technique that is much faster than a three-dimensional numerical technique if the amplitude is separable in x, y, and t; that is, if

$$u(x,y,t;z) = u_x(x;z)u_y(y;z)u_t(t;z). \qquad (2)$$

This assumption is not precisely valid when intensity-dependent nonlinearities are present, but it is often approximately true for self-mode-locked lasers.

We have shown that if Eq. (2) is valid a beam propagating under the influence of diffraction, second- and third-order dispersion, and Kerr nonlinearity evolves in accordance with the three-coupled differential equations,

$$i\frac{\partial u_x}{\partial z} = -\frac{1}{2\beta_0}\frac{\partial^2 u_x}{\partial x^2} - \frac{2\pi}{\beta_0\delta_y\delta_t}\frac{U}{P_c}|u_x|^2 u_x, \qquad (3a)$$

$$i\frac{\partial u_y}{\partial z} = -\frac{1}{2\beta_0}\frac{\partial^2 u_y}{\partial y^2} - \frac{2\pi}{\beta_0\delta_x\delta_t}\frac{U}{P_c}|u_y|^2 u_y, \qquad (3b)$$

$$i\frac{\partial u_t}{\partial z} = \frac{\beta_2}{2}\frac{\partial^2 u_t}{\partial t^2} + i\frac{\beta_3}{6}\frac{\partial^3 u_t}{\partial t^3} - \frac{2\pi}{\beta_0\delta_x\delta_y}\frac{U}{P_c}|u_t|^2 u_t. \qquad (3c)$$

Here β_2 and β_3 and the group-velocity-dispersion and third-order-dispersion parameters, respectively, U is the pulse energy, and $P_c = 2\pi n_0/\beta_0^2 n_2$ is the critical power.[11] The effective width in the ν dimension, $\delta_\nu = \left(\int_{-\infty}^{\infty}|u_\nu|^4\,\mathrm{d}\nu\right)^{-1}$, accounts for the nonlinear coupling. We can solve Eqs. (3) using the BPM with 1D-FFTs.

We have derived a still faster computational method if the spatial and temporal profiles (e.g., Gaussian, hyperbolic secant) do not change significantly during propagation. The second moment of the width in the ν dimension with respect to the intensity distribution is defined as $\rho_\nu^2 = \langle\nu^2\rangle - \langle\nu\rangle^2$, where $\langle\nu^2\rangle = \int_{-\infty}^{\infty}\nu^2|u_\nu|^2\,\mathrm{d}\nu$ and $\langle\nu\rangle = \int_{-\infty}^{\infty}\nu|u_\nu|^2\,\mathrm{d}\nu$. The rms width of the beam ρ_ν is the square root of the second moment.

Neglecting third-order dispersion and assuming the initial condition $\langle\nu\rangle = 0$, we can show that the evolution of the beam is governed by six coupled equations,

$$\rho_\nu^2(z_1+h)/\rho_{\nu 1}^2 = \left(1-\frac{C_{\nu 1}h}{z_{d\nu 1}}\right)^2 + \frac{h^2}{z_{d\nu 1}^2}\left(\sigma_\nu^2 - \frac{\epsilon_\nu^{(3)}\eta_{xyt}}{d_\nu\beta_0}\frac{U}{P_c}\right), \quad (4a)$$

$$C_\nu(z_1+h) = C_{\nu 1}\left(1-\frac{C_{\nu 1}h}{z_{d\nu 1}}\right) - \frac{h}{z_{d\nu 1}}\left(\sigma_\nu^2 - \frac{\epsilon_\nu^{(3)}\eta_{xyt}}{d_\nu\beta_0}\frac{U}{P_c}\right), \quad (4b)$$

where ν equals x, y, or t. Here h is the (small) step size, $d_x = d_y = 1/\beta_0$ and $d_t = -\beta_2$ are the dispersion-diffraction parameters, $z_{d\nu} = 2\rho_\nu^2/d_\nu$ is the dispersion-diffraction distance (which may be negative), and the subscript "1" indicates that a parameter is evaluated at the initial position z_1. The chirp parameter C_ν is related to the radius of curvature by $R_\nu = -z_{d\nu}/C_\nu$. The three-dimensional ellipticity factor $\epsilon_\nu^{(3)} = \rho_\nu^2/2\sqrt{\pi}\rho_x\rho_y\rho_t$ provides the nonlinear coupling in the equations. The quantity σ_ν^2 is the beam-quality factor (also known as the times-diffraction-limit number or M^2).[12] The three-dimensional nonlinear shape factor is $\eta_{xyt} = \eta_x\eta_y\eta_t$, where $\eta_\nu = \delta_{g\nu}/\delta_\nu$ and g indicates a Gaussian profile. For a beam that has a Gaussian profile in x, y, and t, $\sigma_\nu^{(3)} = 1$ and $\eta_{xyt} = 1$.

III. RESULTS

Equations (3) or Eqs. (4) may be used to determine how a beam (pulse) evolves both in space and time. For simplicity, however, we here consider the example of a self-mode-locked laser operating in the quasi-cw regime in which the pulse width inside the cavity is approximately constant (a reasonable assumption for a 100-fs laser). In this regime, we may neglect the action of the prism pair. We let the length of the Ti:sapphire crystal be 1.5 cm, the distances from the folding mirrors to the crystal be 4.85 cm and 4.95 cm, and the distances from the folding mirrors to the flat end mirrors be 80 cm. We let the radii of curvature of the folding mirrors be 10 cm, the angles of the folding mirrors be 27°, and the power be half the critical power.

Figure 1 shows the results of the calculations. We see that, when nonlinear coupling is neglected, the laser has two modes that are stable against perturbation, but that when nonlinear coupling is included, the laser has only one mode. Such large effects are not restricted to the example given here, but may be seen in many different cavities, both near the centers and the edges of the laser stability regions. The numerical results obtained for Fig. 1(b) using the BPM and the second-moment equations were found to agree to within 1% at all points.

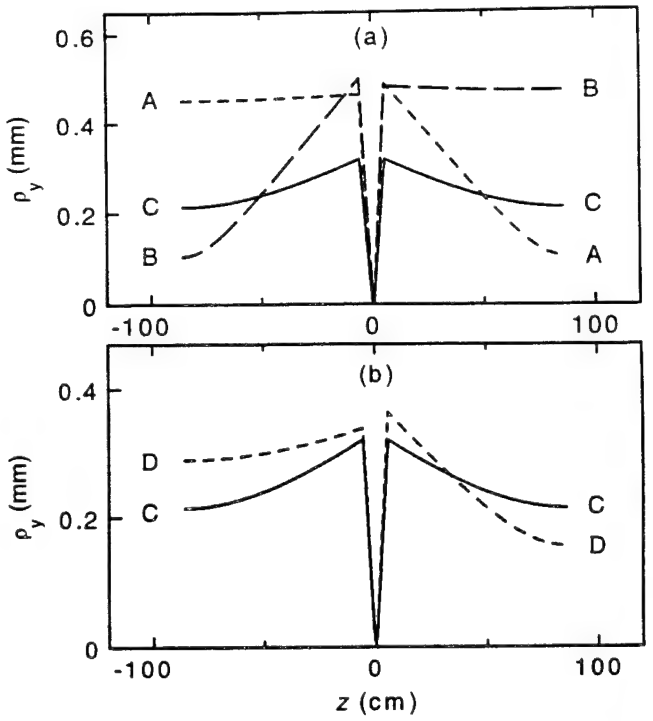

FIG. 1. Beam width ρ_y in the sagittal plance of a Ti:sapphire laser. Continuous-wave (cw) operation is indicated by the solid curves C. (a) Two stable modes (dashed curves A and B) are obtained when nonlinear coupling is neglected. (b) Only one stable mode (dashed curve D) is obtained when nonlinear coupling is included.

ACKNOWLEDGMENTS

This research was supported by the U.S. Army Research Office through a University Research Initiative Center and by IMRA America.

[1] D. E. Spence, P. N. Kean, and W. Sibbett, Opt. Lett. **16,** 42 (1991).
[2] J. Zhou, G. Taft, C.-P. Huang, M. M. Murnane, and H. C. Kapteyn, Opt. Lett. **19,** 1149 (1994).
[3] V. Magni, G. Cerullo, and S. De Silvestri, Opt. Commun. **96,** 348 (1993).
[4] T. Brabec, P. F. Curley, Ch. Spielmann, E. Wintner, and A. J. Schmidt, J. Opt. Soc. Am. B **10,** 1029 (1993).
[5] F. Salin and J. Squier, Opt. Lett. **17,** 1352 (1992).
[6] J. F. Cormier, M. Piché, F. Salin, Opt. Lett. **19** 1225 (1994).
[7] R. E. Bridges, R. W. Boyd, and G. P. Agrawal, Opt. Lett. **18,** 2026 (1993).
[8] I. P. Christov, M. M. Murnane, H. C. Kapteyn, J. Zhou, and C.-P. Huang, Opt. Lett. **19,** 1465 (1994).
[9] J. L. A. Chilla and O. E. Martínez, J. Opt. Soc. Am. B **10,** 638 (1993).
[10] G. P. Agrawal, *Nonlinear Fiber Optics,* 2nd ed. (Academic, Boston, 1995), Chap. 2.
[11] J. H. Marburger, Prog. Quant. Electr. **4,** 35 (1975).
[12] M. A. Porras, J. Alda, and E. Bernabeu, Appl. Opt. **30,** 6389 (1992).

PERIODIC ANTIPHASED STATES IN INTRACAVITY SECOND HARMONIC GENERATION

Paul Mandel and J.-Y. Wang
Optique Nonlinéaire Théorique, Université Libre de Bruxelles,
Campus Plaine C.P.231, B-1050 Bruxelles, Belgium
fax: +32 2 650 5824 Email: PMANDEL(JWANG)@ULB.AC.BE

We report on the study of a model for intracavity second harmonic generation introduced by the group of Roy [1]. The modal intensities I_p and the population differences G_p are determined by the evolution equations

$$\eta dI_p/dt = I_p\left(G_p - \alpha + g\varepsilon I_p - 2g\varepsilon \sum_{r=1}^{M} I_r - 2g_1\varepsilon \sum_{r=1}^{P} I_r \right) \tag{1}$$

$$dG_p/dt = \gamma - G_p\left(1 + (1 - \beta)I_p + \beta \sum_{r=1}^{M+P} I_r \right) \tag{2}$$

where α is the cavity loss parameter, γ is the small signal gain which is related to the pump rate, β is the cross-saturation parameter and g is a geometrical factor whose value depends on the phase delays of the amplifying and doubling crystals and on the angle between the fast axes of these two crystals. We have assumed that α, β and γ are mode-independent, in good agreement with the experimental results [1, 2]. The parameter η equals τ_c/τ_f where τ_c and τ_f are the cavity round trip time and fluorescence lifetime, respectively. The electric field modes can oscillate in one of two orthogonal polarizations. There are M modes in one field polarization and P = N - M modes in the orthogonal polarization. The mode-mode coupling is characterized by the parameter g when the two modes have the same polarization and by the parameter $g_1 = 1 - g$ when the two modes have orthogonal polarizations.
From the experimental data it has been determined that

$$0 < \varepsilon << 1, \qquad \alpha, \beta, \gamma, \eta/\varepsilon = O(1) \tag{3}$$

The physical constraints $0 < g < 1$ and $0 < \beta < 1$ have also to be imposed.

Eqs.(1, 2) have a simple steady solution in which all modal intensities are equal in a given polarization: $I_p = I$ for $1 \le p \le M$ and $I_q = J$ for $1 \le q \le P$. The same degeneracy holds for the population differences. For the range of parameters (3), the steady state is destabilized by a Hopf bifurcation [3]. We report on the analysis of this Hopf bifurcation in the domain

$$\delta^2 = |\gamma - \gamma_h| << 1, \qquad \varepsilon = \varepsilon_0 + \delta\varepsilon_1 + O(\delta^2) \tag{4}$$

where γ_h is the linear gain at the bifurcation. A different domain of parameters was studied in [4] without leading to an answer for the stability of the periodic solutions. However the same classification of the solutions emerges in the present analysis. Let us introduce the expansions

$$I_p = I_h + \delta[\, \alpha_p(\sigma)e^{iT} + \text{c.c.}\,] + O(\delta^2), \qquad p = 1, \ldots, M \tag{5}$$

$$J_q = J_h + \delta[\, \beta_q(\sigma)e^{iT} + \text{c.c.}\,] + O(\delta^2), \qquad q = 1, \ldots, P \tag{6}$$

where $\sigma = \delta^2 t$ is a slow time while $T = \omega t$ with $\omega = O(1/\sqrt{\varepsilon})$. A first result is that

the solutions of (1) and (2) must verify the global sum rule $\sum_p \alpha_p(\sigma) + \sum_q \beta_q(\sigma) = 0$.

AD1 solutions They occur when all modes are in the same polarization (M = N or P = N). The expression $\alpha_p = \rho(\sigma)\exp[2\pi imp/N + i\theta(\sigma)]$ verifies the sum rule with $1 \le m \le M - 1$ and $1 \le p \le M$: all solutions have the same time dependence but are phase shifted by an equal amount $2\pi m/N$. The value of m determines the relative time ordering of the modes. The real amplitude ρ verifies the equation

$$d\rho/d\sigma = \rho[\xi_1(\varepsilon) - \rho^2\xi_3(\varepsilon)], \quad \xi_1(0) \neq 0, \quad \xi_3/\xi_1 \ge 0 \tag{7}$$

The important property is that $\xi_3(0) = 0$ for the AD1 solutions.

AD2 solutions They coexist with the AD1 states and are of the form $\alpha_m(\sigma) = r(\sigma)/Q$ and $\alpha_n(\sigma) = -r(\sigma)/R$, with $1 \le m \le Q$ and $1 \le n \le R = N - Q$. The real amplitude of $r(\sigma)$ verifies eq.(7) with $\xi_3(0) \neq 0$. These solutions cluster into two subgroups, all modes in one subgroup being inphased while the two subgroups antiphase.

AD3 solutions The sum rule must be verified in each polarization: $\sum\alpha_p(\sigma) = 0$, $\sum\beta_q(\sigma) = 0$. Hence, in the particular case M = N - 1, P = 1, we have $\beta = 0$. Seeking a solution of the form $\alpha_p = \rho(\sigma)\exp[2\pi imp/N + i\theta(\sigma)]$ leads to an amplitude equation for ρ which is eq.(7) with $\xi_1(0) \neq 0$. The coefficient $\xi_3(0)$ remains finite for M = 2 but vanishes for M > 2. For M = N - 1 and P = 1, the mode P oscillates at a higher frequency than the modes M.

AD4 solutions The solutions of the global sum rule are of the form $\alpha(\sigma) = \rho(\sigma)/M$ and $\beta(\sigma) = -\rho(\sigma)/P$ where ρ verifies eq.(7) with $\xi_3(0) \neq 0$.

Near the Hopf bifurcation, we can study the scaling law $I_{j,max} - I_{j,h} \sim (\gamma - \gamma_h)^{\mu_j}$ where $I_{j,max}$ is the maximum amplitude of the intensity of mode j and $I_{j,h}$ is its intensity at the Hopf bifurcation. When $\xi_3(0) = 0$, the bifurcation is nearly vertical and the exponent μ_j depends on η. When $\xi_3(0) \neq 0$ for all modes, $\mu_j = 1/2$. This is the case for the AD2 and AD4 states. For AD3 and M = 2 with P = 1, we find $\mu_1 = \mu_2 = 1/2$ but $\mu_3 = 1$ for the mode whose amplitude is β.

[1] R. Roy, C. Bracikowski and G. James in *Recent Developments in Quantum Optics*, R. Inguva ed. (Plenum, New York, 1994) pp.309.

[2] K. Wiesenfeld, C. Bracikowski, G. James and R. Roy, Phys. Rev. Lett. 65 (1990) 1749.

[3] J.-Y. Wang and P. Mandel, Phys. Rev. A 48 (1993) 671.

[4] J.-Y. Wang, P. Mandel and T. Erneux, Quant. & Semiclass. Optics (1995, in press).

THE EFFECT OF NOISE SOURCES CORRELATION ON THE FORM OF LOW-FREQUENCY INTENSITY FLUCTUATIONS SPECTRA IN MULTIMODE CLASS B LASER

Ya.Khanin, P.A.Khandokhin, V.G.Zhislina

Institute of Applied Physics of Russian Academy of Sciences
46 Uljanov Street, 603600 Nizhny Novgorod, Russia
Tel:(8312) 384587 Fax: 363792 Email: Khanin@appl.nnov.su

The dynamic theory of multimode class B lasers involves two types of models. The rate equations approach proposed by S.Tang, H.Statz and G.DeMars [1] ignores the inversion gratings induced in a laser medium by a joint action of different modes and pulsing, therfore, with beat frequencies. Such an approach disregarding phase-sensitive mode-mode coupling is valid when the intermode frequency spacing is large compared with the inversion relaxation- and field decay rates in the cavity [2]. In the opposite limiting case phase-sensitive mode-mode coupling is essential, which noticeably tells on the properties of these models [2,3].

The characteristics features of a multimode laser model without phase-sensitive interactions are:

- only one steady-state solution is globally stable [4];

-the number of relaxation oscillations coincides with the number of lasing modes [5-7];

- the relaxation oscillations frequencies and decrements have a relatively weak dependence on laser parameters.

These properties account for the mutually simple conformity between the systems of optical modes and the relaxation oscillations of laser. As a result, the intensity fluctuation spectra of individual modes acquires a specific form. Most pronounced in the weakest mode spectrum is the resonance peak at the lower relaxation oscillations frequency; in the spectrum of a mode coming next for intensity it is the neighbouring peak that shows up most vividly, etc.

However, regularities in the spectra of low-frequency fluctuations depend not only on the laser parameters, but on the properties of noise sources existing in different modes. For the first time this effect (factor) was noticed in [5]. The experimental works [8-10] in which intensity fluctuations

spectra of solid-state lasers modes were obtained with good resolution put forward a problem of constructing a more exact theoretical model with a view to a qualitative comparison of theoretical and experimental data. This problem is dealt with in our paper.

In this paper we consider a set of rate equations for a multimode laser with Langevin forces included in the right-hand parts of the equations for mode intensities. The power spectra of individual modes and of total intensity for a three-mode model given different correlations between the noise sources are calculated. The numerical results have been compared with the experimental data from [8,9], which has led the authors to a conclusion about the existence of correlation between the noise sources. Possible reasons of correlation, including a likely effect of technical fluctuations of laser parameters are discussed.

References

1. C.L.Tang, H.Statz, G.DeMars, J.Appl.Phys., 34 (1963) 2289.

2. P.A.Khandokhin, Ya.I.Khanin, I.V.Koryukin, P.Mandel, IEEE J. Quant. Electron.

3. P.Mandel, C.Etrich, K.Otsuka, IEEE J. Quant. Electron., QE-29 (1993) 836.

4. A.V.Ghiner, K.P.Komarov, K.G.Folin, Opt.Commun., 19 (1975) 350

5. A.S.Meller,P.A.Khandokhin,Ya.I.Khanin,Sov.J.Quant.Electron., 16 (1986) 1502.

6. P.Mandel, M.Georgiou, K.Otsuka, D.Pieroux, Opt. Commun., 100 (1993) 341.

7. D.Pieroux, P.Mandel, Opt.Commun., 107 (1994) 245.

8. K.Otsuka,M.Georgiou, P.Mandel,Jap.J.Appl.Phys., 31 (1992) 1250.

9. K.Otsuka, D.Pieroux, P.Mandel, Opt. Commun., 108 (1994) 265.

10. P.A.Khandokhin, Ya.I.Khanin, J.-C.Celet, D.Dangoise, P.Glorieux, (Submitted to Opt. Commun.)

CO-OPERATIVE SYNCHRONIZATION IN A LASER ARRAY WITH EIGENFREQUENCIES SPREAD

A.P. Napartovich, S.Y. Kurchatov, V.V. Likhanskii
Troitsk Institute for Innovation and Fusion Research
142092 Troitsk, Moscow region, Russia
(095)334-0450, fax:(095)334-5158,
e-mail: kochet@anet.sovam.com

It is known that the most effective for phase-locking of lasers in an array is global or all-to-all coupling, where an equal part of every laser beam is splitted on N-1 beamlets directed each to the corresponding laser. This complicated schematics can be realized easily, for example, by placing a stop at the common focus of the array radiation. This global coupling permits to keep lasing of all lasers in the array to be coherent inspite of some time independent eigenfrequencies spread. In fact, it is a matter of magnitude of this random spread, which is specified usually by a mean square root detuning, delta. Being delta large in comparison with a coupling strength, M, the phase locked operation violates, and complicated dynamics may occur. In particular, in Ref.1 it was shown that for the globally coupled array with the eigenfrequencies distribution having a Lorentzian form transitions between different dynamic modes may be observed. Authors of [1] neglected an inertia of an active medium. This asssumption is far from being justified in most experiments. Here it is demonstrated that the active medium inertia causes a new effect called by us cooperative field phase-locking.

The system of nonlinear equations for wave field amplitudes in each laser of the array with global coupling and kinetic equations describing the time variation of gain in each laser were calculated numerically. The eigenfrequency in the given laser was taken as the random variable fixed in time. The eigenfrequency detunings were supposed to be uniformly distributed in the interval from $-\Delta/2$ to $+\Delta/2$. The parameters that govern the mode of operation of the laser array are Δ and small-signal gain, g_0, if the kinetic relaxation time is taken fixed.

Along with numerical calculations, analytical studies were carried out which result in explicit expressions for the critical detuning, which were in an excellent agreement with numerical studies. It was shown that for $g_0 - 1 < M$, when independent lasing of the single laser is impossible, the increase of Δ causes the total power of laser array to

diminish and become zero at some critical value for Δ. Below this critical value lasing was phase locked.

For sufficiently high small signal gain, $g_0 - 1 > M$, the critical detuning was found above which the stationary phase locked operation becomes unstable. The dynamic mode depends on the kinetic relaxation time. In particular, when the relaxation oscillation period is close to the average field modulation period a new phenomenon was found. The temporal co-operative phase-locking of lasers was observed in comparatively short pulses almost regularly repeated in time. The peak intensity can be 1.6 times greater than the intensity of the ideal laser array. The time averaged intensity achieved 0.4 of the ideal one. Explanation of this phenomenon and discussion on possibilities of its extension to more realistic situations will be presented in the talk.

1. Z. Jiang, M. McCall, J. Optical Soc. of America, **10**, No. 1, 155 (1993).

Dynamical Characterization of Globally Coupled Optical Systems

Kenju Otsuka
Department of Applied Physics, Faculty of Engineering, Tokai University
1117 Kitakaname, Hiratsuka, Kanagawa, 259-12 Japan
Fax +81 463 58 9461 Email ootsuka@keyaki.cc.u-tokai.ac.jp
Jingyi Wang, Paul Mandel and Thomas Erneux
Universite Libre de Bruxelles, Campus Plaine
Code Postal 231, 1050 Bruxelles, Belgium
Fax +32 2 650 5824 Email jwang (pmandel, terneux)@ulb.ac.be

We propose two correlation functions derived from the ideas of statistical mechanics to characterize generic dynamics including the antiphase states and clustering in globally coupled nonlinear systems. Explicit results are obtained for the case of intracavity second harmonic generation in multimode lasers. Our analysis indicates the formation scenario of antiphase periodic states and dynamical independence of clustered modes. The same analysis is applicable in general to a dissipative dynamical system with many identical or similar elements.

The laser problem can be described by the set of equations

$$dI_k/dt = K(G_k - \alpha - g\epsilon I_k - 2\epsilon \sum_{j\neq k} \mu_{jk} I_j + s_k) I_k, \tag{1}$$

$$dG_k/dt = \gamma - (1 + I_k + \beta \sum_{j\neq k} I_j) G_k, \quad k = 1, 2, 3, ..., N \tag{2}$$

Here, $t = T/\tau_f$ is the normalized time (τ_f: population lifetime), $K = \tau_f/\tau_c$ (τ_c: photon lifetime), I_k is the intensity for the k-th longitudinal mode, G_k is the nonlinear modal gain, s_k is the injection-seed signal and other parameters are the same as those in [1].

The first function we study was proposed recently by Otsuka and Aizawa [2]. It is the gain circulation G_{ij} between modes i and j which is defined as

$$G_{ij} = G_i \dot{G}_j - \dot{G}_i G_j. \tag{3}$$

Its property is that a positive (negative) G_{ij} implies a *gain flow* from mode i (j) to mode j (i). To see how this function can be used, let us consider the pulsed antiphase states which have been recently analyzed numerically [3], where there coexist (N -1)! antiphased solutions with different orderings of the sequence $\{I_k\}$ when all modes are in the same polarization. In Fig.1-a, we display an antiphased solution in the case of single polarization [M, P] = [4, 0]. In Fig.1-b, we display the gain circulations relative to mode 1. At the pulse leading edge $t = a$, all the gain flows from mode 1, $G_{1j}(t = a)$, are positive and practically identical (i.e., uniform coupling). Therefore, all modes except mode 1 are equally probable candidates for the next pulse. However, at the trailing edge of that pulse $t = b$, it is found that only mode 2, which transfers back almost the same amount of gain to the previous mode 1, can emit the next pulse. The same scenario is observed for the gain flows at the leading and trailing edges of each pulse. This implies that a symmetric gain flow path connecting antiphased modes is dynamically created.

When the coupling is uniform, the system admits maximal sensitivity to a mode-dependent selective perturbation. Using this property, we apply an injection-seeding method to switch between the (N -1)! equivalent antiphase states. We inject during a single period of the antiphased state a sequence of N seed square pulses in the desired new sequence. Each pulse is timed to occur at the leading edge of a pulse of the original sequence. Fig.1-c illustrates the transition between the mode sequence { 1, 2, 4, 3 } of Fig.1-a to the mode sequence { 1, 2, 3, 4 }.

As the number of modes increases in the globally coupled system, clustering becomes a prominent feature [4]. Clustering implies that a subset of the modes evolve differently from the other modes. As an example of chaotic clustering, we display in Fig.2 a case where M = 3 and P =2. In Fig.2-a, there is antiphase dynamics with the periodic sequence {1, 5, 2, 4, 3, 5, 1, 4, 2, 5, 3, 4}. This sequence results from the fact that each of the two orthogonal polarizations are periodic and have periods which are in the ratio of the mode numbers 3/2. In Fig.2-b, chaotic clustering takes place and the M modes are chaotic while the P modes seem periodic. Finally, in Fig.2-c, all M + P = N modes are chaotic.

To decribe clustering, we introduce global correlation functions defined as

$$\Gamma_{ij} = \dot{I}_j \prod_{k \neq j} I_k - \dot{I}_i \prod_{k \neq i} I_k = (\dot{I}_j/I_j - \dot{I}_i/I_i) \prod_k I_k. \tag{4}$$

The product $\dot{I}_j \prod_{k \neq j} I_k$ represents the total intensity transfer from all modes to mode j. Γ_{ij} includes the contributions of *all* the mode intensities instead of only those of modes i and j. Hence it describes the global intensity circulation between modes i and j. In the following, we adopt the convention that the indices p and p' refer to the P modes while the indices m and m' refer to the orthogonal M modes. In the antiphase regime of Fig.2-a where all modes are periodic, there is practically no global intensity flow at all: $\Gamma_{mp} \cong \Gamma_{mm'} \cong \Gamma_{pp'} \cong 0$. In the chaotic clustered state displayed in Fig.2-b where the modes P are periodic and the modes M are chaotic, the Γ_{pm} have large positive peaks and small negative peaks, indicating a predominant intensity transfer from the periodic modes towards the chaotic modes. However, the relevant numerical observation is that the sum of the global intensity flows from any periodic mode to all the chaotic modes is strictly positive at any time: $\sum_m \Gamma_{pm}(t) > 0$. Thus, the total intensity flow is unidirectional, from the periodic to the chaotic modes. This supports the concept of dynamical independence of clustered modes [3]. In the fully chaotic situation of Fig.2-c, there are bidirectional global intensity flows between all modes and no cancellation occurs: $\sum_m \Gamma_{pm}(t)$ exhibits positive and negative peaks.

[1] R. Roy, C. Bracikowski, and G. James, in *Proceedings of the International Conference on Quantum Optics*, R. Inguva ed. (Plenum, New York, 1994) pp. 309.

[2] K. Otsuka and Y. Aizawa, Phys. Rev. Lett. **72**, 2701 (1994).

[3] P. Mandel and J.-Y. Wang, Opt. Lett. **19**, 533 (1994).

[4] G. Nicolis and I. Prigogine: *Self-organization in nonequilibrium systems* (Wiley, New York, 1977).

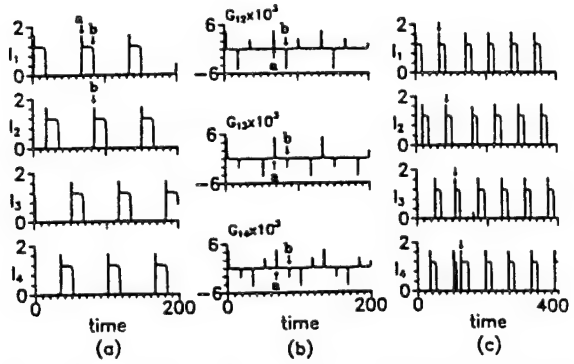

Fig.1 Pulsed antiphased solution (a), gain circulation (b) and injection seeding (c) with [M, P] = [4, 0]. K = 500, α (cavity loss) = 0.02, β (cross-saturation parameter) = 0.292, γ (small-signal gain) = 0.11, ϵ (SHG coefficient) = 0.05 and g (geometrical factor) = 0.5161.

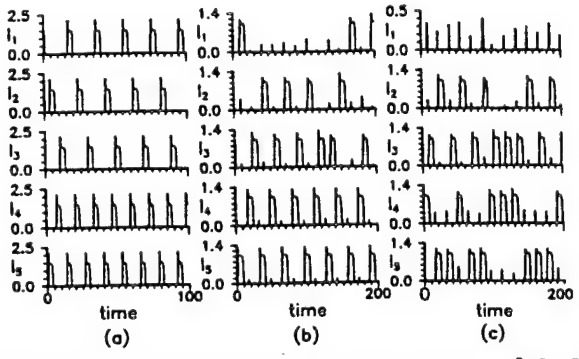

Fig.2 Mode clustering for the partition [M, P] = [3, 2]. (a)γ = 0.14: antiphase periodic state, (b)γ = 0.095: chaotic clustering state, (c) γ = 0.0936: fully chaotic state. Other parameters are the same as those of Fig.1.

Unified Treatment of Spontaneous Pattern Formation in "2+1" Dimensional Optical Systems

Ross F. McIntyre, Weiping Lu and Robert G. Harrison
Department of Physics, Heriot-Watt University,
Edinburgh, EH14 4AS, U.K.,
Tel: 031-451 3056, Fax: 031-451 3136,
E-mail: phyrm@uk.ac.hw.phy

The emergence of transverse spatial patterns in nonlinear passive and also active optical systems is currently a subject of keen interest [1]. Recent theoretical treatments of spontaneous spatial pattern formation in passive optics have been developed for various "2+1" dimensional systems. An interesting feature when one looks collectively at these physical systems is the fact that the equations, used to describe them, all have, in form, striking mathematical similarities. This suggests that a general formulation can be found to describe these and other pattern forming systems and from this the Ginzburg-Landau equation (GLE) may be derived to provide a generalised treatment of bifurcations and pattern formations in these systems. In this paper the focus of attention is to the formulation of such a generalised description and through this to provide a framework for its application to specific systems in nonlinear optics and more generally to pattern forming systems in other fields such as hydrodynamics.

In choosing the form of a general equation one must account for the relevant physical processes in the optical-material interactions. Accordingly, we study the following diffraction-diffusion system

$$\tau \partial_t \mathbf{v} = f(\mathbf{v}, \mu) + D\triangle_\perp \mathbf{v}, \tag{1}$$

where $\mathbf{v} \in \mathbb{R}^n$ is our dependent variables, μ is a scalar parameter, D is the matrix of diffraction-diffusion coefficients, τ is the matrix of relaxation times, f is our nonlinear operator, and $\triangle_\perp$ is the generalised transverse operator which describes all possible transverse spatial operations that allows us to write $\triangle_\perp = -K_c^2$, where K_c^2 is some real function of the critical wavevector k_c^2. Examples of such spatial operators in optics are the ones appearing in Swift-Hohenberg type models, $\triangle_\perp = (\nabla_\perp^2 + k_c^2)^2$, and reaction-diffusion type equations, $\triangle_\perp = \nabla_\perp^2$.

The GLE, which is written in the form of ref [3], is derived from multiple scales analysis using equation (1) in which the real coefficients

$$r = (\mu - \mu_c)m_1, \tag{2}$$

$$h_0 = 2m_2, \tag{3}$$

$$h_1 = \frac{1}{2}m_3 - \frac{5}{6}m_2^2 K_c^{-2}, \tag{4}$$

$$h_2 = m_3 - \frac{1}{4}m_2^2 K_c^{-2}. \tag{5}$$

are determined from relatively straightforward scalar products, m_1, m_2, and m_3, which are related explicitly to the physical paramters of the system. This leads us naturally to reinterpret the well known stability properties for roll and hexagon patterns in terms of our scalar products; the emerging pattern behaviour is found to depend opon the quadratic, m_2, and cubic, m_3, terms as seen in Fig. 1 which displays five distinct pattern forming regions. Apart from the fairly conventional and well studied hexagon roll transition domains we observe regions where there is a direct bifurcation into turbulence. Indeed in one such region we conjecture that the turbulance gives way to stable rolls as the control parameter is increased.

As illustration, we apply this general theory to a thin slice Kerr ring cavity system in a more generalised form and show that pattern formations are altered by the inclusion of diffusion and finite response of the medium, leading to new stable honeycomb patterns for focusing media and further that the inclusion of diffusion alone may lead to a hexagon-roll transition as seen in Fig. 2.

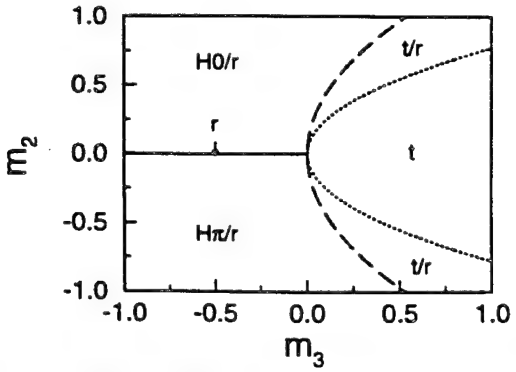

Fig. 1. Pattern behaviour diagram for the diffraction-diffusion system in (m_2, m_3) parameter space.

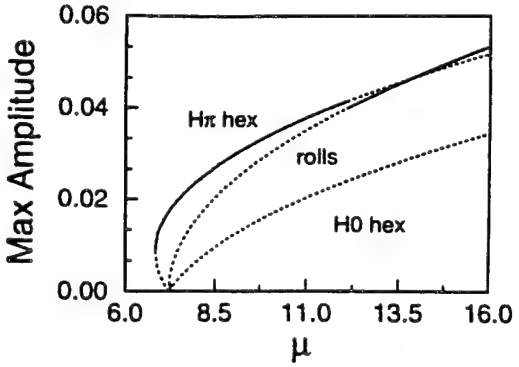

Fig. 2. Bifurcation diagram of the hexagon and roll states as a function of the control paramter.

[1] See for example N. B. Abraham and W. Firth. *J. Opt. Soc. Am. B* **7**, 951 (1990); L. A. Lugiato. *Phys. Rep.* **219**, 293 (1992);

[2] S. Ciliberto, P. Coullet, J. Lega, E. Pampaloni, and C. Perez-Garcia. *Phys. Rev. Lett.* **65**(19), 2370 (1990).

[3] M. Tilde, P. Mandel and R. Lefever. *Phys. Rev. Lett.* **73**(5), 640, (1994).

Spatiotemporal chaos due to attractor merging in a Class-C-Laser

M.Sauer, F. Kaiser

Institute for Applied Physics - Nonlinear Dynamics,Technical University Darmstadt,Hochschulstr.4a,

64289 Darmstadt, FRG

Phone: + 6151 163379, Fax: + 6151 163279, E-mail: markus@optics.iap.physik.th-darmstadt.de

The investigation of transverse laser dynamics has attracted wide interest during the last years. Research effort has mainly been focussed on the investigation of wide-gain-section lasers [1] with large aspect-ratio on the one hand and lasers with stable resonators which can be described by a low number of linear cavity modes and correspond to small aspect ratio on the other hand[2]. Both situations can be adequate descriptions of experiments. In order to clarify the connection between dynamics governed by few cavity modes and situations of wide-gain-section we investigate the behaviour of a Class-C-Laser with a stable resonator. However, we do not restrict the dynamics to only a few modes but perform direct numerical simulation of the Maxwell-Bloch-equations. We observe a transition into spatiotemporal chaos due to merging of two attractors which coexist because of the symmetry breaking induced by left- and right-travelling waves respectively. The model reads [1]:

$$\frac{\partial E}{\partial t} = -\mu E + i\delta(x) - ia\frac{\partial^2 E}{\partial x^2} + \beta_1 P \tag{1}$$

$$\frac{\partial P}{\partial t} = -\gamma_1(1 + i\omega_{ab})P + \beta_2 EN \tag{2}$$

$$\frac{\partial D}{\partial t} = -\gamma_2(D - D_0(x)) - \frac{1}{2}\beta_2(EP^* + E^*P) \tag{3}$$

Here, $\delta(x)$ takes into account the curvature of the cavity mirrors. For explanation of the remaining variables and parameters, see [1]. Since the cavity modes in general oscillate with different frequencies depending on their order, they can individually be tuned to resonance with the atomic transition frequency. Slightly above the first laser threshhold, the behaviour of the system is then governed by the cavity mode whose oscillation frequency lies nearest to the atomic line. For higher pump levels instabilities for modes higher than the ground mode occur which are due to spatial hole burning. These solutions involve contributions of a high number of linear resonator modes and are reminiscent of the recently reported travelling wave solutions in geometries where the influence of transverse boundaries is strong [3]. The wave

travelling in one specific direction accounts for symmetry-breaking of the beam profile (left). For higher pump strength, the dynamics of the system involves periodic and quasiperiodic states, however, with the wave travelling to one direction only (Fig. 1 (center)). Of course, an attractor with a right-travelling wave coexists. These two coexisting attractors merge at a certain point due to an attactor crisis and the system performs intermittent jumps between the now merged attractors (Fig.1 (right)). It is therefore an example of crisis-induced intermittency due to attractor merging in a spatially extendend system as has previously reported for the Ikeda-system [4]. At the same time, the crosscorrelation of the signal decreases significantly. The merged situation can thus be classified as spatiotemporally chaotic.

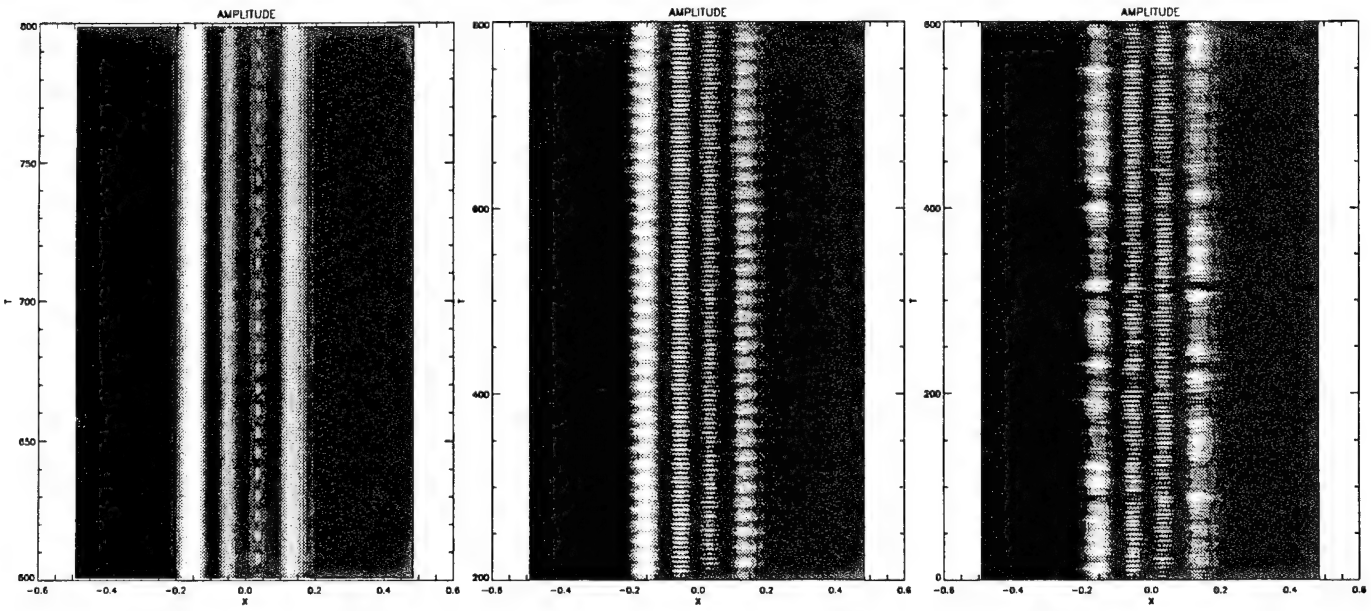

Figure 1: left: time evolution a GH(3)-Mode with left-travelling wave, center: just before merging with the coexisting state, right: just after merging of the coexisting states

References

[1] P.K.Jakobsen et. al., Phys.Rev. A 45 (1992), p.8129

[2] M.Brambilla et. al., Phys.Rev.A 49 (1994), p.1427

[3] Q.Feng et. al., Phys.Rev.A (1994), p.R3601

[4] M.Sauer et. al., Chaos,Solitons Fractals, 4 (1994), p.1461

Controlling the unstable steady-states of lasers using continuous feedback

Daniel J. Gauthier, Duke University, Department of Physics
and Center for Nonlinear and Complex Systems, Durham, NC 27708 USA
Voice: (919) 660-2511, FAX: (919) 660-2525, e-mail: gauthier@phy.duke.edu

In many cases of practical importance, it is desirable to stabilize chaotic lasers by applying only small perturbations to some accessible system parameter. An efficient scheme for achieving such control was proposed by Ott, Grebogi, and Yorke (OGY) [1] and variations of the scheme have been used successfully to control the dynamics of lasers [2]. The key idea is to take advantage of the unstable states embedded in the attractor. As the system approaches the unstable state, the size of the feedback signal required to keep it there vanishes and its smallness is limited only by the noise level in the system. We describe an alternative implementation of the OGY scheme that efficiently stabilizes the unstable steady-states (USS) of a dynamical system and it can be easily applied to high-speed optical systems.

The control scheme for stabilizing USS's is a specific case of a general feedback algorithm recently introduced for stabilizing unstable periodic orbits (UPO's) [3]. Stabilization of UPO's is achieved by feedback of a continuous error signal

$$\epsilon(t) = \vec{c}_f \cdot [\vec{\xi}(t) - (1-R)\sum_{k=1}^{\infty} R^{k-1}\vec{\xi}(t-k\tau)] \quad , \tag{1}$$

that is proportional to the difference between the present value of an accessible state variable $\vec{\xi}(t)$ and an infinite series of values of the state variable delayed by integral multiples of the period of the orbit τ, where $0 \leq R \leq 1$, and $\vec{c}_f$ is a gain vector. Note that the form of Eq. 1 is closely related to the amplitude of light reflected from a Fabry-Pérot interferometer suggesting an all-optical implementation. The case $R = 0$ corresponds to the scheme investigated by Pyragas [4] and Lu and Harrison [5], and it was used successfully to control UPO's in a laser [6]. The more general scheme ($R \neq 0$) can stabilize highly unstable orbits and it is capable of extending the domain of effective control significantly [3].

Optimal control of USS's using the continuous feedback scheme can be achieved when the feedback loop is adjusted such that $\tau \to 0$, $R \to 1$, with the ratio $(1-R)/\tau$ finite. Under these conditions, the feedback signal is determined approximately by the differential equation

$$\frac{d\epsilon}{dt} = -\gamma_f \epsilon + \vec{c}_f \cdot \frac{d\vec{\xi}(t)}{dt} \quad , \tag{2}$$

where $\gamma_f = (1-R)/\tau$. Equation 2 is closely related to the transmission of an high-pass filter and the amplitude of light reflected from a high-finesse Fabry-Pérot interferometer with a short mirror spacing. We emphasize that $\epsilon(t)$ vanishes when the system is on the USS since $d\vec{\xi}(t)/dt = 0$. *Thus, there is no power dissipated in the feedback loop when control is successful.* Lu and Harrison [5] found that USS's of a laser could be stabilized theoretically using a feedback signal given by Eq. 1 with $R = 0$ for some values of $\vec{c}_f$ and τ; however, the general case when $R \neq 0$ was not addressed.

To confirm theoretically the effectiveness of the proposed feedback scheme, we have used it to stabilize the two non-zero USS's of the resonant, homogeneously broadened two-level laser. The domain of control is determined by performing a linear stability analysis of the laser equations including the effects of the feedback signal. In the first example, we investigated 'coherent control' where the feedback signal is generated by filtering a fraction of the optical field with a Fabry-Perot interferometer and control is initiated by injecting the filtered field into the laser. The injected field is given by

$$\frac{dE_{inj}}{dt} = -\gamma_f E_{inj} - c\frac{dE}{dt} \quad , \tag{3}$$

where E represents the laser field. The domain of control for coherent feedback is shown in Fig. 1a where it is seen that stabilization of the USS is effective for arbitrarily large pump rates. The domain of control is the same for both phases of the field; the initial conditions determine the phase that is stabilized successfully. In the second example, we investigated 'incoherent control' where the pump rate w_p is adjusted about its nominal value w_p^o by a feedback signal that is generated by high-pass-filtering a signal proportional to the intensity I of the laser. The pump rate with control is given by $w_p = w_p^o + \epsilon(t)$ where

$$\frac{d\epsilon}{dt} = -\gamma_f \epsilon + c\frac{dI}{dt} \quad . \tag{4}$$

The domain of control for incoherent feedback is shown in Fig. 1b where it is seen that control is also possible for arbitrarily large pump rates and that the range of feedback strengths that give rise to successful control is finite.

We acknowledge discussions of this work with R. Roy and J. Socolar and support from the U.S. ARO through contract No. DAAL03-92-G-0286 and the National Science Foundation through Grant No. PHY-9357234.

[1] E. Ott, C. Grebogi, and J. Yorke, Phys. Rev. Lett **64**, 1196 (1990).
[2] R. Roy, T. W. Murphy, Jr., T. D. Maier, Z. Gills, and E. R. Hunt, Phys. Rev. Lett. **68**, 1259 (1992).
[3] J. E. S. Socolar, D. W. Sukow, and D. J. Gauthier, Phys. Rev. E **50**, 3245 (1994).
[4] K. Pyragas, Phys. Lett. A **170**, 421 (1992).
[5] W. Lu and R. G. Harrison, Opt. Commun. **109**, 457 (1994).
[6] S. Bielawski, D. Derozier, and P. Glorieux, Phys. Rev. A **47**, R2492 (1993).

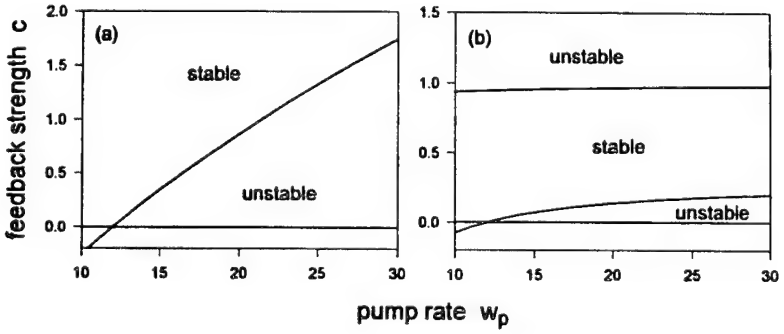

Figure 1 Domain of control for (a) coherent and (b) incoherent feedback with $\kappa/\gamma_\perp = 4$, $\gamma_\parallel/\gamma_\perp = 0.5$, and $\gamma_f/\gamma_\perp = 0.1$. The laser becomes unstable when $w_p = 13$.

Instabilities and Synchronization of Coupled Solid-State Lasers

K. Scott Thornburg, Jr., Michael Möller*, and Rajarshi Roy
Georgia Institute of Technology, School of Physics
Atlanta, GA 30332-0430
Phone: (404) 853-0027 Fax: (404) 853-9958
e-mail: scott@socrates.physics.gatech.edu

Chaotic intensity fluctuations of two pump modulated, multimode infrared lasers generated in one Nd:YAG crystal pumped by a pair of spatially-separated Argon-ion laser beams have been investigated earlier as an example of synchronized chaotic systems. There is an interaction between these lasers due to the overlap of the infrared fields which depends on their spatial separation [1-2].

We report here the results of measurements on an experimental system with single mode, similarly polarized lasers. The pump optics have been modified to optimize the range and reproducibility of the laser coupling. The mode structure, spatial separation, and intensities of both lasers now can be measured simultaneously, as well as their relative frequency detuning. We now present further insights into the behavior of both the autonomous (unmodulated) and chaotic, non-autonomous laser systems.

Theoretical analysis of the weak-coupling equations [2] for the autonomous case predicts an instability in the vicinity of the phase-locking threshold [3]. Experimental measurements confirm the existence of an instability at the spatial separation value predicted. For the non-autonomous case, theoretical predictions of the model [see Fig. 1] are compared with experimental data, yielding quantitative agreement, particularly for the minimum coupling necessary to achieve synchronization for loss-modulation. Fig. 1(a) shows the visibility of the far field interference fringes for the superimposed laser beams, $V = (I_{max} - I_{min})/(I_{max} + I_{min})$, which is a measure of phase-locking. Fig. 1(b) shows the correlation coefficient $r = \mu_{12}/(\sigma_1\sigma_2)$, μ_{12} is the covariance of the intensity fluctuations of laser 1 and laser 2 and σ_i denote the respective standard deviations. Measurements of the extent of synchronization as a function of coupling for different modulation schemes are presently underway.

Another set of experiments investigates synchronization using time-delayed bidirectional or unidirectional coupling, in contrast to the lateral coupling described previously. Recent theoretical work has proposed a possible application of such a scheme in encoding messages in the background of a chaotic signal using synchronized lasers [4-6], which has not been demonstrated in an experiment yet.

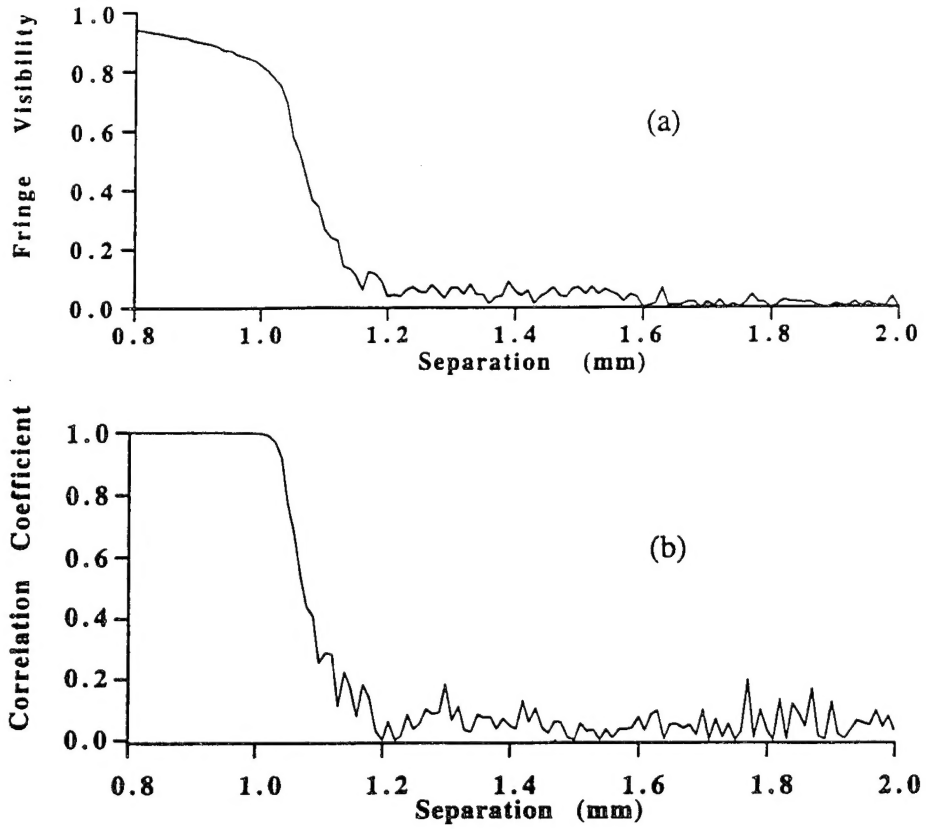

Figure 1. Theoretical prediction of (a) far-field fringe visibility and (b) correlation coefficient versus spatial separation for two loss-modulated, laterally coupled Nd:YAG lasers. A visibility of one indicates perfect phase-locking; a correlation coefficient of one indicates perfect synchronization of intensity fluctuations.

* Permanent Address: Westfälische Wilhelms-Universität, Institut für Angewandte Physik, Corrensstraße 2/4, 48149 Münster, Germany.

References

1. R. Roy and K. S. Thornburg, Jr., Phys. Rev. Lett. 72, 2009 (1994).
2. L. Fabiny, P. Colet, R. Roy, and D. Lenstra, Phys. Rev. A47, 4287 (1993).
3. T. W. Carr, T. Erneux, and R. Li, (private communication).
4. K. V. Cuomo and A. L. Oppenheim, Phys. Rev. Lett. 71, 65 (1993).
5. L. M. Pecora and T. L. Carroll, Phys. Rev. A44, 2374 (1991).
6. P. Colet and R. Roy, Opt. Lett. 19, 2056 (1994).

Author Index